Glycosylation of PrP and the Transmissible Spongiform Encephalopathies species barrier

Frances Wiseman

Ph.D. by Research
The University of Edinburgh
2006

Declaration

I declare that this thesis has been composed entirely by myself and that the work presented herein is my own, except where otherwise stated. All experiments were designed by myself, in collaboration with my supervisors. No part of this thesis has or, will be, submitted for any other degree, diploma or qualification.

Frances Wiseman

Acknowledgement

None of this work could have been carried out without the kind permission of the families of the variant and sporadic CJD patients that were studied here. Thank you.

Many thanks to my supervisors, Dr. Enrico Cancellotti, Professor Jean Manson, Professor James Ironside and Professor David Price, for their continuing help, support and belief.

Much thanks to Irene McConnell, Val Thomson, Mary Brady, Simon Cummings, Shona Herd, Lynsey Doyle, Carol Blain, Leeann Frame, Emma Murdoch, Stuart Dunlop, Kris Hogan, Rebecca Greenan and Sally Shillinglaw for all there help with the transgenic lines and *in vivo* experiments. Thanks to Aileen Boyle and Wingee Lui for lesion profiling and to Gillian McGregor and Sandra Coupar for sectioning the Category Three material for me. Many thanks to all those in the Pathology department at NPU, especially Anne Suttie for their help and advice on all things histological. Thanks also to the unending patience, advice and kindness of all the staff in the TSE division at Edinburgh and Compton. In particular thanks to Dr. Nadia Tuzi, Dr. Rona Barron and Dr. Patricia Hart for listening, encouraging, reading and correcting during the past three years, and all in the Mouse and Sheep Genetics group especially for the loans of gels (Dec, Chris, Barry, Lorna, Gwen and Angie), antibodies (Bridget and Rona) and most importantly protocols (Tricia, Rona, Nadia, Angie, Dec, Chris, Herbert and Barry). Thanks to Val Finlayson for help with sourcing of obscure references. Thank you to Dr. Jill Sales for advice on all things statistical.

At the CJD Surveillance Unit many thanks to Dr. Mark Head, Helen Yull, Dr. Alex Peden and Diane Ritchie for their help during my time there. Thank you, to Dr. Paul Monaghan, Jennifer and Pippa at Bioimaging in Pirbright, for all their help detecting PrP by Confocal and making my time in Surrey so fun, and to Virginine and Eleanor for letting take over their box room. Many thanks to Professor Claudio Soto, Dr.

Joaquin Castilla, Paula, Jorge, Rodrigo, Lisbell, Karim, June and Becky at University of Texas Medical Branch for making me so welcome, helping me so much and pushing me to do the apparently impossible (and for footing the bill for all those gels). Thanks again to Dr. Rona Barron and Declan King for help with the transportation of Dangerous Goods to the U.S. Thanks to the department of Pathology at the University of Edinburgh for the PAGE bursary for the second trip to Texas. Many thanks to all those in the TSE research community, the discussion with whom have been invaluable in helping me develop the direction of this thesis.

Thanks to Declan for the gift of Europium labelled antibodies. Thanks to Man-Sun Sy, for 7A12 and 8H4 antibodies, to Dr. C.R Birkett for FH11 antibody and Dr. J.M Manser for AH6 and AG4 antibodies that were supplied by Ruth Hennion at the TSE Resource Centre, IAH Compton. Thanks to Dr. Ian Sylvester, IAH Compton for recombinant murine PrP. Many thanks to Dr. Tom Wileman for the gift of anti-ERp60 and anti-βcop antibodies. Thank you to Angela Jen and Professor Roger Morris (Kings College London), Dr. Paulette Zaki (University of Edinburgh) and Enrico (NPU) for showing me the ropes of cell culture, despite it not making it in to this thesis.

Thanks to the organisers of the 4-year Wellcome Program for giving me the opportunity to study at Edinburgh. Big thank you to the Wellcome girls and the 2002 NPU students for tea, sanity and hill-of the-week meetings, to most of all to Andy and Ruth for understanding, and my mum and dad for preventing homelessness, hunger and the use of poor grammar.

Many thanks, to Christine Farquhar, Nick Wiseman, Tricia Hart and Andrew Wheeler for proof-reading this thesis.

This work was supported by the Wellcome Trust at the Institute for Animal Health-Neuropathogenesis Unit Edinburgh, The National CJD Surveillance Unit Edinburgh, The Institute for Animal Health - Bioimaging Facility at Pirbright and the University of Texas Medical Branch, Galveston.

Abstract

Transmissible spongiform encephalopathies (TSEs) are a group of fatal neurodegenerative diseases. They can be readily transmitted within a host species but are rarely transmitted between different species. This "*species barrier*" effect is characterised by reduced susceptibility of exposed novel hosts and an increase in the length and variability of the incubation period. The mechanisms that underlie this barrier are yet to be fully understood; hence it is currently not possible to accurately predict the host range of a novel TSE disease. During TSE pathogenesis the host protein, PrP, misfolds and accumulates within the central nervous system. This misfolded form is denoted PrP^{Sc} to discriminate it from the normal cellular form PrP^{C}. The prion hypothesis proposes that PrP^{Sc} is the TSE infectious agent and propagates its aberrant conformation by inducing PrP^{C} to misfold. PrP is variably glycosylated at two sites *in vivo*, such that di-, mono- and un-glycosylated glycotypes are observed; all of these PrP glycotypes can form PrP^{Sc}. However the role of each glycotype in cross species transmission is unclear. *In vitro* conversion experiments have suggested that PrP^{C}'s N-glycans specifically retard the cross species PrP^{Sc} seeded conversion of PrP^{C}. Thus glycosylation of PrP^{C} may inhibit cross-species TSE transmission.

Previous studies have not examined the role of glycosylation of PrP^{C} in the cross-species transmission of TSE disease. In this study glycosylation deficient transgenic mice [NPU] were challenged with three non-murine TSE agents. A barrier to cross-species transmission was observed in normally glycosylated control mice, although a proportion of animals did develop signs of TSE disease after challenge with hamster scrapie (263K) and variant CJD (vCJD). Transgenic mice that lack both N-glycan attachment sites were resistant to cross-species TSE challenge (263K, vCJD and sporadic CJD). Moreover, absence of N-glycans at the first site only, resulted in a significant decrease in disease incidence after challenge with 263K. These data suggest that glycosylation of the first site mediates the transmission of TSE between species. However, this effect is not unique to cross-species transmission as previous reports have demonstrated that the within-species transmission of TSE is also delayed by the absence of the first N-glycan attachment site. Transgenic mice which lack

glycosylation at the second site were shown to have a higher disease incidence than controls after cross-species challenge with 263K or sporadic CJD. Therefore, glycosylation of the second site inhibits the cross-species transmission of these strains. This effect is specific to cross-species transmission as previous murine TSE transmissions to these mice have not demonstrated an acceleration of disease. Thus the site of glycosylation determines the role of the N-glycan in cross-species transmission. Moreover, here it is shown that mice which lack the second N-glycan attachment site exhibit a reduced disease incidence after challenge with vCJD compared to control mice. Therefore, TSE strain determines the role of N-glycans in disease transmission.

To further interpret these transmission studies, the localisation of PrP^{C} in the glycosylation deficient transgenics was investigated using confocal microscopy. No significant difference in the cellular localisation of PrP^{C} was detected in mice which lack the first or second N-glycosylation sites. Therefore, the effect of N-glycan attachment at these sites on TSE transmission occurs independently of PrP^{C}'s cellular location. Lower levels of anti-PrP signal were detected in the neuropil of mice that lack both N-glycan attachment sites than in control animals, suggesting a possible mechanism for the enhanced resistance of these transgenic mice to TSE challenge.

Normally glycosylated PrP can be induced to adopt a misfolded conformation *in vitro*, by exposure to infected brain homogenate, mimicking the *in vivo* formation of PrP^{Sc}. Using an *in vitro* conversion assay, the ability of PrP derived from the glycosylation deficient transgenic to misfold was studied. PrP that lacks the first N-glycan attachment site did not misfold, suggesting a potential cause of the enhanced resistance of the transgenic mice that lack this site to TSE transmission. PrP that lacks the second N-glycan attachment site adopted a misfolded form *in vitro*, with efficiency equal to that of normally glycosylated PrP. Therefore the higher disease incidence observed in the transgenic mice, which lack the second PrP glycosylation site, did not occur because PrP in these animals is more readily misfolded. This suggests that other aspects of PrP biology, such as PrP^{Sc} toxicity or clearance, are influenced by glycosylation of PrP's second site and that these can alter TSE disease.

Abbreviations

129/Ola	inbred wild type mouse strain 129/Ola, murine PrP^a
BAC	bacterial artificial chromosome
bp	base pair
BSA	bovine serum albumen
BSE	bovine spongiform encephalopathy
C57/B6	inbred wild type mouse strain C57/B6, murine PrP^a
CDI	Conformational Dependent Immunoassay
CJD	Creuztfeldt-Jacob Disease
CL	transgenic control line, carrying a *loxP* site downstream of wild type *Prnp*
CNS	central nervous system
CSF	cerebrospinal fluid
CV	F1 cross of inbred wild type C57/B6 and VM mouse strains,
CWD	Chronic Wasting Disease
ctyPrP	Cytoplasmatic PrP
(k)Da	(Kilo)Dalton
DELFIA	Differential Extraction Lanthanide Fluorometric Immunoassay
dH_2O	distilled water
DNA	deoxyribonucleic Acid
d.p.i	days post inoculation
EDTA	ethylenediaminetetracetic Acid
ER	Endoplasmatic Reticulum
ERAD	ER associated degradation
FFI	Fatal Familial Insomnia
FSE	feline spongiform encephalopathy
G1	PrP glycosylation deficient transgenic, lacking the first N-glycan attachment site (N180T)
G2	PrP glycosylation deficient transgenic, lacking the second N-glycan attachment site (N196T)

G3	PrP glycosylation deficient transgenic, lacking both N-glycan attachment sites (N180T, N196T)
GFAP	glial fibrillary acidic protein
Gnd HCl	guanidine hydrocholoride
GSS	Gerstmann-Stäussler Scheinker (Syndrome)
GPI	Glycosyl-phosphatidylinositol
HLA	Human Leukocyte Antigen
HPRT	hypoxanthine phosphorbosyl transferase
IAH	Institute for Animal Health
ic	inter cerebral
IHC	immunohistochemistry
ip	inter peritoneal
iv	intra venous
Kb	kilobase
LRP	laminin receptor precursor
mRNA	messenger RNA
NaPTA	sodium phosphotungstic acid
Neo/TK	LoxP neomycin/thymidine kinase-selectable cassette
NIH	National Institute of Health
NP40	nonidet P40
NPU	Neuropathogenesis Unit
ORF	open reading frame
PAGE	Polyacrylamide Gel Electrophoresis
PBS	phosphate buffered saline
PBST	phosphate buffered saline 0.5% Tween
PCR	Polymerase Chain Reaction
PIPLC	phoshatidylinosital phospholipase C
PK	proteinase K
PI	proteinase inhibitor
PMCA	Protein Misfolding Cyclic Amplification
PMSF	phenylmethysulforyfluoride
PNGase	Peptide: N-Glycosidase F

POD	peroxidase substrate
Prnp	PrP gene encoding murine PrP
PRNP	PrP gene encoding human PrP
PrP	Prion related protein
PrP*	theoretical subset of PrP^{Sc} that corresponds to the TSE agent
PrP^{a}	murine PrP 108L and 189T
PrP^{b}	murine PrP 108 F and 189V
PrP^{C}	PrP-cellular; native, uninfectious form of PrP
PrP^{Ctm}	transmembrane PrP with the C-terminus within the ER lumen
PrP^{d}	PrP-disease; TSE challenge associated PrP deposited *in vivo*
PrP^{Ntm}	transmembrane PrP with the N-terminus within the ER lumen
PrP^{Sc}	PrP-Scrapie; infectious form of PrP equivalent to a prion
PrP^{Res}	PK resistant form of PrP generated *ex vivo*
rPrP	recombinant PrP
PVDF	Polyvinylidine fluoride
NMR	Nuclear Magnetic Resonance
RNA	Ribonucleic Acid
SDS	Sodium Dodecyl Sulphate
TBE	Tris boric acid/EDTA buffer
TBS	Tris buffered saline
TBST	TBS 1 % Tween
TME	Transmissible Mink Encephalopthy
TSE	transmissible spongiform encephalopathy
vCJD	Variant Creuztfeldt-Jacob Disease
UPR	unfolded protein response
UV	Ultraviolet light
VM	Inbred wild type mouse strain VM, murine PrP^{b}

Contents

Figure List

Chapter 1

Chapter 2

Chapter 3

Chapter 4

Chapter 5

Chapter 6

Chapter 7

Tables

Chapter 1

Chapter 2

Chapter 5

Chapter 6

Chapter 7

Introduction

Table 1.1 History of TSE Research (References in body of text)

1732 Scrapie first identified in sheep
1883 Report of scrapie-like disease in a cow
1937 Transmission of scrapie to other sheep
1939 Report of scrapie in a goat
1940 Transmission of scrapie via pasture
1942 Experimental transmission of scrapie from sheep to goat
1947 TME identified
1957 Kuru first studied
1959 Kuru identified as a TSE
1961 Experimental transmission of scrapie to mice
1961 Multiple strains of scrapie identified in goats
1965 TSE species barrier proposed
1965 TME outbreak linked to a downer cow
1966 Transmission of Kuru to Chimpanzees
1967 Scrapie resistant to UV/ theory for non-nucleic acid replication
1967 CWD emergence
1968 Host genetic factor (*Sinc*) controls murine scrapie incubation period
1977 CWD identified as TSE
1980 Infectivity associated with a protease resistant component
1981 Familial TSE infectious
1982 Prion hypothesis
1985 PrP identified as host factor putative prion
1986 First case of BSE identified in the United Kingdom
1989 PrP mutation linked to familial TSE
1989 Transmissibility of TSE linked to PrP amino acid homology
1990 Over-expressing tgPrP develop TSE signs
1991 PrP* not PrP^{Sc} the infectious agent
1992 PrP non-essential gene
1993 PrP knockout TSE resistant
1993 Efficient PrP conversion *in vivo* requires additional cellular factors
1993 Conformational difference between PrP^{C} and PrP^{Sc}
1994 TSE strains differ in PrP^{Sc} conformations
1994 Cell free conversion of PrP^{C} to PrP^{Sc}
1996 vCJD identified
1997 BSE causes vCJD
1997 BSE primary pass in the absence of detectable PrP^{Sc}
2002 Species barrier correlates with conformational change in PrP^{Sc}
2003 synthetic prions shown to be infectious
2005 *in vitro* generated PrP^{Res} shown to be infectious

1.1 Overview of TSE disease

Transmissible Spongiform Encephalopathies (TSEs) are a diverse group of relatively rare diseases which include: scrapie in sheep and goats; transmissible mink encephalopathy (TME); chronic wasting disease (CWD) in North American deer and elk; and bovine spongiform encephalopathy (BSE) which has been reported to have naturally infected cattle, exotic ungulates, cats (Feline Spongiform Encephalopathy FSE), non-human primates, and to date 195 human patients world wide (variant CJD - vCJD) (Table 1.2 and 1.3). A number of other human TSEs have also been identified. These include: Creutzfeldt-Jakob disease (CJD) that has been shown to have idiopathic, familial and iatrogenic aetiologies; Fatal Familial Insomnia (FFI) that also has been observed in a sporadic form; Gerstmann-Staussler-Scheinker disease (GSS), and Kuru which was an epidemic disease in the Eastern Highlands of New Guinea during the first half of the last century (Table 1.3).

These fatal neurodegenerative diseases are characterised by long incubation periods and present with symptoms such as ataxia, trembling, dementia, hallucinations, depression, visual abnormalities and insomnia in human patients. A number of types of TSE have been observed that have differing combinations of clinical symptoms and rate of disease progression, although all share a common underlying pathology of spongiform vacuolation of the brain. Neuronal loss, astrocytic proliferation and activation are also commonly observed in these conditions.

Disease is frequently but not always associated with the accumulation of a protease resistant form of the host glycoprotein PrP, denoted PrP^{Sc}, within the central nervous system and in some cases peripheral lymphoid tissue (Bolton et al., 1982; Bruce et al., 1989; DeArmond et al., 1993; Hill et al., 1997b; van Keulen et al., 1996). The normal form of this host protein (PrP^{C}) is required for the development of TSE disease as mice that lack it are refractory to infection (Bueler et al., 1993; Manson et al., 1994b). Currently there is no effective treatment, prophylaxis or accurate pre-mortem test for TSEs. Therefore a greater understanding of this group of diseases

Table 1.2 TSEs of animal species

TSE	Natural host Species	Route of Transmission	First Identified
Scrapie	domestic sheep (*Ovis aries*), moufflon (*Ovis musimon*), goats (*Capra hirus*)	Unknown	1732 (Chelle, 1942)
Atypical scrapie	domestic sheep (*Ovis aries*),	Unknown	(Benestad et al., 2003)
TME	mink (*Mustela vison*)	Putatively oral	(Hartsough and Burger, 1965)
BSE	cattle (*Bos primigenius familiaris taurus*), greater kudu (*Tragelaphus strepsiceros*), eland (*Taurotragus oryx*), 3 oryx spp. (*Oryx spp.*), nyala (*Tragelaphus angasi*), bison (*Bison bison*), goats (*Capra hirus*); rhesus macaque (*Macaca mulatta*), 3 lemur spp. (*Eulemur spp.*)	Oral recycling of CNS material	(Bons et al., 1999; Bons et al., 1996; Eloit et al., 2005; Kirkwood and Cunningham, 1994; Wells et al., 1987)
FSE	domestic cat (*Felis catus*), cheetah (*Acinonyx jubatus*), puma (*Felis concolor*), ocelot (*Felis pardalis*), tiger (*Panthera tigris*), lion (*Leo panthera*)	Oral recycling of CNS material	(Kirkwood and Cunningham, 1994; Wyatt et al., 1991)
Atypical BSE (L or H)	cattle (*Bos primigenius familiaris taurus*)	Unknown	(Biacabe et al., 2004; Casalone et al., 2004)
CWD	white tailed deer (*Odocoileus virginianus*), mule deer (*Odocoileus hemionus*), elk (*Cervus elaphus nelosini*)	Unknown	(Williams and Young, 1980)

Table 1.3 TSEs of humans

TSE	Clinical Features	Route of Transmission	First Identified
Sporadic CJD	Dementia, visual abnormalities, ataxia, cognitive impairment, psychiatric signs	Unknown (spontaneous)	Creutzfeldt 1920 Jakob 1921
fCJD		Associated with familial mutations in *PRNP*	Meggendorfer 1930
Iatrogenic CJD		dura mater, cornea grafts and hGH,	(Duffy et al., 1974)
FFI	Ataxia, insomnia	Familial mutation in *PRNP* (D178N linked to 129M)	(Lugaresi et al., 1986)
Sporadic FI	Ataxia, insomnia	Unknown sporadic	(Mastrianni et al., 1999)
GSS	Ataxia, late onset dementia	Associated with familial mutation in *PRNP*	Gerstmann 1938
Kuru	Ataxia, loss of lumbar control	Oral (endocannabilism)	(Gajdusek and Zigas, 1957)
vCJD	Psychiatric signs, ataxia and dementia	Oral (consumption of BSE contaminated beef), intravenous (IV by blood transfusion)	(Will et al., 1996)

and the role of PrP in them is important for the development of both diagnostics and treatments.

1.1.1 TSE, spontaneous, familial and acquired

TSE disease unusually occurs in spontaneous, familial and acquired forms. Many of the spontaneous cases of disease have been demonstrated to be transmissible to new hosts, suggesting that the *de novo* synthesis of an infectious agent has occurred (Brown et al., 1994). However, spontaneous or sporadic forms of disease may occur because of an unidentified infectious agent, the source of which may be obscured by the disease's long incubation time (Diringer, 1995). Equally, spontaneous disease may theorectically result from a somatic mutation in *PRNP* (Prusiner, 1991), although no such events have ever been identified. However, familial clusters of TSE disease are clearly associated with mutations in the PrP gene (*PRNP*) (Figure 1.1). These changes may increase the probability of PrP adopting the disease associated misfolded conformation. However, others have suggested that these mutations may enhance susceptibility to external TSE agents, rather than result in pure spontaneous disease (Manson et al., 1999). Moreover, clear evidence demonstrates that susceptibility to acquired TSE disease is influenced by polymorphisms in PrP in a number of host species (Figure 1.1); this is consistent with the known requirement for PrP in TSE disease. TSE disease has only been observed in mammals, although all chordates are proposed to carry *Prnp/PRNP*, and homologs of PrP have been identified at the level of protein in fish, turtles and chickens (Rivera-Milla et al., 2003; Wopfner et al., 1999).

Figure 1.1 Structure, polymorphisms and mutations of PrP

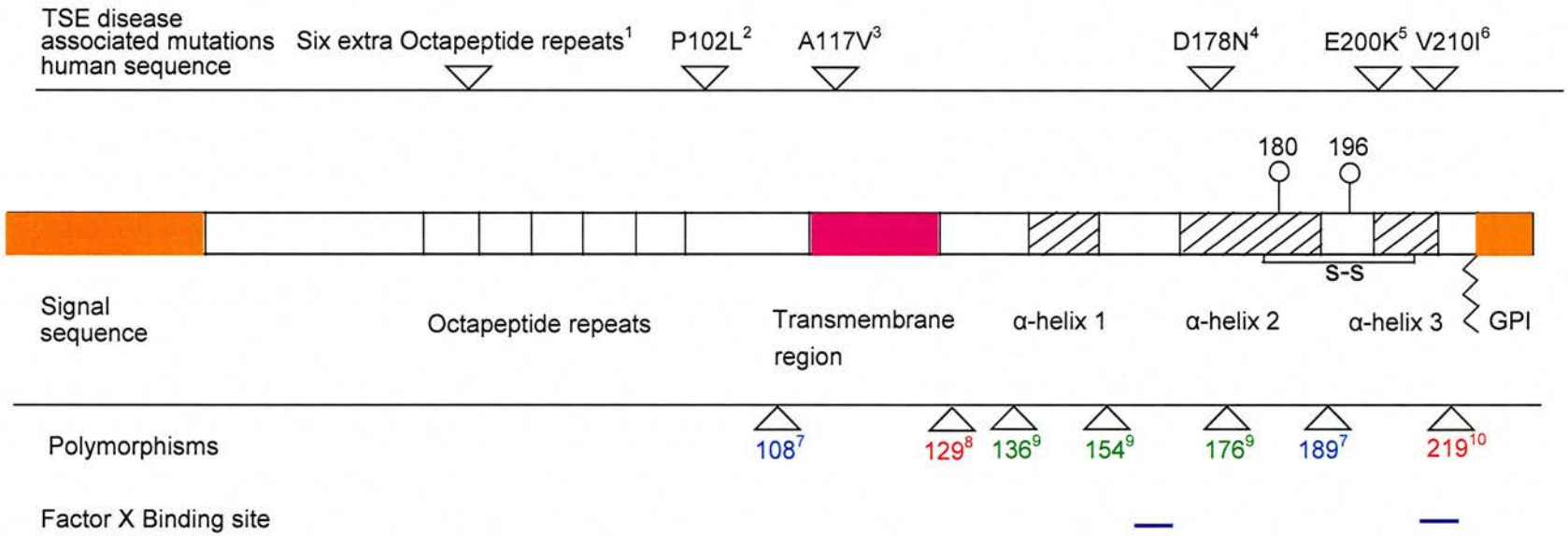

TSE associated mutations key

[1]Owen et al 1989, Polulter et al 1992

[2]Hsiao et al 1989

[3]Doh-Ura et al 1989

[4]Nieto et al 1991

[5]Goldfarb et al 1991

[6]Mouillet-Richard et al 1999

Polymorphisms key
(position in species PrP sequence)

Blue Murine; [7]Westaway et al 1987
Red Human; [8]Palmer et al 1991, [10]Petraroli et al 1996
Green Sheep; [9]Goldmann et al 1994

1.1.2 Natural/iatrogenic TSE transmissions

Natural transmissions of TSE agents have been observed principally via oral routes (Kuru, BSE and vCJD) (Mathews et al., 1968; Ward et al., 2006; Wilesmith et al., 1988) and by undefined contact with infected individuals or a contaminated environment, which may also be orally mediated (scrapie and CWD) (Greig, 1940; Miller and Williams, 2004). Iatrogenic transmission by direct contact with infected CNS material which can be mediated by: cadaver pituitary derived human growth hormone treatment (Koch et al., 1985); dura mater (Hoshi et al., 2000); cornea transplantation (Duffy et al., 1974) and intracerebral EEG electrode recordings (Bernoulli et al., 1977). Recently, transmission of TSE by blood transfusion has been reported (Llewelyn et al., 2004; Peden et al., 2004). Generally, natural TSE transmissions exhibit long incubation periods which complicate epidemiological study. However the majority of acquired TSE diseases have been reported to have an epidemic nature and a number of recorded outbreaks have been self-limiting owing to their poor transmissibility and fatal nature (e.g. TME). However, scrapie in sheep and goats has become established as an endemic disease in a large number of countries, although it too has an epidemic nature at the level of individual flocks (Gubbins et al., 2006). Furthermore, CWD has yet to be successfully controlled and poses a risk of becoming an endemic disease in North America, although current evidence does not suggest it has been transmitted to humans (Belay et al., 2004).

A number of cases of natural TSE disease occurring in different host species from the same geographical location have been recorded including scrapie in sheep and goats (Mackay and Smith, 1961; Toumazos, 1991) and CWD in Mule, White-tailed deer and Elk (Spraker et al., 1997). This suggests that the TSE agent may have been transmitted between these species. Additionally, BSE has been naturally transmitted to fifteen other species including humans (Eloit et al., 2005; Kirkwood and Cunningham, 1994; Will et al., 1996; Wyatt et al., 1991). However cross-species transmissions of TSEs are generally limited. Susceptibility to disease is often observed to be reduced after transmission to a new host species and the incubation period after transmission is often greatly prolonged (Pattison, 1965). This "*species*

barrier" to disease transmission is attenuated on secondary and subsequent passage within the same species, such that a reduction both in length and the variability of incubation period is observed (Pattison, 1965). For conventional infectious agents the species barrier would be interpreted as the requirement for the pathogen to adapt to the new host species via a selection driven accumulation of mutations within the pathogens genome.

1.1.3 Experimental TSE transmission

Experimental transmissions of TSEs to sheep, goats, non-human primates and, most commonly rodents, (hamsters (*Mesocricetus auratus*), mice (*Mus musculus*) and bank voles (*Clethrionomys glareolus*)) have been demonstrated by a variety of routes including: intracerebral (Chandler, 1961); intraperitoneal (Kimberlin and Walker, 1988); intravenous (Hunter et al., 2002); subcutaneous (Kimberlin and Walker, 1978b); skin scarification (Mohan et al., 2004), intraocular (Fraser, 1996) and oral/intragastric (Beekes et al., 1998). TSE infectivity has been observed in the CNS (Chandler, 1961), lymphoid tissues (Kimberlin and Walker 1988), kidneys, liver, lung, eye (Brown et al., 1994), sites of inflammation (Heikenwalder et al., 2005) and blood from both clinical and pre-clinical or sub-symptomatic individuals (Hunter et al., 2002). However, the tissue distribution of infectivity varies between types of TSE disease. Transmission is generally most efficient via direct injection into the brain, such that a high disease incidence and short incubation period are observed, although significant transmission has been reported by other routes.

A number of mammalian species appear to have enhanced resistance to experimental cross-species TSE challenge, including pigs (*Sus domesticus*), rabbits (*Oryctolagus cuniculus*) and guinea pigs (*Cavia porcellus*) (Barlow and Rennie, 1976; Gibbs and Gajdusek, 1973; Wells et al., 2003). Equally other species, such as bank voles, have shown unusual susceptibility to a range of TSE sources (Nonno et al., 2006).

1.1.4 Peripheral pathogenesis

The principal route of natural TSE infection appears to be via peripheral routes. The greatest weight of evidence suggests that the most infection occurs via oral ingestion of TSE-contaminated material. However, other routes may also be important, especially direct introduction of infectivity into the blood via transfusion (1.1.2). It is clear that the peripheral phase of TSE pathogenesis is important to the successful transmission of some TSE agents and eventual fatal invasion of the CNS. However, the target organs and form of the peripheral phase differ between TSE strains. Additionally, the peripheral phase is bypassed when a high dose of TSE infected material is administered in the periphery. Importantly, this stage of TSE disease is not associated with pathological changes or a TSE specific immune response (Mabbott and MacPherson, 2006).

Whether defined cells types are required for specific routes of invasion or whether passive carriage of TSE infectivity via the blood or lymphatic system occurs has yet to be experimentally resolved. Experimental systems have suggested that a number of cell types may be important for the peripheral movement of infectivity, in particular M-cells in the gut and migratory dendritic cells (Heppner et al., 2001; Huang et al., 2002). However the precise *in vivo* importance of these cell types in TSE disease remains to be defined. Clear experimental evidence suggests that after peripheral TSE challenge with some strains the agent accumulates in lymphoid follicles in the spleen and other organs prior to CNS invasion (Fraser and Dickinson, 1970; Mabbott and MacPherson, 2006). This accumulation requires the presence of PrP^{C}-expressing follicular dendritic cells (FDCs) (Brown et al., 1999; Montrasio et al., 2000); these cells are localised in the B cell zone of mature lymphoid follicles, their principal function appears to be to retain antigen for presentation to B cells (Kapasi et al., 1993). TSE accumulation on FDCs appears to be facilitated by complement receptor CR2 and complement components (Klein et al., 2001; Mabbott et al., 2001), although the mechanism of replication is not clear. This FDC accumulation phase is proposed to be important for neuronal invasion, and nearness of the FDCs to peripheral nerves has been linked to incubation time and hence, by

inference, speed of neuronal invasion (Prinz et al., 2003). Work by McBride and colleagues has demonstrated that CNS invasion can occur via both the sympathetic and vagus nerve (Beekes et al., 1998; McBride et al., 2001). Direct invasion from blood across the blood-brain barrier is also feasible as PrP^{Sc} can readily cross the barrier (Banks et al., 2004). However, observed patterns of TSE pathology in the brain are not consistent with direct spread from the blood (Armstrong et al., 2003).

Recent work by Aguzzi and colleagues demonstrated that accumulation of TSE infectivity can also occur in ectoptic lymphoid tissue induced to form via a number of experimental inflammatory models and in the mammary glands of some scrapie infected sheep (Heikenwalder et al., 2005; Ligios et al., 2005; Seeger et al., 2005). Although this does not appear to alter the incubation period in the affected host, it does provide insight into potential transmission routes between hosts, especially as regards inflammation in excretory or secretory organs of TSE infected hosts.

1.2 Pathological hallmarks of TSE disease

1.2.1 Misfolded PrP/PrP^{Sc}

TSE disease-associated PrP (PrP^{Sc}) has the same primary amino acid sequence as the normal cellular form of PrP (PrP^{C}). However, its secondary structure is enriched in ß-sheets/ß-helix compared to the α-helical form of PrP^{C} (Oesch et al., 1985; Pan et al., 1993; Riek et al., 1996) (1.4). These differences in conformation have also been demonstrated using more detailed structural studies which have suggested that PrP^{Sc} may be in the form of trimers, in which amino acids 89-175 form a β helical structure (Govaerts et al., 2004; Wille et al., 2002). This change in conformation is inferred to lead to the unusual biochemical properties that define PrP^{Sc} including its partial protease resistance, resistance to GPI anchor cleavage by PIPLC treatment, detergent and chaotrophes insolubility and tendency to form aggregates and fibrils (Caughey et al., 1990; Oesch et al., 1985; Safar et al., 1998).

The pattern and type of PrP^{Sc} deposition varies both with host and source of the TSE agent (Brown et al., 2003; Bruce et al., 1989). In addition the biochemical properties of PrP^{Sc} also differ between TSE sources. These properties include the extent of resistance to proteinase K, both in terms of time to complete digestion and size of the C-terminal resistant core, relative solubility in destabilising agents and structural signatures (Bessen and Marsh, 1992a; Bessen and Marsh, 1994; Collinge et al., 1996; Kascsak et al., 1985; Parchi et al., 1996). Additionally, clinical TSE disease in both experimental models and natural cases can occur in the apparent absence of detectable PrP^{Sc} as assayed by standard proteinase K resistance criteria (Dorandeu et al., 1998; Lasmezas et al., 1997; Manson et al., 1999). In other models PrP^{Sc} deposition is closely associated with TSE pathological hallmarks such as vacuolation (DeArmond et al., 1993). However, clear dissociation of PrP^{Sc} and vacuolation has also been reported in other systems, suggesting that PrP^{Sc} may not directly cause neurodegeneration (Foster et al., 2001; Nitrini et al., 1997). Additionally, significant deposition of PrP^{Sc} in peripheral lymphoid tissue occurs in the apparent absence of a pathological effect (Hill et al., 1997b; Sigurdson et al., 2002; van Keulen et al., 1996).

1.2.2 Spongiosis of the CNS

Vacuolar pathology or spongiosis of the CNS is the defining characteristic of TSE disease (Brownlee, 1940; Hadlow, 1959). However, in some cases of familial disease associated with mutations in *PRNP,* particularly GSS (P102L), significant spongiform change does not occur (Brown et al., 1994). The vacuoles are principally observed in the dendrites and axons of both grey and white matter and occasionally within the cell bodies. TSE vacuoles range from 5- 15 μm, although in areas that are densely affected vacuoles may coalesce to form larger holes up to 40 μm (Baker et al., 1990). Vacuolation is occasionally observed in healthy animals (Zlotnik and Rennie, 1958). However, the frequency of vacuoles is much lower than that observed in TSE affected animals. The degree and extent of vacuolation observed varies between TSE sources and host species (Fraser and Dickinson, 1968). In some cases vacuolation is highly restricted to small regions of the brain or cannot be detected at clinical endpoint (Foster et al., 1996). Additionally, vacuolation is not unique to TSE disease, as

similar pathology has been reported for murine retroviral infections and in some cases of Alzheimer's disease (Dimcheff et al., 2003; Hansen et al., 1989; Kim et al., 2004). However, the distribution of the spongiform changes differs from that normally observed in TSE.

The underlying molecular mechanisms driving the formation of vacuoles are unknown, as is their relationship to neurodegeneration. Some authors have suggested they are derived from lysosomes as a consequence of accumulation of misfolded PrP (Laszlo et al., 1992). This over-filling of the lysosome is proposed to compromise the lysosomal membrane leading to the spilling of the compartment's cytotoxic contents into the cytoplasm (Laszlo et al., 1992). Others postulate that vacuoles originate from the ER because of ultrastructural similarities and hence may be a consequence of elevated autophagy of cellular contents (Baker et al., 1990). Alternatively, DeArmond and colleagues have proposed that vacuolation may be the result of *"focal plasma abnormalities of electrolyte and water homeostasis"* resulting in membrane damage and vacuole formation (DeArmond et al., 1997).

Early authors demonstrated that vacuolation increased linearly during the TSE incubation period (Fraser and Dickinson, 1968), suggesting their generation reflects an ongoing disease process. Work by Mallucci and colleagues suggested that vacuolar change in the early stages of TSE disease was reversible, and is dependent upon the expression of neuronal PrP (Mallucci et al., 2003). Interestingly, null mutations in an E3 ubiquitin ligase (mahogunin) and a transmembrane protein involved in pigment regulation (attractin) lead to targeted age-dependent vacuolation in the CNS that reassembles TSE spongiosis (Gunn et al., 2001; He et al., 2003). Whether the pathology observed in these mutant mice is related to that observed in TSE disease has yet to be experimentally demonstrated, although PrP^{Sc} is not detected in zitter rats in which the attractin gene is mutated (Gomi et al., 1994).

Vacuolation is often targeted to specific areas of the brain. The pattern and type (vacuolar size and proximity) of vacuolation is reproduced on subpassage of the TSE to hosts with the same genetic background (Fraser and Dickinson, 1967; Fraser and

Dickinson, 1968). This may reflect targeting of the agent to specific cell types within the CNS. Thus, by examining the region and density of vacuolation it is possible to recognise different strains of TSE disease. This idea was formalised by Fraser and Dickinson who defined nine grey matter and 3 white matter areas in inbred murine hosts which can be easily delineated by anatomical features in which the extent of TSE could be scored on a semi-quantitative scale (Fraser and Dickinson, 1968). This allows the systematic and reproducible comparison of an agent/host specific lesion profile between experimental challenges. However, different TSE sources/strains may share the same pattern of vacuolar pathology despite having different clinical presentations, duration of the disease or incubation periods.

1.2.3 Neuronal death and dysfunction

Neuronal death has been observed in TSE disease in both experimental and natural infections (Fairbairn et al., 1994; Giese et al., 1995; Gray et al., 1999; Jamieson et al., 2001; Lucassen et al., 1995). Synaptic loss and dendritic abnormalities are often observed to precede neuronal death in TSE disease, often by long periods (Belichenko et al., 2000; Jamieson et al., 2001). The brain regions in which neuronal loss occurs differs between TSE strains (Cunningham et al., 2005; Fraser, 2002), however a number of subsets of neurons appear to be particularly vulnerable to TSE-induced death including granular neurons of the cerebellum in sporadic CJD and a group of parvalbumin positive GABAergic inhibitory neurons (Budka, 2003). Most evidence suggests that TSE neuronal loss occurs via apoptosis (Budka, 2003; Fairbairn et al., 1994; Giese et al., 1995; Gray et al., 1999; Jamieson et al., 2001; Lucassen et al., 1995), although death by autophagy has also been proposed as potentially important (Liberski et al., 2004). Although a number of PrP murine transgenic models exhibit dramatic apoptotic phenotypes (Chiesa et al., 2000; Hachiya et al., 2005), the relevance of these models to natural TSE disease is unclear. Apoptosis is mediated by a cascade of cysteine proteases/ caspases through which intracellular or extracellular death signals are transduced to effector caspases which result in the ordered demise of the cell, characterised by endonuclease DNA cleavage. No inflammatory response is linked to this ordered cell death.

The death signal which elicits neuronal apoptosis during TSE has not been categorically determined. PrP^{Sc} is an obvious candidate; some authors have report a correlation of PrP^{Sc} and cell death *in vivo* (1.4.3). Work using transgenic mice, in which neuronal PrP expression was eliminated after the onset of TSE pathology by Cre-lox gene-excision or in which expression was limited to astrocytes, has suggested that neuronal death requires the expression of neuronal PrP^{C} (Brandner et al., 1996; Mallucci et al., 2003), although another study did not replicate this finding (Jeffrey et al., 2004). The work of Brandner *et al*, Mallucci *et al*, has led to the suggestion that the death signal may be generated by the interaction of PrP^{C} with PrP^{Sc}. Furthermore, antibody crosslinking of PrP causes cell death in support of PrP^{C}'s role in the transduction of death signals (Solforosi et al., 2004). Others have suggested that apoptotic signals may be elicited by ER in response to PrP misfolding in this compartment (Hetz et al., 2003). However, there is limited evidence for accumulation of PrP^{Sc} in this compartment *in vivo* apart from in some very rare inherited forms of TSE. Thus the probability of this mechanism being relevant to the majority of transmitted TSE disease appears remote.

1.2.4 Astrogliosis and activation of microglia

Activation (upregulation of specific proteins including glial fibrillary acidic protein) and proliferation of astrocytes are commonly observed during TSE disease. Although astrogliosis is also a common feature of many other brain diseases including viral infections such as HIV, the regulatory pathway by which astrocytes are activated has been suggested to differ in TSE disease (Titeux et al., 2002). Importantly, once activated and recruited, astrocytes will remain in the damaged region, even after resolution of the acute phase of the astrocyte response, where they may permanently alter the local environment. The normal function of astrocytes within the brain includes the maintenance of a homeostatic extracellular environment, particularly the concentration of glutamate, and the coupling of blood flow and supply of metabolic substances to neurones (Sofroniew, 2005). In contrast the role of activated astrocytes

is less clearly defined, and the context of activated astrocytes greatly influences their precise function *in vivo*.

More recently, the activation of microglial, and an atypical inflammatory response characterised by the upregulation of a subset of microglial-associated cytokines, has been shown to occur during CNS TSE pathogenesis (Cunningham et al., 2002; Felton et al., 2005; Williams et al., 1997b; Williams et al., 1994; Williams et al., 1995). TSE incubation periods are slightly prolonged in mice that lack some of these factors, supporting a specific role of microglia in TSE disease (Felton et al., 2005; Schultz et al., 2004). Additionally, activation of microglia has been shown to precede neuronal cell loss in a mouse scrapie model, suggesting that their activation may mediate TSE neurodegeneration (Williams et al., 1997a). Activated microglia have also been shown to correlate with the type of PrP^{Sc} deposited *in vivo* (Puoti et al., 2005). Furthermore, PrP^{Sc} has been reported within microglial in mouse-passaged scrapie suggesting that these cells may have a PrP^{Sc}-clearance function (Bruce et al., 1989).

1.3 TSE strains and strain typing

The great diversity of clinical signs and pathology observed in natural cases of TSE in genetically identical hosts illustrates the existence of multiple strains of the agent (1.1). The idea of TSE strains was first proposed by Pattison and Millison after they isolated two distinct clinical phenotypes (scratching and drowsy) of scrapie in goats (Pattison and Millson, 1961), the clinical symptoms of which could be reproduced upon transmission to new hosts. Later work developed the definition of scrapie strain by transmission to two inbred strains of mice (VM and C57/B6) and their F1 cross (Bruce, 2003). These wild type mice have differing susceptibilities to TSEs principally because of polymorphisms at amino acid 108 and 189 in PrP (Moore et al., 1998). Repeat repassage of the original TSE isolate in mice is usually required prior to strain definition because of the species barrier effect, as stabilisation of the incubation period is required prior to strain classification. By comparison of this reproducible incubation period and the associated pattern of vacuolar targeting (lesion

profile) in the mice it is possible to categorise the nature of the original TSE agent (Fraser and Dickinson, 1967; Fraser and Dickinson, 1968). By this method, the TSE agent causing both BSE and vCJD was demonstrated to be caused by an identical strain, formally proving that BSE could cross the species barrier to humans (Bruce et al., 1997). Over twenty different TSE strains have been isolated by this method from a range of TSE sources (Bruce and Dickinson, 1987). In addition to differing in lesion profile and incubation period, the pattern and type of PrP^{Sc}-deposition also differs between strains (Brown et al., 2003).

Multiple strains have been isolated from single TSE sources suggesting the concurrence of multiple strains in natural hosts, or that strain isolation results in a change of the TSE agent (Kimberlin and Walker, 1978a). A few strains have been repeatedly isolated, whereas others have only been observed on a single occasion (Bruce and Dickinson, 1987). This suggests that either the frequencies of strains vary within hosts or natural population or that some strains are more able to establish infection in murine hosts. Most TSE strains are stable when passaged within an inbred host population, whereas transmission to a new host population often results in a change in strain characteristics (Bruce and Dickinson, 1987). However, strain characteristics have been observed to alter even after multiple stable passages within an inbred population (Bruce and Dickinson, 1987). Some TSE strains exhibit dominance or an interference effect in co-infections of hosts or in cell culture systems (Dickinson et al., 1975; Dickinson et al., 1972; Nishida et al., 2005). In some cases infection with a dominant but slow strain with a long incubation prevented the establishment of infection with a more virulent TSE strain, effectively prolonging the lifespan of the challenged host. These data suggest that TSE strains may compete for some limited *in vivo* resource.

1.4 The nature of the TSE agent

1.4.1 The prion hypothesis

The characteristic long incubation periods of TSE disease led to early suggestions that the causative agent was a slow virus (Gibbs et al., 1965). However, unlike conventional viruses, infectivity of the TSE agent is not greatly diminished by treatment with radiation or nucleases (Alper et al., 1967; Alper et al., 1966; Hunter and Millson, 1967; Latarjet et al., 1970; Millson et al., 1976; Prusiner et al., 1980). However, TSE infectivity was shown to be sensitive to phenol, proteases and urea (Hunter et al., 1969; Hunter and Millson, 1967). This led to the suggestion that the agent does not have a nucleic acid component but may be a self-replicating protein (Griffith, 1967). This idea was refined by Prusiner (1982) who hypothesised that the TSE agent is a form of infectious protein or prion (proteinaceous infectious particle), based upon its unusual biochemical properties. Subsequent work identified a host protein PrP (prion related protein) as the prime prion candidate and demonstrated that it was expressed at similar levels in the brains of both TSE diseased and healthy individuals (Bolton et al., 1982; Oesch et al., 1985). It had been previously known that an inherited host gene influenced the scrapie incubation in mice (*Sinc*) (Dickinson et al., 1968). Two alleles were postulated, s7 (short scrapie incubation time) and p7 (prolonged scrapie incubation time), based upon the segregation of ME7 incubation periods in the F1 cross of the RIII and VM inbred mouse strains. Further work demonstrated that the incubation period of other TSE strains also differed between these two lines of mice (Bruce et al., 1991). It was later shown using gene-targeted replacement of the PrP gene *Prnp,* that *Prnp* was synonymous with the murine scrapie susceptibly factor *Sinc* (Moore et al., 1998). The s7 phenotype was demonstrated to be caused by the $Prnp^a$ (108L and 189T) allele and the p7 phenotype by $Prnp^b$ (108F and 189V) allele.

It was proposed that the host protein PrP could exist in both a normal cellular state (PrP^C) and a prion or scrapie-associated state (PrP^{Sc}) and that PrP^{Sc} was autocatalytic

(Prusiner, 1991). The prion hypothesis thus suggests that PrP^{Sc} is infectious by causing PrP^{C} to adopt its pathogenic state, that PrP^{Sc} can spontaneously form *de novo* and that changes in the primary sequence of PrP predispose this to occur. This model then neatly explains the observed infectious, apparently spontaneous and familial cases of TSE disease as the only factor required for the diseased state is expression and subsequent misfolding of a host protein. *In vitro* conversion assays using purified radio-labelled normal PrP^{C} substrate and a vast excess of PrP^{Sc} have demonstrated that PrP^{Sc} can induce PrP^{C} to adopt its aberrant biochemical characteristics and hence presumably its conformation, providing evidence of the autocatalytic nature of PrP^{Sc} (Kocisko et al., 1994).

PrP is essential for TSE disease, as mice in which *Prnp* had been ablated ($PrP^{0/0}$ or PrP null) are completely resistant to TSE disease (Bueler et al., 1993; Manson et al., 1994b). Additionally, overexpression of PrP in mice has been linked to spontaneous spongiform neurodegeneration and shortening of TSE incubation periods (Westaway et al., 1994). The identification of mutations in the human PrP gene, *PRNP*, in familial clusters of TSE disease, provided further evidence of a link between PrP and the TSE disease (Figure 1.1) (Doh-Ura et al., 1989; Goldfarb et al., 1991; Hsiao et al., 1989; Mouillet-Richard et al., 1999; Owen et al., 1989). Additionally, polymorphisms in the *Prnp/PRNP* have been linked to TSE disease incidence in natural populations, and to susceptibility to, and incubation periods after, experimental TSE challenge (Barron et al., 2005; Bishop et al., 2006; Goldmann et al., 1994; Moore et al., 1998; Palmer et al., 1991).

However, these conventional genetic data do not prove that PrP is sufficient for TSE disease development, only that it is necessary. Overexpression of human *PRNP,* carrying a GSS linked mutation, in transgenic mice led to the development of transmissible spontaneous TSE disease, providing evidence that PrP was sufficient for development of disease (Hsiao et al., 1994; Hsiao et al., 1990). However, the failure to replicate this result in a comparable model with a low expression level or in an alterative murine transgenic system questioned the validity of the original conclusions (Barron et al., 2001; Manson et al., 1999; Nazor et al., 2005).

Figure 1.2 Model of misfolding of PrP (based on Baskakov *et al* 2002 and Bocharova *et al* 2006)

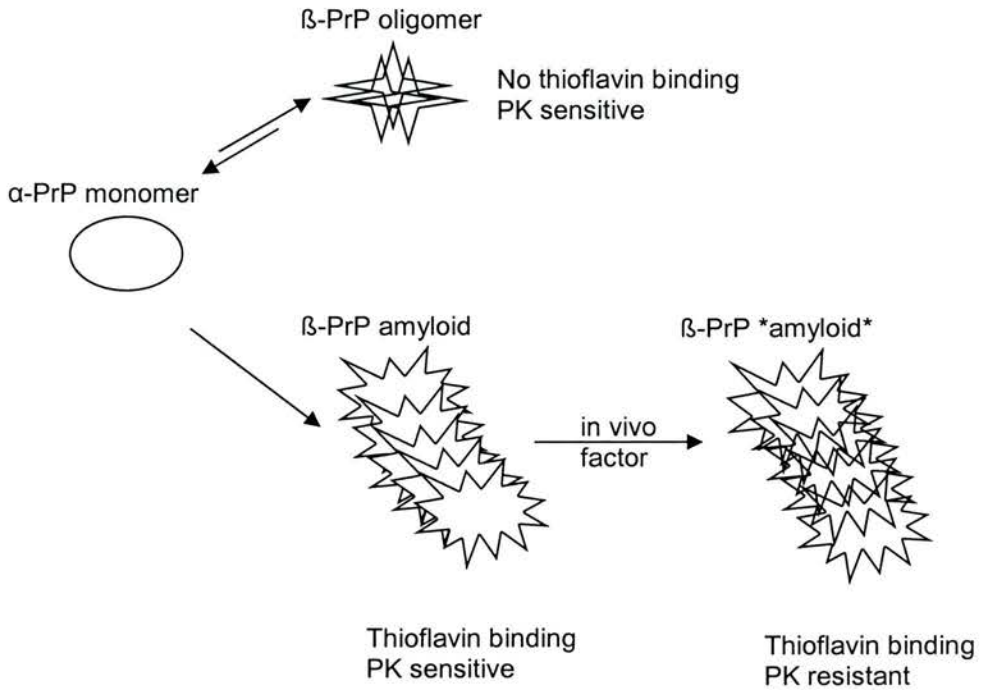

Recently, two novel methods of generating TSE infectivity *ex vivo* have provided strong evidence in support of the prion hypothesis. TSE infectivity was reported to be generated *de novo* by inducing recombinant PrP to misfold *in vitro* (Legname et al., 2004; Legname et al., 2005). However, this form of artificial prion was only infectious to transgenic mice which overexpress a truncated form of PrP. Moreover, the titre of infectivity generated in this experiment was very low compared to the amount of misfolded PrP used to challenge the animals. *Ex vivo* replication of TSE infectivity has also been demonstrated in an independent system (Castilla et al., 2004). In this case PrP^{C} was induced to misfold using Protein Misfolding Cyclic Amplification (PMCA), the reaction was seeded with clinical endpoint TSE infected hamster brain and repeat rounds of incubation at 37 °C and sonication were used to mediate amplification of proteinase K resistant PrP (Chapter 7). Many rounds of serial PMCA were undertaken to significantly dilute the original TSE material. A significant increase in infectivity was detected in the PMCA generated PrP^{Res}. However, similarly to the synthetic prion work the level of infectivity was found to be less than that predicted by the amount of PrP^{Res} formed (Castilla et al., 2005).

The discrepancy between the amount of misfolded PrP and TSE infectious titre presented in these works suggests that the classical definition of the prion as proteinase K resistant PrP may be flawed. Many previous pieces of evidence also support this conclusion; both TSE infectivity in the absence of PrP^{Sc} and PrP^{Sc} in the absence of infectivity have been previously reported in a range of experimental and natural systems (Lasmezas et al., 1997; Manson et al., 1999; Prusiner et al., 1990). A discussion paper presented by Weissmann in 1990 suggested that the prion may correspond to a subset of misfolded PrP, which he named PrP^{*} (Weissmann, 1991). The conformation and biophysical properties of PrP* remain to be determined. However, recent work has suggested that TSE infectivity correlates with PrP aggregate size and that mid-sized (14-28 PrP molecules) oligomers are more infectious than those that are very small or larger aggregates of PrP^{Sc}, raising the possibility that size in addition to conformation defines the prion (Silveira et al., 2005).

An early model of PrP replication suggested that that PrP^{Sc} acts as a template to overcome the energy barrier of conversion of PrP^{C} to PrP^{Sc} and that PrP^{Sc} is unique to TSE disease (Prusiner, 1991). An alternate theory suggested that PrP^{C} and PrP^{Sc} are in reversible thermodynamic equilibrium and that introduced PrP^{Sc} seeds stabilize and sequester endogenous PrP^{Sc} favouring its further production (Jarrett and Lansbury, 1993). This model hence suggests that PrP^{Sc} is not unique to TSE disease. Recent experimental evidence has suggested that the PrP misfolding pathway may consist of multiple steps, which include the formation of a ß-rich structure, followed by extensive structural rearrangement that may involve domain swapping between PrP molecules (Figure 1.2) (Baskakov and Bocharova, 2005; Baskakov et al., 2002; Bocharova et al., 2006). These *in vitro* experiments support the autocatalytic nature of PrP^{Sc} and further suggest that the misfolded form's ability to induce PrP^{C} to misfold may be important to prion propagation (Baskakov and Bocharova, 2005). Further experimentation is required to determine which of these forms of misfolded PrP most closely resemble the *in vivo* TSE agent.

Data from *in vitro* conversion assays suggest that the conversion of PrP^{C} to PrP^{Sc} may be facilitated by additional factors *in vivo* (Deleault et al., 2005; Deleault et al., 2003; Saborio et al., 1999). In particular a number of polyanionic molecules, including RNA, have been suggested as potent promoters of conversion in some systems (Deleault et al., 2005; Deleault et al., 2003). PrP^{Sc} is often tightly associated with a poly-glucose scaffold *in vivo* which is distinct from the glycans that are conjugated to the protein via asparagine 180 and 196 (Dumpitak et al., 2005). This scaffold may be important in the formation or stabilisation of the misfolded form *in vivo*. Other groups have suggested that the conversion factor is a brain and muscle specific protein which fractionates with lipid rafts (Soto, 2006). Although there is clear evidence that these factors can promote conversion *in vitro*, *in vivo* evidence of their efficacy has yet to be presented. However given the crowded nature of the cellular environment it would seem probable that additional factors influence the *in vivo* generation and stabilisation of PrP^{Sc}.

Propagation of the aberrant conformation of PrP^{Sc} *in vivo* requires that its rate of formation exceeds its rate of clearance. Despite the proteinase resistance of PrP^{Sc}, it is relatively efficiently degraded. Estimates of its half life range from 15-36 hours (Borchelt et al., 1990; Peretz et al., 2001; Safar et al., 2005). Indeed, in a transgenic murine model in which PrP^{C} expression and hence *de novo* PrP^{Sc} formation can be reversibly regulated, clearance of a significant load of PrP^{Sc} from the CNS has been reported (Safar et al., 2005). Numerous pharmacological studies have suggested that degradation of PrP^{Sc} principally occurs in lysosomes and acid endosomes (Doh-Ura et al., 2000; Gilch et al., 2001; Supattapone et al., 1999; Supattapone et al., 2001), although both the precise mechanism and the effect of TSE strain on this process have yet to be elucidated.

The mechanism of cell to cell spread of PrP^{Sc} within the CNS has yet to be determined and may occur by diffusion. Recent work has suggested that cell to cell spread may be mediated by exosomes that are derived from the fusion of multi-vesicular bodies with the plasma membrane (Fevrier et al., 2004). This hypothesis is supported by data that suggest that PrP conversion occurs most efficiently when PrP^{C} and PrP^{Sc} are inserted in contiguous membranes (Baron et al., 2002). Work by Pinheiro and colleagues has suggested that the lipid composition of membranes greatly influences the preferred conformation of PrP (Pinheiro, 2006). Thus localisation within in the cell membrane may contribute to PrP^{Sc} propagation.

Opponents of the prion hypothesis have long cited the great number of TSE strains as a major flaw in the hypothesis (Bruce and Dickinson, 1987; Farquhar et al., 1998). This is mainly owing to the molecular biology dogma that polypeptide sequence defines protein conformation, based upon the seminal work of Anfinsen (Anfinsen, 1973), and hence the diversity of TSE strains can not be encoded by a single protein sequence. However, many protein sequences can adopt more than one conformation, often as part of their normal function.

Experimental evidence suggests that multiple conformations of PrP^{Sc} do exist and that these may correlate with different TSE strains. The first evidence for this was

presented by Bessen and Marsh, who isolated two clinically distinct strains of TSE in hamsters that also reproducibly differed in the biophysical properties of PrP^{Sc} (Bessen and Marsh, 1992a; Bessen and Marsh, 1994). Most notably the size of the PK-resistant core significantly differed between the two strains (Bessen and Marsh, 1992a). N-terminal amino acid sequencing after PK digestion has demonstrated that these size differences are the result of an alteration in the extent of proteinase sensitivity of the N-terminus. This difference in N-terminal cleavage is proposed to occur because of conformational differences in PrP^{Sc} that results in variation in the PK accessibility (Bessen and Marsh, 1994). Similar differences in the size of the PK resistant core or PrP^{Sc} types have also been reported for different isolates of bovine and human TSE diseases (Biacabe et al., 2004; Casalone et al., 2004; Collinge et al., 1996; Parchi et al., 1996), and inconsistently for sheep scrapie (Hill et al., 1998; Hope et al., 1999; Sweeney et al., 2000). Difference in the conformation of PrP^{Sc} from TSE strains has also been demonstrated by an independent method based upon variation in the sensitivity of PrP from different strains to undergo denaturation in guanidine hydrochloride, as detected by the availability of an internal epitope which is shielded in PrP (Safar et al., 1998). Propagation of PrP^{Sc} conformation *ex vivo* has been demonstrated, providing evidence of the feasibility of TSE strain being maintained *in vivo* by PrP^{Sc} conformation (Bessen et al., 1995; Soto et al., 2005). However, significant co-occurrence of multiple PrP^{Sc} types in the same host has been demonstrated in sporadic CJD patients (Head et al., 2004; Puoti et al., 1999). This suggests that either PrP^{Sc} type, and hence potentially conformation, does not categorically define TSE strain or that multiple strains of TSE coexist in the same host.

In addition to variation in the size of the PK resistant core, differences in the glycoform (ratio of glycotypes) of PrP^{Sc} have also been shown to correlate with TSE strain (Collinge et al., 1996; Parchi et al., 1996). For example, BSE in cattle, vCJD from human patients and both isolates passaged in mice display a very distinctive, predominantly di-glycosylated glycoform (Collinge et al., 1996; Hill et al., 1997a). This reproducibility of PrP^{Sc} glycoform in numerous hosts infected with the same TSE source led to the suggestion that glycoform itself may encode TSE strain

characteristics (Collinge et al., 1996). However this observation has a number of alternative explanations, as glycoform may equally be a consequence of strain rather than its cause. The glycoform of PrP^{C} varies between regions of the brain (Somerville, 1999) and PrP^{Sc} glycoform may occur as a result of the regional targeting of PrP^{Sc} formation observed in TSE disease (Bruce et al., 1989). Similarly, subcellular differences in the localisation of PrP glycotype may influence resultant PrP^{Sc} glycoform. Additionally, a PrP^{Sc} glycotype will represent an equilibrium state determined not only by rate of formation but also rate of clearance. It is also important to emphasise that glycoform analysis of PrP^{Sc} is generally made after proteinase K (PK) digestion and thus assumes that the different glycotypes of PrP^{Sc} have equal resistance to PK. Alternatively, TSE infection may alter the glycosylation of all proteins including PrP^{C} (1.8). Glycoforms may result from variation in the propensity of each glycotype to adopt the misfolded conformation of a TSE strain; thus the resultant glycoform will be determined by the relative abundance of each glycotype at the site of conversion and the probability of each converting, as suggested by *in vitro* conversion assays (Vorberg and Priola, 2002).

Although significant evidence supports the prion hypothesis a number of major questions regarding it remain to be addressed. For example how does PrP^{Sc} conformation result in the manifestation of TSE strain characteristics? Additionally, what confers the transmissibility of PrP^{Sc} as compared to other similarly misfolded proteins that are not infectious (Aß, Huntingtin)? Moreover, what aspects of PrP^{Sc} dictate TSE host range?

1.4.2 The Virino hypothesis

An alternative to the prion hypothesis has been proposed by some TSE workers (Bruce and Dickinson, 1987; Farquhar et al., 1998). This virino hypothesis proposes that TSE strain characteristics are conferred by an "*agent specific replicable information molecule*" (nucleic acid) tightly associated with a form of PrP, and that PrP is a disease rate limiting host factor (Farquhar et al., 1998). The observed resistance of the TSE agent to UV non-penetrating radiation may be attributable to shielding of this hypothesized nucleic acid by PrP, as is observed in the viroid subgroup of plant viruses (Diener, 1972). This unusual property is explained by energy transfer between the nucleic acid and protein which elevates the dose of UV tolerated (Millson et al., 1976). Similarly, X-ray radiation inactivation studies can be interpreted to show that the TSE agent may contain between 2-4 kilobases of nucleic acid, if results are calibrated against known viruses that displayed enhanced resistance to radiation (Chesebro, 1999). Furthermore, radiation tolerance may be further enhanced if the agent can self repair as is observed for human immunodeficiency virus (Chesebro, 1999). Thus the inactivation evidence which originally suggested that the TSE agent may be devoid of nucleic acid, does not disprove that the agent may be viral in nature. However, there is a lack of any experimental evidence for the existence of a TSE specific nucleic acid despite numerous attempts to identify it.

1.4.3 The neurotoxic form of PrP

The form of PrP which causes neural degeneration may differ from that which transmits TSE disease to new hosts (Hill and Collinge, 2003). The neurotoxicity of a number of forms of PrP has been demonstrated in cell culture, including peptides that correspond to amino acid 106-126 of human PrP, N-terminal truncated PrP^{Sc}, fibrillar or β-oligimeric recombinant PrP (Forloni et al., 1993; Hetz et al., 2003; Novitskaya et al., 2006). Alternative localisations of PrP, including in the cytoplasm (cytPrP) or across the Golgi membrane (PrP^{Ctm}) may be neurotoxic *in vivo* (Hegde et al., 1998; Hegde et al., 1999; Ma et al., 2002; Stewart and Harris, 2005). However the relevance of these forms of PrP to natural TSE disease is unclear, although an up

regulation of PrP^{Ctm} has been suggested in some human familial TSE cases (Hegde et al., 1998). The subcellular localisation of a particular PrP conformation is likely to affect its behaviour and may also modify conformation itself. Indeed, the conformation of huntingtin protein, the causative agent of Huntington's disease, has been previously reported to be affected by its cellular localisation (Rousseau et al., 2004).

1.4.4 Non PrP prions

Many other proteins adopt disease-associated misfolded conformations *in vivo*, indeed some have suggested that all proteins have an innate tendency to misfold (Stefani and Dobson, 2003). However, only a limited number of proteins have been observed to exhibit autocatalytic prion-like properties *in vivo*. In particular, a number of yeast proteins exhibit prion-like properties. These prions are able to propagate their misfolded conformation to daughter cells and mating partners (Ross et al., 2005). Although the prion state in yeast has a clear phenotype, it is not associated with reduced host fitness in an experimental setting and appears to be highly conserved (Lindquist, 1997). Thus although yeast prions may reflect the proposed propagation of PrP^{Sc} they do not share its pathogenic role. The yeast prions have diverse functions including catabolic regulation (Ure2 associated with the [*URE3*] prion trait) and suppression of nonsense mutations (Sup35 associated with the [*PSI+*] prion trait) (Stansfield et al., 1995; Wickner, 1994). These proteins encode a domain that adopts a specific conformation associated with the prion like state. This region of the protein is separate from the protein's functional domains. In contrast, the PrP putative functional domain is also that which adopts the prion state (Lindquist, 1997). Despite these differences, studies of yeast prions may be informative as to the propagation of the PrP^{Sc} state.

Propagation of the [*PSI+*] prion state in budding yeast is influenced by the expression level of chaperones (Chernoff et al., 1995), implicating the regulation of protein folding as a key determinate of prions. Work in yeast has demonstrated that the conformation variation in prions correlates with phenotypic differences, lending

support to the hypothesis that misfolded PrP could encode TSE strain diversity (Tanaka et al., 2004). King and colleagues have presented data demonstrating that *in vitro* generated misfolded Sup35p can infect yeast cells and cause them to change phenotype in support of the prion hypothesis (King and Diaz-Avalos, 2004). Additionally, Chien and colleagues have demonstrated a species barrier to yeast prion propagation and that propagation of the prion state between species is associated with a change in prion structure (Chien et al., 2003; Chien and Weissman, 2001), supporting the similar finding for PrP^{Sc} (Peretz et al., 2002).

1.5 The cell biology and function of PrP^{C}

Prnp is a single copy gene located on the short arm of human chromosome twenty. Proximal to the *Prnp* is the related gene *Prnd* (Doppel) and the putative tumour suppressor *RASSF2* (Deloukas et al., 2001). The open reading frame is located within a single exon such that no splice variants of the gene occur. Consistent with its role in neurodegenerative disease, PrP^{C} is predominately expressed in neurons from early in development, although it is observed at lower levels in many other tissues (Manson et al., 1992b) (1.5.2). Some studies have reported that the expression of PrP displays a circadian rhythm, with a peak of expression occurring 2 hours after onset of the active dark period in rats (Cagampang et al., 1999). The normal biological function of PrP^{C} has yet to be elucidated, as $PrP^{0/0}$ mice have only subtle phenotypes which differ between lines of transgenic mice; these include alterations in circadian rhythms, sleep regulation, synaptic transmission and impaired long-term-potentiation (LTP) (Bueler et al., 1992; Manson et al., 1994a; Tobler et al., 1996). A number of biological roles for PrP^{C} have been suggested including: a role in copper homeostasis (Brown et al., 1997), resistance to oxidative stress (Brown et al., 1998), cell survival and neurite outgrowth (Chen et al., 2003; Kuwahara et al., 1999), apoptosis (Brandner et al., 1996; Solforosi et al., 2004) and signal transduction (Mouillet-Richard et al., 2000).

PrP^C contains two structural domains: an N-terminal region of around 100 amino acids which is highly flexible during nuclear magnetic (NMR) spectroscopy and a C-terminal region which forms a globular structure amenable to NMR (Donne et al., 1997; Riek et al., 1997). The structure of recombinant PrP^C from different species, including those with low amino acid identity, is remarkably similar (Calzolai et al., 2005; Donne et al., 1997; Lysek et al., 2005; Riek et al., 1997). Replication of this structure using native glycosylated bovine protein has also been shown, validating use of recombinant protein to investigate PrP structure (Hornemann et al., 2004). PrP^C from all species contains three α-helices (144-154, 175-193 and 200-219 in human PrP) the length of the third is species specific (Calzolai et al., 2000). Additionally, the extent of the structural rigidity of the loop between helix one and two, and the length of a short parallel ß-sheet (160-163 in hamster) also varies between species (Calzolai et al., 2000; Gossert et al., 2005).

1.5.1 Post-translational processing of PrP^C

PrP contains two N-glycan attachment sequences (N-X-T) at amino acids 180 and 196 in mice (Figure 1.1) (Locht et al., 1986). These sites are variably glycosylated *in vivo* such that un-, mono- and di-glycosylated glycotypes are observed (Rudd et al., 1999; Stimson et al., 1999). Although there are a number of potential O-glycosylation sites in PrP, none is utilised *in vivo* (Rudd et al., 2001). The relative ratio of the N-glycotypes varies between areas of the brain and species, however the species variation observed may be caused by differences in antibody binding (Betemps and Baron, 2001; Somerville, 1999; Zanusso et al., 1998). Both N-glycosylation sites are conserved in *Prnp/PRNP* from all species, suggesting the N-glycans play an important role in the protein's function (Rivera-Milla et al., 2003; van Rheede et al., 2003; Wopfner et al., 1999). The biological significance of each of the glycotypes of PrP (un-, mono- and di-glycosylated) is unknown. However, protein attached glycans have been shown to have a wide range of biological functions in other proteins, most notably conformational stabilisation and control of cellular trafficking. Additionally, glycosylation of host proteins has been implicated in

resistance to infectious disease, principally by a prevention of protein-protein interactions (Marin et al., 2003; Wentworth and Holmes, 2001).

PrP is targeted to the endoplasmic reticulum (ER) by its hydrophobic N-terminal signal sequence (amino acids 1-23), which is subsequently cleaved (Turk et al., 1988). Recent work has suggested that PrP's signal sequence is complex and less efficient compared to that of other proteins, suggesting that *in vivo* a proportion of PrP may not be translocated into the ER but remain un-glycosylated and cytoplasmatic (Rane et al., 2004). Indeed cytoplasmic but nucleus-excluded PrP (cytPrP) has been observed in a subset of cells in murine brains (Barmada et al., 2004; Mironov et al., 2003). These cytPrP cells are interneuronal in character, have a normal distribution of another GPI-anchored protein, Thy-1, and do not display any signs of apoptosis (Mironov et al., 2003). Thus PrP appears to have a cell type specific localisation pattern *in vivo*.

Within the oxidising environment of the ER, a disulphide bond between cysteine residues 179 and 214 (hamster sequence) is formed (Turk et al., 1988). Also within this compartment a glycosyl-phosphatidylinositol (GPI) anchor is attached to serine 231 of PrP with the concurrent cleavage of the carboxy terminus (amino acids 232-254), leading to membrane anchorage of the protein (Stahl et al., 1990; Stahl et al., 1987). Although GPI anchorage is the predominant method of PrP membrane attachment *in vivo*, other mechanisms also occur. A small proportion of PrP exhibits transmembrane topology, in which amino acids 111-134 are inserted across the membrane, such that only the N-terminus of PrP reaches the ER lumen (PrP^{Ntm}) and hence is not glycosylated (Hegde et al., 1998). Additionally, transmembrane PrP is also observed in the reverse orientation, with its C-terminal within the ER lumen and a cytoplasmic N-terminal that retains the ER signal sequence (PrP^{Ctm}) (Hegde et al., 1998). The normal function of these forms of PrP is unknown, although PrP^{Ctm} has been suggested to have a role in the pathogenesis of some inherited forms of TSE (Hegde et al., 1998), although its production is not elevated by the majority of TSE associated PrP mutations (Stewart and Harris, 2001).

Early work suggested that membrane anchorage is essential for the glycosylation of PrP (Walmsley et al., 2001). However further studies revealed that these results were an artefact and attributable to a requirement for the site of N-glycan attachment to access the oligosaccharyltransferase prior to detachment of the ribosome (Walmsley and Hooper, 2003). This enzyme transfers the core high mannose N-glycan (Glc_3-Man_9-$GlcNAc_2$) from its dolichol carrier to the amide nitrogen of asparagines (Taylor and Drickamer, 2003). The final glycotype of PrP is thus determined at this early stage in the ER. *In vitro* translation has suggested that PrP^C may be preferentially glycosylated at the first site, suggesting that PrP^C may be predominately mono-glycosylated at the first attachment site (Walmsley and Hooper, 2003), consistent with the *in vivo* observation of preferential glycosylation of the first site (Stahl et al., 1993). However, antibody binding experiments have suggested that both mono-glycosylated forms of PrP^C occur in sheep and mice (Moudjou et al., 2004). Rapid folding of PrP may prevent access of asparagines to the active site of oligosaccharyltransferase and hence lead to the un- or mono-glycosylated forms (Ermonval et al., 2003). Inhibition of the formation of the Cys^{179}-Cys^{214}disulphide bond that is likely to slow the rate of folding has been linked to an increase in PrP glycosylation (Capellari et al., 1999). Equally, N-glycan attachment at the first site has been shown to facilitate formation of the disulphide bond, demonstrating the close link between glycosylation and protein folding (Bosques and Imperiali, 2003).

The attached glycans are then trimmed in the ER, first glucose molecules are removed by ER glucosidase I and II and then the terminal mannose by ER α 1,2 mannosidase (Taylor and Drickamer 2003). Following this, correctly folded proteins are transported to the Golgi apparatus for further glycan modification. Within the Golgi, further mannose residues are removed in the *cis* compartment such that mature PrP^C contains no oligomannose species, in contrast to many glycoproteins found in the brain (Rudd et al., 1999). Further sugars are then added to the core N-glycan moiety, resulting in a great diversity of mature glycotypes of PrP^C, over 50 of which have been identified by 2-D electrophoresis (Pan et al., 2002). These N-glycans are heavily sialylated and contain bisecting GlcNAc, a typical pattern for brain sugars (Rudd et al., 1999; Stimson et al., 1999). The profile of the glycans attached to the

two sites is broadly similar, however the second site carries more highly processed acidic structures which result in a different range in molecular weight at this site (2000-3020 kDa) as compared to the first (1600-2340 kDa) (Stimson et al., 1999).

1.5.2 Localisation of PrP^C

In the central nervous system wild type PrP^C is principally observed within the neuropil (dendrite-axon-synapse complex) (Barmada et al., 2004; Fournier et al., 2000; Haeberle et al., 2000; Mironov et al., 2003; Moya et al., 2000; Sales et al., 1998). Early reports that suggested PrP was principally localised within only a subset of cell bodies can be attributed to the destruction of plasma membrane associated PrP^C during tissue embedding and dehydration (Bendheim et al., 1992; DeArmond et al., 1987; Ford et al., 2002a; Manson et al., 1992b; Piccardo et al., 1990). The amount of PrP detected varies between regions of the brain, high levels have been consistently reported in the cortex and hippocampus (Barmada et al., 2004; Mironov et al., 2003; Sales et al., 1998), although species and antibody differences in the pattern (Liu et al., 2001; Moya et al., 2000; Sales et al., 1998) and regional differences in glycoform (Liu et al., 2001; Somerville, 1999) have also been reported.

A number of groups have reported a preferential localisation to the synapse *in vivo* (Fournier et al., 2000; Haeberle et al., 2000; Moya et al., 2000; Sales et al., 1998). However, other studies have not reproduced this result (Laine et al., 2001; Mironov et al., 2003). Others have reported preferential localisation of PrP^C to cellular processes associated with intraparenchymal blood vessels (Verghese-Nikolakaki et al., 1999). Specific PrP localisation to Purkinje cells has also been reported (DeArmond et al., 1987; Ford et al., 2002a; Manson et al., 1992a; Piccardo et al., 1990), although a number of other groups have not observed this (Bendheim et al., 1992; Mironov et al., 2003; Sales et al., 1998). Additionally, some groups have reported PrP^C localisation to glial cells (Laine et al., 2001), although this has not been consistently observed (Mironov et al., 2003). In addition to CNS, PrP^C is also observed in peripheral nerves and has also been reported in the FDCs in the spleen and other organs, in circulating

leuckocytes, in muscle (particularly cardiac) and in lung, although the levels observed in peripheral tissues are much lower than in the CNS (Bendheim et al., 1992; Ford et al., 2002b; Manson et al., 1992a; McBride et al., 1992).

PrP^C plasma membrane staining is patchy, consistent with biochemical studies which have demonstrated that PrP is localised in lipid rafts (Madore et al., 1999; Vey et al., 1996). These domains are enriched for cholesterol, sphinolipids and other GPI anchored proteins and are classically defined by their resistance to extraction in cold non-ionic detergent (Brown and Rose, 1992). Lipid rafts are proposed to act as signal centres that transduce extracellular information into the cells interior (Helms and Zurzolo, 2004). Specific localisation of PrP^C may occur as early as in the Golgi apparatus, as has been reported for other GPI anchored proteins (Simons and van Meer, 1988). Work has shown that PrP^C is localised to a subtype of rafts (Madore et al., 1999; Sunyach et al., 2003). These rafts differ from those in which the common neuronal raft protein Thy-1 is found. Moreover, a proportion of PrP^C is found outside of lipid rafts, this may be related to the mechanism of PrP internalisation. Work in cell cultures has suggested that glycosylation of PrP is not required for its normal localisation to rafts, however, the N-terminal of the protein does appear to be required (Walmsley and Hooper, 2003).

In cell culture models, in which PrP is normally glycosylated, all glycotypes of PrP^C have been shown to reach the plasma membrane, however un-glycosylated PrP^C is transported more slowly to the cell surface (Caughey et al., 1989; Petersen et al., 1996). Experimental results from conventional PrP glycosylation deficient transgenic mice, in which the transgene copy number and site of integration in the genome are not controlled (1.8), have suggested that removal of the first N-glycan attachment site (T183A) leads to a dramatic alteration in the cellular localisation of PrP^C, either when expressed alone or in the double mutant (T183A, T199A) (DeArmond et al., 1997). In this model PrP^C was observed to accumulate in the nerve cell bodies and only a little was observed within the neuropil. Subtle changes in cellular localisation were also observed in the transgenic mice in which the second N-glycan attachment site was disrupted (T199A) (DeArmond et al., 1997). However, two different amino acid

changes (hamster N181Q and mouse T182N), which also disrupt glycosylation of the first site, do not alter the cellular localisation of PrP^C (Capellari et al., 2000b; Neuendorf et al., 2004) (appendix table 1). Therefore the observed change in the localisation of PrP^C in DeArmond and colleagues' model is attributable to the mutation they used to disrupt glycosylation rather than an effect of absence of a N-glycan at the first site, however, the rate of export of PrP^C was not explored in these experiments and may be altered. In normal central nervous tissues, intracellular PrP^C is also observed. However it only makes up a small fraction of the total PrP^C and has only been detected by sensitive experimental techniques. In the CNS of uninfected wild type mice, PrP^C is observed principally in the Golgi and endosome compartments and to a lesser extent the ER (Laine et al., 2001; Mironov et al., 2003).

PrP^C is rapidly internalised from the plasma membrane in cultured cells (Shyng et al., 1993; Shyng et al., 1995). Internalised PrP^C colocalises with endosomal markers and rate of internalisation can be elevated by application of copper (Cu^{2+}) or zinc (Zn^{2+}) ions (Pauly and Harris, 1998), although other groups have reported that extensive internalisation is observed in the absence of Cu^{2+} (Sunyach et al., 2003). Endocytosis requires the presence of PrP's N-terminus (Nunziante et al., 2003; Shyng et al., 1995), which may also control the protein's exit from lipid rafts (Taylor et al., 2005). The mechanism by which PrP^C is internalised is controversial. Some groups have suggested that PrP^C is endocytosed via clathrin-coated pits because of observed colocalisation and biochemical isolation of PrP^C with pits and the prevention of endocytosis of PrP^C by specific inhibition of clathrin-mediated endocytosis (Laine et al., 2001; Madore et al., 1999; Shyng et al., 1994; Shyng et al., 1993; Sunyach et al., 2003; Taylor et al., 2005). However, clathrin internalisation of PrP^C requires an unidentified transmembrane cofactors to act as intermediary between extracellular PrP^C and the intracellular clathrin pit machinery (Taylor et al., 2005). Colocalisation of PrP^C and caveolae, flask shaped invagination of the plasma membrane, and cholesterol dependence of internalisation have been reported in non-neuronal cell cultures (Peters et al., 2003). This leads to the suggestion that PrP^C is also internalised by a caveola dependent mechanism in neuronal cells. The intracellular destination of PrP^C appears to differ between that internalised by caveloae which is

primarily targeted to the lysosome and that by clathrin to recycling endosomes (Peters et al., 2003; Sunyach et al., 2003). Thus, perhaps both internalisation mechanisms occur *in vivo*, although neuronal cells have been reported to lack caveolin and caveolae (Shyng et al., 1994).

1.5.3 Degradation of PrP^C

During the folding process within the ER errors can occur such that a protein adopts an aberrant or misfolded conformation. These misfolded proteins are potentially toxic and hence must be removed. This process, the ER associated degradation (ERAD) pathway, is ubiquitous in eukaryotes (Goldberg, 2003). Misfolded proteins are retained within the ER by chaperonins to prevent export to the Golgi by bulk transport. Misfolded proteins that have been resident in the ER for an extended period are recognised by their completely processed glycans (Sitia and Braakman, 2003; Wang and Hebert, 2003). These misfolded proteins are targeted to the retrotranslocation machinery for export into the cytoplasm where they are deglycosylated and ubiquitinated. Ubiquitination targets the protein to the proteasome for complete digestion. If large amounts of unfolded protein are detected in the ER, the unfolded protein response (UPR) is elicited; this leads to the down regulation of protein translation and the up regulation of a number of ER chaperonins and protein degradative machinery (Mori, 2000). Continued accumulation of misfolded proteins leads to the triggering of the ER stress response that leads to apoptosis of the affected cell, via expression of the proapoptotic gene CHOP (Oyadomari and Mori, 2004).

It has been suggested that about 10% of PrP^C is subject to ERAD and that subsequent cytosolic accumulation of PrP is neurotoxic when the proteasome is compromised, such as in an aging brain (Grenier et al., 2006; Jin et al., 2000; Ma and Lindquist, 2001; Ma et al., 2002; Yedidia et al., 2001). These results have been questioned in two papers which found no evidence that PrP^C is a substrate for retrotranslocation (Drisaldi et al., 2003; Fioriti et al., 2005). Others have reported that cytoplasmic accumulation of PrP mediated by proteasome inhibition is not neurotoxic (Kristiansen

et al., 2005; Roucou et al., 2003). N-glycans may have a direct effect on binding to mediators of UPR and ERAD, in addition to their proposed role in stabilising folding of the protein.

Cell culture studies have suggested that the half-life of PrP^C is between 3 and 6 hours (Borchelt et al., 1990; Caughey et al., 1989). Work using a murine transgenic model in which PrP^C production can be halted has suggested the longer half-life of 18 hours *in vivo* (Safar et al., 2005). This may in part be attributable to differences in the half-life of *Prnp* mRNA between cultured cells and *in vivo* (Safar et al., 2005). Blockage of lysosmal function by raising the pH of the compartment demonstrates that PrP^C is normally degraded in the lysosome (Vetrugno et al., 2005). Interestingly it is possible to selectively upregulate the lysosomal degradation of PrP^{Sc} without altering the steady state level of PrP^C, although half-life of PrP^C was not investigated in this work (Ertmer et al., 2004). Cell culture studies have suggested that the half life of PrP^C is significantly reduced in the absence of its N-glycans (Taraboulos et al., 1990a), the *in vivo* relevance and the mechanism this effect is mediated by is currently unclear.

1.5.4 Truncation and secretion of PrP^C in the CNS

A proportion of PrP is cleaved immediately N-terminal to the putative transmembrane domain during endocytosis of the protein in a cell culture system (Shyng et al., 1994; Shyng et al., 1995). This cleavage results in the production of a stable 17 kDa C1 terminal fragment that appears to be recycled to the plasma membrane and the N1 fragment. The cleavage has been suggested to be mediated by a serine protease within an acidic compartment (Shyng et al., 1995). The metalloproteases ADAM10 and ADAM17 have also been suggested to mediate production of the N1 fragment (Vincent et al., 2001). A similar truncated form of PrP^C (C1) is also observed in normal human brain and human neuroblastoma cell lines (Chen et al., 1995). A larger truncated (21 kDa) form of PrP (C2), that is cleaved prior to amino acid 90, has also been reported although this form is rarely observed under normal conditions (Chen et al., 1995). However, this cleavage event is promoted by oxidative stress and

a similar sized fragment is produced by the action of calpains (Watt et al., 2005; Yadavalli et al., 2004).

The N-glycans attached to the C1 and C2 truncated forms differ from those of full-length PrP, as indicated by a lectin binding assay, suggesting that the truncation of PrP may be affected by the protein's glycosylation state (Pan et al., 2002). The authors of this paper also proposed that the majority of lower weight PrP^C observed *in vivo* is truncated di-glycosylated PrP^C, rather than mono- and un-glycosylated forms of the protein.

PrP^C has been detected within the CSF (Tagliavini et al., 1992), consistent with the observed release of PrP into cell culture medium via a cleavage proximal to the GPI anchor (Borchelt et al., 1993). Work in cell culture has suggested that the shedding of PrP^C may occur both via the action of endogenous phospholipases and zinc metalloproteases (Parkin et al., 2004). Additionally, PrP^C is released from the cell in exosomes that form when multivesicular bodies fuse with the plasma membrane (Fevrier et al., 2004). These soluble forms of PrP may not play an important role in TSE pathogenesis as has been suggested by studies in transgenic mice that express PrP which lacks its GPI anchor (Chesebro et al., 2005). TSE challenge in these mice results in the formation of extracellular PrP^{Sc} plaques without the development of TSE disease.

1.5.5 The interaction of PrP^C with other molecules

PrP has been proposed to interact with a large number of other molecules. It immunoprecipitates with the ER resident proteins calnexin, calreticulin and protein disulphide isomerise with which it presumably forms a strong interaction as part of its normal folding (Capellari et al., 1999). An additional number of putative PrP interactors have been identified by yeast two hybrid screens, immunoprecipitation in mammalian cells or by an alkaline phosphatase reporter assay, including: the unidentified protein pint-1, Bcl-2, Heat shock protein 60 (Hsp60), synapsin 1b, Grb2, amyloid precursor protein-like protein 1 (Aplp1) and the laminin receptor precursor

(LRP) (Rieger et al., 1997; Spielhaupter and Schatzl, 2001; Yehiely et al., 1997). However, PrP^{C} is normally associated with membranes, therefore interactions between non-membrane attached PrP^{C} and other molecules may not be representative of *in vivo* (Schmitt-Ulms et al., 2001). However, further work supports the *in vivo* interaction of PrP with LRP, as LRP mediates the internalisation of recombinant PrP^{C} and it is necessary for accumulation of PrP^{Sc} in scrapie infected cells (Gauczynski et al., 2001; Leucht et al., 2003). Other studies using an *in situ* cross-linking technique have suggested that PrP binds a subset of neural cell adhesion molecule (N-CAMs) (Schmitt-Ulms et al., 2001). These interactions has been suggested to be important for the putative role of PrP^{C} in neurite outgrowth (Santuccione et al., 2005).

N-glycans attached to PrP are large and negatively charged and may alter the interactions of PrP with other molecules. Importantly, the N-glycans will also influence each other. Moudjou and colleagues have proposed that when both glycosylation sites are occupied the N-glycans will repel each other, revealing an area of PrP that would otherwise be shielded (Moudjou et al., 2004). Equally the N-glycans on two different PrP molecules may prevent the molecules interacting. Thus the different glycotypes may exhibit very different behaviour in the cell, solely because of potential shielding by the attached N-glycans. Equally, N-glycans may mediate interactions between PrP and other molecules, of particular interest in this regard are the $Lewis^{X}$ epitope carried on the N-glycans attached to Asn^{180} and $Lewis^{X}$ and sialyl-$Lewis^{X}$ epitopes on the Asn^{196} attached N-glycans (Stimson et al., 1999). These epitopes are highly regulated during development of the central nervous system and may have a role in specific ligand recognition (Roberts et al., 1991). Although previous work has demonstrated that glycosylation of PrP^{C} is not required for its interaction with NCAM (Schmitt-Ulms et al., 2001), glycosylation's importance to other key binding partners, such as the laminin receptor, have yet to be explored.

1.6 The TSE species barrier

The TSE species barrier has been experimentally analysed in a wide range of model systems, including *in vitro* PrP conversion assays, TSE infected cell cultures and by experimental transmission to many animal species. *In vivo* there is a clear barrier to replication of the TSE agent both in the CNS and lymphoid tissue of the novel host species (Muramoto et al., 1993). Recent parallels between the factors controlling within and between species spread have led a number of TSE researchers to adopt the term "*transmission barrier*" to describe both the species barrier and factors limiting the spread within-species (Hill and Collinge, 2003). Although some mechanisms may be common to within and between species TSE transmission, the extent of the barrier to transmission is generally far greater between than within-species. Thus consideration of the factors that affect specifically cross-species TSE transmission is important.

1.6.1 Observations of the TSE species barrier

The first reported case of a species other than sheep being infected with a TSE disease occurred in 1883 when a cow exhibiting a scrapie like disease was reported by Sarradett (Sarradett, 1883). However, as no pathological examination was undertaken in this case it may not reflect an actual case of TSE. Subsequently, putative natural transmission of scrapie to a goat was reported (Chelle, 1942). Experimental transmission of scrapie to goats and rodents formally proved that TSEs could infect novel host species (Chandler, 1961; Cuille and Chelle, 1939). Cross-species TSE transmission was observed to be linked with an increase in length and variation of the incubation period, reduction in disease incidence in challenged hosts and an alteration in pathology. On subsequent passage within the new host the incubation period was observed to fall during the second and third passage until a stable or "*fixed*" incubation time was achieved within the new host species. This phenomenon, the "species barrier", was defined by Pattison in 1964 at a Slow Latent

and Temperate Viral Infection Meeting at the National Institute of Health (NIH) (Pattison, 1965).

Extensive efforts to transmit Kuru and other human diseases of the CNS, including a number of TSEs, to animal species were undertaken during the 1960s and 1970s by Gajdusek and colleagues at the NIH (Brown et al., 1994). Successful transmission of Kuru to a number of primate species was demonstrated, but there appeared to be a strong species barrier between human TSE and rodent hosts (Gajdusek et al., 1966; Gibbs and Gajdusek, 1973). Furthermore, a number of human TSE isolates appear relatively untransmissible to other species, providing evidence that the species barrier may be influenced by TSE strain (Brown et al., 1994).

Epidemiological study of three outbreaks of TME that occurred in 1947, 1961-2 and 1963 suggested that this disease of mink resulted from a cross-species TSE transmission via an oral route (Hartsough and Burger, 1965). The most likely TSE source in these and later TME outbreaks was the feeding of "downer" cattle (Hartsough and Burger, 1965; Marsh et al., 1991). The disease incidence approached 100% of adults but no kits exhibited disease on the index farm in the 1947 outbreak; this observation and the occurrence of disease in animals that had been exported to another farms without subsequent spread suggested that mink to mink spread was not responsible for the high disease incidence (Hartsough and Burger, 1965). These data suggests that the species barrier between the TSE source animal (putatively cattle) and mink was small or nonexistent in this natural outbreak. This hypothesis was later provided with experimental support as TME is readily transmissble to cattle (Marsh et al., 1991). Additionally, the resultant bovine TSE is also readily transmissible to mink via the oral route. Moreover both cross-species transmissions were not associated with a significant increase in incubation period at primary passage. Thus TME demonstrates the unpredictable nature of the TSE species barrier.

The BSE epidemic provided categorical evidence that the TSE species barrier is neither absolute nor predictable. The BSE agent transmitted to over fifteen non-cattle animal host species prior to its detection and elimination from the British bovine herd.

The genetic relatedness of the hosts (to date) is somewhat unusual and includes species in distantly related genus from the family Felidae (puma, domestic cats, tigers, cheetahs and lions) but not the similarly exposed Canidae (Kirkwood and Cunningham, 1994; Sigurdson and Miller, 2003). TSE disease linked to BSE exposure was also observed in a number of non-human primates in French zoos (Bons et al., 1999; Bons et al., 1996), in addition to an apparently random subset of Bovinea species. Despite the observed wide dissemination, BSE does display a classic species barrier on transmission to many new hosts species and some host species including pigs are relatively resistant to BSE infection (Wells et al., 2003). The high numbers of infected cows entering the food chain (estimated to be 1-3 million) (Anderson et al., 1996) may have contributed to the wide dissemination of BSE to other species. Additionally, a number of host species exhibited unusually high susceptibility to BSE such as Greater kudu (*Tragelaphus strepsiceros*) (Kirkwood and Cunningham, 1994), although secondary within-species spread may have contributed to the extremely high disease incidence observed in this species (Cunningham et al., 2004). However, the great number of transmissions observed suggested that cross-species transmissibility of BSE may differ from other TSE diseases such as scrapie.

In 1995 the first cases of a new form of human TSE were reported in the UK (Bateman et al., 1995; Britton et al., 1995). Patients were unusually young and had a different clinical and pathological presentation compared to known human TSEs. In 1996 this disease was classified as a new variant of CJD (Will et al., 1996). Clinical illness differed starkly from sporadic CJD, early signs were often psychiatric in nature and early development of ataxia was common. The neuropathology of the variant CJD patients also varied from that of sporadic cases, in particular the extensive deposition of PrP "florid" plaques (surrounded by vacuolation) in the cerebrum and cerebellum (Ironside et al., 2000). The emergence of this novel disease within the UK population led to obvious suspicions about its origin. Similarities in the PrP^{Sc} glycoform from vCJD patients and BSE strengthened the hypothesis that vCJD was the result of transmission of BSE to man (Hill et al., 1997a), and *in vivo* strain typing by Bruce and colleagues demonstrated that vCJD

and BSE were caused by the same TSE strain (Bruce et al., 1997). Thus the human barrier to cross-species TSE transmission had failed and the question now became why?

1.6.2 Subclinical infections

Transmission of TSE diseases to novel host species often results in subclinical TSE infections, in which, despite an absence of outward signs of disease within the hosts natural lifespan, significant replication of the agent has occurred (Hill et al., 2000; Kimberlin and Walker, 1978a; Race et al., 2001; Zlotnik, 1965). Transmissions of TSE from these subclinical individuals has resulted in the development of clinical disease both in hosts of the original species and more importantly hosts of the new species (Hill et al., 2000; Race et al., 2001), thus demonstrating that adaptation to the new host species occurred during the subclinical TSE infection. Thus, the species barrier can be breeched in a two part process: first, by subclinical and therefore undetectable infection in the novel host, and then by onward transmission to further individuals of the novel species, causing significant disease. This phenomenon has obvious public health implications and is informative as to the mechanism of the species barrier. Perhaps there is something unique about the agent in these subclinical cases such that its toxicity is reduced or merely that the replication rate is slowed to such an extent that it does not reach a disease-causing load within the host's natural lifespan.

1.6.3 Species barrier mechanism

The prolongation of incubation period at first passage in a new species leads to the hypothesis of a special zero-phase or period of non-replication in the new host species (Kimberlin and Walker, 1979). They suggested that the zero-phase may occur because of an alteration in TSE replication efficiency in new hosts or the requirement for a different transmission route. Furthermore, successful transmission of TSE disease across a range of species barriers results in a modification of the infectious agent (Bartz et al., 1998; Kimberlin and Walker, 1978a; Kimberlin et al., 1989;

Pattison, 1965). In some cases the agent loses the ability to infect the original host and in others acquires transmissibility to additional species. Additionally, alteration of strain characteristics such as the targeting of vacuolation have also been reported to result from transmission through an intermediate host species (Kimberlin et al., 1989). This suggests that the TSE agent was irreversibly altered when it established an infection in a new host. Equally, in other cases the species barrier effect has been observed in the absence of any detectable change in TSE strain, for example BSE maintained its identity after passage in a number of non-bovine hosts (Bruce et al., 1997). Thus, although passage across the species barrier does not automatically result in an alteration of the agent, transmission to a new host species greatly elevates the chances of TSE agent change. This disparity in the effects of cross-species transmission on the nature of the TSE agent suggests that multiple mechanisms may contribute to the species barrier. The observed resistance to cross-species TSE transmission may be thought of as species barriers rather than a single mechanism. Additionally, there appears to be a uniquely stochastic nature to cross-species transmission of TSE disease as indicated by the variation in incubation period observed at primary passage in a new host species, which is not observed for within-species transmission (Scott et al., 1989).

1.6.3.1 Involvement of the immune system

Preimmunisation of mice with hamster brain prior to peripheral challenge with hamster scrapie both increased the incubation period and decreased disease incidence, suggesting that a peripheral immune response may contribute to the species barrier (Kimberlin et al., 1975). However, the invasive method of TSE challenge used in this experiment (intraperitoneal injection) may not reflect natural transmission events. Thus the suggested immune effect may be artefactual. Limited evidence has been reported that the Human Leukocyte Antigen type DQ7 is more abundantly observed in vCJD patients than would be expected by chance (Jackson et al., 2001), suggesting that this immune molecule may influence the cross-species transmission of BSE. However other groups have not replicated this observation (Laplanche et al., 2003; Pepys et al., 2003).

1.6.3.2 PrP amino-acid sequence

Work using transgenic mice expressing hamster or hamster/murine chimeric PrP suggested that the TSE species barrier was attributable to the degree of PrP sequence homology between the TSE donor species and the new host (Prusiner et al., 1990; Scott et al., 1989; Scott et al., 1993). Indeed, in transgenic mice overexpressing hamster PrP, the usual strong barrier to hamster scrapie transmission was completely absent (Prusiner et al., 1990; Scott et al., 1989). Furthermore, the TSE disease phenotype in these transgenic mice was similar to that observed in hamster (Scott et al., 1989). Similar effects have been reported in PrP *in vitro* conversion assays in which efficiency of conversion was linked to PrP^{Sc} and PrP^{C} sequence homology (Bossers et al., 1997; Horiuchi et al., 2000; Kocisko et al., 1995; Raymond et al., 2000; Raymond et al., 1997). This would suggest that the observed effect of host PrP^{C} sequence on the species barrier is directly related to its ability to form PrP^{Sc}. However, in the chimeric mouse/hamster transgenic system the TSE disease phenotype was influenced by the TSE source species, showing that disease outcome is not purely dictated by PrP^{C} sequence (Prusiner et al., 1990). Additionally, the species barrier effect in this system is influenced by the strain of TSE (Scott et al., 1993). Furthermore, different strains of TSE, in which donor PrP^{Sc} have identical amino acid sequence, can have radically different transmission characteristics to new host species, e.g. variant compared to sporadic CJD (Bruce et al., 1997).

Further transgenic animal studies revealed that increasing the amino acid sequence homology between host and donor can enhance or have no effect on the species barrier (Collinge et al., 1995; Telling et al., 1995). Conversely, single amino acid changes at key residues can have dramatic effects on the species barrier, in some cases without increasing amino acid homology with the TSE source (Barron et al., 2001; Bishop et al., 2006; Manson et al., 1999; Telling et al., 1995). For example, the human methionine/valine polymorphism at amino acid position 129 is a key determinate of susceptibility to BSE. Approximately thirty percent of the UK human population are 129 MM homozygotes, yet all clinical vCJD cases reported to date are

of this genotype (Will, 2003). However, work in transgenic mice expressing either MM, MV or VV human PrP suggests that people who have MV or VV genotypes may be also be susceptible to vCJD infection but may have longer incubation periods than MM individuals (Asante et al., 2006; Bishop et al., 2006). The pattern and type of PrP^{Sc} which accumulated after cross-species transmission also differed between mice expressing the methionine and valine forms of PrP (Bishop et al., 2006), consistent with the observed accumulation of PrP^{Sc} in peripheral tissues of an MV individual suspected to have subclinical vCJD (Peden et al., 2004). This suggests that the differences in incubation period and/or susceptibility observed in these animals may be related to the formation of PrP^{Sc}. Importantly, the same single amino acid change can render a host more susceptible to cross-species infection with some TSE sources and enhance resistance to others, demonstrating that the change does not simply just destabilise PrP (Barron et al., 2001; Manson et al., 1999).

1.6.3.3 Species specific conversion factors

One group proposed that the TSE species barrier may be contributed to by a requirement for species specific factors to promote the conversion of PrP to PrP^{Sc} (Telling et al., 1994; Telling et al., 1995). This work was based on data which demonstrated that endogenous murine PrP specificity inhibited the transmission of human TSE agents to transgenic mice expressing human PrP. This led to the hypothesis of a murine specific factor "Protein X" that is essential for the PrP conversion process and TSE transmission. This factor is proposed to have higher affinity for murine PrP than the transgenic HuPrP and hence to preferentially interact with it. However, the ability of chimeric murine/human PrP (murine amino acids 1-95 and 168-231) to support the transmission of human TSE agents is not greatly affected by the expression of endogenous murine PrP (Telling et al., 1995). The authors thus proposed that "Protein X" specifically interacts with the murine component of PrP and suggest that the protein's binding site is in PrP C-terminal, via an epitope that includes murine amino acids 167, 171, 214 and 218 which are on the opposite face of PrP to its attached N-glycan (Kaneko et al., 1997; Telling et al., 1995). An alternative explanation of this result is that a direct interaction between

endogenous murine PrP and transgenic hamster PrP caused the prolongation of the incubation period. The authors argued against this hypothesis on the basis of the presence of an excess of the hamster PrP in their murine transgenic model. However small amounts of heterologous PrP could disrupt the formation of PrP^{Sc}.

Despite this there is growing evidence from other systems of the importance of factors both in the CNS and the periphery, other than PrP, which influence the TSE disease process. Cross-species transmission of BSE to mice suggests that four identified loci influence the TSE disease incubation period in mice (Manolakou et al., 2001). The authors of this paper suggested a number of immune system genes as likely candidates at these loci. However, the loci identified in this work were large and contain many genes thus it is currently unclear which molecules other than PrP influence cross-species TSE transmission. Additionally, only half of the incubation period heritability was accounted for in this study suggesting that additional loci of small effect may also be important.

1.6.3.4 Conformational compatibility

A kinetic model of the TSE species barrier proposed by Kellershohn and Laurent suggested that a PrP^{Sc} conformational adaptation step may underlie the species barrier (Kellershohn and Laurent, 1998). In particular the authors proposed the production of an intermediary conformation of PrP during cross-species TSE infection prior to the production of host specific PrP^{Sc} that differed from that of the donor. This was based on experimental work that demonstrated PrP^{Sc} could not be detected at primary and secondary passage of BSE in mice (Lasmezas et al., 1997), and was consistent with observations *in vitro* of a change in PrP^{Res} size during cross-species conversions (Kocisko et al., 1995). Complementary to this idea is recent experimental work by Peretz and colleagues who elegantly demonstrated that the TSE species barrier effect is correlated with an alteration in the conformation of PrP^{Sc} (Peretz et al., 2002). In this work, transmission of a TSE across a species barrier required the emergence of a novel PrP^{Sc} conformation. The authors propose that delay in incubation period, associated with the species barrier, occurs because of this conformational-

transition/adaptation stage; akin to the zero-phase proposed by Kimberlin in 1979 (Kimberlin and Walker, 1979). This hypothesis has been further supported by work in a yeast prion model that showed a correlation between the ability to transmit the prion state to novel yeast species and protein conformation (Chien et al., 2003; Chien and Weissman, 2001). Additionally, *in vitro* conversion of the N-terminus of PrP demonstrated that cross-species seeding compatibility is determined by conformation not primary sequence (Jones and Surewicz, 2005).

This model would suggest that factors that affect the conformational adaptability of host PrP will also influence the TSE species barrier, and provides a mechanistic understanding for the observed strain dependence of the species barrier. Thus destabilising amino acid mutations, removal of post-translational stabilisers such as the di-sulphide bond or PrP's N-glycans will render the host more susceptible to cross-species TSE challenge. However, the species barrier effect has also been observed in the absence of a change in the nature of the agent (Bruce et al., 2002) and thus by inference the conformation of PrP^{Sc}. Thus conformational compatibility may be part of the species barrier but other mechanisms may also be important.

1.7 PrP's N-glycans and TSE transmission

1.7.1 Alteration of glycosylation after TSE transmission

The glycosylation of proteins may be altered by TSE infection, as given the dramatic neuropathology observed in TSE disease an impact on cellular processing would be anticipated. Indeed, glycosylation of the insulin receptor,, but not the insulin-like growth factor, is changed in chronically scrapie infected N2a cells compared to those that are uninfected (Nielsen et al., 2004). However the uninfected and infected cell lines used in this study may represent two clonally distinct populations and thus the difference in glycosylation observed may not be directly related to TSE disease status. Other work has suggested that the amount of dolichol and dolichyl phosphate, key components of the glycosylation machinery, may be altered in TSE infected

individuals (Guan et al., 1996). However this has not been linked to an *in vivo* change in glycosylation. Rudd and colleagues suggested that the differences in glycosylation observed between hamster PrP^{C} and 263K PrP^{Sc} could be most readily explained by a change in the activity of a single glycosylation enzyme, however this hypothesis was not further explored (Rudd et al., 1999).

1.7.2 Role of PrP's N-glycans in TSE disease

Molecular modelling of the importance of N-glycans to the conformation of PrP has suggested they may have a stabilising effect on the protein's structure, via a reduction in water molecule motility (Zuegg and Gready, 2000). However, NMR comparisons of the un-glycosylated and glycosylated PrP show only minimal conformational differences, suggesting that glycosylation of PrP may have a functional rather than a conformational role (Bosques and Imperiali, 2003; Hornemann et al., 2004). In addition, glycosylation of the first site has been linked to the promotion of formation of the disulphide bond and a reduced tendency to form fibrils, suggesting that glycosylation may be important to conformational change rather than conformation per se (Bosques and Imperiali, 2003).

Glycosylation of PrP may influence and be influenced by mutations in the protein, as suggested by molecular modelling (Wong et al., 2000). Indeed, in addition to the changes in PrP glycosylation associated with the rare TSE disease linked T183A mutation, which ablates the second N-glycan attachment site (Grasbon-Frodl et al., 2004; Nitrini et al., 1997), changes at other amino acid positions also correlate with specific PrP^{Sc} glycoforms (Capellari et al., 2000a; Chasseigneaux et al., 2006; Hill et al., 2006; Monari et al., 1994). Little un-glycosylated PrP^{Sc} is observed in familial TSE patients that carry D178N and E200K mutations that lie close to the first N-glycan attachment site. Cell culture studies have suggested that the absence of un-glycosylated PrP in patients carrying these mutations may be attributed to their instability and consequent failure of traffic to the cell surface (Capellari et al., 2000a; Petersen et al., 1996). In addition abnormal glycosylation of the second site was shown to be associated with the E200K mutation (Capellari et al., 2000a). A

mutation at codon 180 (V180I) has been reported to be associated with the absence of di-glycosylated PrP^{Sc} in a CJD patient (Chasseigneaux et al., 2006). Interestingly this mutation does not prevent the glycosylation of PrP^{C} in cell culture, suggesting that this mutation prevents the accumulation of di-glycosylated PrP^{Sc} (Chasseigneaux et al., 2006). A similar, atypical form of sporadic CJD has been recently reported in which no di-glycosylated PrP^{Sc} is observed (Zanusso, 2006). However, no mutations in *PRNP* were detected in this patient. Thus the glycosylation state of PrP^{Sc} may be influenced by factors other than the primary sequence of PrP.

Spontaneous induction of PrP^{Res} formation in cell culture expressing PrP lacking the N-glycan attachment sites and by blockage of N-glycosylation by tunicamycin has been reported (Lehmann and Harris, 1997). However, this may be an artefact of cell stress linked to over expression of PrP or owign to the pathogenic mutations used to disrupt the glycosylation of PrP (Capellari et al., 2000b). Similarly, prevention of complex glycosylation by inhibition of heat shock protein 90 (Hsp90) or α-mannosidase treatment increased the formation of PrP^{Res} in scrapie infected cell culture (Winklhofer et al., 2003). Additionally, an independent study reported more rapid generation of PrP^{Res} in scrapie-infected cell culture when glycosylation was inhibited with tunicamycin or point mutation (Taraboulos et al., 1990a). However, in these experiments overall production of PrP^{Res} was decreased. Moreover, if glycosylation of PrP generically prevented the proteins misfolding, un-glycosylated PrP^{Sc} would be predicted to be the predominant form observed *in vivo*. However, many different PrP^{Sc} glycoforms are observed *in vivo*, including the heavily di-glycosylated signature of BSE and vCJD (Collinge et al., 1996; Parchi et al., 1996; Somerville et al., 1997) (1.4). This indicates that the *in vivo* role of PrP's N-glycans in TSE disease is not to simply prevent the formation of PrP^{Sc}.

Conventional murine transgenics expressing hamster PrP in which the first N-glycan site had been ablated either alone (T183A) or in conjunction with the second site (T183A, T199A) [UCSF] were resistant to challenge with hamster passaged scrapie (DeArmond et al., 1997). Comparable murine transgenics, carrying ablative mutations in the second glycosylation site only, were resistant to strain 139H but

susceptible to strain Sc237, albeit with greatly extended incubation periods compared to controls (DeArmond et al., 1997) (appendix i). Differences in the pattern of PrP^{Sc} deposition were also reported including an absence of deposition in the thalamus, a reduction of deposition in the habenula and hypothalamus in the second site N-glycan deficient transgenic mice, compared to controls. However, these transmissions studies were compounded by the observed overexpression of PrP (2-4 X), the potential aberrant expression of the transgene caused by the random site of integration of the transgene, and the use of hamster PrP in a murine host. Furthermore, altered localisation of PrP^{C} was observed in these experimental models; the first site deficient model exhibited white matter PrP^{C} expression, and the second and both sites deficient model lacked cell surface PrP^{C}. Similar results have also been reported in a cell culture model expressing comparable mutations (Rogers et al., 1990). Additionally, cell culture studies have shown that the T183A mutation used to disrupt the first glycosylation site has pathogenic effects independent of the disruption of N-glycan attachment (Capellari et al., 2000b; Neuendorf et al., 2004). This is consistent with its association with two independent incidences of familial spongiform encephalopathy with this mutation (Grasbon-Frodl et al., 2004; Nitrini et al., 1997). Thus it is not possible to fully interpret the importance of PrP glycosylation state to TSE transmission in this study because of the large number of confounding effects.

Independently generated conventional transgenic mice expressing 3F4-tagged murine PrP lacking the second glycosylation site (T198A) [Riems] were also susceptible to infection with a range of murine TSE strains/isolates (Neuendorf et al., 2004) (appendix ii). These transgenic mice exhibited greatly extended incubation times compared to normally glycosylated controls. However, in contrast to the work of DeArmond and colleagues, disruption of the first N-glycan attachment site (T182N two independent lines) [Riems] did not lead to complete resistance to TSE challenge. These lines were susceptible to infection with murine TSE strains ME7, Chandler (139A) and murine passaged BSE. The differences between the UCSF and Riems glycosylation deficient transgenic mice may be attributed to the different point mutation used to disrupt the glycosylation sites. In particular, that used in the Riems

transgenic models was reported to allow transportation of PrP^C to the plasma membrane in cell culture (Neuendorf et al., 2004).

However, the incubation times for the two independent Riems lines in which the first attachment site was disrupted were significantly different (Neuendorf et al., 2004). For example, in one line the incubation period for Chandler equalled that of the normally glycosylated control, whereas a significant extension was observed in an independent line carrying the same transgene. Thus, the specific role of the first N-glycan site in transmission can not be clearly determined from these data. This discrepancy between independent lines expressing the same transgene, highlights the potential for artefacts caused by copy number and site of transgene integration in conventional transgenic mice.

Work using gene-targeted PrP glycosylation deficient transgenic mice lacking the first glycosylation site (N180T) [NPU] suggests that glycosylation of this site facilitates within-species TSE transmission (Tuzi et al., in preparation) (appendix table ii). Moreover, the requirement for glycosylation of the first site is highly TSE strain dependent. Comparable gene-targeted transgenic mice lacking the second glycosylation site (N196T) [NPU] are also susceptible to a number of murine TSE strains (Tuzi et al, in preparation). Similarly, absence of glycosylation at this site results in an elongation of the incubation period for some strains of TSE only, as previously observed in conventional transgenic mice (DeArmond et al., 1997; Neuendorf et al., 2004). However, in contrast to the absence of disease in UCB un-glycosylated PrP transgenic mice after TSE challenge, gene-targeted un-glycosylated PrP transgenic mice (N180T, N196T) [NPU] are susceptible to TSE disease, albeit only when challenged with one strain (Tuzi et al., in preparation; appendix table ii).

1.7.3 The role of glycosylation of PrP in TSE strain determination

The glycoform of PrP^{Sc} often correlates with TSE strain (Collinge et al., 1996; Parchi et al., 1996), leading to the hypothesis that glycoform itself encodes TSE strain characteristics, such as the targeting of neuropathology and the length of the

incubation period (Collinge et al., 1996). Transmission of TSE to conventional glycosylation deficient transgenic mice has been reported to alter the pattern of PrP^{Sc} deposition *in vivo* (DeArmond et al., 1997) suggesting that the strain of TSE may also have been altered. However the authors of this work did not further examine this possibility. Recent work by Tuzi and colleagues has further investigated the importance of glycosylation of host PrP to strain determination; they suggest that, for some TSE strains, glycosylation at the second site contributes to the maintenance of TSE strain characteristics *in vivo* (Tuzi et al., in preparation; appendix table ii).

1.7.4 The role of glycosylation of PrP^{C} in cross-species TSE transmission

Cell-free conversion studies, in which PrP^{C} is converted to PrP^{Res} by seeding with PrP^{Sc}, have shown that un-glycosylated PrP^{C} appears to be two-to three-fold more efficiently converted to the protease resistant form, compared to that normally glycosylated, when the seeding PrP^{Sc} originates from a different host species (Priola and Lawson, 2001). This suggests that glycosylation of PrP may influence the TSE species barrier. However, this effect has not been replicated in other studies (Raymond et al., 1997) nor investigated *in vivo*. Glycosylation of PrP^{C} could feasibly influence the species barrier by a number of mechanisms including by affecting the accumulation or nature of PrP^{Sc} formed *in vivo* or alternatively by influencing other aspects of TSE pathogenesis. PrP's N-glycans may modify the flexibility of the protein and hence change the range of misfolded conformations that it can adopt, as previously suggested by DeArmond and colleagues (DeArmond et al., 1997). This may be of specific importance to the cross-species transmission of the TSE agent which has been proposed to involve an alteration in the conformation of PrP^{Sc} (1.6.3.4).

Glycosylation of other host proteins has been implicated in cross-species resistance to infection and pathogenic effects (Chu and Whittaker, 2004; Falk et al., 1995; Gambaryan et al., 2003; Griffitts et al., 2003; Kunz et al., 2005; Marin et al., 2003; Wentworth and Holmes, 2001). In some cases this effect is mediated by specific differences in the combination of glycans attached to proteins of different species

with which the host pathogen is adapted to interact (Gagneux et al., 2003; Gambaryan et al., 2003). Alternatively, the effect of glycosylation is to shield the target host protein and hence prevent the pathogen gaining access to them (Chu and Whittaker, 2004; Falk et al., 1995; Griffitts et al., 2003; Kunz et al., 2005). Similar mechanisms may contribute to the potential role of glycosylation of PrP in the cross-species transmission of the TSE agent.

1.8 PrP transgenic mice

Despite recent advances in TSE susceptible cell cultures (Klohn et al., 2003), not all TSE strains can be successfully transmitted *in vitro*; additionally it is not possible to study TSE pathogenesis outside a host. It is thus necessary to use animal models to address questions of all TSE pathogenic processes or strain. PrP transgenic mice have been used to address these issues for over fifteen years. All model systems carry experimental limitations and choice of model has been shown to greatly impact on the experimental interpretation and conclusions

The earliest PrP transgenic animal models were generated by conventional methods, whereby the *Prnp* transgene is introduced into the murine genome at random by microinjection of DNA into fertilised oocytes. The transgene may integrate into the genome at multiple sites. The expression of the transgene in these conventional model systems is therefore regulated differently than the endogenous gene. These mice also exhibited high transgene copy number and over-expressed PrP (Hsiao et al., 1990; Scott et al., 1989). Work by Westaway and colleagues demonstrated that this led to neurodegeneration even if PrP bore no mutations (Westaway et al., 1994). Additionally, in early conventional murine transgenics the *Prnp* /*PRNP* transgene was expressed alongside endogenous murine *Prnp*; and interaction of murine and transgenic PrP altered TSE disease outcome in some models (Telling et al., 1995). The production of PrP knock-out transgenic mice circumvented this problem permitting the production of transgenic animal models using a murine PrP null background (Bueler et al., 1992; Manson et al., 1994a; Moore, 1997; Sakaguchi et al.,

1996). However two of the four knock-out lines generated exhibited an ataxic phenotype, leading to suggestions that loss of PrP function may cause TSE disease (Moore, 1997; Sakaguchi et al., 1996). However the pattern of neurodegeneration in these murine transgenics was unlike that observed in TSE disease. Further characterisation of these mice demonstrated that the gene disruption strategy employed resulted in the ectopic neuronal expression of a nearby gene, Doppel, the expression of which was normally restricted to the testis and heart (Moore et al., 1999). Despite a high degree of homology to PrP, Doppel appears to have little relevance to TSE disease (Tuzi et al., 2002), highlighting the importance of understanding the model system used.

Importantly the site of transgene integration is not controlled during the generation of conventional transgenic models. Gene expression is greatly affected by its genomic context thus aberrant spatial and temporal expression of the transgene may occur. Equally, use of non-*Prnp* promoters and absence of specific regulatory regions may occur at some distance to *Prnp* and could also affect expression pattern. This may lead to spurious effects such as the observed absence of tgPrP expression in Purkinje cells, when the transgene is driven by the endogenous promoters contained in the 6 kb of *Prnp* upstream sequence (Fischer et al., 1996). Such effects may impact on TSE pathogenesis as is clearly demonstrated by the great variation of TSE incubation periods observed in independent conventional PrP transgenics mice which express the same transgene at apparently comparable levels *in vivo* (Neuendorf et al., 2004). Thus comparisons between the effects of changes in *Prnp* are difficult to make, especially if subtle.

PrP gene-targeted transgenic mice in which murine *Prnp* is directly replaced by the *Prnp* transgene circumvent the problems of mis- and over-expression observed in conventional transgenic animal models; this can be achieved using a two step strategy (Moore et al., 1995). Genomic *Prnp* in murine embryonic stem (ES) cells is first replaced with a hypoxanthine phosphorbosyl transferase (HPRT) minigene by homologous recombination. At this first step HPRT positive cell are selected, using specific growth media. Thus in all the selected cells, wildtype *Prnp* exon three has

been replaced by the HPRT minigene. In the second step the HPRT minigene is then itself replaced with the *Prnp* transgene by the use of selective growth media.

An alternative strategy uses a LoxP neomycin/thymidine kinase-selectable cassette (Neo/TK) into which the *Prnp* transgene is ligated (Cancellotti et al., 2005) (Figure 1.3 B). This cassette is used to replace genomic *Prnp* by homologous recombination in ES cells, which can then be selected using gancylovir. The Neo/TK selection marker is flanked by LoxP, so that it can be removed via the action of Cre recombinase, leaving a single LoxP site downstream of the *Prnp* open reading frame. Both selection strategies result in transgenic *Prnp* ES cells in which the transgene has directly replaced the genomic *Prnp* and thus is subject to control by all the appropriate regulatory elements, be they local or distal. These ES cells derived from the inbred 129/Ola strain are then injected into a 3.5 day old C57/B6 blastocyst. If the transgenic cells colonise the blastocyst, a chimeric mouse will result from a successful pregnancy (Manson et al., 1999). Germ line transmission of the 129/Ola transgenic cells then results in the production of the gene targeted line which can be directly compared to other gene targeted *Prnp* lines, avoiding the need for the generation of multiple lines.

This method was used to generate three directly comparable lines of PrP glycosylation deficient transgenic mice used in this thesis (Figure 1.3 C). In these mice the first (G1), second (G2) or both (G3) glycosylation sites have been disrupted by N180T, N196T or N180T and N196T respectively (NPU). All lines are maintained on the 129/Ola inbred genetic background, so they only differ from 129/Ola wild type mice at the outlined amino acid changes and the single 3' LoxP site. To control for the effect of this site a control transgenic mouse line (CL) was also used; these transgenic mice carry the wild type *Prnp* open reading frame and hence produce PrP that is normally glycosylated, however they also carry the single 3' LoxP site. These CL transgenic mice are equivalent to non-transgenic 129/Ola mice save for this non-translated LoxP site.

Figure 1.3 Schematic representation of the production of the PrP glycosylation deficient transgenic mice by double-step *Prnp* gene targeting

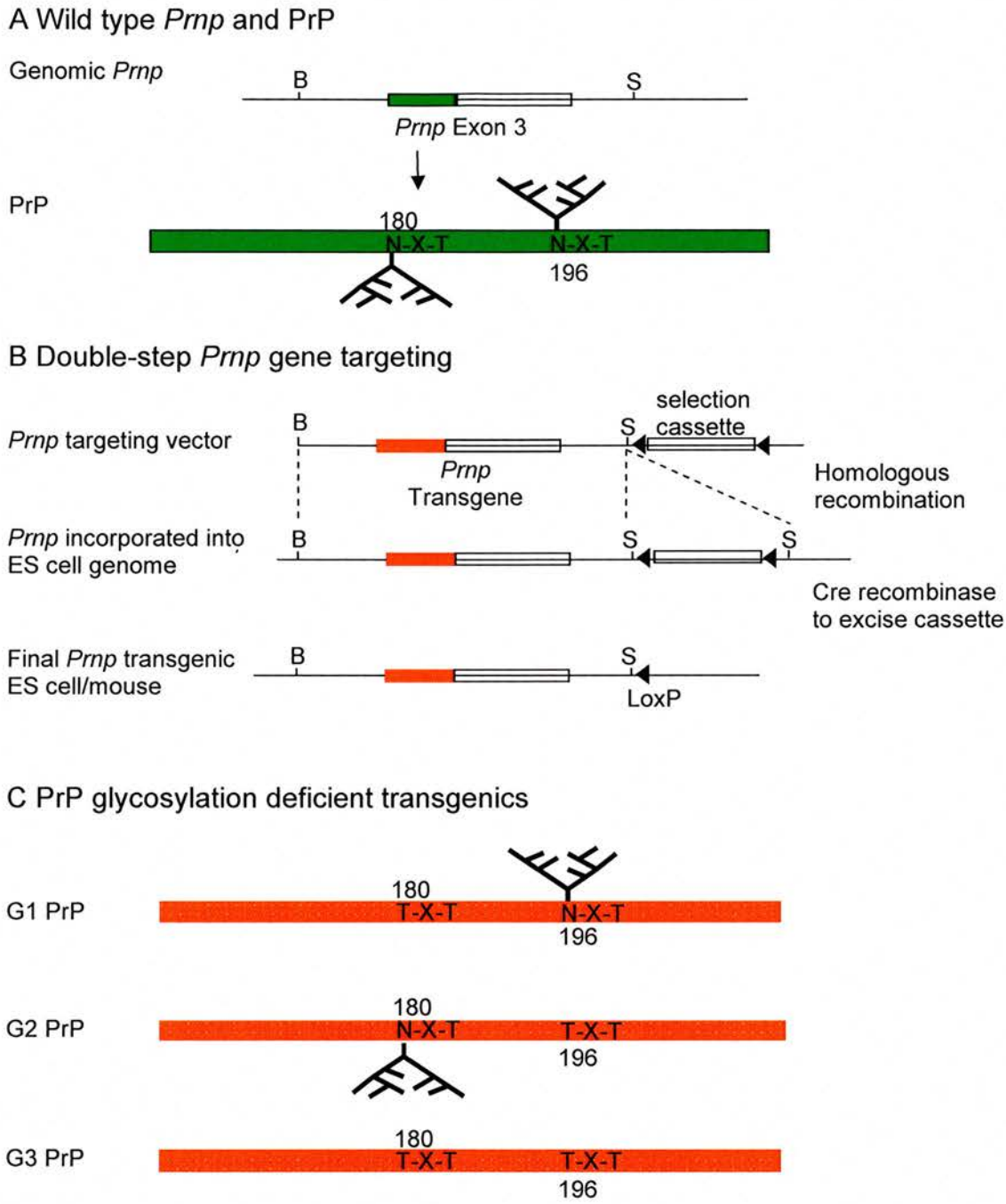

1.9 Thesis aims

In vitro experimental evidence suggests that glycosylation of PrP may specifically inhibit the cross-species transmission of TSE and hence contribute to the TSE species barrier (1.7). The aim of this thesis is to investigate this hypothesis *in vivo*.

Specific Aims

- 1) To validate three lines of gene-targeted PrP glycosylation deficient transgenic mice [NPU] (1.8) as suitable models in which to investigate the effect of glycosylation of PrP on the transmission of TSE between species. This will consist of
  a) establishing that the alteration in the PrP amino acid sequence in these transgenic mice prevents N-glycan attachment to the protein.
  b) establishing whether the alterations in PrP in these transgenic mice changes the steady-state level of the protein in the brain.
  c) determining, using confocal microscopy, if the localisation of PrP^{C} in the brains of the glycosylation deficient transgenic mice is altered.
  d) to establish whether the glycosylation deficient transgenic mice develop TSE specific vacuolation, clinical disease or spontaneous formation of PrP^{Sc}, in the absence of TSE challenge.

- 2) To test the hypothesis that glycosylation of PrP^{C} inhibits the cross species transmission of TSE disease, by transmission of one hamster and two human TSE strains to the PrP glycosylation deficient transgenic and normally glycosylated control mice.

- 3) To determine if the change in disease incidence and time to disease onset observed in the glycosylation deficient transgenic mice after cross-species TSE challenge, is linked to an alteration in TSE strain characteristics including, the pattern of vacuolar pathology and PrP^{Sc} deposition.

- 4) To test the hypothesis that the glycosylation of PrP alters its ability to adopt a misfolded form.

2.0 Materials and Methods

All Chemicals are from BDH unless otherwise stated. All experiments were carried out at room temperature unless otherwise stated.

2.1 Murine genomic DNA extraction

2.1.1 Taking of tail snips

Tail snips were taken from live animals under 3 % fluothane (delivered in oxygen) anaesthesia and from culled animals post-mortem. For each live animal the tip of the tail ~0.5 cm long was removed using a flamed scalpel which cauterised the wound. Culled animals also had a larger piece of tail (~3 cm) removed in addition to the small snip; all tail snips were stored at -20 °C for DNA extraction.

2.1.2 Uninfected mice (Qiagen DNeasy Tissue Kit) (All tails from uninfected mice prior to 17th November 2004 and all tails from *prnp*$^{-/-}$ (PrP null) mice)

DNA was extracted from tail snips (0.5 cm) using DNeasy Tissue Kit (all reagents Qiagen, Sussex, UK), as per manufacturer's protocol. Briefly, tissue was lysed in Buffer ATL plus proteinase K (2 mg/ml) for 6-18 hours, with shaking at 55 °C. Double volume of Buffer AL-ethanol (1:1) was added to lysed tissue. The resultant solution was transferred to a DNeasy spin column, the membrane of which selectively binds DNA, and centrifuged at 8000 rpm for 1 minute. Bound DNA was washed two times with Buffer AW1 and AW2, before eluting with 200 µl of Buffer AE. DNA was stored at 4 °C.

2.1.3 Uninfected mice (Jackson Laboratory Direct PCR after lysis method) (All tails from uninfected mice after 17th November 2004 except those to be genotyped for the *prnp* null allele)

DNA was extracted from tail snip fragments (2 mm) by proteinase K (10 mg/ml) digestion for 14-18 hours at 55 °C in polymerase chain reaction (PCR) buffer with non-ionic detergent (50 mM potassium chloride, 10 mM tris-HCl [pH 8.3], 2.5 mM

magnesium chloride, 0.1 mg/ml gelatine, 0.45 % Nonidet P40, 0.45 % Tween 20). Proteinase K was inactivated by heating to 95 °C for 15 minutes. PCR was carried out directly on the resultant solution without further purification, which was stored at 4 °C.

2.1.4 TSE inoculated mice (phenol/chloroform extraction)

Tail snips (0.5 cm) were lysed by shaking over night at 37 °C or for 2-3 hours at 64 °C, in tail lysis solution [15 mM sodium acetate, 1% SDS, 1 mM tris (pH 8), 1 mM EDTA] and PK (200 µg/ml, Qiagen, Sussex, UK). The resultant lysate was thoroughly mixed with phenol (Qbiogene)/chloroform [1 part AquaPhenol (pH 8): 1 part chloroform] before separation of the aqueous phase by centrifugation at 13,000 rpm for 5 minutes at room temperature. DNA was isolated from the aqueous phase by incubation for 10 minutes with sodium acetate (final concentration 50 mM) and an equal volume of isopropanol, followed by separation of the precipitated DNA by centrifugation at 13,000 rpm for 2 minutes. Prior to resuspension in buffer AE (DNeasy Tissue Kit, Qiagen, Sussex, UK) DNA pellet was washed in 70% ethanol (v/v in dH_2O). DNA was then stored at 4 °C.

2.1.5 Quantification of DNA

The concentration of murine genomic DNA solution isolated by phenol/chloroform extraction was assayed by determining optical density at 260 nm (DNA absorption) using a Beckman spectrophotometer and the Beer-Lambert equation [1] to standardise concentration for PCR. If required, DNA stock solution was then diluted in autoclaved ultrapure water prior to PCR analysis. To check for contamination of DNA stock the ratio of 260 nm to 280 nm (protein and single stranded nucleic acid absorption) was also calculated. If a ratio of lower than 1.8 was observed a new DNA sample was extracted prior to PCR.

$$\text{Optical Density} = ebc \qquad [1]$$

Where e = extinction coefficient (~20 g/cm/L), b = spectrophotometer path length (1 cm), c = concentration of DNA

2.2 Genotyping for *Prnp* transgenes by PCR

2.2.1 Detection of the G1, G2, G3 mutant and wild type *prnp* alleles

Presence of the G1 mutant allele was determined by mismatch PCR, using a primer specific for the G1-mutation (G1-mutant) and standard reaction mix (1X magnesium chloride free PCR buffer [200 mM Tris-HCl (pH 8.4), 500 mM KCl; Invitrogen Life Technologies, Paisley, UK]; 1.5 mM Magnesium chloride [Invitrogen Life Technologies, Paisley, UK]; 200 µM deoxynucleotide 5′-phosphate (dNTP) mix [equal parts deoxyadenosine, deoxyguanosine, deoxythymidine and deoxycytidine; Promega, Southampton, UK]; 30 units/ml Taq DNA polymerase [Invitrogen Life Technologies, Paisley, UK]; 1 µl of a three primer mix [9910 (48.8 pmol/µl), G1-mutant (48.8 pmol/µl), 9912 (2.4 pmol/µl)] (Table 2.1) to which 1-2 µl of DNA solution was added, dependent on DNA stock concentration. The final volume of 50 µl was achieved by addition of the appropriate volume of distilled water that had also been autoclaved.

Cycle conditions were 94 °C for 3 minutes, followed by 30 cycles, of 50 seconds at 94 °C, 30 seconds at 60 °C and 1 minute at 72 °C. This was followed by a final 10 minutes at 72 °C (Biometra Triblock). The reaction was then stored at 4 °C, prior to size separation of DNA product by gel electrophoresis (1% Agarose). In the presence of the G1-mutant allele a 268 base pair fragment is amplified (G1-mutant and 5′), in addition to the control 585 base pair fragment (5′ and 3′) which is produced in the presence of both wild type and G1-mutant *Prnp*.

Similarly, presence of the G1- wild type, G2- mutant and G2- wild type allele was determined using the same PCR reaction conditions and mix, save the primer combination. For detection of the G1 wild type allele 5′ (48.8 pmol/µl), G1-wild type (48.8 pmol/µl) and 3′ (2.4 pmol/µl) primers were used (Table 2.1). In the presence of the wild type allele a 268 base pair product was amplified in addition to the control 585 base pair fragment (5′ and 3′). For detection of the G2 mutant allele

5′ (48.8 pmol/µl), G2-mutant (48.8 pmol/µl) and 3′ (2.4 pmol/µl) primers were used. In the presence of DNA containing the G2 mutant *Prnp* allele a 320 base pair fragment in addition to the control 585 base pair fragment (5′ and 3′) was observed. For detection of the G2 wild type allele 5′ (48.8 pmol/µl), G2-wild type (48.8 pmol/µl) and 3′ (2.4 pmol/µl) primers were used (Table 2.1). In the presence of DNA containing the G2 wild type allele a 320 base pair fragment in addition to the control 585 base pair fragment (5′ and 3′) was observed. G3 mice were genotyped for presence of the G1-mutant, G2-mutant, G1-wild type and G2-wild type alleles.

2.2.2 Detection of the 3′ *lox-P* site of the *Prnp* allele present in all the Cre-loxP generated transgenic mice used including the control line (CL)

Presence of the 3′ *lox-P* site was determined by PCR using a standard reaction mix (1X magnesium chloride free PCR buffer [200 mM Tris-HCl (pH 8.4), 500 mM KCl; Invitrogen Life Technologies, Paisley, UK]; 1.5 mM magnesium chloride [Invitrogen Life Technologies, Paisley, UK]; 80 µM deoxynucleotide 5′-phosphate (dNTP) mix [equal parts deoxyadenosine, deoxyguanosine, deoxythymidine and deoxycytidine; Promega]; 20 units/ml Taq DNA polymerase [Invitrogen Life Technologies, Paisley, UK]; 1 µl of a two primer mix [CreA (100 pmol/µl) and CreB (100 pmol/µl) (Table 2.1)] to which 1-2 µl of DNA solution was added, dependent on DNA stock concentration. The final volume of 50 µl was achieved by addition of the appropriate volume of distilled water that had also been autoclaved.

Cycle conditions were 94 °C for 3 minutes, followed by 30 cycles of 45 seconds at 94 °C, 45 seconds at 60 °C and 45 seconds at 72 °C. This was followed by a final 10 minutes at 72 °C (Biometra Triblock). The reaction was then stored at 4 °C, prior to size separation of DNA product by gel electrophoresis (2 % Agarose). In the presence of the 3′ *lox-P* site a 342 base pair fragment is amplified, in the absence of the site a 322 base pair fragment is observed.

2.2.3 Screening of the NPU *Prnp*$^{-/-}$ mice

The NPU *Prnp*$^{-/-}$ mice have a neomycin resistance gene (*neo*), inserted into exon 3 of *Prnp*. To detect this insert, primers specific to a region in the *neo* cassette were used. A standard PCR reaction mix was used (1X magnesium chloride free PCR buffer [200 mM Tris-HCl (pH 8.4), 500 mM KCl; Invitrogen Life Technologies, Paisley, UK]; 1.5 mM magnesium chloride [Invitrogen Life Technologies, Paisley, UK]; 200 µM deoxynucleotide 5′-phosphate (dNTP) mix [equal parts deoxyadenosine, deoxyguanosine, deoxythymidine and deoxycytidine; Promega]; 12 units/ml Taq DNA polymerase [Invitrogen Life Technologies, Paisley, UK]) in addition to 1 µl of a two primer mix (Null A (100 pmol/µl) and Null B (100 pmol/µl) Table 2.1) and 1-2 µl of DNA solution.

Cycle conditions were 94 °C for 3 minutes, followed by 30 cycles of 50 s at 94 °C, 50 seconds at 57 °C and 50 seconds at 72 °C. This was followed by a final 10 minutes at 72 °C (Biometra Triblock). The reaction was then stored at 4 °C, prior to size separation of DNA product by gel electrophoresis (1% Agarose gels). In the presence of the NPU *Prnp*$^{-/-}$ template a 1200 base pair fragment is amplified.

2.1 Table of primers used for PCR (All supplied by MWG Biotech)

Primer	Sequence (5′ to 3′)	T_m (°C)
G1-wildtype	GCTGCTTGATGGTGATAT	51.4
G1-mutation	GCTGCTTGATGGTGATAG	53.7
G2-wildtype	CATCGGTCTCGGTGAAGT	56
G2-mutation	CATCGGTCTCGGTGAAGG	58.2
9910	AACCTCAAGCATGTGGCAGGGGCTGCGGCAGCTGG	>75
9912	TCAGTGCCAGGGGTATTAGCCTATGGGGGACACAG	74.2
CreA	AGACAGGTCTGACCACACTGGTT	66
CreB	AATGGTTAAACTTCGTTAAGGAT	58.5
NullA	GCCATCACGAGATTTCGATT	63.8
NullB	ATCCCACGATCAGGAAGATG	63.8

2.2.4 Gel electrophoresis of PCR products

Glycerol loading buffer (5 µl; 30 % glycerol, 0.25 % bromophenol blue, 0.25 % xylene cyanol FF) was added to the total PCR reaction. This was then run on a 1 or 2 % agarose (Roche Diagnostics, Basel, Switzerland) gel [1X TBE (89 mM Tris, 89

mM Orthoboric acid, 2 mM EDTA (pH 8 with NaOH)]; 1 mM ethidium bromide, Sigma-Aldrich Company Ltd, Dorset, UK], dependent upon PCR reaction product size, at 100 V for approximately 2 hours in 1X TBE. A 1 Kb ladder (12216 - 75 base pair fragments; Invitrogen Life Technologies, Paisley, UK) was used as a standard. DNA bands were visualised under UV and photographed (The Imager; Appligene).

2.3 Preparation of total protein from murine brain

2.3.1 Tissue sources used for biochemical analysis of PrP

Uninfected wild type 129/Ola, PrP null (*Prnp*$^{-/-}$), CL (control line), G1 (homozygous for N180T), G2 (homozygous for N196T) and G3 (homozygous for N180T and N196T) all on a 129/Ola genetic background, sourced from breeding stock maintained at NPU, Edinburgh.

PrP^{Sc} positive control; ME7 mouse (129/Ola) passaged scrapie; experiment (NPU experiment number 522D-2P/animal number 26) kind gift of Dr. Rona Barron NPU, Edinburgh.

Experimentally infected animals, that were challenged with hamster scrapie 263K (experiment 568C-1A), variant CJD (experiment 567G-1A), sporadic CJD MM type 2A (experiment 567H-1A).

2.3.2 Preparation of post-nuclear brain tissue homogenate for biochemical analysis

After sacrifice, brain was removed (in some cases saggitally divided in half), flash frozen in liquid nitrogen and then stored at -70 °C until required. Half or whole brains were weighed and mechanically homogenised from frozen in nine volumes of ice cold NP40 lysis buffer [1% Nonidet 40, 0.5% sodium deoxycholate, 150 mM sodium chloride, 50 mM Tris (pH 7.5 with HCl)] with the addition of phenylmethylsulfonyl fluoride (PMSF) [final concentration 1 mM; Sigma-Aldrich Company Ltd, Dorset, UK] to prevent protein degradation by endogenous proteases. PMSF was not added if the homogenate was intended for Proteinase K treatment. The homogenate was centrifuged at 8000 rpm for 10 minutes to remove

unhomogenised debris. The resultant protein containing supernatant was aliquoted and flash frozen in liquid nitrogen for storage at -70 °C.

2.3.3 Preparation of brain tissue homogenate in physiological saline (inoculum) for biochemical analysis

An equal volume of 2 X NP40 lysis Buffer (2% Nonidet 40, 1% sodium deoxycholate, 150 mM sodium chloride, 100 mM Tris (pH 7.5 with HCl)) was added to 10 % brain homogenates in physiological saline and mixed by vortexing prior to biochemical analysis.

2.3.4 Serial dilution of brain homogenate

Homogenate was diluted in an equal volume of NP-40 lysis buffer and mixed by vortexing.

2.3.5 PNGase F treatment of brain homogenate

Total brain protein (10 % brain homogenate; NP-40 lysis buffer, 10 mM PMSF) was diluted 2-fold in NP-40 lysis buffer prior to denaturation in 1 X Glycoprotein Denaturing Buffer [0.5 % sodium dodecyl sulphate (SDS), 1 % β-mercaptoethanol; New England Biolabs, Ipswich, MA, USA] at 100 °C for 10 minutes prior to incubation with Peptide: N-Glycosidase F (PNGase F) (30,000 units/ml; New England Biolabs, Ipswich, MA, USA) in 1 % Nonidet 40 (New England Biolabs, Ipswich, MA, USA) and 1 X G7 Reaction Buffer [50 mM $NaPO_4$ (pH 7.5); New England Biolabs, Ipswich, MA, USA] at 37 °C for 2-4 hours with shaking. The reaction was stopped by freezing at -20 °C or by SDS denaturation.

2.3.6 Proteinase K digestion of brain homogenate

Brain homogenate (5 % or 10 % in NP-40 lysis buffer) was incubated with Proteinase K (PK) (20, 10, 5 or 1 μg/ml, 100mM Tris-HCl, 1mM Ca Cl_2, pH 7; Roche Diagnostics, Basel, Switzerland) (PK) at 37 °C for one hour. Reaction was stopped by the addition of the PMSF (final concentration 10 mM) and by freezing at -20 °C or by SDS denaturation.

2.3.7 Sodium phosphotungstic acid (NaPTA) concentration of PrP^{Sc}

Total brain protein (10 % or 5 % brain homogenate in NP-40 lysis buffer) was mixed with an equal volume of 4 % sarkosyl /phosphate buffered saline (Oxoid, Basingstoke, UK) (PBS) by shaking at 37 °C for 5 minutes. The homogenate was then incubated with PK (20 μg/ml, 100mM tris-HCl, 1mM Ca Cl_2, pH 7 Roche Diagnostics, Basel, Switzerland) for 1 hour at 37 °C with shaking. The reaction was stopped by the addition of PMSF (final concentration 10 mM). NaPTA stock solution was added (4 % NaPTA; 10 mM magnesium chloride; pH 7.4) (final concentration 0.3 % NaPTA). The reaction was briefly vortexed and incubated at 37 °C for 20 minutes with shaking. The precipitated PrP^{Sc} was then collected by centrifugation at 13,000 rpm for 20 minutes at room temperature. The resultant supernatant was removed and retained at – 70 °C and the pellet washed with 0.1% sarkosyl/PBS. The pellet was then re-isolated by centrifugation at 13,000 rpm for 20 minutes, the wash solution discarded and the pellet stored at – 70 °C or directly resuspended in 1 X Novex Tris-Glycine SDS Sample Buffer (Invitrogen Life Technologies, Paisley, UK) and 1 X NuPage Sample Reducing Agent (Invitrogen Life Technologies, Paisley, UK) by denaturation at 95 °C.

2.4 Characterisation of glycosylation deficient transgenic mice and analysis of cross species transmission studies by western blotting

2.4.1 Protein denaturation and separation by Sodium Dodecyl Sulphate Polyacrylamide gel electrophoresis (SDS-PAGE)

Total brain protein was denatured in 1 X Novex Tris-Glycine SDS Sample Buffer (Invitrogen Life Technologies, Paisley, UK) and 1 X NuPage Sample Reducing Agent (Invitrogen Life Technologies, Paisley, UK) for 30 minutes at 95 °C. Proteins were size/charge separated by gel electrophoresis at 125V using Novex Pre-cast Tris-Glycine gel (12 or 14 % acrylamide, tris-glycine; Invitrogen Life Technologies, Paisley, UK) which were run for between 1 hour 40 minutes and 2 hours 15 minutes in 1 X Running Buffer [24 mM tris, 0.19 M glycine, 0.1 % SDS]. SeeBlue Pre-Stained standard (Invitrogen Life Technologies, Paisley, UK) was used to estimate the molecular weight of the separated proteins (250 kDa myosin, 98 kDa

bovine serum albumin, 64 kDa glutamic dehydrogenase, 50 kDa alcohol dehydrogenase, 36 kDa carbonic anhydrase, 30 kDa myoglobin, 16 kDa lysozyme, 6 kDa aprotinin, 4 kDa insulin, B chain).

2.4.2 Western blotting semi-dry transfer of separated protein to a membrane

Proteins in the acrylamide gel were transferred to polyvinylidene fluoride (PVDF) membrane (Hybond-P, Amersham Biosciences, Buckinghamshire, UK) at a current of 125 A/gel (25 V) using a semi-dry transfer blotter (BioRad Laboratories, Hemel Hempstead, UK) in 1 X Transfer Solution (48 mM tris, 39 mM glycine, 0.375 % SDS, 20 % methanol); a maximum of 2 gels per blotter were simultaneously transferred.

2.4.3 Identification of membrane bound PrP and Tubulin by immunodetection

The amount of protein bound to the PVDF membrane was checked by staining with Ponceau S solution (0.1 % Ponceau S, 5 % acetic acid; Sigma-Aldrich Company Ltd, Dorset, UK) for 5 minutes in order to confirm that transfer was successful. After destaining with TBS/Tween [50 mM tris, 150 mM sodium chloride, (pH to 7.5 with HCl), 1 % Tween 20] (TBST) the membrane was blocked with 1 X Western Blocking reagent (10 X, supplied by Roche Diagnostics, Basel Switzerland) diluted in TBS [50 mM Tris, 1.5 M sodium chloride, (pH to 7.5 with HCl)] for 1 hour at room temperature. To allow use of the anti-tubulin control the PVDF membrane was cut between 50 and 36 kDa markers (for non-proteinase K treated samples) and the two parts processed separately. The upper portion (~45-250 kDa) was incubated with anti-tubulin rat antibody ab6160 (1/4000; Abcam, Cambridge) which was used as a control for protein loading, in 0.5 X Western Blocking Reagent (10 X, supplied by Roche Diagnostics, Basel, Switzerland), diluted in TBS, rocking overnight at room temperature. The lower portion of the membrane (~45-4 kDa) was incubated with the anti-PrP mouse monoclonal antibodies 7A12, 8H4 (1/20,000; kind gift of M.S. Sy, Cleveland) or 6H4 (1/20,000, Prionics, Schlieren Switzerland) in 0.5 X Western Blocking Reagent (10X supplied by Roche Diagnostics, Basel, Switzerland) TBS, rocking overnight at room temperature (Table 2.2). The membrane was washed with TBS/Tween to remove

excess primary antibody and blocked for 20 minutes with 0.5 X Western Blocking Reagent (supplied by Roche Diagnostics, Basel, Switzerland)/TBS. Membranes treated with anti-tubulin were then incubated with peroxidase-conjugated AffiniPure rabbit anti-rat antibody (1/10,000; Jackson ImmunoResearch, West Grove, PA, USA) in 0.5 X Western Blocking Reagent (10X supplied by Roche Diagnostics, Basel, Switzerland) TBS, for 30 minutes, rocking at room temperature. Membranes treated with anti-PrP antibodies were then incubated with peroxidase-conjugated AffiniPure rabbit anti-mouse antibody (1/10,000; Jackson ImmunoResearch West Grove, PA, USA) in 0.5 X Western Blocking Reagent (10X, supplied by Roche Diagnostics, Basel) TBS, for 30 minutes, rocking at room temperature. Membranes were washed 4 times for 15 minutes in TBST to remove excess secondary antibody. Bound secondary antibody was detected on film (Lumi-Film; Roche Diagnostics, Basel, Switzerland) by light emission from the BM Chemiluminescece Blotting Substrate POD (Roche Diagnostics, Basel, Switzerland). Typically 30 second, 3 minute and 10 minute exposures were taken. Film was developed manually using developer and fixative (AGFA, Mortsel, Belgium).

2.2 Table of antibodies used in western blotting

Antibody	Antigen	Type	Epitope	Source
8H4	PrP	Mouse monoclonal (IgG1)	a.a 175-185 of helix B	Gift of M.S. Sy, Case Western Reserve University, Cleveland, USA (Zanusso et al., 1998)
7A12	PrP	Mouse monoclonal	a.a 143-155 of helix B	Gift of M.S. Sy, Case Western Reserve University, Cleveland, USA (Kang et al., 2003)
ab6160	α tubulin	Rat monoclonal	C-terminal Gly-Gly-Tyr	Abcam, Cambridge, UK (Kilmartin et al., 1982)
6H4	PrP	Mouse monoclonal (IgG1)	a.a. 143-151 of helix B DYEDRYYRE	Prionics, Schlieren, Switzerland (Korth et al., 1997)
3F4	PrP	Mouse monoclonal (IgG2a)	a.a. 109-112 human and hamster only	Signet Laboratories, Inc, Dedham, USA (Kascsak et al., 1987)
6D11	PrP	Mouse monoclonal (IgG2a)	a.a. 93-109	Signet Laboratories, Inc, Dedham, USA (Pankiewicz et al., 2006)

2.5 Analysis of the amount of PrP in murine brain homogenate by Dissociation Enhanced Lanthanide Fluoroimmunoassay (DELFIA®)

2.5.1 Preparation of brain homogenate for DELFIA

PrP^C was extracted from total protein brain homogenate (100 mg/ml ; NP-40 lysis buffer; 1 mM PMSF) by mechanical homogenisation in 1M guandine hydrocholoride (Gnd HCl) solution (25 mM tris; 1M Gnd HCl, Sigma-Aldrich Company Ltd, Dorset, UK; 0.5 % Triton X-100, Sigma-Aldrich Company Ltd, Dorset, UK). This was then diluted in DELFIA Assay Buffer (supplied by Perkin Elmer Life Sciences), leading to final concentration equivalent to 10 mg/ml of original tissue. Proteins insoluble in 1 M Gnd HCl (PrP^{Sc}) were separated from those that were soluble (PrP^c) by centrifugation 13000 rpm for 10 minutes. The resultant pellet was resuspended in 6 M Gnd HCl prior to dilution in DELFIA Assay Buffer to a concentration equivalent to 10 mg/ml original tissue.

2.5.2 Preparation of recombinant PrP standard for DELFIA

Murine recombinant PrP (kind gift from Dr. Ian Sylvester, IAH Compton) was serially diluted 2-fold in DEFLIA Assay Buffer (25 – 0.781 ng/ml) for use as a standard.

2.5.3 DELFIA time-resolved fluorescence immunoassay

The method is an adaptation of that of Barnard and colleagues (Barnard et al., 2000). Capture antibody (1/200; FH11 and AG4; TSE Resource Centre, IAH Compton) was bound to 96 well plates by overnight incubation, at 4 °C. Plates were then blocked with 2 % bovine serum albumin (BSA) (Roche Diagnostics, Basel, Switzerland) in sterile 1 X PBS (Oxoid, Basingstoke, UK) with 3 M NaN_3 for 1 hour with shaking at room temperature. The blocking solution was discarded and the plate was then incubated with samples and standards, shaking at room temperature for one hour. Samples and standards were then discarded and the plate was then incubated with europhium (Eu^{3+}) labelled detector antibody (7A12 or

8H4, 1/3000, kindly labelled by Mr. Declan King, NPU, Edinburgh), with shaking at room temperature for one hour. The plate was then incubated with DELFIA Enhancement Solution, to facilitate the formation of Eu-(2-NTA)$_3$(TOPO)$_{2-3}$. After shaking for 5 minutes at room temperature Eu emission was read (615 nm), using a time-resolved technique. Between each step, plate was washed in 1 X DELFIA Wash Concentrate (supplied by; PerkinElmer Life Sciences) using the DELFIA automatic plate washer (Wallac). The programme WorkOut was used to analyse absorbance from standard and samples and to produce the standard curve (based on a linear model of emission).

2.6 Localisation of PrP^C in murine brain by confocal microscopy

This work was carried out at Institute of Animal Health Bioimaging Facility, at Pirbright, UK, under the guidance of Dr. Paul Monaghan.

2.6.1 Fixation and sectioning of brain tissue

Post-mortem tissues were fixed, by immersion, in a range of fixatives (4 % paraformaldehyde/PBS or 4 % paraformaldehyde/0.25 % gluteraldehyde/PBS or 4 % paraformaldehyde/0.025 % gluteraldehyde/PBS or periodate-lysine-paraformaldehyde (PLP) for 3-5 hours. Fixed tissues were then stored at 4 °C in sterile PBS (Sigma-Aldrich Company Ltd, Dorset, UK) for transport before the cutting of 70 µm coronal sections using a vibrating microtome (Leica Microsytems, Milton Keynes, UK).

2.6.2 Immunofluorescence on free-floating thick brain sections

Tissue sections were permeabilised for 1 hour at room temperature with 0.1 % Triton-X100 in phosophate buffered saline (PBS) (0.01 M phosphate buffer, 0.0027 M potassium chloride and 0.137 M sodium chloride, pH 7.4; Sigma-Aldrich Company Ltd, Dorset, UK). The sections were then blocked at room temperature overnight in a humid chamber in 0.5 % bovine serum albumin (BSA) (Sigma-Aldrich Company Ltd, Dorset, UK), 1X PBS. To eliminate non-specific cross-reactivity of the anti-PrP mouse monoclonal antibody sections were then blocked for a further hour with mouse on mouse (MOM) Ig blocking reagent (Vector

Laboratories, California, UK). To remove this reagent sections were washed for 10 minutes in PBS/ protein concentrate (Vector Laboratories, California, UK), before incubated with primary antibody in protein concentrate/PBS at either room temperature or 37 °C for 90 minutes. Sections were then washed in 1 X PBS 10 times, each for 2 minutes; before incubating with the appropriate Alexa conjugated goat secondary antibody (1/200; Molecular Probes, Cambridge, UK) in 0.5% protein concentrate/1X PBS for 90 minutes at room temperature or 37 °C. Unbound secondary antibody was removed by washing with 1X PBS for 2 minutes, 10 times. Sections were then stained for DNA using 4',6-diamidino-2-phenylindole (DAPI) (1 μg/ml; Molecular Probes, Cambridge, UK) dissolved in ultra pure water (Sigma-Aldrich Company Ltd, Dorset, UK, Dorset, UK) for 30 minutes. Sections were then washed 5 times in ultra pure water, each for 1 minute, before mounting in Vectashield (Vector Laboratories, Burlingame, CA, USA) and sealing with nail varnish.

2.6.3 Immunofluorescence on free-floating thick brain sections to colocalise PrP and intracellular markers

Colocalisation experiments were carried out using the same basic method as 2.6.2 with some modifications. For ERp60/8H4 the primary antibodies were mixed in 1 X PBS/protein concentrate so that the tissue was incubated with them simultaneously. Similarly the secondary antibodies Alexa^{488} conjugated goat anti-mouse antibodies and Alexa^{568} conjugated goat anti-rabbit antibodies were simultaneously incubated. Controls for cross reactivity were used and none was detected. For PDI/8H4 cross reactivity was detected; to eliminate it a sequential staining method was used. For the two-step staining technique, sections were first incubated with 8H4, washed in 1 X PBS then incubated with Alexa^{488} conjugated goat anti-mouse using a method identical to that for single 8H4 labelling. Sections were then washed 10 times in 1X PBS before being blocked for one hour in MOM Ig blocking reagent. Block was removed by washing for 10 minutes in 1 X PBS/protein concentrate before incubation of the section with anti-PDI in PBS/ protein concentrate. The sections were then washed and incubated with Alexa^{568} conjugated goat anti-mouse (PDI) as above. The sections were washed, stained with DAPI and mounted for analysis.

Cross reactivity between 23C and Alexa^{488} conjugated goat anti-mouse was also detected. To eliminate this either the sequential staining technique (8H4, Alexa^{488} conjugated goat anti-mouse; 23C, Alexa^{568} conjugated goat anti-rat) or an isotype specific secondary (Alexa^{488} conjugated goat anti-mouse IgG1) was used.

2.3 Table of antibodies used in immunofluorescence

Antibody	Type	Antigen/ Epitope	Source
8H4	Mouse monoclonal (IgG1)	PrP a.a. 175-185 of helix B	Gift of Dr. Sy, Case Western Reserve University, Ohio (Zanusso et al., 1998)
Anti-PDI Clone 1D2	Mouse monoclonal (IgG1)	PDI raised against rat PDI synthetic peptide (a.a. 497-508, CT), conjugated to KLH	Stressgen Bioreagents, Victoria, Canada. (Huovila et al., 1992)
Anti-ERp60	Rabbit polyclonal	Raised against porcine ERp60 C-terminal peptide PIIQEEKPKKKKKA QEDL	Gift of Dr. T. Wileman, IAH Pirbright. (Rouiller I *et al* 1998)
23C	Rat monoclonal (IgG2c)	Golgi coatomer p102B' COP subunit	Gift of Dr. P. Monaghan IAH Pirbright. (Willison K *et al*, 1989)
Anti-α tubulin (DM1A)	Mouse monoclonal (IgG1)	α-tubulin a.a. 426-430	Sigma-Aldrich, Saint Louis, Missouri (Blose et al., 1984)
Anti-GM130 (2C10/1)	Mouse monoclonal	Raised against full length recombinant Rat GM130	Abcam, Cambridge, UK (Nakamura et al., 1995)
Anti-ßcop	Rabbit polyclonal	Golgi coatomer raised against ßcop	Gift of Dr. T. Wileman, IAH Pirbright.

2.6.4 Confocal imaging

Sections were imaged with a Leica TCS SP2 laser scanning confocal microscope using argon 405, 488 and 568 lasers to excite the Alexa-flourophores. Sequential imaging of each channel was undertaken if bleed through of DAPI emission into the 488 channel was observed. All images were analysed using Leica confocal software and prepared for presentation at 300 dpi, RGB in Adobe Photoshop.

2.7 Cross species transmission of TSEs

All experiments were approved by the Neuropathogenesis Unit's Local Ethical Review Committee. All inoculations were kindly performed by Mrs Val Thomson, in accordance with Health and Safety recommendations in Category 2 (263K) or 3 (variant and sporadic CJD) facilities under sterile conditions.

2.7.1 Tissue sources used in cross species transmissions

Hamster passaged scrapie strain 263K: NPU experiment 263K-5L (clinical end point female Syrian hamster whole brain).

Variant CJD, 129MM (NHBY0/0003 10% homogenate in 0.25M sucrose; National Institute for Biological Standards and Controls; corresponding to CJD surveillance unit sample number RU 98/148).

Sporadic CJD 129MM type (CJD surveillance unit, tissue sample number RU 98/73).

2.4 Summary table of TSE transmissions to the glycosylation deficient transgenics

Source	Concentration	Genotypes Injected	Protocol
263K (263K-5L1/3)	10 %	G1, G2, G3, CL	568C-1A
vCJD (RU 98/148)	1 %	*G2, G3, CL	567G-1A
Sporadic CJD (RU 98/73)	1 %	*G2, G3, CL	567H-1A

*Breeding problems with the G1 transgenic line from November 2002 such that insufficient experimental G1 mice were available for protocols 567G-1A and 567H-1A until March 2006, when these mice were inoculated.

2.7.2 Preparation of TSE infected inoculum

Brain tissue (263K and sporadic CJD MM) was weighed and mechanically homogenised using a pestle with nine volumes of sterile physiological saline solution (Martindale Pharmaceuticals, UK) to prepare a 10 % unspun homogenate.

The NIBSC variant CJD sample was supplied as a 10% homogenate. Previous inoculations at NPU of 10 % NIBSC vCJD homogenate had led to unacceptable toxicity to mice (NPU protocol; toxicity testing at 10^{-1}; experiment number 553A-1A). Thus both this and the comparative sporadic CJD isolate were diluted a further 10 fold with sterile physiological saline solution (Martindale Pharmaceuticals, UK) for inoculations. After preliminary homogenisation and dilution all the inoculum was passed through a 26 gauge needle to ensure it could be injected safely. Excess inoculum was frozen at -70 °C.

2.7.3 Intra-cerebral inoculation of mice

Mice were anaesthetised with 3 % fluothane gas (delivered in oxygen) before injection of 20 µl of the inoculum in the right hemisphere of the brain using a 26 gauge needle. A needle sheath, exposing 2 mm of the needle, was used so that inoculum was consistently injected into the mid-temporal cortex. Animals were then monitored and any not recovering as normal from the procedure were culled (Home Office Schedule 1) and excluded from experimental analysis.

2.7.4 TSE clinical assessment

After inoculation animals were numerically coded to blind for genotype, such that all clinical assessments were carried out with no reference to transgenic genotype. Animals were monitored daily, and formally assessed for clinical TSE disease weekly, as previously defined by Dickinson, from 100 days after inoculation, by experienced animal technicians (Miss Emma Murdoch and Miss Sally Shillinglaw) (Dickinson et al., 1968). Clinical signs were reviewed by Mrs Val Thomson, Mrs Irene McConnell (senior animal facility staff) as required and frequently monitored by F. Wiseman. Animals were scored as TSE "unaffected", "possibly affected" or "definitely affected" using standard criteria (pronounced spinal hunching, ataxia or paralysis and "freezing" behaviour or hyperactivity). "Unaffected animals" exhibited no signs of clinical TSE disease. Animals that displayed signs of disease but also exhibited an aging phenotype (kyphosis, reduced activity, weight loss and loss of condition) were classified as "possibly affected" which can be misdiagnosed as a TSE clinical state. Animals with standard clinical signs but no aging phenotype

were classified as "definitely affected" In some cases clinically affected animals also displayed weight loss and urinary incontinence. Disease endpoint was defined as occurring 1) after two consecutive "definitely affected" score were observed on the formal scoring day, 2) after the third "definitely affected" score (on the weekly formal scoring day) within a four week period 3) if the animal was culled on welfare grounds linked to a "definitely affected" score or 4) if the animal was found dead after receiving a "definitely affected" score in the previous week. Other causes of death are defined as inter-current deaths (either found dead or culled on welfare grounds) and are allocated a clinical negative score.

Table 2.5 Clinical scoring criteria

TSE Clinical Status	Clinical Criteria
Unaffected	no signs of neurological disease
Probably Affected	pronounced spinal hunching, ataxia or paralysis and "freezing" behaviour or hyperactivity (TSE signs) AND kyphosis (curvature of upper spine), weight loss, loss of condition, reduced activity (ageing phenotype)
Definitely Affected	pronounced spinal hunching, ataxia or paralysis and "freezing" behaviour or hyperactivity (TSE signs)

All animals were culled in accordance with the Animals (Scientific Procedures) Act 1986 (Home Office Schedule 1-cervical dislocation). After cull, brains of both inter-current deaths and TSE disease endpoint animals were removed under aseptic conditions and divided asymmetrically saggitally. The brain was then assigned a unique number such that all subsequent experiments could be carried out blind to transgenic genotype and TSE strain. However, for reasons of health and safety all brain material is also labelled with a letter code (B for biohazard category 2 and C for biohazard category 3). The larger half of the brain was then fixed in 10 % formal saline for 48 hours. Biohazard category 3 material was then treated with

formic acid, for 90 minutes, to reduce TSE infective titre further as a biosafety measure. The tissue was then incubated for a further 2 hours in 10 % formal saline before being cut into five defined areas for embedding (Figure 2.1). The smaller half of the brain was flash frozen in liquid nitrogen for storage at -70 °C. Two pieces of tail were also removed post-mortem from which DNA was extracted by the phenol/chloroform method to confirm the animals genotype.

2.7.5 Embedding and sectioning of murine brain for lesion profiling and immuno-histo-chemistry

After fixation and trimming brain tissue was taken through an industrial methylated spirits (IMS) (70-99 %) and xylene gradient before embedding in paraffin wax using an automated Leica Tissue Processor (TP1050). Excess wax was removed from embedded tissue using a Histogical Microtome. The cutting surface was then rehydrated and softened, after trimming, up placing trimmed side down on wet ice for 2-3 hours. Sections (6 μm thick) were then cut. To assist mounting sections were briefly floated in a waterbath (40 °C), to flatten and soften the wax before attaching them to Superfrost or Superfrost^{+} (for PrP^{d} detection) ground slides (VWR International). Mounted sections were allowed to dry overnight at 37 °C. Category 3 material was kindly trimmed and sectioned by trained and experienced histological staff (Mrs Sandra Coupar and Mrs Gillian MacGregor) in accordance with NPU Health and Safety Policy.

2.7.6 Lesion profiling of TSE vacuolar pathology in murine brain

Sections of paraffin wax embedded brain tissue (6 μm thick) were stained with haematoxylin and eosin using a Leica XL automatic staining machine. Briefly, mounted sections were taken down a xylene and IMS (99-95%) gradient, washed and stained with haematoxylin (3 minutes) followed by 2 minutes in Scott's Tap Water Substitute (sodium hydrogen carbonate 42 mM; magnesium sulphate 160 mM in tap water). After washing sections were counter stained with eosin, washed, and taken up an IMS (70-99 %) and xylene gradient before mounting in Pertex. Vacuolation density in nine grey matter regions were scored on a scale of 0-5 and three white matter regions on a scale of 1-3 by trained and experience histology

staff (Miss Wingee Liu and Mrs Aileen Boyle) blinded to animal genotype or TSE agent and reviewed by F. Wiseman (Figure 2.1, 2.2) (Fraser and Dickinson, 1967; Fraser and Dickinson, 1968).

2.7.6.1 TSE vacuolation scoring scale

Grey matter 0; indicating an absence of vacuolation,

Grey matter 1; limited vacuolation may be caused by ageing,

Grey matter 2 /white matter 1; definite but uneven vacuolation,

Grey matter 3 /white matter 2; even vacuolation of entire brain area,

Grey matter 4 /white matter 3; heavier vacuolation defined but some merging of small vacuoles to form larger holes,

Grey matter 5; severe vacuolation many vacuoles merged.

2.7.6.2 TSE vacuolation scoring areas

Nine grey matter areas (Grey1 dorsal medulla; Grey2 cerebellar cortex; Grey3 superior colliculus; Grey4 hypothalamus; Grey5 thalamus: Grey6 hippocampus; Grey7 septum; Grey8 retrosplenial and adjacent motor cortex; Grey9 cingulate and adjacent motor cortex) and 3 white matter areas (White1 inferior and middle cerebellar peduncles; White2 decussation of the superior cerebellar peduncles; White3 cerebral peduncles) were scored.

Figure 2.1 TSE vacuolation scoring areas in the brain

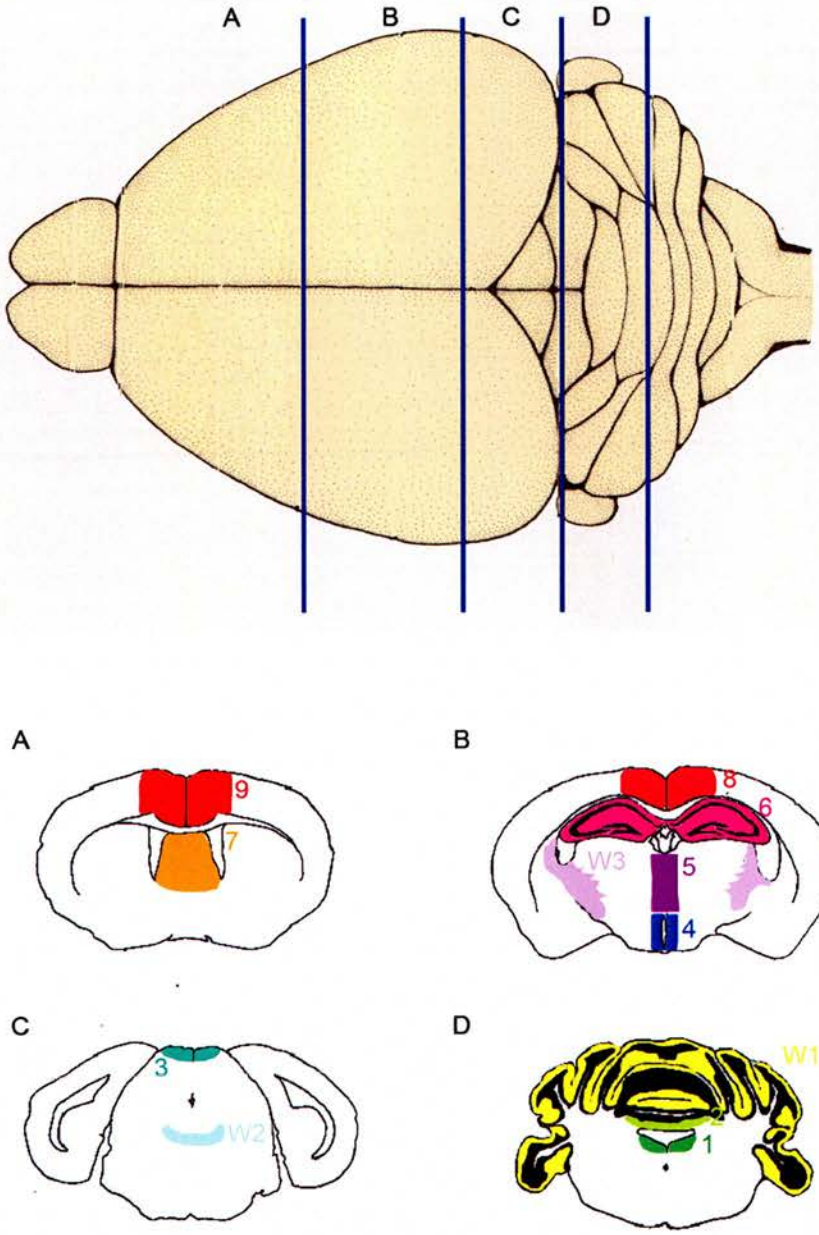

A) Forebrain, B) Caudal Midbrain, C) Rostral Midbrain, D) Hindbrain. TSE vacuolation scoring areas 1) dorsal medulla; 2) cerebellar cortex; 3) superior colliculus; 4) hypothalamus; 5) thalamus: 6) hippocampus; 7) septum; 8) retrosplenial and adjacent motor cortex; 9) cingulate and adjacent motor cortex; W1) inferior and middle cerebellar peduncles; W2) decussation of the superior cerebellar peduncles; W3) cerebral peduncles.

Figure 2.2 Examples of TSE vacuolation scores 0-5 (hypothalamus)

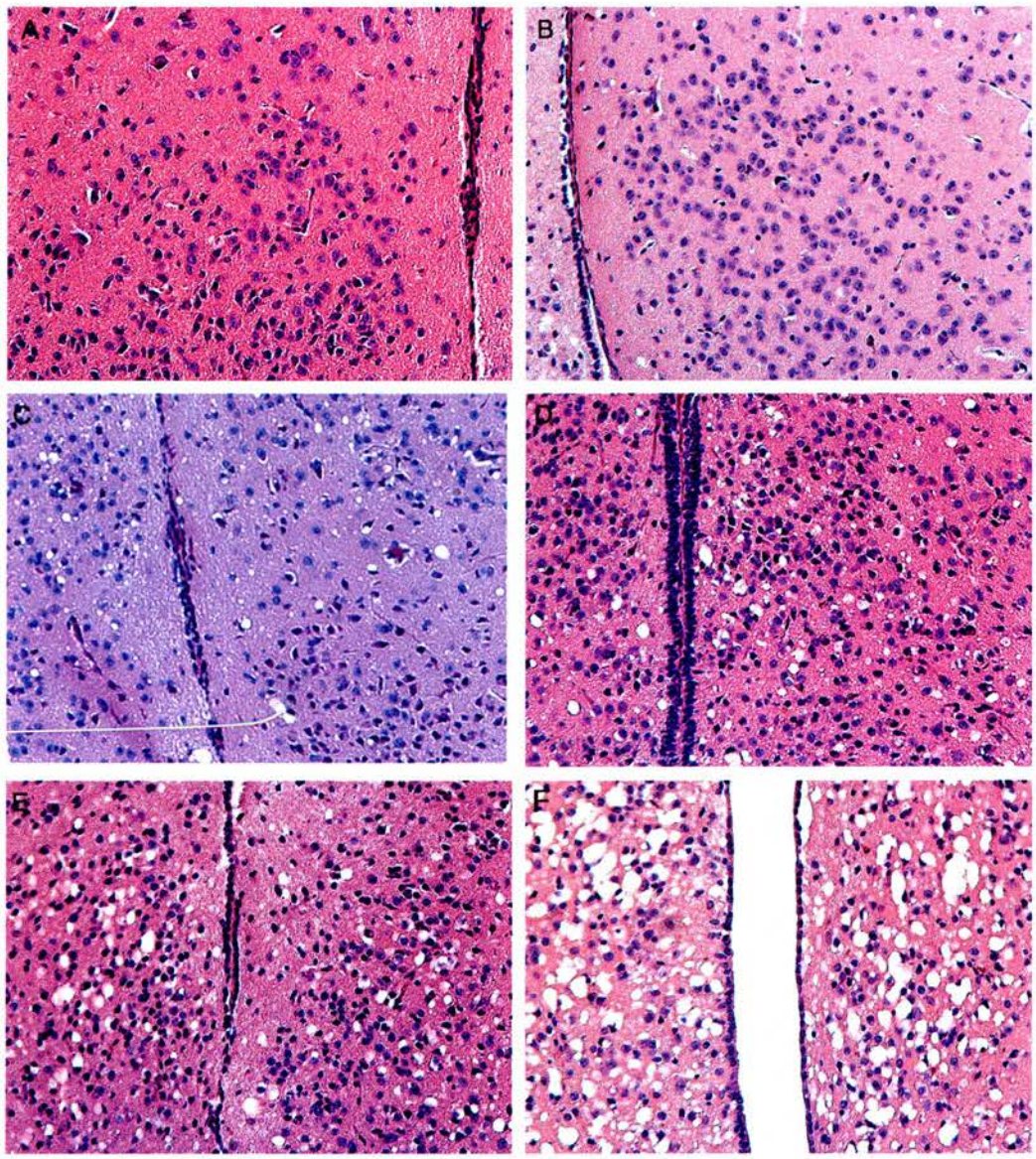

TSE vacuolation in the hypothalamus score 0 (A), 1 (B), 2 (C), 3 (D), 4 (E), 5(F).

2.8 Immuno-histo-chemistry of brain tissue experimental infected with TSE

2.8.1 CSA signal amplification method for the detection of PrP

All reagents were from DakoCytomation Inc, California, USA, Catalyzed Signal Amplification (CSA) System. All reactions were carried at room temperature unless otherwise stated.

Slide mounted paraffin embedded sections were de-paraffinized in xylene and rehydrated in an 99-70 % ethanol gradient, before blocking for endogenous peroxidases in 1 % hydrogen peroxide (Sigma-Aldrich Company Ltd, Dorset, UK)/ methanol (BDH) for 30 minutes. PrP antigen was retrieved from the highly fixed sections by wet autoclaving at 121 °C for 15 minutes and treatment with 98 % formic acid for 5 minutes. Sections were then washed in TBS/Tween (tris pH 7.6; sodium chloride 150 mM; 1% Tween 20) prior to blocking for 20 minutes with normal rabbit serum (Jackson ImmunoResearch, West Grove, PA, USA; 1/1000) diluted in TBS/ Tween; Avidin-D (Vector Laboratories, Burlingame, CA USA) for 15 minutes and biotin (Vector Laboratories, Burlingame, CA, USA) for 15 minutes to remove endogenous rabbit antigens, biotin and streptavidin respectively. Slides were then incubated with anti-PrP primary antibody for 1-2 hours (6H4 1/20,000 or 8H4 1/5000). Unbound primary antibody was removed by washing in TBS/ Tween. The CSA kit uses a multiple step approach to amplify the signal from each bound primary antibody molecule fifty fold. Sections were incubated with biotinylated rabbit anti-mouse antibody for 15 minutes, washed, then incubated with streptavidin-biotin conjugated to horseradish peroxidase for 15 minutes. After further washing the sections were then incubated with amplification reagent (biotinyl tyramide and hydrogen peroxide in PBS) and washed again before the final incubation with peroxidase conjugated streptavidin for 15 minutes. Sections were incubated with hydrogen peroxide activated 3,3'-diaminobenzidine (DAB) (Sigma-Aldrich Company Ltd, Dorset, UK) which converts to a brown precipitate upon contact with the peroxidase conjugated streptavidin. Sections were counter stained with haematoxylin before dehydrating in an 70- 99% ethanol gradient and 100 % xylene before mounting in pertex (CellPath, Hemel Hempstead, UK).

2.8.2 Avidin-Biotinylated peroxidase complex (ABC) immuo-histo-chemistry for the detection of astrocytes

Slide mounted paraffin embedded sections were de-paraffinized in xylene and rehydrated in an 99-70 % ethanol gradient, before blocking for endogenous peroxidases in 1 % hydrogen peroxide (Sigma-Aldrich Company Ltd, Dorset, UK)/ methanol (BDH) for 10 minutes. Sections were then blocked with normal goat serum (1/20) diluted in 1 X PBS/ 2% BSA (Sigma-Aldrich Company Ltd, Dorset, UK) for 15 minutes. Then sections were incubated with rabbit anti-cow glial fibrillary acid protein (1/500; DakoCytomation Inc, California, USA) diluted in 1 X PBS/ 2% BSA for 1 hour. Unbound primary antibody was removed by washing in 1 X PBS/ BSA before incubation with biotinylated goat anti-rabbit antibody (Jackson) diluted in 1 X PBS/ 2% BSA for 1 hour. Excess secondary antibody was removed by washing before incubation for 30 minutes with an Avidin-Biotinylated conjugated peroxidase complex (Vectastain Elite ABC Kit, Vector Laboratories, California, USA). Peroxidase was detected by incubation with hydrogen peroxide activated 3,3'-diaminobenzidine (DAB) (Sigma-Aldrich Company Ltd, Dorset, UK), sections were then counter stained with haematoxylin before dehydrating in an 70- 99% ethanol gradient and xylene for mounting in pertex (CellPath, Hemel Hempstead, UK).

2.9 Thioflavin treatment of paraffin embedded sections for the detection of amyloid

Slide mounted paraffin embedded sections were de-paraffinized in xylene and rehydrated in an 99-70 % ethanol gradient before staining in Haematoxylin for 5 minutes prior to incubation with Thioflavin-S (10mg/ml) for 5 minutes, then 70 % ethanol for 5 minutes before rinsing in water and mounting in Fluoresecent Mounting Medium (DakoCytomation Inc, California, USA). Fluorescence was analysed using a Nikon eclipse (E400) microscope illuminated with a mercury bulb.

2.10 Diagnostic western blotting of human TSE samples

The standard diagnostic protocol (National CJD Surveillance Unit (NCJDSU)) for western blotting of suspect human TSE cases was used to examine the Parchi type (mobility in SDS-PAGE of the un-glycosylated band) and glycoform of the inocula used in the cross species transmission experiments. All work was carried out in the category 3 laboratory at the, NCJDSU using methods adapted from Collinge *et al* 1996 under the supervision of Dr. Mark Head. Dissection of standard reference samples was kindly carried out by Dr. Mark Head.

2.10.1 Preparation (dilution, proteinase K treatment and denaturation) of human TSE samples and reference standards

Diagnostic reference standards were prepared from frozen tissue dissected from the frontal cortex. Briefly, tissues was mechanically homogenised using a pestle in nine volumes of sterile saline solution (0.9 % w/v) (Martindale Pharmaceuticals, UK) to prepare a 10% homogenate. This was then diluted a further 10 fold in sterile physiological saline solution (Martindale Pharmaceuticals, UK) to form a 1% homogenate comparable to the inocula prepared at NPU. Protein from standards and inocula was then extracted by the addition of saline free Extraction Buffer (0.5 % NP-40, 0.5 % sodium deoxycholate, TBS [pH7.4]; all Sigma-Aldrich Company Ltd, Dorset, UK) and centrifugation at 2000 rpm for 5 minutes at 4 °C. The supernatant was then removed from the pellet and treated with PK at 37 °C for 1

hour (50 µg/ml; Merck). Reaction was stopped by the addition of Pefabloc (1mM; Roche Diagnostics, Basel, Switzerland) and freezing at – 20 °C. In some cases samples were concentrated prior to SDS-PAGE separation by centrifugation at 14,000 rpm for 1 hour at 4 °C. The supernatant was discarded and the pellet resuspended in 1 X Extraction Buffer (0.5 % NP-40, 0.5 % sodium deoxycholate, TBS [pH7.4]; all Sigma-Aldrich Company Ltd, Dorset, UK)

2.10.2 Sodium Dodecyl Sulphate Polyacrylamide gel electrophoresis (SDS-PAGE)

Samples were denatured by heating at 102 °C for 10 minutes with NuPAGE LDS 4 X Sample Buffer (final concentration glycerol 10 %, tris 157 mM, lithium dodecyl sulphate 2 %, EDTA 0.51 mM, SERVA Blue G250 0.22 mM, Phenol Red 0.175 mM [pH 8.5]; Invitrogen, Paisley, UK). Proteins were then separated on the basis of weight and charge by gel electrophoresis at 200 V for 50 minutes using NuPAGE Novex 10 % Bis-Tris Gels (1.0 mm Invitrogen Life Technologies, Paisley, UK) in NuPAGE 1 X MES SDS running buffer (MES 50 mM [pH 7.2], tris 50mM, SDS 0.1 %, EDTA 1 mM; Invitrogen Life Technologies, Paisley, UK). Extraction buffer and NuPAGE LDS 4 X Sample Buffer blanks were used as negative controls. A mixture of SeeBlue (Invitrogen Life Technologies, Paisley, UK) and Magic-marker (Invitrogen Life Technologies, Paisley, UK) were used as molecular weight markers.

2.10.3 Transfer of separated proteins to a membrane

Proteins separated by SDS gel electrophoresis were transferred to PDVF membrane (Hybond-P, Amersham Biosciences, Piscataway, NJ, USA) at 30 V for 1 hour, using the NuPAGE transfer system, in 1 X NuPAGE Transfer Buffer (Invitrogen Life Technologies, Paisley, UK; final concentration, bicine 25 mM, bis-tris (free base) 25 mM, EDTA 1.0 mM, chlorobutanol 0.05 mM) and 20 % methanol.

2.10.4 Detection of PrP protein bound to a membrane

Membrane was washed 2 X 3 minutes in TBST before blocking in 5 % milk (Safeway non-fat dried milk powder)/ TBST (Sigma-Aldrich Company Ltd, Dorset,

UK) overnight, shaking at 4 °C. After blocking the membrane was washed with TBST prior to incubation with the primary anti-PrP antibodies 3F4 (1/20,000; Dako) or 6H4 (1/20,000; Prionics, Schlieren, Switzerland) in TBST for 1 hour. Membrane was then washed to remove excess primary antibody before incubation with HRP-conjugated secondary antibody (goat anti-mouse IgG (Fab-specific) peroxidase conjugate 1/40,000; Sigma-Aldrich Company Ltd, Dorset, UK) in TBST. Membrane was washed with TBST to remove excess secondary antibody prior to incubation with chemiluminescent substrate for 5 minutes (ECL plus, Amersham Biosciences, Piscataway, NJ, USA) followed by exposure to X-ray film (Hyperfilm ECL; Amersham Biosciences, Piscataway, NJ, USA). Films were developed using an automatic film processor (Hyperprocessor™; Amersham Biosciences, Piscataway, NJ)). Digital images of the chemiluminescence were also recorded when the signal was adequate using a Storm860 digital imager (Molecular Dynamics, Sunnyvale, CA).

2.10.5 Strain typing, densitometry and glycoform analysis

After X-ray films had been developed they were scanned using a GS-700 Densitometer (BioRad). Densitometry was performed using the Quantity One (4.4.1) programme. Band density was confirmed to be within the linear range by reference to previous standards kindly provided by Dr. Mark Head, and was recorded for glycoform analysis. Band width was determined manually by intensity minima. Samples were compared to standard reference samples for both glycoform analysis and typing of the size of the un-glycosylated band (Parchi *et al* 1996)

2.11 Protein misfolding cyclic amplification (PMCA)

PMCA was undertaken in the laboratory of Dr. Claudio Soto, under the supervision of Dr. Joaquin Castilla, University of Texas Medical Branch (UTMB), Galveston, Texas, USA. Infectious materials were transported on dry ice in accordance with IATA Dangerous Goods requirements from NPU to UTMB. This was kindly arranged by Dr. Rona Barron and Mr. Declan King. All chemicals supplied by Fisher Scientific, unless otherwise stated.

2.11.1 TSE infected samples used in PMCA

263K (Syrian Hamster NPU protocol 263K-5Z animal number 33; B34853 and animal number 3; B34855)

ME7 (129/Ola mouse NPU protocol 5666G-1A; animal number 52, C11147 and animal number 53, C11172) kind gift of Dr. Nadia Tuzi, NPU, Edinburgh.

79A (129/Ola mouse NPU protocol 567C-1A animal number 40, C10760 and animal number 50, C10759) kind gift of Dr. Nadia Tuzi, NPU, Edinburgh.

2.11.2 Normal brain homogenate preparation for PMCA

Whole brains were taken post mortem, rinsed in PBS and immediately snap frozen in liquid nitrogen for transport on dry ice to UTMB. The brains were weighed separately and homogenized in glass homogenisers with a plastic pestle on ice in nine volumes of conversion buffer (1 X Dulbecco's phosphate buffered saline (136.9 mM sodium chloride, 8.1 mM sodium phosphate, 1.5 mM potassium phosphate, 1.5 mM potassium chloride (supplied by Sigma-Aldrich Company Ltd, St. Louis, MO, USA; D-PBS), 150 mM sodium chloride, 1% Triton X-100 [Sigma-Aldrich Company Ltd, St. Louis, MO, USA, T8787] with 1 X Complete Protease Inhibitor Cocktail containing 1 mM EDTA [Roche Diagnostics, Basel, Switzerland]). Cell debris was removed by brief centrifugation at 2000 rpm for 45 seconds (Harrier 18/10 SANYO). The resultant supernatant was either directly frozen at – 80 °C in 450 µl aliquots or mixed with additional EDTA [Promega, Madison, WI, V4231, (final concentration 5 mM)] prior to aliquoting and freezing.

Normal hamster brain homogenate was a kind gift of Dr. Paula Prieto Saa, UTMB, Galveston.

2.11.3 TSE infected brain homogenate preparation for PMCA

Partial brains were weighed and homogenized in nine volumes of 1 X D-PBS (with 1X Complete Protease Inhibitor Cocktail that contains 1 mM EDTA (Roche Diagnostics, Basel, Switzerland 1836 145) (PBS/PI). Un-spun homogenate was then aliquoted for storage at -80 °C. Prior to PMCA, aliquots of 263K were heated at 55 °C for 10 minutes, with shaking, to denature any PrP^c rendering it incompetent as substrate for PMCA. It was necessary to purify the mouse ME7 and 79A infected brain homogenates further. They were mixed with an equal volume of 20% sarkosyl and centrifuged at 100,000g for 1 hour. The resultant pellet was washed in PBS/PI and centrifuged for 30 minutes at 100,000g in polycarbonate tubes before resuspension in PBS by manual sonication (40 X 1 second pulses at 10% power output) using a Sonoplus HD 2070 sonicator with a titanium microtip MS73 (Bandelin Electronic, Berlin, Germany).

2.11.4 Automatic protein misfolding cyclic amplification

Optimisation experiments were performed to determine the conditions under which PrP^{Sc} (263K, ME7, 79A) seeded the *in vitro* conversion of PrP^c to the protease resistance form (PrP^{Res}) would occur. The ratio of TSE infected brain homogenate to the normal brain homogenate, the concentration of EDTA and the number of cycles were examined to determine optimum conditions for *in vitro* generation of PrP^{Res}. Control samples of the normal brain homogenate/ TSE infected brain homogenate mix were either directly frozen or incubated at 37 °C for the same period of time as PMCA was performed. An equal volume of mix (80 µl) was used for PMCA and 37 °C control samples as amplification may be volume dependent (personal communication, J. Castilla). PMCA was performed in a bath sonicator using a microplate horn (Misonix 3000), such that the ultrasound is applied to the samples indirectly. Thin wall PCR tubes (GeNunc, Nalge Nunc International, 0.2 ml tubes) were used to permit adequate penetration of ultrasound into the PMCA samples. Each cycle consists of a 30 minute incubation at 37 °C followed by 40

second pulse at power output 6. Samples were frozen at – 80 °C prior to analysis by gel electrophoresis and western blotting.

2.11.6 Proteinase K treatment and sample denaturation for western blotting

Samples subjected to PMCA and controls which had either been frozen or incubated at 37 °C without sonication were treated with 50 μg/ml Proteinase K (Roche Diagnostics, Basel, Switzerland) for one hour at 37 °C. The reaction was stopped with NuPAGE LDS Sample Buffer (Invitrogen, Carlsbad, CA, USA) followed by immediate denaturation by heating to 100 °C for 10 minutes or freezing at – 20 °C for denaturation later. Control samples not treated with PK were similarly denatured in NuPAGE LDS Sample Buffer prior to electrophoresis.

2.11.7 Sodium Dodecyl Sulphate Polyacrylamide gel electrophoresis (SDS-PAGE)

LDS denatured total proteins were separated by size and charge in NuPAGE 12 4% Bis-Tris Gels (15 minutes at 70 V; 50-70 minutes at 150 V) using 1 X NuPAGE MES Running Buffer (Invitrogen, Carlsbad, CA, USA) using the Invitrogen cassette system. SDS-PAGE prestained low-range molecular weight markers (phosphoylase B 103 kDa, bovine serum albumin 81 kDa, ovalbumin 48 kDa, carbonic anhydrase 36 kDa, soybean trypsin inhibitor 27 kDa and lysozyme 19 kDa; BioRad, Hercules CA, USA) was used.

2.11.8 Western blotting and detection of membrane bound proteins

Total proteins were transferred to Hybond-ECL nitrocellulose membrane (Amersham Biosciences, Piscataway, NJ, USA) in 1 X Tris-glycine transfer Buffer (20 % Methanol; 25 mM tris; 200 mM glycine) at 0.8 Amps, for 1 hour, using a BioRad immersion blotter cooled by ice. Membranes were blocked in 5 % non-fat milk (Carnation) PBS/0.05 % Tween 20 (PBST) for 1 hour, rocking at room temperature, prior to incubation with anti-PrP mouse monoclonal antibodies 3F4 (1/5000) for the detection of hamster PrP, and 6H4 (1/5000 Prionics, Schlieren, Switzerland) or 6D11 (1/5000 Signet, Dedham, MA, USA) for the detection of murine PrP, in 2 % milk PBST, rocking either for 1 hour at room temperature or

overnight at 4 °C. Membranes were washed in PBST (once for 10 minutes and three times for 5 minutes), prior to incubation with ECL sheep horseradish peroxidase linked anti-mouse antibody (Amersham Bioscience, Piscataway, NJ, USA) for 1 hour rocking at room temperature. Excess secondary antibody was removed by washing in PBST (once for 10 minutes and three times for 5 minutes). Bound HRP-conjugated secondary antibody was detected using ECL plus Western Blotting Detection System (Amersham Bioscience, Piscataway, NJ, USA) and the EpiChemi^3 Darkroom (UVP BioImaging Systems; California, USA) linked to LabWorks program via a Hamamatsu Camera, with exposures of 30 seconds and 15 minutes.

2.11.9 Stripping of bound antibody from nitrocellulose membranes

To permit re-probing of western blots with a second antibody, the blots were stripped with Western Stripping solution (100 mM ß-Mercaptothanol; 2 % SDS; 62.5 mM Tris pH 6.7) by shaking at 50 °C for 30-45 minutes. Prior to reprobing, blots were washed in distilled water and PBST, and blocked in 5 % milk/PBST for 1 hour at room temperature.

3.0 Characterisation of PrP in uninfected PrP glycosylation deficient transgenic mice

3.1 Aim to characterise the biochemistry of PrP^{C}, the spontaneous formation of PrP^{Sc} and development of spontaneous TSE clinical disease in the glycosylation deficient transgenic mice.

3.2 Introduction and experimental techniques

In order to interpret the importance of the glycosylation status of PrP^{C} to cross-species TSE transmission, it is necessary to understand the influence of glycosylation of PrP on the protein's normal biochemistry. The N-linked glycosylation of proteins is known to influence multiple aspects of their biochemistry. These include the protein's half-life, folding efficiency and identification of misfolded forms in the ER, functionality (catalytic ability) and interactions with other molecules (Mitra et al., 2006). The relative importance of glycosylation to these parameters varies between individual proteins and it is not possible to predict the biochemical effects of N-linked glycan attachment. Therefore altering the glycosylation of PrP may change the ability of the protein to fold or misfold, its steady state or lead to the spontaneous formation of PrP^{Sc} (Rudd et al., 2001).

These potential changes may have a major impact on the key role of PrP in TSE disease, perhaps via an influence on the conversion of PrP^{C} to PrP^{Sc}. Equally, PrP's glycosylation state may change the tendency of the protein to form dimers or be truncated, which may also impact on disease phenotype or incidence. Thus it is necessary to determine which of these factors are influenced by the change in N-linked glycosylation of PrP *in vivo* in the transgenic model system employed here [NPU]. To validate the model, the disruption of glycosylation by the amino acid changes in PrP will be investigated. Additionally, it is important to ascertain if the models used here develop spontaneous TSE disease. This will provide a baseline

against which experimental TSEs transmission can be compared. Thus both the spontaneous development of TSE neurological signs as defined by Dickinson and Fraser (1968) and subclinical TSE specific vacuolar pathology were investigated by standard methods over the normal lifespan of the PrP glycosylation deficient transgenic mice.

The alteration of glycosylation state in the PrP glycosylation deficient murine transgenics may reduce the stability or turnover of PrP^C such that its steady state is altered, as has been demonstrated for other proteins (Chen et al., 2006; Li et al., 2004). Previous work has demonstrated that the level of *Prnp* mRNA in the PrP glycosylation deficient transgenic mice [NPU] is comparable to that in normally glycosylated wild type mice (Cancellotti et al., 2005; Wiseman, 2003). Consistent with previous models generated using PrP gene-targeting (Moore et al., 1998), this indicates that the point mutations introduced into the *Prnp* transgene in these transgenics do not alter the amount of *Prnp* mRNA in the CNS. Further experimentation is required to assess if these changes alter the amount of PrP^C produced in the CNS of these transgenic murine models. The level of PrP^C greatly affects the disease incubation period for many TSE strains (Manson et al., 1994b; Prusiner et al., 1990), thus these data are important to correctly interpret TSE transmission studies in the glycosylation deficient transgenic mice.

Preliminary studies to determine PrP level in the unchallenged glycosylation deficient transgenic mice using western blot analysis produced ambiguous results because of the semi-quantitative nature of the assay (data not shown). This approach was abandoned in favour of a quantitative analysis using Dissociation Enhanced Lanthanide Fluoroimmunoassay (DELFIA) adapted from the method of Barnard and colleagues (Barnard et al., 2000). This technique uses pairs of PrP specific antibodies. An N-terminal specific antibody (FH11 or AG4) captures PrP and anchors it to an ELISA plate such that is concentrated. A second detector antibody (8H4 or 7A12) labelled with the lanthanide, europium, which can be spectometrically detected is then used to detect bound PrP. The amount of PrP in each sample can then be determined by comparison with a known recombinant PrP

standard. As this system uses monoclonal antibodies, comparison of multiple pairs is required as PrP may exist in more than one conformation or in truncated forms *in vivo*. Thus a specific epitope may only be available for binding in a fraction of the total PrP molecules. Importantly, the binding of PrP to antibodies may be influenced by its glycosylation state.

Expression of mutant or truncated forms of PrP *in vivo* has led to the development of spontaneous neurological dysfunction in a number of models (Castilla et al., 2005; Chiesa et al., 1998; Hsiao et al., 1990; Ma et al., 2002; Muramoto et al., 1997; Shmerling et al., 1998). However only in limited cases has TSE spongiosis been observed (Castilla et al., 2005; Hsiao et al., 1990). These neurodegenerative phenotypes can confound TSE transmission studies, as it is difficult to determine whether neurological signs are the result of expression of the transgene, TSE transmission or a combination of both. Neurological phenotypes have only been previously observed when the PrP transgene is over expressed (Nazor et al., 2005). Thus in the gene-targeted transgenic mice used here the development of spontaneous TSE disease is unlikely. Despite this, it is important to experimentally demonstrate this so that any observed cases of TSE disease, after cross-species TSE challenge, can be attributed to the experimental TSE exposure (Chapters 5 and 6). This is particularly pertinent to cross-species transmission studies for which long incubation periods are anticipated as spontaneous disease is particularly apparent in older mice. Additionally, these data are informative regarding the mechanism of non-acquired TSE disease which includes both familial and sporadic forms, some of which are associated with PrP^{Sc} that is abnormally glycosylated (Capellari et al., 2000a; Grasbon-Frodl et al., 2004; Monari et al., 1994; Nitrini et al., 1997; Zanusso, 2006).

Spontaneous formation of PrP^{Sc} or partial PrP^{Sc}-like properties may occur in the absence of overt clinical signs in the glycosylation deficient transgenic mice. This would also confound cross-species TSE transmission studies, as PrP^{Sc} formation will be used as a marker of disease susceptibility (Chapters 5 and 6). Spontaneous formation of misfolded PrP, including that which is PK sensitive, has been reported in a number of experimental systems in which primary amino acid sequence of PrP

has been altered (Castilla et al., 2005; Chiesa et al., 1998; Hsiao et al., 1994; Hsiao et al., 1990; Lehmann and Harris, 1996a; Lehmann and Harris, 1996b; Lehmann and Harris, 1997; Ma and Lindquist, 2002; Ma et al., 2002; Nazor et al., 2005; Singh et al., 1997). However, spontaneous formation of misfolded PrP *in vivo* has only been demonstrated when PrP is highly expressed (Chiesa et al., 1998; Hsiao et al., 1990; Manson et al., 1999; Nazor et al., 2005). In some experiments, changes in the biochemistry of PrP, such as enhanced PK resistance, have been observed even in young animals (Chiesa et al., 1998).

Previous studies have suggested that glycosylation of PrP contributes to the stability of the protein's conformation and its resistance to misfolding (Lehmann and Harris, 1997; Rudd et al., 2001). Cell culture studies have suggested that, in the absence of its N-glycans, PrP spontaneously exhibits some biochemical properties of PrP^{Sc}, including enhanced insolubility and resistance to protease digestion (Lehmann and Harris, 1997). This led these authors to conclude that this partially misfolded PrP may resemble an intermediate pre-PrP^{Sc} like state. Furthermore, the authors suggest this effect may be mediated by reduced solubility, or an enhancement of the ability of the un-glycosylated form to adopt a partially misfolded conformation. Thus the *in vivo* effect of the absence of PrP's N-glycans on the biochemical properties of PrP was investigated in the PrP glycosylation deficient transgenic mice.

To investigate the folding status of PrP, a standard PK digestion and a solubility assay were employed. PrP^{Sc} is resistant to digestion with relatively high concentrations of PK, compared to PrP^{C} (Buschmann et al., 1998). A range of PK concentrations was thus investigated to determine if PrP^{C} from the glycosylation transgenic mice had enhanced resistance to digestion. Previous studies have demonstrated that not all misfolded forms of PrP are PK resistant (Nazor et al., 2005). To determine if such forms of PK sensitive PrP^{Sc} spontaneously formed in glycosylation deficient murine transgenics, a solubility assay was additionally used. Misfolded PrP is insoluble at low guanidine hydrochloride (Gnd HCl) concentrations (1 M), at which PrP^{C} is predominately soluble, but soluble at higher concentrations of the chaotroph (6 M) (Barnard et al., 2000; Safar et al., 1998). Thus total brain

proteins were separated on the basis of their solubility in Gnd HCl and the amount of PrP in each fraction determined quantitatively.

3.3 Optimisation of experimental techniques

3.3.1 PNGase deglycosylation of PrP^C

Optimum conditions for the enzymatic deglycosylation of normally glycosylated PrP^C, in total brain homogenate were experimentally determined using commercially available PNGase enzyme derived from *Chryseobacterium [Flavobacterium] menigosepticum*. De-glycosylation of PrP^C was incomplete using conditions recommended by the enzyme manufacture (New England Biolabs) (data not shown). Increasing the incubation time resulted in the formation of truncated forms of PrP, irrespective of the presence of PNGase, perhaps because of the action of endogenous proteinases (data not shown). Increasing the ratio of PNGase to total brain protein for short incubation periods was found to facilitate complete deglycosylation of normally glycosylated PrP^C without the formation of truncated forms. This experimental method was thus used to investigate the glycosylation state of PrP^C in the PrP glycosylation deficient transgenics.

3.3.2 Western blot tubulin loading control

A rat anti-α tubulin monoclonal antibody was used to confirm that equal amounts of total protein were loaded in each lane of western blots, as has been previously used by other workers (Allen et al., 2005). The optimum anti-tubulin antibody concentration was experimentally determined to be 1/4000 (appendix iii).

3.4 Experimental results

3.4.1 Threoine for asparagine substitution at position 180 and 196 prevent the attachment of N-glycans to PrP

To confirm that the N180T and N196T substitutions in the PrP glycosylation deficient transgenics altered the glycosylation of PrP *in vivo*, the sensitivity of PrP^C to enzymatic deglycosylation was investigated. A three hour treatment of total brain protein with PNGase (30,000 Units/ml) resulted in the complete deglycosylation of wild type PrP such that predominant ~35-37 kDa forms, and the minor ~31-34 kDa forms, were observed to disappear with a concurrent increase in the amount of the previously minor ~30 kDa form (Figure 3.1 A, n = 4 8H4 and 7A12). This observed change in molecular weight is consistent with the well documented variable glycosylation of PrP^C *in vivo*, and supports the proposal that the 35-37, 31-34 and 30 kDa forms correspond to di-, mono- and un-glycosylated forms of PrP^C respectively. Minimal truncated forms of PrP were detected by this method in samples in which PrP was normally glycosylated, supporting the hypothesis that the 31-34 kDa forms are mono-glycosylated PrP and not truncated forms as has been previously suggested (Chen et al., 1995). The molecular weight of β-tubulin was unchanged by the PNGase treatment consistent with its un-glycosylated state.

Similar treatment of total brain protein with PNGase from G1 and G2 glycosylation deficient transgenic mice resulted in the disappearance of ~31-34 KDa PrP^C and an increase in ~30 KDa PrP^C (Figure 3.1 A). This change in molecular weight after enzymatic deglycosylation is consistent with a single site of N-glycan attachment being utilised in these transgenic lines. The molecular weight of PrP^C from the brains of G3 PrP glycosylation deficient transgenic mice was unchanged by enzymatic deglycosylation, consistent with PrP^C not being glycosylated in this transgenic model (Figure 3.1 A).

Figure 3.1 Western blots of total brain proteins from glycosylation deficient transgenic and control mice

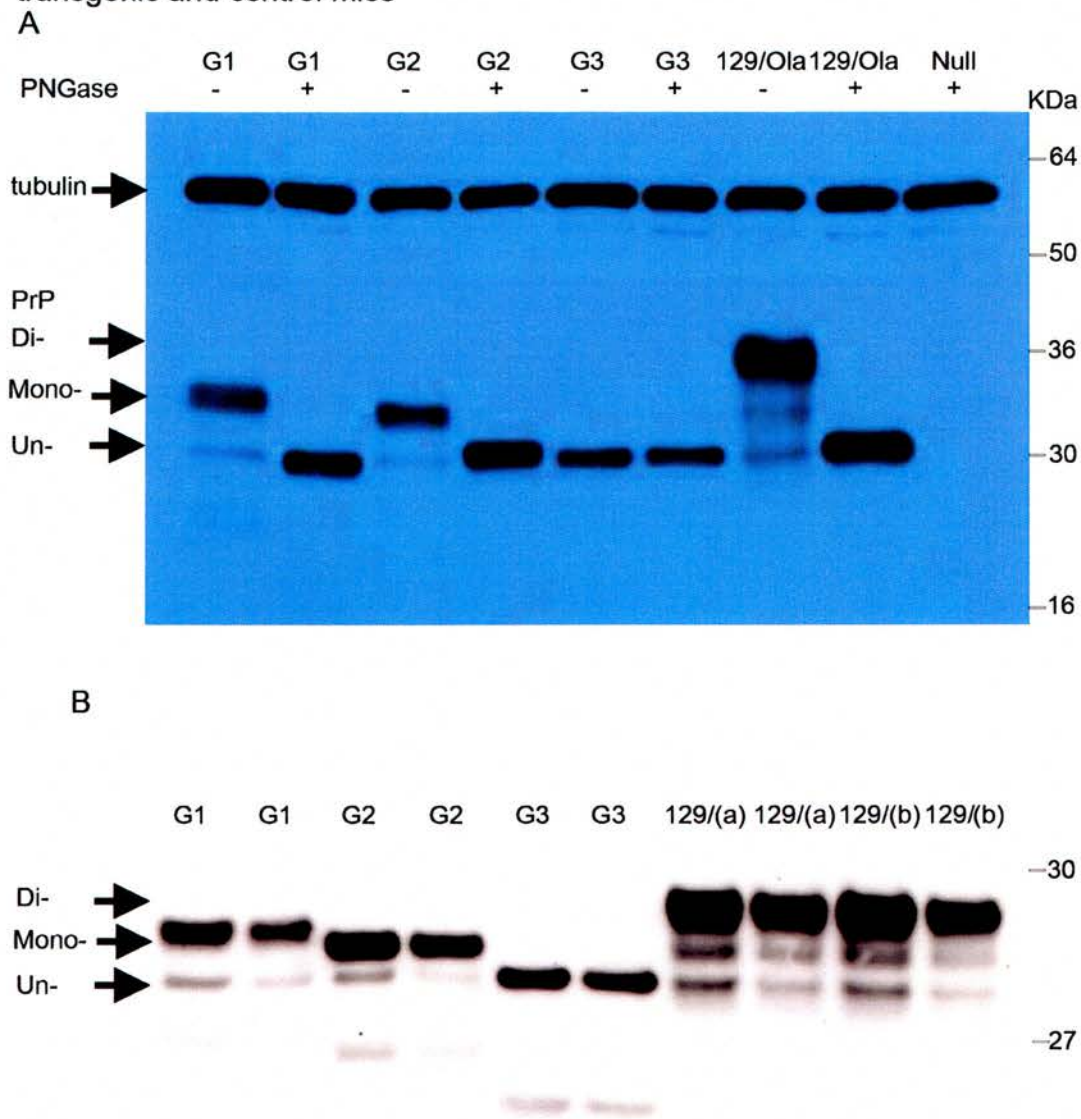

3.1 (A) Western blot of PNGase deglycosylated total brain protein (3 hours 37 °C 30,000 Units/ml) from uninfected PrP glycosylation deficient transgenic and normally glycosylated control (129/Ola) mice demonstrates that the N180T (G1 and G3) and the N196T (G2 and G3) substitution disrupt the first and second PrP glycosylation site of PrP respectively. PrP detected using anti-PrP mouse monoclonal 8H4, antibody specificity demonstrated by the use of PrP null mice total brain homogenate control (Null). Upper band indicated by arrow anti-β-tubulin loading control (rat monoclonal). (B) Western blot demonstrating the difference in the electrophoretic mobility of mono-glycosylated PrP from G1 and G2 transgenic murine brain. Total brain protein from uninfected PrP glycosylation transgenic (single samples assayed in duplicate) and two independent normally glycosylated 129/Ola control (129/(a) and 129/(b)) mice run under denaturing conditions. PrP detected using anti-PrP monoclonal 6H4.

3.4.2 The molecular weight of mono-glycosylated PrP^C differs between G1 (T180N) and G2 (T196N) transgenic mice

Visual inspection of western blots suggests that the electrophorectic mobility of mono-glycosylated PrP^C differs between G1 and G2 transgenic mice (Figure 3.1 B). This was examined further using densitometry (Figure 3.2). Normally glycosylated wild type PrP exhibits three peaks of PrP densitometry that correspond to the di- , mono- and un-glycosylated forms of the protein. Both G1 and G2 PrP glycosylation deficient transgenic mice exhibit two major peaks, however the predominate heavier peak (mono-glycosylated) from G1 transgenic mice reproducibly ran slower than that of either G2 transgenic mice or normally glycosylated controls (Figure 3.2 6H4 n = 3). This supports the hypothesis that the combination of sugars attached to G1 and G2 PrP^C differ and suggests that those attached to G2 PrP more closely resemble the predominate wild type mono-glycosylated form. However further experimental investigation is required to confirm this as the prevention of glycosylation at one site may alter the combination of sugars attached to the other.

Figure 3.2 Densitometry profile of western blot of PrP from PrP glycosylation deficient transgenic and normally glycosylated control (129/Ola) mice

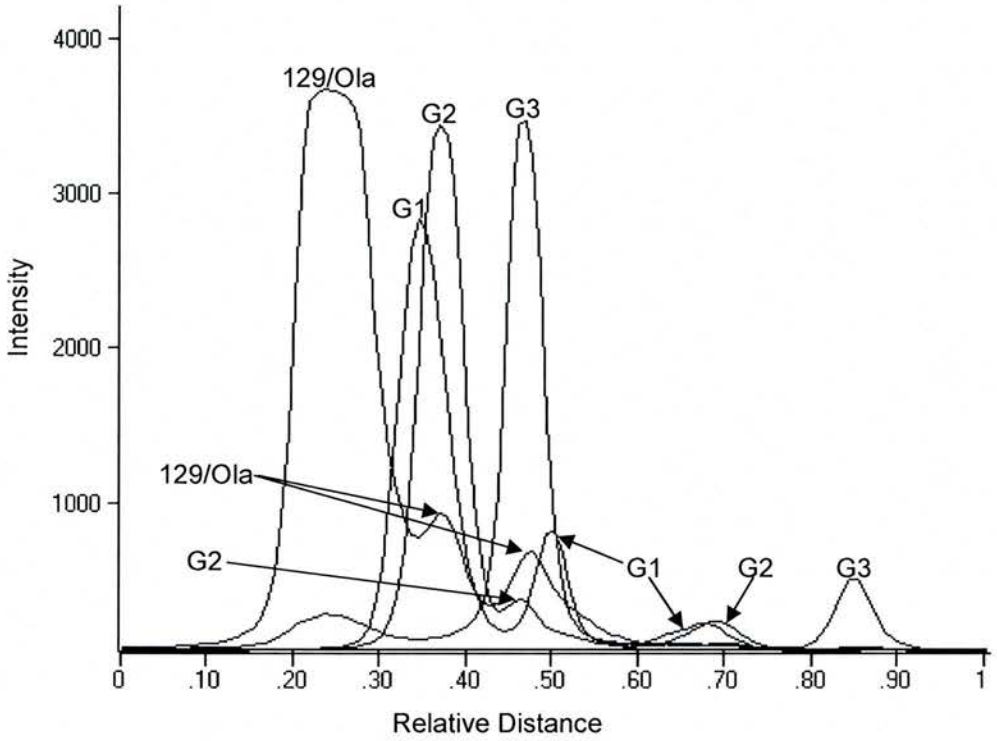

PrP detected using anti-PrP monoclonal 6H4 and corresponds to the that represented in western blot 3.1 B. Intensity of anti-PrP signal displayed on y-axis, relative distance from top of gel on the x-axis. Predominate 129/Ola (129/Ola (a) in figure 3.1B) PrP control peak observed at approximately 25 units on x-axis, minor peaks observed at 37 units and 47 units; G1 PrP major peak observed at 34 units and minor peak at 50 units; G2 PrP major peak at 37 units and minor peak at 46 units; G3 PrP major peak at 47 units, as indicated by arrows. This data supports the hypothesis that the electrophorectic mobility of mono-glycosylated PrP^C differs between G1 and G2 transgenic mice and that from G2 animals most closely reassembles mono-glycosylated PrP^C from normally glyco-

3.4.3 Comparison of the amount of PrP^C in the glycosylation deficient transgenic and normally glycosylated control mice

To investigate if alteration of the glycosylation state of PrP in the G1, G2, and G3 transgenic mice changed the overall amount of the protein *in vivo*, the amount of PrP^C in the brains of transgenic mice and normally glycosylated controls was compared by Dissociation Enhanced Lanthanide Fluoroimmunoassay (DELFIA). For this assay PrP^C was solubilised in a weak solution of guanidine hydrocholoride (Gnd HCl; 1M) in which PrP^{Sc} is insoluble. The amount of PrP^C in the sample is then determined using an un-glycosylated recombinant PrP standard. The apparent amount of normally glycosylated PrP detected varied by a factor of 10 between antibody pairs, in particular the capture antibody AG4 was associated with higher anti-PrP signals (Figure 3.3, compare A and B to C). Thus the ratio of detectable recombinant and native PrP displays antibody dependence. This may either reflect enhanced detection of the normally glycosylated form or reduced detection of recombinant PrP. A higher signal was detected in the assay buffer negative control than in the PrP null brain homogenate negative control when the capture antibody FH11 was used (Figure 3.3 A and B). This suggests that molecules in the murine brain homogenate act to block non-specific interactions between FH11 and both 8H4 and 7A12 capture antibodies. A similar effect is not observed when AG4 is used as the capture.

For antibody pair FH11-7A12, no significant difference in the amount of PrP^C was observed between the PrP glycosylation deficient murine transgenics and normally glycosylated controls (Figure 3.3 A, n = 2-4, assayed three times in duplicate, ANOVA $p = 0.177$). In contrast, significantly more PrP^C was detected in G1 and G3 transgenic mice than in wild type controls using the FH11-8H4 antibody pair (Figure 3.3 B, n = 2-4, assayed twice in duplicate, ANOVA $p = 0.004$). However, a difference in the amount of PrP^C was also observed between the two normally glycosylated controls (wild type and control line) which was not observed using the other antibody pairs.

Figure 3.3 Amount of soluble and insoluble PrP detected by DELFIA

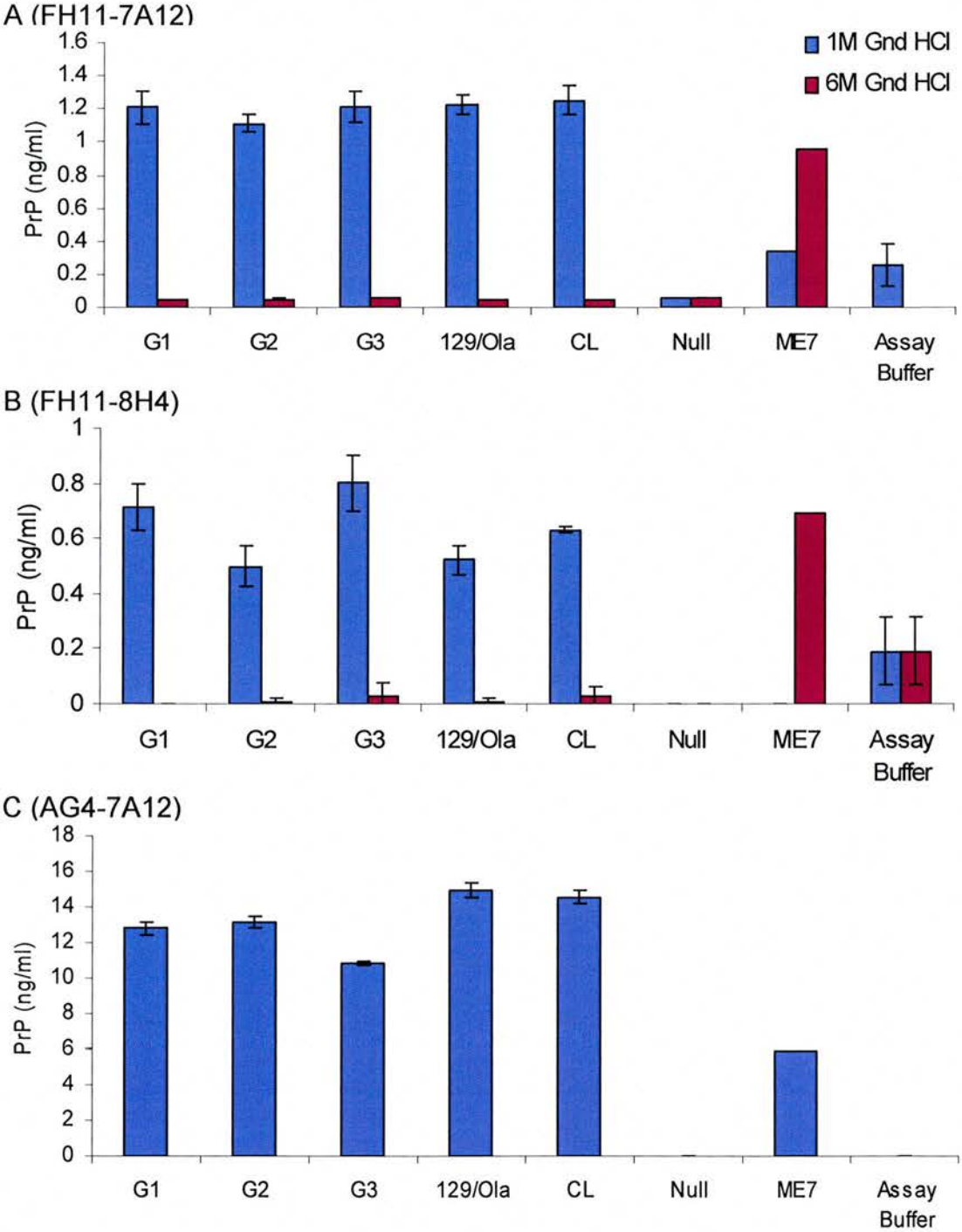

PrP detected by DELFIA using an anti-PrP capture (A & B) FH11 or (C) AG4 and a europhium labelled detector antibody (A &C) 7A12 or (B) 8H4, in brain homogenates from uninfected G1 (N180T), G2 (N196T) and G3 (N180T, N196T) PrP glycosylation deficient transgenic, normally glycosylated control (129/Ola, and transgenic control line (CL) that expresses normally glycosylated PrP but carry a LoxP site downstream of exon 3), PrP null (Null) and murine scrapie infected 129/Ola mice (ME7). Recombinant PrP^a used as the standard, to determine relative amount of soluble (1 M Gnd HCl) and insoluble (1 M Gnd HCl insoluble 6 M soluble) PrP. Mean amount of PrP detected for 3 (A) or 2 (B and C) DELFIA experiments using n independent samples (G1 n = 2, G2 n = 4, G3, 129/Ola and CL n = 3, Blank, ME7 and PrP Null n = 1) each sample assayed in duplicate during each experiment. Error bars indicate the standard deviation between individual animals and the assay buffer between different experiments. Significantly more soluble PrP was detected using FH11-8H4 in G1 and G3 brain homogenates than in the 129/Ola control (B, ANOVA $p = 0.0004$) and significantly less soluble PrP was detected using AG4-7A12 in G1, G2 and G3 brain homogenates than in the 129/Ola control (C, ANOVA $p < 0.001$).

This result questions the validity of the differences between the wild type control and glycosylation deficient transgenic mice observed using this antibody pair. The anti-PrP signal was particularly low when using FH11-8H4, this may have contributed to the apparent inaccuracy of this combination of antibodies. A significant but small reduction in the amount of G1, G2 and G3 PrP^{C} detected as compared to the normally glycosylated controls was observed using the AG4-7A12 antibody pair (Figure 3.3 C, n = 2-4 assayed twice in duplicate, ANOVA $p < 0.001$). Interestingly, the AG4-7A12 antibody pair did not detect any (1M guanidine hydrochloride insoluble 6 M soluble PrP) PrP^{Sc} in the ME7 clinical endpoint positive control, suggesting it cannot bind misfolded forms of PrP. Thus the reduced level of protein observed in the glycosylation deficient transgenic mice using AG4-7A12 may be the result of only a subset of total PrP being captured by AG4.

The same group of age and sex matched mice were assayed using each antibody pair, thus the observed differences between pairs are not attributable to intra-animal variation and are likely to result from differential antibody recognition of the glycotypes in each transgenic line. Thus these data do not suggest that there are underlying differences in the amount of PrP^{C} between the murine PrP glycosylation deficient transgenics and normally glycosylated controls, but that variation in antibody recognition between PrP glycotypes occurs. In particular, there is no evidence of a reproducible reduction in the amount of PrP^{C} detected in any of the PrP murine glycosylation deficient transgenics, suggesting that *in vivo* an absence of N-glycans does not compromise the overall amount of PrP^{C} in the CNS.

3.4.4 Absence of PrP's N-glycans does not lead to the spontaneous formation of PrP^{Sc} like properties *in vivo*.

Previous cell culture studies have suggested that un-glycosylated or partially glycosylated PrP spontaneously adopts PrP^{Sc}–like properties (Lehmann and Harris, 1997). These biochemical changes included enhanced insolubility and resistance to PK. To investigate if this occurred *in vivo* in the PrP murine glycosylation deficient transgenics, a number of biochemical features of PrP where examined. Misfolded PrP, as assayed by low concentration Gnd HCl insolubility (1M insoluble), was not observed in any of the uninfected murine PrP glycosylation deficient transgenics, suggesting that PrP^{Sc} had not spontaneously formed in these mice (Figure 3.3 A and B).

Additionally, no PK resistant PrP was observed in uninfected murine PrP glycosylation deficient transgenics as assayed by standard PK digested (20 µg/ml 37 °C for 1 hour) and measured by western blot using two anti-PrP monoclonal antibodies (8H4 n = 3, 7A12 n = 3). In contrast, PK resistant PrP can be clearly detected in TSE infected mice (murine scrapie strain ME7) at clinical endpoint by this method (Figure 3.4 A). Moreover, even using low concentrations of PK (10 µg/ml 37 °C for one hour), resistant PrP was not detected in the murine PrP glycosylation deficient transgenics (Figure 3.4 B, 8H4 n = 2, 7A12 n = 3). The use of lower concentrations of PK (5 or 1 µg/ml 37 °C for one hour) resulted in the incomplete digestion of normally glycosylated and glycosylation deficient PrP, consistent with previous reports (Figure 3.4 C, 7A12 n = 2, 8H4 n = 3) (Buschmann et al., 1998). No significant differences in the amount of PrP remaining were apparent between transgenic mice and normally glycosylated controls by this method. No PK resistant PrP (20 µg/ml 37 °C for 1 hour) was detected in G3 transgenic mice that were in excess of 800 days old (Figure 3.5 A, 8H4 n = 3).

Figure Legend 3.4 PK resistance of PrP from the glycosylation deficient transgenic and normally glycosylated control mice as analysed by western blot. Total brain proteins from murine scrapie strain ME7 infected clinical endpoint and uninfected glycosylation deficient transgenic (G1 N180T; G2 N196T; G3 N180T and N196T), normally glycosylated control (129/Ola and control line (CL) mice that express murine wild type PrP but carry a single transgenic LoxP site downstream of exon three) and PrP null mice (Null) were treated for 1 hour at 37 °C with (A) 20 µg/ml (B) 10 µg/ml or (C) 1 µg/ml PK; the reaction was stopped with PMSF and samples were denatured and western blotted. Di-, mono- and un-glycosylated PrP was detected with anti-PrP mouse monoclonal 8H4 (indicated by small arrows) and the control for protein loading ß-tubulin of approximately 50 kDa was detected with a rat monoclonal anti-ß-tubulin (indicated by large arrow).

Figure 3.4 PK resistance of PrP from PrP glycosylation deficient transgenic and normally glycosylated control mice as analysed by western blot

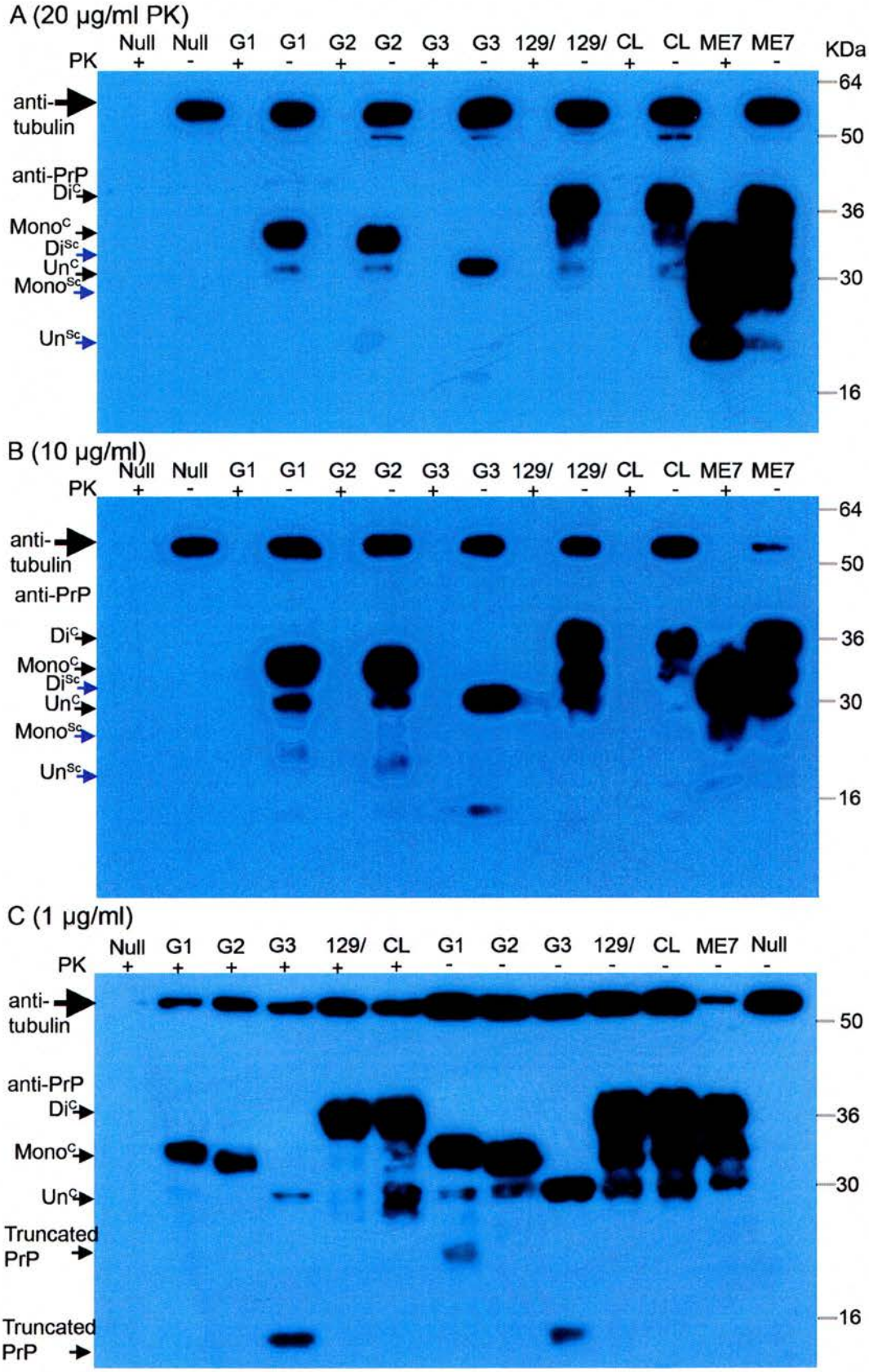

Figure 3.5 The PK resistance of PrP in aged G3 transgenic and control (CL) mice

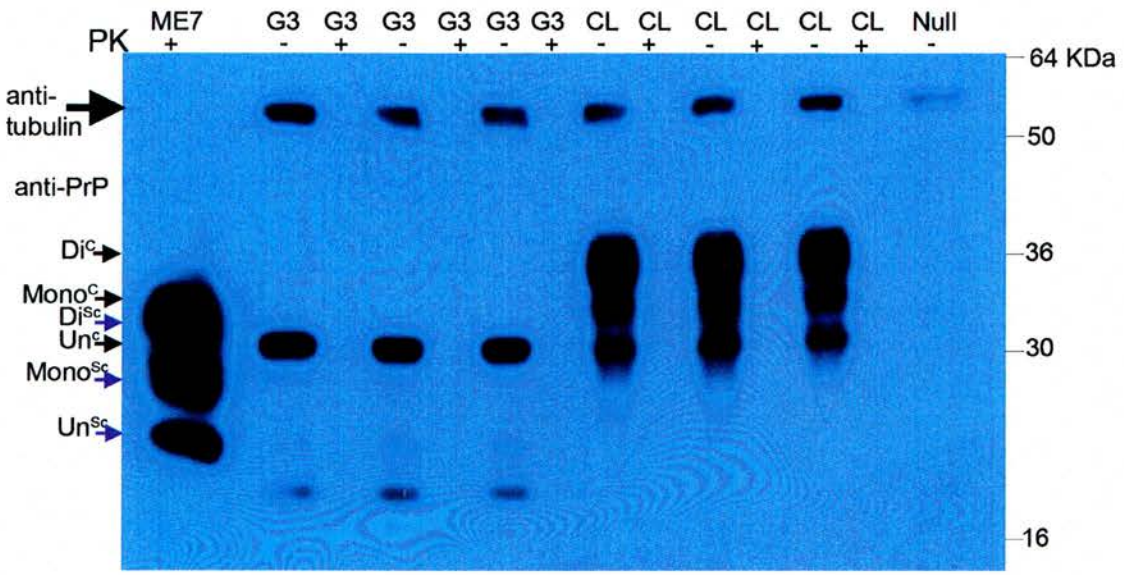

To investigate the PK resistance of PrP in aged G3 transgenic mice, total brain proteins from aged G3 transgenic and normally glycosylated (CL) control mice were treated for 1 hour at 37 °C with 20 µg/ml PK as indicated, denatured and western blotted, no PK resistant PrP was detected by this method in either the aged G3 or CL mice, despite clear detection of di-, mono- and un-glycosylated PrP^{C} in corresponding samples which were not treated with PK (indicated by small black arrows) and β-tubulin which was used as a control for the amount of total brain proteins loaded in each lane (large black arrow). A normally glycosylated control mouse, infected with ME7, which was at TSE clinical endpoint, was used as a control for PrP PK resistance, di-, mono- and un-glycosylated PrP^{Sc} (indicated with blue arrows).

3.4.5 The effect of glycosylation on PrP^C truncation

An increased incidence and quantity of PrP truncated forms were observed in the glycosylation deficient transgenic mice compared to normally glycosylated control mice (Figure 3.1 B, 3.4 and 3.5 A). The size difference observed between the truncated forms in the transgenic mice is likely to reflect the different predominant glycotypes of PrP in these mice. However, these truncated forms were not always observed in the murine PrP glycosylation deficient transgenics (Figure 3.1 A) and appeared more frequently in samples that had experienced longer storage at -80 °C. This variability suggests that the truncated products may be a result on the action of endogenous proteases in the total brain homogenate samples as has previously been reported (Jimenez-Huete et al., 1998). Furthermore, it appears that partially or completely un-glycosylated PrP is more sensitive to their action. Further experimentation is required to investigate this hypothesis and to asses whether if the processing of PrP^C is influenced by its N-glycosylation state *in vivo*.

3.4.6 Absence of PrP's N-glycans does not lead to the development of spontaneous clinical signs or TSE vacuolar pathology

Groups of twelve male and twelve female PrP glycosylation deficient transgenic mice, and normally glycosylated controls, were aged and assessed for the spontaneous development of TSE clinical signs over the natural life span of the animals using standard techniques (Dickinson et al., 1968). A number of animals of all genotypes survived in excess of 700 days (G1 = 5, G2 = 6, G3 = 5) and none exhibited clinical TSE disease. The brains from all aged animals were removed post-mortem and sagitally divided in two asymmetrically. The larger right halves were fixed for assessment of TSE vacuolar pathology by standard methods (Fraser and Dickinson, 1967; Fraser and Dickinson, 1968). No TSE specific vacuolation was detected in any genotype of the glycosylation deficient transgenic mice over the course of the aging experiment (n = 24 data not shown).

3.4.7 Results summary

These data demonstrate that the absence of PrP's N-glycans does not lead to spontaneous formation PrP^{Sc}-like properties *in vivo* or to a reduction in the steady state of PrP^{C}.

- The N180T and N196T substitutions prevent the *in vivo* glycosylation of PrP's first and second glycosylation site respectively and support the hypothesis that the combination of sugars attached at each site differ.
- Absence of PrP's N-glycans does not lead to the spontaneous formation of PrP^{Sc}-like properties but may elevate truncation of the protein.
- Absence of PrP's N-glycans does not lead to the spontaneous development of TSE clinical signs or TSE specific vacuolar pathology.

3.5 Discussion

3.5.1 Discussion of experimental techniques

Significance of the antibody dependent detection of PrP^{Sc}

Detection of PrP by DELFIA demonstrated significant antibody dependence in the detection of soluble and insoluble forms of PrP, and of different PrP glycotypes. This suggests that the antibodies used in these experiments may recognise subsets of PrP, consistent with their monoclonal nature. In particular, AG4 does not appear to recognise PrP that is insoluble in low concentrations of Gnd HCl. This suggests that in this form of PrP, that may be equivalent to PrP^{Sc}, the AG4 epitope is hidden. Thus this epitope is conformational and is irreversibly disrupted by the higher concentration of Gnd HCl used to solubilise the low concentration insoluble fraction; alternatively, the epitope may be shielded in the PrP^{Sc}-like form.

The apparent amount of PrP detected using AG4 appeared to be ten-fold higher than when FH11 was used to probe identical samples. Thus the ratio of wild type PrP relative to recombinant PrP differs between these antibodies. The structure of recombinant PrP has been reported to reflect that of mammalian PrP^{C} (Hornemann et al., 2004), suggesting that the observed difference in antibody recognition is not caused by differences in the conformation of the two forms. This differential recognition may be attributable to the absence of N-glycans or the GPI anchor from recombinantly produced PrP. However, as a similar difference in the ratio of FH11 to AG4 signal is also apparent for samples from G3 transgenic mice, in which PrP is un-glycosylated, it seems unlikely that the difference is caused by the un-glycosylated state of recombinant PrP. Alternatively, the binding of native PrP to the capture antibody may be modified by other molecules in the total brain homogenate used in this assay; experimental data measuring the binding of recombinant PrP in the presence of PrP null brain homogenate are required to investigate this possibility.

The observed antibody dependence of the amount of PrP detected in the glycosylation deficient transgenic mice may be caused by differences in the interaction of PrP in these samples with other cellular factors. Further experimentation is required to address this possibility. Equally the antibodies used in these studies may differentially recognise G1, G2, G3 and wild type PrP or the predominant glycotypes in these samples. In particular, the epitope of 8H4 is located between amino acid 175 and 185 (Zanusso et al., 1998). Therefore the N180T substitution in the G1 and G3 transgenic mice may alter the interaction of these transgenic forms of PrP with this antibody. Indeed, the amount of PrP^C (1M Gnd HCl soluble) detected using 8H4 is increased in both the G1 and G3 transgenic mice relative to normally glycosylated controls. Previous reports have suggested that 8H4 recognises un-glycosylated recombinant PrP as well as the glycosylated form, although PrP in this study did not carry the N180T substitution (Zanusso et al., 1998). Similarly, the reduced level of PrP^C detected in the murine PrP glycosylation deficient transgenics, as compared to controls when an AG4 capture antibody is used, may reflect a partial glycosylation requirement for this antibody's epitope. Alternatively, this result may be attributable to the apparent inability of AG4 to recognise all conformations of PrP.

3.5.2 Discussion of experimental results

3.5.2.1 Differences in the molecular weight of G1 and G2 mono-glycosylated PrP^C

Previous studies have demonstrated that the molecular weight of the sugars attached at the first and second site differs (Moudjou et al., 2004; Stimson et al., 1999). Electro-spray mass spectrometry analysis has suggested this is owing to a different subset of sugars being attached at the two sites, in particular the preferential addition of sialyl Lewis-x residues at the second site (Stimson et al., 1999). The difference in molecular weight of mono-glycosylated PrP^C in the G1 and G2 transgenic mice is consistent with the observed molecular weight of the first and second site mono-

glycosylated form in normally glycosylated PrP^C (Stimson et al., 1999). This suggests that the glycans attached to PrP^C in G1 and G2 transgenic mice are representative of the wild type mono-glycosylated forms. However, further experimentation is required to determine the precise glycan composition attached at the two sites in the PrP transgenic mice and during normal CNS glycosylation of PrP. Previous work has demonstrated that more than forty different combinations of glycans are attached to PrP *in vivo* (Pan et al., 2002), although some of this diversity may represent cell type specific forms, although multiple glycan combinations are likely to occur in the same cells. Additionally, the relative abundance of the two mono-glycosylated forms for normally glycosylated PrP is unknown. N-Glycan addition is governed by the local primary sequence surrounding the glycan attachment site and by the folding dynamics and global conformation of the protein, in addition to cell type specific variation in the N-glycan pool (Petrescu et al., 2004). These differences in glycan composition will impact on the interaction of the entire N-glycan with other molecules, including the protein to which it is attached. Hence they may have a major impact on the function of PrP^C.

3.5.2.2 Glycosylation of PrP does not affect the steady state levels of the protein *in vivo*

Glycosylation is known to increase the half life of a number of proteins (Chen et al., 2006; Li et al., 2004). This may occur via a number of mechanisms including enhanced resistance to proteolytic attack or reduced endocytosis and lysomal targeting. Glycosylation is also known to specifically contribute to the stability of mutant protein forms (Buck et al., 2004). This is thought to occur by N-glycan mediated interactions with ER chaperones preventing the ERAD export of proteins that are slow to fold or are misfolded. In particular, a number of pathological mutant forms of PrP are stabilised by the attachment of N-glycans in cell culture systems (Capellari et al., 2000a; Lehmann and Harris, 1996a; Petersen et al., 1996; Singh et al., 1997).

However, here we show, by direct comparison with normally glycosylated PrP, that the steady state level of PrP^C is unchanged by the absence of the first, second or both glycosylation sites *in vivo*. Thus either the half-life of wild-type PrP is independent of its glycosylation state or a compensatory up-regulation of PrP translation occurs in these transgenic mice. Previous work has shown that the *Prnp* mRNA levels in these transgenic mice are comparable to the level in wild type mice of the same genetic background, negating the second scenario (Cancellotti et al., 2005; Wiseman, 2003). Therefore glycosylation of PrP does not appear to be necessary to prevent ERAD or post-ER degradation of wild type PrP. Therefore, any influence of the absence of the first, second or both glycosylation sites on PrP^C function or role in TSE disease pathogenesis in these models will not be mediated by differences in the amount of PrP^C.

3.5.2.3 Absence of PrP's N-glycans does not lead to spontaneous formation of PrP^{Sc} *in vivo*.

Cell culture studies have suggested that, in the absence of its N-glycans, PrP adopts a PrP^{Sc}–like form, displaying enhanced PK resistance and insolubility (Lehmann and Harris, 1997). A number of transgenic PrP murine models have also demonstrated that PrP can spontaneous misfold *in vivo* in the absence of exposure to the TSE agent; however, in all these models spontaneous PrP^{Sc} formation was only observed when PrP was highly overexpressed (Castilla et al., 2005; Chiesa et al., 1998; Hsiao et al., 1990; Ma et al., 2002; Muramoto et al., 1997; Nazor et al., 2005; Shmerling et al., 1998). No spontaneous misfolded PrP was detected in the glycosylation deficient transgenic mice including by a PK independent method of insolubility in a low concentration of Gnd HCl. Furthermore, no spontaneous PK resistance was observed even in aged G3 transgenic mice, in which maximal accumulation of misfolded forms might be anticipated to occur owing to the age related decline of protein folding and clearance mechanisms (Erickson et al., 2006). Thus when expressed at endogenous levels, glycosylation of PrP is not required to prevent the spontaneous misfolding of the protein *in vivo* within the normal lifespan of the mouse. These data suggest that the primary role of PrP's highly conserved N-

glycans is not to stabilise the protein. However, this does not negate the possibility that the glycans prevent conformational change under perturbed conditions, as may occur when a host is exposed to the TSE agent. Additionally, glycosylation of PrP may help stabilise the soluble PrP conformation in the presence of pathogenic mutations in the primary amino acid sequence as has been previously suggested (Capellari et al., 2000a; Petersen et al., 1996). Consistent with these conclusions is the observation that the glycosylation deficient transgenic mice do not spontaneously develop TSE clinical signs. Thus these models can validly be used to investigate the importance of PrP's N-glycans to the TSE species barrier.

Recent work has suggested that PrP's N-glycans retard the formation of dimeric PrP in cell culture, as indicated by slower electrophorectic mobility of a fraction of total PrP (Biswas et al., 2006). During the characterisation studies of PrP^C in the glycosylation deficient transgenic mice, no form of dimeric PrP were observed. In the original cell culture study, glycosylation of PrP^C was disrupted by removal of the C-terminus of the protein including the GPI anchor. The observed enhanced dimerisation in this model therefore may be attributable to the absence of the anchor rather than a direct effect of glycosylation status. Indeed, previous work has suggested that dimerisation of PrP may be promoted by glycosylation of the protein (Meyer et al., 2000). Further specific experimental investigations are required to investigate the effect of glycosylation state on the occurrence of PrP dimers *in vivo* in the murine glycosylation deficient transgenics, such as the use of cross-linkers or size exclusion chromatography.

In conclusion, the biochemistry of PrP in the murine glycosylation deficient transgenics resembles that of wild type mice, save for the alteration of the protein's glycosylation state. Thus these murine transgenic models are a valid system in which to investigate the role of PrP's N-glycans in the cross-species transmission of the TSE agent.

4.0 Glycosylation of PrP^C and the localisation of the protein *in vivo*

4.1 Aim To determine if the cellular location of PrP^C is altered *in vivo* by absence of the protein's N-glycans.

4.2 Introduction and experimental technique

The cellular localisation of PrP^C is thought to be key in determining the protein's misfolding during TSE disease, in addition to its importance to the protein's native function (Caughey et al., 1991; Rudd et al., 2001). Experiments in which the subcellular location of PrP^C has been altered have demonstrated changes in TSE disease susceptibility or the ability to form PrP^{Sc} (Caughey et al., 1991; DeArmond et al., 1998; Taraboulos et al., 1992b; Verghese-Nikolakaki et al., 1999; Vetrugno et al., 2005). However, the *in vivo* location of the PrP^C to PrP^{Sc} conversion event is currently unknown, although a number of potential site have been suggested including lysosomes, endosomes and the plasma membrane (Caughey et al., 1991; Taraboulos et al., 1992b; Taraboulos et al., 1995). Furthermore, the preferred site of conversion within the cell may differ between TSE strains. Additionally, experimental studies using transgenic models have suggested that aberrant localisation of PrP to the cytoplasm is neurotoxic, although this finding has been contested by a number of other published works (Drisaldi et al., 2003; Fioriti et al., 2005; Ma et al., 2002; Roucou et al., 2003).

Previous work has shown that normally glycosylated PrP^C is principally located on the plasma membrane within lipid rafts *in vivo* (Barmada et al., 2004; Haeberle et al., 2000; Laine et al., 2001; Mironov et al., 2003; Sales et al., 1998; Vey et al., 1996). Limited amounts of intracellular PrP^C are also apparent in the majority of cells and a minor subpopulation of cells have high levels of PrP^C throughout the cytoplasm (Barmada et al., 2004; Mironov et al., 2003). Glycosylation of PrP^C has been suggested to influence the cellular localisation of the protein (Capellari et al., 2000b;

DeArmond et al., 1997; Korth et al., 2000; Lehmann and Harris, 1997; Neuendorf et al., 2004; Rodolfo et al., 1999; Rogers et al., 1990; Russelakis-Carneiro et al., 2002) (Chapter 1). The localisation of PrP^C may be altered in the murine PrP glycosylation deficient transgenics [NPU]; this could affect the ability of the protein to participate in TSE disease.

Subcellular localisation of PrP^C in uninfected murine glycosylation deficient transgenics (NPU) was investigated in sections of adult brain. Immunofluorescence and confocal microscope analysis was used; as immunohistochemistry would not have provided the degree of resolution required to assess the subcellular localisation. Paraffin embedding and dehydration of brain materials have been suggested to disrupt the plasma membrane and reduce detectable PrP^C (Laine et al., 2001; Mironov et al., 2003). Indeed, standard embedding and dehydration techniques completely eliminate detectable PrP in uninfected murine brains, even when signal amplification kits are employed (Chapter 5). To avoid elimination of detectable PrP, whole uninfected brains were lightly fixed and rapidly processed. Sections were not mounted and immunofluorescence was carried out using a free-floating method (Monaghan et al., 2001). GPI proteins like PrP are prone to antibody mediated rearrangement in conventionally fixed tissues (Mayor et al., 1994). Although previous studies have suggested this is not the case for PrP^C, a range of fixation conditions were investigated (Laine et al., 2001; Mironov et al., 2003). A number of antibodies were screened to identify those which could successfully and specifically detect endogenous expression of PrP^C *in vivo*. Colocalisation studies using a marker of the ER (Endoplasmic Reticulum) or Golgi were then undertaken to determine if in the absence of its N-glycans, PrP^C accumulated in these compartments.

4.3 Optimisation and validation of experimental technique

4.3.1 Anti-PrP antibody screen

Seven anti-PrP monoclonal and polyclonal antibodies were screened for the effective and specific detection of PrP^C by immunofluorescence in whole brain sections from 129/Ola wild type and PrP null mice. No specific signal was detected for the polyclonals 1B3, 1A8 or mouse monoclonals 7A12, FH11 or AG4 (data not shown). A strong and specific signal was observed for 8H4 in accordance with previous reports (Laine et al., 2001; Liu et al., 2001; Mironov et al., 2003) (Figure 4.1 A). Optimum 8H4 antibody concentration was experimentally determined to be 1/1000 for staining of PrP alone and 1/500 for colocalisation experiments (data not shown). The IgG1 isotype of 8H4 was experimentally confirmed for use in colocalisation experiments (Liu et al., 2001) (Figure 4.2 C and D). A weaker specific anti-PrP signal was observed for AH6 (Figure 4.1 B). The staining pattern of Ah6 observed in 129/Ola mice was similar to that observed for 8H4. However the signal was too weak for complete confocal analysis.

4.3.2 Use of the Mouse on Mouse blocking kit

During preliminary experiments, non-specific binding of the anti-mouse Alexa conjugated secondary antibody to blood vessels was observed (Figure 4.1 C and D). This may be mediated by interaction of the antibody with murine immunoglobulins carried in the blood. The effectiveness of the Mouse on Mouse (MOM) blocking kit (Vector Laboratories) to reduce this non-specific background was investigated. This kit is designed to specifically block the interaction of anti-murine secondary antibodies with mouse immunoglobulins. The observed non-specific interaction of the anti-mouse secondary antibody with the brain sections was reduced by the MOM blocking kit. However use of the blocking kit also reduced the detection of PrP^C by 8H4, but, because of the great reduction in non-specific staining the kit was used in all experiments (Figure 4.2 A and B).

Figure 4.1 Immunofluorescent localisation of PrP in sections of the hippocampus using different anti-PrP monoclonals.

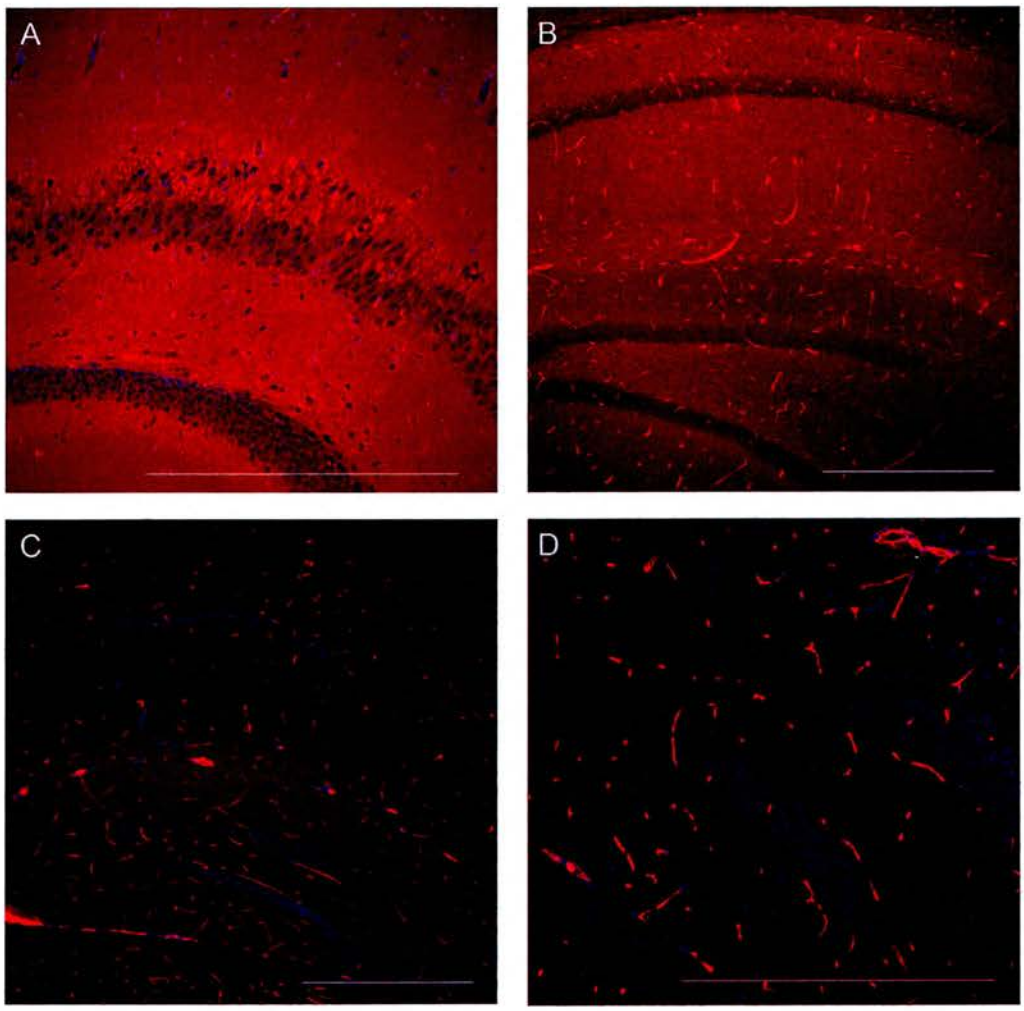

Localisation of PrP in the hippocampus was examined in (A & B) 129/Ola 70 µm sections using equivalent (C & D) PrP null sections as controls for specificity of antibody binding. Two anti-PrP mouse monoclonal antibodies were investigated (A & C) 8H4 1/1000 and (B & D) AH6 1/1000 both were detected using 1/200 anti-mouse Alexa568. Scale bar 500 µm.

Figure 4.2 Comparison of anti-PrP (8H4) staining in 129/Ola brain sections using different methods.

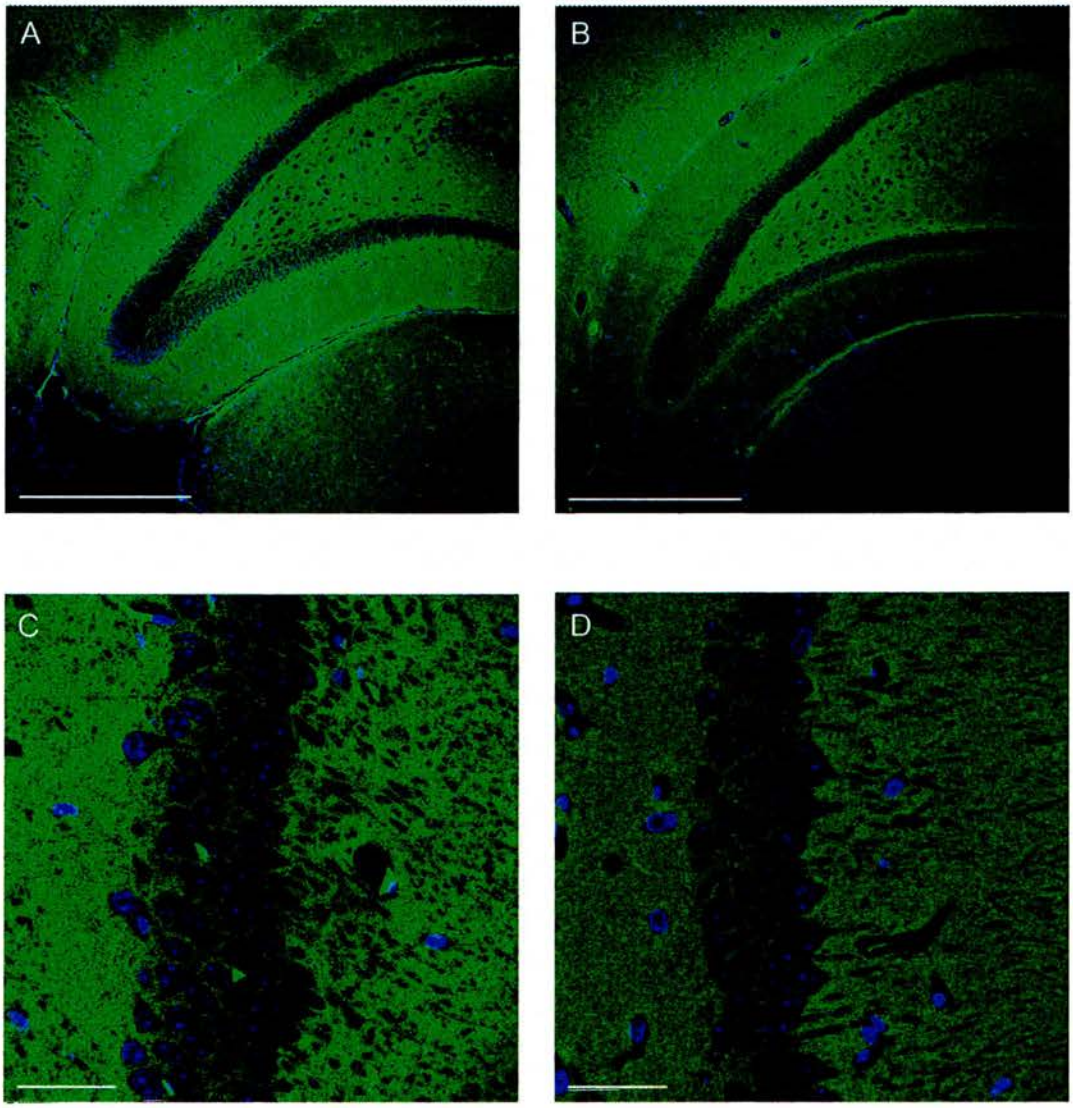

Comparison of 8H4 staining in the dentate gyrus and portion of the thalamus (1/1000 8H4, 1/200 anti-mouse Alexa488) with (B) and without (A) use of the MOM blocking kit. Note the absence of blood vessel staining within the thalamus in B. Binding of IgG1 specific Alexa488 antibody (C) to 8H4 is less efficient that that of 1/200 anti-mouse Alexa488 (C). Area shown is the pyramidal cell layer and adjacent neuropil similar results observed for other brain regions. Scale bar (A & B) 500 µm, (C & D) 50 µm.

4.3.3 Comparison of tissue fixation conditions

The cellular localisation of GPI anchored proteins, like PrP, may be altered by the fixation conditions used (Mayor et al., 1994). To investigate the importance of fixation to PrP immunofluorescence whole brains were fixed by post-mortem immersion: in 4 % paraformaldehyde; 0.025 % glutaraldehyde 4 % paraformaldehyde; 0.25 % glutaraldehyde 4 % paraformaldehyde; or periodate-lysine-paraformaldehyde (PLP). No alteration in the subcellular localisation of normally glycosylated PrP^C was observed under the different fixation conditions investigated, consistent with previous reports (Laine et al., 2001; Liu et al., 2001; Mironov et al., 2003). In contrast to previous reports, PLP did not enhance PrP^C antigenicity, perhaps because of the different antibody used here (DeArmond et al., 1987).

However a dramatic decrease in detectable PrP^C at the surface of the brain was observed when the fixative contained glutaraldehyde (Figure 4.3 B). The area of PrP^C signal decrease was greater for the higher concentration of glutaraldehyde and for longer fixation intervals, indicating that this effect may be caused by the degree of penetration of glutaraldehyde. This surface decrease in signal was not observed for detection of tubulin in glutaraldehyde fixed tissue (Figure 4.3 C). Thus the use of low concentrations of glutaraldehyde fixation appeared to selectively eliminate the 8H4 epitope. Previous reports have observed a reduction in the detection of murine PrP^C by using 8H4 and hamster PrP^C by 3F4 after glutaraldehyde fixation (Laine et al., 2001; Moya et al., 2000). Indeed one group has generated specific antibodies against glutaraldehyde fixed PrP to circumvent this problem (Ford et al., 2002a). However, the use of glutaraldehyde during fixation generated a hard edge to the tissue which facilitated the cutting of sections and prevented the break-up of sections during the experiment. All tissue was fixed in 0.025 % glutaraldehyde and 4 % paraformaldehyde to facilitate experimental manipulation and fixation time was reduced to 3 hours 30 minutes to minimise surface loss of PrP^C signal owing to use of glutaraldehyde. PrP^C localisation data were not collected from areas in which 8H4 signal was reduced because of fixation.

Figure 4.3The effect of glutaraldehyde fixation on 8H4 epitope availability

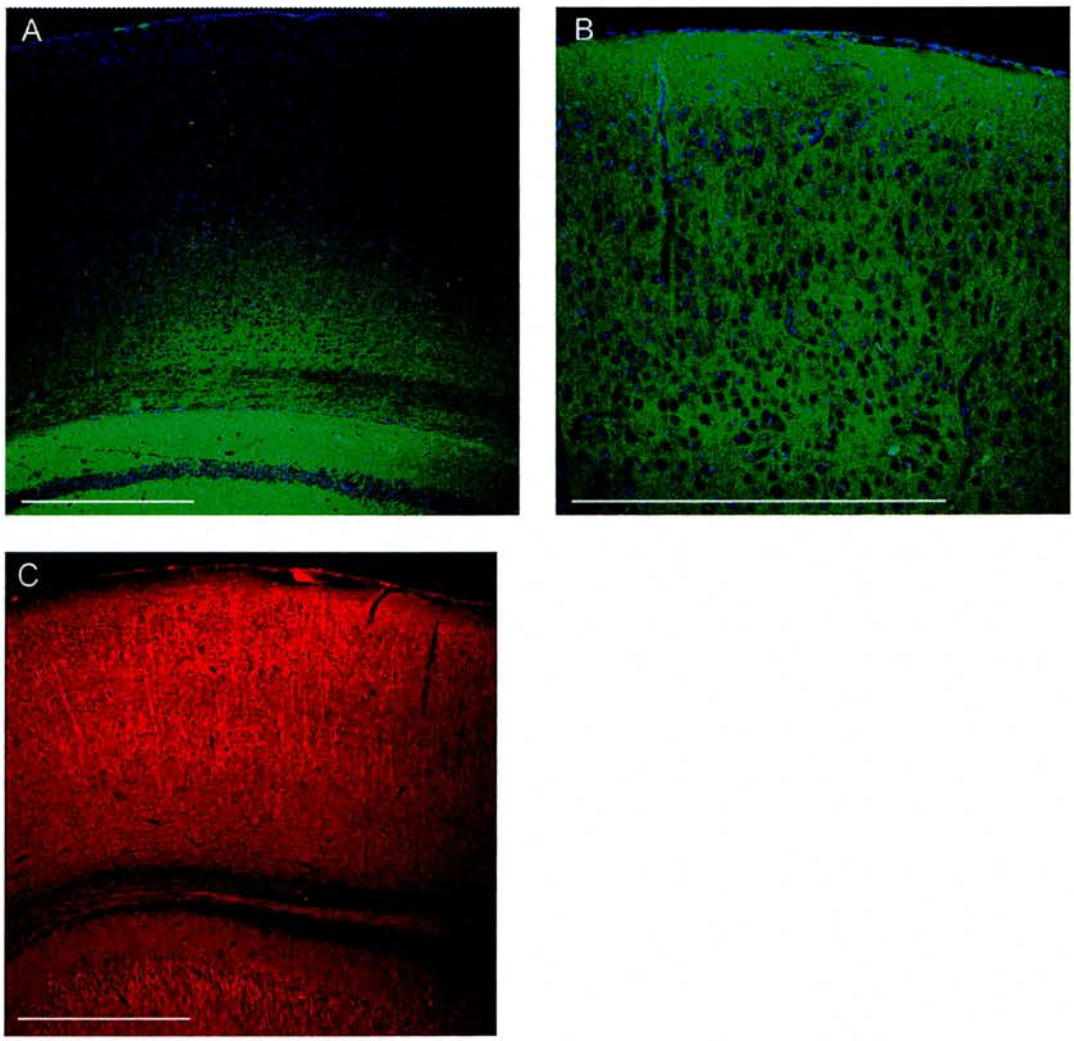

Use of glutaraldehyde during fixation of brain tissue selectively destroys the 8H4 PrP epitope (A) but not that of tubulin (C). The 8H4 epitope is maintained if tissue is fixed by paraformaldehyde alone (B). A & B) 1/1000 anti-PrP 8H4, 1/200 anti-mouse Alexa488 C) 1/1000 anti-tubulin, 1/200 anti-mouse Alexa568. A & B) 129/Ola; C) PrP null. Tissue fixed in A & C) 4% paraformaldehyde, 0.25 % gluteraldehyde; B) 4% paraformaldehyde. Scale bar 500 µm.

4.3.4 Antibody screen markers of the ER and Golgi

Two ER lumen marker antibodies, anti-PDI, a mouse, monoclonal antibody, and anti-ERp60, a rabbit polyclonal antibody (kind gift of T. Wileman, IAH-Pirbright), were investigated to determine if they were compatible with 8H4 for immunofluorescence. Clear anti-PrP and anti-ERp60 staining were observed on wild type brain sections (Figure 4.4 A). Additionally, no cross reactivity between 8H4 and the anti-rabbit secondary antibody, nor anti-ERp60 and the anti-mouse secondary antibody was detected (Figure 4.4 B and C). Thus anti-ERp60 was an 8H4 compatible ER marker. As both 8H4 and anti-PDI are mouse monoclonal antibodies a two part staining strategy was employed. Sections were first incubated with anti-PDI antibody, then the first anti-mouse secondary antibody. These sections were then blocked with MOM kit, incubated with 8H4 and finally the second anti-mouse secondary antibody. Alternatively, 8H4 was used first and anti-PDI second. Despite the two-step staining technique, cross reactivity between these two mouse monoclonal antibodies was apparent (data not shown). Thus anti-PDI was unsuitable to determine if PrP^C was localised in the ER *in vivo* and only anti-ERp60 was used for further study.

Three Golgi marker antibodies were investigated. The signals for rabbit polyclonal anti-ß-cop (kind gift of T. Wileman, IAH-Pirbright) and GM130 antibodies on murine brain sections were too weak and non-specific for confocal analysis and thus were not used for the PrP^C colocalisation study (data not shown). A low level of cross reactivity occurred between the 23C anti-ß-cop, which is a rat monoclonal antibody, and the anti-mouse secondary antibody used (data not shown). Thus it was necessary to use an anti-mouse IgG1 subclass specific secondary antibody for 8H4 detection for these experiments, which eliminated cross reactivity (Figure 4.4), or to carry out a two-step staining strategy (data not shown). The IgG1 specific secondary antibody was less efficient in its detection of 8H4 compared to the general anti-mouse secondary antibody (Figure 4.3). Despite this lower sensitivity, apparently intracellular PrP could still be detected in the 23C colocalisation experiment. Thus this antibody was suitable to use in the PrP^C colocalisation study.

Figure 4.4 Antibody screen for markers of the ER and Golgi

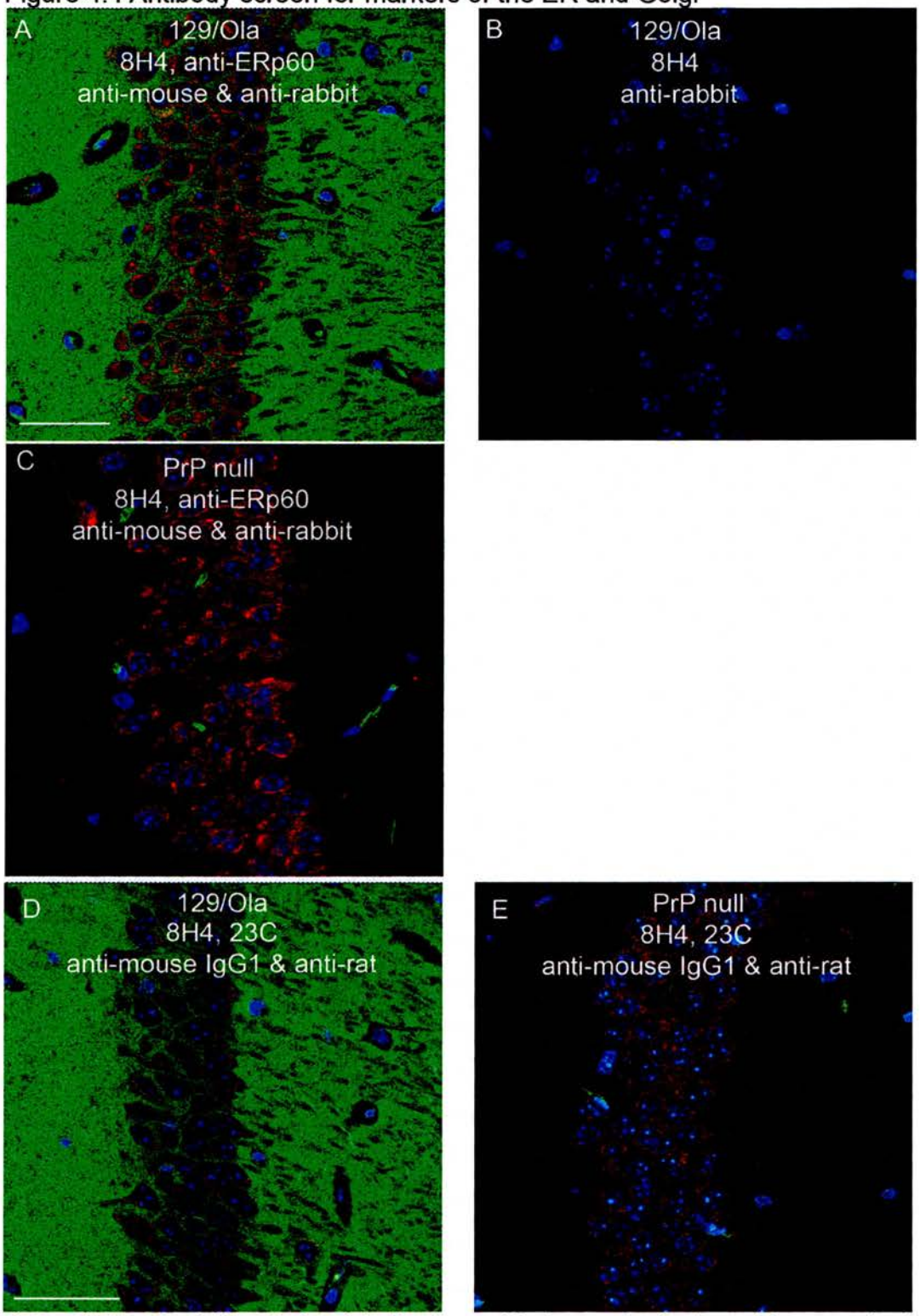

The anti-ERp60 rabbit polyclonal antibody can bind to murine brain and is recognised by an anti-rabbit Alexa568 conjugated secondary antibody (red channel A & C). The anti-rabbit Alexa568 conjugated secondary antibody does not interact with 8H4 (red channel B) and the anti-mouse Alexa488 conjugated secondary antibody does not interact with anti-ERp60 (green channel C). Therefore anti-ERp60 and 8H4 are suitable for colocalisation studies. The antibody 23C which recognises beta-cop on the outer leaflet of the Golgi apparatus can bind to murine brain and is recognised by anti-rat Alexa568 conjugated secondary antibody (red channel D and E). Anti-mouse IgG1 Alexa488 conjugated secondary antibody does not interact with 23C (green channel E). Therefore 23C and 8H4 are suitable for colocalisation studies. Scale bar 50 µm

4.4 Experimental results

4.4.1 The role of glycosylation of PrP^C in the protein's *in vivo* localisation

Previous work has suggested that subcellular localisation of PrP^C may be altered by the protein's glycosylation state (Capellari et al., 2000b; DeArmond et al., 1997; Korth et al., 2000; Lehmann and Harris, 1997; Neuendorf et al., 2004; Rodolfo et al., 1999; Rogers et al., 1990; Russelakis-Carneiro et al., 2002). The localisation of PrP^C in whole coronal brain sections was compared between PrP glycosylation deficient transgenic [NPU] and 129/Ola control mice, to determine if the protein's localisation was influenced by its glycosylation state *in vivo*. The animals from which the brain tissue was taken were age and sex matched, and were between 6-32 weeks old. PrP null brain sections, incubated with 8H4, were used in all experiments to determine the level of specific anti-PrP signal. Analysis was principally focussed on the hippocampus, as previous work has demonstrated this is an area of high PrP^C expression (Bendheim et al., 1992; DeArmond et al., 1987; Liu et al., 2001; Manson et al., 1992a; Mironov et al., 2003; Moya et al., 2000; Sales et al., 1998; Taraboulos et al., 1992a). Also, by using the clear anatomical features of the hippocampus, equivalent areas from transgenic and control mice could be matched. The intracellular localisation of PrP^C was analysed in the clearly defined hippocampal cell layers (pyramidal and granular). Additionally, previous studies examining the importance of glycosylation state to PrP^C's localisation have focussed on this region (DeArmond et al., 1997). Three sections were examined from each brain to control for potential regional differences in PrP^C localisation.

In 129/Ola controls, in which PrP is normally glycosylated, anti-PrP specific staining was observed throughout the neuropil (axon-synapse-dendrite complex) of the hippocampus, cerebral cortex and thalamus (Figure 4.5). Some anti-PrP signal was observed in the corpus collosum but the signal was weaker than the surrounding neuropil. The staining pattern was consistent with surface localisation of PrP^C on axons.

Figure 4.5 Comparison of anti-PrP (8H4) staining intensity between the PrP glycosylation deficient transgenics and controls in the neuropil.

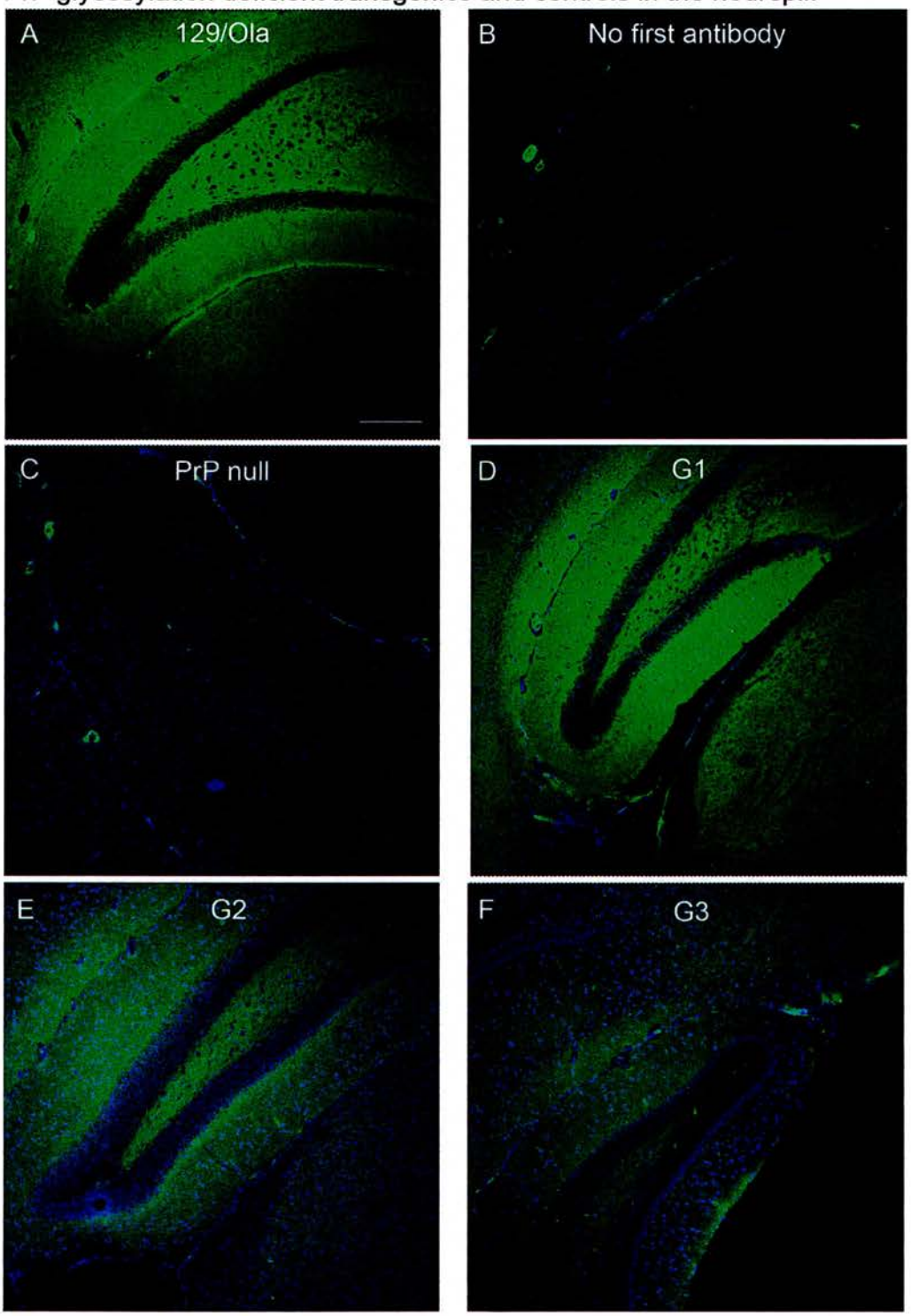

The amount of PrP detectable using 8H4 (1/1000) and anti-mouse Alexa488 (1/200) differs between the hippocampi of normally glycosylated 129/Ola mice (A) and some PrP N-glycan deficient G2 (E) and all G3 (F) transgenic mice. The amount and localisation of PrP detected in the hippocampi of G1 transgenic mice (D) is similar to that observed in control mice (A). All images were taken using the same microscope settings. Specificity of anti-mouse Alexa488 secondary antibody is demonstrated by the absence of signal in a 129/Ola section incubated with anti-mouse Alexa488 (1/200) only (B) and the PrP null section (C) incubated with 8H4 (1/1000) and anti-mouse Alexa488 (1/200). Scale bar 250 μm.

Variation in the intensity of PrP^C staining was observed in the neuropil of the hippocampus. Higher levels of signal were detected in the neuropil adjacent to the granular cell layer of the dentate gyrus. In some cases slightly higher anti-PrP signal was detected in the stratum oriens and stratum radium than the stratum molecular. However this was not consistently observed in contrast to the clear results reported for hamster PrP^C (Mironov et al., 2003; Moya et al., 2000). No consistent difference in the staining intensity or pattern was observed between the anterior and posterior sections, although section to section differences in staining intensity were apparent (data not shown). This is likely to reflect variations in experimental technique rather than differences in PrP^C expression level.

Low levels of specific anti-PrP signal were detected within both the pyramidal and granular cell layers in 129/Ola brain sections. In the cell layers staining was principally observed in a pattern consistent with the expect localisation of PrP^C at the plasma membrane. At high magnification this staining was observed to be clustered in patches, in a pattern consistent with lipid raft localisation on the plasma membrane (Figure 4.6 A). Furthermore, low levels of intracellular signal were observed. The anti-PrP signal was excluded from the nucleus and formed discrete clusters in the cell, consistent with localisation within a subcellular compartment (Figure 4.6 A). The staining pattern observed is similar to previous work investigating the localisation of PrP^C *in vivo* (Barmada et al., 2004; Mironov et al., 2003; Moya et al., 2000; Sales et al., 1998). Thus this method is valid to analyse the effect of PrP^C's glycosylation state on its localisation *in vivo*.

A clear and consistent reduction of PrP signal in the neuropil was detected in transgenic mice expressing un-glycosylated PrP^C (G3) as compared to normally glycosylated PrP^C controls (Figure 4.5) (n = 3, assayed in triplicate). The ratio of intracellular to plasma membrane associated signal in the cell layer appeared to be elevated in the G3 transgenic mice and a pattern of staining consistent with plasma membrane localisation was not detected (Figure 4.6). This alteration in staining suggests that in the G3 transgenic mice little PrP is found at the plasma membrane.

Figure 4.6 Comparison of anti-PrP staining pattern in the molecular layer of the dentate gyrus and adjacent neuropil.

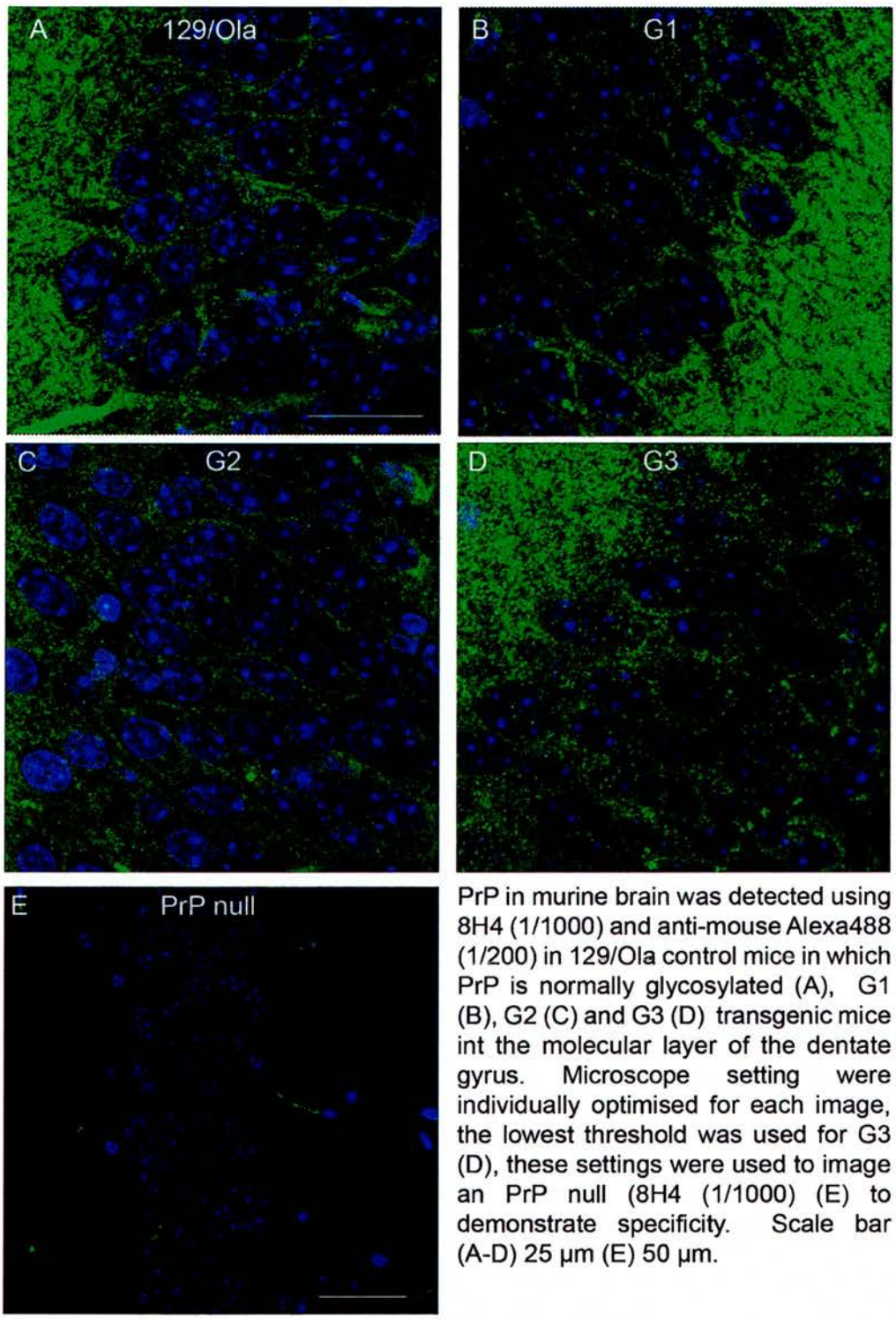

PrP in murine brain was detected using 8H4 (1/1000) and anti-mouse Alexa488 (1/200) in 129/Ola control mice in which PrP is normally glycosylated (A), G1 (B), G2 (C) and G3 (D) transgenic mice int the molecular layer of the dentate gyrus. Microscope setting were individually optimised for each image, the lowest threshold was used for G3 (D), these settings were used to image an PrP null (8H4 (1/1000) (E) to demonstrate specificity. Scale bar (A-D) 25 µm (E) 50 µm.

However specific anti-PrP signal above background was observed in the neuropil of G3 transgenic mice (Figure 4.5). This suggests that some PrP^C may be localised to the plasma membrane in the G3 transgenic mice, however further biochemical studies are required to investigate this.

Some variation was observed in the intensity of PrP^C detected in the neuropil on sections from G1 transgenic mice (n = 4). This is likely to reflect section to section variation rather than any underlying biological difference, as both higher and lower intensities than the wild type controls were observed. G2 sections generally displayed lower 8H4 neuropil staining intensity but the effect was not as dramatic that seen on G3 sections, and in some instances the intensity of anti-PrP staining in the neuropil was equivalent to that observed in 129/Ola controls (n = 4).

4.4.2 The role of glycosylation of PrP^C in the protein's cellular localisation

To determine if the pattern of intracellular localisation was changed in the G3 transgenic mice, colocalisation studies were undertaken. The absence of its N-glycans may lead to the retention of PrP^C in the ER/Golgi. This may occur via a direct effect on recognition of PrP^C for export out of the compartment, as a N-glycan may act as "tag for transport" (Rudd et al., 2001). Alternatively, the attached N-glycans may facilitate the folding of PrP^C within the ER and thus in their absence the protein may accumulate in this compartment because of its less efficient folding (Rudd et al., 2001). Therefore the colocalisation of anti-PrP signal with markers of both the ER and Gogli apparatus was studied.

4.4.2.1 Colocalisation of PrP^C and ER marker ERp60

Localisation of PrP^C within the ER has only been reported in one previous study (Laine et al., 2001). Colocalisation of PrP (8H4) with a marker of the ER lumen ERp60 (rabbit polyclonal, a kind gift of T. Wileman, Insitute for Animal Health (Pirbright)) was undertaken (Figure 4.7). The pattern of ERp60 staining differed between the pyramidal and molecular cell layers (Figures 4.8 and 4.9).

Figure 4.7 Absence of colocalisation of PrP (8H4) and a marker of the ER (anti-ERp60) in the pyramidal cell layer

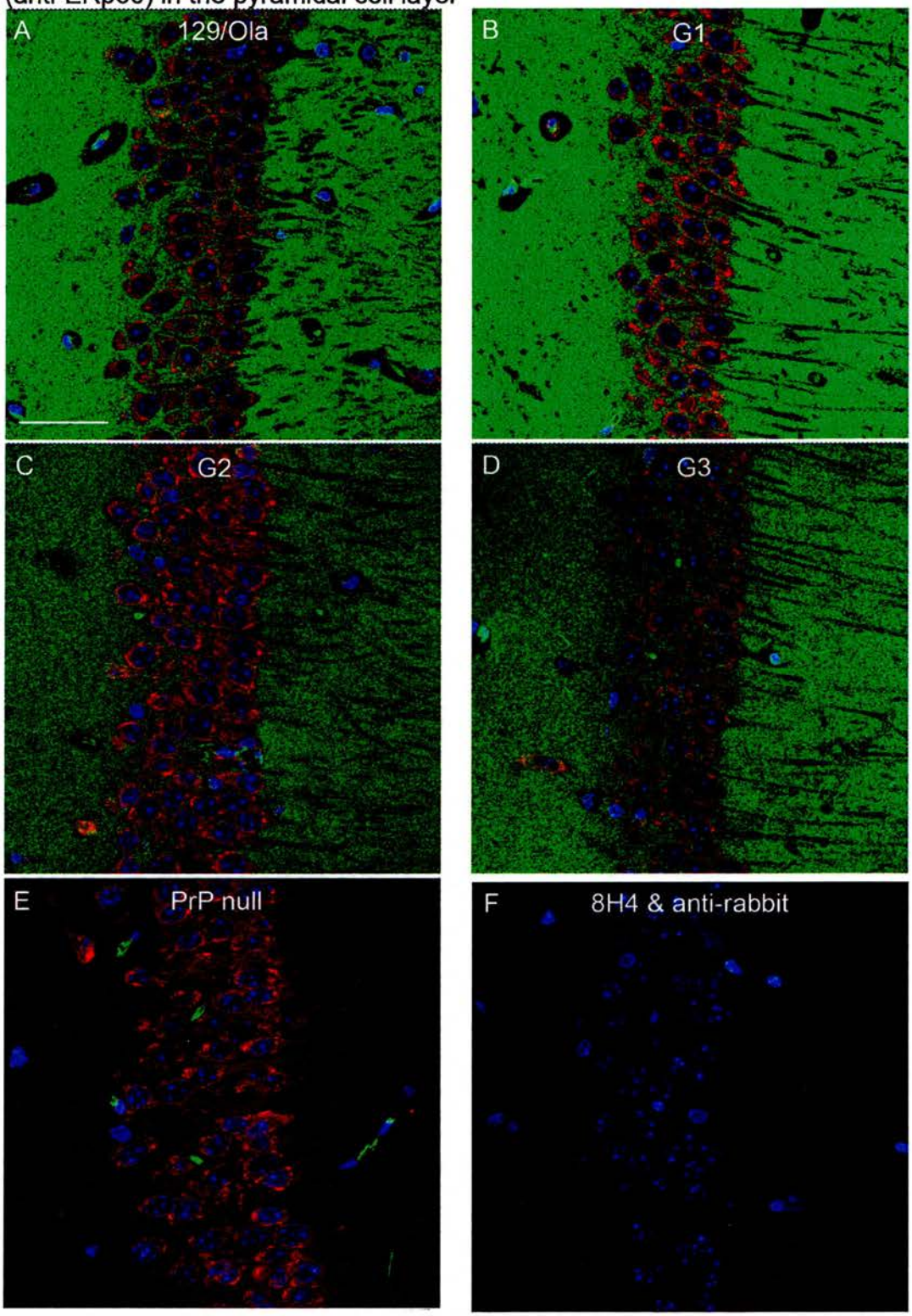

PrP (8H4 (1/500) anti-mouse Alexa488 (1/200) green) does not colocalise with a marker of the ER (anti-ERp60 (1/400), anti-rabbit Alexa568 (1/200) red) in normally glycosylated 129/Ola (A) nor PrP N-glycan deficient G1 (B), G2 (C) or G3 (D) transgenics in the pyramidal cell layer of the hippocampus. Microscope setting were individually optimised for each image, the lowest threshold was used for G3 (D); these settings were used to image an PrP nul (8H4 (1/500) and anti-mouse Alexa488 (1/200)) stained section (E). No cross reaction of 8H4 with the anti-rabbit secondary (8H4 (1/500), anti-rabbit Alexa568 (1/200)) was detected (F). Scale bar 50 µm

Figure 4.8 Close up of anti-PrP staining (8H4) and a marker of the ER (anti-ERp60) in the pyramidal cell layer of the hippocampus.

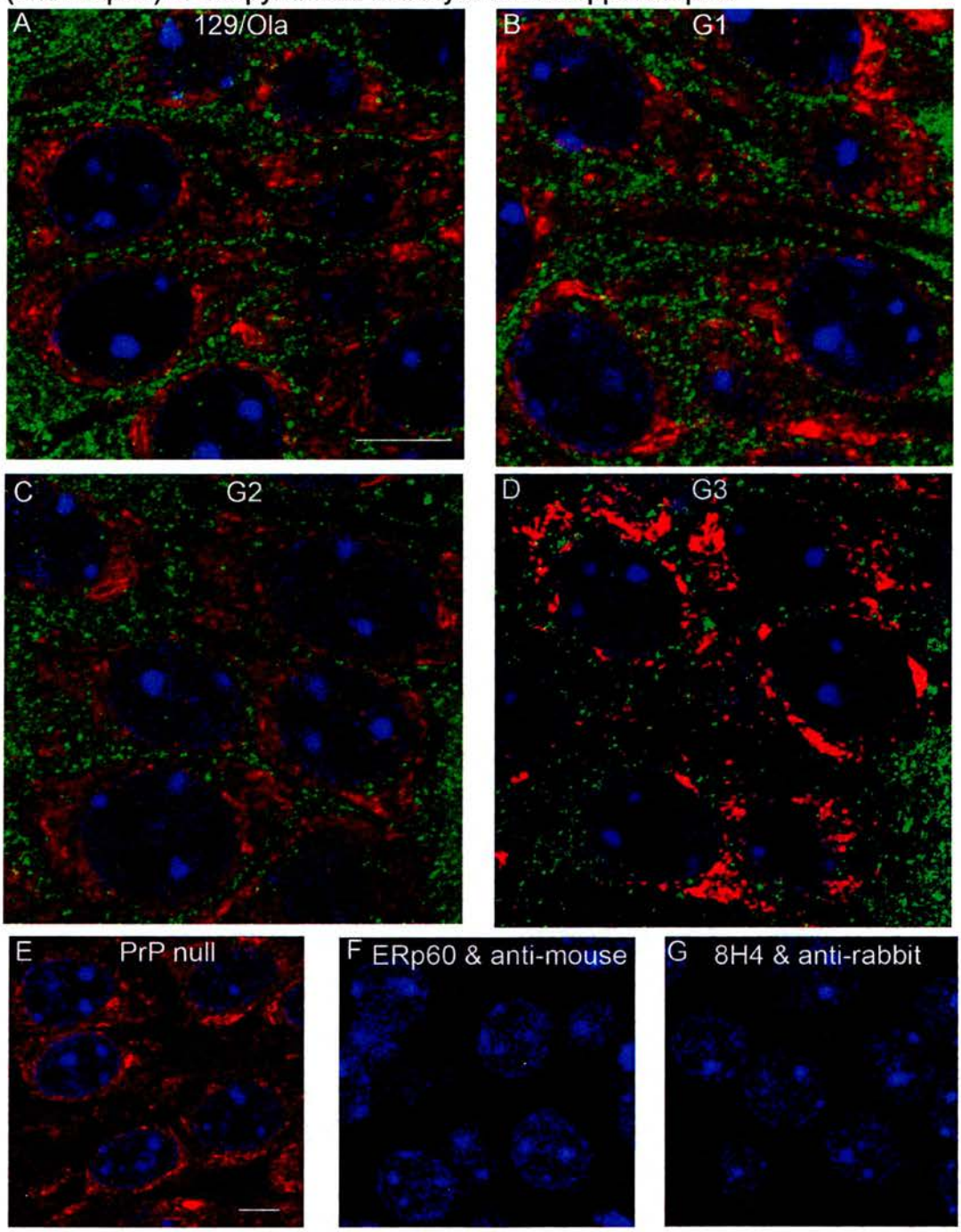

No colocalisation of an ER marker (anti-ERp60 (1/400), anti-rabbit Alexa568 (1/200) red) and PrP (8H4 (1/500) anti-mouse Alexa488 (1/200) green) (see arrows) is detected in normally glycosylated 129/Ola (A) nor PrP N-glycan deficient G1 (B), G2 (C) or G3 (D) transgenic mice in the pyramidal cell layer of the hippocampus. Microscope setting were individually optimised for each image, the lowest threshold was used for G3 (D); these settings were used to image an PrP null (8H4 (1/1000) and anti-mouse Alexa488 (1/200)) stained section (E). No cross reaction of anti-ERp60 and anti-mouse secondary (anti-ERp60 (1/1000), anti-mouse Alexa488 (1/200)) (F) nor 8H4 with the anti-rabbit secondary (8H4 (1/500), anti-rabbit Alexa568 (1/200)) (G) was detected. Scale bar 25 µm.

Figure 4.9 Close up of anti-PrP (8H4) staining and a marker of the ER (anti-ERp60) in the molecular cell layer of the dentate gyrus

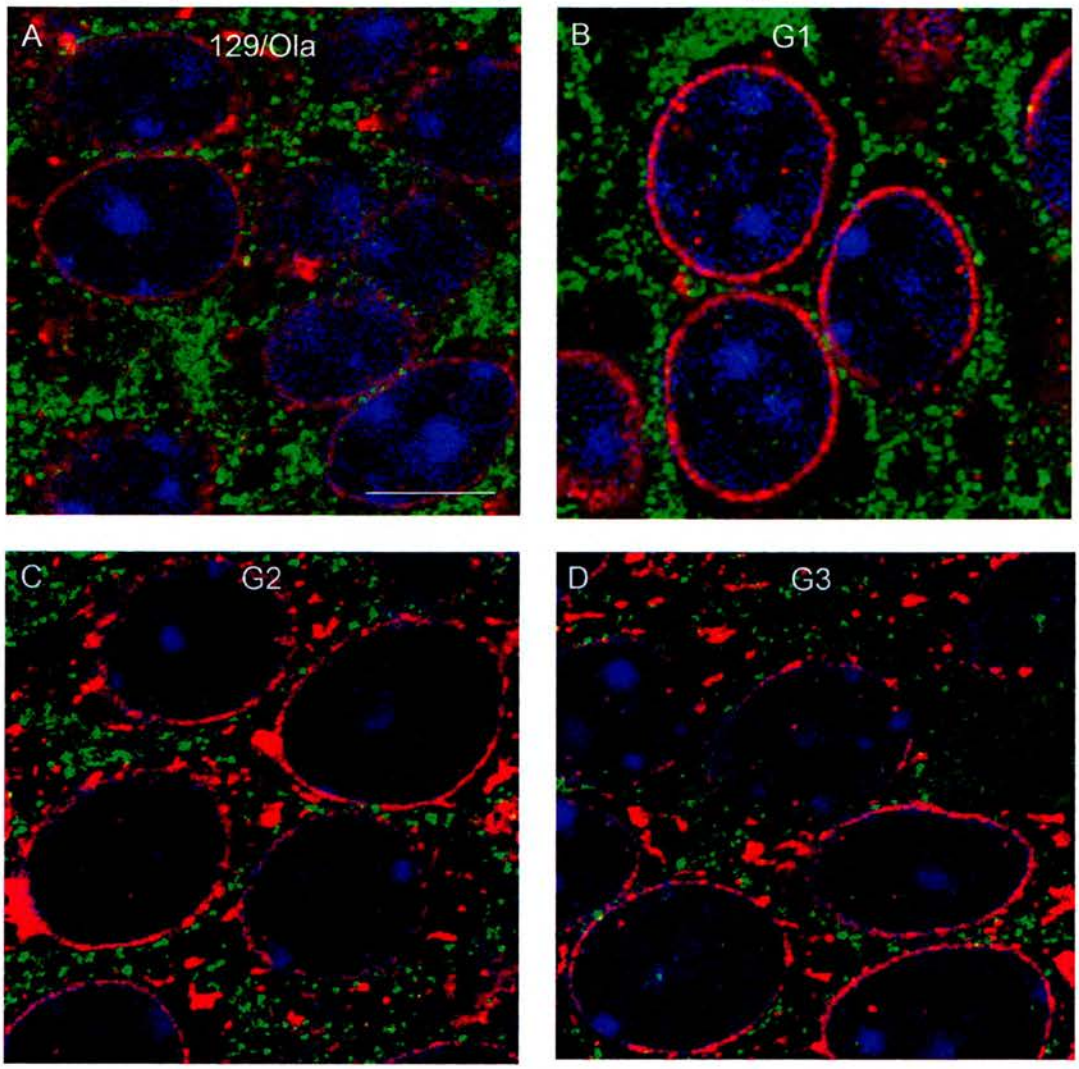

No colocalisation of an ER marker ERp60 (anti-ERp60 (1/400), anti-rabbit Alexa568 (1/200) red) and intracellular PrP (8H4 (1/500) anti-mouse Alexa488 (1/200) green) is detected in normally glycosylated 129/Ola (A) nor PrP N-glycan deficient G1 (B), G2 (C) or G3 (D) transgenic mice in the molecular cell layer of the dentate gyrus. Scale bar 25 μm.

In the molecular layer of the dentate gyrus ERp60 was localised almost exclusively surrounding the nucleus, in the classic ER pattern. In the pyramidal cell layer, in addition to perinuclear staining, extensive staining was observed in the cytoplasm of the cell body, in a pattern consistent with layered ER cisternae. No difference in pattern or intensity of ERp60 was observed between the controls and PrP glycosylation deficient transgenic mice. The pattern of 8H4 staining in these ERp60 colocalisation experiments was similar to that observed for single staining experiments, including the reduced neuropil intensity and higher intracellular to plasma membrane associated ratio observed in G3 sections. A higher threshold intensity was required to successfully image G3 sections compared to that needed for imagining the other transgenic mice and 129/Ola controls. In all cases the microscope settings used to image the G3 sections were also used to image all the negative controls.

No colocalisation or significant association of ERp60 and 8H4 was observed in the wild type or any of the PrP glycosylation deficient transgenic lines, in the cells of the hippocampus, overlying cortex or thalamus (Figures 4.8, 4.9 and data not shown) (n = 3). Indeed significant amounts of non-ER associated PrP^C could be observed in all sections, suggesting that the un- and mono-glycosylated PrP^C in the NPU murine PrP glycosylation transgenics is not retained the ER.

4.5.2.2 Colocalisation of PrP^C and Golgi/associated vesicles marker ß-cop

Colocalisation of PrP^C and a marker of the outer membrane of the Golgi and associated vesicles, ß-cop (rat monoclonal, 23C), was undertaken. 23C staining displayed a Golgi-like pattern of punctuate intracellular dots which were predominately located on one side of the nucleus in any one cell (Figure 4.10 and 4.11). These dots were observed to form rings in some cells which would appear to delineate the Golgi compartment (Figure 4.11). No difference in 23C staining pattern or intensity was observed between the control and transgenic brain sections.

Figure 4.10 Colocalisation of PrP (8H4) and a marker of the Golgi (23C) in the pyramidal cell layer.

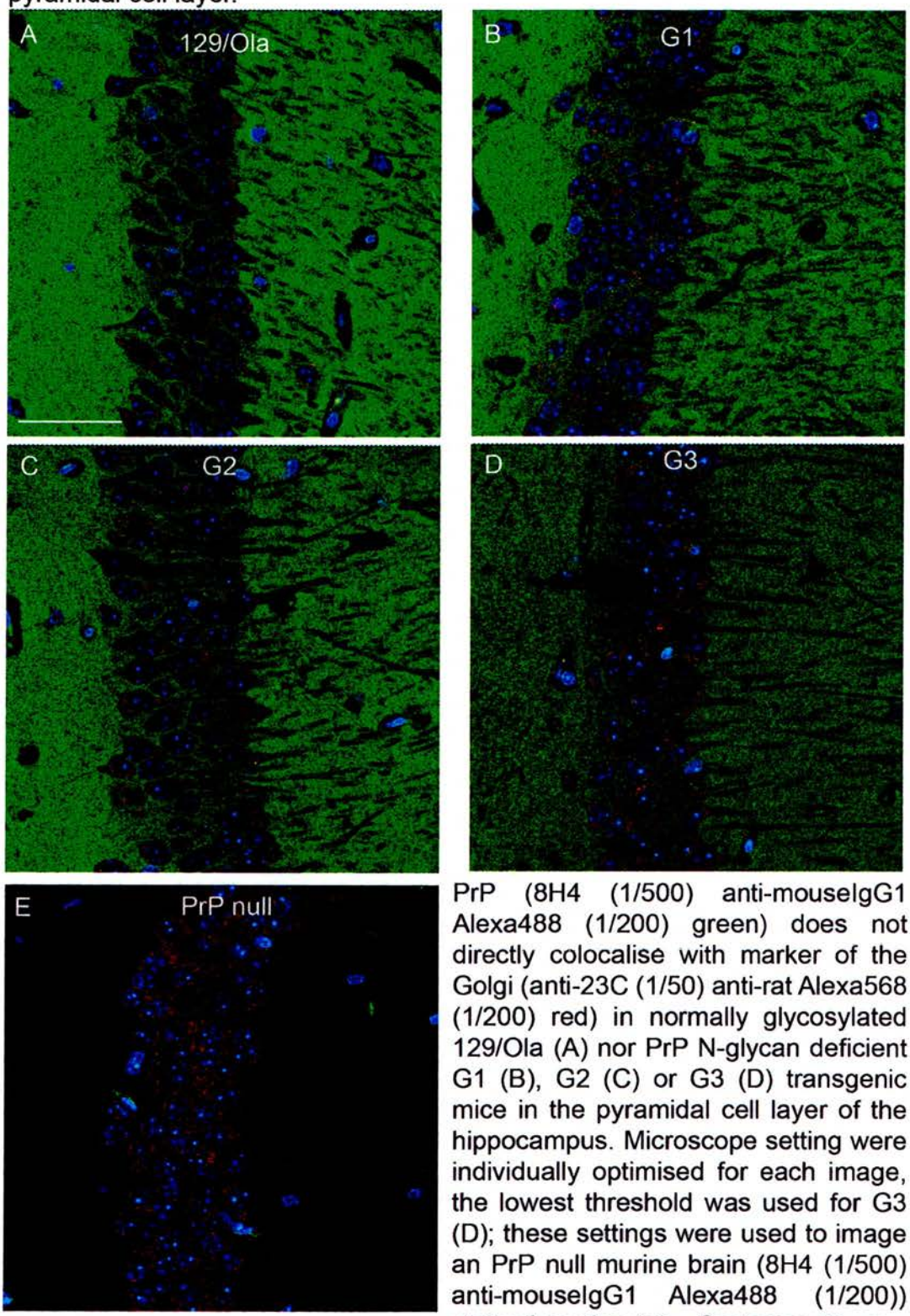

PrP (8H4 (1/500) anti-mouseIgG1 Alexa488 (1/200) green) does not directly colocalise with marker of the Golgi (anti-23C (1/50) anti-rat Alexa568 (1/200) red) in normally glycosylated 129/Ola (A) nor PrP N-glycan deficient G1 (B), G2 (C) or G3 (D) transgenic mice in the pyramidal cell layer of the hippocampus. Microscope setting were individually optimised for each image, the lowest threshold was used for G3 (D); these settings were used to image an PrP null murine brain (8H4 (1/500) anti-mouseIgG1 Alexa488 (1/200)) stained section (E) . Scale bar 50 µm

Figure 4.11 Close up of anti-PrP staining (8H4) and a marker of the Golgi (23C) in the pyramidal cell layer of the hippocampus

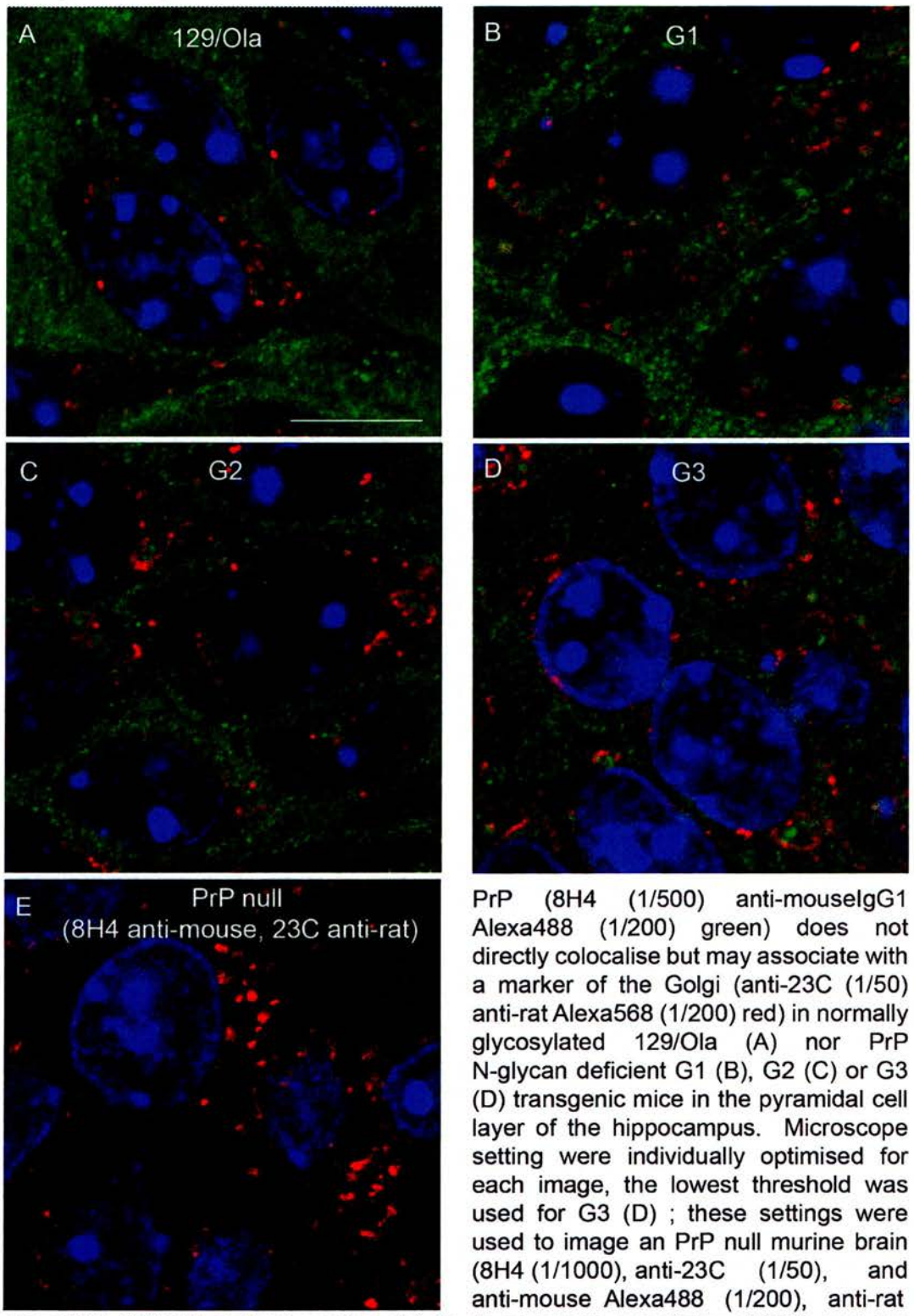

PrP (8H4 (1/500) anti-mouseIgG1 Alexa488 (1/200) green) does not directly colocalise but may associate with a marker of the Golgi (anti-23C (1/50) anti-rat Alexa568 (1/200) red) in normally glycosylated 129/Ola (A) nor PrP N-glycan deficient G1 (B), G2 (C) or G3 (D) transgenic mice in the pyramidal cell layer of the hippocampus. Microscope setting were individually optimised for each image, the lowest threshold was used for G3 (D) ; these settings were used to image an PrP null murine brain (8H4 (1/1000), anti-23C (1/50), and anti-mouse Alexa488 (1/200), anti-rat Alexa568 (1/200)) stained section (E) to demonstrate specificity of 8H4 and the absence of cross reactivity of 23C with anti-IgG1mouse Alexa488. Scale bar 25 µm

Intracellular anti-PrP and anti-β-cop staining were associated, however no direct colocalisation was observed (Figure 4.11). The β-cop labelling appeared to surround a significant proportion of PrP^C in both wild type control and the glycosylation deficient transgenic mice (Figure 4.11). This pattern is consistent with a proportion of PrP^C being localised in the Golgi lumen surrounded by the β-cop staining outer membrane, although further experimentation is required to confirm this conclusion. No difference in either the frequency or the intensity of Golgi-associated PrP^C was observed between brain sections from PrP glycosylation deficient transgenic and 129/Ola control mice, suggesting that the alteration of localisation of PrP^C observed is not linked to an accumulation or reduction of the protein within the Golgi (Figure 4.11) (n = 2, assayed in duplicate).

4.4.2.3 Cytoplasmatic PrP^C

In the majority of cells there was no evidence that PrP^C was located in the cytoplasm. In the majority of cells anti-PrP^C staining was observed to have a discrete clustered distribution consistent with localisation within subcellular compartments, consistent with localisation of PrP in endosomes, lysosomes or associated endocytic vesicles, as previously reported (Laine et al., 2001; Mironov et al., 2003). However, occasional cells in which anti-PrP^C staining was strongly detected in the entire cell body (excluding the nucleus) were observed (Figure 4.12). These cells were observed in the neuropil adjacent to, but not in, the granular cell layer of the dentate gyrus and occurred very infrequently. This observation is similar to the cytPrP cells identified by Mironov and colleagues, and those reported by Barmada et al from their work with Green Fluorescent Protein (GFP) tagged PrP (Barmada et al., 2004; Mironov et al., 2003).

Figure 4.12 Cytoplasmic PrP

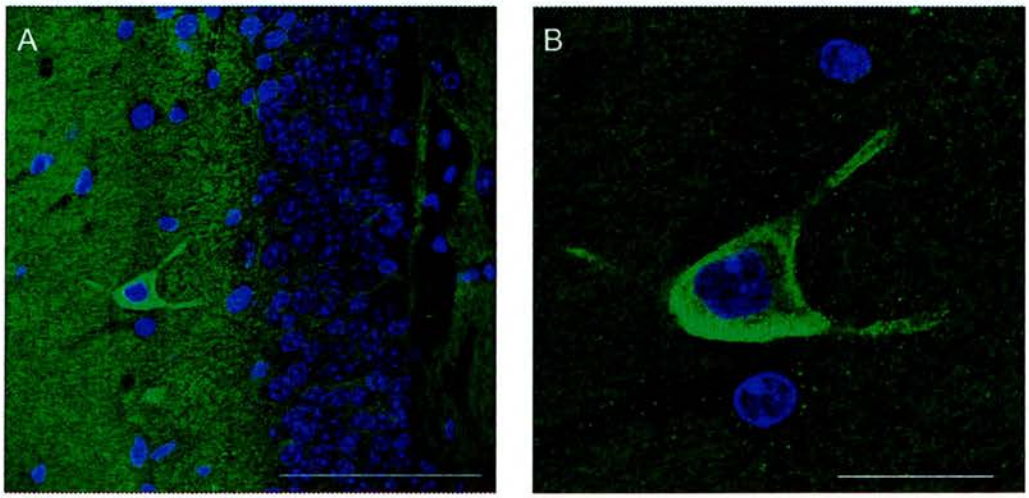

High level of PrP (8H4 (1/500) anti-mouse Alexa488 (1/200)) staining throughout the cell body of a single cell, in the stratum molecular of the hippocampus in a 129/Ola mouse (A & B) were observed. Scale Bar 100 µm (A) 50 µm (B).

4.4.3 Results summary

These data suggest that the glycosylation state of PrP^C may influence the proteins localisation *in vivo*.

- That the absence of a N-glycan at the first attachment site does not significantly alter the cellular localisation of PrP^C.
- That the absence of a N-glycan at the second attachment site may reduce the amount of PrP^C localised in the neuropil.
- That the complete absence of PrP^C's N-glycans greatly reduces the amount of PrP^C detected in the neuropil.
- That the pattern of intracellular localisation of PrP^C does not appear to be altered by the partial or complete lack of the protein's N-glycans.
- That *in vivo* some cells expressing high levels of PrP^C in the cytoplasm are observed.

4.5 Discussion

4.5.1 Technical discussion

Early work suggested that normally glycosylated PrP^C was principally localised within the cell bodies and that PrP was only detected in a subset of CNS cells (Bendheim et al., 1992; DeArmond et al., 1987; Ford et al., 2002a; Manson et al., 1992a; Piccardo et al., 1990). This contrasts with the ubiquitous localisation of PrP^C within the neuropil observed here and by others (Barmada et al., 2004; Fournier et al., 2000; Haeberle et al., 2000; Mironov et al., 2003; Moya et al., 2000; Sales et al., 1998). Early experimental investigations into the localisation of PrP^C used embedding and alcohol dehydration techniques to prepare CNS material for immunohistochemical analysis. This method will disrupt the cells' plasma membrane where PrP^C is predominately localised and is thought to lead to the loss of the antigen (Laine et al., 2001; Mironov et al., 2003). The free-floating immuno-detection method used here, and by others, eliminates the problem allowing plasma

membrane PrP^C to be localised (Laine et al., 2001; Mironov et al., 2003; Moya et al., 2000; Sales et al., 1998). The cell body PrP^C reported in papers in which embedding tissue preparation was used may represent the instances of cytPrP, as described here and by Mirnovo and Barmada (Barmada et al., 2004; Mironov et al., 2003).

Anti-PrP staining intensity observed in the molecular layer of the dentate gyrus was only slightly lower and inconsistently observed than that in the stratum oriens and stratum radium, in contrast to previous reports from hamsters and baboons (Mironov et al., 2003; Moya et al., 2000). This difference may be caused by species differences in PrP^C levels between the regions of the hippocampus, as no difference in staining intensity between the hippocampal regions has been reported for reported for humans, macaques and murine GFP-tagged PrP^C (Barmada et al., 2004; Moya et al., 2000; Sales et al., 1998). Alternatively these differences may be a result of the antibody used, as the variation in hippocampal staining intensity observed in hamsters has shown antibody dependence (Moya et al., 2000).

It was not possible to accurately quantify the amount of plasma membrane associated PrP^C in the glycosylation deficient transgenic and the 129/Ola control mice because of the confocal method used. Further experiments using other techniques are required to address this issue fully. This could be explored using primary neuronal cell cultures from the glycosylation deficient transgenic and control mice such that surface biotinalytion or PIPLC digestion of surface PrP^C could be used. Alternatively cell-fractionation techniques could be used determine the relative proportion of PrP^C within each cellular compartment.

4.5.2 Discussion of experimental results

These data show that the overall pattern of PrP^C localisation is altered in G3 PrP glycosylation deficient transgenic mice, in a manner consistent with a significant reduction but not a complete elimination of PrP^C within the neuropil. This work is consistent with previous reports of the intracellular localisation of un-glycosylated PrP^C both in transgenic animals and cell culture (DeArmond et al., 1997; Neuendorf

et al., 2004; Rogers et al., 1990). However, un-glycosylated PrP^C has been observed at the surface of cultured cells (Borchelt et al., 1990; Caughey et al., 1989; Lehmann and Harris, 1997; Neuendorf et al., 2004; Petersen et al., 1996). However, in these cases un-glycosylated PrP^C, was expressed in the presence of endogenous glycosylated PrP^C, which may facilitate trafficking of the un-glycosylated form to the cell surface, as PrP^C may form dimers *in vivo* (Bendheim and Bolton, 1986).

A reduction in anti-PrP^C staining in the neuropil was observed in some sections from G2 PrP glycosylation deficient transgenic mice. However this result was not consistently observed, suggesting that N-glycan attachment at the second site may facilitate localisation of PrP^C to the neuropil in some situations but that it is not absolutely required. The majority of previous work has suggested that glycosylation of the second N-glycan site is not required for the localisation of PrP^C (DeArmond et al., 1997; Korth et al., 2000; Lehmann and Harris, 1997; Neuendorf et al., 2004). However, one paper has reported intracellular localisation of PrP^C in the absence of the second site (Rogers et al., 1990). Differences between the model systems employed may underlie the differences in the importance of the second site to PrP^C location in these studies. This is in accordance with our finding that the relative importance of the second N-glycan site varied, suggesting that factors such as the expression of other cellular components may modify the importance of the second N-glycan attachment site to the protein's localisation. Further investigation is required to determine what these modifying factors are and how they mediate the localisation of PrP^C.

No consistent difference in PrP staining was observed in sections from G1 PrP glycosylation deficient transgenic mice, suggesting that glycosylation of the first site is not required for the normal localisation of PrP^C. A number of published works have demonstrated the contrary (DeArmond et al., 1997; Lehmann and Harris, 1997; Rogers et al., 1990). However, all these works disrupted glycosylation at the first site by the pathogenic T182A mutation that has been shown in three independent studies to alter cellular localisation of PrP^C independently of the prevention of glycosylation at the first site (Capellari et al., 2000b; Korth et al., 2000; Neuendorf et al., 2004).

Thus this work supports the hypothesis that glycosylation of PrP^C at the first site is not required for the localisation of the protein to the plasma membrane, in agreement with the work of Capellari (2000), Korth (2000) and Neuendorf (2005). However, small changes in the localisation of PrP^C which are below the detection limit may occur.

Despite the reduced level of PrP^C detected in the neuropil of sections from G3 transgenic mice, the location of intracellular PrP^C was similar in the PrP glycosylation deficient transgenic and 129/Ola control mice. In all sections examined intracellular PrP^C was excluded from the ER and a proportion of the total was associated with a marker of the Golgi. A similar pattern of localisation has been previously reported for wild type PrP^C *in vivo* validating this finding (Laine et al., 2001; Mironov et al., 2003). Thus the alteration of localisation of un-glycosylated PrP^C is not caused by an accumulation of the protein in the ER or Golgi. Moreover, the data presented here suggest that complete absence of PrP N-glycans does not prevent transport of the protein through the ER and into the Golgi. Furthermore, the amount of PrP^C observed within the Golgi in G3 transgenic mice does not appear to be reduced compared to murine controls, suggesting that ER to Golgi trafficking of PrP^C may not be greatly altered in the absence of PrP N-glycans. However further experimentation is required to test this hypothesis.

There are a number of possible explanations for the decreased level of PrP^C detected in the neuropil of the G3 PrP glycosylation deficient transgenic mice. PrP^C may not be correctly trafficked post-Golgi to the plasma membrane, perhaps being miss-directed to the endosomal or lysosomal compartments. Alternatively, much reduced levels of PrP^C may reach the membrane because of an enhancement of intracellular degradation. This may occur if un-glycosylated PrP^C has a higher probability of misfolding in the ER and hence a greater proportion of it is subjected to retrotranslocation and protease degradation via the ERAD pathway. The ERAD pathway has also been suggested to be important to the normal regulation of glycosylated PrP^C (Jin et al., 2000; Ma and Lindquist 2001; Yedidia et al., 2001). Un-glycosylated PrP^C may be correctly trafficked to the plasma membrane but there

may be subject to an increased rate of turnover or release, perhaps because of the exposure of an enzymatic site usually shielded by the N-glycans. As the level of PrP detected by DELFIA are similar between G3 and 129/Ola controls (Chapter 3), any increase in degradation *in vivo* must be linked to an upregulation of PrP^C synthesis.

Only one anti-PrP monoclonal was suitable for detection of PrP^C by Immunofluorescence, despite the large number investigated. Thus the observed decrease in G3 PrP^C may be caused by a specific alteration in the un-glycosylated PrP 8H4 epitope availability at the membrane. This could conceivably occur, as G3 un-glycosylated PrP^C may interact differently from the glycosylated form with a range of different molecules. G3 PrP^C may even interact differently with the plasma membrane or be localised differently within it, as the regional localisation of GPI anchored proteins within membrane is thought to be mediated via interactions with other membrane proteins. Further experimentation is required to investigate whether G3 PrP^C is located within the same membrane domain as the normally glycosylated protein, and to define the mechanism which underlies the observed difference in PrP distribution in the G3 transgenic mice.

The observation of high levels of cytoplasmatic PrP (cytPrP) within a subset of cells in the hippocampus is consistent with previous reports (Barmada et al., 2004; Mironov et al., 2003). CytPrP has been suggested to be neurotoxic (Ma et al., 2002). However, the observation presented here of high levels of cytoplasmatic PrP, in apparently healthy cells, with intact nuclei, in wild type mice, suggests the contrary. However, further work is required to investigate whether these cells lack signs of apoptosis/necrosis *in vivo*, as has been previously demonstrated in another system (Mironov et al., 2003). The previous reports of cytPrP cells recorded a higher frequency of such cells than observed here (Barmada et al., 2004; Mironov et al., 2003). This may be attributable to the different strains of mice used in this study, 129/Ola compared to FVB and C57/B6 X CBA/J, differences in environmental factors or circadian fluctuations in cytPrP expression. In this regard it important to note that all mice used in the experiments presented here were sacrificed between 08.30-10.00 hours, at the start of the light cycle.

5.0 The role of glycosylation of PrP^C in a TSE species barrier

5.1 Aim To determine if glycosylation of PrP^C influences cross-species TSE transmission.

5.2 Introduction and experimental method

Like many infectious diseases, TSE transmission between species is notably less efficient than that observed within a species. However, cross-species transmission does occur with devastating consequences (Chapter 1). The molecular mechanisms that underlie the barrier to cross-species transmission are poorly understood. Thus it is currently not possible to make accurate predictions about the risk of cross-species transmission of novel TSEs and hence to which host species they pose a threat.

The species barrier to transmission is characterised by a decrease in susceptibility, and an increase in length and variability of the incubation period, in the novel host species (Pattison, 1965). A number of factors are thought to contribute to the barrier, most notably PrP and its interaction with species specific factors (Chapter 1) (Barron et al., 2005; Barron et al., 2001; Manson et al., 1999; Scott et al., 1989; Telling et al., 1994; Telling et al., 1995). The degree of homology of the amino acid sequence of host PrP^C and donor PrP^{Sc} has been reported to influence the extent of the species barrier (Scott et al., 1989). However, PrP also influences cross-species TSE transmission independently of PrP^C-PrP^{Sc} sequence similarity (Barron et al., 2005; Barron et al., 2001; Manson et al., 1999). Current data suggest that conformational compatibility between PrP^C and PrP^{Sc} is a key determinant of the barrier: firstly because of the TSE strain dependence of the barrier and secondly because of the correlation of the transmission barrier effect with an alteration of PrP^{Sc} conformation (Peretz et al., 2002; Scott et al., 1993). However, the observed complexity of the TSE species barrier suggests that it may be composed of multiple mechanisms (Chapter 1).

The TSE species barrier effect is partially replicated in cell-free PrP misfolding reactions (Kocisko et al., 1995). This suggests that innate convertibility of PrP may contribute to the observed transmission barrier, consistent with the conformational compatibility model. In these *in vitro* systems, conversion of PrP^{C} to a proteinase resistant form is induced by the introduction of PrP^{Sc}, derived from a TSE infected animal (Kocisko et al., 1994). The observed conversion efficiency approximately correlates with the relatedness of the amino acid sequence of PrP^{C} and PrP^{Sc}, such that within species conversions occur more readily than cross-species reactions (Kocisko et al., 1995). Glycosylation of PrP^{C} has been suggested to have a specific role in the observed reduced efficiency of cross-species conversion, since removing PrP^{C}'s N-glycans specifically elevates the efficiency of cross-species seeded reactions (Priola and Lawson, 2001). This suggests that the glycosylation of host PrP^{C} may specifically hinder cross-species TSE infection *in vivo*.

The postulated effect of PrP's glycosylation state on cross-species TSE transmission may be mediated by a number of mechanisms. Firstly, reported differences in the glycans attached to PrP^{Sc} between species (Xanthopoulos et al., 2006) may indicate an adaptation or preference of the TSE agent to the predominant PrP glycotypes of a particular host species. Thus the glycosylation of PrP^{C} in other host species may restrict replication of the agent. Alternatively, PrP's N-glycans may have a generic effect on the protein's conformational flexibility, as proposed by (Zuegg and Gready, 2000), such that a glycosylated molecule is less able to adopt the novel conformation of PrP^{Sc} from a different species. Alternatively, glycosylation of PrP^{C} may directly interfere with the protein's ability to interact with PrP^{Sc} (Rudd et al., 2001). Additionally, the glycosylation state of PrP^{C} may mediate the protein's interaction with other cellular factors that influence the conversion of PrP^{C} to PrP^{Sc} *in vivo*. Thus the glycosylation status of PrP^{C} could both directly and indirectly influence PrP^{C} to PrP^{Sc} conversion and hence the TSE transmission barrier.

To investigate the hypothesis that glycosylation of PrP^{C} retards cross-species TSE transmission, PrP glycosylation deficient murine transgenics [NPU] and normally glycosylated mice (CL and 129/Ola) were challenged with the hamster model TSE

strain, 263K, by intracerebral (ic) inoculation. Data presented in chapter 3 demonstrate that these transgenic mice are a valid model in which to investigate the influence of PrP's glycosylation state on cross-species TSE transmission. Direct ic injection is the most efficient route of TSE challenge and thus was used to minimise the number of experimental animals required. However, this method circumvents the peripheral transmission and replication phase of the TSE agent. Thus in these experiments the importance of glycosylation of PrP^C to the peripheral stage of TSE infection is not investigated. Although this phase is a key part of natural cross-species TSE transmissions, the hypothesised influence of glycosylation of PrP^C on the TSE species barrier is via its effect on PrP misfolding efficiency, which will directly effect CNS pathogenesis (Priola and Lawson, 2001). However, further experiments are necessary to investigate if the glycosylation state of PrP has a specific effect on peripheral pathogenesis.

Hamster passaged scrapie strain 263K, and the putative equivalent strain Sc237 (Scott et al., 1989), are much studied TSE models. A strong barrier to transmission exists between 263K and wild type mice. The 263K incubation period is in excess of 700 days in murine hosts in contrast to around 60 days in hamsters and susceptibility is also much reduced in mice (Kimberlin and Walker, 1978a; Race et al., 2001). Thus transmission of 263K to mice provides a model reflecting a classic species barrier, as defined by Pattison in 1965 (Pattison, 1965). Additionally, although clinical disease incidence in 129/Ola mice after challenge with 263K is low, subclinical pathology is observed in a higher proportion of challenged animals (personal communication R. Barron). Thus by comparing the extent of subclinical deposition of misfolded PrP and TSE specific vacuolar pathology between the normally glycosylated control and glycosylation deficient transgenic mice, the influence of PrP glycosylation state on cross-species transmission of 263K can be determined, even in the absence of clinical disease. Therefore, inoculations of 263K into the glycosylation transgenic mice will be a useful model to test the hypothesis that glycosylation of PrP^C retards cross-species transmission of the TSE agent. In particular, given that cell-free conversion work suggests an effect that is equivalent to a two-three log change in titre (Priola and Lawson, 2001; Raymond et al., 2000).

263K was used by Priola and Lawson to demonstrated that glycosylation of PrP^C reduces the efficiency of cross-species TSE misfolding *in vitro* (Priola and Lawson, 2001). Thus, it is of particular relevance to this study of the *in vivo* effects of PrP^C's N-glycans on cross-species TSE transmission. Additionally, 263K/Sc237 haa been used in many previous investigations into the species barrier. It was the strain used to identify the importance of amino acid sequence homology of PrP^C and PrP^{Sc} to cross-species transmission (Scott et al., 1989). Notably it has been used to demonstrate the phenomenon of adaptation of the agent in new hosts, as illustrated by an alteration of strain characteristics (Kimberlin and Walker, 1978a). More recent work has built on this finding and has shown, using the 263K model, a correlation of conformational change of PrP^{Sc} and the species barrier effect (Peretz et al., 2002).

Hamster PrP and hence 263K PrP^{Sc} differs from murine PrP at fourteen amino acid residues (Locht et al., 1986). Three of these differences lie within the N-terminal signal sequence or the C-terminal GPI anchorage motif, and are hence absent from the fully mature protein. Previous work has suggested that the difference in the PrP amino acid sequence between hamster and mice mediates the species barrier (Scott et al., 1989). It is interesting to note that the amino acid sequence surrounding the first glycan attachment site is highly conserved between hamster and mouse. In contrast, proximal to the second site, hamster and mouse PrP differ at amino acids 203 and 205 (hamster sequence). These differences in local amino acid sequence homogeneity may affect the relative importance of the two N-glycan attachment sites to cross-species TSE transmission.

The 263K challenged murine transgenics and normally glycosylated control mice were observed blind to genotype, for 700 days post inoculation, for clinical TSE disease incidence using standard criteria (Dickinson et al., 1968). Thus, the influence of glycosylation of PrP^C on TSE disease transmission and hence the extent of the species barrier was experimentally assessed. Additionally, the incidence and extent of subclinical TSE specific pathology, including vacuolar pathology, deposition of disease associated misfolded PrP (PrP^d) within the brain and formation of PK

resistant PrP (PrP^{Sc}) were also examined by standard methods (Bruce et al., 1989; Fraser and Dickinson, 1968), since significant subclinical disease was anticipated. The disease associated PrP (PrP^{d}) detected by immunohistochemistry (IHC) was not always demonstrated to be PK resistant, hence the term PrP^{d} was used to differentiate it from PK resistant PrP^{Sc}. If PrP^{Sc} was not detected by the standard extraction technique it was concentrated by ultracentrifugation or sodium phosphotungstic acid (NaPTA) precipitation (Safar et al., 1998). In addition to providing information about the extent of TSE infection in the challenged mice, these data also provide mechanistic insight into the role of PrP^{C} glycosylation in formation of PrP^{Sc} *in vivo* after cross-species challenge with 263K.

To further examine the role of glycosylation of PrP^{C} on the TSE disease process, astrocytosis, which is a common but not exclusive TSE pathological hallmark, was also investigated by IHC using an antibody to glial fibrillary acid protein (GFAP) to label activated astrocytes. The glycosylation state of PrP may influence the activation of astrocytes via an effect on the type of PrP^{Sc} formed *in vivo* or by a direct effect on their role in pathogenesis.

Moreover, by comparing the pattern of vacuolation and PrP^{d} deposition, and the type of PrP^{Sc} formed in control and transgenic mice, the influence of PrP^{C}'s N-glycans on TSE strain characteristics could be determined. Passage of TSE in new hosts is linked to the emergence of novel strains which differ in their disease characteristics, including incubation time. Moreover some have postulated that the correlation of PrP^{Sc} glycoform and TSE strain reflects the encryption of TSE strain characteristics by PrP^{Sc} glycoform (Collinge et al., 1996). Thus the alteration of PrP^{C} glycosylation, and hence also that of PrP^{Sc} produced in the murine PrP glycosylation deficient transgenics, may directly cause a change in TSE strain. Hence it is important to determine whether any observed changes in disease incidence or onset occur purely because of a host effect on disease progression (i.e. same pathogen strain, with a species barrier), or owing to an effect of host on the TSE strain able to infect it. Furthermore, it is important to consider that TSE strain and the transmission barrier

may be mechanistically linked and hence it may be artificial to separate them (Hill and Collinge, 2003).

Subpassage of material from glycosylated controls and G2 transgenic mice infected with 263K has been undertaken to further compare which TSE strain caused the disease observed in these mice. TSE vacuolar pathology positive murine brains (two G2 and one CL) were used to challenge G2 transgenic mice, normally glycosylated control mice (CL and 129/Ola) and three additional inbred strains of wild type mice which have been classically used to define TSE strain (Chapter 1.). This work is currently ongoing and not available for analysis.

5.3 Optimisation of experimental methods

5.3.1 CSA kit for the detection of disease associated PrP

To permit analysis of TSE specific vacuolar targeting, all TSE challenged brain tissue was subjected to prolonged fixation in formol-saline, alcohol dehydration and the paraffin embedding process that is required for observation of TSE vacuolation. The fixation and embedding strategy used is known to remove PrP^C epitopes and reduce the levels of detectable PrP^d owing to the extensive cross-linking of proteins that occurs during fixation (Brown et al., 2003; Laine et al., 2001; Mironov et al., 2003). Thus it was necessary to use antigen retrieval (wet autoclaving sections at 115 °C for 15 minutes and 5 minutes in 98 % formic acid) to maximise the amount of PrP^d detectable by IHC to ensure that all subclinical TSE cases were detected, which is key given the low rates of transmission anticipated in this cross-species transmission experiment (Bruce et al., 1989).

To further increase the detection of PrP^d, a catalyzed signal amplification kit from DAKO was used in which an extra amplification step is used. In this system the primary antibody is recognised by a biotinylated secondary antibody, to which a streptavidin-biotin-peroxidase complex then binds. The amplification step is then

mediated by this peroxidase which catalyses the deposition of biotinylated phenol increasing the number of biotins bound at the site of the original antibody binding by approximately fifty-fold. This deposited biotin can then be recognised by a standard streptavidin peroxidise diaminobenzidine/hydrogen peroxide reaction. Normal brain homogenate inoculated $PrP^{a/a}$ mice and PrP null [NPU] mice were used as negative controls to ensure that all signal detected was specific to the TSE challenged animals (PrP^{d}), however these were not aged matched to the experimental TSE challenged aged mice. Two anti-PrP mouse monoclonal antibodies (6H4 and 8H4) were used with the kit, the concentrations of which were determined by titration (appendix iv, v). These monoclonal antibodies recognise epitopes in the central region of the protein and thus should be effective at detecting both C and N terminal truncated forms of PrP (appendix vi). No significant difference in the pattern of normally glycosylated wild type PrP^{d} was observed when the antibodies were used at their optimised concentrations (8H4 (1/5,000) and 6H4 (1/20,000)); indicating that these antibodies are effective at recognising all forms of PrP^{d}. However, in general the level of PrP^{d} detected with 8H4 was lower than 6H4.

5.4 Experimental results

5.4.1 TSE incubation periods and incidence of disease

Age and sex matched PrP glycosylation deficient transgenic [NPU] and normally glycosylated control mice were challenged by ic injection, to a depth of 2-3 mm in the right brain hemisphere, with 20 µl of clinical endpoint 263K infected hamster brain (10 %). Animals were anesthetised for the duration of the experimental procedure, coded after inoculation and examined blind to mouse genotype, daily for general good health and formally assessed by TSE scoring criteria weekly using the definitions of Dickinson and Fraser (1968). All animals which died at time of injection were excluded from the analysis. After the termination of the experiment, mice, for which no material was available for post-mortem genotyping or if the brain material was unsuitable for pathological study, were excluded from experimental

analysis. All these animals were clinical negatives and those for which pathological analysis was possible were also negative for TSE specific vacuolation. Exclusions were necessary because of an excessive post-mortem interval and/or damage during tissue removal which rendered tissue inappropriate for examination of vacuolation or because of accidental discards or inappropriate treatment of CNS material.

No symptoms of clinical disease were observed in either the murine PrP glycosylation deficient transgenics or normally glycosylated control mice challenged with 263K, consistent with a strong 263K/murine species barrier (Table 5.1) (Kimberlin and Walker, 1978a). Animals were sacrificed on welfare grounds during the course of the experiment with non-TSE ailments. These included two scratched eyes, skin abscesses and breathing difficulties in young and middle aged mice. In older animals (550 dpi) profound weight loss and associated loss of condition were the most common reasons for sacrifice; as the animals reached the end of their normal lifespan the rate of sacrifice increased in all genotypes, consistent with normal aging (Figure 5.1 A). No differences in reason for sacrifice were observed between genotypes.

Table 5.1 Summary of TSE disease status in 263K challenged PrP glycosylation deficient transgenic and control mice

Genotype	TSE disease status		
	0 (•)	**1 (■)**	**2 (▲)** (dpi +/- SEM)
G1	9	8	0
G2	2	5*	11 (552 +/- 16.3)
G3	21	1*	0
CL or 129/Ola	3	15	3 (638 +/- 38.6)

TSE disease status key

0, negative for signs of TSE disease (PrP^d deposition, vacuolation, clinical signs)
1, only positive for PrP^d deposition
2, positive for both PrP^d deposition and TSE specific vacuolation

* In these groups, in one animal, PrP^d was limited to a plaque in the corpus callosum.

Figure 5.1 Survival and TSE disease status of PrP glycosylation deficient transgenic and control mice challenged with 263K

A

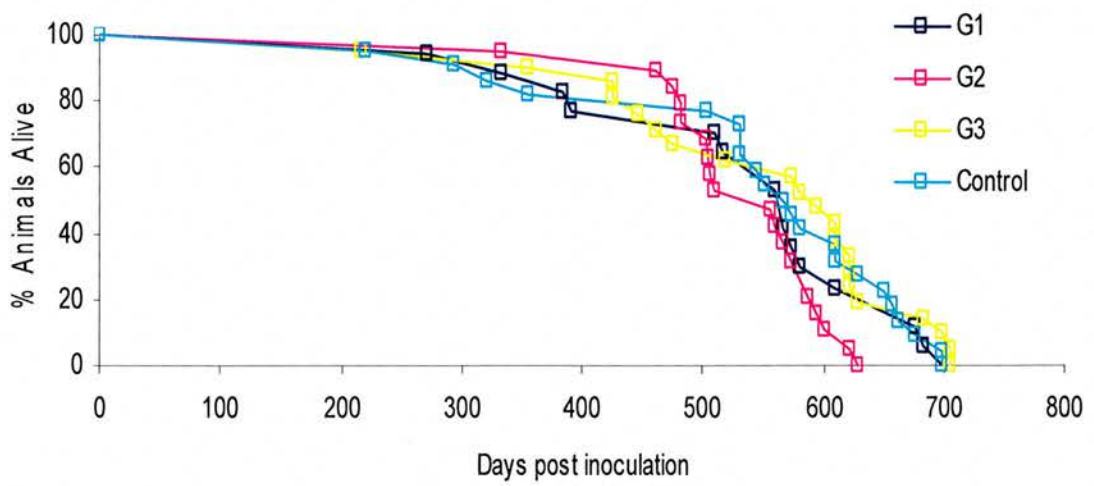

B

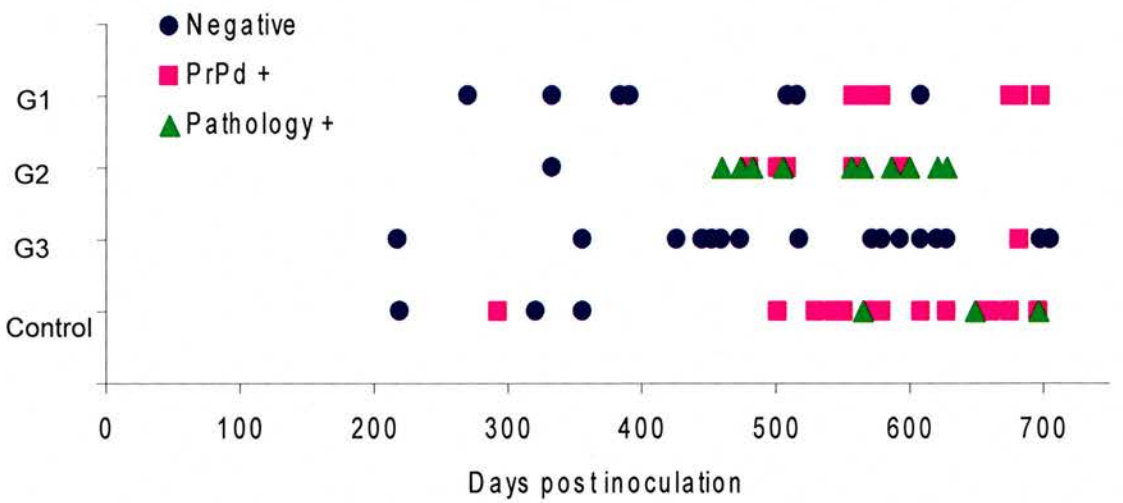

(A) The number of G1, G2, G3 transgenic and normally glycosylated control mice surviving after TSE challenge was plotted against time from inoculation, to determine if life expectancy after 263K exposure differed between host genotypes. (B) The TSE disease status (clinical signs, vacuolar pathology and PrP^d deposition +/-) of G1, G2, G3 transgenic and normally glycosylated control (CL or 129/Ola) mice after challenge with 263K was plotted against the number of days post inoculation at which the animal was euthanized, to demonstrate the effect of PrP's N-glycans on TSE disease incidence and onset. The incidence of sub-clinical TSE disease is significantly lower in the G3 ($p < 0.001$) and G1 ($p < 0.025$) transgenic mice than in normally glycosylated control mice, and the incidence of subclinical TSE disease is significantly higher in G2 transgenic mice than in normally glycosylated control animals ($p < 0.001$).

Within the normally glycosylated control group (CL = 16, 129/Ola = 5) three of the twenty-one challenged mice exhibited no evidence of TSE pathology or PrP^d deposition, fifteen mice exhibited PrP^d deposition in the absence of pathology and only three of the challenged mice developed specific TSE vacuolar pathology (Table 5.1, Figure 5.1 B). Thus overall, eighteen of the twenty-one normally glycosylated controls challenged with 263K and available for analysis exhibited evidence of TSE infection.

No TSE specific vacuolation was observed in the 263K challenged G3 transgenic mice. A small PrP^d deposit was visible in the corpus callosum of one 263K challenged G3, this may be an injection related accumulation of PrP^{Sc} as this region is proximal to the site of injection in the hippocampus (5.4.3). PrP^d was not detected in any other 263K challenged G3 transgenic mice. Thus G3 mice have enhanced resistance to 263K, or greatly increased incubations after infection with this agent, compared to normally glycosylated murine controls (Chi-squared = 28.742, degrees of freedom = 2, $p < 0.001$). Thus glycosylation of PrP^C facilitates the successful transmission of hamster passaged scrapie strain 263K across a species barrier.

Reduced 263K disease incidence or significantly extended incubation periods were also apparent in the G1 transgenic mice which lack the first N-glycan attachment site (Table 5.1) (Chi-square = 7.796, degrees of freedom = 2, $p < 0.025$). Nine G1 transgenic mice neither displayed deposition of PrP^d nor vacuolar pathology; in eight, limited deposition of PrP^d was observed and no G1 mice displayed any specific TSE vacuolar pathology or signs of CNS dysfunction (Figure 5.1 B). The absence of vacuolation and the reduced incidence and extent of PrP^d deposition (5.4.3) in the G1 compared to the control mice, demonstrates that glycosylation of PrP^C at the first N-glycan attachment site specifically mediates transmission of hamster TSE strain 263K to mice.

In contrast to the enhanced resistance apparent in G1 and G3 transgenic mice, G2 murine transgenics were more susceptible to or had significantly shortened times to disease onset after 263K challenge than normally glycosylated control mice (Table

5.1) (Chi-squared = 10.264, degrees of freedom = 2, $p < 0.001$). The incidence of TSE specific vacuolation was significantly higher (eleven of the eighteen animals challenged) and the first case of vacuolation was observed earlier in the G2 transgenic mice than in normally glycosylated murine controls. However, as animals were not sacrificed at serial time points, it is not possible to precisely define when the onset of vacuolar pathology occurred in the two genotypes and the differences observed in the current data set are not significant. In addition to the cases exhibiting subclinical vacuolation, a further five G2 transgenic mice exhibited PrP^d deposition in the absence of pathology. Overall, sixteen of the eighteen challenged G2 animals available for analysis exhibited signs of TSE infection. The G2/263K challenge experiment suggests that glycosylation of PrP at the second site retards the cross-species transmission of hamster passaged scrapie strain 263K.

However a barrier to the cross-species transmission of 263K is still observed in the complete absence of glycosylation at the second site since G2 transgenic mice do not develop clinical disease, even after 700 days, in contrast to the approximately 60 day incubation period observed in hamsters after 263K challenge (Kimberlin and Walker, 1978a). This indicates that factors in addition to the glycosylation state of PrP^C are important to the murine species barrier to 263K infection. To further investigate the extent of the barrier, material from two vacuolation positive G2 mice and a normally glycosylated control mouse are being subpassed into G2 transgenic and normally glycosylated wild type mice.

The differences in the disease incidence observed in G1 and G2 transgenic mice after 263K challenge, indicates that the site of N-glycan attachment greatly influences the role that glycosylation of PrP^C plays in cross-species TSE transmission. Indeed the attachment of an N-glycan to asparagine 180 appears to facilitate the cross-species transmission of 263K to mice, whereas attachment at the second site reduces the incidence and decreases the time to disease onset after 263K challenge. Moreover, the apparent resistance of G3 transgenic mice and enhanced susceptibility of G2 transgenic mice to 263K, suggests that absence of glycosylation of the second site only promotes

cross-species transmission of 263K to mice in the presence of an N-glycan at the first site.

5.4.2 The pattern of TSE vacuolar pathology

The correlation of PrP^{Sc} glycoform and TSE strain characteristics, such as the targeting of vacuolar pathology, has led some to suggest that TSE strain maybe encrypted by the glycoform of PrP^{Sc} (Collinge et al., 1996). Thus the observed differences in the disease incidence in the murine PrP glycosylation deficient transgenics after cross-species transmission may be caused by differences in the TSE strains able to colonise the transgenic hosts, rather than a direct effect of glycosylation on disease progression. To investigate this possibility, the targeting of TSE vacuolar pathology was examined. The brains of TSE challenged animals were removed post-mortem and saggitally divided in two asymmetrically. The larger right halves into which the inoculum was originally introduced were assessed for TSE vacuolar pathology, by standard methods (Fraser and Dickinson, 1967; Fraser and Dickinson, 1968).

The pattern of sub-clinical vacuolar pathology observed after 263K challenge appeared similar in G2 and normally glycosylated control animals, (Figure 5.2 A), although a slightly lower pathology score was observed in the hypothalamus in the control group (Figure 5.2 A, B and D). This may be due to differences in the stage of TSE disease development between the groups; given the later onset of pathology in the CL group, it is also likely that these mice died at an earlier stage of the sub-clinical disease. In both groups particular targeting to the dorsal medulla (grey area 1) and septum (7) (Figure 5.2 C and E) was observed and little pathology was observed in the cerebellar cortex (2), hippocampus (6), or cerebral cortex (8 & 9). The pattern of targeting observed was comparable to previous reports of the transmission of murine passaged/263K to normally glycosylated 129/Ola mice, (Barron et al., 2001). This further validates the interpretation that the absence of glycosylation of PrP^{C} at the second site does not influence the targeting of 263K TSE specific vacuolation.

Figure 5.2 Lesion profile and examples of vacuolar pathology in 263K challenged G2 transgenic and normally glycosylated control mice

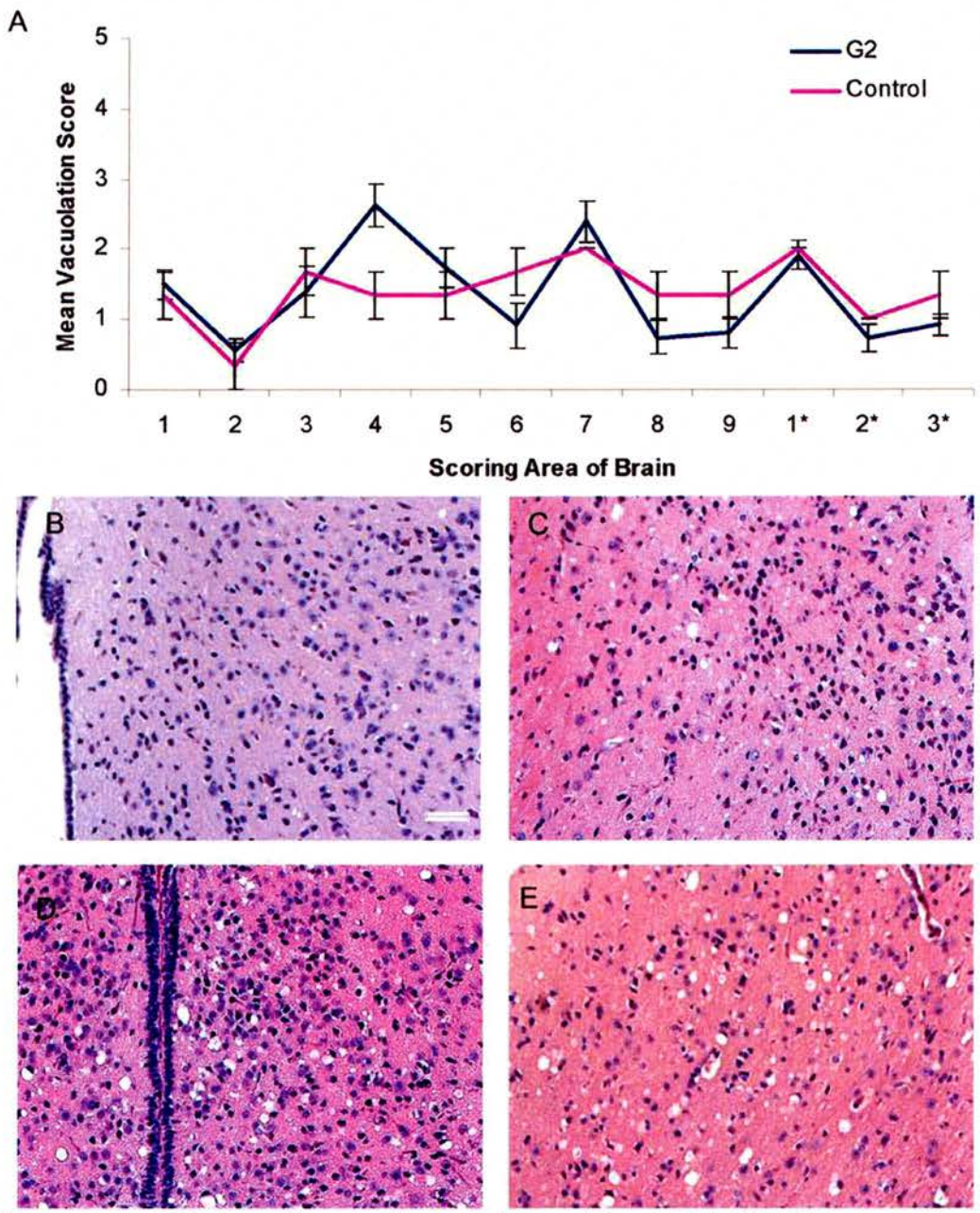

The pattern of TSE specific vacuolar pathology evident in G1, G2, G3 transgenic and normally glycosylated control mice after 263K challenge was semi-quantatively scored, blind to mice genotype and TSE agent, on a scale of 0-5 in nine grey areas (1 dorsal medulla; 2 cerebellar cortex; 3 superior colliculus; 4 hypothalamus; 5 thalamus; 6 hippocampus; 7 septum; 8 retrosplenial and adjacent motor cortex; 9 cingulate and adjacent motor) and three white matter areas of the brain (1* inferior and middle cerebellar peduncles; 2* decussation of the superior cerebellar peduncles; 3* cerebral peduncles) by standard methods. The experiment was then decoded and a lesion profile of the mean vacuolation score for each genotype constructed. This demonstrates that the pattern and density of vacuolation in G2 and normally glycosylated control mice is similar apart from in the hypothalamus (A). No vacuolation was detected in the G1 or G3 transgenci mice. B-E) Examples of haematoxylin and eosin stained brain sections showing TSE vacuolar pathology in the hypothalamus (B & D) and septum (C & E) of normally glycosylated (B & C) and G2 transgenic (D & E) mice. Scale bar 50 µm (B-E).

The intensity of vacuolation observed was lower than that previously reported for clinically sick animals infected with murine passaged 263K, consistent with the subclinical TSE state of the mice studied here (Barron et al., 2001).

The similarity of the targeting of TSE vacuolar pathology in the G2 transgenic and normally glycosylated control mice suggests that they were infected with the same TSE strain. Further experimental investigation, including an examination of the pattern of PrP^d deposition and strain typing by bioassay, is required to support this conclusion. However, the observed conservation of the pattern of vacuolar targeting between the G2 transgenic and normally glycosylated control mice infected with 263K suggests that the observed alteration of disease incidence and onset is the result of a specific role of second site glycosylation of PrP^C on disease progression in mice.

5.4.3 Pattern of TSE associated PrP deposition in the CNS

To further investigate if other TSE strain characteristics differed between the murine PrP glycosylation deficient transgenics and normally glycosylated controls, the pattern of disease associated PrP (PrP^d) deposition was determined. PrP^d deposition was examined at five defined levels at which vacuolar pathology was scored (Chapter 2) using an anti-PrP antibody 6H4. Normal brain inoculated $Prnp^{a/a}$ mice and PrP null mice were used as negative controls, although these controls were not aged matched to experimental mice. A subset of brains were stained with an additional anti-PrP antibody 8H4, to determine if the results were antibody dependent. Furthermore, the extent of PrP^d deposition was used to assess the relationship between PrP^d accumulated *in vivo* and the extent of other TSE pathological features.

The pattern of early PrP^d deposition was broadly similar between vacuolation positive G2 transgenic and normally glycosylated control mice challenged with 263K as assayed by 6H4 and 8H4 (Figure 5.3 (i, ii)). Targeted synaptic type PrP^d deposition was observed in the thalamus, habenula and in some cases in the septum at the early stages in both G2 (Figure 5.3 E-H, I) and normally glycosylated controls (Figure 5.3 A-D, J).

Figure 5.3 Early stage PrP^d deposition in vacuolation positive G2 transgenic and control mice challenged with 263K. Early stage PrP^d deposition after 263K challenge was examined at five defined brain levels of which four are shown here (A & E) medulla and cerebellum, (B & F) midbrain including superior collicullus (Sc) (just seen B), cerebral cortex and hippocampal formation, (C & G) hippocampus (Hp), habenula (Hb), thalamus (Th), hypothalamus, cerebral cortex and corpus callosum (cc), (D & H) forebrain including corpus callosum and septum (Sp). PrP^d was detected after wet autoclaving and formic acid treatment using anti-PrP antibodies 6H4 (i) and 8H4 (ii). The signal was amplified using a CSA kit and visualised with DAB; nuclei were counter stained with haematoxylin. Synaptic PrP deposition can be observed in habenula and thalamus (C & G) using both antibodies (i, ii) and the septum (D & H) using 6H4 (i) in both G2 transgenic (E-H) and normally glycosylated control mice (A-D). Pattern of synaptic staining in the thalamus is similar in normally glycosylated controls (iI enlargement of C) and G2 transgenic mice (iJ, enlargement of G). Specificity of signal was determined using PrP null [NPU] and normal brain homogenate challenged $PrP^{a/a}$ negative control sections (i-K) and (ii-I). Sections (A-D) from a single CL mouse, (E-H) two G2 transgenic mice were analysed (E, G & H animal one; F animal two). Scale bar 500 μm (A-H), scale bar 25 μm (I & J).

Figure 5.3 (i) Early stage PrP^d deposition in vacuolation positive G2 transgenic and control mice challenged with 263K (6H4)

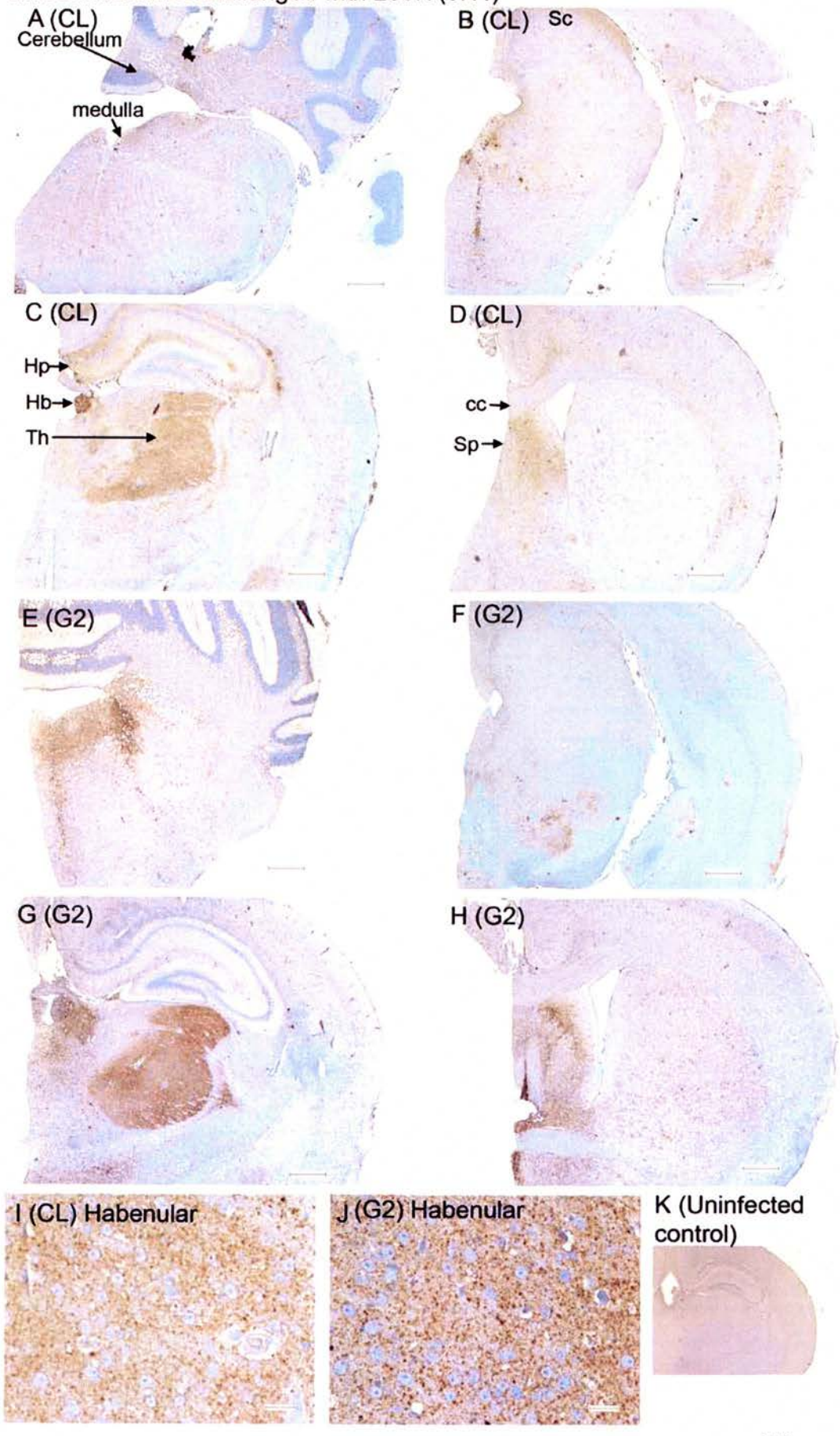

Figure 5.3 (ii) Early stage PrP^d deposition in vacuolation positive G2 transgenic and control mice challenged with 263K (8H4)

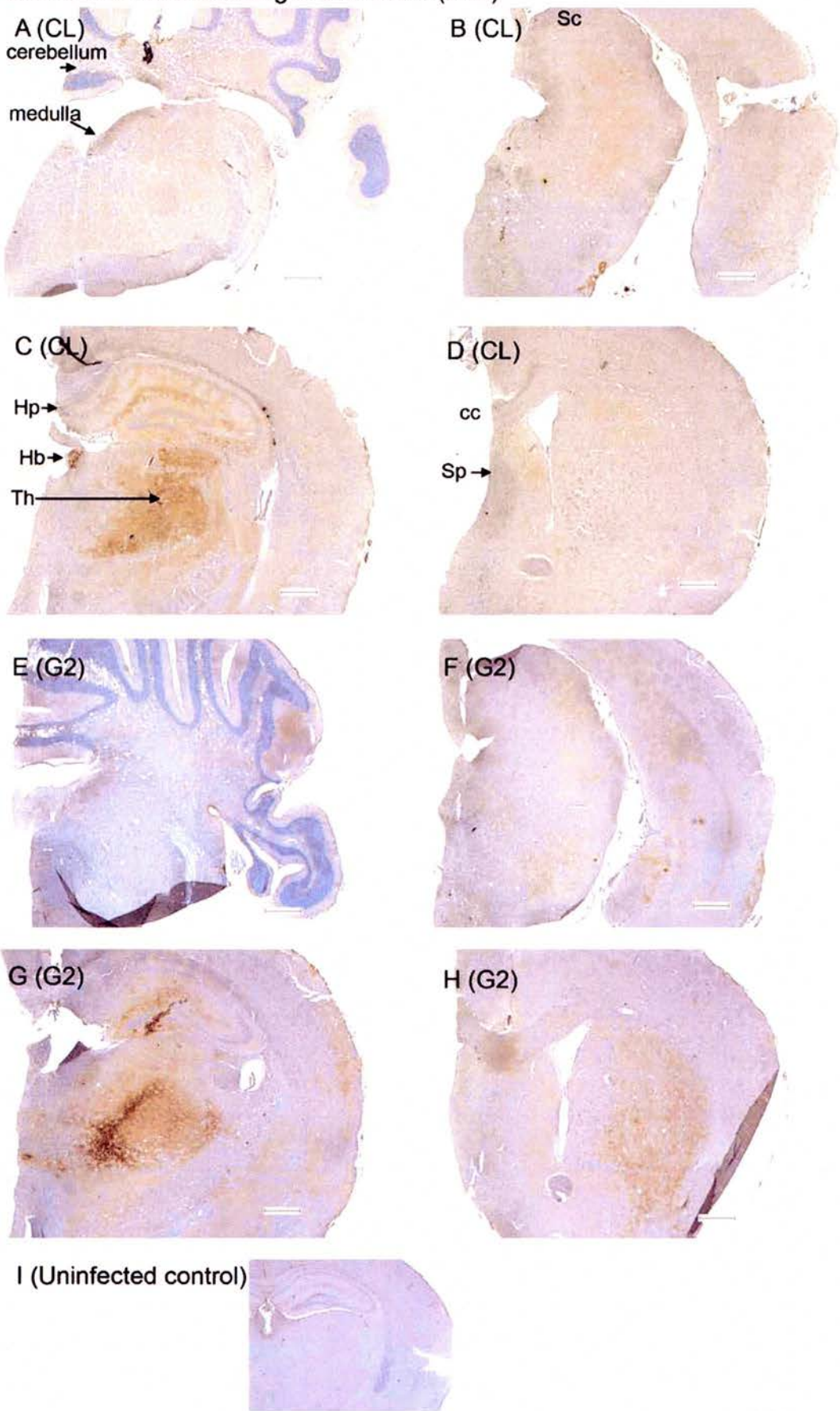

Additionally, more extensive synaptic type deposition was also observed in the cerebral cortex and forebrain in some G2 and control animals that were sacrificed at later time points (more than 600 days post ic challenge) (Figure 5.4, 5.5). Despite this variability, G2 transgenic mice challenged with 263K appeared to exhibit more extensive PrP^d deposition than controls (Figure 5.5, table 5.2), however this difference was not statistically significant (Chi square = 2.09, df = 3, $p < 1$). PrP^d amyloid plaques were observed in five G2 transgenics in the thalamus, septum, cerebral cortex and hippocampus as confirmed by thioflavin-s treatment (Figure 5.6). This formation of amyloid plaques within these G2 transgenic mice may be a result of the higher density of PrP^d deposition observed, which may favour the formation of higher order aggregates. These data suggest that glycosylation of PrP^C at the second site influences the amount/rate but not the pattern of PrP^d accumulation after cross-species TSE challenge with 263K. This further supports the hypothesis that TSE strain does not differ between the G2 transgenic and normally glycosylated control mice but that the rate and probability of disease progression is changed, indicative of an alteration in the TSE species barrier.

Table 5.2 Extent of PrP^d deposition in the brains of 263K challenged mice

Murine Genotype	Extent of PrP^d deposition (semi-quantitatively scored)			
	None	Limited	Moderate	Extensive
G1	9	8	0	0
G2	2	6	4	6
G3	21	1	0	0
CL/129/Ola	3	10	5	3

The brain regions in which PrP^d was detected using anti-PrP antibody (6H4), in 263K challenged mice, was scored blind to genotype. Then the extent of PrP^d deposition was categorised as limited (PrP^d observed in the habenular and associated neuropil; ventral midbrain and midline of the medulla and/or pons), moderate (PrP^d observed additionally in the thalamus) or extensive (PrP^d additionally observed in the cerebral cortex, septum, and caudate-putamen). The experiment was decoded and tabulated.

Figure 5.4 More extensive PrP^d deposition is observed in control mice after challenge with 263K at later time points. Early stage PrP^d deposition in a normally glycosylated control after 263K challenge was examined at five defined brain levels of which four are shown here (A & E) medulla and cerebellum, (B & F) midbrain including superior collicullus (Sc) (just seen B), cerebral cortex and hippocampal formation, (C & G) hippocampus (Hp), habenula (Hb), thalamus (Th), hypothalamus, cerebral cortex and corpus callosum (cc), (D & H) forebrain including corpus callosum and septum (Sp). PrP^d was detected after wet autoclaving and formic acid treatment, using anti-PrP antibody 6H4. The signal was amplified using a CSA kit and visualised with DAB; nuclei were counter stained with haematoxylin. Synaptic-type PrP^d deposition can be observed in habenula, medulla, cerebral cortex (C & G) the septum and caudate putamen (D & H). Boxed area in A = B, C = D, E = F and G = H. Sections shown are from a single normally glycosylated control mouse a further two animals also exhibited a similar pattern of extensive deposition. Specificity of signal was determined using PrP null [NPU] and normal brain homogenate challenged $PrP^{a/a}$ negative control sections (I). Scale bar 500 μm (A, C, E, G), 25 μm (B, D, F, H).

Figure 5.4 More extensive of PrP^d deposition is observed in control mice after 263K challenge at later time points (6H4)

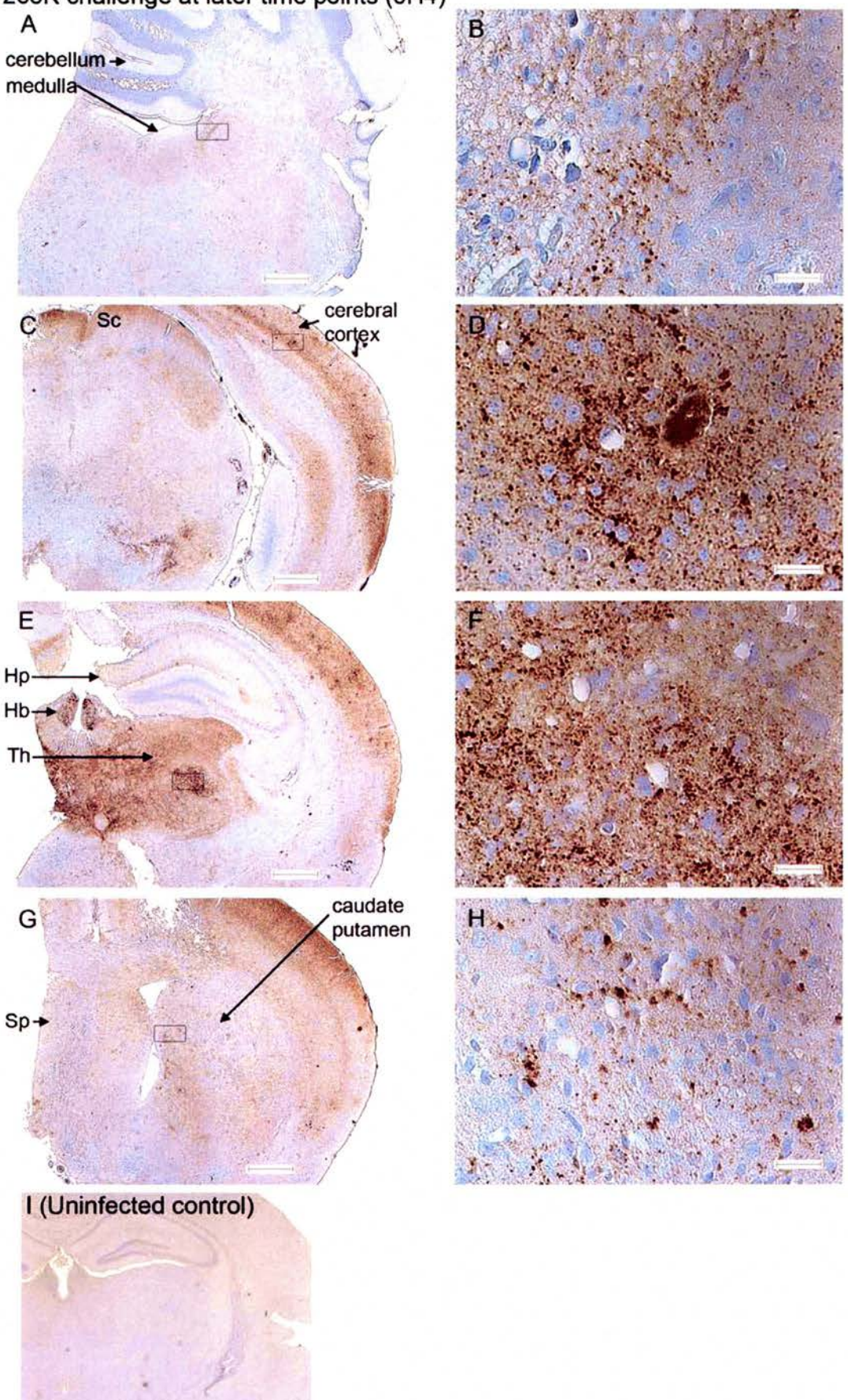

Figure 5.5 Extensive PrP^d synaptic-type deposition and plaques were observed in G2 transgenic mice challenged with 263K. PrP^d deposition in G2 transgenic mice after 263K challenge was on average more extensive than that observed in normally glycosylated controls. The deposition of PrP^d was examined at five defined brain levels of which four are shown here (A & B) medulla and cerebellum, (C & D) midbrain including superior colliculus (Sc), cerebral cortex and hippocampal formation, (E & F) hippocampus (Hp), habenula (Hb), thalamus (Th), hypothalamus, cerebral cortex and corpus callosum (cc), (G & H) forebrain including corpus callosum and septum. Extensive PrP^d deposition was detected throughout the brain, after wet autoclaving and formic acid treatment, using anti-PrP antibody 6H4. The signal was amplified using a CSA kit and visualised with DAB; nuclei were counter stained with haematoxylin. Large PrP^d plaques can be observed in the thalamus (E). Boxed area in A = B, C = D, E = F and G = H. Figures show the results from a single G2 transgenic mouse, a further five G2 animals exhibited a similar extent of deposition. Specificity of signal was determined using PrP null [NPU] and normal brain homogenate challenged $PrP^{a/a}$ negative control sections (I). Scale bar 500 μm (A, C, E, G), 25 μm (B, D, F, H).

Figure 5.5 Extensive PrP^d synaptic-type deposition and plaques were observed in G2 transgenic mice challenged with 263K (6H4)

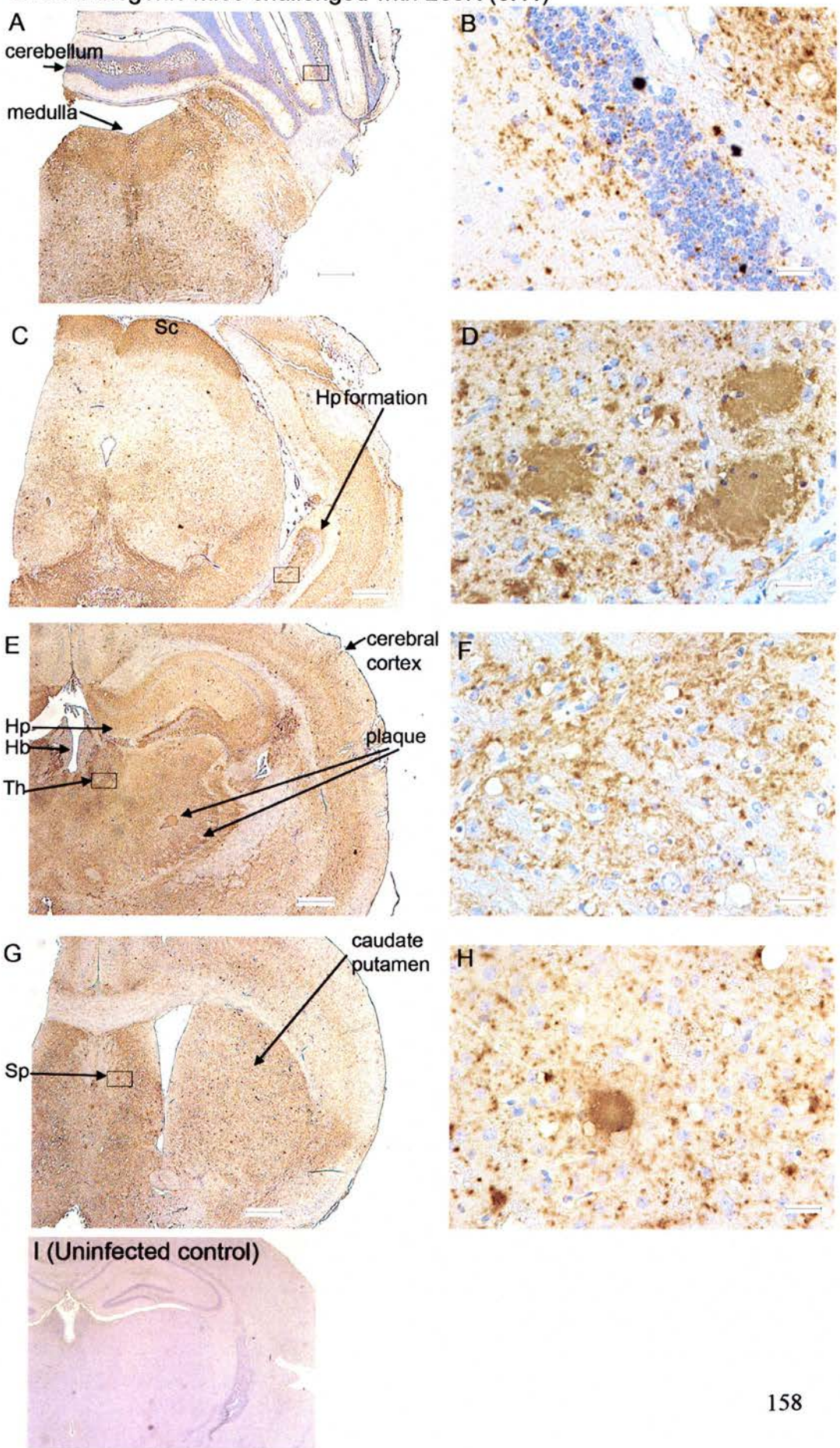

Figure 5.6 PrP^d amyloid plaques are formed in the thalamus and hippocampus in G2 transgenic mice after challenge with 263K.

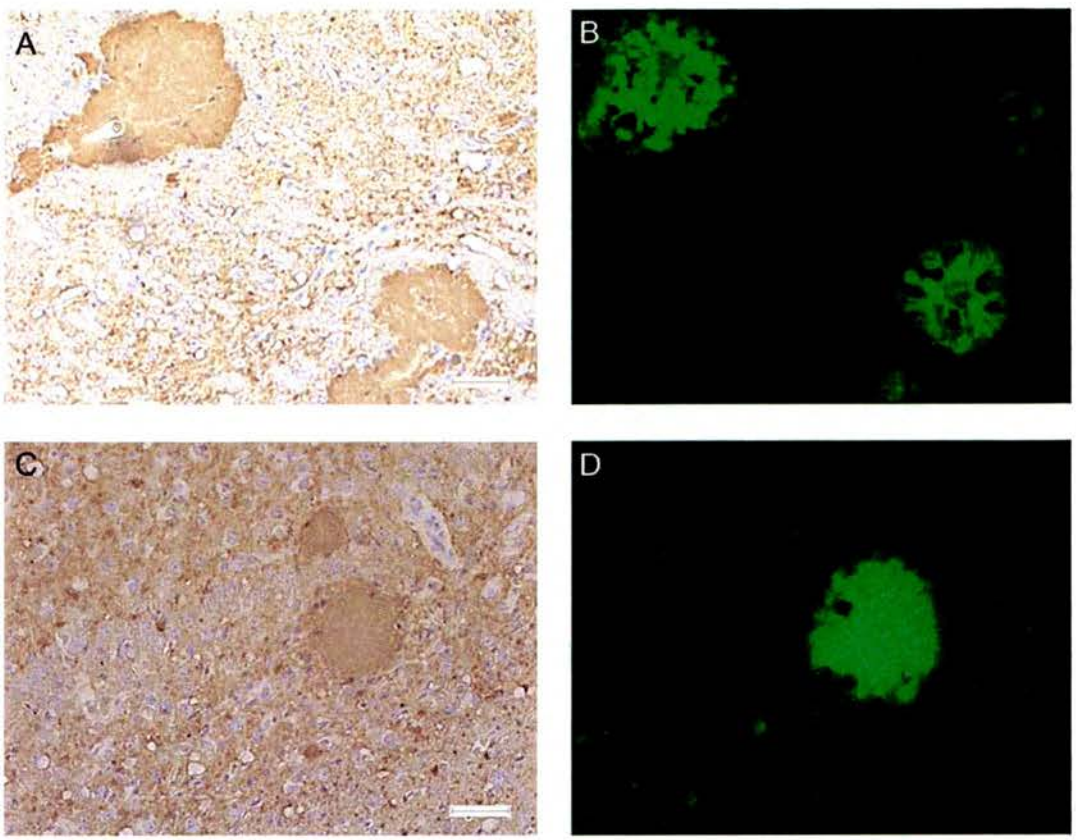

PrP^d plaques were observed in the thalamus (A) and hippocampus (C) of G2 transgenic mice that were challenged with 263K, using the anti-PrP antibody 6H4, on brains sections that had be treated with formic acid and wet autoclaving to mediate antigen detection. To determine if these plaques contained amyloid protein, serial sections were treated with thioflavin-s (B & D). The plaques interacted with thioflavin-s demonstrating the formation of amyloid *in vivo*. Scale-bar 50 µm.

The extent of PrP^d deposition was reduced in the G1 glycosylation deficient transgenic mice compared to the normally glycosylated controls (Figure 5.7, table 5.2) (Chi-square = 10.922, degrees of freedom = 3, $p < 0.25$). In the majority of G1 transgenic mice, PrP^d was only observed in the habenula and surrounding thalamic neuropil; occasionally, very limited synaptic staining was also observed in the hypothalamus or medulla. This pattern of deposition is similar to the earliest deposition observed in 263K challenged G2 transgenic mice and normally glycosylated controls (data not shown). These data demonstrate that the absence of the first glycosylation site retards the accumulation of PrP^d in the brain after cross-species 263K challenge, but does not appear to alter its pattern. This is consistent with the hypothesis that the strain of TSE does not differ between the G1 transgenic and normally glycosylated mice. The contrasting effect of N-glycans attached at the first site (G2), which may promote PrP^d accumulation and at the second site (G1) that inhibits the accumulation, of PrP^d *in vivo* after 263K challenge, suggests that the N- glycans attached to the two sites play very different roles in the accumulation of PrP^d.

Apart from a single corpus callosum PrP^d plaque in one G3 transgenic mouse (Figure 5.8 I) no other PrP^d deposition was observed in 263K challenged G3 transgenic mice as assayed by 6H4 or 8H4 (Figure 5.8 A-G). These data suggest that glycosylation of PrP^C facilitates the accumulation of PrP^d *in vivo*. Furthermore, this demonstrates that the effect of absence of glycosylation at the second site on the promotion of PrP^d accumulation *in vivo* requires that the first site is glycosylated.

Figure 5.7 Little PrP^d deposition was observed in G1 transgenic mice after challenge with 263K.

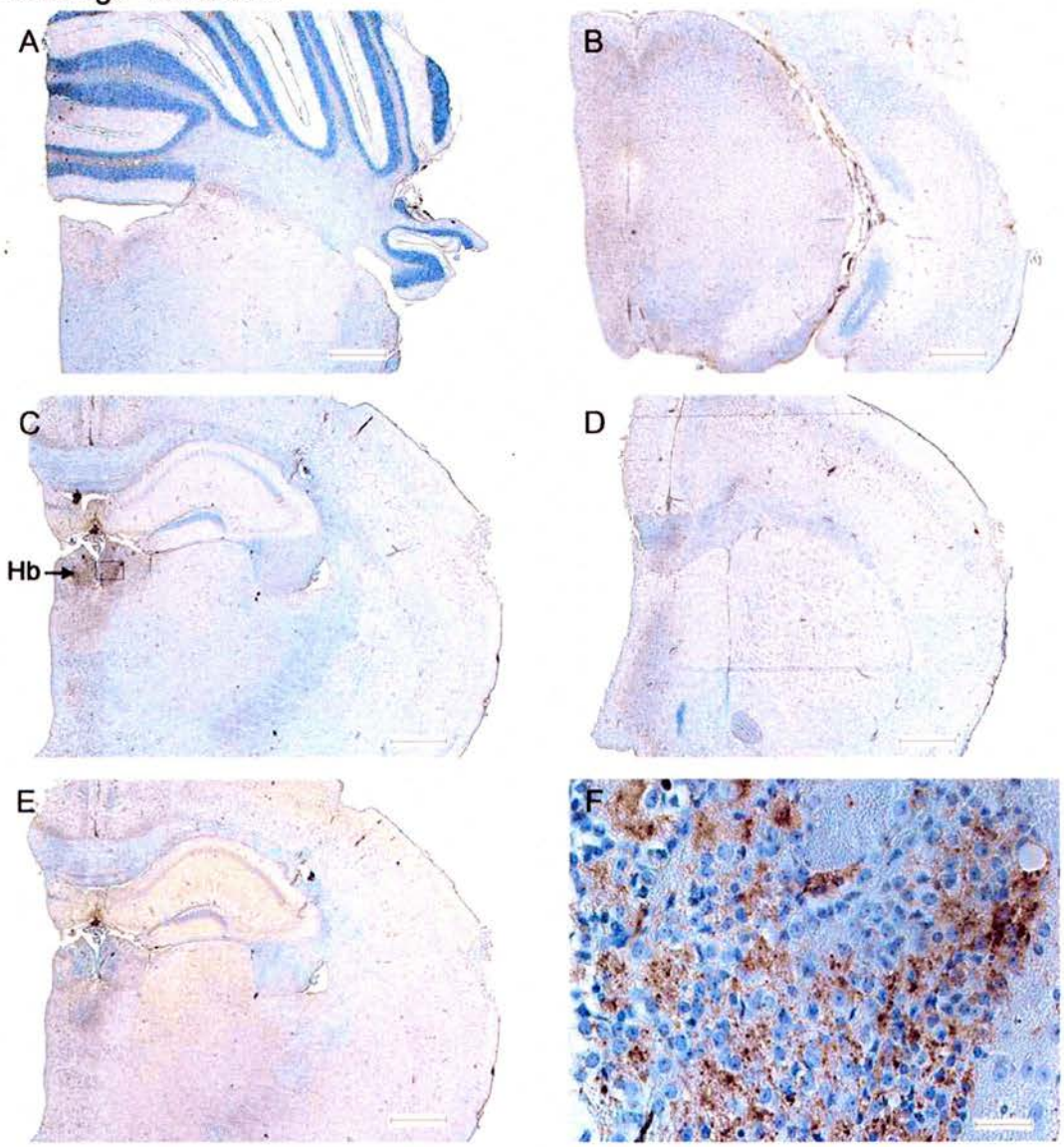

PrP^d deposition in G1 transgenic mice after 263K challenge was very limited, deposition was examined at five defined brain levels of which four are shown here (A) medulla and cerebellum, (B) midbrain including superior colliculus, cerebral cortex and hippocampal formation, (C) hippocampus, habenula, thalamus, hypothalamus cerebral cortex and corpus callosum, (D) forebrain including corpus callosum and septum, close up of deposition in habenula (Hb) (F). PrP^d deposition was only detected in the habenula and surrounding thalamus using anti-PrP antibody 6H4 (C and F) but not in normal mouse serum negative control (E). Tissue was pretreated by wet autoclaving and formic acid treatment, anti-PrP signal was amplified using a CSA kit and visualised with DAB, nuclei were counter stained with haematoxylin. Specificity of signal was determined using PrP null [NPU] and normal brain homogenate challenged PrP^a negative control brain sections. Scale bar 500 µm (A-E), 25 µm (F).

Figure 5.8 PrP^d deposition was generally not observed in G3 transgenic mice challenged with 263K. PrP^d deposition in G3 transgenic mice after 263K challenge was examined at five defined brain levels of which four are shown here (A & E) medulla and cerebellum, (B & F) midbrain including superior colliculus (B), cerebral cortex and hippocampal formation, (C & G) hippocampus, habenula, thalamus, hypothalamus, cerebral cortex and corpus callosum, (D & H) forebrain including corpus callosum and septum. PrP^d deposition was generally not detected, even after PrP antigen retrieval by wet autoclaving and formic acid treatment, using anti-PrP antibody 6H4 (A-D) or 8H4 (E-H), and use of signal amplification by CSA kit. Sections from two G3 transgenic mice (animal one, A-D; animal two, E-H) did not exhibit detectable PrP^d but in one G3 transgenic mouse, PrP^d was detected in the corpus callosum (I). Nuclei were counter stained with haematoxylin. A 263K challenged G2 transgenic mouse was used as a PrP^d positive control (6H4-J, 8H4-K). Scale bar 500 μm (A-H).

Figure 5.8 PrP^d deposition was generally not observed in G3 transgenic mice challenged with 263K

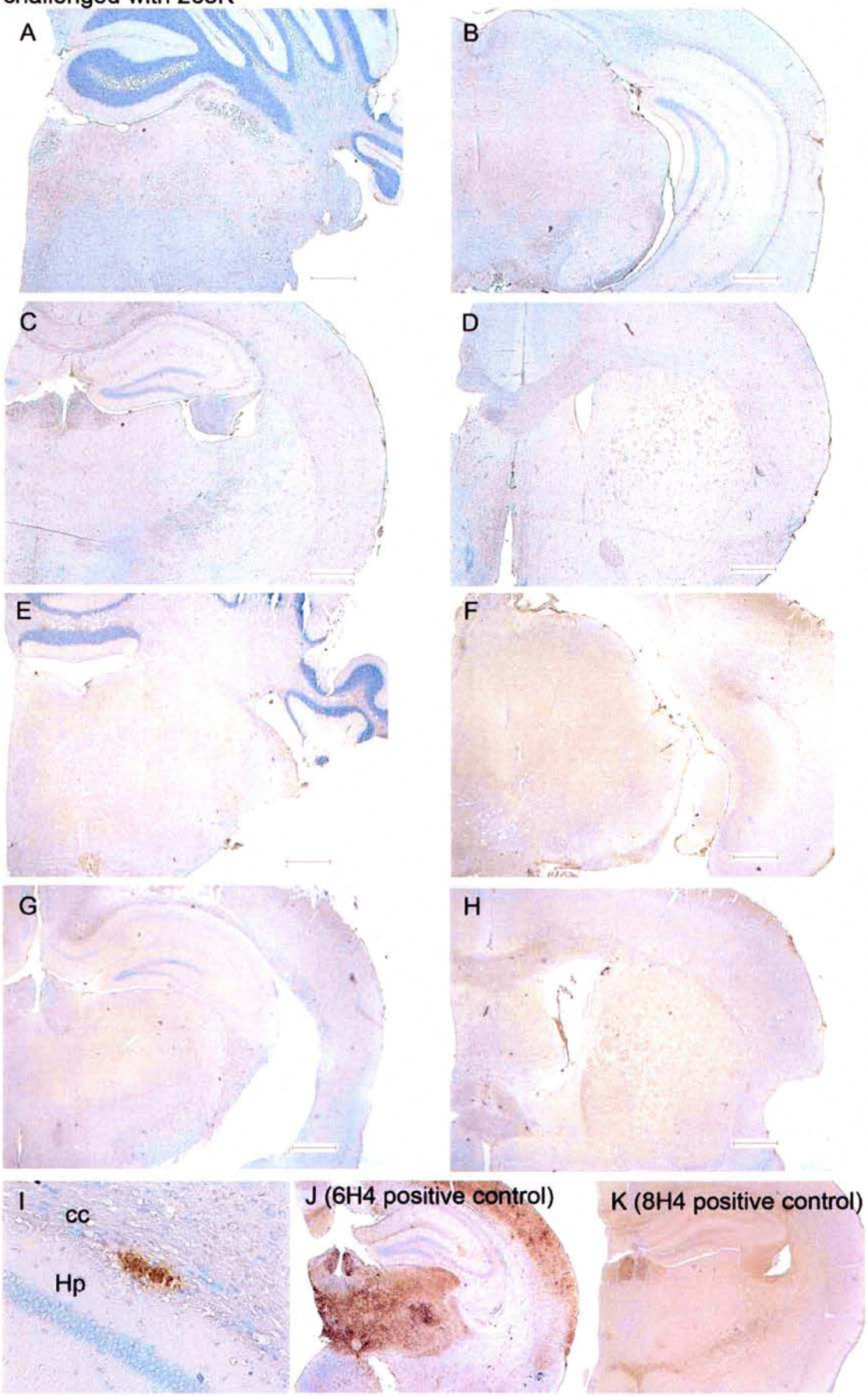

5.4.4 TSE associated PK resistant PrP^{Sc}

To further investigate the effect of host PrP glycosylation state on TSE strain, the PrP^{Sc} type was examined by limited PK digestion and western blot, after cross-species challenge with 263K. This allowed the molecular weight of the PK resistant core to be compared between 263K challenged glycosylation transgenic and normally glycosylated control mice. This parameter correlates with a number of TSE strains and is proposed to reflect the conformation of PrP^{Sc} (Bessen and Marsh, 1992a; Collinge et al., 1996; Parchi et al., 1996; Somerville et al., 1997). These experiments also permitted an estimate of the amount of misfolded PrP that had accumulated after 263K challenge. Brain material was either prepared in sterile physiological saline (for subpassage) then extracted in detergent containing Tris buffered lysis solution (NP40 lysis buffer) or directly in NP40 lysis buffer to facilitate isolation of PrP^{Sc}. The same batch of PK (aliquoted and stored a –20 °C) was used for all digestion under standard conditions (20 µg/ml, 37 °C for 1 hour) to ensure enzyme consistency; uninfected negative controls of the appropriate genotype and corresponding PrP^{Sc} positive controls were used for all digestions.

The PK resistance of PrP^{Sc} in 263K challenged animals was determined using standard digestion conditions and western blotting under denaturation conditions. PrP was detected using anti-PrP monoclonal antibodies 8H4 and 7A12; similar results were observed with both antibodies (Figure 5.9 and data not shown). Proteinase K resistant PrP (PrP^{Sc}) was observed in 263K challenged G2 transgenic mice (n = 5) and normally glycosylated control mice (n = 7), but not in 263K challenged G1 (n = 5) or G3 (n = 5) transgenic mice or uninfected murine controls, even after twenty fold concentration by NaPTA precipitation or high speed centrifugation (Figure 5.9 B-E). This would suggest that either the G1/263K PrP^{d} observed by IHC is PK sensitive or below the level of detection possible by these techniques. Further investigation is required using a more sensitive assay and lower concentrations of PK to assess these possibilities experimentally.

Figure 5.9 Western blots of PrP^{Sc} from PrP glycosylation deficient transgenic mice, murine and hamster controls challenged with 263K

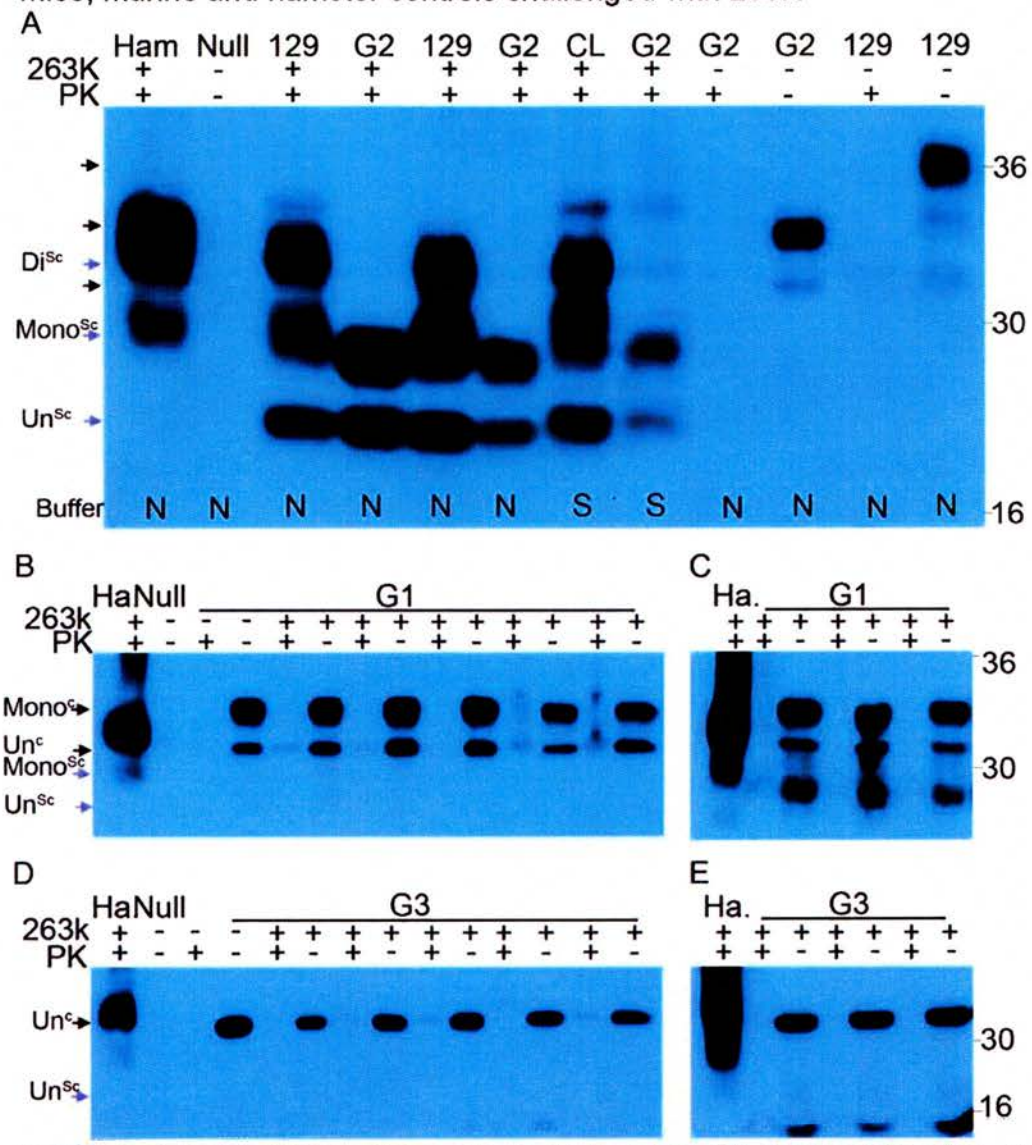

PrP^{Sc} was isolated from three 263K challenged G2 transgenic mice and three normally glycosylated control mice (CL or 129/Ola) and one hamster, that exhibited TSE specific vacuolation and/or PrP^{d} deposition, by standard PK digestion (20 µg/ml, 37 °C, one hour) of total brain homogenate (A) that ahd been prepared in saline (S) or NP40 tissue lysis buffer (N). No consistent difference in electrophorectic mobility of un-glycosylated PrP^{Sc} (blue arrow un^{Sc}) is observed between G2 transgenic and normally glycosylated control mice, however differences in the mobility of mono-glycosylated PrP^{Sc} (blue arrow $mono^{Sc}$) between the G2 transgenic and control mice are apparent. In five G1 transgenic mice (B and C) in which PrP^{d} was observed and five G3 transgenic mice (D and E) in which no PrP^{d} was observed, PrP^{Sc} was concentrated twenty-fold by NaPTA mediated precipitation (B and D) or high speed centrifugation (C and E); after standard PK digestion (20 µg/ml, 37 °C, one hour). No PrP^{Sc} was detected in any of these samples, despite clear PrP^{C} signal . PrP was detected with anti-PrP antibody 8H4 and horseradish conjuagated anti-mouse secondary antibody (Jackson ImmunoResearch, West Grove, USA). Secondary was detected using POD solution (Roche Diganostics, Basel, Switzerland) and the resultant chemiluminescence was detected using X-ray film.

Slight variation was observed in the electrophoretic mobility of PrP^{Sc} between samples. In particular, tissue that was prepared for inoculation by homogenisation in physiological saline produced un-glycosylated PrP^{Sc} after PK digestion of a slightly lower electrophoretic mobility, which may indicate a greater molecular weight than that directly homogenesised in NP40 buffer. However, PrP^{Sc} isolated from 263K challenged G2 transgenic mice was not of a consistently different molecular weight than that from normally glycosylated controls. This is consistent with the observed similarity of deposition pattern of PrP^{d} in G2 and control mice *in vivo* and suggests that the conformation of PrP^{Sc} is similar in the transgenic and control mice, which is indicative of these animals being infected with the same TSE strain.

However, the mono-glycosylated PrP^{Sc} from G2 transgenic mice consistently exhibited significantly higher electrophoretic mobility than that from normally glycosylated animals. This indicates that the combination of sugars attached to mono-glycosylated PrP^{Sc} differs between G2 transgenic and normally glycosylated control mice. Further investigation is required to determine how the glycans attached to G2/263K PrP^{Sc} and CL/263K PrP^{Sc} differ, and if these differences affect the conformation of PrP^{Sc}.

In both G2 and normally glycosylated controls, the ratio of glycotypes appeared to be shifted towards the less glycosylated forms when compared to that of hamster 263K glycoform (Figure 5.9). However, this result is compounded by known differences in the amino acid sequence and putative differences in the N-glycans attached to hamster and mouse PrP, which may alter antibody binding to the different glycotypes of protein as highlighted by results presented in Chapter 3. Hence although this observation does not provide strong evidence for preferential conversion of un- and mono-glycosylated murine PrP^{C} by hamster 263K PrP^{Sc}, it further supports the hypothesis that PrP's N-glycans may retard the conversion of murine PrP^{C} by hamster 263K.

Furthermore, G2/263K CNS material appeared to contain more PrP^{Sc} than was observed in 263K challenged normally glycosylated mice, as higher dilution factors were required to produce equivalent western blot signals (Figure 5.9 A). This is consistent with the observation of heavier and more extensive PrP^{d} deposition in the murine G2 transgenics

than in normally glycosylated mice. Thus providing further evidence that glycosylation of PrP's second site reduces the rate of PrP^{d} accumulation in mice after cross-species infection with hamster passaged scrapie strain 263K. However, differential antibody recognition of misfolded PrP from G2 transgenic and normally glycosylated control mice could conceivably also explain these observations. Moreover, the concentration of PrP^{Sc} isolated from 263K/G2 transgenic mice was always lower than that observed in the clinical endpoint 263K hamsters. Thus, even in the absence of glycosylation at the second site, a strong barrier to *in vivo* 263K seeded PrP^{Sc} accumulation is apparent in mice.

5.4.5 TSE associated astrogliosis

Astrogliosis is a typical pathogenic response to TSE infection, although it is not observed in all types of disease. To determine if its occurrence after cross-species TSE challenge was influenced either directly or indirectly by the glycosylation state of PrP^{C}, its extent was examined in 263K challenged glycosylation deficient transgenic mice and normally glycosylated controls. What mediates the observed up regulation of astrocytes in TSE disease is currently unclear; they may be responding to the deposition of misfolded PrP, a subset of PrP forms (PrP*), directly to neuronal damage or dysfunction independently of PrP, or may be independently interacting with the TSE agent. An antibody against glial fibrillary acid protein (GFAP) was used. In a healthy brain nascent astrocytes express GFAP at low levels, however during the astrocytic response the number of astrocytes increases, their morphology alters and the level of GFAP they express rises (Sofroniew, 2005). A subset of brains was selected from each experiment and the presence of an astrocytic response was scored blind using three possible categories (no response, limited response, extensive response). Brain sections from normal murine brain homogenate inoculated and uninfected wild type mice were used as negative controls for astrogliosis. Brain sections from clinical endpoint mice infected with ME7 were used as the positive control for astrogliosis

Vacuolation positive 263K challenged G2 transgenic and normally glycosylated control mice exhibited extensive astrocytosis throughout the brain suggesting that glycosylation

of PrP at the second site is not required for the TSE disease activation of astrocytes (Figure 5.10). G1 transgenic mice, in which only PrP^d was observed in the absence of vacuolation, did not exhibit detectable astrogliosis (Figure 5.10 E, F). This suggests that either the misfolded PrP deposited in the G1 transgenic mice was of an insufficient quantity to induce an astrocytic response or it was of a different type to that which formed in the G2 transgenic mice. Alternatively, the absence of astrogliosis in the G1 transgenic mice may also occur independently of misfolded PrP, perhaps via a direct effect of PrP^C glycosylation state on astrocytes or via a change in neuronal damage or dysfunction. No astrocytosis was observed in G3 263K challenged transgenic mice consistent with absence of other TSE signs in these animals (data not shown)

Figure 5.10 Extent of astrocyte activation in glycosylation deficient transgenic and control mice challenged with 263K

Astrogliosis in 263K challenged mice was examined using immunohistochemistry for GFAP. Clinical endpoint ME7 challenged mice were used a positive control and normal brain homogenate challenged and unchallenged mice were used to determine baseline level of astrocyte activation in healthy brains. Extensive astrogliosis was observed in TSE vacuolation positive normally glycosylated controls (A and B) and G2 transgenic mice (G and H). In G1 transgenic mice (E and F) in which limited PrP^d was observed in the absence of vacuolation, the distribution of astrocytes was comparable to that observed in uninfected control (C and D). Scale bar 500 μm (A, C, E, G), 50 μm (B, D, F, H).

Figure 5.10 Extent of astrocyte activation in glycosylation deficient transgenic and control mice challenged with 263K

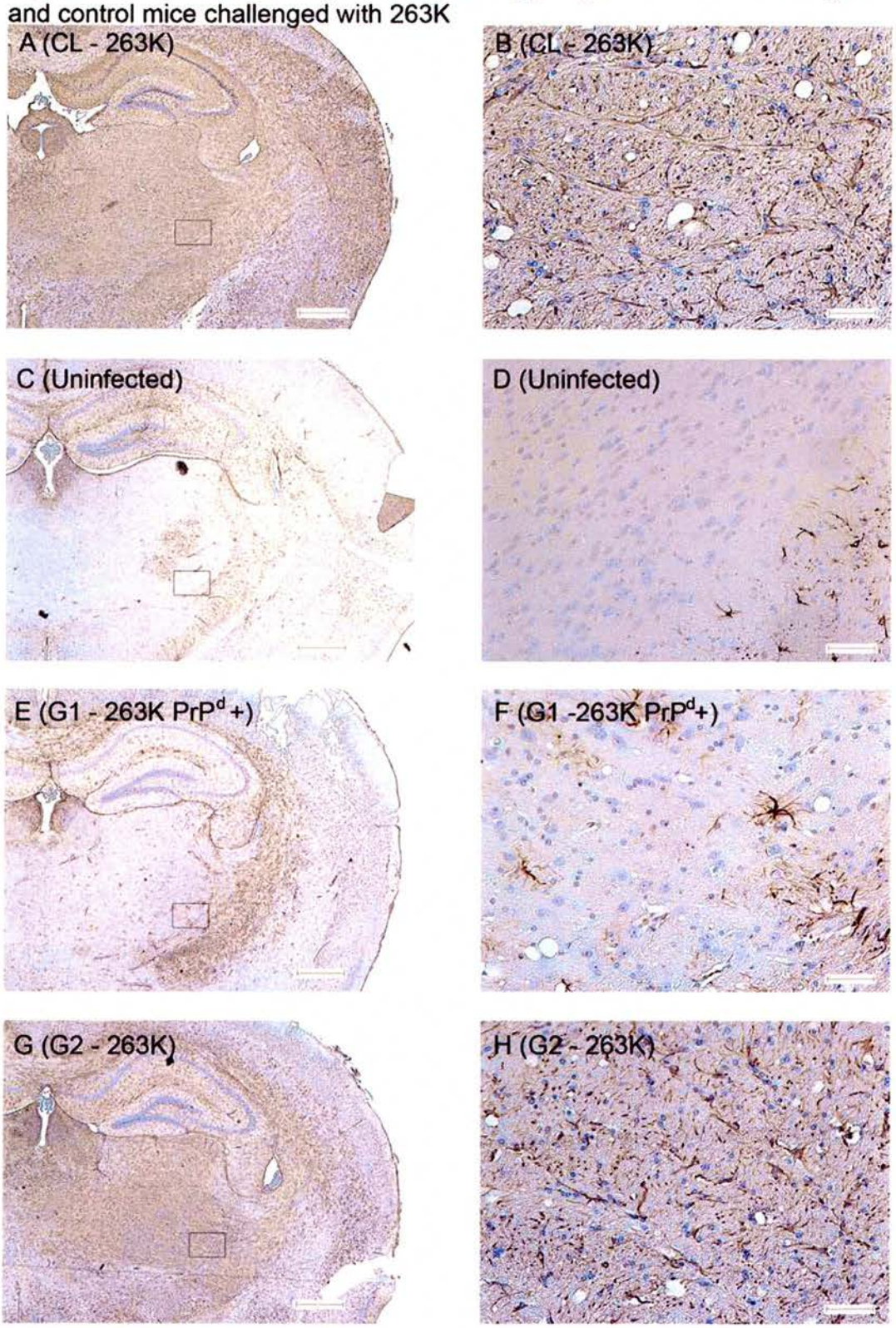

5.4.6 Results summary

These data demonstrate that the glycosylation state of host PrP greatly influences the incidence and progression of TSE disease after cross-species transmission of 263K to mice. However, other strain characteristics of the resultant infection do not appear to be altered by the glycosylation state of host PrP. Moreover, the effect of glycosylation is dependent on the site of N-glycan attachment.

- Mice expressing only un-glycosylated PrP are resistant to 263K transmission and do not form significant PrP^{Sc}.
- Absence of the first N-glycan attachment site increases resistance to, or extends the incubation period, of 263K but does not completely prevent the formation of misfolded PrP in mice.
- Absence of the second N-glycan attachment site enhances the susceptibility of mice to 263K, as illustrated by the higher attack rate and decreased time to disease onset. Additionally, the accumulation of PrP^{Sc} *in vivo* appears to be promoted.
- Glycosylation of host PrP^{C} does not influence the pattern of vacuolar pathology, pattern of PrP^{d} deposition or the PrP^{Sc} type resultant from the transmission of 263K to murine hosts.

5.5 Discussion

5.5.1 Technical discussion

A number of hamster scrapie challenged mice, particularly G2 transgenic mice, exhibited relatively severe TSE specific pathology (PrP^{d} deposition and widespread vacuolation) and extensive astrocytosis in the absence of any neurological signs or significant reduction in life span. This sub or preclinical disease state is consistent with previous reports of cross-species TSE transmissions (Hill et al., 2000; Race et al., 2001). These data also support the hypothesis that the neurotoxic PrP species may not be PrP^{Sc} (Weissmann, 1991), given the substantial amounts tolerated in clinically unaffected mice. Additionally, this work questions a direct link between TSE specific vacuolation

and neuronal dysfunction as has been previously postulated (Laszlo et al., 1992). Equally, these data may be explained by compensation of a damaged neurons function by surrounding cells. However, as only standard clinical signs were assessed, subtle changes in behaviour, as have been previously reported associated with the pre-clinical TSE phase (Deacon et al., 2001; Guenther et al., 2001), may have been overlooked. Thus the observed pathological changes may have resulted in undetected alterations in the behaviour of infected mice.

5.5.2 Discussion of experimental results

These data demonstrate that glycosylation of PrP^C specifically affects the cross-species transmission of hamster scrapie strain 263K, as indicated by an alteration in the incidence and time to development of TSE specific pathology. However, other TSE strain characteristics such as the pattern of vacuolar targeting and PrP^d deposition are not significantly affected by changes in the glycosylation status of PrP^C. Moreover, the influence of PrP's glycosylation state on disease is dependent upon the site of N-glycan attachment. Glycosylation of asparagine 180 is linked to the facilitation of cross-species transmission of 263K, as demonstrated by the reduced incidence and extent of TSE disease observed in challenged G1 and G3 transgenic mice. In contrast, glycosylation of asparagine 196 retards the cross-species transmission of hamster 263K to murine hosts, but only in the presence of a glycan at the first site, as demonstrated by the higher disease incidence in G2 transgenic mice compared to wild type murine controls and the G3 transgenics. These data raise the question of why glycosylation of the two sites has such dramatically different effects on 263K transmission, and why the glycosylation state of first site modifies the importance of glycan attachment to the second.

Importantly, the facilitating effect of the absence of glycosylation of PrP^C's second site on TSE transmission appears to be limited to cross-species challenge, as G2 transgenic mice and comparable conventional murine transgenics are not more susceptible to murine passaged scrapie or murine passaged BSE (Neuendorf et al., 2004) (Tuzi et al, in preparation, appendix ii). Indeed, extensive prolongation of the incubation period has been observed in G2 transgenic mice challenged with the murine TSE strains 301C,

ME7 and Chandler (appendix ii.). This suggests that the mechanism underlying the inhibitory role of second site PrP glycosylation in TSE transmission is dependent upon a species barrier specific function. However, the inhibitory effect of disrupting the first glycosylation site, or both sites, on TSE disease is not limited to cross-species transmissions (Tuzi et al, in preparation, appendix ii), suggesting that the observed reduced disease incidence and the apparent extended time to disease onset in the G1 and G3 transgenic mice may be the result of a generic effect on TSE disease.

The extent of the species barrier to 263K transmission correlates with the observed accumulation of PrP^{Sc} *in vivo*, for example the TSE pathology negative G3 transgenic mice also exhibit no significant misfolded PrP. Thus, either G3 PrP^{Sc} does not form *in vivo*, or it forms but does not accumulate or is undetectable by conventional methods. These results differ from *in vitro* PrP^{C} to PrP^{Res} conversion assay data presented by Priola and Lawson, which showed that un-glycosylated murine PrP was more readily converted to PrP^{Res} by hamster scrapie (263K) than the normally glycosylated protein (Priola and Lawson, 2001). This discrepancy may be the result of the experimental differences between the work presented here and the *in vitro* conversion assay, such as the method of producing un-glycosylated PrP or the amino acid sequence of murine PrP^{C} used. Alternatively this difference may be the result of an *in vivo* specific effect of PrP's N-glycans on TSE disease pathogenesis and PrP^{Sc} accumulation. Further experimentation is required to determine if the innate convertibility of G3 un-glycosylated PrP resembles or differs from that of Priola and Lawson's construct, and hence if the absence of PrP^{Sc} formation in the G3 transgenic mice reflects an inability of G3 PrP to misfold (Chapter 7).

Similarly, the differences in the role of the first and second site of N-glycosylation on the cross-species transmission of 263K to mice correlated with the accumulation of misfolded PrP *in vivo*. This may be related to the differing effect of glycosylation of the two sites on the efficiency of PrP^{Sc} formation. Computational modelling experiments have suggested that N-glycan attachment to PrP^{C} at the second site may enhance the protein's conformational stability (Zuegg and Gready, 2000). Thus in the absence of glycosylation at the second site, the energy barrier to generate the misfolded

conformation may be reduced and hence conversion may occur more readily. This mechanism may be specific to cross-species TSE challenge because of the unique conformational transition of PrP^{Sc} which is proposed to underlie the species barrier (Peretz et al., 2002). Equally, the relative proximity of the second site to two murine/hamster amino acid differences may underlie the observed inhibitory effect of glycosylation at this site on the cross-species transmission of 263K to mice. Further experimentation is required to explore the feasibility of these scenarios.

The effect of PrP glycosylation state on the accumulation of PrP^{Sc} *in vivo* may be mediated by an effect on the stability of PrP^{Sc}, such that its rate of clearance in the CNS is modified. This could occur if the sensitivity of the N-glycan deficient forms to enzymatic digestion was directly changed or if they are differently targeted for clearance. The absence of glycosylation of the second site does not appear to alter the conformation of PrP^{Sc}, as assayed by PK digestion. However, the effect of the absence of glycosylation at the first or both sites on the conformation of misfolded PrP unknown since no detectable PrP^{Sc} formed in either the G1 or G3 transgenic mice. A change in conformation may affect the stability of PrP^{Sc}, as has been experimentally suggested for different TSE strains (Safar et al., 1998), and hence its ability to accumulate *in vivo*. The glycosylation state of PrP^{Sc} may equally affect the protein's ability to aggregate that could result in a change in its *in vivo* stability. All these possible effects could feasibly result as a direct effect on the behaviour of an individual PrP molecule or via higher order interactions between PrP and itself or other cellular components.

Alternatively, the difference between the *in vitro* and *in vivo* data may reflect a TSE specific role of the glycosylation state of PrP independent of its TSE disease associated misfolding. This putative function may either be upstream of the *in vivo* formation of PrP^{Sc}, or it may act in addition to a change in convertibility. Glycosylation of PrP^{C} may influence the turnover or trafficking of the protein, despite the comparable steady state of the PrP^{C} in the CNS in the PrP glycosylation deficient transgenic and normally glycosylated mice (Chapter 3). These factors could directly affect the ability of PrP to play its essential role in TSE pathogenesis. Equally they may affect the subcellular distribution of PrP^{C} in the murine PrP glycosylation deficient transgenics, as has been

previously demonstrated in other systems (DeArmond et al., 1993; Neuendorf et al., 2004). Cellular localisation of PrP^C has been suggested as important to both PrP misfolding and TSE pathogenesis (Chesebro et al., 2005; Taraboulos et al., 1995; Trifilo et al., 2006). The localisation of PrP^C may be altered in the G3 PrP glycosylation deficient transgenics (Chapter 4) and this may contribute to the resistance of these mice to cross-species TSE transmission.

Transgenic mice which express PrP that lacks the GPI anchor also do not develop classical TSE disease, but do form PrP^{Sc} after TSE challenge (Chesebro et al., 2005; Trifilo et al., 2006). The PrP in this transgenic model is also not fully glycosylated, presumably because of the known requirement for a specific distance between the N-glycan attachment site and PrP's C-terminus (Walmsley and Hooper, 2003). The formation of PrP^{Sc} in the GPI anchor deficient transgenic mice suggests that the mechanisms underlying TSE disease resistance differ between the PrP glycosylation and GPI anchor deficient transgenic mice. Enhanced resistance to cross-species transmission is also caused by the endogenous expression of murine PrP^C in over-expressing hamster PrP^C transgenic mice (Telling et al., 1994; Telling et al., 1995). The authors of this paper suggested that this result occurred because of a requirement for a species specific PrP conversion factor, which they postulate interacts with an area of the C-terminus of PrP that is not normally shielded by the protein's N-glycans (Telling et al., 1995). Thus interactions with this proposed factor would be anticipated to be equivalent in the G1 and G3 murine transgenics to those in wild type mice, although interaction of conversion factors with other regions of PrP may be affected by the absence of glycosylation of the protein in the transgenic mice.

Alternatively, the results of Telling and colleagues can be explained by heterologous PrP conversion interference, as has been observed *in vitro* systems (Horiuchi et al., 2000). Similarly, heterozygosity for PrP polymorphisms is linked to enhanced resistance to TSE transmission (reduced disease incidence and increased incubation periods) (Barron et al., 2005; Collinge et al., 2006). The G1 and G3 transgenic mice used in these experiments were homozygous for the introduced changes in the first and second glycan

attachment site and thus heterologous interference would not have contributed to the observed changes in cross-species transmission.

These data demonstrate that the absence of glycosylation of PrP at the first or both N-glycan attachment sites greatly reduces the formation of PrP^{Sc} and prevents the development of TSE disease after cross-species challenge with hamster scrapie strain 263K. Replication of TSE infectivity in the absence of detectable PrP^{Sc} or the development of TSE pathology has been previously observed (Barron et al., 2001; Hill et al., 2000; Lasmezas et al., 1997; Race et al., 2001). Thus, subpassage of material from TSE challenged G3 and G1 transgenic mice into the G3 mice, G1 mice, wild type mice and hamsters is required to experimentally assess whether the complete lack of PrP's N-glycans prevents the replication of TSE infectivity in addition to its influence on PrP misfolding and development of TSE disease.

In conclusion these data demonstrate that the glycosylation state of murine PrP can have a dramatic influence on disease incidence and time to disease onset after challenge across a species barrier with hamster scrapie strain 263K. The effect of PrP^{C}'s N-glycans on the rate of disease progression occurs in the absence of an alteration of other strain characteristics. Further experimentation is required to determine the mechanism by which this modification of transmission occurs and if PrP's glycosylation state also affects transmission of other TSE strains between species.

6.0 TSE strain and the effect of glycosylation of PrP^C on cross-species transmission

6.1 Aim To determine if the proposed role of PrP's N-glycans in the TSE species barrier is dependent upon TSE strain.

6.2 Introduction and experimental method

Data presented in Chapter 5 demonstrates that the N-linked glycosylation of PrP^C has a major influence on the transmission of hamster scrapie, strain 263K to mice. In particular, glycosylation of asparagine 180 enhances the cross-species transmission of 263K, whilst N-glycan attachment to asparagine 196 hindered it. Thus the glycosylation state of host PrP^C modulates the ability of a TSE agent to elicit disease in a novel host species. Previous host factors that influence the cross-species transmission of TSE disease, such as PrP amino acid sequence, have exhibited TSE strain dependence (Manson et al., 1999; Prusiner et al., 1990). Additionally the effect of PrP's glycosylation state on within species transmission is also affected by TSE strain (DeArmond et al., 1997; Neuendorf et al., 2004; Tuzi et al., in preparation) (appendix ii). Thus the effect of N-glycan attachment to PrP^C on cross-species transmission may be similarly influenced by TSE strain.

The potential strain dependence of the role of PrP's N-glycans in the TSE species barrier may be mediated by a number of mechanisms. Experimental work has suggested that the extent of the species barrier may reflect the conformational compatibility between host PrP^C and donor PrP^{Sc}, which will be unique for each strain/host combination (Peretz et al., 2002). This model suggests that the ability of PrP^C from a host species to adopt the misfolded conformation of the challenging TSE strain determines the extent of the species barrier. Thus host factors that influence the conformational flexibility of PrP^C and its ability to misfold may be particularly important to the species barrier. Equally the specific PrP^C glycotypes required for efficient transmission may vary between different strains, as the glycoform of PrP^{Sc}

has been reported to reproducibly correlate with strain (Collinge et al., 1996; Parchi et al., 1996). Moreover other strain specific factors, such as the cells targeted during disease or the method of cell to cell spread of infectivity may also be differentially influenced by the glycosylation state of PrP^{C}. Hence the glycosylation state of PrP^{C} may also influence the barrier, independent of an effect on the accumulation of PrP^{Sc}.

The role of N-glycans in the TSE species barrier may depend upon the relatedness of host and donor of infectivity. In particular, the degree of amino acid sequence homology between the two species may determine the relative importance of N-glycosylation to cross-species transmission. Alternatively the degree of the barrier to cross-species transmission may also modify the importance of N-glycans. Additionally, recent work has suggested that the combination of N-glycans attached to PrP^{Sc} differs between host species (Xanthopoulos et al., 2006). This may reflect an adaptation of the TSE agent to the N-glycans of a particular host, which may also contribute to a specific effect of glycosylation on cross-species transmission.

To investigate if TSE strain influences the role of glycosylation of PrP^{C} in the TSE species barrier, PrP glycosylation deficient murine transgenics [NPU] and normally glycosylated mice (CL) were independently challenged with two human TSE sources, variant CJD and sporadic CJD MM-cortical (type 2). Comparison of these data with that presented in chapter 5 will provide further insight into the importance of TSE donor species and strain. The patients from which the variant CJD and sporadic CJD (MM type 2) TSE sources were derived were methionine homozygote at PrP codon 129 and did not carry other changes in their PrP amino acid sequences. Additionally, the size of PK resistant un-glycosylated PrP^{Sc} is not distinguishable between these patients, suggesting that the conformation of PrP^{Sc} may be similar in these two diseases. Despite having an identical PrP amino acid sequence and PK resistant core size, variant and sporadic CJD (MM type 2) markedly differ in a number of aspects, most notably their clinical and neuropathological features, the glycoform of PrP^{Sc} and their transmissibility to new hosts differs (Brown et al., 1997; Collinge et al., 1996; Ironside et al., 2000; Parchi et al., 1999; Will et al., 1996) (Table 6.1).

Table 6.1 Variant and Sporadic CJD Summary Table (based upon data presented in (Bruce et al., 1997; Ironside et al., 2000; Parchi et al., 1999; Will et al., 1996)

Strain/Isolate	**Variant CJD**	**Sporadic CJD MM-cortical (type 2)**
Clinical signs	Psychiatric symptoms, painful sensory symptoms, later developing ataxia &/ myoclonus, dementia	Cognitive impairment often associated with myoclonus & pyramidal signs
Neuropathology	Severe spongiform change (caudate nucleus & putamen) absent in the hippocampus PrP deposited in florid plaques (cerebral and cerebellar cortex) & wide spread pericellular deposition	Coarse spongiosis (cerebral cortex & thalamus) absent in the brain stem and cerebellum, Perivascular PrP deposited, plaque like non-amyloid deposits
PrP codon 129	methionine/methionine	methionine/methionine
Glycoform of PrP^{Sc}	Predominately **di**-glycosylated	Predominately **un-** & **mono**-glycosylated
Molecular weight of un-glycosylated PrP^{Sc} (KDa)	**19**	**19**
Transmissibility	Good	Poor

The TSE agent which causes variant CJD and the related disorders of BSE and FSE is unusually transmissible to other host species, including to a number of strains of wild type mice (Bruce et al., 1997). Clinical disease is observed in a relatively high proportion of challenged 129/Ola mice and onset is observed from around 400 days after intra-cerebral (ic) inoculation of a 10^{-2} homogenate. The characteristics of vCJD are generally very stable upon passage through novel host species, suggesting it is able to invade a range of hosts without undergoing significant adaptation (Bruce et al., 1997). Consistent with this is the observation of the maintenance of the PrP^{Sc} glycoform (predominantly di-glycosylated) after passage in new host species (Collinge et al., 1996; Hill et al., 1997a). However, the molecular mechanisms that permit the wide host range of this TSE strain are not well understood. In contrast, sporadic CJD MM-cortical (type 2) is relatively untransmissible to wild type or humanized transgenic mice (Korth et al., 2003; Taguchi et al., 2003) (Personal communication, Professor Moira Bruce and Mr. Matthew Bishop). Thus a classical

species barrier to the transmission of sporadic CJD (MM type 2) to mice is observed; where as the murine barrier to variant CJD transmission appears far weaker.

Both variant and sporadic (MM type 2) CJD generally exhibit a relatively long clinical phase that is in excess of one year. However, on average variant CJD patients are far younger than those with sporadic CJD (MM) type 2 (Parchi et al., 1999; Will et al., 1996). The clinical features and neuropathology also differ between the two diseases, although the age distribution of the two patients groups may also contribute to the observed variation in the pattern and progress of disease. The distribution and pattern of PrP^{Sc} deposition also varies between the two conditions (Ironside et al., 2000; Parchi et al., 1999). This difference suggests that the conformation of PrP^{Sc} may also differ, consistent with the radically different PrP^{Sc} glycoform observed in variant and sporadic CJD (MM type 2) patients (Figure 6.1). Despite these diseases occurring in individuals with identical PrP amino acid sequences, they have dramatically different phenotypes and are likely to be caused by different TSE strains.

Thus by transmitting these two TSE sources to the PrP glycosylation deficient transgenic and control mice, the importance of TSE strain to the role of PrP's N-glycans in the TSE species barrier can be specifically investigated. Furthermore, as the PrP^{Sc} from both TSE sources differ from murine PrP^{C} at the same twenty-seven amino acids, these experiments will be independent of the known effect of PrP^{C}/PrP^{Sc} amino acid sequence homology on the barrier.

Figure 6.1 Variant CJD and sporadic CJD MM type 2 differ in PrP^{Sc} glycoform but not size of the un-glycosylated band

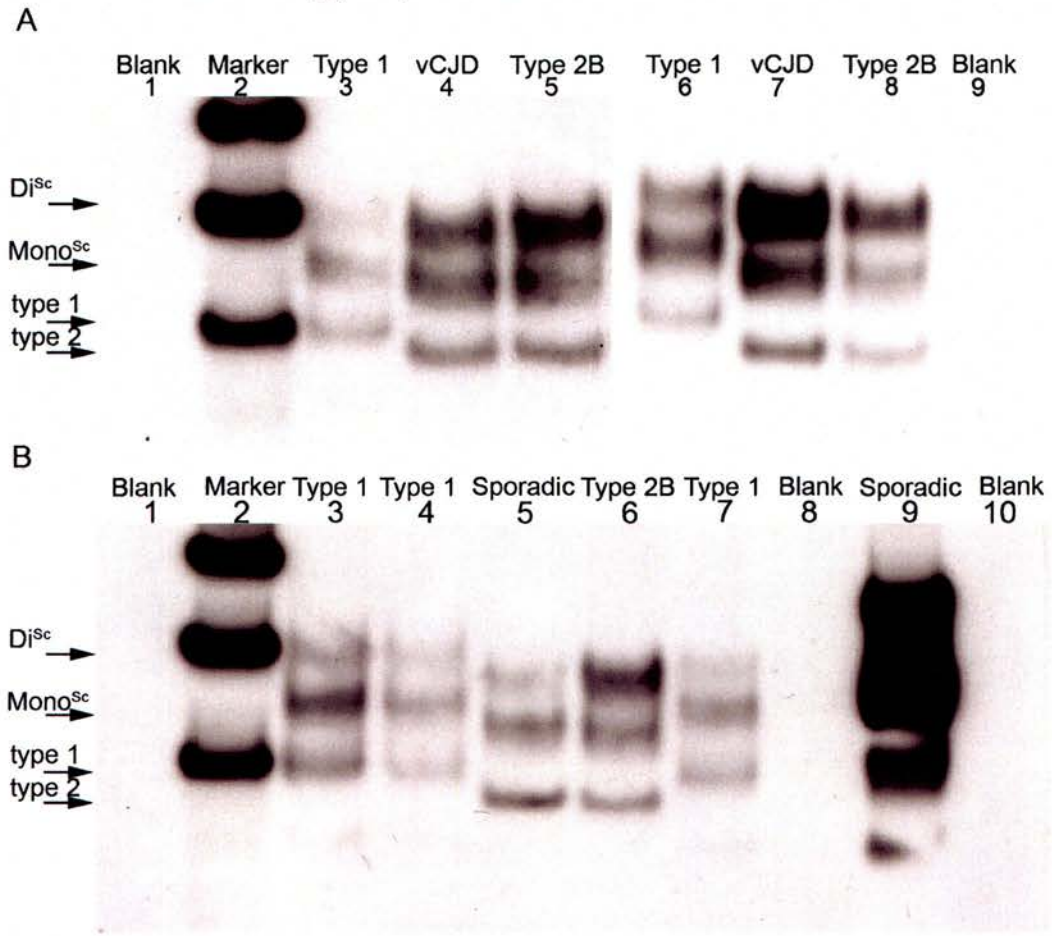

Western blots of PrP^{Sc} isolated from sporadic and variant CJD patients by limited PK digest (50 µg/ml 1 hour 37 °C) (A, all lanes but 2, and B, all lanes but 2 and 9). PrP^{Sc} type 1 (un-glycosylated PrP^{Sc} approximately 19 kDa) and type 2 (un-glycosylated PrP^{Sc} approximately 21 kDa) reference samples were used to determine the electrophoretic mobility of PrP^{Sc} found in (A) variant CJD NIBSC remainder inocula (lane 4 and 7) and (B) sporadic CJD type 2 remainder inocula (lane 5). Both samples have type 2, un-glycosylated, PrP^{Sc}. The PrP^{Sc} glycoform differs between variant and spordic CJD MM type 2. PrP^{Sc} from the variant CJD patient is predominately di-glycosylated and PrP^{Sc} from the sporadic CJD patient is predominately mono-glycosylated. The sporadic CJD sample was concentrated ten-fold compared to references samples, by high speed centrifugation. PrP detected with anti-PrP specific antibodies 6H4 (A, lanes 1-5, and B) and 3F4, (B, lanes 6-9).

The WHO reference vCJD isolate supplied by National Institute of Biological Standards as a 10 % homogenate was used as the source of vCJD challenge material (Minor et al., 2004). This isolate has full ethical approval for research. The sporadic CJD isolate used was kindly provided by Professor Ironside, The National CJD Surveillance Unit, Edinburgh, and also has research use ethical approval. The NIBSC sporadic CJD reference cases are unsuitable for this study because of their mixed PrP^{Sc} type, which may represent the coexistence of multiple TSE strains that would compound the study presented here (Minor et al., 2004). The sporadic CJD MM type 2 sample selected has been previously studied on multiple occasions and had been shown to only contain type 2 PrP^{Sc} of predominate mono-glycosylated glycotype (personal communication, Dr. Mark Head). This was reconfirmed experimentally for the frontal cortex sample used in these transmission experiments (Figure 6.1).

Previous transmission of the NIBSC vCJD isolate to mice by inter-cerebral (ic) inoculation at the concentration supplied, lead to ethically unacceptable levels of injection related deaths (personal communication Irene McConnell). This may be linked to the previously reported bacterial bioburden of 200-600 colony forming units/ml in the NIBSC sources (Minor et al., 2004). A further ten-fold dilution of the inoculum was required to remediate this toxicity problem. The sporadic CJD isolate was likewise inoculated as a 1 % homogenate so that the two human transmissions would be directly comparable. Full ethical approval for the use of the experimental animals was granted by the local review panel.

6.3 Experimental results

6.3.1 TSE incubation periods and incidence of disease

Aged and sex matched PrP glycosylation deficient transgenic [NPU] and normally glycosylated control line (CL) mice were challenged by intracerebral (ic) injection with 20 µl of TSE source infected brain homogenate (1 %) and monitored for the development of TSE clinical disease (Chapter 2 and 5). Only challenged animals that

exhibited clinical signs and TSE vacuolar pathology were classified as confirmed TSE clinical cases, as other non-TSE conditions may lead to the development of neurological signs. All challenged animals were examined for TSE specific vacuolation and the deposition of misfolded PrP within the brain.

Table 6.2 Summary of the outcome of cross-species transmissions to the PrP glycosylation deficient transgenic mice

TSE	Genotype	TSE Disease status			
		0 (•)	**1 (■)**	**2 (▲)**	3 (◊) (dpi +/- SEM)
Sporadic CJD type 2	CL	18	0	1†	0
Sporadic CJD type 2	G3	17	0	0	0
Sporadic CJD type 2	G2	5	2	6	7 (404 +/- 7.8)
Variant CJD	CL	2	10	2	9 (491+/-24.5)
Variant CJD	G3	22	0	0	0
Variant CJD	G2	9	8*	0	5 (536 +/- 16.3)

TSE disease status key (Corresponds to data presented in Figure 6.2)

0, negative for signs of TSE disease (PrP^d deposition, vacuolation, clinical signs)

1, only positive for PrP^d deposition

* In these experiments, in one animal, PrP^d was limited to a plaque in the corpus collosum

2, positive for both PrP^d deposition and TSE specific vacuolation

†No PrP^d was visible in the brain of this animal.

3, confirmed TSE clinical case (clinical signs and vacuolation)

6.3.1.1 Sporadic CJD

Sporadic CJD MM type 2 did not appear to transmit to normally glycosylated (CL) mice. Animals were observed for 707 days after challenge and none displayed TSE clinical signs (Table 6.2, Figure 6.2 A). Limited TSE specific vacuolation in the thalamus was observed in one sporadic CJD challenged normally glycosylated control, however PrP^d deposition was not observed in this or any other normally glycosylated control. These results are consistent with previous findings that have shown this TSE source is poorly transmitted to wildtype and transgenic mice (Korth et al., 2003; Taguchi et al., 2003) (Personal communications Mr. Matthew Bishop and Professor Moira Bruce).

No sporadic CJD challenged G3 transgenic mice developed clinical signs, TSE vacuolar pathology or PrP^d deposition during 707 days of observation post inoculation (d.p.i.). Survival of CL sporadic CJD challenged mice and G3 transgenic mice was comparable (Figure 6.2 C). Thus, the complete absence of PrP's N-glycans does not appear to reduce the resistance of mice to sporadic CJD challenge or reduce the incubation period of disease.

In contrast, the absence of glycosylation at the second site only (G2) permitted the development of clinical TSE disease after sporadic CJD challenge (Figure 6.2 A). Seven of the G2 challenged mice developed clinical TSE (mean 404 d.p.i., +/- 7.8 days (SEM)). Fourteen of the twenty-four challenged G2 mice survived until the first clinical case. Thus the incidence of sporadic CJD transmission at 10^{-2} dilution was 50 % (7/14). Three of these G2 mice were found dead, unexpectedly soon after exhibiting clinical symptoms. Additionally, a further seven sporadic CJD challenged G2 animals with no definite signs of TSE clinical disease were also found dead. TSE vacuolar pathology and PrP^d was detected in five of these animals and PrP^d in the absence of vacuolation was observed in the sixth. Therefore these animals may have died of undetected TSE disease. Thus the G2 transgenic mice may have higher susceptibility to sporadic CJD than was experimentally observed. However, animals were also found dead in genotypes of mice that were resistant to TSE challenge.

Figure 6.2 TSE status and survival-time of challenged animals

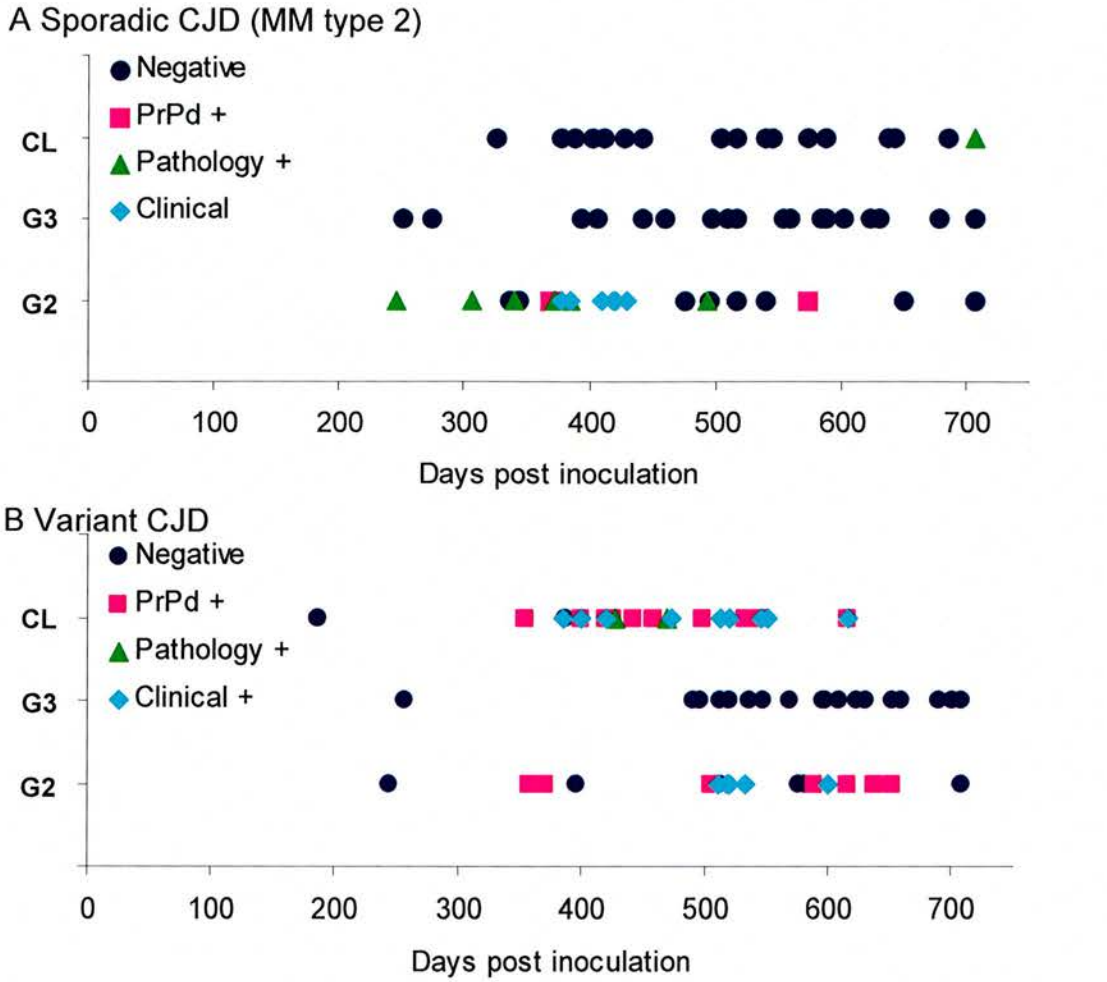

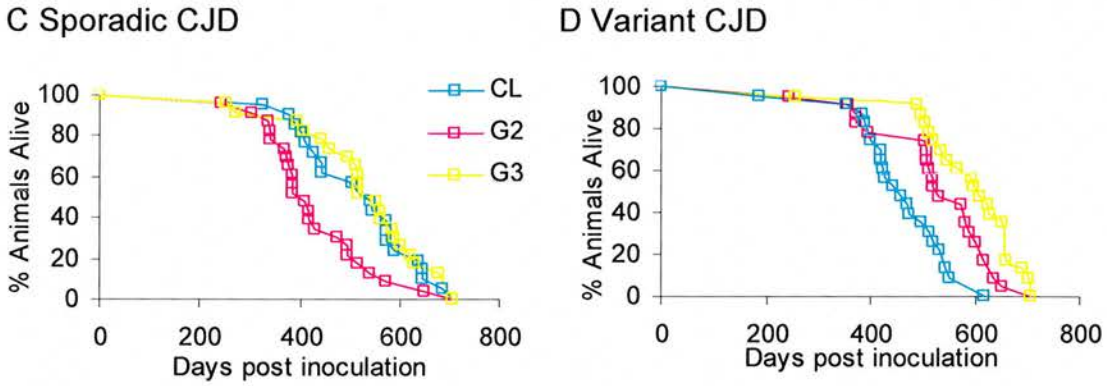

The TSE disease status (clinical signs, vacuolar pathology and PrP^d deposition +/-) of G1, G2, G3 transgenic and normally glycosylated control (CL) mice after challenge with (A) sporadic CJD MM type 2 or (B) variant CJD was plotted against the number of days post inoculation at which the animal was euthanized. The incidence of TSE disease after challenge with sporadic CJD was significantly higher in G2 transgenic mice than in control mice ($p < 0.001$). The incidence of disease after challenge with vCJD was significantly lower in G2 ($p = 0.032$) and G3 ($p < 0.001$) transgenic mice than in controls. Percentage of animals surviving after challenge with (C) sporadic CJD MM type 2 or (D) variant CJD was plotted against the number of days since TSE challenge .

Thus it is only possible to speculate that the G2 transgenics that did not exhibit overt TSE clinical signs, died as a result of their TSE pathology.

A number of sporadic CJD challenged G2 animals, including three animals which survived for more that 650 days post inoculation, did not exhibit clinical disease, vacuolar pathology or PrP^d deposition. Although the barrier to the cross-species transmission of sporadic CJD to mice was greatly reduced by the absence of glycosylation of PrP's second site, the incidence of disease was not 100 % indicating that the species barrier was not completely eliminated. Subpassage of sporadic CJD affected G2 transgenic mice into G2 transgenic and normally glycosylated, wild type mice are being undertaken to determine the extent of the species barrier (6.4.8).

6.3.1.2 Variant CJD

TSE clinical disease signs was observed in nine of the twenty-three vCJD challenged normally glycosylated controls (CL) between 386 and 616 d.p.i. with a mean incubation period of 491 days (+/- 24.5 days SEM) (Table 6.2, Figure 6.2 B). Two of the control mice died prior to the first clinical case thus the CL disease incidence was 43 % (9/21) for a 10^{-2} vCJD challenge. This moderate disease incidence and the high variance in incubation period are attributable to the murine species barrier to infection with a human TSE agent and are consistent with previous reports. Two additional CL transgenic mice had TSE specific vacuolation in the brain but did not show clinical signs. In both cases the vacuolation was less dense and extensive than that observed in brain sections from clinical end point mice. This suggests that had these mice lived they may have gone on to develop clinical signs (data not shown). In ten of the vCJD challenged mice PrP^d deposition was observed in the absence of significant vacuolar pathology.

Both the G2 and G3 transgenic mice had a lower disease incidence or longer incubation period after vCJD challenge than the CL mice (Figure 6.2 B, Figure 6.2 D) (G2 versus CL control Chi-sq = 6.908, df = 2, $p = 0.032$; G3 versus CL control Chi-sq = 37.663, df = 2, $p < 0.001$). No vCJD challenged G3 mice exhibited signs of TSE

clinical disease, nor was vacuolation or PrP^d deposition seen in brain sections from these mice. Thus glycosylation of host PrP^C is required for the successful cross-species transmission of vCJD from humans to mice. There were only five clinical cases in the twenty-two G2 transgenic mice challenged with vCJD. Sixteen of the total twenty-two challenged mice survived after the first clinical case, givin g an disease incidence of 31 % (5/16). The mean incubation period in the G2 transgenic mice (536 days +/- 16.3 (SEM)) after vCJD challenge was 45 days longer than that observed in the CL mice. However, this difference in incubation period is not statistically significant. In addition to the clinically sick G2 transgenic mice a further eight G2 animals exhibited PrP^{Sc} deposition in the absence of vacuolar pathology.

In summary, thirteen of the twenty-two vCJD challenged G2 transgenic mice exhibited evidence of TSE disease, in contrast to twenty-one of the twenty-three vCJD challenged normally glycosylated controls. Therefore the G2 transgenics which lack the second glycosylation site have a lower disease incidence after vCJD ic inoculation than normally glycosylated controls. This suggests that glycosylation of PrP^C at the second site facilitates the cross-species transmission of vCJD, in contrast to its inhibitory effect on the transmission of 263K and sporadic CJD to mice. Thus the role of the second glycosylation site in cross-species TSE transmission is dependent upon TSE strain.

6.3.2 The pattern of TSE vacuolar pathology

To examine if the change in disease incidence and incubation period observed in the G2 transgenic mice compared with the CL mice after cross-species TSE challenge, was linked to an alteration of other disease characteristics, the pattern of TSE vacuolar pathology was investigated. The brains of clinically sick animals challenged with variant and sporadic CJD (MM type 2), were analysed, blind to mouse genotype and TSE agent, for the extent and distribution of vacuolation by standard methods (Fraser and Dickinson, 1967; Fraser and Dickinson, 1968) (2.7.6). The mean results were compared between the normally glycosylated control (CL) and G2 transgenic mice.

6.3.2.1 Sporadic CJD MM type 2

TSE vacuolar pathology was relatively evenly spread through-out the brains of sporadic CJD challenged G2 transgenic mice and was of a relatively low intensity (Figure 6.3). Some targeting to the superior colliculus and the hippocampus was observed (Figure 6.3 A, B, C). The posterior brain areas such as the dorsal medulla (1) and cerebellar cortex (2) were relatively spared and little vacuolation was observed in the hypothalamus (4). Vacuolation in the cerebral cortex (8 and 9) was unusually coarse (large vacuole size) and was predominately localised in the inner layers. Cortical vacuolation was associated within regions in which deposition of plaques was also observed, although direct association of plaques and vacuoles, i.e. florid plaques, was not apparent (Figure 6.3 D and E).

Figure 6.3 Lesion profile and examples of vacuolar pathology in sporadic CJD challenged G2 transgenic mice at clinical endpoint

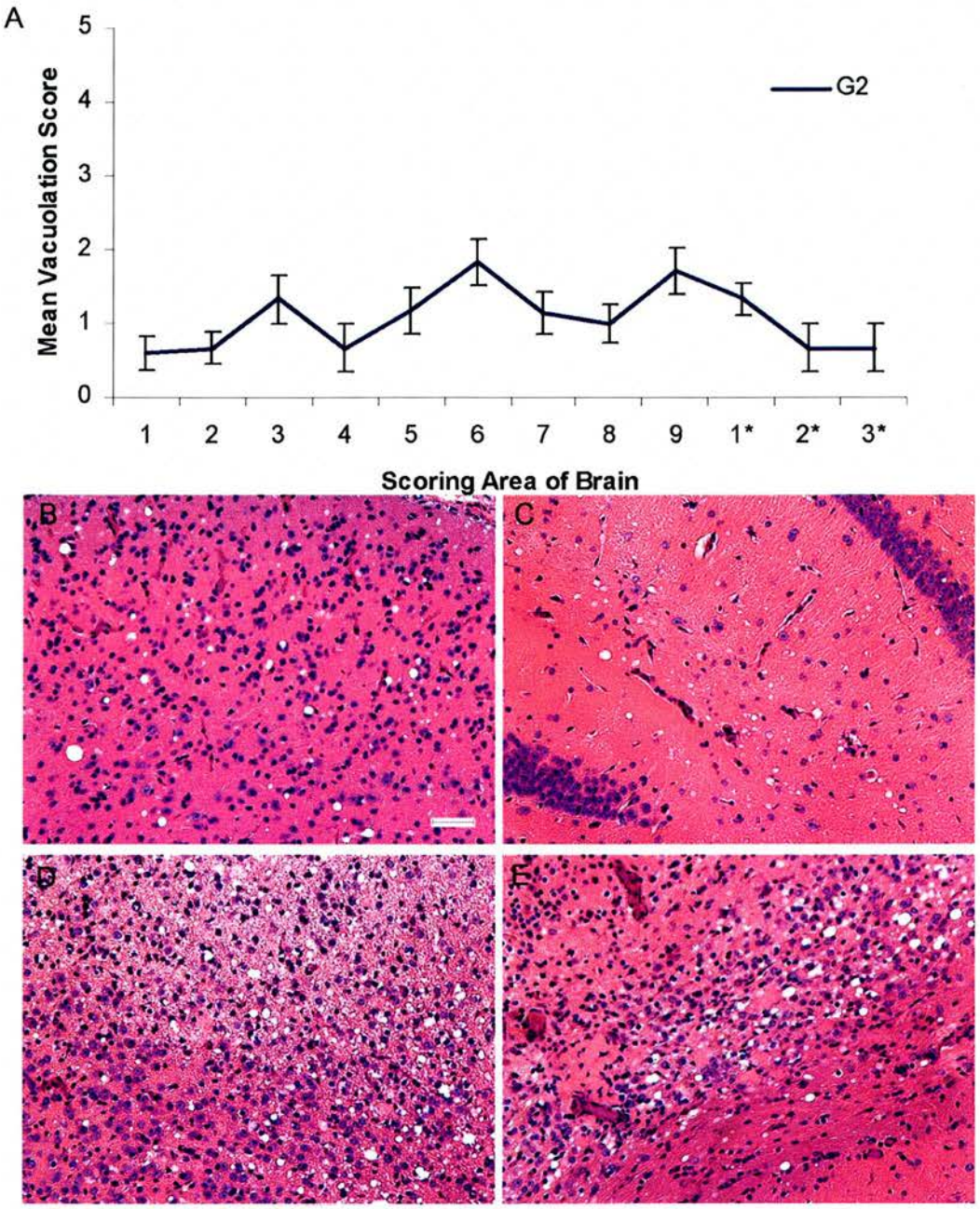

The pattern of TSE specific vacuolar pathology in G2, G3 transgenic and normally glycosylated control (CL) mice after sporadic CJD MM type 2 challenge was semi-quantatively scored, blind to genotype and TSE agent, on a scale of 0-5 in nine grey areas (1 dorsal medulla; 2 cerebellar cortex; 3 superior colliculus; 4 hypothalamus; 5 thalamus; 6 hippocampus; 7 septum; 8 retrosplenial and adjacent motor cortex; 9 cingulate and adjacent motor cortex) and three white matter areas of the brain (1* inferior and middle cerebellar peduncles; 2* decussation of the superior cerebellar peduncles; 3* cerebral peduncles). The experiment was then decoded and a lesion profile of the mean vacuolation score for G2 transgenic mice that developed clinical TSE disease was plotted (A). Error bars indicate standard error of the mean. B-E) Examples of haematoxylin and eosin stained brain sections showing TSE vacuolar pathology in the superior colliculus (B), hippocampus (C) and cerebral cortex (D & E) of G2 transgenic mice. Scale bar 50 µm (B-E).

6.3.2.2 Variant CJD

The targeting and density of vacuolar pathology at clinical endpoint was similar in vCJD challenged G2 and CL transgenic mice, and to previous reports (Figure 6.4 A) (Barron et al., 2001; Bruce et al., 1997). Vacuolation was particularly targeted to the dorsal medulla (1) and the hypothalamus (4) in both genotypes; whereas the superior colliculus (3), the hippocampus (6) and the cerebral cortex (8 and 9) were not significantly vacuolated (Figure 6.4 A-E). Vacuolation targeted to the cochlear nucleus was observed in both G2 and CL mice (data not shown), as has been previously reported for $PrP^{a/a}$ mice challenged with the analogous source BSE (Brown et al., 2003). However, it was not possible to examine this nucleus in a number of animals because of damage to the area or sections at the correct level not being available. Despite decreasing the disease incidence after vCJD challenge, absence of glycosylation at PrP^{C}'s second N-glycan attachment site does not appear to alter the pattern of targeting or intensity of vacuolation at clinical endpoint. This suggests that the TSE strain was not altered by the absence of PrP's second glycosylation site.

Figure 6.4 Lesion profile and examples of vacuolar pathology in vCJD challenged G2 transgenic and control mice at clinical endpoint

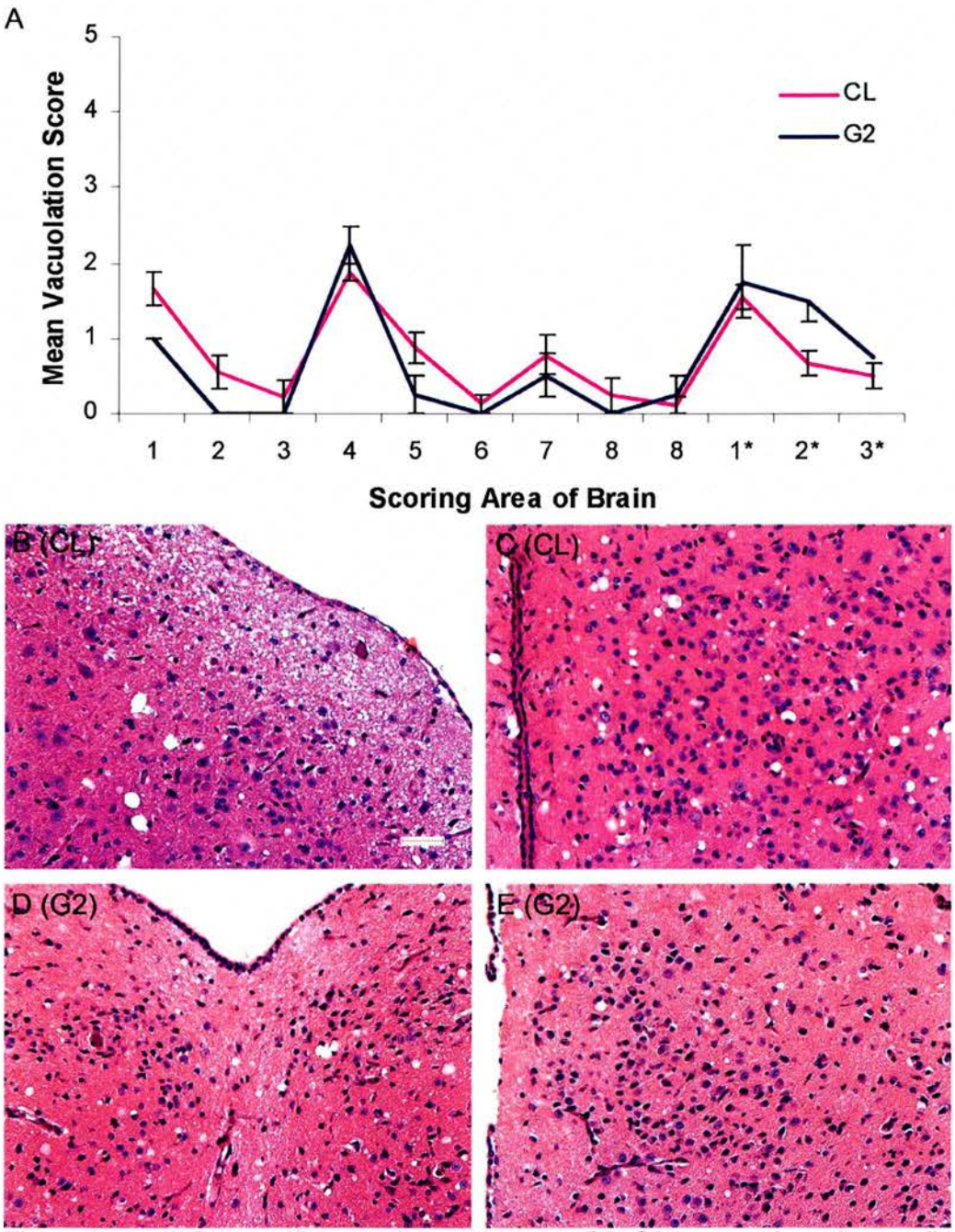

The pattern of TSE specific vacuolar pathology in G2, G3 transgenic and normally glycosylated control (CL) mice after vCJD challenge was semi-quantatively scored, blind to mice genotype and TSE agent, on a scale of 0-5 in nine grey areas (1 dorsal medulla; 2 cerebellar cortex; 3 superior colliculus; 4 hypothalamus; 5 thalamus; 6 hippocampus; 7 septum; 8 retrosplenial and adjacent motor cortex; 9 cingulate and adjacent motor) and three white matter areas of the brain (1* inferior and middle cerebellar peduncles; 2* decussation of the superior cerebellar peduncles; 3* cerebral peduncles). The experiment was decoded and a lesion profile of the mean vacuolation score observed in animals with clinical TSE disease was plotted by mouse genotype (A). Error bars indicate standard error of the mean. This demonstrates that the pattern and density of vacuolar targeting in G2 transgenic and CL control mice challenged with vCJD are indistinguishable. Examples of haematoxylin and eosin stained brain sections showing vacuolar pathology in the medulla (B & D) and hypothalamus (C & E), of normally glycosylated (B & C) and G2 transgenics (D & E). Scale-bar 50 µm (B-E).

6.3.3 The pattern of TSE associated PrP deposition in the CNS

To investigate if the glycosylation state of PrP^C affected the deposition of misfolded PrP in the CNS after cross-species TSE challenge with variant or sporadic CJD, brain sections from all TSE challenged animals were examined blind for disease associated PrP (PrP^d) at five defined levels (Chapter 2). PrP was detected using anti-PrP antibody 6H4. Normal brain inoculated $PrP^{a/a}$ mice and PrP null mice [NPU] were used as negative controls, using the CSA method (Chapter 2 and 5). Sections from a subset of the brains were independently stained using the anti-PrP antibody 8H4, to determine whether the results were antibody dependent. Antibody concentrations were determined by titration (appendix vii-x).

6.3.3.1 Sporadic CJD type 2

PrP^d deposition in G2 mice challenged with type 2 sporadic CJD exhibited a distinct pattern, which was similar for both 6H4 and 8H4 stained sections, although significantly higher non-specific background staining was observed with 8H4 (Figure 6.5 i and ii). Aggregated PrP^d deposition was observed in the thalamus in all G2 animals in which PrP^d was detected. Additionally, multicentric plaque-like deposits were observed in the cerebral cortex in the majority of PrP^d positive animals and in the hippocampus in some G2 mice (Figure 6.5). A similar pattern of deposition was observed in all PrP^d positive sporadic CJD challenged G2 transgenic mice, whether or not clinical signs or vacuolation were apparent. Extensive deposition was observed even at early time points (data not shown).

The plaque-like deposits in sporadic CJD challenged G2 mice interacted weakly with thioflavin-s compared to the plaques observed in G2 animals that were challenged with 263K (Figure 6.6). This suggests that the plaques which formed in G2 mice affected with sporadic CJD did not contain significant amounts of amyloid. Limited synaptic PrP^d deposition was also observed in G2 sporadic CJD challenged brains in association with these plaque-like deposits (Figure 6.5 i F).

Figure 6.5 (i, ii) PrP^d deposition was observed in G2 transgenic mice after challenge with sporadic CJD MM type 2. The deposition of PrP^d was examined in G2 transgenic mice challenged with sporadic CJD MM type 2, at five defined brain levels of which four are shown here (A) medulla and cerebellum, (C) midbrain including superior collicullus, cerebral cortex and hippocampal formation, (E hippocampus, habenula, thalamus, hypothalamus, cerebral cortex and corpus callosum, (G) forebrain including corpus callosum and septum. Aggregated PrP^d deposition was detected in the thalamus (Th) and multicentric plaques were observed throughout the cerebral cortex (A and C); after wet autoclaving and formic acid treatment using anti-PrP antibody 6H4 (i) or 8H4 (ii); signal was amplified using a CSA kit and visualised with DAB, nuclei were counter stained with haematoxylin. Upper boxed area in C corresponds with A, lower boxed area in C with D, upper boxed area in E with F and the lower boxed area in E with H. Specificity of signal was determined using negative control sections from a PrP null [NPU] mouse and a normal brain homogenate challenged normally glycosylated control mouse (I). Sections shown are from one G2 transgenic mouse (A-H). Scale-bar 500 μm (A, C, E, G) and 25 μm (B, D, F, H).

Figure 6.5(i) PrP^d deposition was observed in G2 transgenic mice after challenge with sporadic CJD (MM type 2) (6H4)

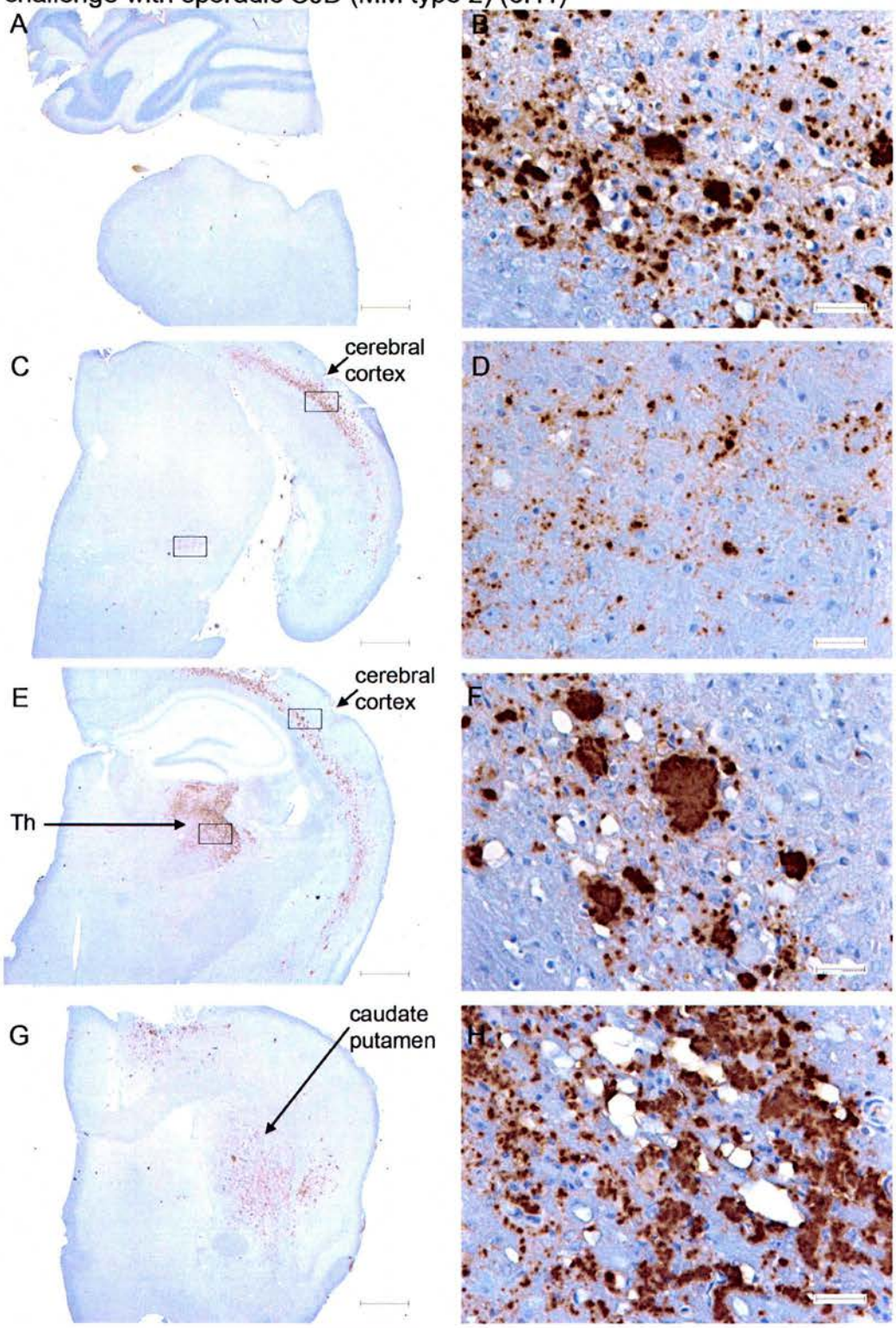

Figure 6.5(ii) PrP^d deposition was observed in G2 transgenic mice after challenge with sporadic CJD (8H4)

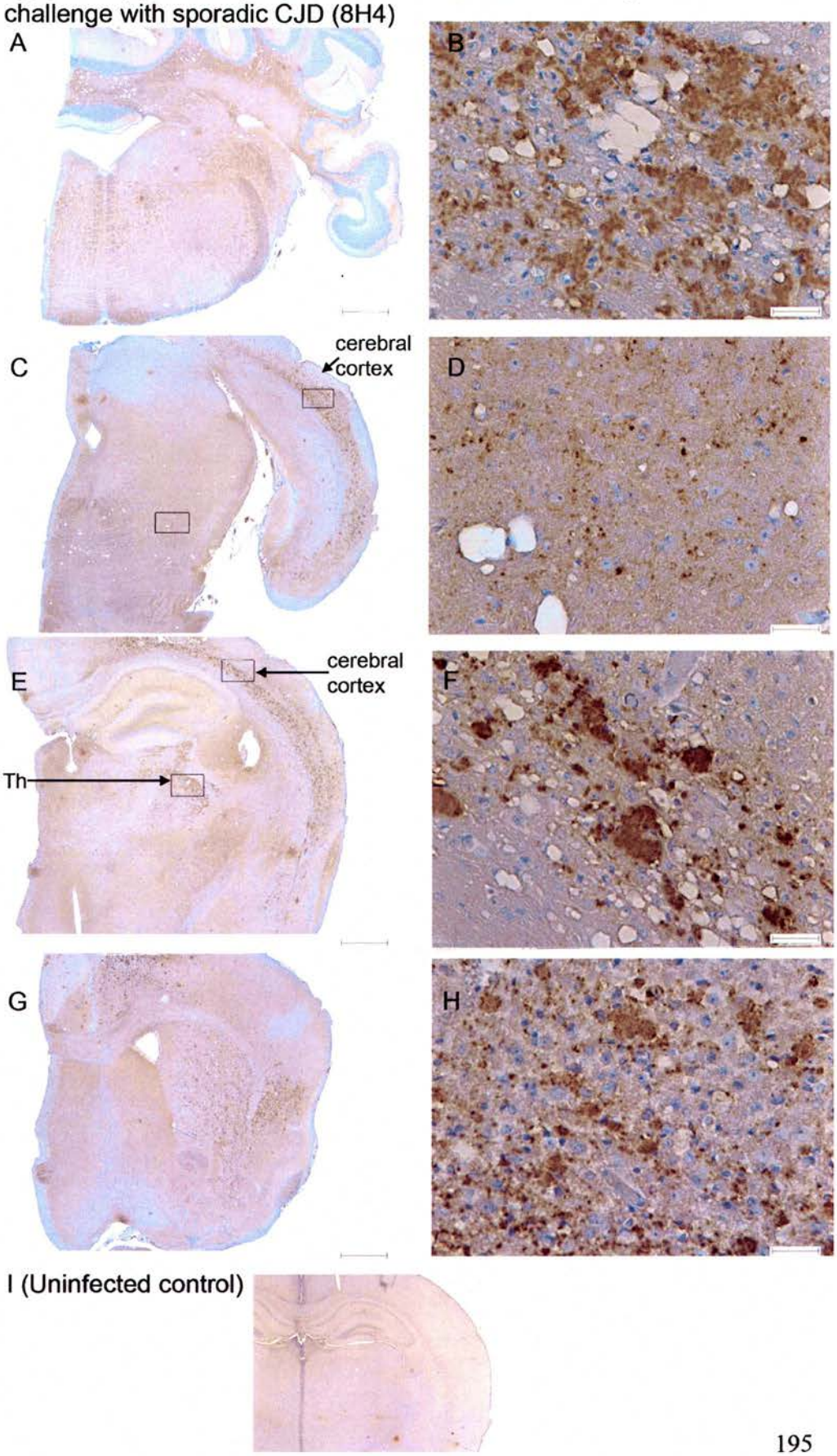

Figure 6.6 PrP^d plaque like deposits in G2 transgenic mice after sporadic CJD challenge did not interact strongly with thioflavin-s

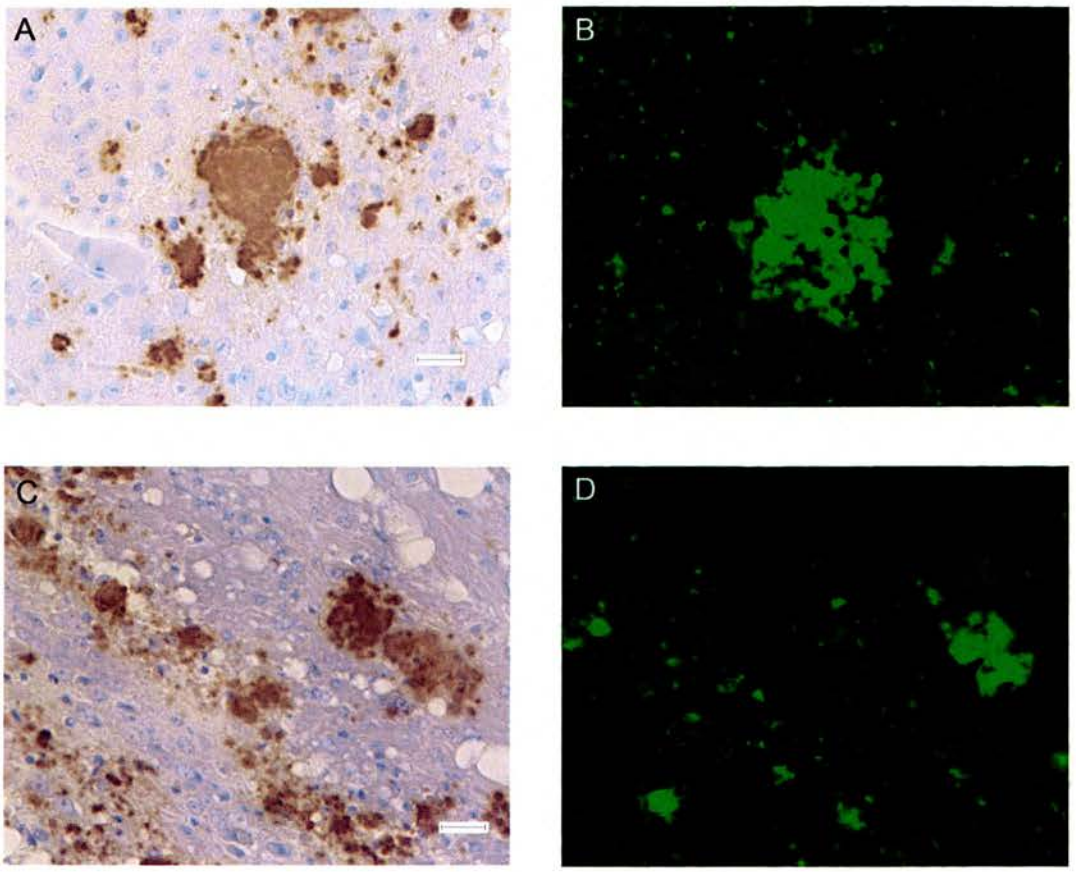

Multicentric PrP^d plaque-like deposits in the cerebral cortex (A, C), were detected with anti-PrP antibody 6H4 in brain sections subjected to formic acid and wet autoclaving, in G2 transgenic mice (results from two individual mice shown) that were challenged with sporadic CJD. To determine if these deposits contained amyloid, serial sections were treated with thioflavin-s. G2 transgenic mice that were challenged with 263K and contained amyloid plaques were used as a positve control (Figure 5.6). The PrP^d deposits in the sporadic CJD challeged mice did not strongly interact with thioflavin-s (B, D). Scale-bar 35 µm.

No PrP^d deposition was observed in either CL normally glycosylated control or G3 transgenic mice challenged with sporadic CJD (Figure 6.7, 6.8).

Figure 6.7 PrP^d deposition was not observed in normally glycosylated control mice challenged with sporadic CJD The deposition of PrP^d was examined in normally glycosylated controls challenged with sporadic CJD MM type 2, at five defined brain levels of which four are shown here (A & E) medulla and cerebellum, (B & F) midbrain including superior collicullus (B), cerebral cortex and hippocampal formation, (C & G) hippocampus, habenula, thalamus, hypothalamus cerebral cortex and corpus callosum, (D & H) forebrain including corpus callosum and septum. PrP^d deposition was not detected even after PrP antigen retrieval by wet autoclaving and formic acid treatment using anti-PrP antibodies 6H4 (A-D) or 8H4 (E-H), anti-PrP signal was amplified using a CSA kit and visualised with DAB, nuclei were counter stained with haematoxylin. Sections shown are from one normally glycosylated control mouse (CL). A sporadic CJD challenged G2 transgenic mouse was used as a PrP^d positive control (figure 6.5 i and ii). Scale bar 500 μm.

Figure 6.7 PrP^d deposition was not observed in normally glycosylated control mice challenged with sporadic CJD

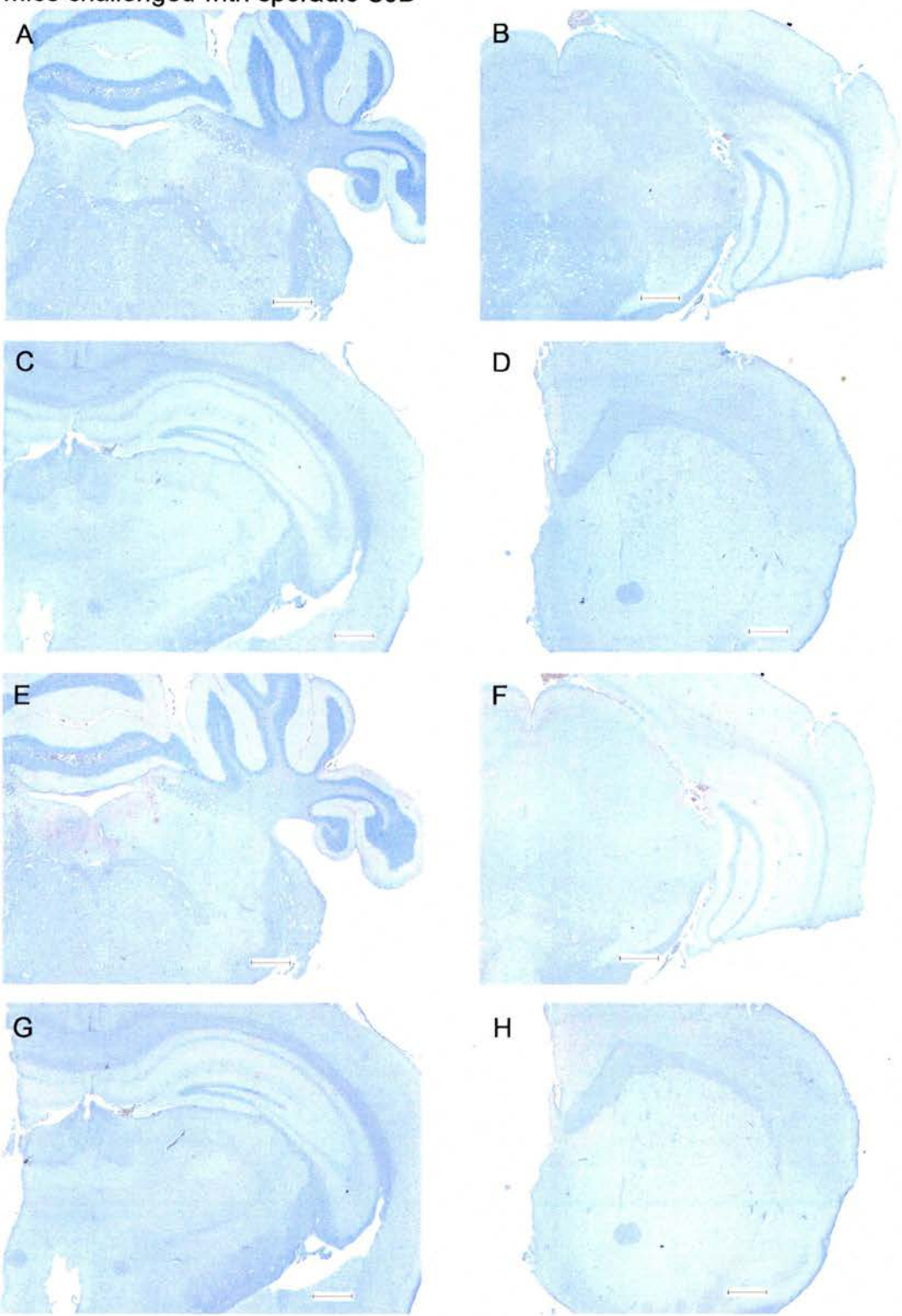

Figure 6.8 PrP^d deposition was not observed in G3 transgenic mice challenged with sporadic CJD MM type 2. The deposition of PrP^d was examined in G3 transgenic mice challenged with sporadic CJD MM type 2, at five defined brain levels of which four are shown here (A & E) medulla and cerebellum, (B & F) midbrain including superior collicullus (B), cerebral cortex and hippocampal formation, (C & G) hippocampus, habenula, thalamus, hypothalamus cerebral cortex and corpus callosum, (D & H) forebrain including corpus callosum and septum. PrP^d deposition was not detected when PrP antigen retrieval, by wet autoclaving and formic acid treatment, using anti-PrP antibodies 6H4 (A-D) or 8H4 (E-H). Anti-PrP signal was amplified using a CSA kit and visualised with DAB, nuclei were counter stained with haematoxylin. Sections shown are from one G3 transgenic mouse. A sporadic CJD challenged G2 transgenic was used as a PrP^d positive control (figure 6.5 i and ii). Scale bar 500 μm.

Figure 6.8 PrP^{d} deposition was not observed in G3 transgenic mice challenged with sporadic CJD

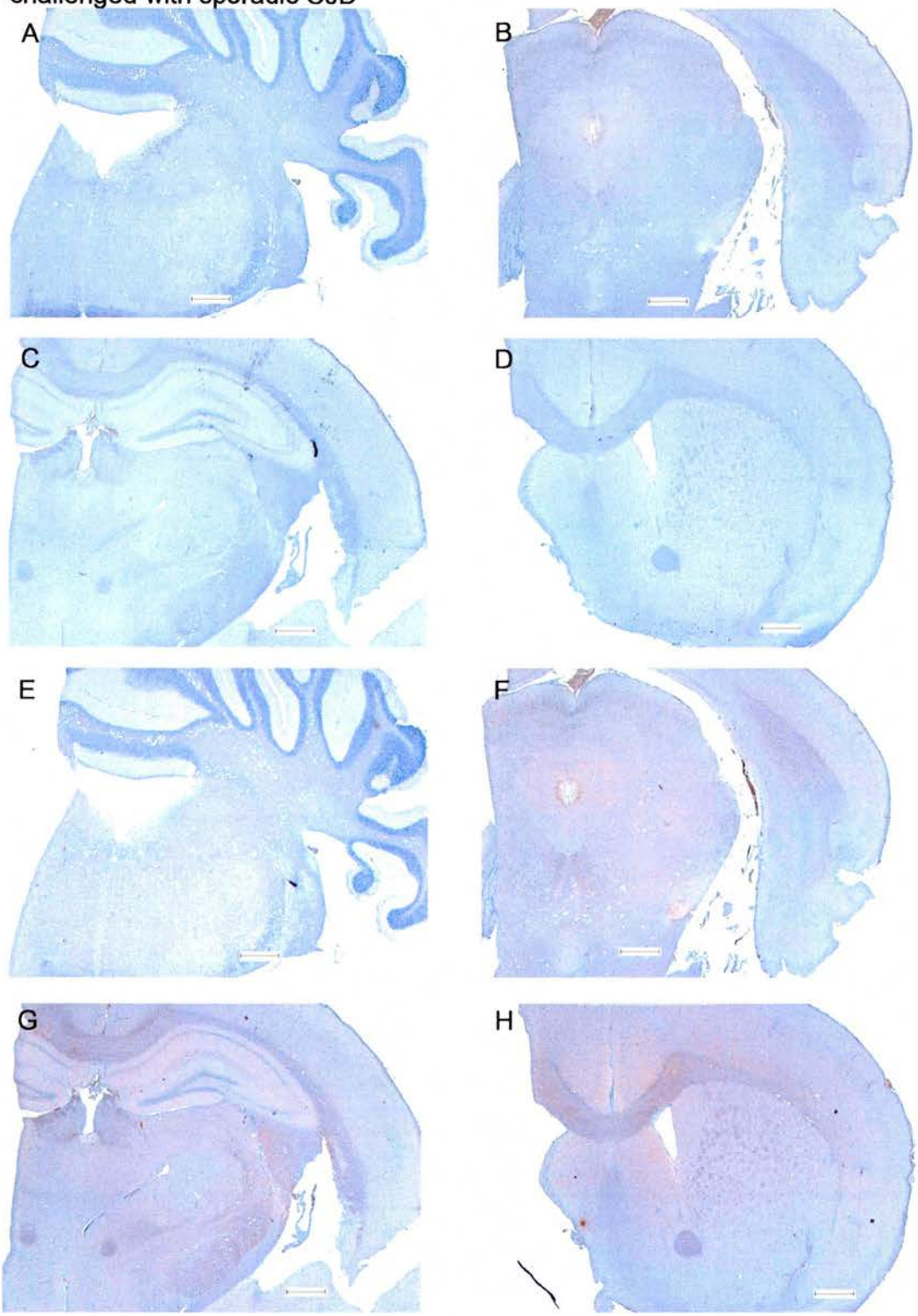

6.3.3.2 Variant CJD

The pattern of disease associated PrP^d deposition in the variant CJD inoculated normally glycosylated controls (CL) at clinical endpoint was similar to that previously reported in 129/Ola wild type mice using both anti-PrP monoclonals (Figure 6 .9 and 6.10) (Barron et al., 2001). Extensive synaptic type deposition throughout the thalamus, hypothalamus, pons and medulla, with particular targeting to the habenula, weaker synaptic type deposition in the forebrain and the hallmark targeting to the neuropil of the CA2 hippocampal cell layer was observed. Additionally, animals with the heaviest PrP^d deposition also exhibited limited synaptic type deposition in the cortex; no plaques were observed (Figure 6.9 E). PrP^d deposition in pre/subclinical CL controls was in general less extensive but of a similar pattern compared to that observed at clinical endpoint (data not shown). Earliest deposition occurred in the habenula and the ventral midbrain (data not shown).

In contrast, the pattern of PrP^d in clinical end point G2 glycosylation deficient transgenic mice was markedly different from that in normally glycosylated controls, as detected both by 8H4 and 6H4 (Figure 6.10, Figure 6.11). Extensive small focal deposits were seen throughout the pons, medulla, thalamus, septum and hypothalamus, and occasionally in the cortex. Additionally to the presence of focal deposits, clinical endpoint G2 mice exhibited lighter and less extensive synaptic type deposition than control mice in the hypothalamus, the thalamus, and occasionally the medulla and pons. Significantly, targeted PrP^d deposition in the CA2 associated neuropil was completely absent in all clinical endpoint G2 cases. The pattern of PrP^d was generally similar in the TSE vacuolation negative animals, although often it was far less extensive. In several G2 transgenic mice deposition was only observed in the habenula. Overall these data demonstrate that the absence of glycosylation of PrP at the second attachment site can modify the pattern of PrP^d accumulation *in vivo*.

Figure 6.9 PrP^d deposition was observed in normally glycosylated control mice challenged with variant CJD. The deposition of PrP^d was examined in normally glycosylated controls challenged with variant CJD, at five defined brain levels of which four are shown here (A) medulla and cerebellum, (C) midbrain including superior collicullus, cerebral cortex and hippocampal formation, (E) hippocampus, habenula, thalamus, hypothalamus cerebral cortex and corpus callosum, (G) forebrain including corpus callosum (cc) and septum (Sp). Synaptic-like PrP^d deposition was detected in the medulla, pons (data not shown), habenula (Hb), ventral midbrain, hypothalamus (Hy), thalamus (Th) and CA2 region of the hippocampus (Hb); after wet autoclaving and formic acid treatment using anti-PrP antibody 6H4, signal was amplified using a CSA kit and visualised with DAB, nuclei were counter stained with haematoxylin. Boxed areas in A corresponds with B, C with D, E with F and G with H. Sections (A,B E-H) are from one normally glycosylated control mouse (CL) and sections (C and D) from another CL animal. Both CL animals were sacrificed at TSE clinical endpoint and exhibited vacuolar pathology. Specificity of signal was determined using negative control sections from a PrP null [NPU] mouse and a normal brain homogenate challenged normally glycosylated control mouse (I). Scale bar 500 μm (A, C, E, G) and 50 μm (B, D, F, H).

Figure 6.9 PrP^d deposition was observed in normally glycosylated control mice challenged with variant CJD

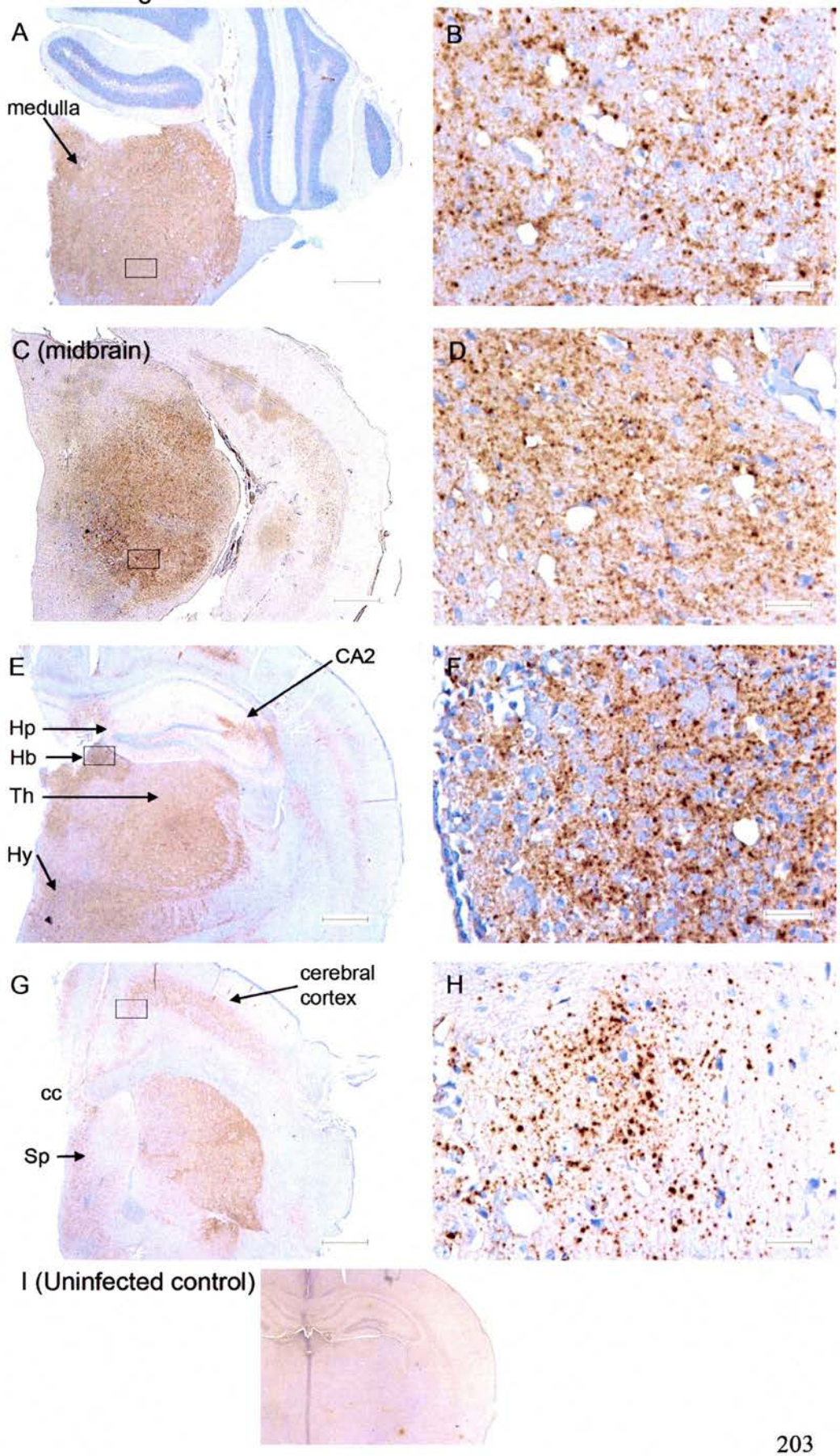

Figure 6.10 PrP^d deposition pattern observed in G2 transgenic mice challenged with variant CJD. PrP^d deposition in G2 transgenic was examined at five defined brain levels of which four are shown here (A) medulla and cerebellum, (C) midbrain including superior collicullus, cerebral cortex and hippocampal formation, (E) hippocampus, habenula, thalamus, hypothalamus cerebral cortex and corpus callosum, (G) forebrain including corpus callosum and septum. Focal PrP^d deposits were detected in the medulla, pons, ventral midbrain, hypothalamus, thalamus and septum. Light synaptic-type deposition was observed in the medulla, ventral midbrain, hypothalamus (Hy) and septum (Sp). Deposition of PrP^d in the habenula (Hb) of G2 transgenic mice was indistinguishable from that observed in normally glycosylated controls. PrP was detected after antigen retrieval by wet autoclaving and formic acid treatment using anti-PrP antibody 6H4, signal was amplified using a CSA kit and visualised with DAB, nuclei were counter stained with haematoxylin. The boxed area in A corresponds with B, C with D, E with F and G with H. All sections shown are from a single G2 transgenic that was sacrificed with clinical TSE disease and exhibited vacuolar pathology. Specificity of signal was determined using brain sections from a PrP null [NPU] mouse and a normal brain homogenate challenged mouse (I). Scale-bar 500 μm (A, C, E, G) and 50 μm (B, D, F, H).

Figure 6.10 PrP^d deposition pattern observed in G2 transgenic mice challenged with variant CJD

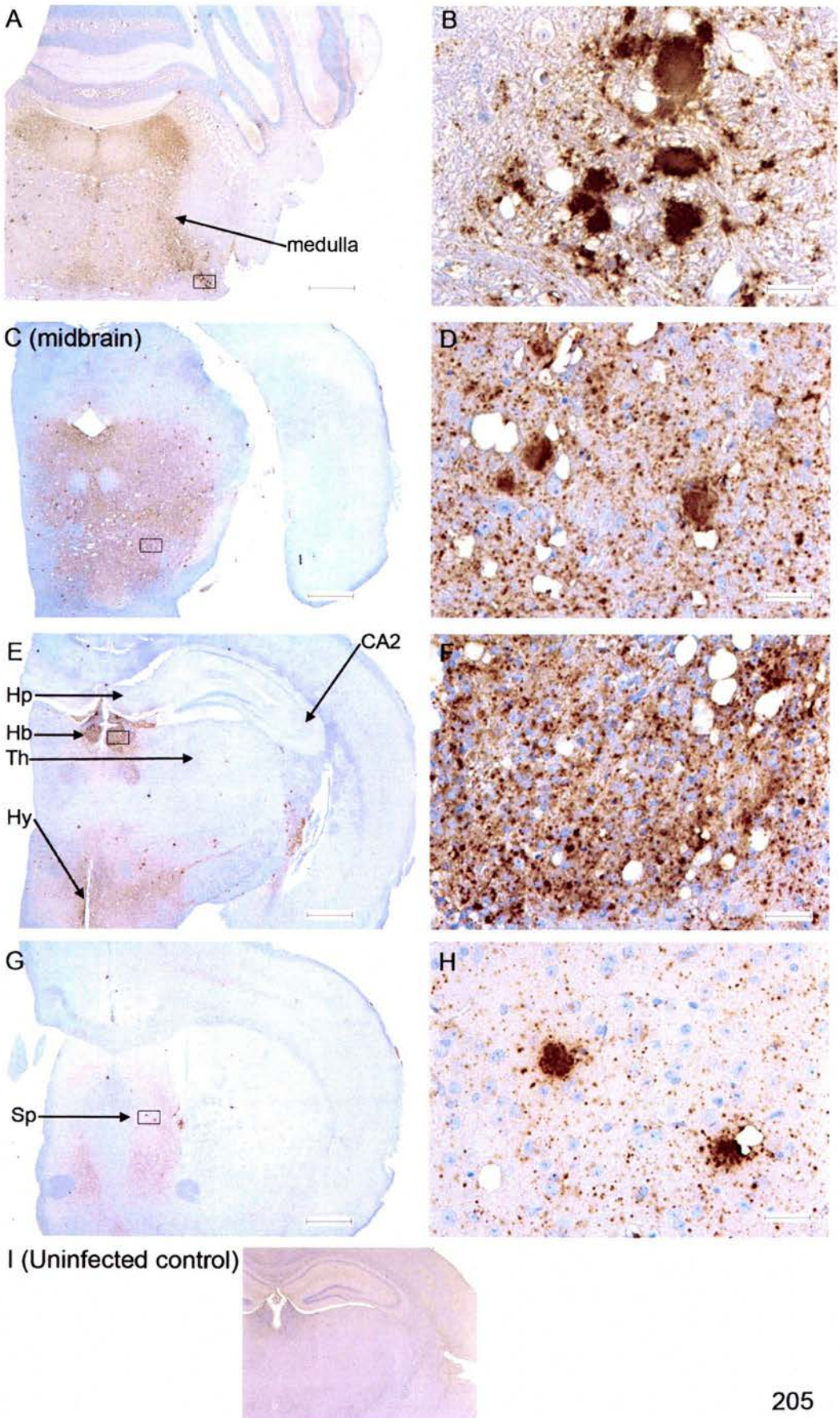

Figure 6.11 The PrP^d deposition pattern observed in G2 transgenic and control mice after variant CJD challenge did not depend on anti-PrP antibody PrP^d deposition was examined at five defined brain levels of which four are shown here (A) medulla and cerebellum, (C) midbrain including superior collicullus, cerebral cortex and hippocampal formation, (E) hippocampus (Hp), habenula (Hb), thalamus (Th), hypothalamus (Hy), cerebral cortex and corpus callosum, (G) forebrain including corpus callosum and septum (Sp). PrP was detected after antigen retrieval by wet autoclaving and formic acid treatment, using anti-PrP antibody 8H4, signal was amplified using a CSA kit and visualised with DAB, nuclei were counter stained with haematoxylin. Clear differences in the PrP deposition pattern can be observed between a G2 transgenic (E-H) and a normally glycosylated control mouse (CL) (A-D), figures shown are representative of four further vCJD challenged G2 transgenics, which developed clinical TSE disease, and the further eight CL animals that developed TSE clinical disease after challenge with vCJD. Specificity of signal was determined using negative control brains sections from a PrP null [NPU] mouse and a normal brain homogenate challenged normally glycosylated control mouse (I). Scale bar 500 μm.

Figure 6.11 The PrP^d deposition pattern observed in G2 transgenic and control mice after variant CJD challenge did not depend on anti-PrP antibody

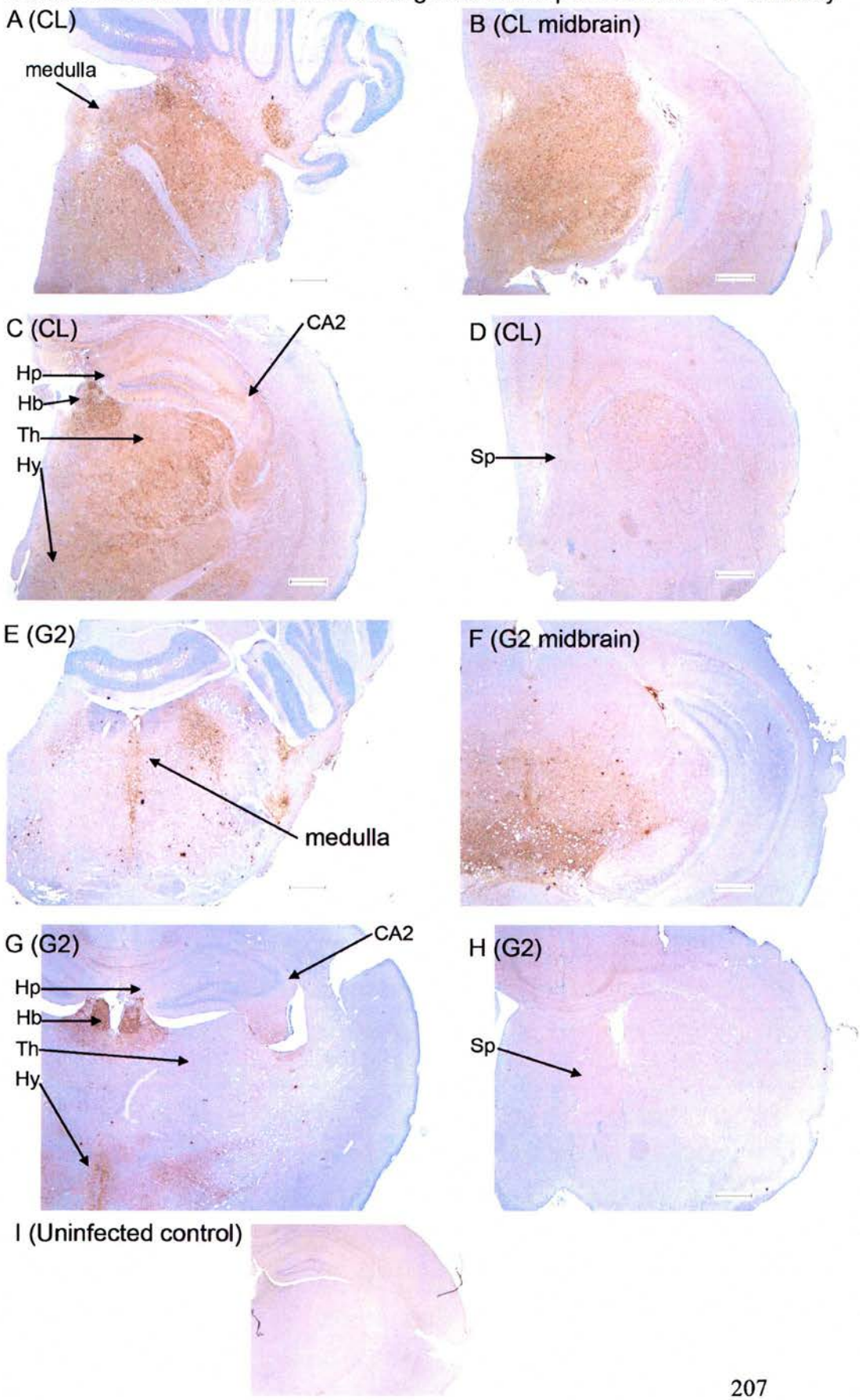

However, PrP^d deposition in the habenula was indistinguishable in the CL and G2 transgenic mice (compare figure 6.9 E and F with 6.10 E and F), demonstrating that brain region specific factors modify the importance of glycosylation of PrP to its TSE disease associated accumulation *in vivo*. This difference in PrP^d deposition may indicate that a different conformation of misfolded PrP is accumulating in the G2 transgenic mice challenged with variant CJD than in normally glycosylated controls.

No deposition of PrP^d was observed in any vCJD challenged G3 mice (6.12), demonstrating that the absence of PrP^C's N-glycans prevents the formation of misfolded PrP after vCJD challenge.

Figure 6.12 No PrP^d deposition was observed in G3 transgenic mice challenged with variant CJD. PrP^d deposition was examined at five defined brain levels of which four are shown here (A and E) medulla and cerebellum, (B and F) midbrain including superior collicullus, cerebral cortex and hippocampal formation, (C and G) hippocampus, habenula, thalamus, hypothalamus cerebral cortex and corpus callosum, (D and H) forebrain including corpus callosum and septum. PrP signal was recovered using antigen retrieval by wet autoclaving and formic acid treatment and detected using anti-PrP antibody 6H4 (A-D) and 8H4 (E-H) on sections from two G3 transgenics (animal one A-D, animal two E-H)), signal was amplified using a CSA kit and visualised with DAB, nuclei were counter stained with haematoxylin. Variant CJD challenged normally glycosylated control (CL) was used as positive controls for the detection of PrP^d using 6H4 (I) and 8H4 (J) antibodies. Scale bar 500 μm.

Figure 6.12 No PrP^d deposition was observed in G3 transgenic mice challenged with variant CJD

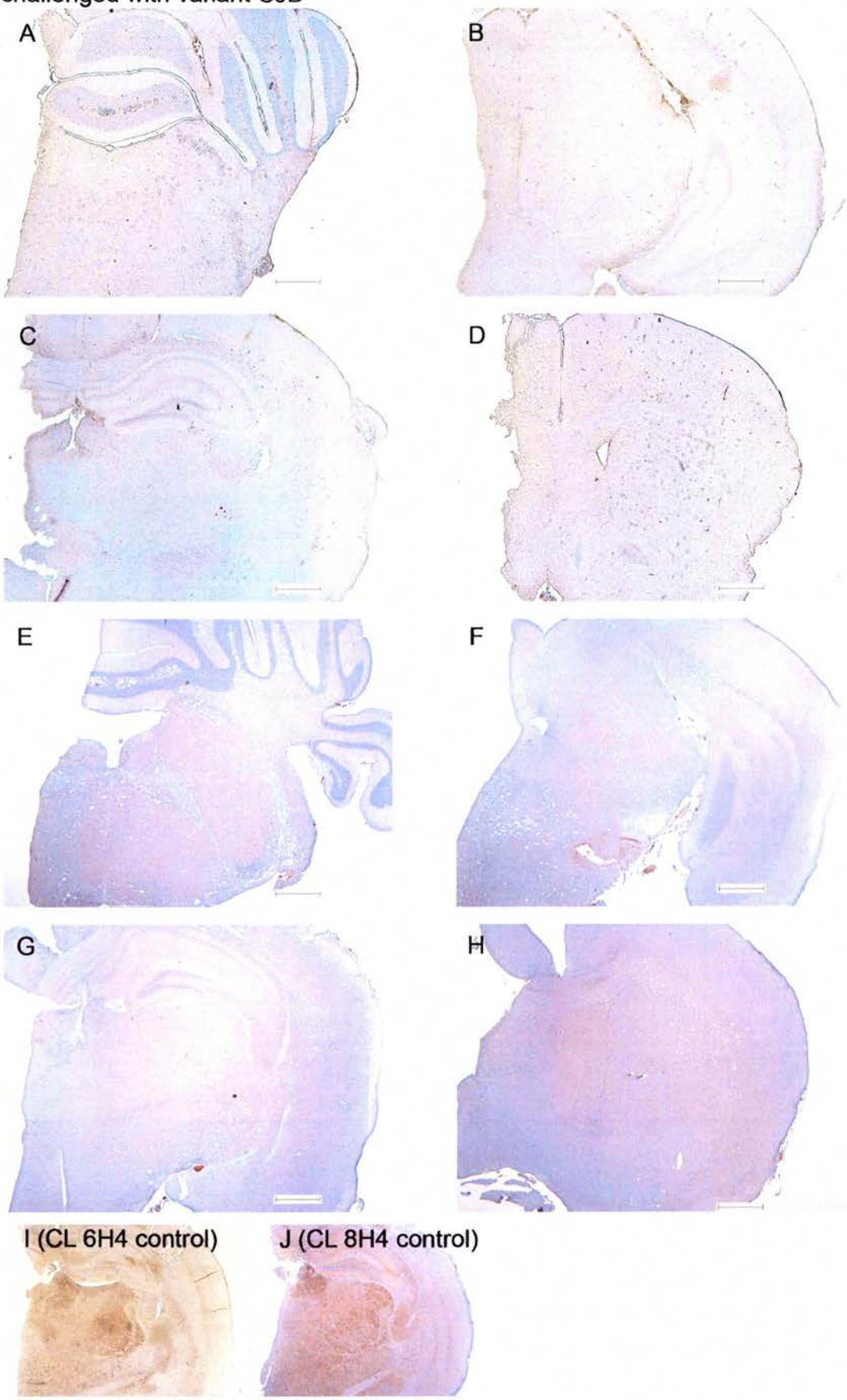

6.3.4 TSE associated PK resistant PrP^{Sc}

To investigate if the conformation of misfolded PrP differed between the G2 transgenic and normally glycosylated control mice challenged with variant CJD the size of PK resistance core of PrP was investigated by standard methods, as outlined in chapters 2 and 5 Additionally the PK resistance of the misfolded PrP observed in G2 transgenic mice challenged with sporadic CJD and in a subset of PrP^{d} negative animals was also determined. When PrP signal was not low or undetectable by standard methods, PrP^{Sc} was concentrated by NaPTA precipitation. High speed centrifugation was not used, as preliminary experiments demonstrated that this method did not sufficiently separate PrP^{Sc} from other PK resistant components resulting in electrophorectic artefacts because of protein overloading of the gel (appendix xi).

6.3.4.1 Sporadic CJD MM type 2

PrP^{Sc} was isolated from one early preclinical and three clinical endpoint sporadic CJD G2 transgenic mice, by standard PK digestion and NaPTA precipitation (Figure 6.13 A; n = 4, 8H4). Similar to the result observed for murine PrP^{Sc} produced after 263K challenge (chapter 5) un-glycosylated PrP^{Sc} isolated from brains prepared in physiological saline for subpassage appeared to have lower electrophoretic mobility to that isolated directly in NP40 lysis buffer (Figure 6.13 A). No PrP^{Sc} was observed 600 d.p.i. in G3 or CL mice that were challenged with sporadic CJD, even after forty-fold NaPTA mediated concentration (Figure 6.13 B and C; n = 5, 8H4). This is consistent with the absence of detectable PrP^{d} by IHC. However, some undigested PrP^{C} was apparent in a number of samples.

Figure 6.13 Western blots of PrP^{Sc} from PrP glycosylation deficient transgenic and control mice challenged with sporadic CJD.

(A) PrP^{Sc} was isolated from four sporadic CJD challenged G2 transgenic mice; one vCJD challenged G2 transgenic (assayed in duplicate), one vCJD challenged normally glycosylated control (CL) (assayed in duplicate), one 263K normally glycosylated challenged control (CL), one uninfected CL mouse and one uninfected G2 transgenic mouse by standard PK digestion (20 μg/ml, 37 °C, one hour). PrP^{Sc} was concentrated by NaPTA mediated precipitation. Original brain samples were prepared in physiological saline (S) or NP40 lysis buffer (N). The electrophoretic mobility of PrP differed between samples prepared by the two methods.

(B) Brain samples from five PrP^{d} and vacuolation negative normally glycosylated controls and (C) five G3 transgenic mice which had survived for at least 600 dpi, were concentrated forty-fold, by NaPTA mediated precipitation, after standard PK digestion (20 μg/ml, 37 °C, one hour). However, no PrP^{Sc} was detected in any of these samples, despite a clear PrP^{C} signal prior to concentration and the concentration of PrP^{Sc} from a sporadic CJD challenged G2 transgenic brain sample. PrP was detected with anti-PrP antibody 8H4 and horseradish conjugated anti-mouse secondary antibody (Jackson ImmunoResearch, West Grove, USA). Secondary was detected using POD solution (Roche Diagnostics, Basel, Switzerland) and the resultant chemiluminescence was detected using X-ray film.

Figure 6.13 Western blots of PrP^{Sc} from PrP glycosylation deficient transgenic and control mice challenged with sporadic CJD

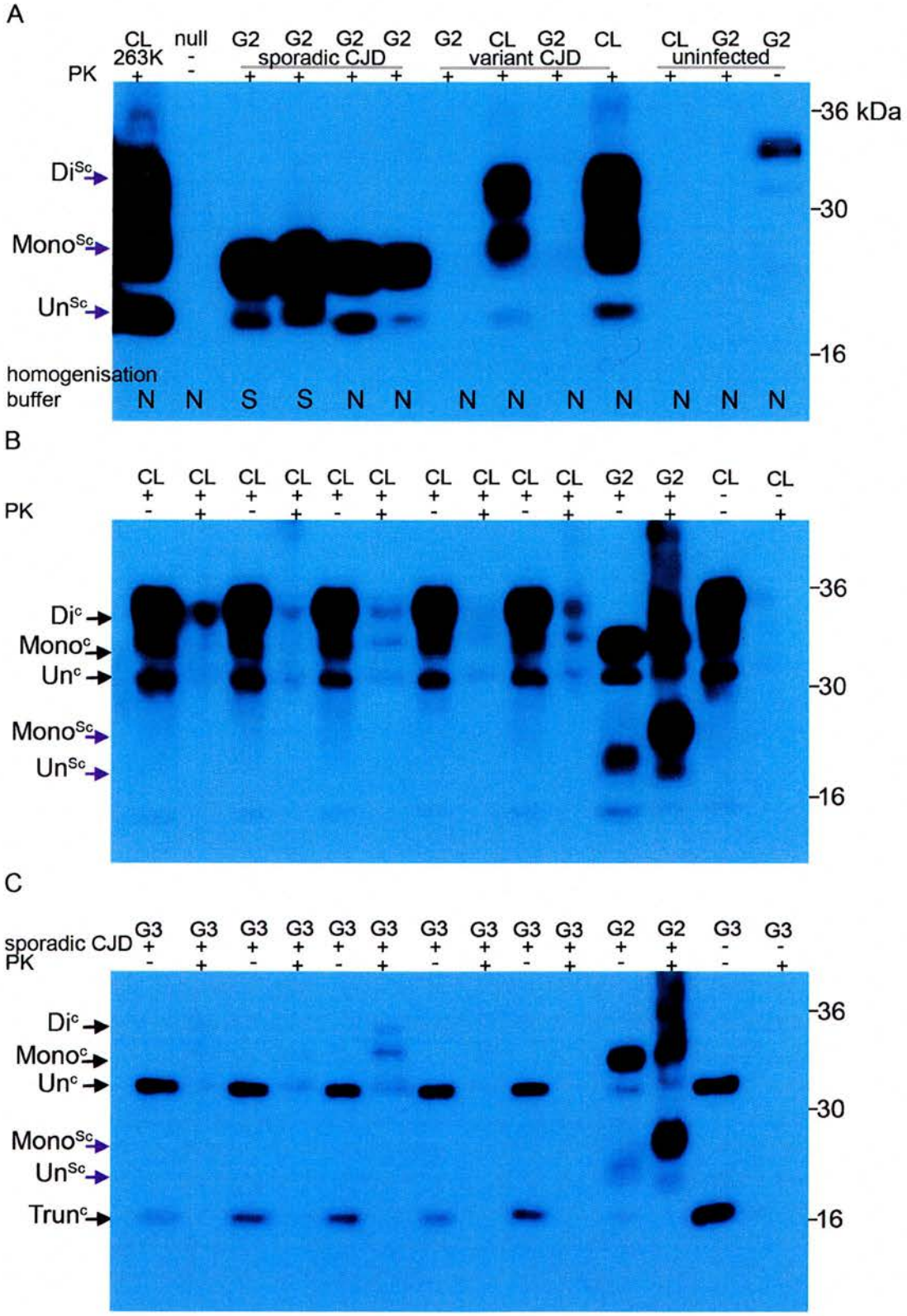

6.3.4.2 Variant CJD

PrP^{Sc} could be isolated from clinical endpoint vCJD normally glycosylated control mice (CLs) by standard methods without the need for NaPTA precipitation (n = 5, data not shown). However, PrP^{Sc} was only detected in one of the four vCJD challenged G2 clinical endpoint animals (Figure 6.13 A and data not shown). Ten-fold NaPTA mediated concentration was required to detected PrP^{Sc} in the other G2 clinical endpoint animals; such that the equivalent of 5 µg of total brain (wet weight) was run per G2 well (Figure 6.14 A). Both vCJD challenged G2 and CL brain homogenates were concentrated after PK digested by NaPTA precipitation, to ensure equivalent populations of PrP^{Sc} were compared. Equal PrP signal was then achieved by diluting CL PrP^{Sc} ten-fold prior to electrophoresis. This data demonstrates that a lower level of PrP^{Sc} accumulates at clinical endpoint after vCJD challenge in G2 transgenic mice despite the longer incubation period in these animals.

However, by Ponceau-s staining it was apparent that the total protein loaded per G2 lane was significantly higher than that loaded for the CL controls, which may have effected the electrophoretic separation of the proteins. This indicates that NaPTA precipitation was not completely selective for PrP^{Sc} and that other PK resistant proteins were also concentrated by this method. Additionally, significant carry-over of undigested PrP^{Sc} or PrP^{C} during NaPTA precipitation was apparent in both the G2 and CL vCJD challenged brain homogenates but not in uninfected controls.

In one subclinical and one clinical endpoint G2 transgenic mouse the size of un-glycosylated PrP^{Sc} was similar to that observed in the CL control mice (Figure 6.14 A, lanes 7 and 9). In the other clinical G2 animals the un-glycosylated PrP^{Sc} exhibited slower electrophoretic mobility than that of the CL controls which may indicate that the PK resistant PrP core was larger in these samples. Although all samples were prepared by identical methods, the greater amount of protein loaded per well for the G2 PrP^{Sc} samples may have affected the electrophoretic mobility of PrP^{Sc}.

Figure 6.14 Western blots of PrP^{Sc} from PrP glycosylation deficient transgenic and control mice challenged with variant CJD

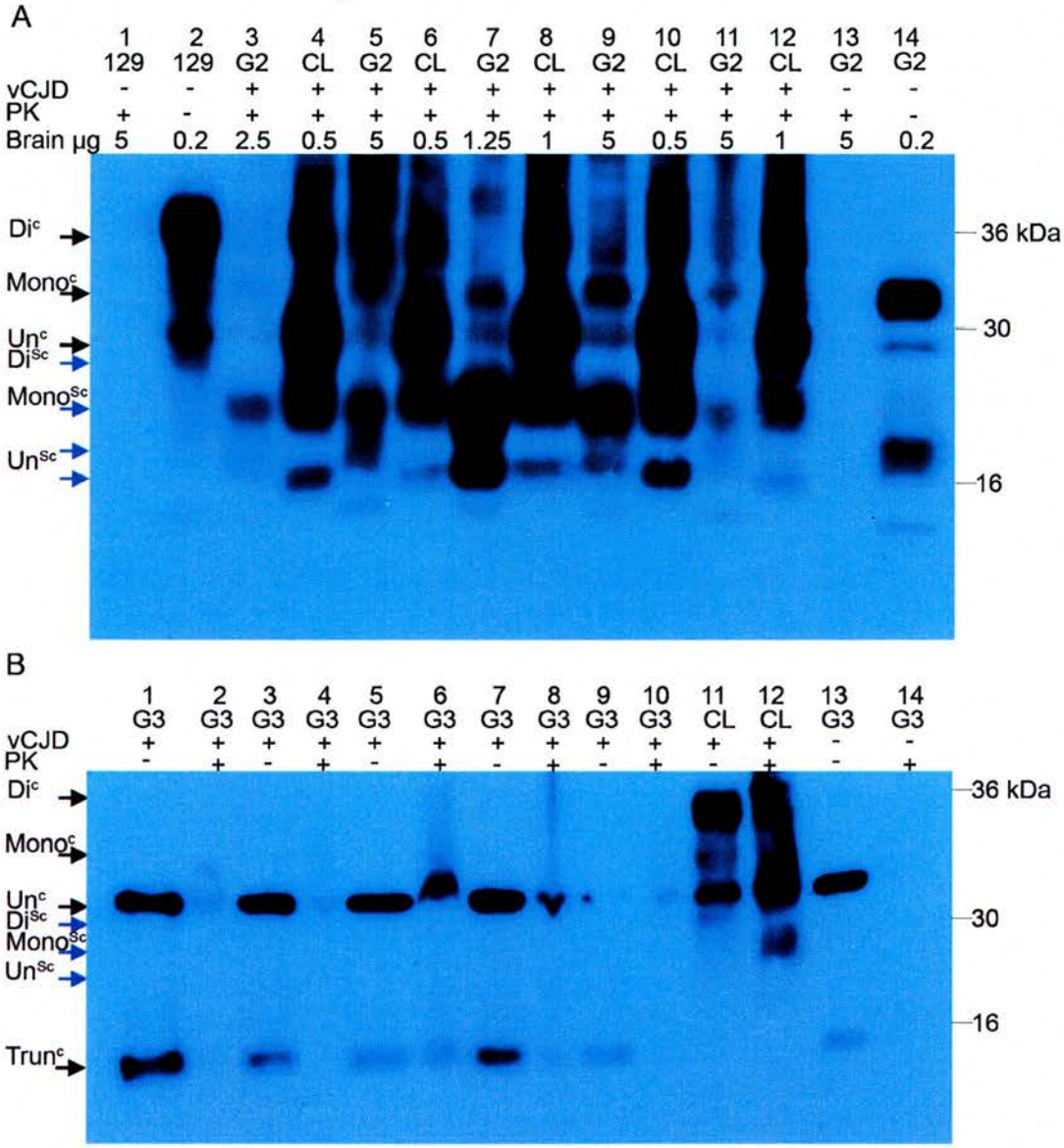

(A) PrP^{Sc} was isolated from vCJD challenged pre-clinical and clinical endpoint G2 transgenic and normally glycosylated control (CL) mice by standard PK digestion (20 µg/ml, 37 °C, one hour) and NaPTA mediated concentration from total brain homogenate. Amount of PrP^{Sc} was equalised between lanes by dilution of samples after NaPTA precipitation to permit comparison of samples. In two G2 transgenic mice (A, lane 7 & 9) electrophoretic mobility of un-glycosylated PrP^{Sc} was comparable to that in normally glycosylated control mice, in three G2 transgenic samples (A, lane 3, 5 & 11) the electrophoretic mobility of un-glycosylated PrP^{Sc} was reduced compared to that of controls, suggesting that the conformation of PrP^{Sc} may also differ. In five PrP^{d} and vacuolation negative variant CJD challenged G3 transgenic mice (B), total brain proteins were concentrated forty-fold by NaPTA mediated precipitation after standard PK digestion; no PrP^{Sc} was detected in any of these samples, despite clear PrP^{C} signal in all samples and a clear PrP^{Sc} signal in the CL/vCJD postive control (B, lane 12). PrP was detected with anti-PrP antibody 8H4 and horseradish conjugated anti-mouse secondary antibody (Jackson ImmunoResearch, West Grove, USA). Secondary was detected using POD solution (Roche Diganostics, Basel, Switzerland) and the resultant chemiluminescece was detected using X-ray film.

Thus although the difference in size of PrP after PK digestion may reflect a difference in the conformation of PrP^{Sc}, this could also be an artefact caused by the difference in the amount of PrP^{Sc} between the samples. Glycosylation of the second site may mediate the maintenance of the misfolded conformation of PrP/vCJD in murine hosts, however further investigation is required to confirm this.

No PrP was detected in G3 transgenic mice challenged with vCJD after 600 d.p.i., even after forty-fold by NaPTA mediated concentration (Figure 6.14 B; n = 5) consistent with the absence of detectable PrP^{d} by IHC.

6.3.5 TSE associated astrogliosis

The number and distribution of astrocytes in the brains of cross-species TSE challenged murine PrP glycosylation deficient transgenics and normally glycosylated control mice was investigated to determine if PrP^{C}'s glycosylation state influenced the development of astrogliosis (for method see chapters 2 and 5).

6.3.5.1 Sporadic CJD MM type 2

Astrocytosis was observed throughout the cerebral cortex, hippocampus, thalamus and hypothalamus of clinical endpoint sporadic CJD challenged G2 transgenic mice but not in challenged normally glycosylated controls or G3 transgenic mice consistent with the absence of TSE pathology in these mice (Figure 6.15). Interestingly, the astrocytosis observed in the clinical endpoint sporadic CJD challenged G2 was less extensive than that observed in 263K vacuolation positive G2 transgenic mice which exhibited no overt signs of clinical disease (Chapter 5).

Figure 6.15 Astrogliosis was apparent at clinical endpoint in sporadic CJD challenged G2 transgenic mice but not in control mice

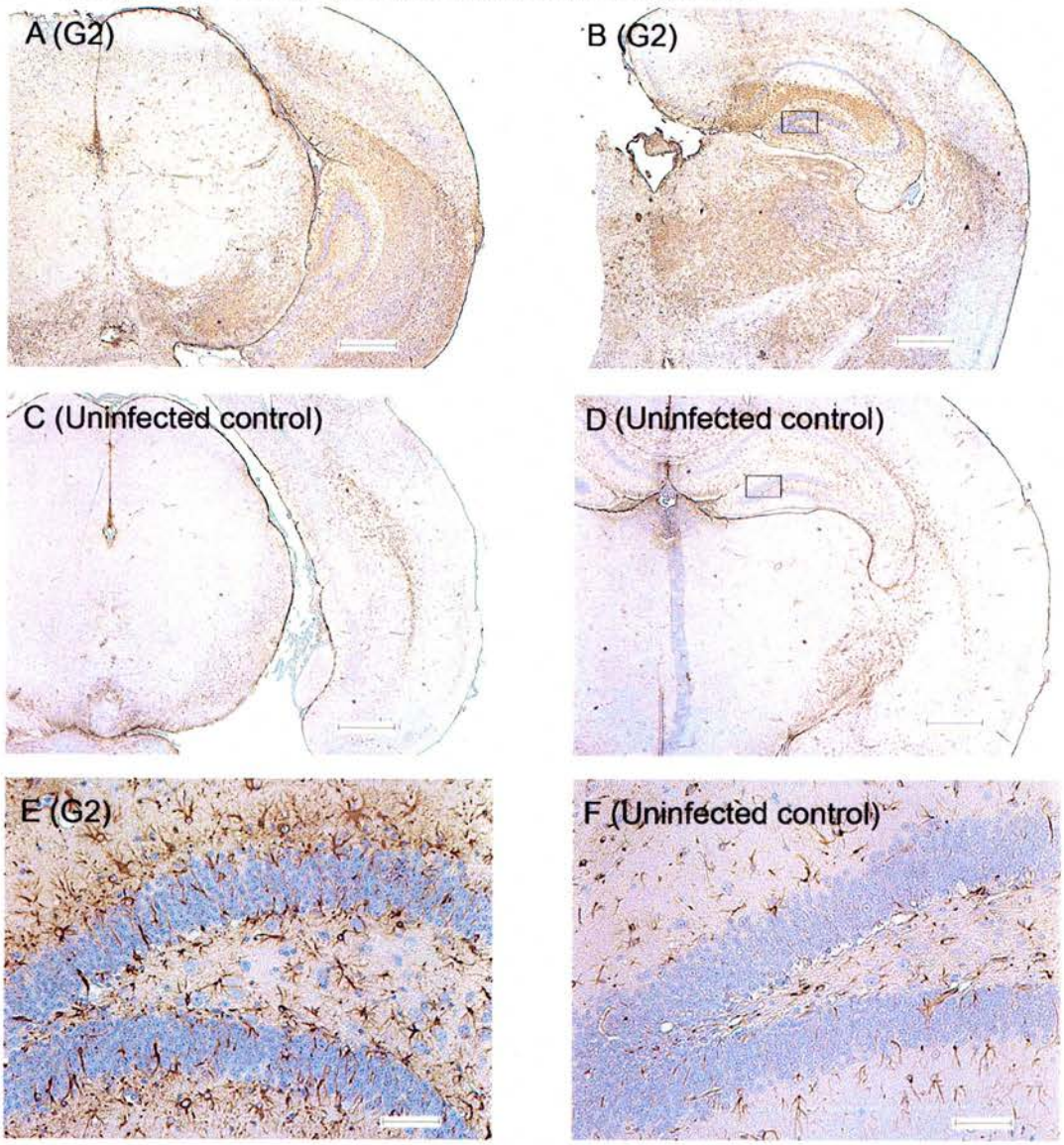

Extensive astrogliosis was apparent in sporadic CJD challenged clinical endpoint G2 transgenics (A, B and E) as compared to uninfected controls (C, D & F); assayed by IHC using anti-GFAP antibody. Figures show sections taken from one G2 transgenic mouse and one uninfected control. Boxed area in B = E and in D = F. Scale bar 500 µm (A-D), 50 µm (E & F).

6.3.5.2 Variant CJD

At clinical endpoint, extensive astrocytosis was observed in all normally glycosylated (CL) vCJD challenged controls examined (n = 7) (Figure 6.17 A and B). Astrocyte activation was observed in the thalamus and throughout the mid-brain and to a more limited extent in the hippocampus and cerebral cortex. In contrast, extensive astrocytosis was not consistently observed in vCJD challenged G2 transgenic mice at clinical endpoint (4/5 astrocytosis negative, 1/5 limited astrocytosis) (Figure 6.17 E and F).

This demonstrates that not only is disease incidence and the pattern of PrP^d deposition altered by the absence of an N-glycan at the second site, but other elements of the pathological response to TSE infections are changed. Interestingly these data also demonstrate the independence of the development of vacuolar pathology and the astrocytic response.

Figure 6.16 Astrogliosis was apparent in clinical endpoint variant CJD challenged control mice but not in G2 transgenic mice

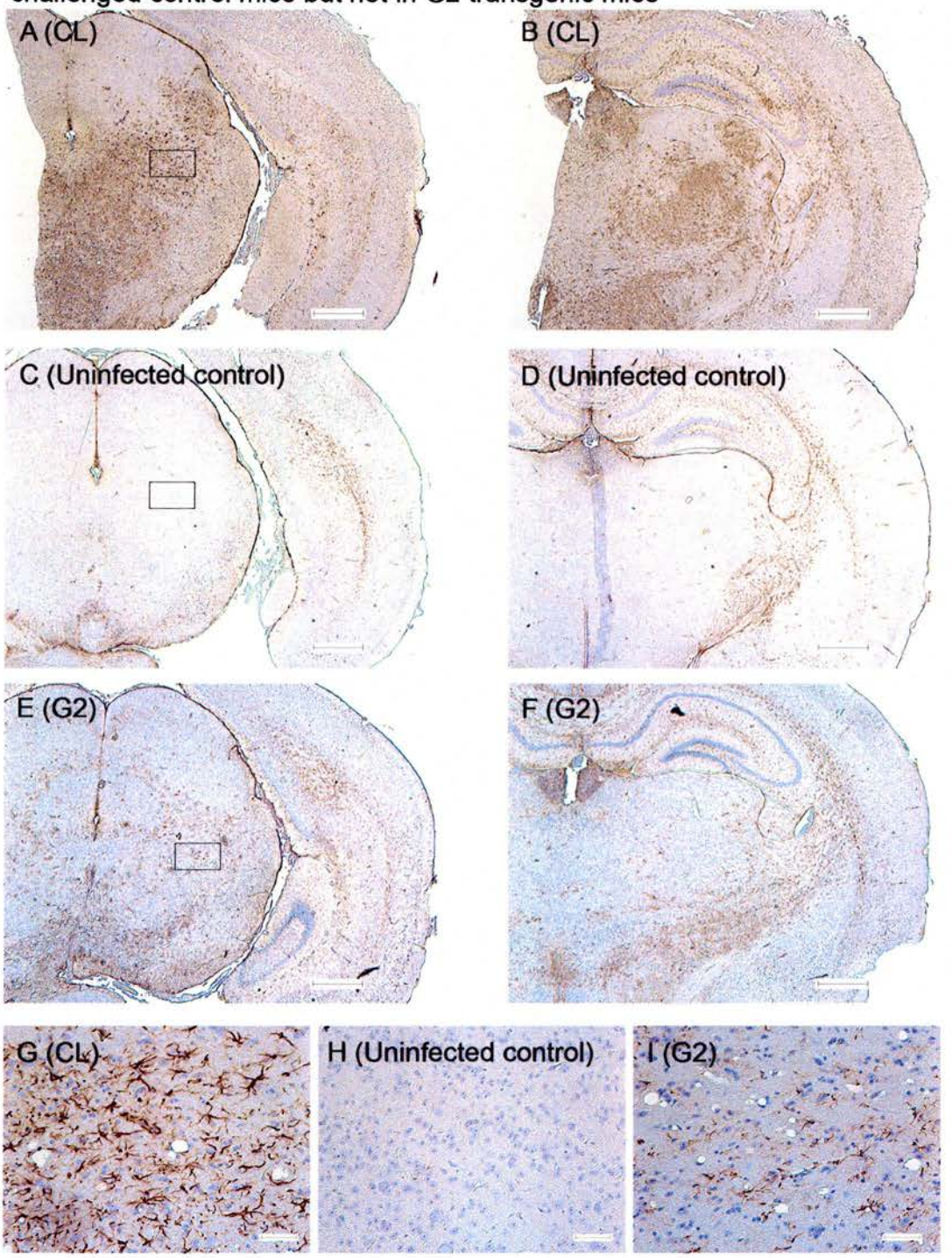

Extensive astrogliosis was apparent in variant CJD challenged clinical endpoint normally glycosylated controls (CL) (A, B & G) but not clinical endpoint G2 transgenics (E, F & I) nor uninfected controls (C, D & H), as assayed by IHC using an anti-GFAP antibody. Figures show results from one vCJD challenged CL control, one vCJD challenged G2 transgenic and one uninfected normally glycosylated control. Boxed area in A = G, in C = H and in E = I. Scale bar 500 µm (A-F), 50 µm (G-I).

6.3.6 Subpassage of CNS material from cross-species challenged G2 transgenic and normally glycosylated control mice

To define the extent of the species barrier between murine hosts and the human TSE agents studies subpassage experiments were undertaken. Material from G2 transgenic and normally glycosylated control mice challenged with vCJD or sporadic CJD MM type 2 was inoculated ic into normally glycosylated and G2 transgenic mice, by standard methods, such that any difference in incubation period between first and second passaged could be defined. A reduction in the incubation period between the first and second passage formally demonstrates that a species-barrier to transmission was observed during the primary passage.

In a complementary experiment, material from the first passage was used to challenge two strains of wild type mice (C57BL, VM) and their F1 cross (CV) [TSE strain typing panel]. The primary amino acid sequence of PrP^{C} differs between C57 ($PrP^{a/a}$) and VM mice ($PrP^{b/b}$) (Moore et al., 1998; Westaway et al., 1987). TSE disease develops differently in these mouse strains (Bruce, 1993). Thus by comparing the incubation period and lesion profile in these mice, the TSE strain isolated during the primary passage can be classified (Chapter 1). This experiment will examine whether the strain of TSE infecting the murine PrP glycosylation deficient transgenic and control mice at first passaged differed, and hence if the observed differences in transmission are attributable to strain selection rather than a direct effect on the extent of the species-barrier.

For secondary passage animals were challenged with 1 % brain homogenate from clinical endpoint sporadic CJD challenged mice. Material from two G2 transgenics that exhibited similar CNS pathology and clinical disease symptoms were used. Experimental procedures were identical to those for primary challenge, as described in chapters 2 and 5. This experiment is ongoing and is currently not available for complete analysis.

However, ic inoculation of brain material from the G2/sporadic CJD clinical-endpoint animals led to the development of TSE clinical disease in all challenged G2 mice. For the two samples assayed, the incubation period observed upon second passage was reduced approximately three fold compared to that of the primary transmission (Table 6.3). This is consistent with the existence of a substantial barrier to the transmission of this source to the G2 transgenic mice, despite their dramatically increased disease incidence compared to normally glycosylated controls at first passage. The mean incubation period was slightly longer for one sample (Table 6.3). This may reflect a marginally lower infectious titre in this sample, titration experiments will be required to investigate this possibility.

Table 6.3 Subpassage of CNS material from G2 transgenic and normally glycosylated control mice

Inoculum	Second passage host number of clinical animals/ total number challenged animals (incubation period +/- SEM)	
	129/Ola	G2
G2/sporadic CJD-1 (incubation period at 1° 418 dpi)	0/12 >300 days	12/12 (146.9 +/- 2.97)
G2/sporadic CJD-1 (incubation period at 1° 409 dpi)	0/12 > 280 days	12/12 (129.58 +/- 2.44)

Importantly no disease has yet been observed in the normally glycosylated controls challenged with G2/sporadic CJD (200 dpi); this demonstrates that G2 transgenic mice are particularly permissive for the strain of TSE isolated after sporadic CJD challenge. Absence of glycosylation at the second site appears to produce an intra-species transmission barrier as has been previously observed for PrP polymorphisms (Barron et al., 2005).

The pattern of TSE vacuolar targeting was very similar between the groups but differed from that observed at first passage (Figure 6.17).

Figure 5.17 Lesion profile of G2/sporadic CJD challenged G2 transgenic mice

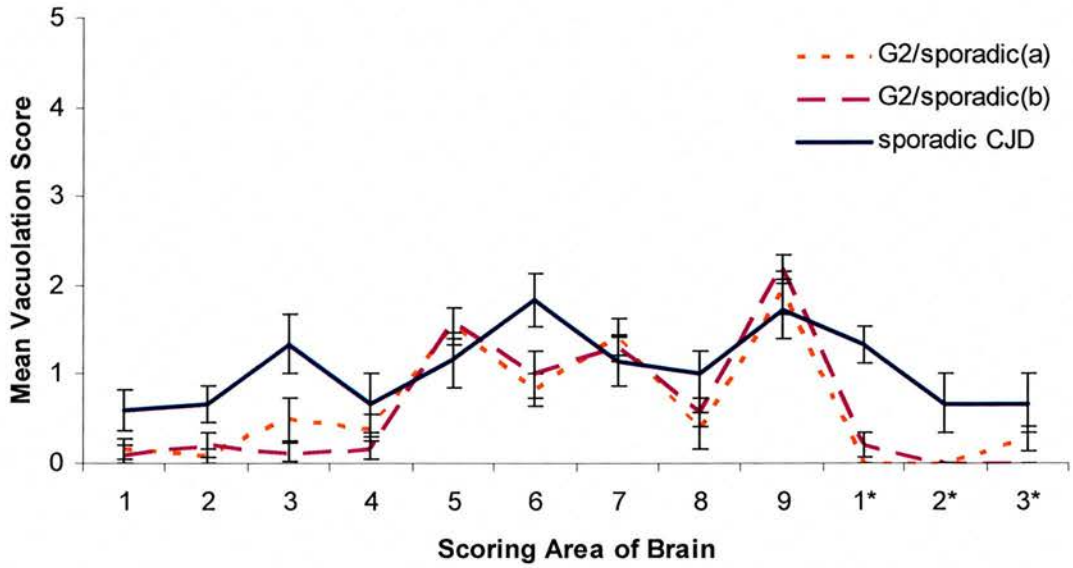

The pattern of TSE specific vacuolar pathology was semi-quantatively scored blind on a scale of 0-5 in nine grey areas (1 dorsal medulla; 2 cerebellar cortex; 3 superior colliculus; 4 hypothalamus; 5 thalamus; 6 hippocampus; 7 septum; 8 retrosplenial and adjacent motor cortex; 9 cingulate and adjacent motor) and three white matter areas of the brain (1* inferior and middle cerebellar peduncles; 2* decoction of the superior cerebellar peduncles; 3* cerebral peduncles) by standard methods, the experiment was then decoded and a lesion profile of the mean vacuolation score constructed. This demonstrates that the pattern and density of vacuolation in G" transgenic mice infected with the two G2/sporadic CJD samples investigated is very similar but that the patterns differs from that observed at primary passage of sporadic CJD in G2 mice.

This provides strong evidence that the same TSE strain was isolated in both the G2 transgenic mice after sporadic CJD challenge, although this conclusion awaits the results of the TSE strain typing experiment which has yet to be finalised. Furthermore, the alteration of lesion profile between primary and secondary passage suggests that TSE agent has undergone a process of adaptation to the G2 transgenic mice; as has previously occurred in other cross-species TSE transmissions (Bruce et al., 2002). This further supports the existence of a species barrier in the G2 transgenic mice to sporadic CJD transmission, despite the greatly elevated disease incidence observed in these mice compared to normally glycosylated controls.

6.4.7 Results summary

These data demonstrate that the role of PrP^{C}'s N-glycans in the cross-species transmission of TSE disease in greatly influenced by TSE strain and can not be predicted by the amino acid homology of PrP^{C} and donor PrP^{Sc}.

- Mice expressing only un-glycosylated PrP^{C} are resistant to vCJD and sporadic CJD transmission and do not permit the accumulation of PrP^{Sc}.
- Glycosylation of the second attachment site alters disease incidence and/or incubation period after cross-species TSE transmission in a strain dependent manner.
- Glycosylation of host PrP^{C} does not influence the strain specific targeting of vacuolar pathology but does alter the rate and pattern of accumulation of PrP^{Sc} *in vivo* after cross-species transmission for some TSE strains
- Glycosylation of host PrP^{C} influences the activation of astrocytes elicited by some TSE strains.

6.4 Discussion

6.4.1 Technical discussion

6.4.1.1 Disparity of clinical symptoms, vacuolation and PrP^d

Clinical signs were observed in a number of animals (11/136) in the absence of TSE specific vacuolar pathology. For experimental analysis all of these animals were defined as false positives, as vacuolation is a diagnostic criterion for TSE disease and the neurological signs in these mice are non-specific. In five of these animals no PrP^d was detected adding further support to these animals being false positives. Non-TSE CNS diseases or a dysfunction of unknown aetiology may have caused the clinical signs in these mice in the absence of TSE pathogenesis. In the remaining six animals PrP^d deposition was apparent, although relatively scant. It remains a theoretical possibility that the clinical signs observed in these animals were caused by misfolded PrP, however for the purposes of this study this scenario was not further explored.

The density of vacuolation varied between the different challenge experiments. In particular the density of subclinical vacuolation after 263K challenge (chapter 5) was much greater than the density observed at clinical endpoint in either the variant or sporadic CJD challenges. The extent and amount of vacuolation in identical hosts is known to vary among different strains of TSE disease (Bruce, 2003). The data presented here is consistent with this, and the hypothesis that vacuolation itself is not the principal cause of clinical signs during TSE disease.

Despite the significant difference in the pattern of PrP^d deposition and type of PrP^{Sc} in G2 transgenic mice as compared to normally glycosylated controls challenged with vCJD the targeting of vacuolar pathology was unchanged. This suggests that PrP^d is not directly responsible for the generation of vacuolation in agreement with previous reports (Barron et al., 2001; Foster et al., 2001). These data support the hypothesis of the existence of a subtype of misfolded PrP that is neurotoxic.

6.4.1.2 Variation in size of PrP^{Sc}

Slight variation in the electrophoretic mobility of un-glycosylated PrP^{Sc} between animals in the same experimental group was observed. In particular, a clear difference in the electrophoretic mobility of the PrP^{Sc} was apparent between the samples which were prepared for subpassaged by homogenisation in physiological saline and those directly extracted in NP40 buffer. The different history of detergent exposure may have altered the binding of PrP^{Sc} to SDS, and hence altered its charge and electrophoretic migration. Additionally, the material prepared for subpassage in physiological saline was disrupted by repeated passage through a 26 gauge needle, resulting in disruption of nuclei and mixing of its contents (DNA and nuclear proteins) with PrP^{Sc}. Interaction of PrP^{Sc} with these components may also have altered its electrophoretic mobility.

Equally, electrophoretic mobility will also be influenced by the ratio of protein to SDS or the amount of protein per lane. In particular, the significant concentration of G2/vCJD samples may have also resulted in electrophoresis artefacts. NaPTA precipitation was not totally selective for PrP^{Sc} and other partially PK resistant proteins were also concentrated. Hence in the G2 lanes approximately ten-fold more protein was loaded than in the normally glycosylated PrP control lanes. This larger amount of total protein may reduce the separation all proteins, including PrP, during electrophoresis. Thus the difference in electrophoretic mobility observed may not be a consequence of differential PK digestion but reflect the ratio of PrP^{Sc} to total protein.

Alternatively, the observed differences in electrophorectic mobility of PrP^{Sc} may have resulted from differences in the extent of PK digestion. The extent of PK digestion of PrP^{Sc} is dependent on a number of experimental factors particularly the pH and PK concentration (Notari et al., 2004). The samples were prepared with 50 mM tris which may be an insufficient concentration to fully buffer variation in pH between samples (Notari et al., 2004). Concentration of PK used should be uniform between all reactions as a single batch of PK which was aliquoted and stored at – 20 °C, was

used for all digestions. However the ratio of PK to protein will have differed between 5 and 10 % homogenates, as the amount of PK which was added was determined by reaction volume rather than the total amount of protein in each sample. Additionally, differences in the pH of homogenates may have contributed to the observed variation in PK digestion. However pH variation is unlikely to have affected the size of PrP^{Sc} in the NaPTA prepared samples, as PK digestions were carried out in the presence of 2 % sarkosyl which eliminates the effect of pH on PrP^{Sc} digestion size (Notari et al., 2004). If additional material were available, it would be desirable to repeat the preparation of infected brain material in a buffer containing 100 mM tris and monitor the pH of homogenates prior to digestion to investigate whether the variation observed was attributable to variation in the pH of samples.

6.4.2 Discussion of experimental results

6.4.2.1 Enhanced resistance of G3 transgenic mice to cross-species TSE challenge

Similarly to the enhanced resistance/increased incubation period of G3 transgenic mice to hamster scrapie 263K challenge (Chapter 5), these murine PrP glycosylation deficient transgenics did not exhibit any sign of TSE disease after cross-species challenge with vCJD or sporadic CJD (MM type 2). These data demonstrate that both the 263K-hamster/murine and human/murine TSE species barriers are enhanced in the absence of glycosylation of host PrP^{C}. However, as only three cross-species TSE sources have been investigated here, it is not possible to determine if the resistance of G3 transgenic mice to cross-species TSE infection is a generic effect or dependent on TSE source or strain. The evidence to date however would suggest the G3 transgenic mice are resistant to cross-species TSE infection irrespective of strain of agent. Transmission of hamster adapted 79A (79A-H) to the G3 transgenic mice may provide data pertinent to this issue (Kimberlin et al., 1989); as G3 mice are susceptible to the murine version of this strain (Tuzi et al., in preparation, appendix ii).

Additionally, further investigation is required to determine if the absence of PrP^{C}'s N-glycans has a similar effect on cross-species transmission of TSE to other host species. In particular, in longer lived animals absence of glycosylation of PrP may not be sufficient to prevent TSE disease development altogether, although it is likely to significantly extend the TSE incubation period, given its dramatic effect in mice. PrP^{d} deposition and PrP^{Sc} formation was also dramatically reduced in G3 transgenic mice compared to normally glycosylated murine controls after cross-species TSE challenge. The absence of accumulated misfolded PrP in G3 transgenic may underlie the observed barrier to TSE transmission.

A strong intra-species transmission barrier has also been observed in the G3 transgenic mice and comparable conventional PrP murine transgenics (DeArmond et al., 1997; Tuzi et al., in preparation) (appendix ii). However, clinical disease in the G3 transgenics has been observed, albeit with greatly increased incubation periods and reduced disease (Tuzi et al., in preparation). Thus the influence of PrP's N-glycans on TSE transmission is not unique to the species barrier. These factors may include the effect of PrP's N-glycans on the subcellular localisation of the protein (chapter 4) or the interaction of the protein with *in vivo* factors that promote its misfolding (chapter 7) or clearance.

Replication of TSE infectivity in the absence of detectable PrP^{Sc} or the development of TSE pathology has been previously observed (Barron et al., 2001; Hill et al., 2000; Lasmezas et al., 1997; Race et al., 2001). Therefore despite the absence of TSE pathology or PrP^{Sc} in the G3 transgenic mice challenged with variant CJD and sporadic CJD, subpassage of CNS material is required to experimentally assess whether replication of TSE infectivity also did not occur in these mice.

6.4.2.2 The effect of glycosylation at the second site on cross-species transmission is TSE source dependent

G2 transgenic mice which lack the second N-glycan attachment site display an altered disease incidence and/or incubation time after cross-species TSE challenge with three

TSE sources (chapter 5 and this chapter). For two sources (hamster 263K and sporadic CJD MM type 2) disease incidence was greater than in CL mice and time to disease onset appeared to be reduced; conversely in the case of vCJD, absence of the second site led to a reduction in disease incidence. Thus the role of glycosylation of PrP's second site in cross-species TSE transmission is dependent upon TSE strain. However, neither the species from which the TSE agent is derived nor the glycoform of the infecting PrP^{Sc} predicts the role of PrP^{C} glycosylation status in transmission between species.

Importantly, as previously discussed in Chapter 5, the absence of second site glycosylation specifically promotes cross-species TSE transmissions. However, an extension of the incubation period in G2 transgenic mice is observed for both vCJD and the related mouse passaged BSE strain, 301C (Tuzi et al, in preparation; appendix ii). Therefore the strain dependence of the role of the second site in cross-species TSE transmission observed here may reflect a common effect of a strain requirement for the second site, independent of the species barrier.

Glycosylation of asparagine 196 significantly contributes to the barrier to transmission of hamster 263K and sporadic CJD (MM type 2) to mice. However, the species-barrier to these agents is not completely eliminated by absence of the second site, as G2 transgenic mice are not 100% susceptible to these agents and a shortening in the incubation period is observed at second passage. This suggests that glycosylation of PrP^{C}'s second site contributes to the barrier to cross-species TSE transmission for some strains, but that other factors are also key to limiting the cross-species spread of the TSE agent.

The data also suggest that the rate of PrP^{d} deposition in the CNS in response to challenge with 263K or sporadic CJD is increased in the absence of glycosylation of PrP's second site. Thus glycosylation of the second N-glycan attachment site appears to inhibit the accumulation of some conformations of misfolded PrP *in vivo*. In contrast, the amount of PrP^{d} detected by IHC and PrP^{Sc} by western blot is reduced in clinical endpoint G2 transgenic mice compared to normally glycosylated controls

challenged with vCJD. Therefore for this TSE strain the second site glycosylation appears to promote the accumulation of PrP^{Sc} *in vivo*. These techniques discriminate TSE disease associated misfolded PrP from PrP^{C} by different methods (fixation-denaturation and PK digestion), and thus the lower amount of misfolded PrP observed is unlikely to be an experimental artefact, although the possibility of the G2/PrP^{Sc} being more liable to degradation by both methods can not be formally discounted. These data suggest that the kinetics of accumulation of PrP^{Sc} after vCJD challenge is altered by the absence of glycosylation of PrP at the second site.

PrP^{Sc} may be a surrogate marker for the neurotoxic form of PrP. Therefore the low level of PrP^{Sc} detected in clinical endpoint G2 transgenic mice challenged with vCJD may not reflect a lower level of neurotoxic PrP (Hill et al., 2000). Further investigation is required to ascertain if the misfolded PrP generated in this challenge is more neurotoxic than that which is normally glycosylated. This could be achieved by comparison of the neurotoxicity of the two forms in neuronal cell cultures.

Titration of TSE affected brain in G2 and wild type mice is required to ascertain if the titre of TSE infectivity produced after vCJD challenge is equivalent in G2 and normally glycosylated control mice.

The size of the PK resistant PrP core appears to be altered in some G2 transgenic mice compared to normally glycosylated controls after vCJD challenge, although this result may be an experimental artefact (6.4.2.2). Alteration in the size of the PK resistant core is thought to be caused by differences in the conformation of PrP^{Sc}, such that less of the N-terminal is available for PK digestion (Bessen and Marsh, 1992a). Thus glycosylation of PrP at the second site may alter the conformation of PrP^{Sc} generated after vCJD challenge. Previous work has suggested that glycosylation may influence PrP conformation, indeed some have suggested that PrP^{Sc}'s N-glycans may encode TSE strain information (Collinge et al., 1996; Rudd et al., 2001). Transmission of murine scrapie strain 79A through the G2 transgenic mice has been shown to alter some strain characteristics (Tuzi et al, in preparation). Further investigation is required to determine if the conformation of PrP^{Sc} has been

altered upon cross-species transmission of TSE in the PrP^{C} glycosylation deficient transgenic mice. A similar change in PrP^{Sc} type has been reported upon passage of vCJD in normally glycosylated transgenic mice (Asante et al., 2006; Hill et al., 1997a; Korth et al., 2003). In these reports, the electrophoretic mobility of the un-glycosylated PK resistant core was observed to be lower in a proportion of the challenged animals. However, no difference in the amount of PrP^{Sc} was reported in these studies in contrast to the dramatic results observed here.

In addition to the amount and size of PK resistant PrP varying, the pattern of PrP^{d} deposition was also significantly different in G2 transgenic mice as compared to normally glycosylated murine controls challenged with vCJD. Similarly, within species TSE transmission to a conventional murine transgenic lacking the second glycosylation site was reported to result in an altered pattern of misfolded PrP deposition (DeArmond et al., 1997). In this experiment both the targeting and type of PrP^{Sc} deposition was changed, in particular the specific formation of amyloid plaques in the murine transgenics was reported. In contrast to the model used here the pattern of PrP^{C} localisation in the CNS also differed in the murine glycosylation deficient transgenics compared to normally glycosylated controls, which may have contributed to the change in deposition observed (DeArmond et al., 1997).

The pattern of PrP^{d} deposition *in vivo* is influenced by PrP's amino acid sequence and attachment of the GPI anchor (N-glycan attachment) (Bruce et al., 1991; Chesebro et al., 2005). The glycosylation of PrP's second site plays a key role in determining the PrP^{d} deposition after cross-species transmission of some strains of TSE. Differences in the type of PrP^{d} deposited may be caused both by its conformation and rate of formation *in vivo*. Indeed in some TSE models a longer incubation period is associated with the formation of PrP^{d} plaques (Brown et al., 2003). Similarly here in the longer incubation period model (vCJD challenged G2's) focal deposits were observed in contrast to the more diffuse or synaptic pattern of PrP^{d} in the normally glycosylated controls. Alternatively, the absence of glycosylation at the second site may have directly altered the deposition of PrP^{d} and may even have caused the observed change in incubation period.

Different TSE sources have different pathogenic requirements and target different regions of the brain, peripheral nerves and lymphoid tissue (Bruce, 1993). Glycosylation of PrP^C differs between regions of the brain and in the periphery; both in terms of the combination of sugars attached and the relative occurrence of the un-, mono- and di-glycosylated forms (Russelakis-Carneiro et al., 2002; Somerville, 1999). Equally the expression and localisation of other cellular components important to cross-species TSE pathogenesis or PrP conversion may differ between TSE target regions. The requirement for PrP^C's N-glycans for successful TSE pathogenesis may regionally differ because of variation in the availability of cofactors. Thus the difference in the importance of the second site to TSE transmission between TSE sources may be the result of differences in the pathogenesis and the tissues targeted by each source. In particular, th e apparent requirement for a replication phase in peripheral lymphoid tissue prior to the development of full CNS disease, even after direct inter-cerebral inoculation, differs between sources (Bruce et al., 1994). Peripheral pathogenesis may be altered in the G2 glycosylation deficient transgenic mice.

The glycosylation state of PrP^C may also impact on other aspects of TSE pathogenesis that are known to differ between TSE sources, such as the extent of neuronal death, microglial activation or astrogliosis. Indeed, after vCJD challenge, the glycosylation state of murine PrP clearly influenced the activation of astrocytes. This effect may be mediated indirectly via a change the conformation of PrP^{Sc}. However, an effect on astrocyte function directly via the change in PrP^C glycosylation state may also occur; as work has suggested that PrP^C is expressed at low levels in astrocytes, although this has not been replicated in all studies (DeArmond et al., 1987; Ford et al., 2002a; Laine et al., 2001; Manson et al., 1992a; Mironov et al., 2003; Verghese-Nikolakaki et al., 1999). Thus it is feasible that the global alteration of the glycosylation of PrP^C in these studies may alter astrocyte activation in a TSE source specific manner, although given the massive effect on PrP^{Sc} deposition in this model it appears a rather unlikely scenario. PrP^C has been reported to have both pro- and anti-apoptotic functions in cell culture systems (Bounhar et al., 2001; Brown et al.,

2002; Milhavet and Lehmann, 2002; Solforosi et al., 2004). The glycosylation state of host PrP^C may alter the proteins role in TSE disease related apoptosis. The extent and pattern of cell death differs between TSE strains. The importance of glycosylation of PrP to the protein's pro- or anti-apoptotic role may also differ between TSE strains.

Surprisingly, G2 transgenic mice are more susceptible to variant CJD and sporadic CJD than comparable gene-targeted murine transgenics which express the human PrP under control of the murine PrP promoter (Bishop et al., 2006; Personal communication Matthew Bishop), despite the comparable level of PrP^C in the G2 and humanised transgenic mice. This provides strong evidence that amino acid sequence homology does not determine the barrier to infecting mice with human TSE sources. Furthermore these data emphasise the likely existence of murine specific PrP conversion factors which facilitate PrP misfolding or accumulation *in vivo*.

Importantly, both the targeting of vacuolation and the clinical signs were not significantly altered in G2 transgenic mice compared to normally glycosylated murine controls after vCJD challenge, despite the differences in PrP^d deposition. This demonstrates that not all aspects of TSE pathogenesis correlate with PrP^d deposition. However, the activation of astrocytes was not detected in the G2 clinical endpoint vCJD animals, suggesting that the alteration in PrP^d deposition does alter disease pathogenesis. Astrocytosis has been clearly observed in G2 animals challenged with both sporadic CJD and 263K indicating that in this case the absence of astrocyte activation must a specific to the TSE source.

In conclusion, the PrP's N-glycans greatly influence the cross-species transmission of a number of TSE agents, demonstrating that this post-translational modification has an important species barrier role. However, the nature of this role is strain dependent. Additionally, the N-glycosylation state of PrP^C alters both the rate of accumulation and the pattern of misfolded PrP deposition *in vivo*. Further investigation is required to determine if the observed changes in PrP^{Sc} directly underlie the effect of PrP's glycosylation status on cross-species TSE transmission.

7.0 The role of PrP^C's N-glycans in the protein's misfolding determined using Protein Misfolding Cyclic Amplification (PMCA)

7.1 Aim To determine if the role of PrP^C glycosylation state in the TSE transmission barrier can be attributed to a direct influence of the N-glycans on the conversion of PrP^C to PrP^{Res}.

7.2 Introduction and experimental technique

Glycosylation of PrP^C has a dramatic influence on TSE transmission both within and between species (Chapter 4 and 5; Tuzi et al., in preparation; DeArmond et al., 1997; Neuendorf et al., 2004). However the nature of the influence of PrP^C's N-glycans varies both with TSE strain and the site of attachment. The role of glycosylation of PrP^C in TSE transmission may occur via a number of potential mechanisms. In particular, the glycosylation state of PrP^C may alter its interaction with other molecules and may influence the key PrP^C to PrP^{Sc} conversion event, which is thought to lie at the heart of TSE disease.

Some studies have suggested that the glycosylation state of PrP^C has little influence on its *in vitro* convertibility (Kocisko et al., 1994; Kocisko et al., 1995). Others have suggested that un-glycosylated PrP^C is more readily converted than the normally glycosylated protein (Bossers et al., 1997; Lawson et al., 2001; Priola and Lawson, 2001; Raymond et al., 1997; Vorberg and Priola, 2002). In some cases this inhibitory effect of glycosylation was only observed for cross-species conversions or when the N-terminus of PrP^C was truncated (Lawson et al., 2001; Priola and Lawson, 2001). However all these *in vitro* investigations utilised cell culture derived PrP^C and/or global glycosylation inhibition strategies such as the use of tunicamycin.

Glycosylation of PrP^C in cell culture differs from that *in vivo* and is greatly influenced by the culture conditions (Monnet et al., 2003). In particular PrP produced in N2a cells has been reported to be overglycosylated and under sialyated

(Bossers et al., 1997). Thus, studies using cell-culture-derived PrP^C, which will not be natively glycosylated, may not reflect the true role of glycosylation of PrP^C *in vivo*. Global inhibition of glycosylation may alter conversion efficiency independently of the role of PrP^C N-glycans, as the glycosylation state of other cellular factors including any involved in conversion will also be altered. Moreover, use of tunicamycin in cell cultures both increases the incidence of protein misfolding and greatly alters cellular expression pattern, both of which may affect PrP convertibility independently of the role of the glycosylation (Benedetti et al., 2000). Use of the PrP glycosylation deficient transgenic mice [NPU] as the source of PrP^C circumvents these issues, as partially and completely un-glycosylated PrP^C can be produced without the use of enzymatic or chemical deglycosylation. Additionally, the relative importance of glycosylation, at each attachment site, to conversion can be investigated by a comparison of G1 and G2 derived PrP^C. Furthermore, the *in vitro* data generated can be directly comparable to the *in vivo* transmission experiments to these PrP glycosylation deficient transgenic mice.

To examine the role of PrP's N-glycans in the conversion of PrP^C to PrP^{Res} the *in vitro* conversion technique Protein Misfolding Cyclic Amplification (PMCA) was used (Saborio et al., 2001). Unpurified murine brain homogenate was used as the source of PrP^C, mixed with PrP^{Sc} and subjected to PMCA. This conversion technique utilises repeat round of incubation at 37 °C and sonication to induce the amplification of the misfolded conformation of PrP. During the incubation step PrP^{Sc} from a TSE infected host binds to and induces the conformational conversion of the normally folded PrP^C substrate, leading to an amplification of the misfolded PK resistant form. To increase the amplification level the reaction is sonicated after each 37 °C incubation period, to break-up the misfolded PrP aggregates into smaller fragments which are then able to bind and induce further conversion of PrP^C to a PK resistant form (Figure 7.1 adapted from Saborino et al 2001).

Figure 7.1Schematic representation of PMCA (Adapted from Saborino *et al* 2001)

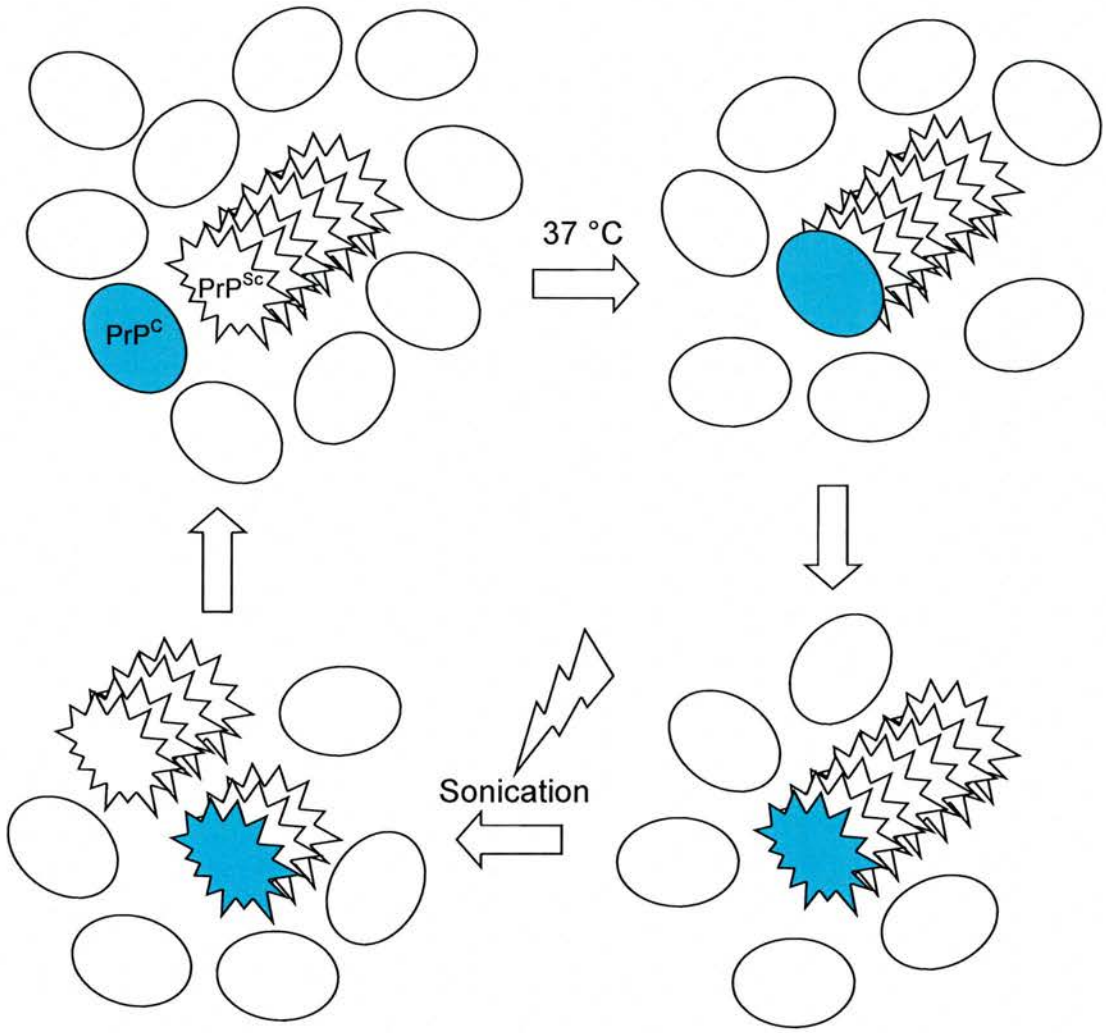

The PMCA technique requires that PrP^{C} misfolding is seeded by the presence of PrP^{Sc}, as has been previously demonstrated by conventional *in vitro* conversion assays (Kocisko et al., 1994). Additionally the theory underlying PMCA would suggest that seeded misfolding leads to an increase in the size of PrP^{Res} aggregates, as the application of ultrasound, which mechanically breakdowns large molecules, facilitates amplification. This apparent requirement for aggregate breakdown suggests that seeding efficiency is proportional to the surface area of misfolded protein, perhaps because of a requirement for a direct interaction between PrP^{Sc} and PrP^{C}. This may be consistent with the observations of Silveira and colleagues who demonstrated that oligomeric PrP^{Sc} was associated with higher levels of TSE infectivity than larger aggregates (Silveira et al., 2005). However the optimum size of PrP^{Res} aggregate to mediate PMCA conversion has yet to be determined.

The standard *in vitro* conversion method is relatively inefficient and requires a great excess of PrP^{Sc} to seed conversion (Kocisko et al., 1994). Thus, in order to detect the newly formed PrP^{Res}, PrP^{C} must either be radiolabelled or have a specific epitope which is not present in the seeding PrP^{Sc}. Radiolabelling of *in vivo* derived protein is not experimentally viable and the introduction of a novel antibody epitope into PrP may alter the behaviour of the protein, as has been previously highlighted (Barron et al., 2005). Thus the standard conversion technique is not suitable for the study of the role of *in vivo* glycosylation of PrP in the convertibility of the protein to PrP^{Res}. In contrast *in vivo* derived PrP^{C} can be utilised as a substrate for PMCA mediated conversion. Higher PrP^{Res} amplification levels are possible using PMCA rather than standard *in vitro* conversion. Therefore, it is possible to identify newly formed PrP^{Res} purely on the basis of its resistance to PK because it is formed in excess of the seeding PrP^{Sc} (Castilla et al., 2004). Therefore, it is not necessary to specifically label the PrP^{C} substrate.

PMCA mediates the seeded misfolding of PrP to the disease associated form in the presence of all cellular components of the central nervous. In fact these components are essential for successful PMCA mediated PrP^{Res} amplification (Saborio et al.,

1999). This demonstrates that the PrP^{C} to PrP^{Res} conversion event is mediated by other cellular factors. In the PMCA system all cellular components can freely mix and thus novel interactions may occur between molecules from different cell types and subcellular compartments which would not normally occur *in vivo*. Thus the *in vitro* mechanism of PrP^{C} to PrP^{Res} conversion may differ from that *in vivo* because of the influence of non-specific factors or the absence of a sufficient concentration of a required factor. Equally, sonication is known to mediate the misfolding of a number of proteins that are not amylogenic *in vivo*, which may alter their role in conversion (Stathopulos et al., 2004). Despite these caveats, PMCA generated PrP^{Res} has similar physical properties to PrP^{Sc} including its secondary structure (Castilla et al., 2005). Furthermore, PMCA does appear to mimic a number of *in vivo* TSE characteristics, most notably the replication of infectivity and also some aspects of the species barrier (Castilla et al., 2005; Piening et al., 2006), suggesting that fundamental aspects of TSE disease are dictated at the molecular, rather than the cellular level and validating the use of PMCA to investigate the importance of PrP's N-glycans to TSE transmission.

For all the experiments performed in this chapter, automated PMCA was carried-out in tubes which were sealed for the duration of the experiment, such that sonication was applied indirectly via a water bath (Castilla et al., 2004). Uninfected brain homogenate was prepared by standard procedures to ensure of retention of cellular membranes, as this has been suggested to be important for successful PMCA amplification (Castilla et al., 2004). This PrP^{C} containing substrate was then seeded by an experimentally determined ratio of infected brain homogenate that contained PrP^{Sc}. This master mix was divided into aliquots after vigorous vortexing to ensure homogeneity. Control aliquots were frozen or incubated at 37 °C in the absence of sonication for the duration of the experiment, multiple aliquots were then subjected to PMCA. Each PMCA cycle consisted of a 30 minute incubation at 37 °C followed by 30 second pulse of sonication, multiple cycles were undertaken as determined by optimisation experiments.

The amount of newly formed PrP^{Res} was assayed by standard proteinase K digestion and western blot densitometry, which permitted the separate quantification of the un-, mono- and di-glycosylated PrP glycotypes. Bands were delineated manually using peak minima to determine band limits. The level of PrP^{Res} amplification was calculated by dividing the amount of PrP^{Res} detected after experimental treatment by the amount of PrP^{Sc} used to seed the reaction, as detected in the frozen sample. In this way both the relative amplification level of each individual glycotypes and the total increase in PrP^{Res} could be determined. Thus the specificity of amplification could be checked by comparing the amplification level of the PrP glycotypes which were present in the uninfected brain homogenate with those which were not. For example, when using a G3 PrP^{C} homogenate, non-specific amplification of the mono- and di-glycosylated forms can be compared against the specific amplification of the un-glycosylated PrP^{Res}, to confirm that any observed reaction was specific to the PrP^{C} supplied.

Additionally, it was also possible to score the reactions as positive or negative for PrP^{Res} amplification by comparison with the experimental controls. Positive reactions were those which exhibited a two-fold increase of the predominate PrP^{Res} glycotype over that observed in the PrP null [NPU] control, as determined by western blot densitometry. This allowed low but specific amplification of un-glycosylated PrP^{Res} to be detected. Amplification occurrence may reflect the likelihood of a PrP to PrP^{Res} nucleation event occurring, whereas the total amplification level may reflect the efficiency of PrP^{Res} generation after nucleation.

To investigate the importance of PrP N-glycans to TSE transmission, two murine TSE strains (ME7 and 79A) and one hamster TSE strain (263K) were used to seed PMCA reactions. This was performed to investigate both the role of TSE strain and the species barrier on conversion. ME7 and 79A differ in PrP^{Sc} glycoform, in addition to the pattern vacuolar pathology in the brain and disease incubation periods (Somerville et al., 1997) (Figure 7.2 B and C). The glycoform of 263K is similar but not identical to that of ME7, as both are predominantly di-glycosylated (Bruce and Dickinson, 1987; Somerville et al., 1997) (Figure 7.2 A). 263K is poorly

transmissible to wild type normally glycosylated mice (Chapter 5) (Kimberlin and Walker, 1978a). In contrast the murine adapted strain like ME7 and 79A are readily transmitted to mice (appendix ii). Additionally, all these strains have different transmission characteristics to the glycosylation deficient transgenic mice (Chapter 4; Tuzi et al., in preparation; appendix ii). 263K is more readily transmitted to G2 transgenic mice and less readily transmitted to G1 and G3 transgenic mice than to normally glycosylated mice (Chapter 5). Whereas, 79A is transmissible to G1 transgenic mice but ME7 is not (Tuzi et al., in preparation; appendix ii). These differences may be caused by innate differences in the ability of the different PrP glycotypes to adopt the misfolded conformation of each of these strains.

It was not possible to investigate the relative convertibility of variant and sporadic CJD MM type 2 PrP^{Sc} seeded PMCA reactions because of USDA restrictions on the import and work with category three TSE material in the United States, and the lack of a category three located automated sonicator in the United Kingdom at the time of investigation. Additionally, to address the role of PrP's N-glycans in the variant and sporadic CJD seeded PMCA reactions, a relatively large amount of infected brain material would have been required. Approximately 1 gram of infected brain material of each TSE strain was used in the experiments presented here and a larger amount may have been required for variant or sporadic CJD seeded reactions as a higher ratio of PrP^{Sc} to PrP^{C} or additional optimisation experiments may have been required. Using such a large volume of category three infected brain material would have posed both a health and safety risk and ethical issues.

7.3 Optimisation of experimental technique

7.3.1Characterisation of PrP^{Sc} containing seed

Half brains from murine passaged scrapie strains ME7 and 79A clinical end point 129/Ola murine brain were a kind gift of Dr. Nadia Tuzi (NPU). TSE strain was confirmed by incubation period and lesion profile. Two whole brains from a clinical

end point hamster infected with TSE strain 263K were sourced from the NPU-IAH strain bank. All TSE infected brains were homogenised in PBS/proteinase inhibitors (PI) by standard methods (Castilla et al., 2004). The expected PrP^{Sc} glycoform for these strains was confirmed by western blot densitometry (Figure 7.2 and 7.3).

Preliminary PMCA studies demonstrated variable background non-specific amplification of PrP^{Res} for all TSE strains investigated. An apparent amplification of PrP^{Res} was observed in some PrP null controls, which lack any PrP^{C} conversion substrate (data not shown). Additionally, amplification of non-specific PrP glycotypes that were not present in the PrP^{C} containing substrate from the glycosylation deficient transgenic mice was observed (e.g. di-glycosylated PrP^{Res} amplification in a G2 substrate (data not shown). This could be attributable to either amplification of the PrP^{C} contained in the unpurified infected brain homogenate or variability in the amount of PrP^{Sc} in each reaction.

7.3.2 Purification of ME7 and 79A seed

The ME7 and 79A clinical endpoint infected brain 10 % homogenate that were prepared in sterile PBS/PI, were then centrifuged in 10 % sarkosyl to separate PrP^{C} from PrP^{Sc}. Purification of PrP^{Sc} prevents contamination of the reaction with normally glycosylated PrP^{C} from the infected brain homogenate, which may convert to PrP^{Res} elevating the non-specific signal. Not all PrP^{Sc} was recovered by the technique, as demonstrated by the higher concentration of purified sample required to obtain detect similar levels of PrP^{Res} by western blot (Figure 7.2). However, the glycoform of PrP^{Sc} was unchanged by this purification procedure, suggesting that purification did not lead to enrichment for a subset of PrP^{Sc} (Figure 7.2 A, B and 7.3). Furthermore the pattern of amplification observed did not differ between the reactions seeded with purified or unpurified PrP^{Sc} such that these data sets could be validly combined for analysis (Tables 7.1 and 7.2). This purification procedure did not significantly reduce the background for either the ME7 nor 79A seeded PMCA reactions, suggesting that the background observed in the preliminary reactions was not caused by conversion of PrP^{C} associated with the seed.

Figure 7.2 Western Blots of PrP^{Sc} used to seed PMCA reactions

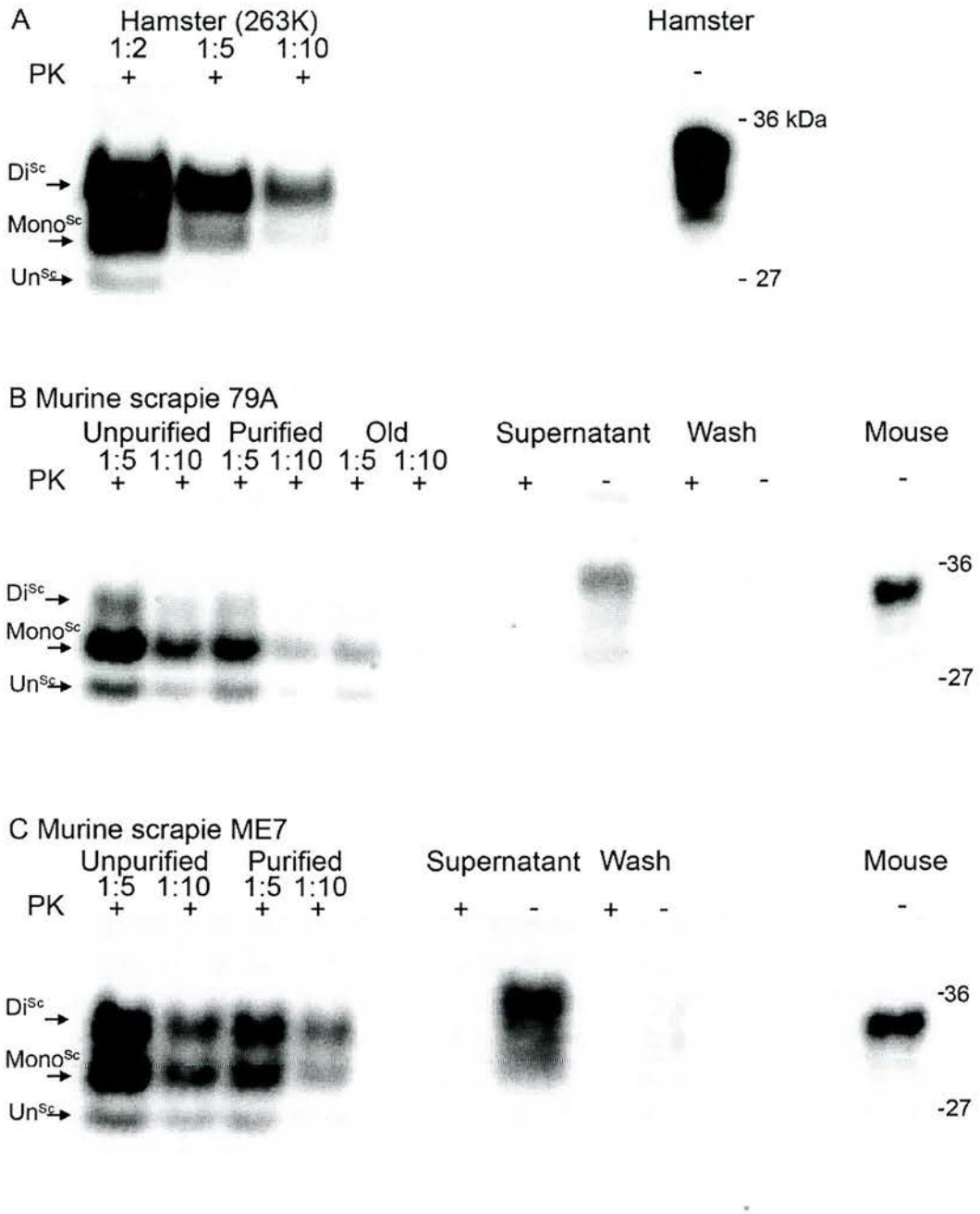

Western blots of total brain proteins, treated with 50 µg/ml PK at 55 °C (A) or 37 °C (B & C) for 1 hour shaking at 300 rpm, as indicated to isolate PrP^{Sc} from total brain homogenate from a (A) clinical endpoint 263K infected hamster, (B) clinical endpoint 79A infected 129/Ola mouse or (C) ME7 clinical endpoint 129/Ola mouse. Infected brain homogenates were diluted in PrP null brain homogenate at the ratio indicated prior to PK digestion. Western blots were probed with PrP specific antibodies 6H4 (A) and 6D11 (B and C).

Figure 7.3 Densitometry was carried out on western blots to quantify the glycoform of murine PrP^{Sc} before and after purification

A (79A)

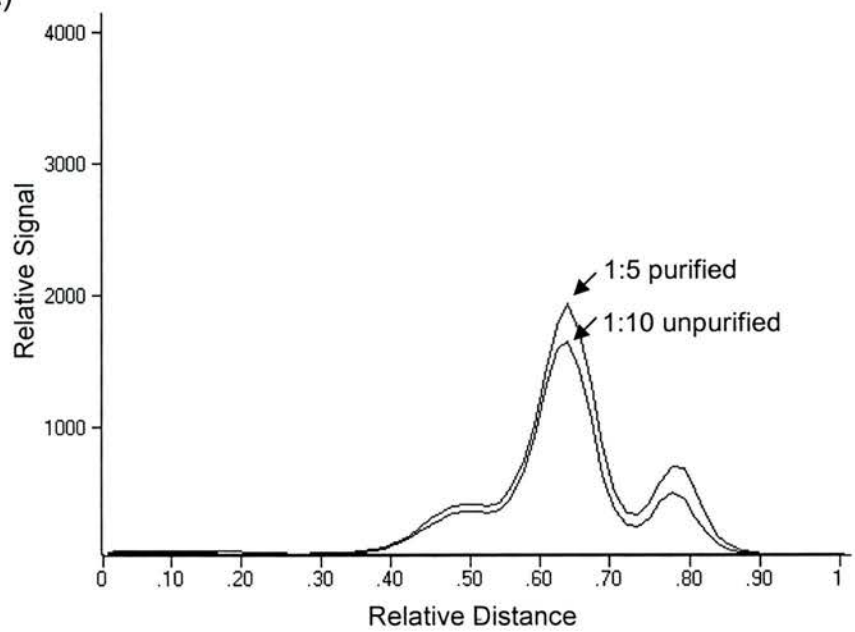

B (ME7)

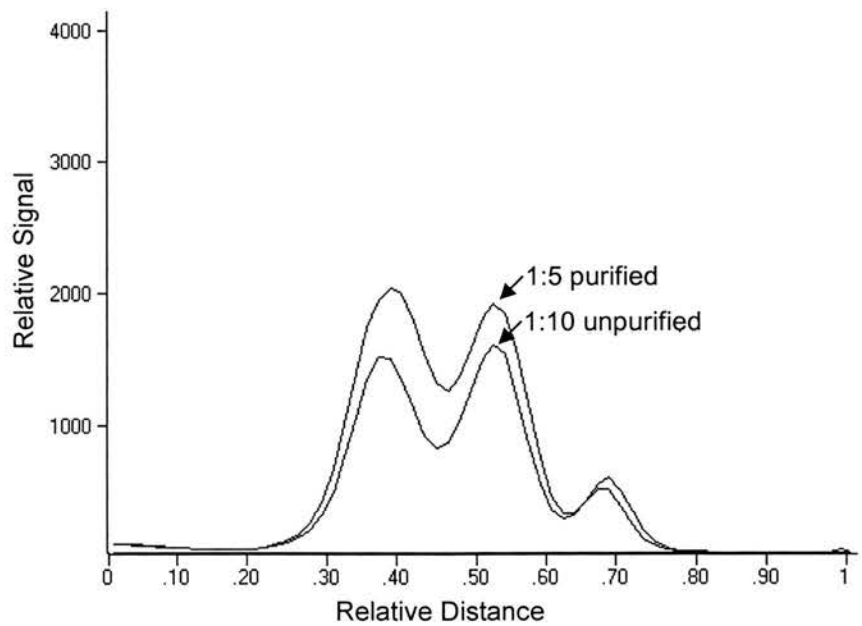

Y-scale intensity of signal, X-scale relative distance from top of lane. PrP^{Sc} concentration and purification state as indicated. A) clinical endpoint 79A infected 129/Ola murine brain homogenate, used to seed PMCA reactions. B) ME7 clinical endpoint 129/Ola murine brain homogenate, used to seed PMCA reactions.

Table 7.1 Mean overall amplification of PrP^{Res} seeded by 79A

PrP^{C} Genotype	PrP^{Res} Amplification¶		
	Un-purified +/- SEM (# positives†/total number reactions)	Purified +/- SEM (# positives†/total number reactions)	Combined +/- SEM (# positives†/total number reactions)
129/Ola	2.99 +/- 0.32 (31/36 ≈ 10/12*)	2.5 +/- 0.28 (21/33 ≈ 7/11*)	**2.76 +/- 0.21 (≈ 17/23)**
G1	1.64 +/- 0.14 (2/12)	1.48 +/- 0.13 (2/9)	**1.57 +/- 0.10 (4/21)**
G2	2.52 +/- 0.34 (7/12)	2.93 +/- 0.26 (9/12)	**2.72 +/- 0.21 (16/24)**
G3	1.43 +/- 0.16 (12/12)	1.72 +/- 0.14 (8/12)	**1.46 +/- 0.11 (20/24)**
PrP Null	0.87 +/- 0.05 (0/36 ≈ 0/12*)	1.04 +/- 0.9 (0/33 ≈ 0/11*)	**0.95 +/- 0.05 (≈ 0/23)**

Table 7.2 Amplification of PrP^{Res} seeded by ME7

PrP^{C} Genotype	PrP^{Res} Amplification¶		
	Un-purified +/- SEM (# positives†/total number reactions)	Purified +/- SEM (# positives†/total number reactions)	Combined +/- SEM (# positives†/total number reactions)
129/Ola	2.42 +/- 0.31 (2/6 ≈ 1/2*)	2.94 +/- 0.19 (58/78 ≈ 19/26*)	**2.90 +/- 0.18 (20/28)**
G1	1.36 +/- 0.09 (0/2)	1.30 +/- 0.10 (3/27)	**1.31 +/- 0.08 (3/27)**
G2	1.73 +/- 0.00 (2/2)	2.54 +/- 0.27 (17/27)	**2.46 +/- 0.25 (19/29)**
G3	0.77 +/- 0.3 (0/2)	1.41 +/- 0.11 (1/25)	**1.36 +/- 0.11 (1/27)**
PrP Null	1.20 +/- 0.24 (0/6 ≈ 0/2*)	1.01 +/- 0.05 (0/69 ≈ 0/23*)	1.02 +/- **0.04 (0/25)**

¶Amplification was calculated by dividing amount of total amount of PrP^{Res} after PMCA by the total amount of PrP^{Res} in the frozen control, as detected by western blot densitometry (anti-PrP antibody 6D11).

† Positive amplifications were those which exhibited two fold amplification of the predominant glycotype compared to that observed for the PrP null controls within that experiment. Additionally, for G1, G2 and G3 samples amplification level of the predominant glycotype also exceed 1.5 fold of that of non-specific glycotypes; i.e. for G1 and G2 samples the amplification level of the mono-glycosylated band had to exceed that of the di-glycosylated band.

*Each independent control sample (129/Ola and PrP null) was run in triplicate, such that each could be directly compared to the PrP glycosylation deficient experimental

samples, thus the 36 samples of 129/Ola seeded with unpurified 79A equate to 12 independent PMCA reactions.

7.3.3 Controlling amplification of hamster PrP^C by pre-heat treating the 263K infected brain homogenate

Consistent with the observed TSE species barrier, *in vitro* PrP conversion efficiency is far higher if the PrP^{Sc} seed and PrP^C substrate are derived from the same species (Kocisko et al., 1995; Piening et al., 2006; Priola and Lawson, 2001; Raymond et al., 2000; Raymond et al., 1997). Thus hamster PrP^C, contained in the seeding infected brain homogenate, may amplify in preference to the murine PrP^C, increasing non-specific amplification, as was observed in preliminary experiments. To remove hamster PrP^C from the infected brain homogenate the material was incubated with shaking for 10 minutes at 55 °C before each PMCA reaction. This procedure does not remove PrP^C from the reaction but renders it incompetent for amplification (personnel communication, Dr. Joaquin Castilla).

Amplification experiments were carried out with both heat treated and untreated 263K seed. The treatment was observed to reduce background non-specific amplification. However heat treatment did significantly alter the mean amplification level observed within each genotype (Table 7.3). The heat treatment appeared to reduce the amplification level of 263K/hamster PrP^{Res} (Table 7.3). However, the amplification level of 263K seeded G2, G3 and normally glycosylated murine PrP^{Res} was significantly enhanced by heat treatment (REML variance component analysis, Wald test for fixed effects, Wald statistic = 10.17, degrees of freedom = 1, Chi-pr = 0.001). Despite these changes the overall pattern of amplification of murine PrP^{Res} was not altered by the heat-treatment (Table 7.3).

Table 7.3 Total amplification of PrP^{Res} for reactions seeded with 263K

PrP^{C} Genotype	PrP^{Res} Amplification¶	
	Un-heated +/- SEM (# positives†/total number reactions)	Heated (55 °C 10 mins) +/- SEM (# positives/total number reactions)
129/Ola	3.55 +/- 0.26 (14/33 ≈ 5/11*)	5.44 +/- 0.98 (26/42 ≈ 9/14*)
G1	1.75 +/- 0.17 (0/11)	1.39 +/- 0.23 (1/14)
G2	3.18 +/- 0.91 (6/11)	5.40 +/- 1.73 (9/14)
G3	1.36 +/- 0.12 (6/11)	2.56 +/- 0.58 (8/14)
PrP Null	1.47 +/- 0.11 (0/9)	0.89 +/- 0.14 (0/12)
Hamster	9.98 +/- 4.86 (3/3)	4.00 +/- 2.90 (1/3)

¶Amplification was calculated by dividing amount of total amount of PrP^{Res} after PMCA by the total amount of PrP^{Res} in the frozen control, as detected by western blot densitometry (anti-PrP antibody 6H4).

† As greater variability between individual samples within each group was observed for the 263k seeded PMCA reactions and the amplification level within each null control was only assayed once, background levels where set using the highest background observed for the experimental conditions rather than on an within experiment basis.

To determine if amplification of hamster PrP^{Res} occurred in the 263K seeded PMCA reactions, a further control step was used. After detection of PrP^{Sc} using the PrP specific antibody 6H4, western blots were stripped and reprobed with a hamster specific antibody 3F4. Thus the generation of hamster PrP^{Res} could be assessed (Figure 7.4). Variability in the amount of hamster PrP^{Res} was observed and it was reduced but not eliminated by heat pre-treatment. Overall, hamster specific amplification levels were low compared to the total amplification detected; demonstrating the specific amplification of murine PrP^{Res}.

Figure 7.4 Western blots of optimisation of 263K seeded PMCA reactions

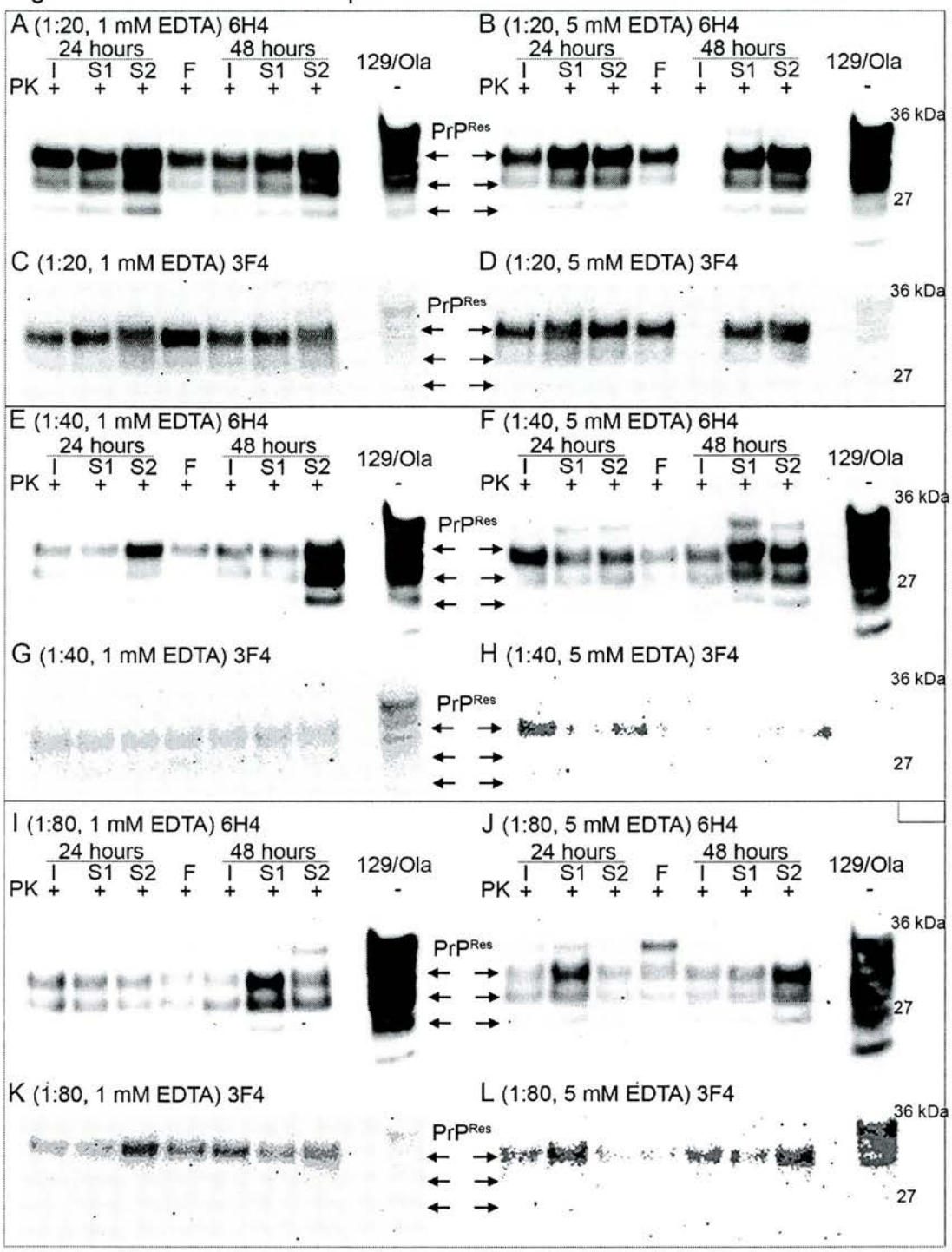

Western blots of PMCA reactions in duplicate (lanes S1, S2), non-sonicated controls incubated at 37 °C (lane I) or frozen (lane F); time on sonicator as indicated. PMCA carried out in the presence of (A, C, E, G, I, K) 1 mM EDTA or (B, D, F, H, J, L) 5 mM EDTA. Ratio of 263K infected brain homogenate to uninfected 129/Ola brain homogenate (A, B, C, D) 1:20, (E, F, G, H) 1:40, (I, J, K, L) 1:80. Samples treated with 50 µg/ml PK at 37 °C for 1 hour shaking at 300 rpm, as indicated. Maximal amplification of PrP^{Res} (F) (5 mM, 1:40, 48 hours). A, B, E, F, I, J) probed with murine and hamster PrP specific antibody 6H4. C, D, G, H, K, L) correspond to membrane above (i.e C = A) which had been stripped and reprobed with hamster specific PrP antibody 3F4 and thus shows minimal amplification of hamster PrP^{Res}.

7.3.4 Use of EDTA in the uninfected brain homogenate

Murine brains were not perfused prior to sacrifice; thus the brain homogenate contained blood in addition to cells of the central nervous system. A constituent of blood is thought to inhibit the PMCA mediated conversion of PrP^{C} to PrP^{Res} (Castilla et al., 2004). The metal chelator EDTA has been shown to reverse this inhibitory effect. To investigate the impact of EDTA concentration on PMCA conversion efficiency, reactions were carried out in presence of either 5 mM or 1 mM EDTA. For 263K seeded reactions, both the amplification efficiency and frequency were higher in the presence of 5 mM EDTA (Figure 7.4). Thus all 263K seeded PMCA reactions were carried out at this EDTA concentration. No effect of EDTA concentration was discernible for reactions seeded by either ME7 or 79A and all reactions were carried out at 5 mM EDTA (Figure 7.5 and 7.6).

7.3.5 Optimisation of the ratio of infected brain homogenate to uninfected brain homogenate

Optimisation of PMCA experimental conditions was carried out using normally glycosylated PrP^{C} from 129/Ola mouse brain homogenate. The optimum ratio of 263K infected brain homogenate to uninfected was experimentally determined to be 1:40 (Figure 7.4). At the lower 1:20 dilution, amplified PrP^{Res} was swamped by the signal from the starting material and at a higher dilution (1:80) a lower proportion of total PMCA reactions exhibited PrP^{Res} amplification. The amplification of PrP^{Res} seeded by 263K, was greater after 48 hours (96 PMCA cycles), compared to the level of amplification observed after 24 hours (48 cycles). The optimum ratio of both ME7 and 79A purified PrP^{Sc} seed to uninfected homogenate was determined to be 1:100 (Figure 7.5 and 7.6). In contrast to the 263K experiments, increasing the number of PMCA cycles performed did not increase the PrP^{Res} amplification level for either of the murine scrapie strains investigated (7.6 and data not shown). Thus ME7 and 79A seeded PMCA reactions were carried out for 24 and 48 cycles respectively.

Figure 7.5 Western blots of optimisation of ME7 seeded PMCA reactions

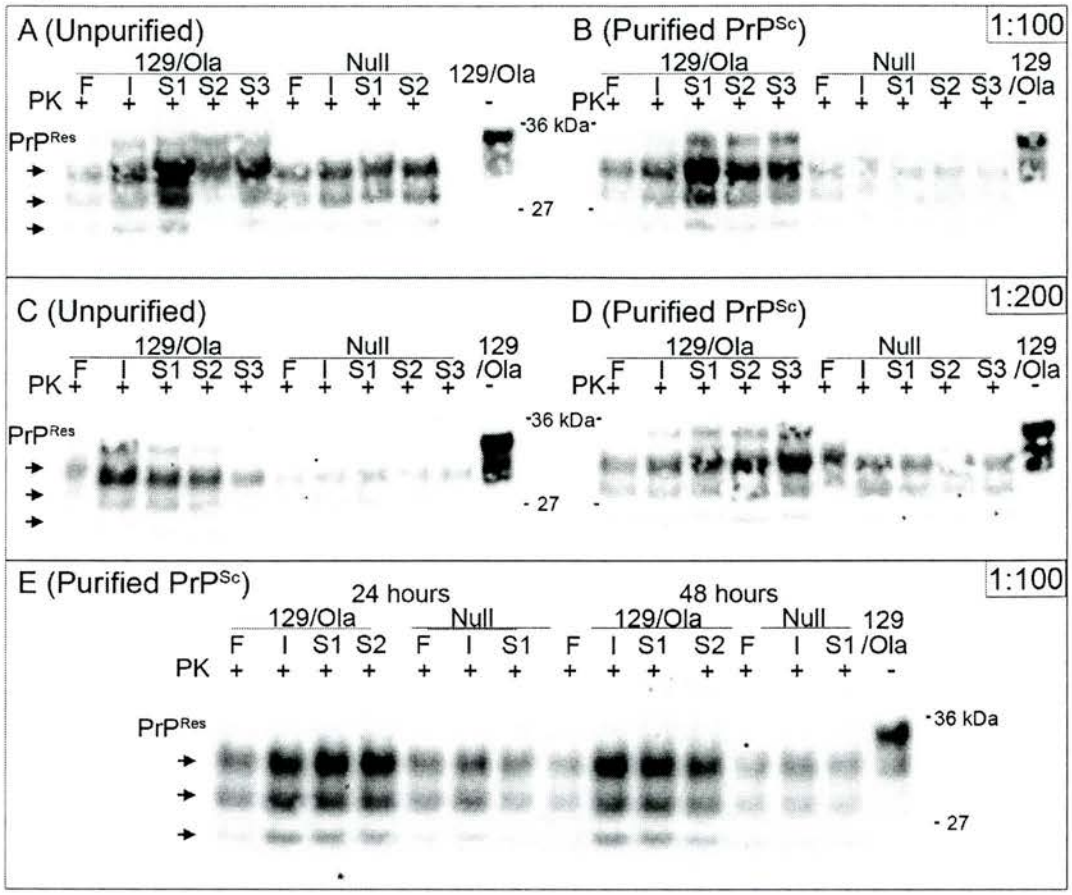

Western blots of PMCA reactions in triplicate (lanes S1, S2, S3), non-sonicated controls incubated at 37 °C (lane I) or frozen (lane F) for duration of experiment; time on sonicator as indicated or if not indicated 12 hours. PMCA substrate PrP^{C} containing normal brain homogenate from 129/Ola mice or PrP null mice as indicated, seeded with unpurified ME7 brain homogenate (A & C) or purified PrP^{Sc}/ME7 (B, D & E). PMCA carried out in the presence of (A, B C, D) 5 mM EDTA or (E) 1 mM EDTA. Ratio of seed to uninfected 129/Ola brain homogenate (A, B, E) 1:100 or (C, D) 1:200. Samples treated with 50 µg/ml PK at 37 °C for 1 hour shaking at 300 rpm, as indicated. Maximal amplification of PrP^{Res} (B) (5 mM, purified, 1:100). PrP^{Res} detected with anti- PrP antibody 6D11.

Figure 7.6 Western blot of optimisation of 79A seeded PMCA reactions

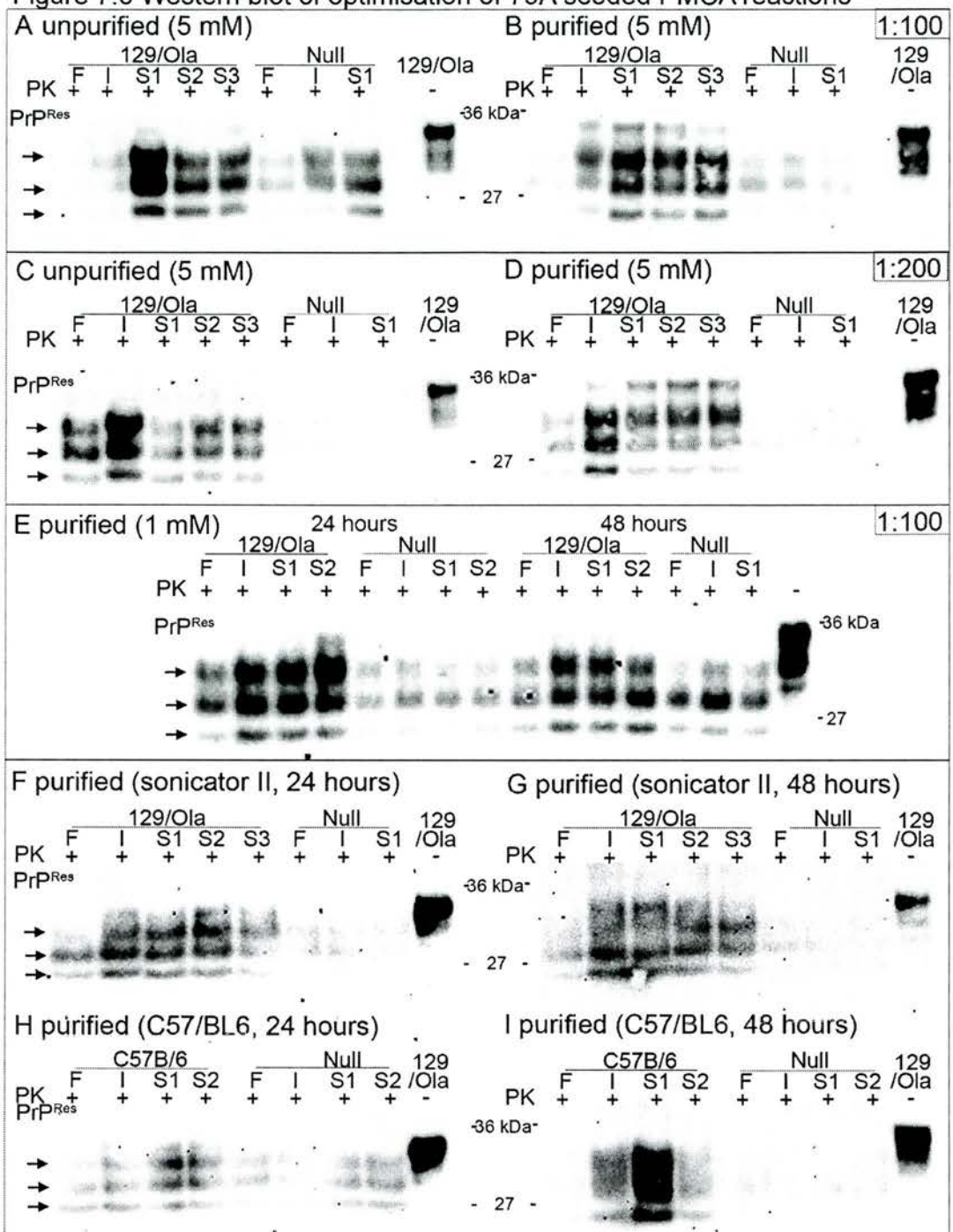

Western blots of 79A seeded PMCA reactions in triplicate (lanes S1, S2, S3), non-sonicated controls incubated at 37 °C (lane I) or frozen (lane F). PrP^{C} containing normal brain homogenate 129/Ola mice (A-G), C57/BL6 (H & I) or brain homogenate of PrP null mice as indicated, seeded with unpurified 79A brain homogenate (C & D) or purified PrP^{Sc}/79A (A, B, E-I). PMCA carried out in the presence of (A-D & F-I) 5 mM EDTA or (E) 1 mM EDTA. Ratio of seed to uninfected 129/Ola brain homogenate A, B, E, F-I) 1:100; C, D) 1:200. Time on sonicator as indicated or A-D, F, H) 24 hours and G & I) 48 hours A-E, H, I) sonicator 1; F & G) sonicator 2. Samples treated with 50 µg/ml PK at 37 °C for 1 hour shaking at 300 rpm, as indicated. Maximal amplification of PrP^{Res} (B) (5 mM, purified 1:100) not (A) (5 mM, unpurified 1:100). PrP^{Res} detected with anti-PrP antibody 6D11.

Both the predominant di-glycosylated PrP^{Res} glycoforms of 263K and ME7 were reproduced in the PMCA reactions. However, despite manipulation of a number of experimental factors, including EDTA concentration, purification of seeding material, number of PMCA cycles and sonicator used, it was not possible to reproduce the predominant mono-glycosylated PrP^{Res} glycoform of 79A (Figure 7.6). To determine if this was attributable to the source of PrP^{C}, 79A seeded PMCA using an alternative PrP^{C} source was undertaken (perfused C57BL/6J uninfected brain homogenate a kind gift of Dr. Joaquin Castilla UTMB, TX). The predominant mono-glycosylated glycoform of 79A was also not reproduced using the C57/B6 PrP^{C} substrate (Figure 7.6 H and I), indicating that the failure to reproduce the characteristic glycoform of 79A was a general result and was not attributable to the quality of the 129/Ola derived brain homogenate or strain of mouse used.

Table 7.4 Optimised PMCA conditions

TSE Strain	Ratio of seed:substrate	Number of PMCA Cycles	EDTA (mM)
79A	1:100	48	5
ME7	1:100	24	5
263K	1:40	96	5

7.4 Validation of experimental technique

7.4.1 Amplification of PrP^{Res} in the absence of seed

Previous cell culture studies have suggested that absence of PrP N-glycans leads to the spontaneous adoption of PrP^{Sc}–like properties; although, no such formation of PrP^{Res} has been observed in the PrP glycosylation deficient transgenic mice *in vivo* (Cancellotti et al., 2005; Lehmann and Harris, 1997) (Chapter 3). To investigate the possible spontaneous formation of PrP^{Res} during PMCA; PMCA reactions were undertaken using the optimised experimental conditions without the inclusion of infected brain homogenate or PrP^{Sc}. A preliminary study demonstrated that no spontaneous formation of PrP^{Res} occurred after 96 PMCA cycles in unseeded

substrate from the glycosylation deficient transgenic [NPU] or normally glycosylated 129/Ola control mice (two independent brains, assayed in duplicate, data not shown). A more detailed study was then undertaken, in which samples were also examined after 24 and 48 cycles. No PrP^{Res} was detected after standard PK digestion and western blot (Figure 7.7, three independent brains in triplicate), demonstrating that absence of PrP N-glycans does not lead to the spontaneous formation of the PK resistant conformation under the experimental conditions used. Thus all PMCA mediated amplification of PrP^{Res} described here is dependent upon seeding by PrP^{Sc}.

7.4.2 Stability of PrP^{C} substrate in the reaction conditions used

The removal of PrP N-glycans may render the protein more liable to degradation (Petersen et al., 1996; Rudd et al., 2001). To investigate the relative stability of PrP^{C} from the glycosylation deficient transgenic and 129/Ola control mice in PMCA, PMCA reactions without the addition of infected brain homogenate were undertaken. The amount of PrP^{C} remaining after 24, 48 and 96 PMCA cycles was assayed by western blot densitometry (Figure 7.8 E, four independent brains assayed in triplicate). The relative fold-change was calculated by division of the amount of PrP^{C} detected after PMCA by the amount detected in a sample frozen for the duration of the experiment (Figure 7.8 A-D). Neither the normally glycosylated controls nor the glycosylation deficient transgenic samples exhibited a decrease in detectable PrP^{C}. Thus the stability of normally glycosylated wild type PrP^{C} and partially glycosylated PrP^{C} from transgenic murine brains were comparable.

However, although no decrease in detectable PrP^{C} was observed in several incidences, average PrP^{C} signal was higher than in the frozen control after PMCA. These changes were significantly different from one but the increases in detectable PrP^{C} were relatively small (REML variance component analysis Wald test for fixed effects, Wald statistic = 10.65, degrees of freedom = 3, Chi pr = 0.014). Additionally, the detected change in PrP^{C} did not correlate positively with the number of PMCA cycles for either G1 or 129/Ola derived substrates, suggesting that the observed differences may represent variability in detection rather than a PMCA dependent

Figure 7.7 Western blot of PrP^{Res} generation in unseeded PMCA reactions

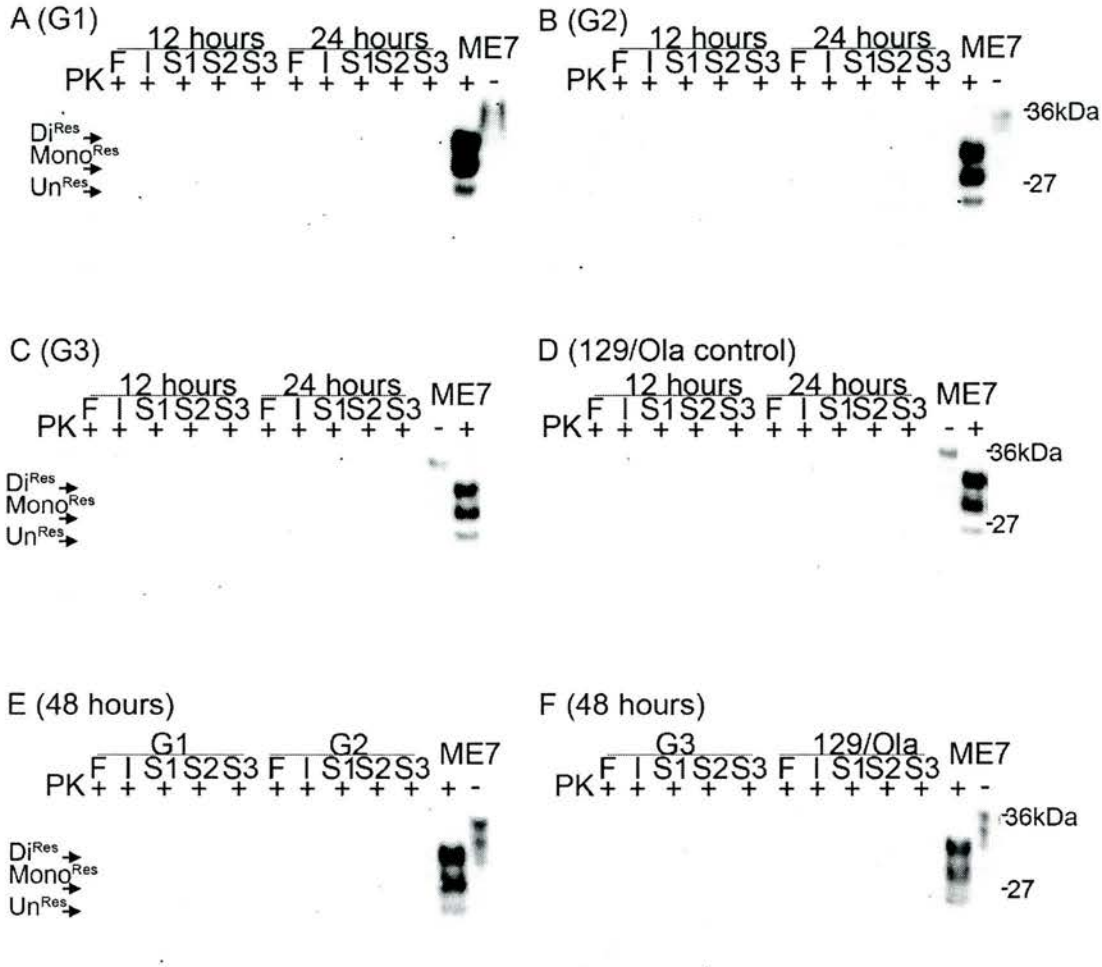

Western blots of unseeded PMCA in triplicate (lanes S1, S2, S3), non-sonicated controls incubated at 37 °C (lanes I) or frozen (lanes F) and ME7 infected brain homogenate, PK resistance controls. A-D) Time on sonicator as indicated or (E & F) 48 hours. PMCA substrate used; normal brain homogenate from the G1 (A), G2 (B), G3 (C) glycosylation deficient transgenic or normally glycosylated 129/Ola mice (D) and as indicated (E & F). All PMCA reactions carried out in 5 mM EDTA. A-F) probed with anti-PrP specific antibody 6H4.

Figure 7.8 PrP^C stability in unseeded PMCA reactions

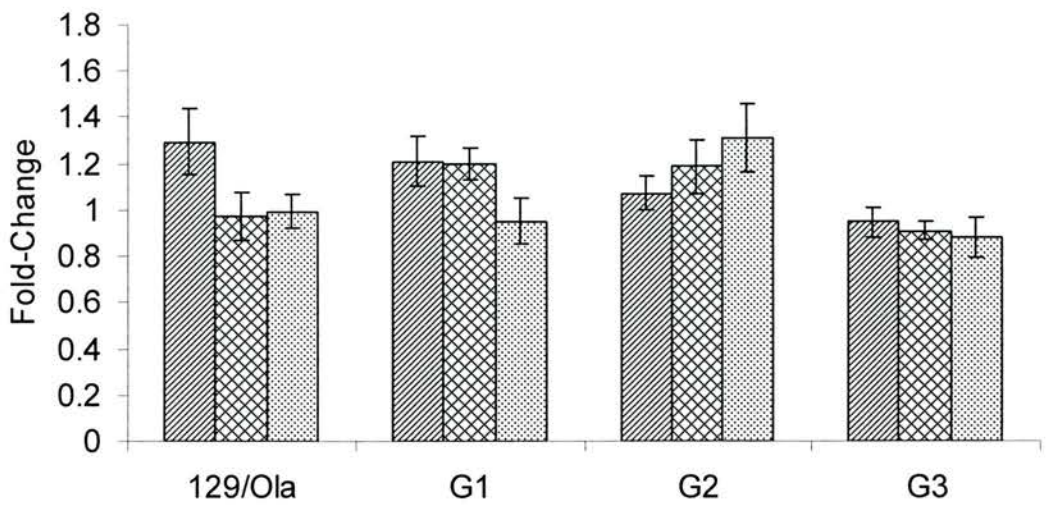

The stability of PrP^C under PMCA conditions in the absence of PrP^{Sc} seed was determined by densitometry on western blots using anti-PrP specific antibody (6H4), on samples that had been subjected to 24 (hatched), 48 (double hatched) and 96 (dotted) PMCA cycles. Error bars indicate standard error of the mean (n = 4 assayed in triplicate), a small but significant difference in PrP^C stability is detected between normally glycosylated control (129/Ola) and G1, G2 and G3 transgenic murine brain homogenate samples (REML variance components analysis, Chi-pr = 0.014). However, the change in amount of PrP^C detected does not correlate with the number of PMCA cycles.

increase in PrP^C signal. Interestingly, little variability in the amount of G3-PrP^C detected after PMCA was observed (Figure 7.8), indicating that PrP's N-glycans may contribute to the observed western blot detection variability.

7.4.4 263K seeded amplification level of hamster PrP

In accordance with the species barrier effect, previous *in vitro* conversion reactions have shown that 263K amplification is more efficient when a hamster rather than murine PrP^C is used as substrate (Kocisko et al., 1995; Piening et al., 2006; Priola and Lawson, 2001). To investigate this in the system used here, 263K seeded PMCA reactions using uninfected hamster brain homogenate as substrate (kind gift of Dr. Paula Prieto Saá) were under taken (Figure 7.9 D, Table 7.3). The mean amplification level of normally glycosylated hamster PrP^{Res} was higher than that observed for normally glycosylated murine PrP when the 263K seed had not been heat treated (REML variance component analysis, Wald statistic = 10.17, degrees of freedom = 1, Chi pr = 0.001). Thus the experimental system used here replicated the *in vivo* hamster-mouse species barrier phenomena. However, heat treatment of the 263K seed appeared to reduce the total level of amplification observed for hamster PrP, in contrast to the effect on cross-species conversion efficiency.

7.4.5 The effect of sonication on amplification of PrP^{Res}

The level of 263K seeded PrP^{Res} amplification was significantly higher in samples subjected to sonication as compared to that in the non-sonicated controls incubated at 37 °C (Table 7.7) (REML variance component analysis, Wald statistic = 9.69, degrees of freedom = 1, Chi pr = 0.002). In contrast, sonication had only a small facilitating effect on amplification in ME7 and 79A seeded reactions (Table 7.5 and 7.6) (ME7, REML variance component analysis, Wald statistic = 3.81, degrees of freedom = 1, Chi pr = 0.048; 79A REML variance component analysis, Wald statistic = 2.24, degrees of freedom = 1, Chi pr = 0.134). This would suggest that further refinements to the experimental conditions are required for these TSE strains and underlines the differences in PrP^{Sc} derived from different TSE strains.

Table 7.5 Mean overall amplification of non-sonicated 37 °C controls seeded with 79A

PrP^C Genotype	Unpurified +/- SEM (n)	Purified +/- SEM (n)
129/Ola Mouse	2.36 +/- 0.16 (12 ≈ 4)	2.07 +/- 0.16 (11 ≈ 4)
G1 Transgenic Mouse	1.72 +/- 0.24 (4)	1.36 +/- 0.18 (3)
G2 Transgenic Mouse	1.96 +/- 0.06 (4)	1.92 +/- 0.33 (4)
G3	1.31 +/- 0.16 (4)	1.18 +/- 0.11 (4)
PrP Null	0.98 +/- 0.09 (12 ≈ 4)	0.68 +/- 0.11 (11 ≈ 4)

Table 7.6 Mean overall amplification of non-sonicated 37 °C controls seeded with ME7

PrP^C Genotype	Unpurified +/- SEM (n)	Purified +/- SEM (n)
129/Ola	2.44 +/- 0.15 (3 ≈ 1)	2.49 +/- 0.17 (26 ≈ 9)
G1	1.71 (1)	1.33 +/- 0.06 (9)
G2	1.53 (1)	2.02 +/- 0.31 (9)
G3	1.01 (1)	1.31 +/- 0.10 (8)
PrP Null	1.31 +/- 0.27 (3 ≈ 1)	1.09 +/- 0.06 (26 ≈ 9)

Table 7.7 Mean overall amplification of non-sonicated 37 °C controls seeded with 263k

PrP^C Genotype	Unheated +/- SEM (n)	Heated+/- SEM (n)
129/Ola	1.74 +/- 0.23 (9 ≈ 3)	2.48 +/- 0.53 (12 ≈ 4)
G1	1.20 +/- 0.09 (3)	2.00 +/- 0.61 (4)
G2	1.97 +/- 0.60 (3)	1.58 +/- 0.20 (4)
G3	1.75 +/- 0.23 (3)	1.52 +/- 0.43 (4)
PrP Null	1.40 +/- 0.14 (9 ≈ 3)	1.03 +/- 0.11 (12 ≈ 4)

7.5.1 Experimental Results

7.5.1 The ability of mono-glycosylated PrP^{C} to convert PrP^{Res}

TSE transmission to the PrP glycosylation deficient transgenic mice [NPU] has demonstrated that the site of PrP N-glycan attachment has a great influence on the role of glycosylation of PrP in TSE disease (Chapter 5; Tuzi et al., in preparation, appendix ii). To investigate the importance of site of N-glycan attachment on the ability of mono-glycosylated PrP to convert to the disease associated form, PMCA using PrP^{C} derived from the G2 and G1 transgenic murine brain as the conversion substrate were undertaken. Strong and specific amplification of PrP^{Res} mono-glycosylated at the first N-glycan attachment site (G2) was observed for all TSE strains investigated (Figure 7.9-7.12) (79A REML variance component analysis, difference between G2 and negative control mean = 0.2097, standard error = 0.0445, significant at p = 0.05; ME7 REML variance component analysis, difference between G2 and negative control mean = 0.2321, standard error = 0.0590, significant at p = 0.05; 263K REML variance component analysis, difference between G2 and negative control mean = 0.4036, standard error = 0.0441, significant at p = 0.05) . However, the conversion frequency and the overall amplification level differed between strains. Additionally, for each seeding strain the size of un-glycosylated PrP^{Res} generated did not differ between the G2 and the 129/Ola substrates. Thus the conformation of PrP^{Res}, as assayed by the extent of the protein resistant to PK, did not appear to be altered by the absence of second site glycosylation.

The majority of the within-species conversion reactions, seeded by ME7 or 79A, produced positive PrP^{Res} amplification of PrP mono-glycosylated at the first site (79A 16/24, ME7 22/29). The mean overall amplification of PrP^{Res} (irrespective of glycoform) seeded by ME7 was slightly lower in the G2 derived substrate than in 129/Ola control, in which PrP was normally glycosylated (129/Ola = 2.90 +/-0.18 fold; G2 = 2.46+/-0.25 fold), however this was not significantly different (REML variance component analysis, difference between G2 and positive control mean = 0.1097, standard error = 0.0586, not significant at p = 0.05).

Figure 7.9 Western blots of 263K seeded PMCA reactions

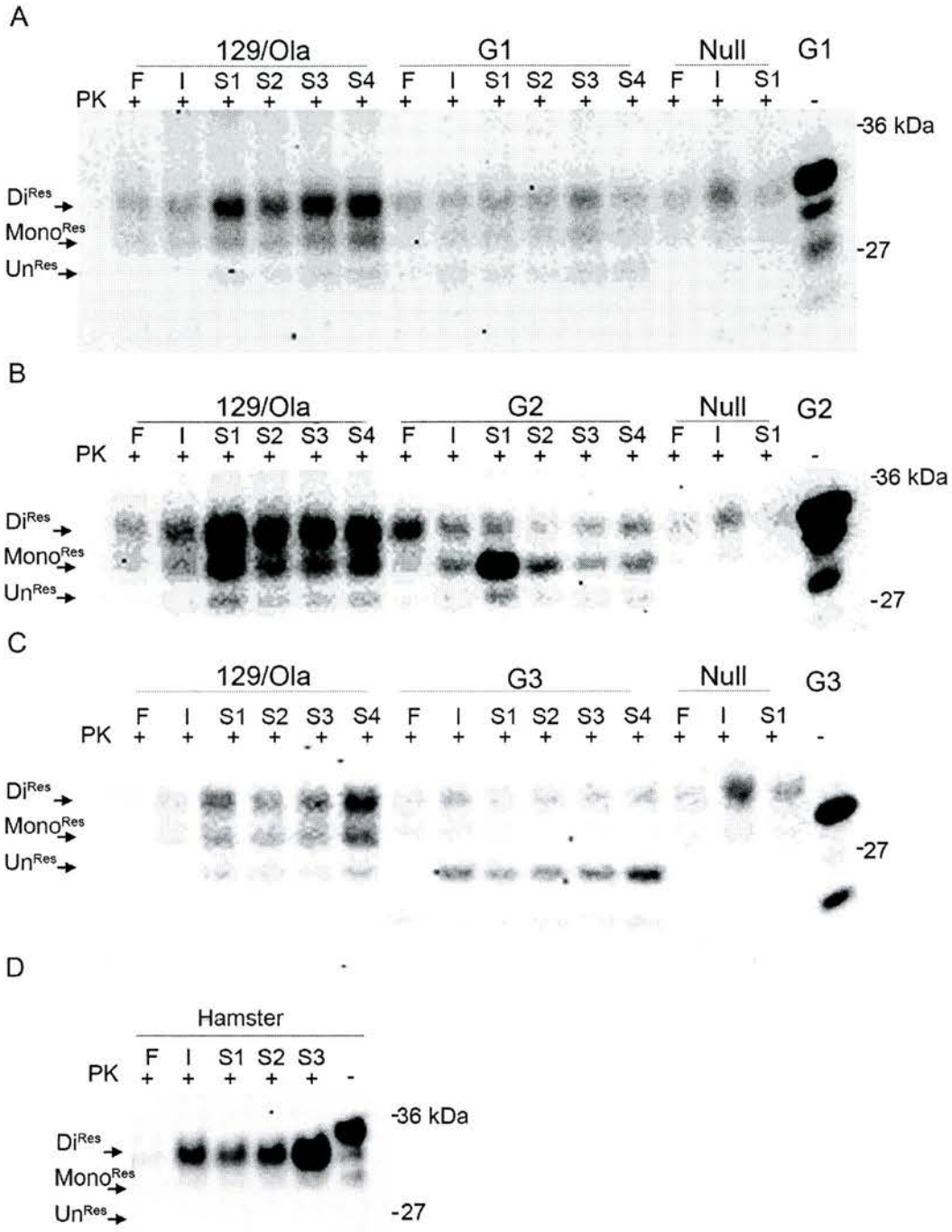

Western blots of example 263K seeded PMCA reactions in quadruplet (lanes S1, S2, S3, S4), non-sonicated controls incubated at 37 °C (lanes I) or frozen (lanes F) for duration of experiment. Ratio of 263K clinical endpoint infected brain homogenate to uninfected brain homogenate (1:40). Normal brain homogenate derived from a PrP null mouse, the PrP glycosylation transgenic mice, a normally glycosylated 129/Ola mouse and pooled hamster brain (kind gift of Paula Prieto Saa) as indicated. PMCA reaction carried out in the presence of 5 mM EDTA, for 96 cycles over 48 hours. PMCA reactions treated with PK (50 µg/ml 37 °C, 1 hour). PrP^{Res} detected by western blot using anti-PrP antibody 6H4.

Figure 7.10 Western blots of 79A seeded PMCA reactions

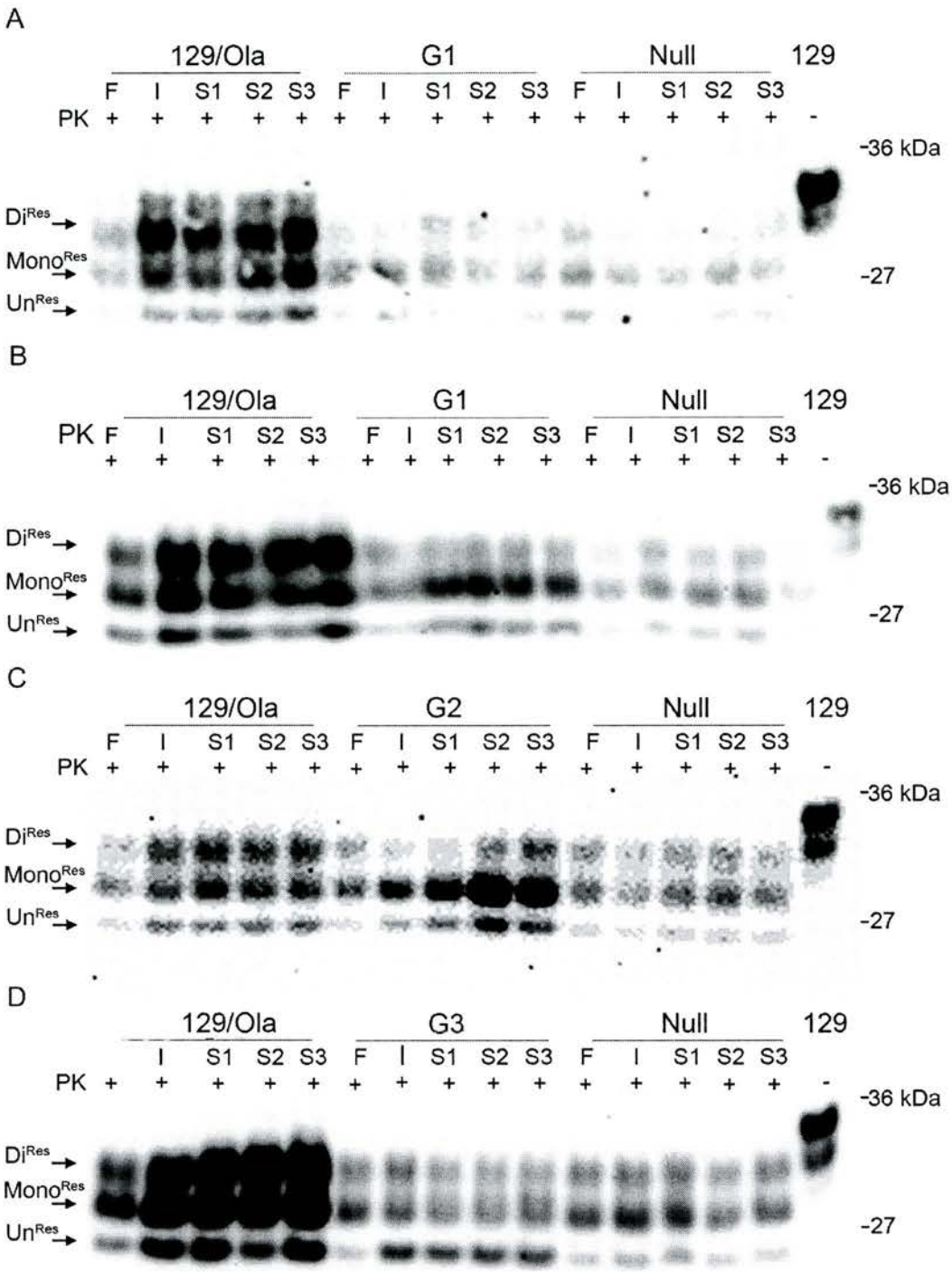

Western blots of example 79A seeded PMCA reactions in triplicate (lanes S1, S2, S3), non-sonicated controls incubated at 37 °C (lanes I) or frozen (lanes F) for duration of experiment. Ratio of purified 79A/PrP^{Sc} to uninfected brain homogenate (1:100). Normal brain homogenate derived from a PrP null mouse, the PrP glycosylation transgenic mice and a normally glycosylated 129/Ola mouse as indicated. PMCA reaction carried out in the presence of 5 mM EDTA, for 48 cycles over 24 hours. Reactions treated with PK (50 µg/ml 37 °C, 1 hour). PrP^{Res} detected by western blot using anti-PrP antibody 6D11.

Figure 7.11 Western blot of ME7 seeded PMCA reactions

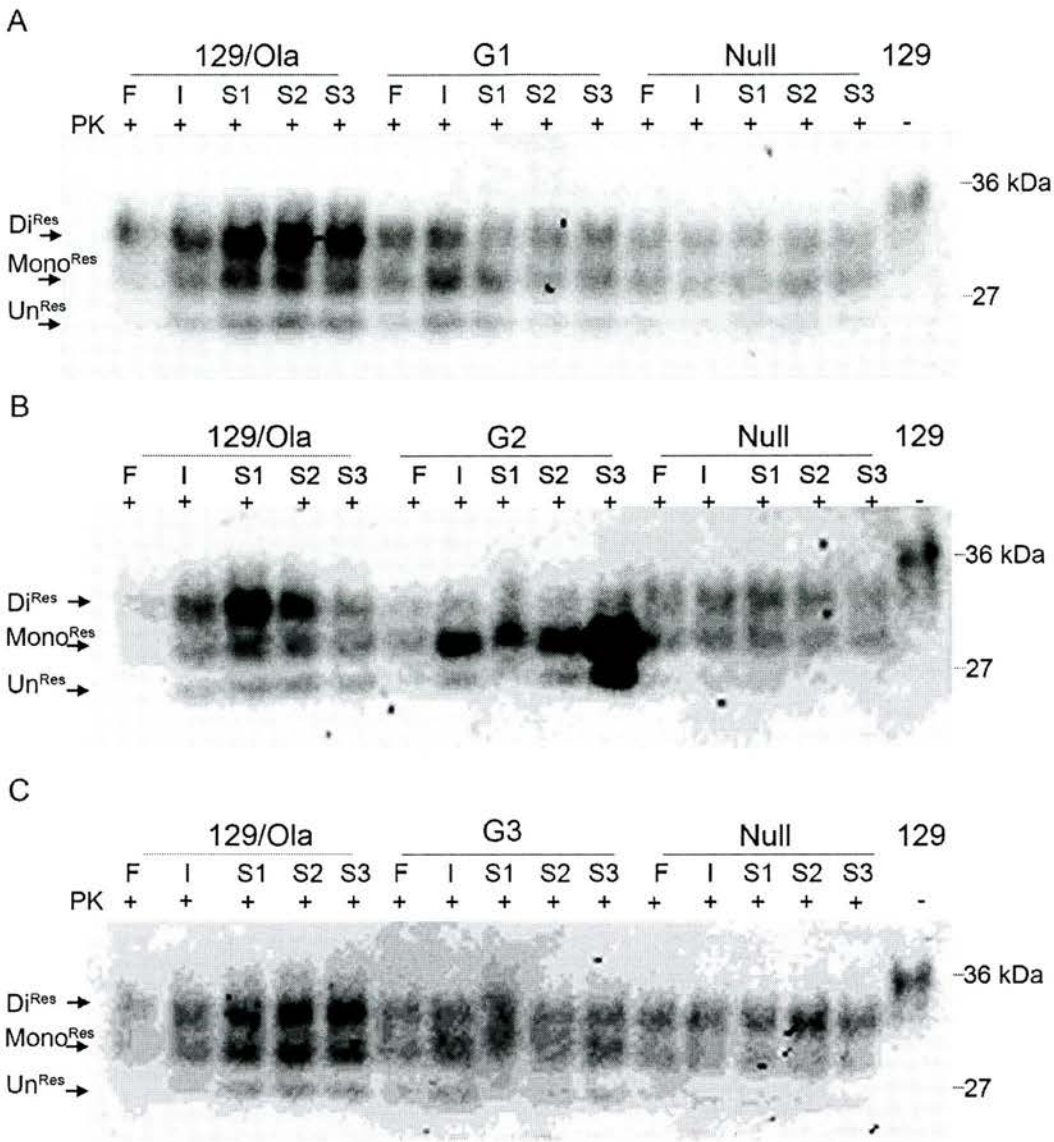

Western blots of example ME7 seeded PMCA reactions in triplicate (lanes S1, S2, S3), non-sonicated controls incubated at 37 °C (lanes I) or frozen (lanes F) for duration of experiment. Ratio of purified ME7/PrP^{Sc} to uninfected brain homogenate (1:100). Normal brain homogenate derived from a PrP null mouse, the PrP glycosylation transgenic mice and a normally glycosylated 129/Ola mouse as indicated. PMCA reaction carried out in the presence of 5 mM EDTA, for 24 cycles over 12 hours. Reactions treated with PK (50 µg/ml 37 °C, 1 hour) and PrP detected using anti-PrP antibody 6D11.

Figure 7.12 Amplification of 263K, 79A and ME7 seeded PMCA reactions by PrP^{Res} glycotype

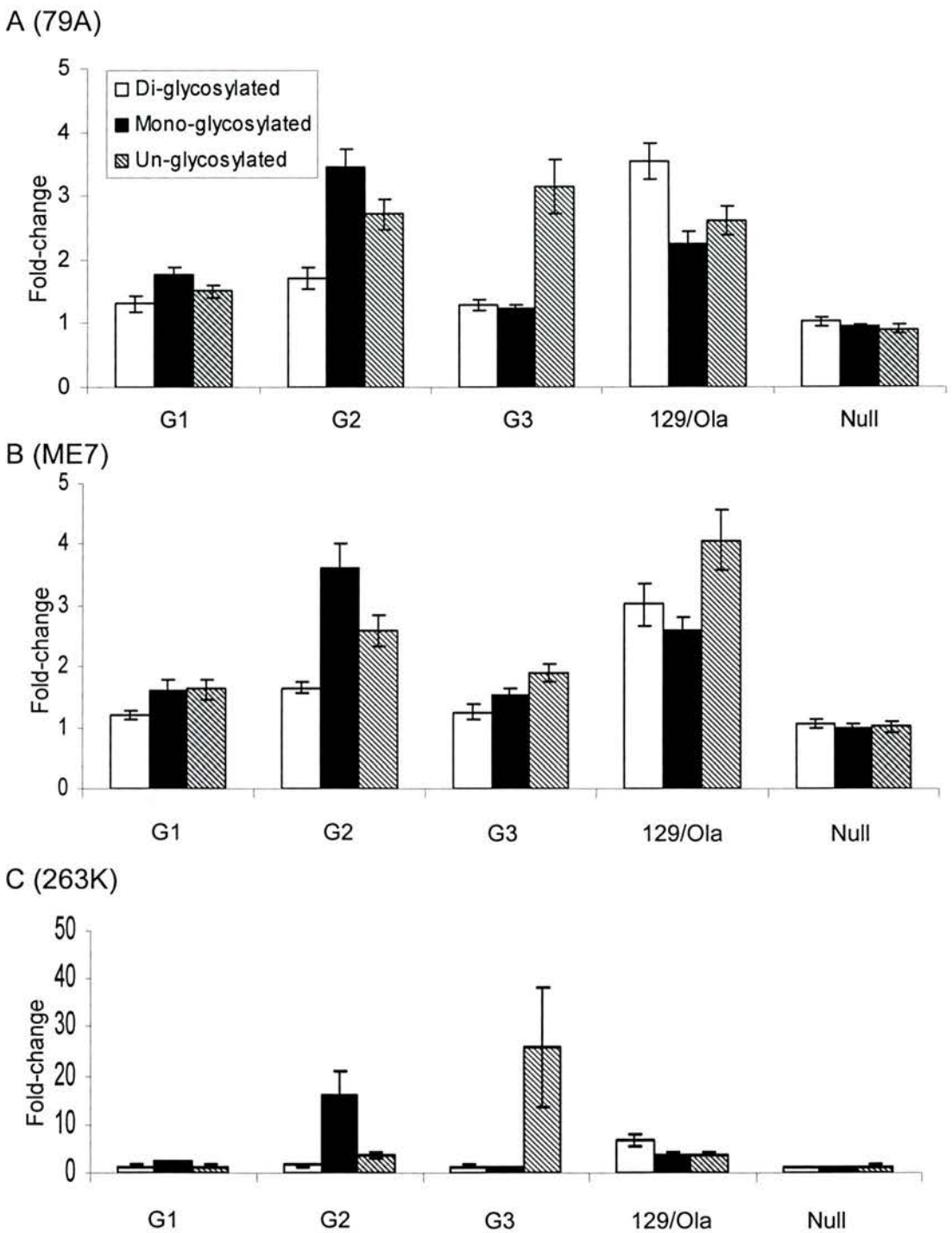

Total amplification of PrP^{Res} by glycotype after PMCA; as determined by western blot densitometry, using the PrP specific antibodies (6H4 or 6D11). All reactions carried in the presence of 5 mM EDTA. (A) 1:100 79A to PrP^{C} brain homogenate, 48 PMCA cycles, (5 independent samples assayed in triplicate), (B) 1:100 ME7 to PrP^{C} brain homogenate, 24 PMCA cycles, (5 independent samples assayed in triplicate), (C) 1:40 263K to brain homogenate, 96 PMCA cycles, (7 independent samples assayed in triplicate/ quadruplet). Error bars standard error of the mean.

Similarly, the total amplification levels of PrP^{Res} seeded by 79A PrP^{Sc} did not significantly differ between the G2 and 129/Ola substrates (129/Ola = 2.76 +/-0.21 fold, G2 = 2.72 +/-fold) (REML variance component analysis, difference between G2 and positive control mean = 0.0341, standard error = 0.0445, not significant at p = 0.05).

G2 derived PrP^{C} also converted to PrP^{Res} when seeded by PrP^{Sc} from a different species (hamster 263K). Both the overall total amplification of PrP^{Res} (irrespective of glycoform) and the frequency of positive amplification reactions were not significantly different between the G2 and the normally glycosylated 129/Ola substrate (Table 7.3) (REML variance component analysis, difference between G2 and positive control mean = 0.0348, standard error = 0.0441, not significant at p = 0.05). Although the mean amplification level of the predominate mono-glycosylated PrP^{Res} seeded by 263K is much greater than that observed for the mono-glycosylated form in the normally glycosylated control (Figure 7.12). This apparent discrepancy is caused by the majority of seeding 263K PrP^{Sc} being di-glycosylated, so that the fold-change in the mono-glycosylated form is magnified compared to the overall amplification level.

In contrast, PrP derived from G1 glycosylation deficient transgenic mice, in which N-glycans can only be attached at the second site, did not convert to PrP^{Res} when seeded by ME7 and 263K (Table 7.2, 7.3 Figure 7.10-7.12). Two of G1/ME7 PMCA reactions which scored as positives are attributable to the failure of the control sample to correctly separate during electrophoresis, perhaps because of a sub-optimum PK digestion (appendix xi). This lead to an unrepresentative low densitometry reading for the frozen mono-glycosylated glycotype, that resulted in an apparently higher than background amplification level for the corresponding PMCA reactions. Thus although these samples scored positive by the densitometric criteria, they do not represent specific amplification of mono-glycosylated PrP^{Res}.

Furthermore, only weak amplification of G1 PrP^{Res} was occasionally observed in reactions seeded by 79A (Table 7.1 Figure 7.10). However, owing to the infrequency

of these conversion events and low amplification levels observed, the mean amplification level of PrP^{Res} mono-glycosylated at the second site was only slightly and not significantly above background levels (Table 7.1 Figure 7.10 B) (REML variance component analysis, difference between G1 and negative control mean = 0.0681, standard error = 0.0490, not significant at p = 0.05). Thus demonstrating that murine PrP mono-glycosylated at the second N-glycan attachment site has greatly reduced convertibility to PrP^{Res}. However, at least one TSE strain may induce this glycotype to adopt the misfolded conformation, albeit with a very low frequency and amplification level. The differences in convertibility of PrP from the G1 and G2 PrP glycosylation deficient transgenic mice demonstrate that the site of N-glycan attachment to PrP greatly affects the role of glycans during PrP^{C} to PrP^{Res} conversion.

7.5.2 The ability of un-glycosylated PrP to convert to PrP^{Res} in the absence of other glycotypes

In the presence of other converting glycotypes (e.g. when using normally glycosylated 129/Ola PrP^{C}), un-glycosylated PrP was observed to form PrP^{Res} with all TSE strains investigated. This is consistent with the formation of un-glycosylated PrP^{Sc} during TSE disease *in vivo* (Collinge et al., 1996; Parchi et al., 1996; Rudd et al., 1999; Somerville et al., 1997; Stahl et al., 1993; Stimson et al., 1999). To investigate the ability of un-glycosylated PrP^{C} to convert to PrP^{Res} in the absence of other PrP^{C} glycotypes, PMCA reactions using G3 derived PrP^{C}, in which all PrP was un-glycosylated, were undertaken. Un-glycosylated PrP formed PrP^{Res} when seeded with either murine passaged scrapie 79A or hamster passaged scrapie 263K but not when seeded by ME7 (Figure 7.9-7.12 and Table 7.1-3). This demonstrates that the PMCA mediated conversion of un-glycosylated PrP is dependent upon TSE strain.

Although the frequency of un-glycosylated PrP to PrP^{Res} conversions seeded with 79A or 263K were comparable to those observed with normally glycosylated PrP, the overall amplification levels (irrespective of the glycotypes) were significantly lower than the wild type control (Table 7.3) (263K REML variance component analysis,

difference between G3 and negative control mean = 0.1978, standard error = 0.0441, significant at p = 0.05; 79A REML variance component analysis, difference between G3 and negative control mean = 0.2125, standard error = 0.0490, significant at p = 0.05). However, total amplification of G3-PrP in 263K seeded reactions was significantly higher than that observed in the negative control (REML variance component analysis, difference between G3 and positive control mean = 0.2406, standard error = 0.0428, significant at p = 0.05). Moreover, G3-PrP amplification in 79A seeded reactions was not significantly higher than background (Table 7.1) (REML variance component analysis, difference between G3 and negative control mean = 0.0313, standard error = 0.0490, not significant at p = 0.05). Therefore although un-glycosylated PrP is as likely to initiate conversion to PrP^{Res} as normally glycosylated PrP (similar conversion frequency) when seeded by 79A or 263K, it is unable to sustain significant amplification of PrP^{Res} in the absence of other glycotypes. Furthermore the size of un-glycosylated PrP^{Res} did not differ between the 129/Ola and G3 reactions, indicating that complete absence of PrP's N-glycans did not alter the PrP^{Res} conformation adopted.

7.5.3 Species barrier specificity of the influence of PrP glycosylation on conversion to PrP^{Res}

Previous work had suggested that PrP's N-glycans specifically play a role in cross-species conversions but not for conversion seeded with PrP^{Sc} from the same species (Priola and Lawson, 2001). In contrast, these data demonstrate that the PrP^{C} glycosylation state is important both to cross-species and within species conversions. Furthermore, the TSE strain rather than the species of the PrP^{Sc} donating TSE host is the major influence in determining the relative importance of PrP^{C}'s glycosylation state to conversion.

7.5.4 Results summary

These data demonstrate that PrP^{C}'s N-glycans do influence the convertibility of the protein to the disease associated form.

- That the site of N-glycan attachment influences the importance of glycosylation of PrP^{C} to its conversion to PrP^{Res}, as demonstrated by the differential convertibility of G1 and G2 PrP.

- That the total absence of PrP^{C}'s N-glycans either inhibits or reduces convertibility to PrP^{Res}, in a TSE strain specific manner.

- That the absence of PrP^{C}'s N-glycans did not alter the conformation of PrP^{Res} generated, as assayed by the size of the un-glycosylated band after PK digest.

- That the importance of PrP^{C}'s N-glycans to conversion events does not display a species barrier specific affect in contrast to previously published work (Priola and Lawson, 2001), but does display a TSE strain specific affect.

7.6 Discussion

7.6.1 Technical discussion

The use of purified PrP^{Sc} as the seeding material did not reduce the background increase in the PrP^{Res} signal (Table 7.1 and 7.2). This suggests that no detectable amplification of PrP^{C} from the infected brain homogenate occurred for the PMCA conditions used. The purified and un-purified infected brain homogenates were manually sonicated (10, 1 second pulses power output 20 %) prior to mixing with the uninfected substrate. This step was not used during the preliminary tests. Thus the variability in background levels observed in the preliminary experiments may be attributable to insufficient dispersal of the infected brain homogenate in the master mix.

The heat treatment of the 263K infected hamster brain homogenate, used to render the hamster PrP^{C} incompetent for PMCA conversion, was observed to inhibit the conversion of hamster PrP^{C} to the PK resistant form, in accordance with the observations of others (Dr. Joaquin Castilla, personal communication). However the opposite was true for murine derived PrP^{C} substrate, as the heat treatment of 263K facilitated these cross-species conversion reactions. This suggests that the heat-treated PrP^{C} or other cellular components may inhibit the conversion of homologous hamster PrP but not heterologous murine PrP. Alternatively the heat-treatment may have specifically modified the conversion ability of $263K/PrP^{Sc}$. The 55 °C treatment of normally folded mammalian proteins such as PrP^{C} is likely to lead to the destabilisation of secondary structure and aggregation. Whereas, this mild heat treatment has been shown to have little effect on TSE infectivity (Somerville et al., 2002) and thus, by inference, also may have little effect on the ability of PrP^{Sc} to seeded conformational conversion. Thus it appears more probable that the observed species-specific inhibitory effect is mediated by PrP^{C} or another cellular component rather than a modification of PrP^{Sc}.

The average amplification level for ME7 and 79A seeded reactions was lower than that observed for cross-species reactions seeded by 263K. This contrasts with the higher transmissibility of the murine strains to mice and results from conventional PrP conversion assay (Kimberlin and Walker, 1978a; Kocisko et al., 1995). Additionally, for the murine seeded PMCA reactions, mean PMCA amplification levels were not significantly higher than control reactions incubated at 37 °C. Also, no increase in amplification level was observed after a greater number of PMCA cycles or by addition of EDTA for the murine seeded experiments, in contrast to those seeded by 263K. This evidence would suggest that although amplification was achieved during the experiments, further optimisation is required for these strains. This however does not invalidate any conclusions drawn from these data as although not maximised, significant amplification of PrP^{Res} did occur for both the murine TSE strains. This result highlights the differing nature of TSE strains.

Despite the manipulation of a number of experimental parameters it was not possible to reproduce the predominantly mono-glycosylated 79A PrP^{Res} glycoform by PMCA using normally glycosylated PrP^{C}. This was consistent with the experimental data presented here, which showed that mono-glycosylated PrP does not amplify more readily than the normally glycosylated protein, when seeded with 79A PrP. Previous studies have reported reproduction of the seeding PrP^{Sc} glycoforms during *in vitro* generation of PrP^{Res} (Soto et al., 2005; Vorberg and Priola, 2002). However, the glycosylation status of PrP^{C} was also shown to influence PrP^{Res} glycoform in one study (Vorberg and Priola, 2002). Thus, TSE strain specific *in vivo* factors other than innate convertibility of PrP glycotypes govern the generation of the characteristic PrP^{Res} glycoform of 79A. These may include the abundance of PrP glycotypes or glycotype specific conversion factors at the site of conversion. This result does not negate the maintenance of 79A strain characteristics during PMCA amplification, as maintenance of TSE strain may be independent of PrP^{Sc} glycoform.

Although the predominately di-glycosylated glycoforms of ME7 and 263K were reproduced by PMCA, the failure to reproduce the glycoform of 79A suggests that this is a generic effect, rather than a true maintenance of strain specific glycoform.

The apparent preferential formation of di-glycosylated PrP^{Res} during PMCA could either be because it is innately more convertible or because there is a vast excess in the normally glycosylated *in vivo* derived substrate (Chapter 3). Thus it may dominate the conversion reaction by virtue of its abundance, in normally glycosylated controls. Convertibility of normally glycosylated PrP^{C} was comparable to that of PrP mono-glycosylated at the first attachment site. However, the convertibility of normally glycosylated PrP^{C} was enhanced compared to un-glycosylated PrP^{C} or PrP^{C} mono-glycosylated at the second attachment site. Thus a higher innate convertibility of the di-glycosylated form could contribute to its preferential production *in vitro*. However, as the stoichiometry of the two possible forms of mono-glycosylated PrP^{C} *in vivo* is unknown, it is not possible to determine whether the convertibility of mono-glycosylated PrP in normally glycosylated hosts differs from that of the di-glycosylated form.

7.6.1 Discussion of experimental results

Our data shows that PrP mono-glycosylated at the second site (G1) is relatively unable to form PrP^{Res} *in vitro*; suggesting that this glycotype may not play a role in TSE disease. However, further experimentation is required to determine if G1 PrP can form PrP^{Res} in the presence of other glycotypes of PrP that can convert. Conversion of G1 PrP may be facilitated by the misfolding of more convertible PrP glycotypes under normal glycosylation conditions. Equally G1 PrP may be more readily converted by PrP^{Sc} from other TSE strains. Alternatively G1 PrP may inhibit the conversion of other conversion competent glycotypes of PrP. Previous studies that have investigated the importance of the glycosylation of PrP to conversion, have not addressed the importance of site of N-glycan attachment to the protein's *in vitro* misfolding (Kocisko et al., 1994; Kocisko et al., 1995; Lawson et al., 2001; Priola and Lawson, 2001; Raymond et al., 1997). Although, *in vivo* transmission studies using PrP glycosylation deficient mice have highlighted the importance of site of attachment to TSE disease (Chapter 4; Neuendorf et al., 2005; Tuzi et al., in preparation). Additionally, no study has thoroughly addressed the importance of the

site of N-glycan attachment to the generation of mono-glycosylated PrP^{Sc} in hosts in which PrP is normally glycosylated.

Several studies have observed variable attachment of N-glycans to PrP^{Sc} at both sites (Rudd et al., 1999; Stahl et al., 1993; Stimson et al., 1999), although in these studies the majority of PrP^{Sc} was shown to be di-glycosylated (Rudd et al., 1999; Stahl et al., 1993; Stimson et al., 1999). The latter result is attributable to the strains of TSE used, ME7 and 263K/Sc237, in which PrP^{Sc} is predominately di-glycosylated (Somerville et al., 1997). Higher site occupancy of the first N-glycan site compared to the second has been observed using mass-spectrometry (with N-glycan attachment detected at greater than 90% of asparagines at the first site, compared to at 80% at the second) (Stahl et al., 1993), consistent with the finding that N-glycan attachment to PrP is determined by the distance from the C-terminus (Walmsley and Hooper, 2003). Others have not observed preferential glycosylation of PrP at the first site; although no experimental data was shown in this case (Rudd et al., 1999). Two prominent mono-glycosylated PrP^{Sc} bands are observed in a number of TSE strains, these may correspond to the first and second site mono-glycosylated forms (Somerville, 1999). However, this has not been experimentally demonstrated and these prominent forms may correspond to different combinations of glycans attached at one site.

However, work on PrP^{Sc}/ME7 has clearly demonstrated that the combination of glycans attached at each site reproducibly differ (Stimson et al., 1999). This translates into clear differences in molecular weight; consistent with our observations of size differences in the G1 and G2 mono-glycosylated form and previous works (Moudjou et al., 2004; Stimson et al., 1999). This is consistent with evidence from 263K infected normally glycosylated hamsters and a conventional transgenic murine model, which also suggest that site specific glycosylation of PrP^{Sc} occurs (DeArmond et al., 1997; Endo et al., 1989). These works are in agreement with the two PrP^{Sc} predominant mono-glycosylated forms observed *in vivo* corresponding to site specific glycotypes. Despite this, there is no clear evidence of the existence of second site mono-glycosylated PrP^{Sc} *in vivo* generated during acquired TSE disease.

The data presented here would suggest that this form of PrP^{Sc} is not readily generated and thus has little or no role in TSE disease, although there is evidence for the existence of mono-glycosylated forms of PrP^{C} attached at both glycosylation sites, in normally glycosylated sheep and mice (Moudjou et al., 2004).

Why PrP mono-glycosylated at the second site is relatively unable to convert to PrP^{Res}, when both di-glycosylated and un-glycosylated PrP can convert, presents a conundrum. These data suggest that this failure to convert is neither attributable to glycosylation at the second site per se, nor owing to absence of N-glycans at the first. The nature of the N-glycans attached at the second site may vary between G1 and 129/Ola PrP such that those attached to G1 PrP may specifically inhibit conversion. Alternatively the interaction of N-glycans attached at the first and second site may alter the behaviour of each. Indeed Moudjou and colleagues have suggested that repulsion between the N-glycans may lead to the unmasking of a region of the PrP surface, which would otherwise be covered if only one of the sites was glycosylated (Moudjou et al., 2004). These potential differences may directly affect both the conformational flexibility of PrP^{C}, its ability to bind PrP^{Sc} or may indirectly effect its interaction with a secondary molecule. Further experimentation is required to determine which of these effects underlies the observed poor convertibility of G1 PrP.

Alternatively, un-glycosylated and glycosylated PrP may convert to PrP^{Res} via different mechanisms. As the complete absence of N-glycans on G3 derived PrP^{C} may alter the protein's folding *in vivo*, as this form of PrP will no longer interact with glycosylation specific folding pathway/chaperones. Differential interaction of PrP with chaperones has been previously demonstrated to be dependent on presence or absence of the di-sulphide bound (Capellari et al., 1999). The G3 PrP folding pathway may also be different from that of the normally glycosylated form, as has been shown for other proteins (Oliver et al., 1997; Swanton et al., 2003). If this is the case the successful conversion of glycosylated forms of PrP may require glycosylation of the first site. Further experimentation is required to ascertain whether the conformation of PrP^{C} glycotypes differs and what impact this may have

on the conversion to PrP^{Sc}. Additionally, experiments are required to investigate whether successful conversion of G1 PrP can be mediated by PrP^{Sc} from another TSE source.

Equally, the conformation or aggregation status of PMCA generated PrP^{Res} may differ between the glycotypes. TSE strain is often biochemically determined by the size of the un-glycosylated band after PK digest. According to this parameter, absence of PrP N-glycans did not alter TSE strain during PMCA (Collinge et al., 1996; Parchi et al., 1996). This result could have been further confirmed by either PNGase digestion or Endman protein sequencing of PrP^{Res}. Additionally, a further investigated either by a conformational study of PrP^{Res} or strain typing bioassay. Previous work has suggested that removal of the second glycosylation site is linked to changes in the strain characteristics of 79A (Tuzi et al., in preparation). The maintenance of size of G2 PMCA generated un-glycosylated PrP^{Res} presented here is compatible with this finding, as *in vivo* the PK resistant band size was also unchanged despite the alteration of other strain characteristics.

The complete absence of PrP^{C}'s N-glycans led to a significant reduction in the level of PrP^{Res} generated for both within and cross-species conversion reactions. Additionally, for one TSE strain, ME7, PrP^{Res} formation was completely inhibited when the PrP substrate was not glycosylated. Previous *in vitro* studies using the standard method have either suggested that the absence of PrP^{C} N-glycans increased or had no effect on conversion efficiency (Kocisko et al., 1995; Priola and Lawson, 2001; Raymond et al., 1997). These differences may be attributable to either the *in vivo* glycosylation of the PrP^{C} substrate used in the experiments outlined here; the influence of other cellular factors on conversion; or the different TSE strains used in these experiments to seed the reactions.

Transfection of scrapie infected cell lines with a construct expressing composite hamster-murine un-glycosylated PrP ($MHM2_{Ala182/Ala198}$) have also demonstrated lower levels of un-glycosylated PrP^{Res} formation than that observed with normally glycosylated controls. Interestingly this study also showed that although the level of

un-glycosylated PrP^{Res} formed was lower, misfolding occurred quicker (Taraboulos et al., 1990a). Similarly more rapid formation of un-glycosylated PrP was detected in a cell culture infection experiment, although no data on amount of PrP^{Res} generated was presented in this paper (Korth et al., 2000). Further studies are required to investigate if the rate of PrP^{Res} formation is altered in the system described here. The data presented here demonstrate that the conversion of un-glycosylated PrP is influenced by the presence of other conversion competent glycotypes. In previous cell culture experiments un-glycosylated PrP was over-expressed in the presence of the normally glycosylated PrP (Korth et al., 2000; Taraboulos et al., 1990a), which may have facilitated the conversion of the un-glycosylated form.

The complete failure of un-glycosylated PrP to adopt the conformation of ME7/PrP^{Res}, counter-intuitively suggests that un-glycosylated PrP is less conformationally flexible than that which is normally glycosylated PrP, in contrast to previous suggestions (Rudd et al., 2002; Rudd et al., 2001). However, G3-PrP may have failed to convert because of an indirect mechanism. PrP's N-glycans may mediate conversion to PrP^{Res} by stabilisation of misfolding intermediates, by interacting with PrP^{Sc} conversion factors or by maintaining the protein in a required environment for successful conversion, perhaps in association with membranes. Similarly, the reduced levels of un-glycosylated PrP^{Res} generated in 79A and 263K seeded reactions demonstrates that although able to initially misfold, un-glycosylated PrP could not sustain significant PrP^{Res} amplification. This result suggests that un-glycosylated PrP^{Res} may not be able to seed further conversion and thus may have little relevance to the transmission of TSE disease. Further experimentation is required to explore this hypothesis and to define the structural characteristics of PMCA PrP^{Res}. Additionally, the seeding ability of un-glycosylated PrP may be altered in the context of other PrP^{Res} glycotypes when mixed aggregates are likely to form.

Previous work has suggested that *in vitro* misfolding of un-glycosylated PrP generates a number of smaller PK resistant forms of PrP (12-14 kDa) in addition to

the major 18-21 kDa form (Lawson et al., 2001; Priola and Lawson, 2001). These works suggest that the misfolded conformation adopted is affected by the glycosylation state of PrP^{C}. In all experiments presented here the size of un-glycosylated PrP^{Res} generated was unaffected by the glycosylation status of the PrP^{C} substrate and no smaller PK resistant forms were observed.

The convertibility of un-glycosylated PrP and to a lesser extent PrP mono-glycosylated at the first site was determined by the strain of TSE used, to seed the PMCA reaction. This implies that the importance of PrP's N-glycans to conversion is dependent upon the novel PrP^{Res} conformation to be adopted. These data support the hypothesis that the precise mechanism and conversion requirements are TSE strain specific. However, the relative PMCA-convertibility of glycan deficient PrP by different TSE strains does not exactly mirror the transmissibility of these agents to the PrP glycosylation deficient transgenics. In particular, no significant difference in the 79A/PrP^{Sc} seeded conversion efficiency of G2/PrP was observed in these studies, whilst the incubation period of 79A in G2 transgenics was significantly increased compared to normally glycosylated controls (Tuzi et al., in preparation, appendix ii). Thus the effect of N-glycan attachment to PrP on TSE transmission is not simply caused by a direct effect on the innate convertibility of the protein.

In contrast to previously published work, the role of PrP N-glycans in determining convertibility to PrP^{Res} is not limited to cross-species seeded reactions (Priola and Lawson, 2001). In particular the experiments presented here demonstrate that PrP's N-glycans do not pose a barrier to cross-species *in vitro* conversion, since partial or total absence of murine PrP N-glycans did not facilitate the formation of PrP^{Res} when seeded by hamster passaged scrapie. In fact, cross-species conversion was inhibited (G1) or reduced (G3) by the partial or complete absence of attached N-glycans. Previous work had shown that removal of PrP^{C}'s N-glycans did not lead to 263K seeded conversion of murine PrP using standard conversion technique (Kocisko et al., 1995). However, in contrast to this work, here we show strong conversion of normally glycosylated murine PrP, thus demonstrating the specific reduction in conversion owing to the absence of glycosylation. Additionally, few differences in

the effect of PrP glycosylation state on convertibility of the protein were observed between cross-species and within-species PMCA seeded reactions. Indeed TSE strain appeared more important in determining the role of PrP^{C}'s N-glycans in conversion than PrP^{Sc} source species. These data suggest that the role of PrP^{C}'s second site N-glycan in the cross species transmission of TSE may be mediated by factors other than the innate convertibility of PrP.

8.0 Discussion

8.1 Overview of principal findings

The N-linked glycosylation of PrP at two sites is highly conserved, suggesting that the N-glycans are important to the protein's normal function, as has been reported for numerous other glycoproteins (Gils et al., 2003; Kim et al., 2004; Lee et al., 2003; Rudd et al., 1995; Torres et al., 2003). However, the data in this thesis demonstrate that the absence of glycosylation of PrP's first, second or both sites, does not compromise the health or survival of transgenic mouse models (Chapter 3) (Cancellotti et al., 2005). Furthermore these transgenic mice do not develop spontaneous TSE disease, or accumulate PrP^{Sc} in the CNS in the absence of TSE challenge, counter to previous suggestions based upon findings from a cell culture system (Lehmann and Harris, 1997). Thus the function of PrP's N-glycans is neither essential for life nor required to prevent spontaneous misfolding of PrP *in vivo*. This is the first systematic examination of the influence of PrP^{C}'s glycosylation state on the spontaneous development of TSE disease, despite the previous generation of PrP glycosylation deficient transgenic mice, in PrP null backgrounds, by conventional methods (DeArmond et al., 1997; Neuendorf et al., 2004). Moreover, glycosylation at either site appears to be sufficient for the normal cellular localisation of PrP^{C} *in vivo* (Chapter 4), in contrast to earlier reports (DeArmond et al., 1997; Rogers et al., 1990) (appendix i).

However, these PrP glycosylation deficient transgenic mice [NPU] exhibit a dramatic phenotype when challenged with hamster or human TSE agents across the species barrier (Chapters 5 and 6). Previous work has shown that the glycosylation of PrP promoted the within-species transmission of TSE disease in a strain dependent manner (DeArmond et al., 1997; Neuendorf et al., 2004; Tuzi et al., in preparation). However, the work presented here is the first study to address the role of PrP's N-glycans in cross-species TSE transmission. The results of a cell-free conversion assay had previously suggested that glycosylation of PrP^{C} may play a TSE species barrier specific role (Priola and Lawson, 2001). These *in vitro* data

predicted that the total absence of PrP's N-glycans would render a host more susceptible to cross-species TSE challenge. In contrast, the data presented here demonstrate that *in vivo* the absence of PrP's N-glycans inhibited the cross-species transmission of a range of TSE agents (Chapters 5 and 6). The altered localisation of PrP^C in the G3 transgenic mice may account for the resistance of this model to cross-species TSE challenge (Chapter 4). Additionally, *in vitro* conversion in an independent experimental system failed to replicate Priola and Lawson's findings (Chapter 7). Indeed the data presented here suggest that the innate convertibility of G3/PrP is reduced compared to that of the normally glycosylated protein.

To further understand the role of glycosylation in cross-species TSE transmission, attachment of glycans to the first or second site was also investigated, using the G1 and G2 transgenic mice. Previous studies have demonstrated that the first and second site of N-glycan attachment have differing effects on the transmission of TSE within a species (DeArmond et al., 1997; Neuendorf et al., 2004; Tuzi et al., in preparation). The removal of either site resulted in an increase in incubation period after TSE challenge. However, the relative importance of each site differed between strains; the first site appears particularly important for the transmission of murine scrapie strain ME7 and the second site for murine BSE (Neuendorf et al., 2004; Tuzi et al., in preparation). The data in this thesis uniquely show that the two N-glycan attachment sites also have radically different effects on the cross-species transmission of the TSE agent (Chapter 5).

Absence of glycosylation at PrP's first site retards the cross-species transmission of the hamster TSE strain 263K, as illustrated by a decrease in disease incidence and increase in time to disease onset (Chapter 5). Thus glycosylation of asparagine 180 appears to facilitate TSE transmission across a species barrier. The alteration in transmission of TSE may be attributable to a direct effect on the innate ability of PrP to misfold (Chapter 7). In contrast, glycosylation of PrP's second site protects the host from TSE challenge with 263K or sporadic CJD, since mice lacking glycosylation at this site exhibit a higher disease incidence and shorter time to disease onset than controls (Chapters 5 and 6). The protective effect of

glycosylation of the second site is only observed after challenge across the species barrier, since numerous within-species transmissions to transgenic mice lacking the second site have never exhibited accelerated disease (DeArmond et al., 1997; Neuendorf et al., 2004; Tuzi et al., in preparation) (appendix ii).

Thus could the function of glycosylation of asparagine 196 be to protect the host from infection with TSE strains from other species? Perhaps the role may even be to counter the facilitatory effect of glycosylation of the first site on TSE transmission? However, N-glycosylation at 196 does not protect the host against cross-species challenge with all TSE strains. Indeed glycosylation of the second site appears to facilitate transmission of vCJD to mice (Chapter 6). Thus the effect of the glycosylation of the second site on cross-species transmission does not simply occur because of a global destabilisation of PrP. Moreover, the effect of second site glycosylation on the cross-species transmission of 263K to mice does not appear to be mediated by an alteration in PrP's conversion efficiency (Chapter 7). This suggests that glycosylation of PrP can influence TSE pathogenesis independently of a direct effect on misfolding.

Glycan attachment to PrP was disrupted in these experiments by threonine for asparagine substitutions in the N-glycan attachment sequence. These amino acid changes reduce homology between murine PrP^{C} and donor PrP^{Sc}. The degree of sequence homology between PrP^{C} and PrP^{Sc} has been previously reported to be a key determinate of the species barrier (Scott et al., 1989). Thus the amino acid changes used in the models may influence the TSE species barrier independently of their role in preventing glycosylation of PrP^{C}. However, the only way to selectively disrupt the glycosylation of one protein *in vivo* is by an amino acid substitution within its glycan attachment site. The amino acid changes in PrP used in the experiments described in this thesis are not associated with any known pathogenic mutation. However, these experiments carry the caveat that the effects observed may occur either because of a change of glycosylation or the amino acids.

In conclusion, the data in this thesis uniquely suggest that N-glycan attachment to PrP^C contributes to the barrier to cross-species TSE transmission in a site of attachment and TSE strain dependent manner. These effects appear to be mediated by multiple mechanisms including an alteration in the localisation of PrP^C and a change in the innate ability of the protein to convert to the disease associated form.

8.2 Possible mechanisms for the observed alteration in cross-species transmission to G3 transgenic mice

G3 transgenic mice lack both PrP N-glycan attachment sites. These mice exhibit enhanced resistance to or significantly increased incubation times after cross-species challenge with all TSE agents investigated (Chapters 5 and 6). This alteration in transmission occurred independently of a change in the level of PrP^C or its membrane attachment (Chapter 3), factors that are known to influence TSE disease (Chesebro et al., 2005; Manson et al., 1994b). The G3 transgenic mice studied here, and a comparable conventional murine PrP glycosylation deficient transgenic model [UCSF], also have greatly extended incubation times after and/or increased resistance to within-species TSE challenge (DeArmond et al., 1997; Tuzi et al., in preparation) (appendix ii). This suggests that the resistance of the G3 transgenic mice to cross-species TSE challenge is not caused by a specific affect on the TSE species barrier, but by an affect on all types of TSE transmission. Additionally, G3 transgenic mice do not accumulate significant PrP^{Sc} within the CNS after cross-species TSE challenge; this may cause the observed resistance of these mice to disease (Chapters 5 and 6).

The reduced level of PrP^C detectable in the neuropil of G3 transgenic mice may have resulted in the increased resistance of these mice to TSE challenge and the absence of significant PrP^{Sc} (Chapter 6). A similar explanation was proposed for the observed TSE resistance of conventional un-glycosylated PrP murine transgenics [UCSF] (DeArmond et al., 1997). TSE transmissions to independent conventional un-glycosylated PrP murine transgenics [Riems] have yet to be reported (Neuendorf et al., 2004). The cellular localisation of PrP^C in the Riems model is anticipated to

resemble that of the normally glycosylated protein (Neuendorf et al., 2004). Comparison of the results of TSE transmissions to these mice with those to the G3 transgenic model [NPU] will be very useful to further test the hypothesis that the elevated resistance of the G3 transgenic mice to TSE challenge is a result of altered PrP^{C} localisation.

The localisation of PrP^{C} has been previously reported to be important for the accumulation of PrP^{Sc} and the development of TSE clinical signs in other PrP model systems (Chesebro et al., 2005; Taraboulos et al., 1995; Vetrugno et al., 2005). Although intracellular misfolding of PrP can occur (Ma and Lindquist, 2002), post-Golgi localisation of PrP^{C} may be required for the biologically relevant interaction of PrP^{C} with the TSE agent/PrP^{Sc}. Indeed some authors have suggested that conversion may occur after the endocytosis of PrP, in an endosomal or lysosomal compartment (Laszlo et al., 1992). The observed significant reduction in PrP^{C} detectable in the neuropil, but apparently unchanged ER or Golgi localisation in the G3 transgenic mice, and absence of accumulated PrP^{Sc} in this model, is consistent with conversion principally occurring in a post-Golgi compartment, as has been previously suggested (Taraboulos et al., 1995). The local availability of cofactors or environmental conditions such as pH may change the ability of PrP to misfold in the G3 transgenic mice. Previous work has shown that the subcellular localisation of Huntingtin is known to dramatically influence its aggregation (Rousseau et al., 2004). However, it is clear that conversion can occur in the G3 transgenic mice after TSE challenge (Chapter 5; Tuzi et al., in preparation; appendix ii). This suggests that the site of conversion may be TSE strain dependent and/or localisation of PrP^{C} only affects the probability of conversion rather than being an absolute determinant of it.

However, in addition to the effect on localisation, *in vitro* PrP conversion experiments also suggest that the innate convertibility of PrP^{C} is reduced in the G3 transgenic mice (Chapter 7). Conversion of G3 PrP^{C}, seeded by both heterologous (263K) and homologous (79A or ME7) PrP^{Sc}, occurred less readily than that of normally glycosylated control-PrP^{C}. Thus the glycosylation state of PrP^{C} may also directly contribute to the reduction in cross-species transmission of TSE to the G3

transgenic mice via this effect on the innate convertibility of the protein. This may occur via a direct effect on the ability of G3/PrP to interact with cellular components which mediate conversion. However, the observed alteration in localisation of PrP^{C} and its changed innate convertibility in the G3 transgenic mice may be linked. The localisation of PrP^{C} and PrP^{Sc} in a contiguous lipid membrane (Baron et al., 2002) and the local lipid environment (Pinheiro, 2006) are known to influence the ability of PrP^{C} to convert. The observed alteration in localisation of G3 PrP^{C} may thus directly alter the ability of the protein to convert to the disease associated form.

Alternatively, the observed change in TSE transmission to the G3 transgenic mice may occur independently of the observed alteration in G3/PrP's convertibility. The N-glycans may directly mediate the interaction of PrP with the TSE agent, and hence may be essential for disease development. A number of specific host glycans are similarly known to be key to facilitate the interaction of toxins, bacterial and viral pathogens with the host (Chu and Whittaker, 2004; Falk et al., 1995; Griffitts et al., 2003; Kunz et al., 2005). Equally, the absence of PrP^{Sc} in the TSE challenged G3 transgenic mice may result from a failure of the misfolded form of PrP to accumulate rather than an absence of its formation. Previous work examining the glycosylation state of Alzheimer's Disease associated tau suggested that paired helical filaments, characteristic of the diseased state, dissociated when tau was not glycosylated (Wang et al., 1996). Similarly the nature of PrP^{Sc} may be changed in the G3 transgenic mice and thus it may not be recognised as misfolded by conventional methods. Alternatively, the clearance rate of G3/PrP^{Sc} may be enhanced.

8.3 Possible mechanisms for the altered transmission of 263K to G1 transgenic mice

Transgenic mice which lack PrP's first glycosylation site only (G1 NPU) also exhibit enhanced resistance to or significantly increased incubation periods after cross-species TSE challenge with hamster scrapie 263K (Chapter 5). The results of further cross-species transmission studies are required to determine if the resistance to 263K occurs because of a generic resistance of these transgenic mice to cross-species TSE

transmission. In contrast to G3 transgenic mice, limited amounts of misfolded PrP were observed to accumulate in a number of G1 mice after cross-species challenge (Chapter 5). Thus although both G1 and G3 transgenic mice lack the first glycosylation site, the mechanism(s) responsible for the observed effects on transmission may differ between the two models.

In particular the cellular localisation of PrP^C does not appear to be changed by the absence of glycosylation at the first site (G1 NPU) (Chapter 4). This contrasts with results of one comparable conventional murine transgenics in which PrP^C was reported to be localised predominately in the nerve cell body (DeArmond et al., 1997). However the point mutation used in this conventional model is known to change the biology of PrP^C, including its localisation, independent of its effect on glycosylation (Capellari et al., 2000b). Other conventional murine transgenic models [Riems] that also lack PrP's first N-glycan attachment site are anticipated to exhibit plasma membrane localisation of PrP *in vivo* (Neuendorf et al., 2004), consistent with the results observed in the G1 transgenic mice presented here. Thus the effect of the absence of an N-glycan at the first attachment site on cross-species TSE transmission is not the result of altered localisation of PrP^C. Moreover the amount of PrP^C within the CNS and the membrane anchorage of PrP^C in the G1 transgenic mice also do not differ from normally glycosylated controls (Chapter 3; Cancellotti et al., 2005).

In vitro heterologous PrP conversion reactions seeded with $263K/PrP^{Sc}$ suggested that $G1/PrP^C$ was unable to convert to a PK resistant form *in vitro* (Chapter 7). This may underlie the observed enhanced resistance of G1 murine transgenic mice to challenge with hamster scrapie, since the misfolding of host PrP may be required for the propagation of infectivity. $G1/PrP^C$ is also not converted by $ME7/PrP^{Sc}$ and only weakly and not significantly by $79A/PrP^{Sc}$. However, 79A can be successfully transmitted to G1 transgenic mice, albeit with an increased incubation time, questioning how closely *in vitro* conversion efficiency reflects that which occurs *in vivo*. Further optimisation of PMCA reaction conditions may permit the significant $79A/PrP^{Sc}$ seeded amplification of $G1/PrP^C$. Alternatively, an *in vivo* specific effect

may mediate the transmission of 79A murine scrapie to the G1 transgenic mice. Although the *in vitro* conversion (PMCA) reactions contain total CNS components, these factors are homogenised so that normal *in vivo* concentrations and interactions may be disrupted. Thus *in vitro* conversion may not precisely mimic that *in vivo* because of an absence of factors that would normally be found at the site of conversion, or equally because of the presence of factors that are normally excluded. Despite these caveats, both the *in vivo* and *in vitro* data suggest that the G1/PrP is less able to convert to the disease associated form than that which is normally glycosylated. However G3/PrP which also lacks the first N-glycan attachment site is able to convert to a PK resistant conformation, albeit with reduced efficiency. Thus although glycosylation of PrP's first site appears to facilitate misfolding of PrP, the failure of G1 PrP to convert can not be solely attributable to lack of the first site. Indeed current data would suggest that the N-glycans attached to the second site in G1/PrP may mediate the failure of this glycoform to convert.

8.4 The role of glycosylation of the second site in the TSE species barrier

In contrast to the effect of the first or both glycosylation sites on cross-species TSE transmission, the absence of an N-glycan attached to PrP's second site (G2 NPU) specifically promotes the cross-species transmission of some TSE strains (Chapters 5 and 6). The facilitation of cross-species TSE transmission to the G2 transgenic mice is associated with enhanced PrP^{Sc} accumulation in the CNS (Chapter 5 and 6), suggesting that PrP^{Sc} or its capacity to misfold may have altered in these mice. However, the effect of the second site on cross-species transmission and PrP^{Sc} accumulation is dependent upon TSE strain. Nevertheless, the importance of the glycosylation of PrP^{C} is not determined by the PrP^{Sc} glycoform of the challenging agent alone since the data presented here demonstrate the PrP^{C} glycosylation requirement of vCJD and 263K significantly differ, despite sharing an almost identical PrP^{Sc} glycoform. Thus the importance of PrP^{C} glycosylation to the TSE species barrier is not to simply provide the required PrP^{Sc} glycotype. Equally, species differences in the glycosylation of PrP^{Sc} (Xanthopoulos et al., 2006) also may not solely dictate the importance of PrP^{C}'s glycosylation state to TSE

transmission, as illustrated by differences in the transmission of vCJD and sporadic CJD to the glycosylation deficient transgenic mice.

The site-specific glycosylation of other host proteins is suggested to prevent the cross-species transmission of viruses (Marin et al., 2003; Wentworth and Holmes, 2001). In these cases glycosylation of the resistant receptor directly acted to prevent interaction with the pathogen perhaps by shielding the host protein from the virus. A similar mechanism may determine how second site glycosylation of PrP^{C} prevents transmission of 263K and sporadic CJD to murine hosts. However, in these examples the N-glycan attachment site is unique to the resistant host species. This contrasts with PrP's second site of glycan attachment which is found in all species.

In contrast to the accelerated accumulation of misfolded PrP in the G2 transgenic mice challenged with 263K, the *in vitro* misfolding efficiency of G2/PrP^{C}, seeded by 263K/PrP^{Sc}, was not significantly different from that of normally glycosylated PrP^{C} (Chapters 5 and 7). This difference suggests factors other than misfolding efficiency must mediate the accelerated accumulation of PrP^{Sc} observed *in vivo*. This may be, mediated by a difference in the rate of clearance of G2/PrP^{Sc} compared to normally glycosylated PrP^{Sc}. This may occur if G2/PrP^{Sc} is recognised differently by the cellular clearance machinery. Indeed clearance proteins like the N-glycan specific E3-ligase Fbx2, that recognises and targets proteins for proteasome degradation via their attached N-glycans, may interact differently with G2/PrP^{Sc} (Yoshida et al., 2002). Equally, the different glycosylation state of G2/PrP may directly change the stability of the protein, perhaps by an alteration in its ability to resist proteinase digestion. Alternatively, the absence of glycosylation of the second site may alter the conformation or aggregation of misfolded PrP which may indirectly alter turnover *in vivo*. Indeed the altered pattern of PrP^{d} deposition observed in G2 transgenic mice challenged with vCJD suggests that glycosylation at the second site may be important to the conformation or aggregation of misfolded PrP. However, no such changes in the pattern or type of PrP^{d} deposition were observed in the G2 transgenic mice after challenge with 263K, which also exhibited a dramatically

different transmission phenotype, highlighting that the glycosylation state of PrP may mediate its species barrier role by multiple mechanisms.

8.5 Glycosylation of PrP^C and the TSE species barrier

The barrier to cross-species TSE transmission has been recognised since the 1960's (Pattison, 1965) and it came under renewed interested during the BSE epidemic. The unusually wide host range of BSE and the emergence of new strains, such as CWD, make it increasingly important to accurately predict the extent of the TSE species barrier. PrP^C is a key TSE host susceptibility factor (Bueler et al., 1993; Manson et al., 1994b) and clear evidence links this protein to the extent of the species barrier (Manson et al., 1999; Scott et al., 1989). However, it is still not possible to make accurate predictions of the host range of a new TSE strain. The data presented here demonstrate that glycosylation of host PrP^C, particularly of the second site, is a key determinant of the TSE species barrier.

A number of host factors have been reported to influence the extent of the TSE species barrier, including the degree of amino acid sequence homology between host PrP^C and incoming PrP^{Sc}, and PrP interaction with species specific conversion factors (Scott et al., 1989; Telling et al., 1995). Glycan attachment to PrP^C may specifically modify the effects of PrP amino acid differences between TSE host species and hence their role in cross-species transmission of TSE. However, although two amino acids differ between the hamster and mouse sequence proximal to the second glycan attachment site, these residues are conserved between human and mouse (Locht et al., 1986; Oesch et al., 1985). Thus the effect of second site glycosylation on cross-species transmission would not appear to be the result of the influence of the N-linked glycans on the local amino acid differences between host PrP^C and donor PrP^{Sc}. Interestingly the removal of PrP's second site N-glycan has a greater effect on the cross-species transmission of sporadic CJD MM-cortical (type 2) than the expression of human PRNP-(MM) in a gene-targeted murine transgenic model (Personal communication Mr. Matthew Bishop). This supports the idea of additional species specific factors that interact with PrP having a significant role in

TSE disease pathogenesis and highlight that the species barrier is not purely the result of PrP amino acid homology. Moreover, perhaps PrP's N-glycans influence the interaction of the protein with these factors *in vivo*.

The increased incidence of alteration in TSE strain characteristics after cross-species transmission led to the hypothesis that an adaptation or zero-replication phase may underlie the species barrier (Kimberlin and Walker, 1979). Recent experimental evidence has linked this idea to the alteration in PrP^{Sc} conformation that correlates with TSE transmission across a species barrier (Peretz et al., 2002). Others have suggested that strain differences in cross-species transmission may be the result of the extent of PrP conformational compatibility between host PrP^{C} and TSE PrP^{Sc} (Hill and Collinge, 2003; Kellershohn and Laurent, 1998). Absence of the N-glycan attached to PrP^{C} at the second site may increase the range of conformations that the host protein can adopt (Rudd et al., 2001; Zuegg and Gready, 2000), and hence the range of TSE strains that can induce it to misfold. However, absence of glycosylation at the second site does not result in an increase in 263K-seeded *in vitro* conversion of PrP, nor to enhanced transmission of all strains across the TSE species barrier. Thus the observed increase in transmission to the G2 transgenic mice does not appear to be attributable to a direct effect on conformational compatibility of PrP^{C}. Equally, the species barrier is observed in the absence of significant adaptation of the strain to the new host, suggesting that a change in conformation of PrP^{Sc} has not occurred (Bruce et al., 1997; Kimberlin et al., 1989). Thus it would appear that the TSE species barrier is not solely the result of conformational compatibility of host and donor PrP.

Although the data presented here demonstrate that glycosylation of murine PrP^{C}'s second site leads to an increase in disease incidence and decrease in time to disease onset after challenge with two TSE sources, no cases of acquired/sporadic human TSE disease have been reported associated with an alteration in glycosylation at the second site. The normal development and survival of G2 transgenic mice indicates that loss of the second glycosylation site is not detrimental, thus one would predict occurrence of mutations ablating the second glycosylation site within the human

population. However, the frequency of such individuals may be very low. This, coupled with the low exposure to TSE agents in the environment, may account for the current absence of any reported cases of TSE infected individuals with disruptive mutations in the second N-glycan attachment site. Moreover, transmission of vCJD is hindered by absence of the second glycosylation site. Absence of the second glycosylation site would thus be predicted to be protective against BSE exposure. This may also account for the absence of cases of acquired disease associated with mutations in the second site, since in recent years most environment TSE exposure will have been to BSE in the United Kingdom. Alternatively, the glycosylation state of PrP^C may also effect peripheral replication and transportation of infectivity. Thus absence of glycosylation of the second site may influence cross-species TSE transmission by natural routes of infection differently to those observed in the experimental system examined here.

Three cases of familial CJD have been reported to be associated with loss of the first glycosylation site (Chasseigneaux et al., 2006; Grasbon-Frodl et al., 2004; Nitrini et al., 1997). The transmission studies presented here suggest that this change would protect against acquired TSE disease. However, this effect may display TSE strain dependence. Moreover the point mutation reported to disrupt the glycosylation of PrP differed from those used here and was linked to the development of familial TSE disease, not as a risk factor for acquired infection. Indeed the mutation in two of these kindreds (Grasbon-Frodl et al., 2004; Nitrini et al., 1997), has been reported to have pathogenic effects on PrP's cellular localisation and solubility, independent of its effects on the protein's glycosylation state (Capellari et al., 2000b).

The data presented here demonstrate that the species barrier role of glycosylation of asparagine 196 is TSE strain dependent (Chapters 5 and 6). Specifically, the results demonstrate that the cross transmission of vCJD is hindered by the absence of glycosylation of PrP's second site, whereas N-glycans attached to this site appears to protect the host against the cross-species transmission of other strains of TSE. This suggests that the vCJD TSE agent is adapted to exploit di-glycosylated PrP^C which is the most abundant glycotype, *in vivo,* in all species so far examined. This may

contribute to the unusually wide host range of the strain since the results presented here suggest that glycosylation of PrP^C's second site usually protect the host from infection with TSE from other species. Why an agent that apparently originated in domestic cattle exhibits a preference for PrP glycosylated at its second site is unclear. Further studies are required to ascertain if the effect observed in the murine model system used here is also important in other hosts and whether glycosylation of host PrP^C affects the transmission of other biologically relevant TSE strains such as CWD and atypical BSE.

8.6 Future Work and Ongoing Studies

The work presented here raises many new questions.

Is the cross-species transmission of variant CJD and sporadic CJD influenced by glycosylation of PrP^C's first site?
Does glycosylation of PrP^C alter peripheral TSE pathogenesis and transmission by natural routes?
Is the conformation of PrP^{Sc} altered by the absence of N-glycans at either the first or second site and does this relate to TSE strain and neurotoxicity?
Why is the cross-species transmission of 263K and sporadic CJD promoted by the absence of an N-glycan attached to PrP^C's second site and why is that of vCJD hindered?
Is clearance of PrP^{Sc} affected by its glycosylation state?
Does glycosylation of PrP^C affect the variant CJD and sporadic CJD *in vitro* conversion efficiency?
What prevents the misfolding of G1-PrP?
Why is cellular localisation of PrP^C altered in the G3 transgenic mice?
Does the change in location of PrP^C really underlie the resistance of G3 transgenic mice to cross-species TSE challenge?

Further studies of the effect of glycosylation on cross-species TSE transmission are currently ongoing. G1 transgenic mice have been challenged by ic inoculation with

variant and sporadic CJD. These studies will be analysed by similar methods to those outlined in Chapters 5 and 6 and will permit a fuller understanding of the role of first site glycosylation in cross-species transmission. Additionally, further cross-species transmission studies to the PrP glycosylation deficient transgenic mice could be undertaken, to increase the range of strains investigated. In particular it would be interesting to examine if the transmission of atypical BSE (Biacabe et al., 2004; Casalone et al., 2004) and CWD were also subject to the effects of PrP^C glycosylation state, since the ability of these agents to cross the species barrier to humans is of growing concern.

To investigate if the peripheral pathogenesis of TSE disease after cross-species challenge is affected by the glycosylation state of PrP^C, peripheral transmission experiments to the glycosylation deficient mice could be undertaken. The PrP glycosylation deficient transgenic mice could be challenged either by intraperitoneal injection or by a more natural transmission route, such as the feeding of TSE infected material. Peripheral routes of challenge are often less efficient and may result in longer incubation periods than the direct ic inoculations used here, thus larger experimental groups will be required. Furthermore any such experimental design must take account of the significantly enhanced resistance of G1 and G3 transgenic mice to cross-species transmissions observed in this thesis.

The species barrier is classically defined by the difference in incubation period between first and subsequent passages (Pattison, 1965). Thus CNS material from TSE infected G2 transgenic and normally glycosylated control mice has been used to challenge groups of G2 transgenic and normally glycosylated control animals to assess the extent of the species barrier at primary passage. Moreover, comparison of the pattern of vacuolar pathology at second passage will provide further information regarding the strain of agent that infected the murine models at primary transmission. This is being further investigated by transmission of CNS material infected with vCJD, sporadic CJD and 263K to two strains of wild type mice and their F1 cross (Bruce, 2003). This system has been previously used to show that BSE and vCJD were caused by the same TSE strain (Bruce et al., 1997). Strain typing data will thus

demonstrate if the differences in incubation period observed in the G2 transgenic mice were the result of colonisation by different strains of agent or by an alteration in the rate of disease progression. In addition to these experiments, the effect of glycosylation on the conformation of PrP^{Sc} could also be assessed, so as to further explore the link between strain, the species barrier and PrP^{Sc} as proposed by the experimental work of Peretz (Peretz et al., 2002). In parallel the relative neurotoxicity and stability of the different PrP^{Sc} glycoforms derived from the PrP glycosylation deficient murine transgenics could be investigated by their application to cultured cells.

To further investigate the importance of TSE strain to the ability of different PrP^{C} glycotypes to be converted by heterologous PrP^{Sc}, PMCA reactions seeded with variant or sporadic CJD could be undertaken. These data could be used to further interpret the cross-species transmission studies presented in this thesis. Similarly the relative ability of other TSE sources to seed conversion of different PrP^{C} glycotypes could be explored including the more recently emergent agents of CWD, atypical BSE and scrapie. Equally, PMCA generated glycosylation deficient PrP^{Res} or *in vivo* derived PrP^{Sc} from the G2 transgenic mice could be used to seed further reactions to examine the importance of PrP^{Sc} glycosylation state to its ability to induce PrP^{C} conversion.

The nature of the N-glycans attached to G1-PrP^{C} and G2-PrP^{C} are unknown, although current data suggest the combination of glycans attached differs (Chapter 3). Absence of one of PrP's glycosylation sites may alter the combination of glycans attached to the other site, such that glycans attached to G1-PrP^{C} and G2-PrP^{C} may not resemble those of wild type PrP^{C}. To investigate this and in particular to further understand why G1- PrP^{C} is relatively unable to adopt a PK resistant conformation, the glycans attached to the cellular forms of the proteins could be investigated by mass spectrometry. However, it may be technically challenging to isolate sufficient murine PrP^{C} for this analysis. Alternative, less technically challenging, but less definitive, approaches to this question could also be employed. Differences in lectin binding between the forms of PrP could be examined to estimate differences in

glycan composition (Xanthopoulos et al., 2006). Additionally, 2-D electrophoresis could be used to further determine if the N-glycans moieties differ in size or charge.

An examination of the interaction of glycan deficient PrP^C with candidate PrP binding partners, such as laminin receptor precursor or cellular chaperones (Capellari et al., 1999; Rieger et al., 1997), may provide information regarding the role of PrP's glycosylation state in TSE transmission. Equally, the influence PrP^C's N-glycan on the protein's interaction with other cellular components such as lipids could also be explored; this may be particularly relevant to the observed altered localisation of G3/PrP^C. Cultured cells could additionally be used to further examine the trafficking and turnover of un- and partially glycosylated PrP^C. Primary neurons derived from the PrP glycosylation deficient transgenic mice [NPU] and/or neuronal cell lines transfected with the appropriate *Prnp* constructs could be used. These *ex vivo* systems will allow the influence of N-glycans on the half-life and trafficking of PrP^C to be examined, since such measurements are extremely difficult to make *in vivo*. However it should be remembered that the data acquired in culture are only an estimate of these phenomena *in vivo*. For example the half-life of PrP^C observed in neuronal cells and within the CNS *in vivo* significantly differ (Caughey et al., 1989; Safar et al., 2005). These differences may be the result of culture cells being an unrepresentative subset of those *in vivo* or because of the very different physical environment that cells are exposed to in culture.

To further investigate the role of un-glycosylated and partially glycosylated PrP^C in TSE disease, a murine bacterial artificial chromosomes (BACs) transgenic murine model could be generated. BACs are able to carry several hundred Kb of transgenic DNA (Yang et al., 1997), in contrast to the far smaller constructs which can be used by conventional methods. Thus both a gene's open reading frame and all its surroundings regulatory sequences can be incorporated in the construct. In contrast to gene-targeted transgenic mice, BAC technology permits multiple copies of the construct to be carried (Yang et al., 1999). Thus a BAC PrP transgenic model could express transgenic PrP in the correct spatial and temporal context but at higher levels than in the gene-targeted transgenic mice. Thus they could be used to magnify the

influence of PrP's N-glycans on TSE disease. In particular, BAC transgenic mice could be used to address if absence of disease after TSE challenge, as observed in G3 transgenic mice, is attributable to absolute resistance or increase in the incubation period.

The work presented here suggests that the glycosylation of PrP^{C} influences the cross-species transmission both by a direct effect on formation of PrP^{Sc} and via another undefined mechanism. This highlights that processes other than rate of PrP^{Sc} formation have dramatic effects on TSE pathogenesis and are influenced by PrP^{C}. The TSE disease pathways altered in the G2 glycosylation deficient transgenic mice may also be important to the transmission of TSE to normally glycosylated hosts both within and between species. Thus further study of the G2 murine transgenic model to identify and understand the aspects of TSE pathogenesis, which are altered in the model, may have wide relevance. Equally, study of the G1 and G3 transgenics could be used to further understanding of the link between PrP^{C} cellular localisation, formation of PrP^{Sc} and TSE disease.

Indeed, given the dramatic effect glycosylation of PrP has on TSE disease, the glycosylation of other proteins that misfold during neurodegenerative disorders may also be important to the pathogenesis of these diseases. Previous work has suggested that the glycosylation state of tau may be important to its role in Alzheimer's Disease (Wang et al., 1996). Equally, misfolded neuroserpin, which forms Collins body's, in a form of familial encephalopathy, is N-linked glycosylated, although the importance of this to disease is currently unknown (Davis et al., 1999).

References

Allen, J.D., Zhang, X.D., Scott, C.L., Boyle, G.M., Hersey, P. and Strasser, A. (2005) Is Apaf-1 expression frequently abrogated in melanoma? *Cell Death and Differentiation*, **12**, 680-681.

Alper, T., Cramp, W.A., Haig, D.A. and Clarke, M.C. (1967) Does the agent of scrapie replicate without nucleic acid? *Nature*, **214**, 764-766.

Alper, T., Haig, D.A. and Clarke, M.C. (1966) The exceptionally small size of the scrapie agent. *Biochemical and Biophysical Research Communications*, **22**, 278-284.

Anderson, R.M., Donnelly, C.A., Ferguson, N.M., Woolhouse, M.E., Watt, C.J., Udy, H.J., MaWhinney, S., Dunstan, S.P., Southwood, T.R., Wilesmith, J.W., Ryan, J.B., Hoinville, L.J., Hillerton, J.E., Austin, A.R. and Wells, G.A. (1996) Transmission dynamics and epidemiology of BSE in British cattle. *Nature*, **382**, 779-788.

Anfinsen, C.B. (1973) Principles that govern the folding of protein chains. *Science*, **181**, 223-230.

Armstrong, R.A., Cairns, N.J., Ironside, J.W. and Lantos, P.L. (2003) Does the neuropathology of human patients with variant Creutzfeldt-Jakob disease reflect haematogenous spread of the disease? *Neuroscience Letters*, **348**, 37-40.

Asante, E.A., Linehan, J.M., Gowland, I., Joiner, S., Fox, K., Cooper, S., Osiguwa, O., Gorry, M., Welch, J., Houghton, R., Desbruslais, M., Brandner, S., Wadsworth, J.D. and Collinge, J. (2006) Dissociation of pathological and molecular phenotype of variant Creutzfeldt-Jakob disease in transgenic human prion protein 129 heterozygous mice. *Proceedings of the National Academy of Sciences of the United States of America*, **103**, 10759-10764.

Baker, H.F., Duchen, L.W., Jacobs, J.M. and Ridley, R.M. (1990) Spongiform encephalopathy transmitted experimentally from Creutzfeldt-Jakob and familial Gerstmann-Straussler-Scheinker diseases. *Brain*, **113 (Pt 6)**, 1891-1909.

Banks, W.A., Niehoff, M.L., Adessi, C. and Soto, C. (2004) Passage of murine scrapie prion protein across the mouse vascular blood-brain barrier. *Biochemical and Biophysical Research Communications*, **318**, 125-130.

Barlow, R.M. and Rennie, J.C. (1976) The fate of ME7 scrapie infection in rats, guinea-pigs and rabbits. *Research in Veterinary Science*, **21**, 110-111.

Barmada, S., Piccardo, P., Yamaguchi, K., Ghetti, B. and Harris, D.A. (2004) GFP-tagged prion protein is correctly localized and functionally active in the brains of transgenic mice. *Neurobiology of Disease*, **16**, 527-537.

Barnard, G., Helmick, B., Madden, S., Gilbourne, C. and Patel, R. (2000) The measurement of prion protein in bovine brain tissue using differential extraction and DELFIA as a diagnostic test for BSE. *Luminescence*, **15**, 357-362.

Baron, G.S., Wehrly, K., Dorward, D.W., Chesebro, B. and Caughey, B. (2002) Conversion of raft associated prion protein to the protease-resistant state requires insertion of PrP-res (PrP(Sc)) into contiguous membranes. *The EMBO Journal*, **21**, 1031-1040.

Barron, R.M., Baybutt, H., Tuzi, N.L., McCormack, J., King, D., Moore, R.C., Melton, D.W. and Manson, J.C. (2005) Polymorphisms at codons 108 and 189 in

murine PrP play distinct roles in the control of scrapie incubation time. *Journal of General Virology*, **86**, 859-868.

Barron, R.M., Thomson, V., Jamieson, E., Melton, D.W., Ironside, J., Will, R. and Manson, J.C. (2001) Changing a single amino acid in the N-terminus of murine PrP alters TSE incubation time across three species barriers. *The EMBO Journal*, **20**, 5070-5078.

Bartz, J.C., Marsh, R.F., McKenzie, D.I. and Aiken, J.M. (1998) The host range of chronic wasting disease is altered on passage in ferrets. *Virology*, **251**, 297-301.

Baskakov, I.V. and Bocharova, O.V. (2005) In vitro conversion of mammalian prion protein into amyloid fibrils displays unusual features. *Biochemistry*, **44**, 2339-2348.

Baskakov, I.V., Legname, G., Baldwin, M.A., Prusiner, S.B. and Cohen, F.E. (2002) Pathway complexity of prion protein assembly into amyloid. *Journal of Biological Chemistry*, **277**, 21140-21148.

Beekes, M., McBride, P.A. and Baldauf, E. (1998) Cerebral targeting indicates vagal spread of infection in hamsters fed with scrapie. *Journal of General Virology*, **79 (Pt 3)**, 601-607.

Belay, E.D., Maddox, R.A., Williams, E.S., Miller, M.W., Gambetti, P. and Schonberger, L.B. (2004) Chronic wasting disease and potential transmission to humans. *Emerging Infectious Diseases*, **10**, 977-984.

Belichenko, P.V., Brown, D., Jeffrey, M. and Fraser, J.R. (2000) Dendritic and synaptic alterations of hippocampal pyramidal neurones in scrapie-infected mice. *Neuropathology and Applied Neurobiology*, **26**, 143-149.

Bendheim, P.E. and Bolton, D.C. (1986) A 54-kDa normal cellular protein may be the precursor of the scrapie agent protease-resistant protein. *Proceedings of the National Academy of Sciences of the United States of America*, **83**, 2214-2218.

Bendheim, P.E., Brown, H.R., Rudelli, R.D., Scala, L.J., Goller, N.L., Wen, G.Y., Kascsak, R.J., Cashman, N.R. and Bolton, D.C. (1992) Nearly ubiquitous tissue distribution of the scrapie agent precursor protein. *Neurology*, **42**, 149-156.

Benedetti, C., Fabbri, M., Sitia, R. and Cabibbo, A. (2000) Aspects of gene regulation during the UPR in human cells. *Biochemical and Biophysical Research Communications*, **278**, 530-536.

Benestad, S.L., Sarradin, P., Thu, B., Schonheit, J., Tranulis, M.A. and Bratberg, B. (2003) Cases of scrapie with unusual features in Norway and designation of a new type, Nor98. *Veterinary Record*, **153**, 202-208.

Bernoulli, C., Siegfried, J., Baumgartner, G., Regli, F., Rabinowicz, T., Gajdusek, D.C. and Gibbs, C.J., Jr. (1977) Danger of accidental person-to-person transmission of Creutzfeldt-Jakob disease by surgery. *Lancet*, **1**, 478-479.

Bessen, R.A., Kocisko, D.A., Raymond, G.J., Nandan, S., Lansbury, P.T. and Caughey, B. (1995) Non-genetic propagation of strain-specific properties of scrapie prion protein. *Nature*, **375**, 698-700.

Bessen, R.A. and Marsh, R.F. (1992a) Biochemical and physical properties of the prion protein from two strains of the transmissible mink encephalopathy agent. *Journal of Virology*, **66**, 2096-2101.

Bessen, R.A. and Marsh, R.F. (1992b) Identification of two biologically distinct strains of transmissible mink encephalopathy in hamsters. *The Journal of General Virology*, **73 (Pt 2)**, 329-334.

Bessen, R.A. and Marsh, R.F. (1994) Distinct PrP properties suggest the molecular basis of strain variation in transmissible mink encephalopathy. *Journal of Virology*, **68**, 7859-7868.

Betemps, D. and Baron, T. (2001) Molecular specificities of antibodies against ovine and murine recombinant prion proteins. *Biochemical and Biophysical Research Communications*, **281**, 101-108.

Biacabe, A.G., Laplanche, J.L., Ryder, S. and Baron, T. (2004) Distinct molecular phenotypes in bovine prion diseases. *EMBO Reports*, **5**, 110-115.

Bishop, M.T., Hart, P., Aitchison, L., Baybutt, H.N., Plinston, C., Thomson, V., Tuzi, N.L., Head, M.W., Ironside, J.W., Will, R.G. and Manson, J.C. (2006) Predicting susceptibility and incubation time of human-to-human transmission of vCJD. *Lancet Neurology*, **5**, 393-398.

Biswas, S., Langeveld, J.P., Tipper, D. and Lu, S. (2006) Intracellular accumulation of a 46kDa species of mouse prion protein as a result of loss of glycosylation in cultured mammalian cells. *Biochemical and Biophysical Research Communications*.

Blose, S.H., Meltzer, D.I. and Feramisco, J.R. (1984) 10-nm filaments are induced to collapse in living cells microinjected with monoclonal and polyclonal antibodies against tubulin. *Journal of Cell Biology*, **98**, 847-858.

Bocharova, O.V., Makarava, N., Breydo, L., Anderson, M., Salnikov, V.V. and Baskakov, I.V. (2006) Annealing prion protein amyloid fibrils at high temperature results in extension of a proteinase K-resistant core. *Journal of Biological Chemistry*, **281**, 2373-2379.

Bolton, D.C., McKinley, M.P. and Prusiner, S.B. (1982) Identification of a protein that purifies with the scrapie prion. *Science*, **218**, 1309-1311.

Bons, N., Mestre-Frances, N., Belli, P., Cathala, F., Gajdusek, D.C. and Brown, P. (1999) Natural and experimental oral infection of nonhuman primates by bovine spongiform encephalopathy agents. *Proceedings of the National Academy of Sciences of the United States of America*, **96**, 4046-4051.

Bons, N., Mestre-Frances, N., Charnay, Y. and Tagliavini, F. (1996) Spontaneous spongiform encephalopathy in a young adult rhesus monkey. *Lancet*, **348**, 55.

Borchelt, D.R., Rogers, M., Stahl, N., Telling, G. and Prusiner, S.B. (1993) Release of the cellular prion protein from cultured cells after loss of its glycoinositol phospholipid anchor. *Glycobiology*, **3**, 319-329.

Borchelt, D.R., Scott, M., Taraboulos, A., Stahl, N. and Prusiner, S.B. (1990) Scrapie and cellular prion proteins differ in their kinetics of synthesis and topology in cultured cells. *The Journal of Cell Biology*, **110**, 743-752.

Bosques, C.J. and Imperiali, B. (2003) The interplay of glycosylation and disulfide formation influences fibrillization in a prion protein fragment. *Proceedings of the National Academy of Sciences of the United States of America*, **100**, 7593-7598.

Bossers, A., Belt, P., Raymond, G.J., Caughey, B., de Vries, R. and Smits, M.A. (1997) Scrapie susceptibility-linked polymorphisms modulate the in vitro conversion of sheep prion protein to protease-resistant forms. *Proceedings of the National Academy of Sciences of the United States of America*, **94**, 4931-4936.

Brandner, S., Isenmann, S., Raeber, A., Fischer, M., Sailer, A., Kobayashi, Y., Marino, S., Weissmann, C. and Aguzzi, A. (1996) Normal host prion protein necessary for scrapie-induced neurotoxicity. *Nature*, **379**, 339-343.

Brown, D.A., Bruce, M.E. and Fraser, J.R. (2003) Comparison of the neuropathological characteristics of bovine spongiform encephalopathy (BSE) and variant Creutzfeldt-Jakob disease (vCJD) in mice. *Neuropathology and Applied Neurobiology*, **29**, 262-272.

Brown, D.A. and Rose, J.K. (1992) Sorting of GPI-anchored proteins to glycolipid-enriched membrane subdomains during transport to the apical cell surface. *Cell*, **68**, 533-544.

Brown, D.R., Qin, K., Herms, J.W., Madlung, A., Manson, J., Strome, R., Fraser, P.E., Kruck, T., von Bohlen, A., Schulz-Schaeffer, W., Giese, A., Westaway, D. and Kretzschmar, H. (1997) The cellular prion protein binds copper in vivo. *Nature*, **390**, 684-687.

Brown, D.R., Schmidt, B. and Kretzschmar, H.A. (1998) Effects of copper on survival of prion protein knockout neurons and glia. *Journal of Neurochemistry*, **70**, 1686-1693.

Brown, K.L., Stewart, K., Ritchie, D.L., Mabbott, N.A., Williams, A., Fraser, H., Morrison, W.I. and Bruce, M.E. (1999) Scrapie replication in lymphoid tissues depends on prion protein-expressing follicular dendritic cells. *Nature Medicine*, **5**, 1308-1312.

Brown, P., Gibbs, C.J., Jr., Rodgers-Johnson, P., Asher, D.M., Sulima, M.P., Bacote, A., Goldfarb, L.G. and Gajdusek, D.C. (1994) Human spongiform encephalopathy: the National Institutes of Health series of 300 cases of experimentally transmitted disease. *Annals Neurology*, **35**, 513-529.

Brownlee, A. (1940) Histo-pathological studies of scrapie, an obscure disease of sheep. *The Veterinary Journal*, **96**, 254-255.

Bruce, M.E. (2003) TSE strain variation. *British Medical Bulletin*, **66**, 99-108.

Bruce, M.E., Boyle, A., Cousens, S., McConnell, I., Foster, J., Goldmann, W. and Fraser, H. (2002) Strain characterization of natural sheep scrapie and comparison with BSE. *Journal of General Virology*, **83**, 695-704.

Bruce, M.E. and Dickinson, A.G. (1987) Biological evidence that scrapie agent has an independent genome. *Journal of General Virology*, **68 (Pt 1)**, 79-89.

Bruce, M.E., McBride, P.A. and Farquhar, C.F. (1989) Precise targeting of the pathology of the sialoglycoprotein, PrP, and vacuolar degeneration in mouse scrapie. *Neuroscience Letters*, **102**, 1-6.

Bruce, M.E., Will, R.G., Ironside, J.W., McConnell, I., Drummond, D., Suttie, A., McCardle, L., Chree, A., Hope, J., Birkett, C., Cousens, S., Fraser, H. and Bostock, C.J. (1997) Transmissions to mice indicate that 'new variant' CJD is caused by the BSE agent. *Nature*, **389**, 498-501.

Buck, T.M., Eledge, J. and Skach, W.R. (2004) Evidence for stabilization of aquaporin-2 folding mutants by N-linked glycosylation in endoplasmic reticulum. *American Journal of Physiology - Cell Physiology*, **287**, C1292-1299.

Budka, H. (2003) Neuropathology of prion diseases. *British Medical Bulletin*, **66**, 121-130.

Bueler, H., Aguzzi, A., Sailer, A., Greiner, R.A., Autenried, P., Aguet, M. and Weissmann, C. (1993) Mice devoid of PrP are resistant to scrapie. *Cell*, **73**, 1339-1347.

Bueler, H., Fischer, M., Lang, Y., Bluethmann, H., Lipp, H.P., DeArmond, S.J., Prusiner, S.B., Aguet, M. and Weissmann, C. (1992) Normal development and

behaviour of mice lacking the neuronal cell-surface PrP protein. *Nature*, **356**, 577-582.

Buschmann, A., Kuczius, T., Bodemer, W. and Groschup, M.H. (1998) Cellular prion proteins of mammalian species display an intrinsic partial proteinase K resistance. *Biochemical and Biophysical Research Communications*, **253**, 693-702.

Cagampang, F.R., Whatley, S.A., Mitchell, A.L., Powell, J.F., Campbell, I.C. and Coen, C.W. (1999) Circadian regulation of prion protein messenger RNA in the rat forebrain: a widespread and synchronous rhythm. *Neuroscience*, **91**, 1201-1204.

Calzolai, L., Lysek, D.A., Guntert, P., von Schroetter, C., Riek, R., Zahn, R. and Wuthrich, K. (2000) NMR structures of three single-residue variants of the human prion protein. *Proceedings of the National Academy of Sciences of the United States of America*, **97**, 8340-8345.

Calzolai, L., Lysek, D.A., Perez, D.R., Guntert, P. and Wuthrich, K. (2005) Prion protein NMR structures of chickens, turtles, and frogs. *Proceedings of the National Academy of Sciences of the United States of America*, **102**, 651-655.

Cancellotti, E., Wiseman, F., Tuzi, N.L., Baybutt, H., Monaghan, P., Aitchison, L., Simpson, J. and Manson, J.C. (2005) Altered glycosylated PrP proteins can have different neuronal trafficking in brain but do not acquire scrapie-like properties. *The Journal of Biological Chemistry*, **280**, 42909-42918.

Capellari, S., Parchi, P., Russo, C.M., Sanford, J., Sy, M.S., Gambetti, P. and Petersen, R.B. (2000a) Effect of the E200K mutation on prion protein metabolism. Comparative study of a cell model and human brain. *American Journal of Pathology*, **157**, 613-622.

Capellari, S., Zaidi, S.I.A., Long, A.C., Kwon, E.E. and Petersen, R.B. (2000b) The Thr183Ala Mutation, Not the Loss of the First Glycosylation Site, Alters the Physical Properties of the Prion Protein. *Journal of Alzheimer's Disease*, **2**, 27-35.

Capellari, S., Zaidi, S.I.A., Urig, C.B., Perry, G., Smith, M.A. and Petersen, R.B. (1999) Prion protein glycosylation is sensitive to redox change. *The Journal of Biological Chemistry*, **274**, 34846-34850.

Casalone, C., Zanusso, G., Acutis, P., Ferrari, S., Capucci, L., Tagliavini, F., Monaco, S. and Caramelli, M. (2004) Identification of a second bovine amyloidotic spongiform encephalopathy: molecular similarities with sporadic Creutzfeldt-Jakob disease. *Proceedings of the National Academy of Sciences of the United States of America*, **101**, 3065-3070.

Castilla, J., Saa, P. and Soto, C. (2004) Cyclic Amplification of Prion Protein Misfolding. In Lehmann, S. and Grassi, J. (eds.), *Techniques in Prion Research*. Birkhauser Verlag, Basel/Switerland, pp. 198-213.

Castilla, J., Saa, P. and Soto, C. (2005) Detection of prions in blood. *Nature Medicine*, **11**, 982-985.

Caughey, B., Neary, K., Buller, R., Ernst, D., Perry, L.L., Chesebro, B. and Race, R.E. (1990) Normal and scrapie-associated forms of prion protein differ in their sensitivities to phospholipase and proteases in intact neuroblastoma cells. *Journal of Virology*, **64**, 1093-1101.

Caughey, B., Race, R.E., Ernst, D., Buchmeier, M.J. and Chesebro, B. (1989) Prion protein biosynthesis in scrapie-infected and uninfected neuroblastoma cells. *Journal of Virology*, **63**, 175-181.

Chandler, R.L. (1961) Encephalopathy in mice produced by inoculation with scrapie brain material. *Lancet*, **1**, 1378-1379.
Chasseigneaux, S., Haik, S., Laffont-Proust, I., De Marco, O., Lenne, M., Brandel, J.P., Hauw, J.J., Laplanche, J.L. and Peoc'h, K. (2006) V180I mutation of the prion protein gene associated with atypical PrP(Sc) glycosylation. *Neuroscience Letters*.
Chelle, P.L. (1942) Un cas de tremblante cez de la chevre. *Bulletin Academie Veterinaire Francais*, **15**, 294-295.
Chen, G., Frohlich, O., Yang, Y., Klein, J.D. and Sands, J.M. (2006) Loss of N-linked glycosylation reduces urea transporter UT-A1 response to vasopressin. *The Journal of Biological Chemistry*.
Chen, S., Mange, A., Dong, L., Lehmann, S. and Schachner, M. (2003) Prion protein as trans-interacting partner for neurons is involved in neurite outgrowth and neuronal survival. *Molecular and Cellular Neuroscience*, **22**, 227-233.
Chen, S.G., Teplow, D.B., Parchi, P., Teller, J.K., Gambetti, P. and Autilio-Gambetti, L. (1995) Truncated forms of the human prion protein in normal brain and in prion diseases. *The Journal of Biological Chemistry*, **270**, 19173-19180.
Chernoff, Y.O., Lindquist, S.L., Ono, B., Inge-Vechtomov, S.G. and Liebman, S.W. (1995) Role of the chaperone protein Hsp104 in propagation of the yeast prion-like factor [psi+]. *Science*, **268**, 880-884.
Chesebro, B. (1999) Prion protein and the transmissible spongiform encephalopathy diseases. *Neuron*, **24**, 503-506.
Chesebro, B., Trifilo, M., Race, R., Meade-White, K., Teng, C., LaCasse, R., Raymond, L., Favara, C., Baron, G., Priola, S., Caughey, B., Masliah, E. and Oldstone, M. (2005) Anchorless prion protein results in infectious amyloid disease without clinical scrapie. *Science*, **308**, 1435-1439.
Chien, P., DePace, A.H., Collins, S.R. and Weissman, J.S. (2003) Generation of prion transmission barriers by mutational control of amyloid conformations. *Nature*, **424**, 948-951.
Chien, P. and Weissman, J.S. (2001) Conformational diversity in a yeast prion dictates its seeding specificity. *Nature*, **410**, 223-227.
Chiesa, R., Drisaldi, B., Quaglio, E., Migheli, A., Piccardo, P., Ghetti, B. and Harris, D.A. (2000) Accumulation of protease-resistant prion protein (PrP) and apoptosis of cerebellar granule cells in transgenic mice expressing a PrP insertional mutation. *Proceedings of the National Academy of Sciences of the United States of America*, **97**, 5574-5579.
Chiesa, R., Piccardo, P., Ghetti, B. and Harris, D.A. (1998) Neurological illness in transgenic mice expressing a prion protein with an insertional mutation. *Neuron*, **21**, 1339-1351.
Chu, V.C. and Whittaker, G.R. (2004) Influenza virus entry and infection require host cell N-linked glycoprotein. *Proceedings of the National Academy of Sciences of the United States of America*, **101**, 18153-18158.
Collinge, J., Palmer, M.S., Sidle, K.C., Hill, A.F., Gowland, I., Meads, J., Asante, E., Bradley, R., Doey, L.J. and Lantos, P.L. (1995) Unaltered susceptibility to BSE in transgenic mice expressing human prion protein. *Nature*, **378**, 779-783.
Collinge, J., Sidle, K.C.L., Meads, J., Ironside, J. and Hill, A.F. (1996) Molecular analysis of prion strain variation and the aetiology of 'new variant' CJD. *Nature*, **383**, 685-690.

Collinge, J., Whitfield, J., McKintosh, E., Beck, J., Mead, S., Thomas, D.J. and Alpers, M.P. (2006) Kuru in the 21st century--an acquired human prion disease with very long incubation periods. *Lancet*, **367**, 2068-2074.

Cuille, J. and Chelle, P.L. (1939) Transmission experimentale de la tremblante a la chevre. *Comptes rendus de l'Académie des sciences. La vie des sciences*, **208**, 1058-1060.

Cunningham, A.A., Kirkwood, J.K., Dawson, M., Spencer, Y.I., Green, R.B. and Wells, G.A. (2004) Bovine spongiform encephalopathy infectivity in greater kudu (Tragelaphus strepsiceros). *Emerging Infectious Diseases*, **10**, 1044-1049.

Cunningham, C., Boche, D. and Perry, V.H. (2002) Transforming growth factor beta1, the dominant cytokine in murine prion disease: influence on inflammatory cytokine synthesis and alteration of vascular extracellular matrix. *Neuropathology and Applied Neurobiology*, **28**, 107-119.

Cunningham, C., Deacon, R.M., Chan, K., Boche, D., Rawlins, J.N. and Perry, V.H. (2005) Neuropathologically distinct prion strains give rise to similar temporal profiles of behavioral deficits. *Neurobiology of Disease*, **18**, 258-269.

Davis, R.L., Shrimpton, A.E., Holohan, P.D., Bradshaw, C., Feiglin, D., Collins, G.H., Sonderegger, P., Kinter, J., Becker, L.M., Lacbawan, F., Krasnewich, D., Muenke, M., Lawrence, D.A., Yerby, M.S., Shaw, C.M., Gooptu, B., Elliott, P.R., Finch, J.T., Carrell, R.W. and Lomas, D.A. (1999) Familial dementia caused by polymerization of mutant neuroserpin. *Nature*, **401**, 376-379.

DeArmond, S.J., Mobley, W.C., DeMott, D.L., Barry, R.A., Beckstead, J.H. and Prusiner, S.B. (1987) Changes in the localization of brain prion proteins during scrapie infection. *Neurology*, **37**, 1271-1280.

DeArmond, S.J., Sanchez, H., Yehiely, F., Qiu, Y., Ninchak-Casey, A., Daggett, V., Camerino, A.P., Cayetano, J., Rogers, M., Groth, D., Torchia, M., Tremblay, P., Scott, M.R., Cohen, F.E. and Prusiner, S.B. (1997) Selective neuronal targeting in prion disease. *Neuron*, **19**, 1337-1348.

DeArmond, S.J., Yang, S.L., Lee, A., Bowler, R., Taraboulos, A., Groth, D. and Prusiner, S.B. (1993) Three scrapie prion isolates exhibit different accumulation patterns of the prion protein scrapie isoform. *Proceedings of the National Academy of Sciences of the United States of America*, **90**, 6449-6453.

Deleault, N.R., Geoghegan, J.C., Nishina, K., Kascsak, R., Williamson, R.A. and Supattapone, S. (2005) Protease-resistant prion protein amplification reconstituted with partially purified substrates and synthetic polyanions. *The Journal of Biological Chemistry*, **280**, 26873-26879.

Deleault, N.R., Lucassen, R.W. and Supattapone, S. (2003) RNA molecules stimulate prion protein conversion. *Nature*, **425**, 717-720.

Deloukas, P., Matthews, L.H., Ashurst, J., Burton, J., Gilbert, J.G., Jones, M., Stavrides, G., Almeida, J.P., Babbage, A.K., Bagguley, C.L., Bailey, J., Barlow, K.F., Bates, K.N., Beard, L.M., Beare, D.M., Beasley, O.P., Bird, C.P., Blakey, S.E., Bridgeman, A.M., Brown, A.J., Buck, D., Burrill, W., Butler, A.P., Carder, C., Carter, N.P., Chapman, J.C., Clamp, M., Clark, G., Clark, L.N., Clark, S.Y., Clee, C.M., Clegg, S., Cobley, V.E., Collier, R.E., Connor, R., Corby, N.R., Coulson, A., Coville, G.J., Deadman, R., Dhami, P., Dunn, M., Ellington, A.G., Frankland, J.A., Fraser, A., French, L., Garner, P., Grafham, D.V., Griffiths, C., Griffiths, M.N., Gwilliam, R., Hall, R.E., Hammond, S., Harley, J.L., Heath, P.D.,

Ho, S., Holden, J.L., Howden, P.J., Huckle, E., Hunt, A.R., Hunt, S.E., Jekosch, K., Johnson, C.M., Johnson, D., Kay, M.P., Kimberley, A.M., King, A., Knights, A., Laird, G.K., Lawlor, S., Lehvaslaiho, M.H., Leversha, M., Lloyd, C., Lloyd, D.M., Lovell, J.D., Marsh, V.L., Martin, S.L., McConnachie, L.J., McLay, K., McMurray, A.A., Milne, S., Mistry, D., Moore, M.J., Mullikin, J.C., Nickerson, T., Oliver, K., Parker, A., Patel, R., Pearce, T.A., Peck, A.I., Phillimore, B.J., Prathalingam, S.R., Plumb, R.W., Ramsay, H., Rice, C.M., Ross, M.T., Scott, C.E., Sehra, H.K., Shownkeen, R., Sims, S., Skuce, C.D., Smith, M.L., Soderlund, C., Steward, C.A., Sulston, J.E., Swann, M., Sycamore, N., Taylor, R., Tee, L., Thomas, D.W., Thorpe, A., Tracey, A., Tromans, A.C., Vaudin, M., Wall, M., Wallis, J.M., Whitehead, S.L., Whittaker, P., Willey, D.L., Williams, L., Williams, S.A., Wilming, L., Wray, P.W., Hubbard, T., Durbin, R.M., Bentley, D.R., Beck, S. and Rogers, J. (2001) The DNA sequence and comparative analysis of human chromosome 20. *Nature*, **414**, 865-871.

Dickinson, A.G., Fraser, H., McConnell, I., Outram, G.W., Sales, D.I. and Taylor, D.M. (1975) Extraneural competition between different scrapie agents leading to loss of infectivity. *Nature* **253**, 556.

Dickinson, A.G., Fraser, H., Meikle, V.M.H. and Outram, G.W. (1972) Competition between different scrapie agents in mice. *Nature New Biology*, **237**, 244-245.

Dickinson, A.G., Meikle, V.M.H. and Fraser, H. (1968) Identification of a gene which controls the incubation period of some strains of scrapie agent in mice. *Journal of Comparative Pathology*, **78 (3)**, 293-299.

Diener, T.O. (1972) Is the scrapie agent a viroid? *Nature: New biology*, **235**, 218-219.

Dimcheff, D.E., Askovic, S., Baker, A.H., Johnson-Fowler, C. and Portis, J.L. (2003) Endoplasmic reticulum stress is a determinant of retrovirus-induced spongiform neurodegeneration. *Journal of Virology*, **77**, 12617-12629.

Diringer, H. (1995) Proposed link between transmissible spongiform encephalopathies of man and animals. *Lancet*, **346**, 1208-1210.

Doh-Ura, K., Iwaki, T. and Caughey, B. (2000) Lysosomotropic agents and cysteine protease inhibitors inhibit scrapie-associated prion protein accumulation. *Journal of Virology*, **74**, 4894-4897.

Doh-Ura, K., Tateishi, J., Sasaki, H., Kitamoto, T. and Sakaki, Y. (1989) Pro----leu change at position 102 of prion protein is the most common but not the sole mutation related to Gerstmann-Straussler syndrome. *Biochemical and Biophysical Research Communications*, **163**, 974-979.

Donne, D.G., Viles, J.H., Groth, D., Mehlhorn, I., James, T.L., Cohen, F.E., Prusiner, S.B., Wright, P.E. and Dyson, H.J. (1997) Structure of the recombinant full-length hamster prion protein PrP(29-231): the N terminus is highly flexible. *Proceedings of the National Academy of Sciences of the United States of America*, **94**, 13452-13457.

Dorandeu, A., Wingertsmann, L., Chretien, F., Delisle, M.B., Vital, C., Parchi, P., Montagna, P., Lugaresi, E., Ironside, J.W., Budka, H., Gambetti, P. and Gray, F. (1998) Neuronal apoptosis in fatal familial insomnia. *Brain Pathology*, **8**, 531-537.

Drisaldi, B., Stewart, R.S., Adles, C., Stewart, L.R., Quaglio, E., Biasini, E., Fioriti, L., Chiesa, R. and Harris, D.A. (2003) Mutant PrP is delayed in its exit from the endoplasmic reticulum, but neither wild-type nor mutant PrP undergoes

retrotranslocation prior to proteasomal degradation. *The Journal of Biological Chemistry*, **278**, 21732-21743.

Duffy, P., Wolf, J., Collins, G., DeVoe, A.G., Streeten, B. and Cowen, D. (1974) Letter: Possible person-to-person transmission of Creutzfeldt-Jakob disease. *New England Journal of Medicine*, **290**, 692-693.

Dumpitak, C., Beekes, M., Weinmann, N., Metzger, S., Winklhofer, K.F., Tatzelt, J. and Riesner, D. (2005) The polysaccharide scaffold of PrP 27-30 is a common compound of natural prions and consists of alpha-linked polyglucose. *Biological Chemistry*, **386**, 1149-1155.

Eloit, M., Adjou, K., Coulpier, M., Fontaine, J.J., Hamel, R., Lilin, T., Messiaen, S., Andreoletti, O., Baron, T., Bencsik, A., Biacabe, A.G., Beringue, V., Laude, H., Le Dur, A., Vilotte, J.L., Comoy, E., Deslys, J.P., Grassi, J., Simon, S., Lantier, F. and Sarradin, P. (2005) BSE agent signatures in a goat. *Veterinary Record*, **156**, 523-524.

Erickson, R.R., Dunning, L.M. and Holtzman, J.L. (2006) The effect of aging on the chaperone concentrations in the hepatic, endoplasmic reticulum of male rats: the possible role of protein misfolding due to the loss of chaperones in the decline in physiological function seen with age. *The Journals of Gerontology. Series A, Biological sciences and medical sciences*, **61**, 435-443.

Ermonval, M., Mouillet-Richard, S., Codogno, P., Kellermann, O. and Botti, J. (2003) Evolving views in prion glycosylation: functional and pathological implications. *Biochimie*, **85**, 33-45.

Ertmer, A., Gilch, S., Yun, S.W., Flechsig, E., Klebl, B., Stein-Gerlach, M., Klein, M.A. and Schatzl, H.M. (2004) The tyrosine kinase inhibitor STI571 induces cellular clearance of PrPSc in prion-infected cells. *The Journal of Biological Chemistry*, **279**, 41918-41927.

Fairbairn, D.W., Carnahan, K.G., Thwaits, R.N., Grigsby, R.V., Holyoak, G.R. and O'Neill, K.L. (1994) Detection of apoptosis induced DNA cleavage in scrapie-infected sheep brain. *FEMS Microbiology Letters*, **115**, 341-346.

Falk, P.G., Bry, L., Holgersson, J. and Gordon, J.I. (1995) Expression of a human alpha-1,3/4-fucosyltransferase in the pit cell lineage of FVB/N mouse stomach results in production of Leb-containing glycoconjugates: a potential transgenic mouse model for studying Helicobacter pylori infection. *Proceedings of the National Academy of Sciences of the United States of America*, **92**, 1515-1519.

Farquhar, C.F., Somerville, R.A. and Bruce, M.E. (1998) Straining the prion hypothesis. *Nature*, **391**, 345-346.

Felton, L.M., Cunningham, C., Rankine, E.L., Waters, S., Boche, D. and Perry, V.H. (2005) MCP-1 and murine prion disease: separation of early behavioural dysfunction from overt clinical disease. *Neurobiology of Disease*, **20**, 283-295.

Fevrier, B., Vilette, D., Archer, F., Loew, D., Faigle, W., Vidal, M., Laude, H. and Raposo, G. (2004) Cells release prions in association with exosomes. *Proceedings of the National Academy of Sciences of the United States of America*, **101**, 9683-9688.

Fioriti, L., Dossena, S., Stewart, L.R., Stewart, R.S., Harris, D.A., Forloni, G. and Chiesa, R. (2005) Cytosolic prion protein (PrP) is not toxic in N2a cells and primary neurons expressing pathogenic PrP mutations. *The Journal of Biological Chemistry*, **280**, 11320-11328.

Fischer, M., Rulicke, T., Raeber, A., Sailer, A., Moser, M., Oesch, B., Brandner, S., Aguzzi, A. and Weissmann, C. (1996) Prion protein (PrP) with amino-proximal deletions restoring susceptibility of PrP knockout mice to scrapie. *The EMBO Journal*, **15**, 1255-1264.

Ford, M.J., Burton, L.J., Li, H., Graham, C.H., Frobert, Y., Grassi, J., Hall, S.M. and Morris, R.J. (2002a) A marked disparity between the expression of prion protein and its message by neurones of the CNS. *Neuroscience*, **111**, 533-551.

Ford, M.J., Burton, L.J., Morris, R.J. and Hall, S.M. (2002b) Selective expression of prion protein in peripheral tissues of the adult mouse. *Neuroscience*, **113**, 177-192.

Forloni, G., Angeretti, N., Chiesa, R., Monzani, E., Salmona, M., Bugiani, O. and Tagliavini, F. (1993) Neurotoxicity of a prion protein fragment. *Nature*, **362**, 543-546.

Foster, J., Goldmann, W., Parnham, D., Chong, A. and Hunter, N. (2001) Partial dissociation of PrP(Sc) deposition and vacuolation in the brains of scrapie and BSE experimentally affected goats. *Journal of General Virology*, **82**, 267-273.

Foster, J.D., Wilson, M. and Hunter, N. (1996) Immunolocalisation of the prion protein (PrP) in the brains of sheep with scrapie. *Veterinary Record*, **139**, 512-515.

Fournier, J.G., Escaig-Haye, F. and Grigoriev, V. (2000) Ultrastructural localization of prion proteins: physiological and pathological implications. *Microscopy Research and Technique*, **50**, 76-88.

Fraser, H. and Dickinson, A.G. (1967) Distribution of experimentally induced scrapie lesions in the brain. *Nature*, **216**, 1310-1311.

Fraser, H. and Dickinson, A.G. (1968) The sequential development of the brain lesion of scrapie in three strains of mice. *Journal of Comparative Pathology*, **78**, 301-311.

Fraser, H. and Dickinson, A.G. (1970) Pathogenesis of scrapie in the mouse: the role of the spleen. *Nature*, **226**, 462-463.

Fraser, J.R. (1996) Infectivity in extraneural tissues following intraocular scrapie infection. *Journal of General Virology*, **77 (Pt 10)**, 2663-2668.

Fraser, J.R. (2002) What is the basis of transmissible spongiform encephalopathy induced neurodegeneration and can it be repaired? *Neuropathology and Applied Neurobiology*, **28**, 1-11.

Gagneux, P., Cheriyan, M., Hurtado-Ziola, N., van der Linden, E.C.M.B., Anderson, D., McClure, H., Varki, A. and Varki, N.M. (2003) Human-specific regulation of alpha 2-6-linked sialic acids. *The Journal of Biological Chemistry*, **278**, 48245-48250.

Gajdusek, D.C., Gibbs, C.J. and Alpers, M. (1966) Experimental transmission of a Kuru-like syndrome to chimpanzees. *Nature*, **209**, 794-796.

Gajdusek, D.C. and Zigas, V. (1957) Degenerative disease of the central nervous system in New Guinea; the endemic occurrence of kuru in the native population. *New England Journal of Medicine*, **257**, 974-978.

Gambaryan, A.S., Tuzikov, A.B., Bovin, N.V., Yamnikova, S.S., Lvov, D.K., Webster, R.G. and Matrosovich, M.N. (2003) Differences between influenza virus receptors on target cells of duck and chicken and receptor specificity of the 1997 H5N1 chicken and human influenza viruses from Hong Kong. *Avian Diseases*, **47**, 1154-1160.

Gauczynski, S., Peyrin, J.M., Haik, S., Leucht, C., Hundt, C., Rieger, R., Krasemann, S., Deslys, J.P., Dormont, D., Lasmezas, C.I. and Weiss, S. (2001) The 37-kDa/67-kDa laminin receptor acts as the cell-surface receptor for the cellular prion protein. *The EMBO Journal*, **20**, 5863-5875.

Gibbs, C.J., Gajdusek, D.C. and Morris, H.R. (1965) Viral characteristics of the scrapie agent in mice. In Gadjusek, D.C., Gibbs, C.J. and Alpers, M.P. (eds.), *Slow latent and temperate virus infections*. US Goverment, Washington D.C., pp. 195-202.

Gibbs, C.J., Jr. and Gajdusek, D.C. (1973) Experimental subacute spongiform virus encephalopathies in primates and other laboratory animals. *Science*, **182**, 67-68.

Giese, A., Groschup, M.H., Hess, B. and Kretzschmar, H.A. (1995) Neuronal cell death in scrapie-infected mice is due to apoptosis. *Brain Pathology*, **5**, 213-221.

Gilch, S., Winklhofer, K.F., Groschup, M.H., Nunziante, M., Lucassen, R., Spielhaupter, C., Muranyi, W., Riesner, D., Tatzelt, J. and Schatzl, H.M. (2001) Intracellular re-routing of prion protein prevents propagation of PrP(Sc) and delays onset of prion disease. *The EMBO Journal*, **20**, 3957-3966.

Gils, A., Pedersen, K.E., Skottrup, P., Christensen, A., Naessens, D., Deinum, J., Enghild, J.J., Declerck, P.J. and Andreasen, P.A. (2003) Biochemical importance of glycosylation of plasminogen activator inhibitor-1. *Thrombosis and Haemostasis*, **90**, 206-217.

Goldberg, A.L. (2003) Protein degradation and protection against misfolded or damaged proteins. *Nature*, **426**, 895-899.

Goldfarb, L.G., Brown, P., Mitrova, E., Cervenakova, L., Goldin, L., Korczyn, A.D., Chapman, J., Galvez, S., Cartier, L., Rubenstein, R. and Gadjusek, D.C. (1991) Creutzfeldt-Jacob disease associated with the PRNP codon 200Lys mutation: an analysis of 45 families. *European Journal of Epidemiology*, **7**, 477-486.

Goldmann, W., Hunter, N., Smith, G., Foster, J. and Hope, J. (1994) PrP genotype and agent effects in scrapie: change in allelic interaction with different isolates of agent in sheep, a natural host of scrapie. *Journal of General Virology*, **75 (Pt 5)**, 989-995.

Gomi, H., Ikeda, T., Kunieda, T., Itohara, S., Prusiner, S.B. and Yamanouchi, K. (1994) Prion protein (PrP) is not involved in the pathogenesis of spongiform encephalopathy in zitter rats. *Neuroscience Letters*, **166**, 171-174.

Gossert, A.D., Bonjour, S., Lysek, D.A., Fiorito, F. and Wuthrich, K. (2005) Prion protein NMR structures of elk and of mouse/elk hybrids. *Proceedings of the National Academy of Sciences of the United States of America*, **102**, 646-650.

Govaerts, C., Wille, H., Prusiner, S.B. and Cohen, F.E. (2004) Evidence for assembly of prions with left-handed beta-helices into trimers. *Proceedings of the National Academy of Sciences of the United States of America*, **101**, 8342-8347.

Grasbon-Frodl, E., Lorenz, H., Mann, U., Nitsch, R.M., Windl, O. and Kretzschmar, H.A. (2004) Loss of glycosylation associated with the T183A mutation in human prion disease. *Acta neuropathologica (Berl)*, **108**, 476-484.

Gray, F., Chretien, F., Adle-Biassette, H., Dorandeu, A., Ereau, T., Delisle, M.B., Kopp, N., Ironside, J.W. and Vital, C. (1999) Neuronal apoptosis in Creutzfeldt-Jakob disease. *Journal of Neuropathology and Experimental Neurology*, **58**, 321-328.

Greig, J.R. (1940) Scrapie observation on the transmission of the disease by mediate contact. *The Vetertinary Journal*, **96**, 203-206.

Grenier, C., Bissonnette, C., Volkov, L. and Roucou, X. (2006) Molecular morphology and toxicity of cytoplasmic prion protein aggregates in neuronal and non-neuronal cells. *Journal of Neurochemistry*, **97**, 1456-1466.

Griffith, J.S. (1967) Self-replication and scrapie. *Nature*, **215**, 1043-1044.

Griffitts, J.S., Huffman, D.L., Whitacre, J.L., Barrows, B.D., Marroquin, L.D., Muller, R., Brown, J.R., Hennet, T., Esko, J.D. and Aroian, R.V. (2003) Resistance to a bacterial toxin is mediated by removal of a conserved glycosylation pathway required for toxin-host interactions. *The Journal of Biological Chemistry*, **278**, 45594-45602.

Guan, Z., Soderberg, M., Sindelar, P., Prusiner, S.B., Kristensson, K. and Dallner, G. (1996) Lipid composition in scrapie-infected mouse brain: prion infection increases the levels of dolichyl phosphate and ubiquinone. *Journal of Neurochemistry*, **66**, 277-285.

Gubbins, S., Clark, A.M., Eglin, R.D. and Sivam, S.K. (2006) Results of a postal survey of scrapie in the Shetland Islands in 2003. *Vetertinary Record*, **158**, 255-260.

Gunn, T.M., Inui, T., Kitada, K., Ito, S., Wakamatsu, K., He, L., Bouley, D.M., Serikawa, T. and Barsh, G.S. (2001) Molecular and phenotypic analysis of Attractin mutant mice. *Genetics*, **158**, 1683-1695.

Hachiya, N.S., Yamada, M., Watanabe, K., Jozuka, A., Ohkubo, T., Sano, K., Takeuchi, Y., Kozuka, Y., Sakasegawa, Y. and Kaneko, K. (2005) Mitochondrial localization of cellular prion protein (PrPC) invokes neuronal apoptosis in aged transgenic mice overexpressing PrPC. *Neuroscience Letters*, **374**, 98-103.

Hadlow, W.J. (1959) Scrapie and Kuru. *The Lancet*, **ii**, 289-290.

Haeberle, A.M., Ribaut-Barassin, C., Bombarde, G., Mariani, J., Hunsmann, G., Grassi, J. and Bailly, Y. (2000) Synaptic prion protein immuno-reactivity in the rodent cerebellum. *Microscopy Research and Technique*, **50**, 66-75.

Hansen, L.A., Masliah, E., Terry, R.D. and Mirra, S.S. (1989) A neuropathological subset of Alzheimer's disease with concomitant Lewy body disease and spongiform change. *Acta Neuropathologica* **78**, 194-201.

Hartsough, G.R. and Burger, D. (1965) Encephalopathy of mink. I. Epizootiologic and clinical observations. *Journal of Infectious Diseases*, **115**, 387-392.

He, L., Lu, X.Y., Jolly, A.F., Eldridge, A.G., Watson, S.J., Jackson, P.K., Barsh, G.S. and Gunn, T.M. (2003) Spongiform degeneration in mahoganoid mutant mice. *Science*, **299**, 710-712.

Head, M.W., Bunn, T.J.R., Bishop, M.T., McLoughlin, V., Lowrie, S., McKimmie, C.S., Williams, M.C., McCardle, L., MacKenzie, J., Knight, R., Will, R.G. and Ironside, J.W. (2004) Prion protein heterogeneity in sporadic but not variant Creutzfeldt-Jakob disease: UK cases 1991-2002. *Annals of Neurology*, **55**, 851-859.

Hegde, R.S., Mastrianni, J.A., Scott, M.R., DeFea, K.A., Tremblay, P., Torchia, M., DeArmond, S.J., Prusiner, S.B. and Lingappa, V.R. (1998) A transmembrane form of the prion protein in neurodegenerative disease. *Science*, **279**, 827-834.

Hegde, R.S., Tremblay, P., Groth, D., DeArmond, S.J., Prusiner, S.B. and Lingappa, V.R. (1999) Transmissible and genetic prion diseases share a common pathway of neurodegeneration. *Nature*, **402**, 822-826.

Heikenwalder, M., Zeller, N., Seeger, H., Prinz, M., Klohn, P.C., Schwarz, P., Ruddle, N.H., Weissmann, C. and Aguzzi, A. (2005) Chronic lymphocytic inflammation specifies the organ tropism of prions. *Science*, **307**, 1107-1110.

Helms, J.B. and Zurzolo, C. (2004) Lipids as targeting signals: lipid rafts and intracellular trafficking. *Traffic*, **5**, 247-254.

Heppner, F.L., Christ, A.D., Klein, M.A., Prinz, M., Fried, M., Kraehenbuhl, J.P. and Aguzzi, A. (2001) Transepithelial prion transport by M cells. *Nature Medicine*, **7**, 976-977.

Hetz, C., Russelakis-Carneiro, M., Maundrell, K., Castilla, J. and Soto, C. (2003) Caspase-12 and endoplasmic reticulum stress mediate neurotoxicity of pathological prion protein. *The EMBO Journal*, **22**, 5435-5445.

Hill, A.F. and Collinge, J. (2003) Subclinical prion infection. *Trends in Microbiology*, **11**, 578-584.

Hill, A.F., Desbruslais, M., Joiner, S., Sidle, K.C., Gowland, I., Collinge, J., Doey, L.J. and Lantos, P. (1997a) The same prion strain causes vCJD and BSE. *Nature*, **389**, 448-450, 526.

Hill, A.F., Joiner, S., Beck, J.A., Campbell, T.A., Dickinson, A., Poulter, M., Wadsworth, J.D. and Collinge, J. (2006) Distinct glycoform ratios of protease resistant prion protein associated with PRNP point mutations. *Brain*, **129**, 676-685.

Hill, A.F., Joiner, S., Linehan, J., Desbruslais, M., Lantos, P.L. and Collinge, J. (2000) Species-barrier-independent prion replication in apparently resistant species. *Proceedings of the National Academy of Sciences of the United States of America*, **97**, 10248-10253.

Hill, A.F., Sidle, K.C., Joiner, S., Keyes, P., Martin, T.C., Dawson, M. and Collinge, J. (1998) Molecular screening of sheep for bovine spongiform encephalopathy. *Neuroscience Letters*, **255**, 159-162.

Hill, A.F., Zeidler, M., Ironside, J. and Collinge, J. (1997b) Diagnosis of new variant Creutzfeldt-Jakob disease by tonsil biopsy. *Lancet*, **349**, 99-100.

Hope, J., Wood, S.C., Birkett, C.R., Chong, A., Bruce, M.E., Cairns, D., Goldmann, W., Hunter, N. and Bostock, C.J. (1999) Molecular analysis of ovine prion protein identifies similarities between BSE and an experimental isolate of natural scrapie, CH1641. *Journal of General Virology*, **80 (Pt 1)**, 1-4.

Horiuchi, M., Priola, S.A., Chabry, J. and Caughey, B. (2000) Interactions between heterologous forms of prion protein: binding, inhibition of conversion, and species barriers. *Proceedings of the National Academy of Sciences of the United States of America*, **97**, 5836-5841.

Hornemann, S., Schorn, C. and Wuthrich, K. (2004) NMR structure of the bovine prion protein isolated from healthy calf brains. *EMBO Reports*, **5**, 1159-1164.

Hoshi, K., Yoshino, H., Urata, J., Nakamura, Y., Yanagawa, H. and Sato, T. (2000) Creutzfeldt-Jakob disease associated with cadaveric dura mater grafts in Japan. *Neurology*, **55**, 718-721.

Hsiao, K., Baker, H.F., Crow, T.J., Poulter, M., Owen, F., Terwilliger, J.D., Westaway, D., Ott, J. and Prusiner, S.B. (1989) Linkage of a prion protein missense variant to Gerstmann-Straussler syndrome. *Nature*, **338**, 342-345.

Hsiao, K.K., Groth, D., Scott, M., Yang, S.L., Serban, H., Rapp, D., Foster, D., Torchia, M., Dearmond, S.J. and Prusiner, S.B. (1994) Serial transmission in rodents of neurodegeneration from transgenic mice expressing mutant prion protein. *Proceedings of the National Academy of Sciences of the United States of America*, **91**, 9126-9130.

Hsiao, K.K., Scott, M., Foster, D., Groth, D.F., DeArmond, S.J. and Prusiner, S.B. (1990) Spontaneous neurodegeneration in transgenic mice with mutant prion protein. *Science*, **250**, 1587-1590.

Huang, F.P., Farquhar, C.F., Mabbott, N.A., Bruce, M.E. and MacPherson, G.G. (2002) Migrating intestinal dendritic cells transport PrP(Sc) from the gut. *Journal of General Virology*, **83**, 267-271.

Hunter, G.D., Gibbons, R.A., Kimberlin, R.H. and Millson, G.C. (1969) Further studies of the infectivity and stability of extracts and homogenates derived from scrapie affected mouse brains. *Journal of Comparative Pathology*, **79**, 101-108.

Hunter, G.D. and Millson, G.C. (1967) Attempts to release the scrapie agent from tissue debris. *Journal of Comparative Pathology*, **77**, 301-307.

Hunter, N., Foster, J., Chong, A., McCutcheon, S., Parnham, D., Eaton, S., MacKenzie, C. and Houston, F. (2002) Transmission of prion diseases by blood transfusion. *Journal of General Virology*, **83**, 2897-2905.

Huovila, A.P., Eder, A.M. and Fuller, S.D. (1992) Hepatitis B surface antigen assembles in a post-ER, pre-Golgi compartment. *The Journal of Cell Biology*, **118**, 1305-1320.

Ironside, J.W., Head, M.W., Bell, J.E., McCardle, L. and Will, R.G. (2000) Laboratory diagnosis of variant Creutzfeldt-Jakob disease. *Histopathology*, **37**, 1-9.

Jackson, G.S., Beck, J.A., Navarrete, C., Brown, J., Sutton, P.M., Contreras, M. and Collinge, J. (2001) HLA-DQ7 antigen and resistance to variant CJD. *Nature*, **414**, 269-270.

Jamieson, E., Jeffrey, M., Ironside, J.W. and Fraser, J.R. (2001) Apoptosis and dendritic dysfunction precede prion protein accumulation in 87V scrapie. *Neuroreport*, **12**, 2147-2153.

Jarrett, J.T. and Lansbury, P.T., Jr. (1993) Seeding "one-dimensional crystallization" of amyloid: a pathogenic mechanism in Alzheimer's disease and scrapie? *Cell*, **73**, 1055-1058.

Jeffrey, M., Goodsir, C.M., Race, R.E. and Chesebro, B. (2004) Scrapie-specific neuronal lesions are independent of neuronal PrP expression. *Annals of Neurology*, **55**, 781-792.

Jimenez-Huete, A., Lievens, P.M., Vidal, R., Piccardo, P., Ghetti, B., Tagliavini, F., Frangione, B. and Prelli, F. (1998) Endogenous proteolytic cleavage of normal and disease-associated isoforms of the human prion protein in neural and non-neural tissues. *American Journal of Pathology*, **153**, 1561-1572.

Jin, T., Gu, Y., Zanusso, G., Sy, M., Kumar, A., Cohen, M., Gambetti, P. and Singh, N. (2000) The chaperone protein BiP binds to a mutant prion protein and mediates its degradation by the proteasome. *The Journal of Biological Chemistry*, **275**, 38699-38704.

Jones, E.M. and Surewicz, W.K. (2005) Fibril conformation as the basis of species- and strain-dependent seeding specificity of Mammalian prion amyloids. *Cell*, **121**, 63-72.

Kaneko, K., Zulianello, L., Scott, M., Cooper, C.M., Wallace, A.C., James, T.L., Cohen, F.E. and Prusiner, S.B. (1997) Evidence for protein X binding to a discontinuous epitope on the cellular prion protein during scrapie prion propagation. *Proceedings of the National Academy of Sciences of the United States of America*, **94**, 10069-10074.

Kang, S.C., Li, R., Wang, C., Pan, T., Liu, T., Rubenstein, R., Barnard, G., Wong, B.S. and Sy, M.S. (2003) Guanidine hydrochloride extraction and detection of prion proteins in mouse and hamster prion diseases by ELISA. *The Journal of Pathology*, **199**, 534-541.

Kapasi, Z.F., Burton, G.F., Shultz, L.D., Tew, J.G. and Szakal, A.K. (1993) Induction of functional follicular dendritic cell development in severe combined immunodeficiency mice. Influence of B and T cells. *The Journal of Immunology*, **150**, 2648-2658.

Kascsak, R.J., Rubenstein, R., Merz, P.A., Carp, R.I., Wisniewski, H.M. and Diringer, H. (1985) Biochemical differences among scrapie-associated fibrils support the biological diversity of scrapie agents. *Journal of General Virology*, **66 (Pt 8)**, 1715-1722.

Kascsak, R.J., Rubenstein, R., Merz, P.A., Tonna-DeMasi, M., Fersko, R., Carp, R.I., Wisniewski, H.M. and Diringer, H. (1987) Mouse polyclonal and monoclonal antibody to scrapie-associated fibril proteins. *Journal of Virology*, **61**, 3688-3693.

Kellershohn, N. and Laurent, M. (1998) Species barrier in prion diseases: a kinetic interpretation based on the conformational adaptation of the prion protein. *Biochemistry Journal*, **334 (Pt 3)**, 539-545.

Kilmartin, J.V., Wright, B. and Milstein, C. (1982) Rat monoclonal antitubulin antibodies derived by using a new nonsecreting rat cell line. *The Journal of Cell Biology*, **93**, 576-582.

Kim, B.M., Kim, H., Raines, R.T. and Lee, Y. (2004a) Glycosylation of onconase increases its conformational stability and toxicity for cancer cells. *Biochemical and Biophysical Research Communications*, **315**, 976-983.

Kim, H.T., Waters, K., Stoica, G., Qiang, W., Liu, N., Scofield, V.L. and Wong, P.K. (2004b) Activation of endoplasmic reticulum stress signaling pathway is associated with neuronal degeneration in MoMuLV-ts1-induced spongiform encephalomyelopathy. *Laboratory Investigation*, **84**, 816-827.

Kimberlin, R.H. and Walker, C.A. (1978a) Evidence that the transmission of one source of scrapie agent to hamsters involves separation of agent strains from a mixture. *Journal of General Virolology*, **39**, 487-496.

Kimberlin, R.H. and Walker, C.A. (1978b) Pathogenesis of mouse scrapie: effect of route of inoculation on infectivity titres and dose-response curves. *Journal of Comparative Pathology*, **88**, 39-47.

Kimberlin, R.H. and Walker, C.A. (1979) Pathogenesis of scrapie: agent multiplication in brain at the first and second passage of hamster scrapie in mice. *Journal of General Virology*, **42**, 107-117.

Kimberlin, R.H. and Walker, C.A. (1988) Incubation periods in six models of intraperitoneally injected scrapie depend mainly on the dynamics of agent replication within the nervous system and not the lymphoreticular system. *Journal of General Virology*, **69 (Pt 12)**, 2953-2960.

Kimberlin, R.H., Walker, C.A. and Fraser, H. (1989) The genomic identity of different strains of mouse scrapie is expressed in hamsters and preserved on reisolation in mice. *Journal of General Virology*, **70 (Pt 8)**, 2017-2025.

Kimberlin, R.H., Walker, C.A. and Millson, G.C. (1975) Letter: Interspecies transmission of scrapie-like diseases. *The Lancet*, **2**, 1309-1310.

King, C.Y. and Diaz-Avalos, R. (2004) Protein-only transmission of three yeast prion strains. *Nature*, **428**, 319-323.

Kirkwood, J.K. and Cunningham, A.A. (1994) Epidemiological observations on spongiform encephalopathies in captive wild animals in the British Isles. *Vetertinary Record*, **135**, 296-303.

Klein, M.A., Kaeser, P.S., Schwarz, P., Weyd, H., Xenarios, I., Zinkernagel, R.M., Carroll, M.C., Verbeek, J.S., Botto, M., Walport, M.J., Molina, H., Kalinke, U., Acha-Orbea, H. and Aguzzi, A. (2001) Complement facilitates early prion pathogenesis. *Nature Medicine*, **7**, 488-492.

Klohn, P.C., Stoltze, L., Flechsig, E., Enari, M. and Weissmann, C. (2003) A quantitative, highly sensitive cell-based infectivity assay for mouse scrapie prions. *Proceedings of the National Academy of Sciences of the United States of America*, **100**, 11666-11671.

Koch, T.K., Berg, B.O., De Armond, S.J. and Gravina, R.F. (1985) Creutzfeldt-Jakob disease in a young adult with idiopathic hypopituitarism. Possible relation to the administration of cadaveric human growth hormone. *New England Journal of Medicine*, **313**, 731-733.

Kocisko, D.A., Come, J.H., Priola, S.A., Chesebro, B., Raymond, G.J., Lansbury, P.T. and Caughey, B. (1994) Cell-free formation of protease-resistant prion protein. *Nature*, **370**, 471-474.

Kocisko, D.A., Priola, S.A., Raymond, G.J., Chesebro, B., Lansbury, P.T., Jr. and Caughey, B. (1995) Species specificity in the cell-free conversion of prion protein to protease-resistant forms: a model for the scrapie species barrier. *Proceedings of the National Academy of Sciences of the United States of America*, **92**, 3923-3927.

Korth, C., Kaneko, K., Groth, D., Heye, N., Telling, G., Mastrianni, J., Parchi, P., Gambetti, P., Will, R., Ironside, J., Heinrich, C., Tremblay, P., DeArmond, S.J. and Prusiner, S.B. (2003) Abbreviated incubation times for human prions in mice expressing a chimeric mouse-human prion protein transgene. *Proceedings of the National Academy of Sciences of the United States of America*, **100**, 4784-4789.

Korth, C., Stierli, B., Streit, P., Moser, M., Schaller, O., Fischer, R., Schulz-Schaeffer, W., Kretzschmar, H., Raeber, A., Braun, U., Ehrensperger, F., Hornemann, S., Glockshuber, R., Riek, R., Billeter, M., Wuthrich, K. and Oesch, B. (1997) Prion (PrPSc)-specific epitope defined by a monoclonal antibody. *Nature*, **390**, 74-77.

Kristiansen, M., Messenger, M.J., Klohn, P.C., Brandner, S., Wadsworth, J.D.F., Collinge, J. and Tabrizi, S.J. (2005) Disease-related prion protein forms aggresomes in neuronal cells leading to caspase activation and apoptosis. *The Journal of Biological Chemistry*, **280**, 38851-38861.

Kunz, S., Rojek, J.M., Kanagawa, M., Spiropoulou, C.F., Barresi, R., Campbell, K.P. and Oldstone, M.B. (2005) Posttranslational modification of alpha-dystroglycan, the cellular receptor for arenaviruses, by the glycosyltransferase LARGE is critical for virus binding. *Journal of Virology*, **79**, 14282-14296.

Kuwahara, C., Takeuchi, A.M., Nishimura, T., Haraguchi, K., Kubosaki, A., Matsumoto, Y., Saeki, K., Yokoyama, T., Itohara, S. and Onodera, T. (1999) Prions prevent neuronal cell-line death. *Nature*, **400**, 225-226.

Laine, J., Marc, M.E., Sy, M.S. and Axelrad, H. (2001) Cellular and subcellular morphological localization of normal prion protein in rodent cerebellum. *The European journal of neuroscience*, **14**, 47-56.

Laplanche, J.L., Lepage, V., Peoc'h, K., Deslasnerie-Laupretre, N. and Charron, D. (2003) HLA in French patients with variant Creutzfeldt-Jakob disease. *Lancet*, **361**, 531-532.

Lasmezas, C.I., Deslys, J.P., Robain, O., Jaegly, A., Beringue, V., Peyrin, J.M., Fournier, J.G., Hauw, J.J., Rossier, J. and Dormont, D. (1997) Transmission of the BSE agent to mice in the absence of detectable abnormal prion protein. *Science*, **275**, 402-405.

Laszlo, L., Lowe, J., Self, T., Kenward, N., Landon, M., McBride, T., Farquhar, C., McConnell, I., Brown, J., Hope, J. and et al. (1992) Lysosomes as key organelles in the pathogenesis of prion encephalopathies. *Journal of Pathology* **166**, 333-341.

Latarjet, R., Muel, B., Haig, D.A., Clarke, M.C. and Alper, T. (1970) Inactivation of the scrapie agent by near monochromatic ultraviolet light. *Nature*, **227**, 1341-1343.

Lawson, V.A., Priola, S.A., Wehrly, K. and Chesebro, B. (2001) N-terminal truncation of prion protein affects both formation and conformation of abnormal protease-resistant prion protein generated in vitro. *The Journal of Biological Chemistry*, **276**, 35265-35271.

Lee, T.K., Koh, A.S., Cui, Z., Pierce, R.H. and Ballatori, N. (2003) N-glycosylation controls functional activity of Oatp1, an organic anion transporter. *American journal of physiology. Gastrointestinal and liver physiology*, **285**, G371-381.

Legname, G., Baskakov, I.V., Nguyen, H.O.B., Riesner, D., Cohen, F.E., DeArmond, S.J. and Prusiner, S.B. (2004) Synthetic mammalian prions. *Science*, **305**, 673-676.

Legname, G., Nguyen, H.O.B., Baskakov, I.V., Cohen, F.E., Dearmond, S.J. and Prusiner, S.B. (2005) Strain-specified characteristics of mouse synthetic prions. *Proceedings of the National Academy of Sciences of the United States of America.*

Lehmann, S. and Harris, D.A. (1996a) Mutant and infectious prion proteins display common biochemical properties in cultured cells. *The Journal of Biological Chemistry*, **271**, 1633-1637.

Lehmann, S. and Harris, D.A. (1996b) Two mutant prion proteins expressed in cultured cells acquire biochemical properties reminiscent of the scrapie isoform. *Proceedings of the National Academy of Sciences of the United States of America*, **93**, 5610-5614.

Lehmann, S. and Harris, D.A. (1997) Blockade of glycosylation promotes acquisition of scrapie-like properties by the prion protein in cultured cells. *The Journal of Biological Chemistry*, **272**, 21479-21487.

Leucht, C., Simoneau, S., Rey, C., Vana, K., Rieger, R., Lasmezas, C.I. and Weiss, S. (2003) The 37 kDa/67 kDa laminin receptor is required for PrP(Sc) propagation in scrapie-infected neuronal cells. *EMBO Reports*, **4**, 290-295.

Li, L.B., Chen, N., Ramamoorthy, S., Chi, L., Cui, X.N., Wang, L.C. and Reith, M.E.A. (2004) The role of N-glycosylation in function and surface trafficking of

the human dopamine transporter. *The Journal of Biological Chemistry*, **279**, 21012-21020.

Liberski, P.P., Sikorska, B., Bratosiewicz-Wasik, J., Gajdusek, D.C. and Brown, P. (2004) Neuronal cell death in transmissible spongiform encephalopathies (prion diseases) revisited: from apoptosis to autophagy. *The International Journal of Biochemistry and Cell Biology*, **36**, 2473-2490.

Ligios, C., Sigurdson, C.J., Santucciu, C., Carcassola, G., Manco, G., Basagni, M., Maestrale, C., Cancedda, M.G., Madau, L. and Aguzzi, A. (2005) PrPSc in mammary glands of sheep affected by scrapie and mastitis. *Nature Medicine*, **11**, 1137-1138.

Lindquist, S. (1997) Mad cows meet psi-chotic yeast: the expansion of the prion hypothesis. *Cell*, **89**, 495-498.

Liu, T., Zwingman, T., Li, R., Pan, T., Wong, B.S., Petersen, R.B., Gambetti, P., Herrup, K. and Sy, M.S. (2001) Differential expression of cellular prion protein in mouse brain as detected with multiple anti-PrP monoclonal antibodies. *Brain Research*, **896**, 118-129.

Llewelyn, C.A., Hewitt, P.E., Knight, R.S.G., Amar, K., Cousens, S., Mackenzie, J. and Will, R.G. (2004) Possible transmission of variant Creutzfeldt-Jakob disease by blood transfusion. *Lancet*, **363**, 417-421.

Locht, C., Chesebro, B., Race, R. and Keith, J.M. (1986) Molecular cloning and complete sequence of prion protein cDNA from mouse brain infected with the scrapie agent. *Proceedings of the National Academy of Sciences of the United States of America*, **83**, 6372-6376.

Lucassen, P.J., Williams, A., Chung, W.C.J. and Fraser, H. (1995) Detection of apoptosis in murine scrapie. *Neuroscience Letters*, **198**, 185-188.

Lugaresi, E., Medori, R., Montagna, P., Baruzzi, A., Cortelli, P., Lugaresi, A., Tinuper, P., Zucconi, M. and Gambetti, P. (1986) Fatal familial insomnia and dysautonomia with selective degeneration of thalamic nuclei. *New England Journal of Medicine*, **315**, 997-1003.

Lysek, D.A., Schorn, C., Nivon, L.G., Esteve-Moya, V., Christen, B., Calzolai, L., von Schroetter, C., Fiorito, F., Herrmann, T., Guntert, P. and Wuthrich, K. (2005) Prion protein NMR structures of cats, dogs, pigs, and sheep. *Proceedings of the National Academy of Sciences of the United States of America*, **102**, 640-645.

Ma, J. and Lindquist, S. (2001) Wild-type PrP and a mutant associated with prion disease are subject to retrograde transport and proteasome degradation. *Proceedings of the National Academy of Sciences of the United States of America*, **98**, 14955-14960.

Ma, J. and Lindquist, S. (2002) Conversion of PrP to a self-perpetuating PrPSc-like conformation in the cytosol. *Science*, **298**, 1785-1788.

Ma, J., Wollmann, R. and Lindquist, S. (2002) Neurotoxicity and neurodegeneration when PrP accumulates in the cytosol. *Science*, **298**, 1781-1785.

Mabbott, N.A., Bruce, M.E., Botto, M., Walport, M.J. and Pepys, M.B. (2001) Temporary depletion of complement component C3 or genetic deficiency of C1q significantly delays onset of scrapie. *Nature Medicine*, **7**, 485-487.

Mabbott, N.A. and MacPherson, G.G. (2006) Prions and their lethal journey to the brain. *Nature Reviews Microbiology*, **4**, 201-211.

Mackay, J.M.K. and Smith, W. (1961) A case of scrapie in an uninoculated goat- a natural occurence or a contact infection. *The Veterinary Record*, **73**, 394-396.
Madore, N., Smith, K.L., Graham, C.H., Jen, A., Brady, K., Hall, S. and Morris, R. (1999) Functionally different GPI proteins are organized in different domains on the neuronal surface. *The EMBO Journal*, **18**, 6917-6926.
Mallucci, G., Dickinson, A., Linehan, J., Klohn, P.C., Brandner, S. and Collinge, J. (2003) Depleting neuronal PrP in prion infection prevents disease and reverses spongiosis. *Science*, **302**, 871-874.
Manolakou, K., Beaton, J., McConnell, I., Farquar, C., Manson, J., Hastie, N.D., Bruce, M. and Jackson, I.J. (2001) Genetic and environmental factors modify bovine spongiform encephalopathy incubation period in mice. *Proceedings of the National Academy of Sciences of the United States of America*, **98**, 7402-7407.
Manson, J., McBride, P. and Hope, J. (1992a) Expression of the PrP gene in the brain of Sinc congenic mice and its relationship to the development of scrapie. *Neurodegeneration*, **1**, 45-52.
Manson, J., West, J.D., Thomson, V., McBride, P., Kaufman, M.H. and Hope, J. (1992b) The prion protein gene: a role in mouse embryogenesis? *Development*, **115**, 117-122.
Manson, J.C., Clarke, A.R., Hooper, M.L., Aitchison, L., McConnell, I. and Hope, J. (1994a) 129/Ola mice carrying a null mutation in PrP that abolishes mRNA production are developmentally normal. *Molecular Neurobiology*, **8**, 121-127.
Manson, J.C., Clarke, A.R., McBride, P.A., McConnell, I. and Hope, J. (1994b) PrP gene dosage determines the timing but not the final intensity or distribution of lesions in scrapie pathology. *Neurodegeneration*, **3**, 331-340.
Manson, J.C., Jamieson, E., Baybutt, H., Tuzi, N.L., Barron, R., McConnell, I., Somerville, R., Ironside, J., Will, R., Sy, M.S., Melton, D.W., Hope, J. and Bostock, C. (1999) A single amino acid alteration (101L) introduced into murine PrP dramatically alters incubation time of transmissible spongiform encephalopathy. *The EMBO Journal*, **18**, 6855-6864.
Marin, M., Lavillette, D., Kelly, S.M. and Kabat, D. (2003) N-linked glycosylation and sequence changes in a critical negative control region of the ASCT1 and ASCT2 neutral amino acid transporters determine their retroviral receptor functions. *Journal of Virology*, **77**, 2936-2945.
Marsh, R.F., Bessen, R.A., Lehmann, S. and Hartsough, G.R. (1991) Epidemiological and experimental studies on a new incident of transmissible mink encephalopathy. *Journal of General Virology*, **72 (Pt 3)**, 589-594.
Mastrianni, J.A., Nixon, R., Layzer, R., Telling, G.C., Han, D., DeArmond, S.J. and Prusiner, S.B. (1999) Prion protein conformation in a patient with sporadic fatal insomnia. *New England Journal of Medicine*, **340**, 1630-1638.
Mathews, J.D., Glasse, R. and Lindenbaum, S. (1968) Kuru and cannibalism. *The Lancet*, **2**, 449-452.
Mayor, S., Rothberg, K.G. and Maxfield, F.R. (1994) Sequestration of GPI-anchored proteins in caveolae triggered by cross-linking. *Science*, **264**, 1948-1951.
McBride, P.A., Eikelenboom, P., Kraal, G., Fraser, H. and Bruce, M.E. (1992) PrP protein is associated with follicular dendritic cells of spleens and lymph nodes in uninfected and scrapie-infected mice. *Journal of Pathology*, **168**, 413-418.

McBride, P.A., Schulz-Schaeffer, W.J., Donaldson, M., Bruce, M., Diringer, H., Kretzschmar, H.A. and Beekes, M. (2001) Early spread of scrapie from the gastrointestinal tract to the central nervous system involves autonomic fibers of the splanchnic and vagus nerves. *Journal of Virology*, **75**, 9320-9327.

Meyer, R.K., Lustig, A., Oesch, B., Fatzer, R., Zurbriggen, A. and Vandevelde, M. (2000) A monomer-dimer equilibrium of a cellular prion protein (PrPC) not observed with recombinant PrP. *The Journal of Biological Chemistry*, **275**, 38081-38087.

Miller, M.W. and Williams, E.S. (2004) Chronic wasting disease of cervids. In D., H. (ed.), *Mad cow disease and related spongiform encephalopathies: Current Topics in Microbiology and Immunology*. Springer, Berlin, Vol. 284, pp. 193-214.

Millson, G.C., Hunter, G.D. and Kimberlin, R.H. (1976) The physico-chemical nature of the scrapie agent. In Kimberlin, R.H. (ed.), *Slow virus diseases of animals and man*. North-Holland Publishing Company, pp. 244-266.

Milot, E., Fraser, P. and Grosveld, F. (1996) Position effects and genetic disease. *Trends in Genetics*, **12**, 123-126.

Mironov, A., Jr., Latawiec, D., Wille, H., Bouzamondo-Bernstein, E., Legname, G., Williamson, R.A., Burton, D., DeArmond, S.J., Prusiner, S.B. and Peters, P.J. (2003) Cytosolic prion protein in neurons. *Journal of Neuroscience*, **23**, 7183-7193.

Mitra, N., Sinha, S., Ramya, T.N.C. and Surolia, A. (2006) N-linked oligosaccharides as outfitters for glycoprotein folding, form and function. *Trends in Biochemical Sciencs*.

Mohan, J., Brown, K.L., Farquhar, C.F., Bruce, M.E. and Mabbott, N.A. (2004) Scrapie transmission following exposure through the skin is dependent on follicular dendritic cells in lymphoid tissues. *Journal of Dermatological Science*, **35**, 101-111.

Monaghan, P., Watson, P.R., Cook, H., Scott, L., Wallis, T.S. and Robertson, D. (2001) An improved method for preparing thick sections for immuno/histochemistry and confocal microscopy and its use to identify rare events. *Journal of Microscopy*, **203**, 223-226.

Monari, L., Chen, S.G., Brown, P., Parchi, P., Petersen, R.B., Mikol, J., Gray, F., Cortelli, P., Montagna, P., Ghetti, B. and et al. (1994) Fatal familial insomnia and familial Creutzfeldt-Jakob disease: different prion proteins determined by a DNA polymorphism. *Proceedings of the National Academy of Sciences of the United States of America*, **91**, 2839-2842.

Monnet, C., Marthiens, V., Enslen, H., Frobert, Y., Sobel, A. and Mege, R.M. (2003) Heterogeneity and regulation of cellular prion protein glycoforms in neuronal cell lines. *European Journal of Neuroscience*, **18**, 542-548.

Montrasio, F., Frigg, R., Glatzel, M., Klein, M.A., Mackay, F., Aguzzi, A. and Weissmann, C. (2000) Impaired prion replication in spleens of mice lacking functional follicular dendritic cells. *Science*, **288**, 1257-1259.

Moore, R.C. (1997) Gene targeting studies at the mouse prion protein locus. University of Edinburgh, Edinburgh, Vol. PhD.

Moore, R.C., Hope, J., McBride, P.A., McConnell, I., Selfridge, J., Melton, D.W. and Manson, J.C. (1998) Mice with gene targetted prion protein alterations show that Prnp, Sinc and Prni are congruent. *Nature Genetics*, **18**, 118-125.

Moore, R.C., Lee, I.Y., Silverman, G.L., Harrison, P.M., Strome, R., Heinrich, C., Karunaratne, A., Pasternak, S.H., Chishti, M.A., Liang, Y., Mastrangelo, P., Wang, K., Smit, A.F.A., Katamine, S., Carlson, G.A., Cohen, F.E., Prusiner, S.B., Melton, D.W., Tremblay, P., Hood, L.E. and Westaway, D. (1999) Ataxia in prion protein (PrP)-deficient mice is associated with upregulation of the novel PrP-like protein doppel. *Journal of Molecular Biology*, **292**, 797-817.

Moore, R.C., Redhead, N.J., Selfridge, J., Hope, J., Manson, J.C. and Melton, D.W. (1995) Double replacement gene targeting for the production of a series of mouse strains with different prion protein gene alterations. *Biotechnology (N Y)*, **13**, 999-1004.

Mori, K. (2000) Tripartite management of unfolded proteins in the endoplasmic reticulum. *Cell*, **101**, 451-454.

Moudjou, M., Treguer, E., Rezaei, H., Sabuncu, E., Neuendorf, E., Groschup, M.H., Grosclaude, J. and Laude, H. (2004) Glycan-controlled epitopes of prion protein include a major determinant of susceptibility to sheep scrapie. *Journal of Virology*, **78**, 9270-9276.

Mouillet-Richard, S., Ermonval, M., Chebassier, C., Laplanche, J.L., Lehmann, S., Launay, J.M. and Kellermann, O. (2000) Signal transduction through prion protein. *Science*, **289**, 1925-1928.

Mouillet-Richard, S., Teil, C., Lenne, M., Hugon, S., Taleb, O. and Laplanche, J.L. (1999) Mutation at codon 210 (V210I) of the prion protein gene in a North African patient with Creutzfeldt-Jakob disease. *Journal of the Neurological Sciences*, **168**, 141-144.

Moya, K.L., Sales, N., Hassig, R., Creminon, C., Grassi, J. and Di Giamberardino, L. (2000) Immunolocalization of the cellular prion protein in normal brain. *Microscopy Research and Technique*, **50**, 58-65.

Muramoto, T., Kitamoto, T., Hoque, M.Z., Tateishi, J. and Goto, I. (1993) Species barrier prevents an abnormal isoform of prion protein from accumulating in follicular dendritic cells of mice with Creutzfeldt-Jakob disease. *Journal of Virology*, **67**, 6808-6810.

Nakamura, N., Rabouille, C., Watson, R., Nilsson, T., Hui, N., Slusarewicz, P., Kreis, T.E. and Warren, G. (1995) Characterization of a cis-Golgi matrix protein, GM130. *Journal of Cell Biology*, **131**, 1715-1726.

Nazor, K.E., Kuhn, F., Seward, T., Green, M., Zwald, D., Purro, M., Schmid, J., Biffiger, K., Power, A.M., Oesch, B., Raeber, A.J. and Telling, G.C. (2005) Immunodetection of disease-associated mutant PrP, which accelerates disease in GSS transgenic mice. *The EMBO Journal*, **24**, 2472-2480.

Neuendorf, E., Weber, A., Saalmueller, A., Schatzl, H., Reifenberg, K., Pfaff, E. and Groschup, M.H. (2004) Glycosylation deficiency at either one of the two glycan attachment sites of cellular prion protein preserves susceptibility to bovine spongiform encephalopathy and scrapie infections. *The Journal of Biological Chemistry*, **279**, 53306-53316.

Nielsen, D., Gyllberg, H., Ostlund, P., Bergman, T. and Bedecs, K. (2004) Increased levels of insulin and insulin-like growth factor-1 hybrid receptors and decreased glycosylation of the insulin receptor alpha- and beta-subunits in scrapie-infected neuroblastoma N2a cells. *Biochemistry Journal*, **380**, 571-579.

Nieto, A., Goldfarb, L.G., Brown, P., McCombie, W.R., Trapp, S., Asher, D.M. and Gajdusek, D.C. (1991) Codon 178 mutation in ethnically diverse Creutzfeldt-Jakob disease families. *Lancet*, **337**, 622-623.

Nishida, N., Katamine, S. and Manuelidis, L. (2005) Reciprocal interference between specific CJD and scrapie agents in neural cell cultures. *Science*, **310**, 493-496.

Nitrini, R., Rosemberg, S., Passos-Bueno, M.R., da Silva, L.S.T., Iughetti, P., Papadopoulos, M., Carrilho, P.M., Caramelli, P., Albrecht, S., Zatz, M. and LeBlanc, A. (1997) Familial spongiform encephalopathy associated with a novel prion protein gene mutation. *Annals of Neurology*, **42**, 138-146.

Nonno, R., Bari, M.A., Cardone, F., Vaccari, G., Fazzi, P., Dell'omo, G., Cartoni, C., Ingrosso, L., Boyle, A., Galeno, R., Sbriccoli, M., Lipp, H.P., Bruce, M., Pocchiari, M. and Agrimi, U. (2006) Efficient transmission and characterization of creutzfeldt-jakob disease strains in bank voles. *PLoS Pathogens*, **2**, e12.

Notari, S., Capellari, S., Giese, A., Westner, I., Baruzzi, A., Ghetti, B., Gambetti, P., Kretzschmar, H.A. and Parchi, P. (2004) Effects of different experimental conditions on the PrPSc core generated by protease digestion: implications for strain typing and molecular classification of CJD. *Journal of Biological Chemistry*, **279**, 16797-16804.

Novitskaya, V., Bocharova, O.V., Bronstein, I. and Baskakov, I.V. (2006) Amyloid fibrils of mammalian prion protein are highly toxic to cultured cells and primary neurons. *The Journal of Biological Chemistry*, **281**, 13828-13836.

Nunziante, M., Gilch, S. and Schatzl, H.M. (2003) Essential role of the prion protein N terminus in subcellular trafficking and half-life of cellular prion protein. *The Journal of Biological Chemistry*, **278**, 3726-3734.

Oesch, B., Westaway, D., Walchli, M., McKinley, M.P., Kent, S.B., Aebersold, R., Barry, R.A., Tempst, P., Teplow, D.B., Hood, L.E. and et al. (1985) A cellular gene encodes scrapie PrP 27-30 protein. *Cell*, **40**, 735-746.

Oliver, J.D., van der Wal, F.J., Bulleid, N.J. and High, S. (1997) Interaction of the thiol-dependent reductase ERp57 with nascent glycoproteins. *Science*, **275**, 86-88.

Owen, F., Poulter, M., Lofthouse, R., Collinge, J., Crow, T.J., Risby, D., Baker, H.F., Ridley, R.M., Hsiao, K. and Prusiner, S.B. (1989) Insertion in prion protein gene in familial Creutzfeldt-Jakob disease. *Lancet*, **1**, 51-52.

Oyadomari, S. and Mori, M. (2004) Roles of CHOP/GADD153 in endoplasmic reticulum stress. *Cell death and differentiation.*, **11**, 381-389.

Palmer, M.S., Dryden, A.J., Hughes, J.T. and Collinge, J. (1991) Homozygous prion protein genotype predisposes to sporadic Creutzfeldt-Jakob disease. *Nature*, **352**, 340-342.

Pan, K.M., Baldwin, M., Nguyen, J., Gasset, M., Serban, A., Groth, D., Mehlhorn, I., Huang, Z., Fletterick, R.J., Cohen, F.E. and Prusiner, S.B. (1993) Conversion of alpha-helices into beta-sheets features in the formation of the scrapie prion proteins. *Proceedings of the National Academy of Sciences of the United States of America*, **90**, 10962-10966.

Pan, T., Li, R., Wong, B.S., Liu, T., Gambetti, P. and Sy, M.S. (2002) Heterogeneity of normal prion protein in two- dimensional immunoblot: presence of various glycosylated and truncated forms. *Journal of Neurochemistry*, **81**, 1092-1101.

Pankiewicz, J., Prelli, F., Sy, M.S., Kascsak, R.J., Kascsak, R.B., Spinner, D.S., Carp, R.I., Meeker, H.C., Sadowski, M. and Wisniewski, T. (2006) Clearance and

prevention of prion infection in cell culture by anti-PrP antibodies. *European Journal of Neuroscience*, **23**, 2635-2647.

Parchi, P., Castellani, R., Capellari, S., Ghetti, B., Young, K., Chen, S.G., Farlow, M., Dickson, D.W., Sima, A.A., Trojanowski, J.Q., Petersen, R.B. and Gambetti, P. (1996) Molecular basis of phenotypic variability in sporadic Creutzfeldt-Jakob disease. *Annals of Neurology*, **39**, 767-778.

Parchi, P., Giese, A., Capellari, S., Brown, P., Schulz-Schaeffer, W., Windl, O., Zerr, I., Budka, H., Kopp, N., Piccardo, P., Poser, S., Rojiani, A., Streichemberger, N., Julien, J., Vital, C., Ghetti, B., Gambetti, P. and Kretzschmar, H. (1999) Classification of sporadic Creutzfeldt-Jakob disease based on molecular and phenotypic analysis of 300 subjects. *Annals of Neurology*, **46**, 224-233.

Parkin, E.T., Watt, N.T., Turner, A.J. and Hooper, N.M. (2004) Dual mechanisms for shedding of the cellular prion protein. *The Journal of Biological Chemistry*, **279**, 11170-11178.

Pattison, I.H. (1965) Experiments with scrapie with special reference to the nature of the agent and the pathology of the disease. *NINDB Monograph*, **2**, 249-257.

Pattison, I.H. and Millson, G.C. (1961) Scrapie produced experimentally in goats with special reference to the clinical syndrome. *Journal of Comparative Pathology*, **71**, 101-109.

Pauly, P.C. and Harris, D.A. (1998) Copper stimulates endocytosis of the prion protein. *The Journal of Biological Chemistry*, **273**, 33107-33110.

Peden, A.H., Head, M.W., Ritchie, D.L., Bell, J.E. and Ironside, J.W. (2004) Preclinical vCJD after blood transfusion in a PRNP codon 129 heterozygous patient. *Lancet*, **364**, 527-529.

Pepys, M.B., Bybee, A., Booth, D.R., Bishop, M.T., Will, R., Little, A.M., Prokupek, B. and Madrigal, J.A. (2003) MHC typing in variant Cretzfeldt-Jakob disease. *Lancet*, **361**, 487-489.

Peretz, D., Williamson, R.A., Kaneko, K., Vergara, J., Leclerc, E., Schmitt-Ulms, G., Mehlhorn, I.R., Legname, G., Wormald, M.R., Rudd, P.M., Dwek, R.A., Burton, D.R. and Prusiner, S.B. (2001) Antibodies inhibit prion propagation and clear cell cultures of prion infectivity. *Nature*, **412**, 739-743.

Peretz, D., Williamson, R.A., Legname, G., Matsunaga, Y., Vergara, J., Burton, D.R., DeArmond, S.J., Prusiner, S.B. and Scott, M.R. (2002) A change in the conformation of prions accompanies the emergence of a new prion strain. *Neuron*, **34**, 921-932.

Peters, P.J., Mironov, A., Jr., Peretz, D., van Donselaar, E., Leclerc, E., Erpel, S., DeArmond, S.J., Burton, D.R., Williamson, R.A., Vey, M. and Prusiner, S.B. (2003) Trafficking of prion proteins through a caveolae-mediated endosomal pathway. *The Journal of Cell Biology*, **162**, 703-717.

Petersen, R.B., Parchi, P., Richardson, S.L., Urig, C.B. and Gambetti, P. (1996) Effect of the D178N mutation and the codon 129 polymorphism on the metabolism of the prion protein. *The Journal of Biological Chemistry*, **271**, 12661-12668.

Petraroli, R. and Pocchiari, M. (1996) Codon 219 polymorphism of PRNP in healthy Caucasians and Creutzfeldt-Jakob disease patients. *American Journal of Human Genetics*, **58**, 888-889.

Petrescu, A.J., Milac, A.L., Petrescu, S.M., Dwek, R.A. and Wormald, M.R. (2004) Statistical analysis of the protein environment of N-glycosylation sites: implications for occupancy, structure, and folding. *Glycobiology*, **14**, 103-114.

Piccardo, P., Safar, J., Ceroni, M., Gajdusek, D.C. and Gibbs, C.J., Jr. (1990) Immunohistochemical localization of prion protein in spongiform encephalopathies and normal brain tissue. *Neurology*, **40**, 518-522.

Piening, N., Nonno, R., Di Bari, M., Walter, S., Windl, O., Agrimi, U., Kretzschmar, H.A. and Bertsch, U. (2006) Conversion efficiency of bank vole prion protein in vitro is determined by residues 155 and 170, but does not correlate with the high susceptibility of bank voles to sheep scrapie in vivo. *The Journal of Biological Chemistry*, **281**, 9373-9384.

Pinheiro, T.J. (2006) The role of rafts in the fibrillization and aggregation of prions. *Chemistry and Physics of Lipids*, **141**, 66-71.

Poulter, M., Baker, H.F., Frith, C.D., Leach, M., Lofthouse, R., Ridley, R.M., Shah, T., Owen, F., Collinge, J., Brown, J. and et al. (1992) Inherited prion disease with 144 base pair gene insertion. 1. Genealogical and molecular studies. *Brain*, **115 (Pt 3)**, 675-685.

Prinz, M., Heikenwalder, M., Junt, T., Schwarz, P., Glatzel, M., Heppner, F.L., Fu, Y.X., Lipp, M. and Aguzzi, A. (2003) Positioning of follicular dendritic cells within the spleen controls prion neuroinvasion. *Nature*, **425**, 957-962.

Priola, S.A. and Lawson, V.A. (2001) Glycosylation influences cross-species formation of protease-resistant prion protein. *The EMBO Journal*, **20**, 6692-6699.

Prusiner, S.B. (1991) Molecular biology of prion diseases. *Science*, **252**, 1515-1522.

Prusiner, S.B., Groth, D.F., Cochran, S.P., McKinley, M.P. and Masiarz, F.R. (1980) Gel electrophoresis and glass permeation chromatography of the hamster scrapie agent after enzymatic digestion and detergent extraction. *Biochemistry*, **19**, 4892-4898.

Prusiner, S.B., Scott, M., Foster, D., Pan, K.M., Groth, D., Mirenda, C., Torchia, M., Yang, S.L., Serban, D., Carlson, G.A. and et al. (1990) Transgenetic studies implicate interactions between homologous PrP isoforms in scrapie prion replication. *Cell*, **63**, 673-686.

Puoti, G., Giaccone, G., Mangieri, M., Limido, L., Fociani, P., Zerbi, P., Suardi, S., Rossi, G., Iussich, S., Capobianco, R., Di Fede, G., Marcon, G., Cotrufo, R., Filippini, G., Bugiani, O. and Tagliavini, F. (2005) Sporadic Creutzfeldt-Jakob disease: the extent of microglia activation is dependent on the biochemical type of PrPSc. *Journal of Neuropathology and Experimental Neurology*, **64**, 902-909.

Puoti, G., Giaccone, G., Rossi, G., Canciani, B., Bugiani, O. and Tagliavini, F. (1999) Sporadic Creutzfeldt-Jakob disease: co-occurrence of different types of PrP(Sc) in the same brain. *Neurology*, **53**, 2173-2176.

Race, R., Raines, A., Raymond, G.J., Caughey, B. and Chesebro, B. (2001) Long-term subclinical carrier state precedes scrapie replication and adaptation in a resistant species: analogies to bovine spongiform encephalopathy and variant Creutzfeldt-Jakob disease in humans. *Journal of Virology*, **75**, 10106-10112.

Rane, N.S., Yonkovich, J.L. and Hegde, R.S. (2004) Protection from cytosolic prion protein toxicity by modulation of protein translocation. *The EMBO Journal*, **23**, 4550-4559.

Raymond, G.J., Bossers, A., Raymond, L.D., O'Rourke, K.I., McHolland, L.E., Bryant, P.K., III, Miller, M.W., Williams, E.S., Smits, M. and Caughey, B. (2000) Evidence of a molecular barrier limiting susceptibility of humans, cattle and sheep to chronic wasting disease. *The EMBO Journal*, **19**, 4425-4430.

Raymond, G.J., Hope, J., Kocisko, D.A., Priola, S.A., Raymond, L.D., Bossers, A., Ironside, J., Will, R.G., Chen, S.G., Petersen, R.B., Gambetti, P., Rubenstein, R., Smits, M.A., Lansbury, P.T., Jr. and Caughey, B. (1997) Molecular assessment of the potential transmissibilities of BSE and scrapie to humans. *Nature*, **388**, 285-288.

Rieger, R., Edenhofer, F., Lasmezas, C.I. and Weiss, S. (1997) The human 37-kDa laminin receptor precursor interacts with the prion protein in eukaryotic cells. *Nature Medicine*, **3**, 1383-1388.

Riek, R., Hornemann, S., Wider, G., Billeter, M., Glockshuber, R. and Wuthrich, K. (1996) NMR structure of the mouse prion protein domain PrP(121-321). *Nature*, **382**, 180-182.

Riek, R., Hornemann, S., Wider, G., Glockshuber, R. and Wuthrich, K. (1997) NMR characterization of the full-length recombinant murine prion protein, mPrP(23-231). *FEBS Letters*, **413**, 282-288.

Rivera-Milla, E., Stuermer, C.A.O. and Malaga-Trillo, E. (2003) An evolutionary basis for scrapie disease: identification of a fish prion mRNA. *Trends in Genetics*, **19**, 72-75.

Roberts, C., Platt, N., Streit, A., Schachner, M. and Stern, C.D. (1991) The L5 epitope: an early marker for neural induction in the chick embryo and its involvement in inductive interactions. *Development*, **112**, 959-970.

Rodolfo, K., Hassig, R., Moya, K.L., Frobert, Y., Grassi, J. and Di Giamberardino, L. (1999) A novel cellular prion protein isoform present in rapid anterograde axonal transport. *Neuroreport*, **10**, 3639-3644.

Rogers, M., Taraboulos, A., Scott, M., Groth, D. and Prusiner, S.B. (1990) Intracellular accumulation of the cellular prion protein after mutagenesis of its Asn-linked glycosylation sites. *Glycobiology*, **1**, 101-109.

Ross, E.D., Minton, A. and Wickner, R.B. (2005) Prion domains: sequences, structures and interactions. *Nature Cell Biology*, **7**, 1039-1044.

Roucou, X., Guo, Q., Zhang, Y., Goodyer, C.G. and LeBlanc, A.C. (2003) Cytosolic prion protein is not toxic and protects against Bax-mediated cell death in human primary neurons. *The Journal of Biological Chemistry*.

Rousseau, E., Dehay, B., Ben-Haiem, L., Trottier, Y., Morange, M. and Bertolotti, A. (2004) Targeting expression of expanded polyglutamine proteins to the endoplasmic reticulum or mitochondria prevents their aggregation. *Proceedings of the National Academy of Sciences of the United States of America*, **101**, 9648-9653.

Rudd, P.M., Endo, T., Colominas, C., Groth, D., Wheeler, S.F., Harvey, D.J., Wormald, M.R., Serban, H., Prusiner, S.B., Kobata, A. and Dwek, R.A. (1999) Glycosylation differences between the normal and pathogenic prion protein isoforms. *Proceedings of the National Academy of Sciences of the United States of America.*, **96**, 13044-13049.

Rudd, P.M., Wormald, M.R., Wing, D.R., Prusiner, S.B. and Dwek, R.A. (2001) Prion glycoprotein: structure, dynamics, and roles for the sugars. *Biochemistry*, **40**, 3759-3766.

Russelakis-Carneiro, M., Saborio, G.P., Anderes, L. and Soto, C. (2002) Changes in the glycosylation pattern of prion protein in murine scrapie. Implications for the mechanism of neurodegeneration in prion diseases. *The Journal of Biological Chemistry*, **277**, 36872-36877.

Saborio, G.P., Soto, C., Kascsak, R.J., Levy, E., Kascsak, R., Harris, D.A. and Frangione, B. (1999) Cell-lysate conversion of prion protein into its protease-resistant isoform suggests the participation of a cellular chaperone. *Biochemical and Biophysical Research Communications*, **258**, 470-475.

Safar, J., Wille, H., Itri, V., Groth, D., Serban, H., Torchia, M., Cohen, F.E. and Prusiner, S.B. (1998) Eight prion strains have PrP(Sc) molecules with different conformations. *Nature Medicine*, **4**, 1157-1165.

Safar, J.G., DeArmond, S.J., Kociuba, K., Deering, C., Didorenko, S., Bouzamondo-Bernstein, E., Prusiner, S.B. and Tremblay, P. (2005) Prion clearance in bigenic mice. *Journal of General Virology*, **86**, 2913-2923.

Sakaguchi, S., Katamine, S., Nishida, N., Moriuchi, R., Shigematsu, K., Sugimoto, T., Nakatani, A., Kataoka, Y., Houtani, T., Shirabe, S., Okada, H., Hasegawa, S., Miyamoto, T. and Noda, T. (1996) Loss of cerebellar Purkinje cells in aged mice homozygous for a disrupted PrP gene. *Nature*, **380**, 528-531.

Sales, N., Rodolfo, K., Hassig, R., Faucheux, B., Di Giamberardino, L. and Moya, K.L. (1998) Cellular prion protein localization in rodent and primate brain. *European Journal of Neuroscience*, **10**, 2464-2471.

Santuccione, A., Sytnyk, V., Leshchyns'ka, I. and Schachner, M. (2005) Prion protein recruits its neuronal receptor NCAM to lipid rafts to activate p59fyn and to enhance neurite outgrowth. *Journal of Cell Biology*, **169**, 341-354.

Sarradett. (1883) Un cas de tramblante sur un boeuf. *Revue Veterinarire (Toulouse)*, **3**, 310-312.

Schmitt-Ulms, G., Legname, G., Baldwin, M.A., Ball, H.L., Bradon, N., Bosque, P.J., Crossin, K.L., Edelman, G.M., DeArmond, S.J., Cohen, F.E. and Prusiner, S.B. (2001) Binding of neural cell adhesion molecules (N-CAMs) to the cellular prion protein. *Journal of Molecular Biology*, **314**, 1209-1225.

Schultz, J., Schwarz, A., Neidhold, S., Burwinkel, M., Riemer, C., Simon, D., Kopf, M., Otto, M. and Baier, M. (2004) Role of interleukin-1 in prion disease-associated astrocyte activation. *American Journal of Pathology*, **165**, 671-678.

Scott, M., Foster, D., Mirenda, C., Serban, D., Coufal, F., Walchli, M., Torchia, M., Groth, D., Carlson, G., DeArmond, S.J., Westaway, D. and Prusiner, S.B. (1989) Transgenic mice expressing hamster prion protein produce species-specific scrapie infectivity and amyloid plaques. *Cell*, **59**, 847-857.

Scott, M., Groth, D., Foster, D., Torchia, M., Yang, S.L., DeArmond, S.J. and Prusiner, S.B. (1993) Propagation of prions with artificial properties in transgenic mice expressing chimeric PrP genes. *Cell*, **73**, 979-988.

Seeger, H., Heikenwalder, M., Zeller, N., Kranich, J., Schwarz, P., Gaspert, A., Seifert, B., Miele, G. and Aguzzi, A. (2005) Coincident scrapie infection and nephritis lead to urinary prion excretion. *Science*, **310**, 324-326.

Shmerling, D., Hegyi, I., Fischer, M., Blattler, T., Brandner, S., Gotz, J., Rulicke, T., Flechsig, E., Cozzio, A., von Mering, C., Hangartner, C., Aguzzi, A. and Weissmann, C. (1998) Expression of amino-terminally truncated PrP in the mouse leading to ataxia and specific cerebellar lesions. *Cell*, **93**, 203-214.

Shyng, S.L., Heuser, J.E. and Harris, D.A. (1994) A glycolipid-anchored prion protein is endocytosed via clathrin-coated pits. *The Journal of Cell Biology*, **125**, 1239-1250.

Shyng, S.L., Huber, M.T. and Harris, D.A. (1993) A prion protein cycles between the cell surface and an endocytic compartment in cultured neuroblastoma cells. *The Journal of Biological Chemistry*, **268**, 15922-15928.

Shyng, S.L., Lehmann, S., Moulder, K.L. and Harris, D.A. (1995) Sulfated glycans stimulate endocytosis of the cellular isoform of the prion protein, PrPC, in cultured cells. *The Journal of Biological Chemistry*, **270**, 30221-30229.

Sigurdson, C.J., Barillas-Mury, C., Miller, M.W., Oesch, B., van Keulen, L.J.M., Langeveld, J.P.M. and Hoover, E.A. (2002) PrP(CWD) lymphoid cell targets in early and advanced chronic wasting disease of mule deer. *Journal of General Virology*, **83**, 2617-2628.

Sigurdson, C.J. and Miller, M.W. (2003) Other animal prion diseases. *British Medical Bulletin*, **66**, 199-212.

Silveira, J.R., Raymond, G.J., Hughson, A.G., Race, R.E., Sim, V.L., Hayes, S.F. and Caughey, B. (2005) The most infectious prion protein particles. *Nature*, **437**, 257-261.

Simons, K. and van Meer, G. (1988) Lipid sorting in epithelial cells. *Biochemistry*, **27**, 6197-6202.

Singh, N., Zanusso, G., Chen, S.G., Fujioka, H., Richardson, S., Gambetti, P. and Petersen, R.B. (1997) Prion protein aggregation reverted by low temperature in transfected cells carrying a prion protein gene mutation. *The Journal of Biological Chemistry*, **272**, 28461-28470.

Sitia, R. and Braakman, I. (2003) Quality control in the endoplasmic reticulum protein factory. *Nature*, **426**, 891-894.

Sofroniew, M.V. (2005) Reactive astrocytes in neural repair and protection. *Neuroscientist*, **11**, 400-407.

Solforosi, L., Criado, J.R., McGavern, D.B., Wirz, S., Sanchez-Alavez, M., Sugama, S., DeGiorgio, L.A., Volpe, B.T., Wiseman, E., Abalos, G., Masliah, E., Gilden, D., Oldstone, M.B., Conti, B. and Williamson, R.A. (2004) Cross-linking cellular prion protein triggers neuronal apoptosis in vivo. *Science*, **303**, 1514-1516.

Somerville, R.A. (1999) Host and transmissible spongiform encephalopathy agent strain control glycosylation of PrP. *Journal of General Virology*, **80 (Pt 7)**, 1865-1872.

Somerville, R.A., Chong, A., Mulqueen, O.U., Birkett, C.R., Wood, S.C. and Hope, J. (1997) Biochemical typing of scrapie strains. *Nature*, **386**, 564.

Somerville, R.A., Oberthur, R.C., Havekost, U., MacDonald, F., Taylor, D.M. and Dickinson, A.G. (2002) Characterization of thermodynamic diversity between transmissible spongiform encephalopathy agent strains and its theoretical implications. *The Journal of Biological Chemistry*, **277**, 11084-11089.

Soto, C. (2006) *Prions the new biology of proteins*. Taylor and Francis.

Soto, C., Anderes, L., Suardi, S., Cardone, F., Castilla, J., Frossard, M.J., Peano, S., Saa, P., Limido, L., Carbonatto, M., Ironside, J., Torres, J.M., Pocchiari, M. and Tagliavini, F. (2005) Pre-symptomatic detection of prions by cyclic amplification of protein misfolding. *Federation of European Biochemical Societies Letters*, **579**, 638-642.

Spielhaupter, C. and Schatzl, H.M. (2001) PrPC directly interacts with proteins involved in signaling pathways. *The Journal of Biological Chemistry*, **276**, 44604-44612.

Spraker, T.R., Miller, M.W., Williams, E.S., Getzy, D.M., Adrian, W.J., Schoonveld, G.G., Spowart, R.A., O'Rourke, K.I., Miller, J.M. and Merz, P.A. (1997) Spongiform encephalopathy in free-ranging mule deer (Odocoileus hemionus), white-tailed deer (Odocoileus virginianus) and Rocky Mountain elk (Cervus elaphus nelsoni) in northcentral Colorado. *Journal of Wildlife Diseases*, **33**, 1-6.

Stahl, N., Baldwin, M.A., Burlingame, A.L. and Prusiner, S.B. (1990) Identification of glycoinositol phospholipid linked and truncated forms of the scrapie prion protein. *Biochemistry*, **29**, 8879-8884.

Stahl, N., Baldwin, M.A., Teplow, D.B., Hood, L., Gibson, B.W., Burlingame, A.L. and Prusiner, S.B. (1993) Structural studies of the scrapie prion protein using mass spectrometry and amino acid sequencing. *Biochemistry*, **32**, 1991-2002.

Stahl, N., Borchelt, D.R., Hsiao, K. and Prusiner, S.B. (1987) Scrapie prion protein contains a phosphatidylinositol glycolipid. *Cell*, **51**, 229-240.

Stansfield, I., Jones, K.M., Kushnirov, V.V., Dagkesamanskaya, A.R., Poznyakovski, A.I., Paushkin, S.V., Nierras, C.R., Cox, B.S., Ter-Avanesyan, M.D. and Tuite, M.F. (1995) The products of the SUP45 (eRF1) and SUP35 genes interact to mediate translation termination in Saccharomyces cerevisiae. *The EMBO Journal*, **14**, 4365-4373.

Stathopulos, P.B., Scholz, G.A., Hwang, Y.M., Rumfeldt, J.A.O., Lepock, J.R. and Meiering, E.M. (2004) Sonication of proteins causes formation of aggregates that resemble amyloid. *Protein Science*, **13**, 3017-3027.

Stefani, M. and Dobson, C.M. (2003) Protein aggregation and aggregate toxicity: new insights into protein folding, misfolding diseases and biological evolution. *Journal of Molecular Medicine*, **81**, 678-699.

Stewart, R.S. and Harris, D.A. (2001) Most pathogenic mutations do not alter the membrane topology of the prion protein. *The Journal of Biological Chemistry*, **276**, 2212-2220.

Stewart, R.S. and Harris, D.A. (2005) A transmembrane form of the prion protein is localized in the Golgi apparatus of neurons. *The Journal of Biological Chemistry*, **280**, 15855-15864.

Stimson, E., Hope, J., Chong, A. and Burlingame, A.L. (1999) Site-specific characterization of the N-linked glycans of murine prion protein by high-performance liquid chromatography/electrospray mass spectrometry and exoglycosidase digestions. *Biochemistry*, **38**, 4885-4895.

Sunyach, C., Jen, A., Deng, J., Fitzgerald, K.T., Frobert, Y., Grassi, J., McCaffrey, M.W. and Morris, R. (2003) The mechanism of internalization of glycosylphosphatidylinositol-anchored prion protein. *The EMBO Journal*, **22**, 3591-3601.

Supattapone, S., Nguyen, H.O., Cohen, F.E., Prusiner, S.B. and Scott, M.R. (1999) Elimination of prions by branched polyamines and implications for therapeutics. *Proceedings of the National Academy of Sciences of the United States of America.*, **96**, 14529-14534.

Supattapone, S., Wille, H., Uyechi, L., Safar, J., Tremblay, P., Szoka, F.C., Cohen, F.E., Prusiner, S.B. and Scott, M.R. (2001) Branched polyamines cure prion-infected neuroblastoma cells. *Journal of Virology*, **75**, 3453-3461.

Swanton, E., High, S. and Woodman, P. (2003) Role of calnexin in the glycan-independent quality control of proteolipid protein. *The EMBO Journal*, **22**, 2948-2958.

Sweeney, T., Kuczius, T., McElroy, M., Gomez Parada, M. and Groschup, M.H. (2000) Molecular analysis of Irish sheep scrapie cases. *Journal of General Virology*, **81**, 1621-1627.

Tagliavini, F., Prelli, F., Porro, M., Salmona, M., Bugiani, O. and Frangione, B. (1992) A soluble form of prion protein in human cerebrospinal fluid: implications for prion-related encephalopathies. *Biochemical and Biophysical Research Communications*, **184**, 1398-1404.

Taguchi, Y., Mohri, S., Ironside, J.W., Muramoto, T. and Kitamoto, T. (2003) Humanized knock-in mice expressing chimeric prion protein showed varied susceptibility to different human prions. *American Journal of Pathology*, **163**, 2585-2593.

Tanaka, M., Chien, P., Naber, N., Cooke, R. and Weissman, J.S. (2004) Conformational variations in an infectious protein determine prion strain differences. *Nature*, **428**, 323-328.

Taraboulos, A., Jendroska, K., Serban, D., Yang, S.L., DeArmond, S.J. and Prusiner, S.B. (1992a) Regional mapping of prion proteins in brain. *Proceedings of the National Academy of Sciences of the United States of America.*, **89**, 7620-7624.

Taraboulos, A., Raeber, A.J., Borchelt, D.R., Serban, D. and Prusiner, S.B. (1992b) Synthesis and trafficking of prion proteins in cultured cells. *Molecular Biology of the Cell*, **3**, 851-863.

Taraboulos, A., Rogers, M., Borchelt, D.R., McKinley, M.P., Scott, M., Serban, D. and Prusiner, S.B. (1990a) Acquisition of protease resistance by prion proteins in scrapie-infected cells does not require asparagine-linked glycosylation. *Proceedings of the National Academy of Sciences of the United States of America*, **87**, 8262-8266.

Taraboulos, A., Scott, M., Semenov, A., Avrahami, D., Laszlo, L. and Prusiner, S.B. (1995) Cholesterol depletion and modification of COOH-terminal targeting sequence of the prion protein inhibit formation of the scrapie isoform. *The Journal of Cell Biology*, **129**, 121-132.

Taraboulos, A., Serban, D. and Prusiner, S.B. (1990b) Scrapie prion proteins accumulate in the cytoplasm of persistently infected cultured cells. *The Journal of Cell Biology*, **110**, 2117-2132.

Taylor, D.R., Watt, N.T., Perera, W.S. and Hooper, N.M. (2005) Assigning functions to distinct regions of the N-terminus of the prion protein that are involved in its copper-stimulated, clathrin-dependent endocytosis. *Journal of Cell Science*, **118**, 5141-5153.

Taylor, M.E. and Drickamer, K. (2003) *Introduction to Glycobiology*. Oxford University Press, Oxford.

Telling, G.C., Scott, M., Hsiao, K.K., Foster, D., Yang, S.L., Torchia, M., Sidle, K.C., Collinge, J., DeArmond, S.J. and Prusiner, S.B. (1994) Transmission of Creutzfeldt-Jakob disease from humans to transgenic mice expressing chimeric

human-mouse prion protein. *Proceedings of the National Academy of Sciences of the United States of America*, **91**, 9936-9940.

Telling, G.C., Scott, M., Mastrianni, J., Gabizon, R., Torchia, M., Cohen, F.E., DeArmond, S.J. and Prusiner, S.B. (1995) Prion propagation in mice expressing human and chimeric PrP transgenes implicates the interaction of cellular PrP with another protein. *Cell*, **83**, 79-90.

Titeux, M., Galou, M., Gomes, F.C., Dormont, D., Neto, V.M. and Paulin, D. (2002) Differences in the activation of the GFAP gene promoter by prion and viral infections. *Molecular Brain Research*, **109**, 119-127.

Tobler, I., Gaus, S.E., Deboer, T., Achermann, P., Fischer, M., Rulicke, T., Moser, M., Oesch, B., McBride, P.A. and Manson, J.C. (1996) Altered circadian activity rhythms and sleep in mice devoid of prion protein. *Nature*, **380**, 639-642.

Torres, G.E., Carneiro, A., Seamans, K., Fiorentini, C., Sweeney, A., Yao, W.D. and Caron, M.G. (2003) Oligomerization and trafficking of the human dopamine transporter. Mutational analysis identifies critical domains important for the functional expression of the transporter. *The Journal of Biological Chemistry*, **278**, 2731-2739.

Toumazos, P. (1991) Scrapie in Cyprus. *British Veterinary Journal*, **147**, 147-154.

Turk, E., Teplow, D.B., Hood, L.E. and Prusiner, S.B. (1988) Purification and properties of the cellular and scrapie hamster prion proteins. *European Journal of Biochemistry*, **176**, 21-30.

Tuzi, N.L., Gall, E., Melton, D. and Manson, J.C. (2002) Expression of doppel in the CNS of mice does not modulate transmissible spongiform encephalopathy disease. *Journal of General Virology*, **83**, 705-711.

van Keulen, L.J.M., Schreuder, B.E.C., Meloen, R.H., Mooij-Harkes, G., Vromans, M.E.W. and Langeveld, J.P.M. (1996) Immunohistochemical detection of prion protein in lymphoid tissues of sheep with natural scrapie. *Journal of Clinical Microbiology*, **34**, 1228-1231.

van Rheede, T., Smolenaars, M.M.W., Madsen, O. and de Jong, W.W. (2003) Molecular evolution of the Mammalian prion protein. *Molecular biology and evolution*, **20**, 111-121.

Verghese-Nikolakaki, S., Michaloudi, H., Polymenidou, M., Groschup, M.H., Papadopoulos, G.C. and Sklaviadis, T. (1999) Expression of the prion protein in the rat forebrain--an immunohistochemical study. *Neuroscience Letters*, **272**, 9-12.

Vetrugno, V., Cardinale, A., Filesi, I., Mattei, S., Sy, M.S., Pocchiari, M. and Biocca, S. (2005) KDEL-tagged anti-prion intrabodies impair PrP lysosomal degradation and inhibit scrapie infectivity. *Biochemical and Biophysical Research Communications*, **338**, 1791-1797.

Vey, M., Pilkuhn, S., Wille, H., Nixon, R., DeArmond, S.J., Smart, E.J., Anderson, R.G.W., Taraboulos, A. and Prusiner, S.B. (1996) Subcellular colocalization of the cellular and scrapie prion proteins in caveolae-like membranous domains. *Proceedings of the National Academy of Sciences of the United States of America*, **93**, 14945-14949.

Vincent, B., Paitel, E., Saftig, P., Frobert, Y., Hartmann, D., De Strooper, B., Grassi, J., Lopez-Perez, E. and Checler, F. (2001) The disintegrins ADAM10 and TACE contribute to the constitutive and phorbol ester-regulated normal cleavage of the cellular prion protein. *The Journal of Biological Chemistry*, **276**, 37743-37746.

Vorberg, I. and Priola, S.A. (2002) Molecular basis of scrapie strain glycoform variation. *The Journal of Biological Chemistry*, **277**, 36775-36781.

Walmsley, A.R. and Hooper, N.M. (2003) Distance of sequons to the C-terminus influences the cellular N-glycosylation of the prion protein. *Biochemistry Journal*, **370**, 351-355.

Walmsley, A.R., Zeng, F. and Hooper, N.M. (2001) Membrane topology influences N-glycosylation of the prion protein. *The EMBO Journal*, **20**, 703-712.

Wang, J.Z., Grundke-Iqbal, I. and Iqbal, K. (1996) Glycosylation of microtubule-associated protein tau: an abnormal posttranslational modification in Alzheimer's disease. *Nature Medicine*, **2**, 871-875.

Wang, T. and Hebert, D.N. (2003) EDEM an ER quality control receptor. *Nature structural biology*, **10**, 319-321.

Ward, H.J., Everington, D., Cousens, S.N., Smith-Bathgate, B., Leitch, M., Cooper, S., Heath, C., Knight, R.S., Smith, P.G. and Will, R.G. (2006) Risk factors for variant Creutzfeldt-Jakob disease: a case-control study. *Annals of Neurology*, **59**, 111-120.

Watt, N.T., Taylor, D.R., Gillott, A., Thomas, D.A., Perera, W.S. and Hooper, N.M. (2005) Reactive oxygen species-mediated beta-cleavage of the prion protein in the cellular response to oxidative stress. *The Journal of Biological Chemistry*, **280**, 35914-35921.

Weissmann, C. (1991) Spongiform encephalopathies. The prion's progress. *Nature*, **349**, 569-571.

Wells, G.A., Hawkins, S.A., Austin, A.R., Ryder, S.J., Done, S.H., Green, R.B., Dexter, I., Dawson, M. and Kimberlin, R.H. (2003) Studies of the transmissibility of the agent of bovine spongiform encephalopathy to pigs. *Journal of General Virology*, **84**, 1021-1031.

Wells, G.A., Scott, A.C., Johnson, C.T., Gunning, R.F., Hancock, R.D., Jeffrey, M., Dawson, M. and Bradley, R. (1987) A novel progressive spongiform encephalopathy in cattle. *Vetertinary Record*, **121**, 419-420.

Wentworth, D.E. and Holmes, K.V. (2001) Molecular determinants of species specificity in the coronavirus receptor aminopeptidase N (CD13): influence of N-linked glycosylation. *Journal of Virology*, **75**, 9741-9752.

Westaway, D., DeArmond, S.J., Cayetano-Canlas, J., Groth, D., Foster, D., Yang, S.L., Torchia, M., Carlson, G.A. and Prusiner, S.B. (1994) Degeneration of skeletal muscle, peripheral nerves, and the central nervous system in transgenic mice overexpressing wild-type prion proteins. *Cell*, **76**, 117-129.

Westaway, D., Goodman, P.A., Mirenda, C.A., McKinley, M.P., Carlson, G.A. and Prusiner, S.B. (1987) Distinct prion proteins in short and long scrapie incubation period mice. *Cell*, **51**, 651-662.

Wickner, R.B. (1994) [URE3] as an altered URE2 protein: evidence for a prion analog in Saccharomyces cerevisiae. *Science*, **264**, 566-569.

Wilesmith, J.W., Wells, G.A., Cranwell, M.P. and Ryan, J.B. (1988) Bovine spongiform encephalopathy: epidemiological studies. *Veterinary Record*, **123**, 638-644.

Will, R.G., Ironside, J.W., Zeidler, M., Cousens, S.N., Estibeiro, K., Alperovitch, A., Poser, S., Pocchiari, M., Hofman, A. and Smith, P.G. (1996) A new variant of Creutzfeldt-Jakob disease in the UK. *Lancet*, **347**, 921-925.

Wille, H., Michelitsch, M.D., Guenebaut, V., Supattapone, S., Serban, A., Cohen, F.E., Agard, D.A. and Prusiner, S.B. (2002) Structural studies of the scrapie prion protein by electron crystallography. *Proceedings of the National Academy of Sciences of the United States of America*, **99**, 3563-3568.

Williams, A., Lucassen, P.J., Ritchie, D. and Bruce, M. (1997a) PrP deposition, microglial activation, and neuronal apoptosis in murine scrapie. *Experimental Neurology*, **144**, 433-438.

Williams, A., Van Dam, A.M., Ritchie, D., Eikelenboom, P. and Fraser, H. (1997b) Immunocytochemical appearance of cytokines, prostaglandin E2 and lipocortin-1 in the CNS during the incubation period of murine scrapie correlates with progressive PrP accumulations. *Brain Research* **754**, 171-180.

Williams, A.E., Lawson, L.J., Perry, V.H. and Fraser, H. (1994) Characterization of the microglial response in murine scrapie. *Neuropathology and Applied Neurobiology*, **20**, 47-55.

Williams, A.E., Ryder, S. and Blakemore, W.F. (1995) Monocyte recruitment into the scrapie-affected brain. *Acta neuropathologica (Berl)*, **90**, 164-169.

Williams, E.S. and Young, S. (1980) Chronic wasting disease of captive mule deer: a spongiform encephalopathy. *Journal of Wildlife Diseases*, **16**, 89-98.

Winklhofer, K.F., Heller, U., Reintjes, A. and Tatzelt, J. (2003) Inhibition of Complex Glycosylation Increases the Formation of PrPsc. *Traffic*, **4**, 313-322.

Wiseman, F. (2003) The Role of Glycosylation in the processing and cellular localisation of PrP. *Science and Enginering*. The University of Edinburgh, Edinburgh, Vol. Master of Science by Research.

Wong, N.K.C., Renouf, D.V., Lehmann, S. and Hounsell, E.F. (2000) Glycosylation of prions and its effects on protein conformation relevant to amino acid mutations. *Journal of Molecular Graphics and Modelling*, **18**, 126-134, 163-125.

Wopfner, F., Weidenhofer, G., Schneider, R., von Brunn, A., Gilch, S., Schwarz, T.F., Werner, T. and Schatzl, H.M. (1999) Analysis of 27 mammalian and 9 avian PrPs reveals high conservation of flexible regions of the prion protein. *Journal of Molecular Biology*, **289**, 1163-1178.

Wyatt, J.M., Pearson, G.R., Smerdon, T.N., Gruffydd-Jones, T.J., Wells, G.A. and Wilesmith, J.W. (1991) Naturally occurring scrapie-like spongiform encephalopathy in five domestic cats. *Veterinary Record*, **129**, 233-236.

Xanthopoulos, K., Polymenidou, M. and Sklaviadis, T. (2006) Comparative inter-species carbohydrate characterisation of PrPSc by lectins. *Prion 2006*, Lingotto, Turino, p. 225.

Yadavalli, R., Guttmann, R.P., Seward, T., Centers, A.P., Williamson, R.A. and Telling, G.C. (2004) Calpain-dependent endoproteolytic cleavage of PrPSc modulates scrapie prion propagation. *The Journal of Biological Chemistry*, **279**, 21948-21956.

Yang, X.W., Model, P. and Heintz, N. (1997) Homologous recombination based modification in Escherichia coli and germline transmission in transgenic mice of a bacterial artificial chromosome. *Nature Biotechnology*, **15**, 859-865.

Yang, X.W., Wynder, C., Doughty, M.L. and Heintz, N. (1999) BAC-mediated gene-dosage analysis reveals a role for Zipro1 (Ru49/Zfp38) in progenitor cell proliferation in cerebellum and skin. *Nature Genetics*, **22**, 327-335.

Yedidia, Y., Horonchik, L., Tzaban, S., Yanai, A. and Taraboulos, A. (2001) Proteasomes and ubiquitin are involved in the turnover of the wild-type prion protein. *The EMBO Journal*, **20**, 5383-5391.

Yehiely, F., Bamborough, P., Da Costa, M., Perry, B.J., Thinakaran, G., Cohen, F.E., Carlson, G.A. and Prusiner, S.B. (1997) Identification of candidate proteins binding to prion protein. *Neurobiology of Disease*, **3**, 339-355.

Yoshida, Y., Chiba, T., Tokunaga, F., Kawasaki, H., Iwai, K., Suzuki, T., Ito, Y., Matsuoka, K., Yoshida, M., Tanaka, K. and Tai, T. (2002) E3 ubiquitin ligase that recognizes sugar chains. *Nature*, **418**, 438-442.

Zanusso, G. (2006) Novel prion protein conformation and glycotype in atypical Creutfeldt Jackob Disease. *Prion2006*, Lingotto, Turino, p. 38.

Zanusso, G., Liu, D., Ferrari, S., Hegyi, I., Yin, X., Aguzzi, A., Hornemann, S., Liemann, S., Glockshuber, R., Manson, J.C., Brown, P., Petersen, R.B., Gambetti, P. and Sy, M.S. (1998) Prion protein expression in different species: analysis with a panel of new mAbs. *Proceedings of the National Academy of Sciences of the United States of America*, **95**, 8812-8816.

Zlotnik, I. (1965) Observations on the experimental transmission of scrapie of various origins to laboratory animals. In *Slow latent and temperate virus infections* US Goverment Printing, Washington DC:, pp. 237-248.

Zlotnik, I. and Rennie, J.C. (1958) A comparative study of the incidence of vacuolated neurones in the medulla from apparently healthy sheep of various breeds. *Journal of Comparative Pathology*, **68**, 411-415.

Zuegg, J. and Gready, J.E. (2000) Molecular dynamics simulation of human prion protein including both N-linked oligosaccharides and the GPI anchor. *Glycobiology*, **10**, 959-974.

Appendix i

Summary of published work on the importance of glycosylation state to the cellular localisation of PrP

Model System	Method of N-glycan attachment inhibition	Cellular localisation	Reference
tgSHa PrP in CV1 cells	T183A	No surface staining but observed intracelluarly	Rogers et al., 1990
tgSHa PrP in CV1 cells	T197A	No surface staining but observed intracelluarly	Rogers et al., 1990
tgSHa PrP in CV1 cells	T183A, T197A	No surface staining but observed intracelluarly	Rogers et al., 1990
tgMo(3F4) in CHO cells	T182A	No surface staining, Endo H sensitive	Lehmann and Harris 1997
tgMo(3F4) in CHO cells	T198A	Surface staining, Endo H resistant	Lehmann and Harris 1997
tgMo(3F4) in CHO cells	T182A, T198A	No surface staining,	Lehmann and Harris 1997
tgMo(3F4) in CHO cells	Tunicamycin	Surface staining	Lehmann and Harris 1997
tgSHa PrP in murine $PrP^{0/0}$ (2-4 X)	T183A	Cell bodies *in vivo*	DeArmond et al., 1997
tgSHa PrP in murine $PrP^{0/0}$ (2-4 X)	T199A	Cell surface, white matter and some intracellular *in vivo*	DeArmond et al., 1997
tgSHa PrP in murine $PrP^{0/0}$ (2-4 X)	T183A, T199A	Cell bodies *in vivo*	DeArmond et al., 1997
tgMHM2 PrP in ScN2a	N180Q,N196Q	Surface staining	Korth et al., 2000
tgMHM2 PrP in ScN2a	T182A,T198A	No surface staining but observed intracelluarly	Korth et al., 2000
tg(CEPß-prion) M-17 human neuroblastoma	N181Q	Cell membrane (Endo H resistant – passes ER)	Capellari et al., 2000
tg(CEPß-prion) M-17 human neuroblastoma	T183A	Intracellular (Endo H sensitive - ER retention)	Capellari et al., 2000
tgMo(3F4) in murine $PrP^{0/0}$ (1-4X)	T182N	Cell surface (N2a cells)	Neurodorf et al., 2005
tgMo(3F4) in murine $PrP^{0/0}$ (1-4X)	T198A	Cell surface (N2a cells)	Neurodorf et al., 2005
tgMo(3F4) in murine $PrP^{0/0}$ (1-4X)	T182N, T198A	Cell surface (N2a cells)	Neurodorf et al., 2005

Appendix ii Summary of TSE transmissions to PrP glycosylation deficient transgenics

Model	TSE agent	Incubation Period dpi	Reference
Mouse TgSHaPrP (T183A) or (T183A, T199A)	Sc237 or 139H	Resistant	(DeArmond et al., 1997)
Mouse TgSHaPrP (T199A) #1 or #2	Sc237	>500	
Mouse TgSHaPrP (T199A)	139H	555	
Mouse TgSHaPrP (T199A)	139H	548	
Mouse SHaPrP	Sc237	55	
Mouse SHaPrP	139H	64	
Mouse TgMoPrP (T182N) #1	Chandler	163	(Neuendorf et al., 2004)
Mouse TgMoPrP (T182N) #2	Chandler	240	
Mouse TgMoPrP (T182N) #1	ME7	308	
Mouse TgMoPrP (T182N) #2	ME7	323	
Mouse TgMoPrP (T182N) #1	Murine BSE	169	
Mouse TgMoPrP (T182N) #2	Murine BSE	224	
Mouse TgMoPrP (T198A) #1	Chandler	305	
Mouse TgMoPrP (T198A) #2	Chandler	390	
Mouse TgMoPrP (T198A) #1	ME7	408	
Mouse TgMoPrP (T198A) #2	ME7	405	
Mouse TgMoPrP (T198A) #1	Murine BSE	390	
Mouse TgMoPrP (T198A) #2	Murine BSE	392	
Mouse (C57/B6)	Chandler	164	
Mouse (C57/B6)	ME7	172	
Mouse (C57/B6)	Murine BSE	197	
Mouse gtMoPrP (N180T)	79A	194	Tuzi et al., in preparation
Mouse gtMoPrP (N180T)	ME7	>600	
Mouse gtMoPrP (N196T)	79A	167	
Mouse gtMoPrP (N196T)	ME7	160	
Mouse gtMoPrP (N196T)	301C	354	
Mouse gtMoPrP (N180T, N196T)	79A	435 *	
Mouse gtMoPrP (N180T, N196T)	ME7	>700	
Mouse (129/Ola)	79A	148	
Mouse (129/Ola)	ME7	163	
Mouse (129/Ola)	301C	166	

*Disease incidence 4/21

Appendix iii Titration of anti-tubulin antibody (rat monoclonal)

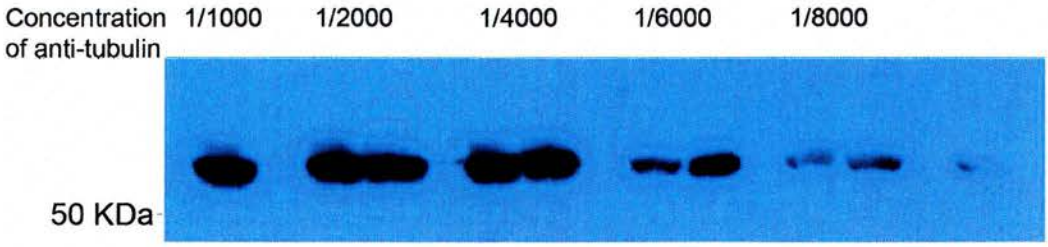

Western blot of total brain proteins was used to determine required concentration of anti-tubulin rat monoclonal required for clear signal.

Appendix iv Titration of anti-PrP antibody 6H4 in 263K challenged mice

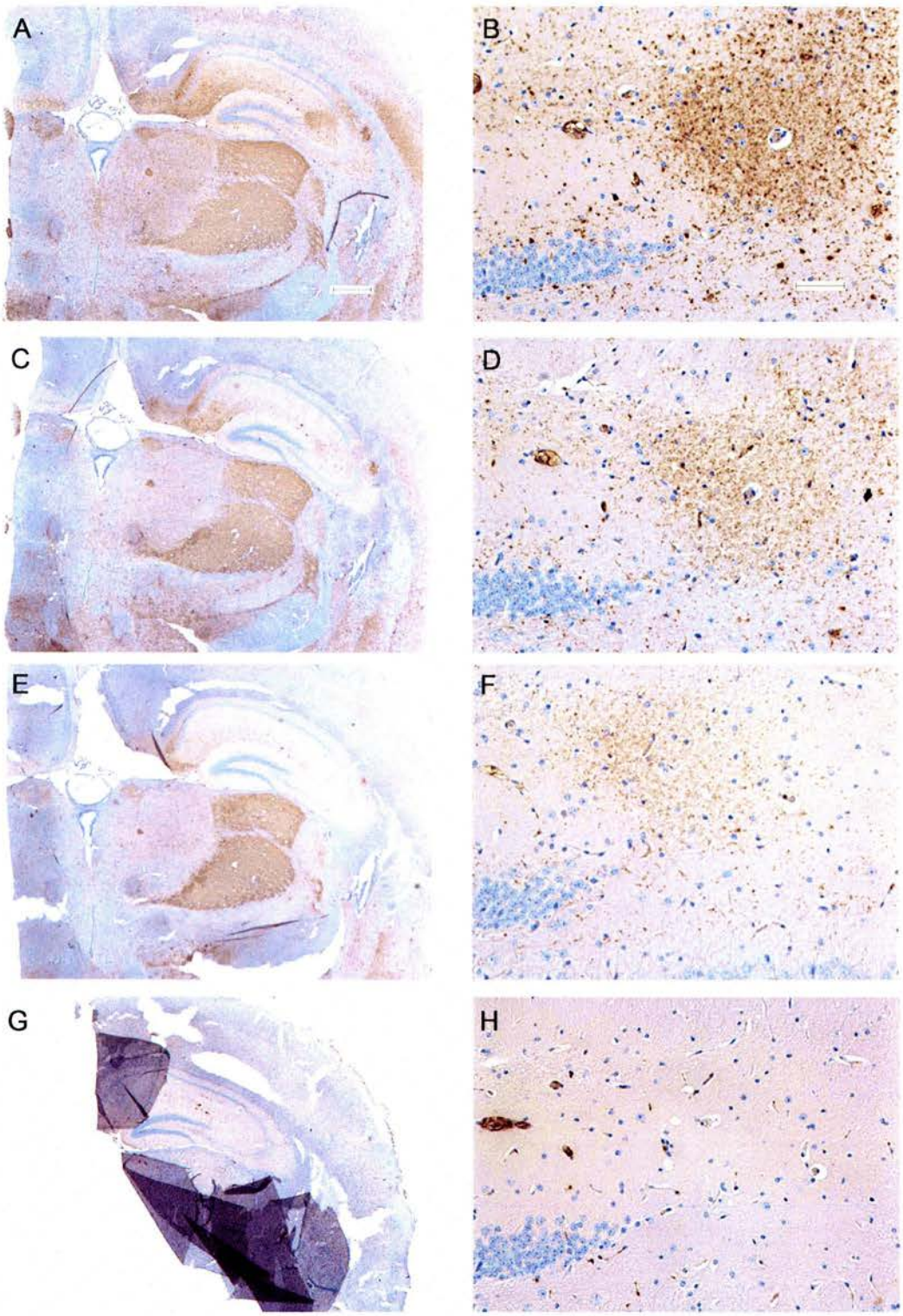

IHC performed on sections from a G2 transgenic challenged with 263K that were subjected to antigen retrival. Anti-PrP antibody (6H4) used at (A, B) 1/20,000, (C & D) 1/40,000, (E & F) 1/80,000. Normal mouse serum (1/20,000) used as negative control (G & H). Scale bar 500 µm (A, C, E, G) and 50 µm (B, D, F, H).

Appendix v Titration of anti-PrP antibody 8H4 in 263K challenged mice

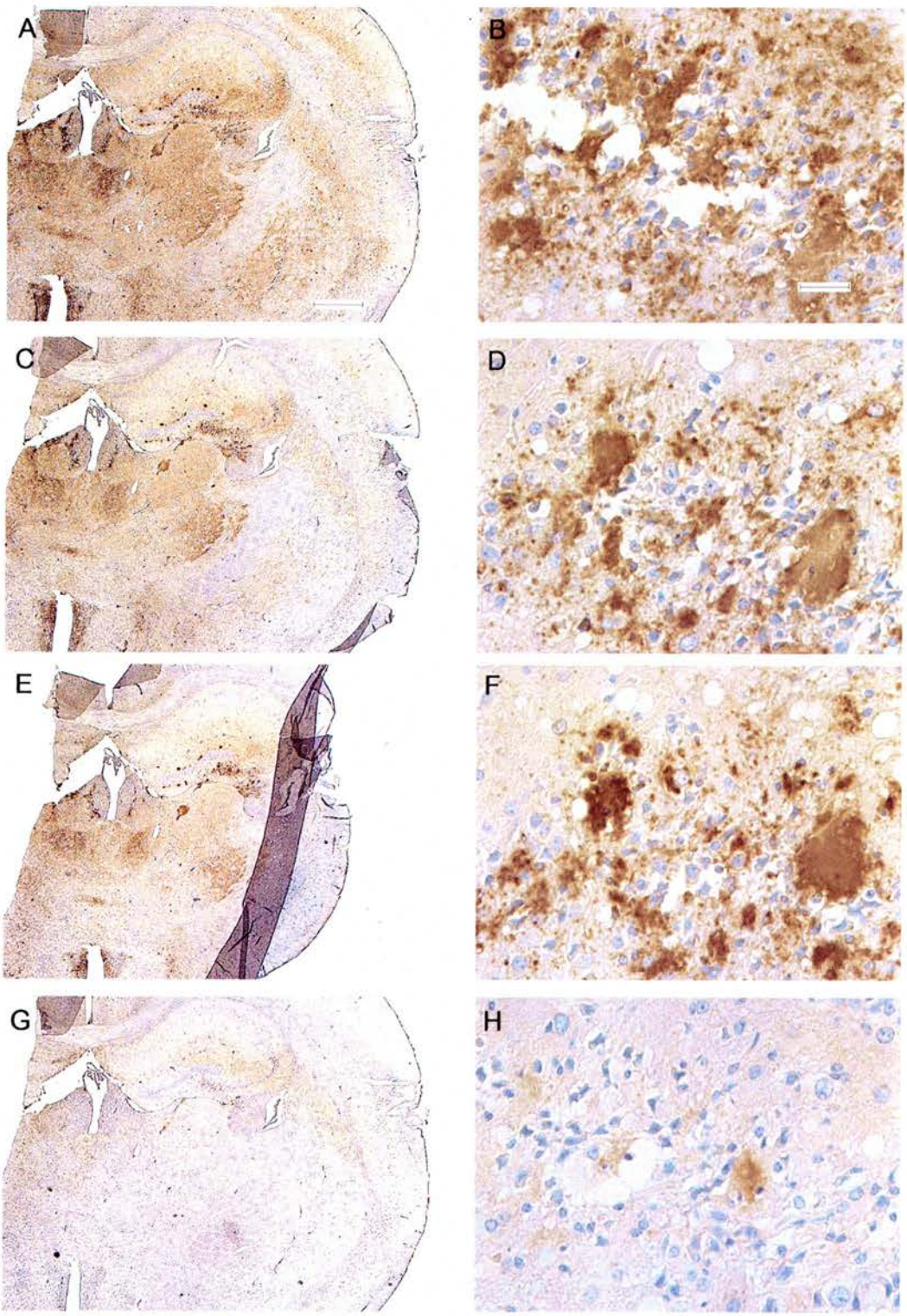

IHC performed on sections from a G2 transgenic challenged with 263K that were subjected to antigen retrival. Anti-PrP antibody (8H4) used at (A, B) 1/5000, (C & D) 1/10,000, (E & F) 1/20,000. Normal mouse serum (1/10,000) used as negative control (G & H). Scale bar 500 µm (A, C, E, G) 50 µm (B, D, F, H).

Appendix vi

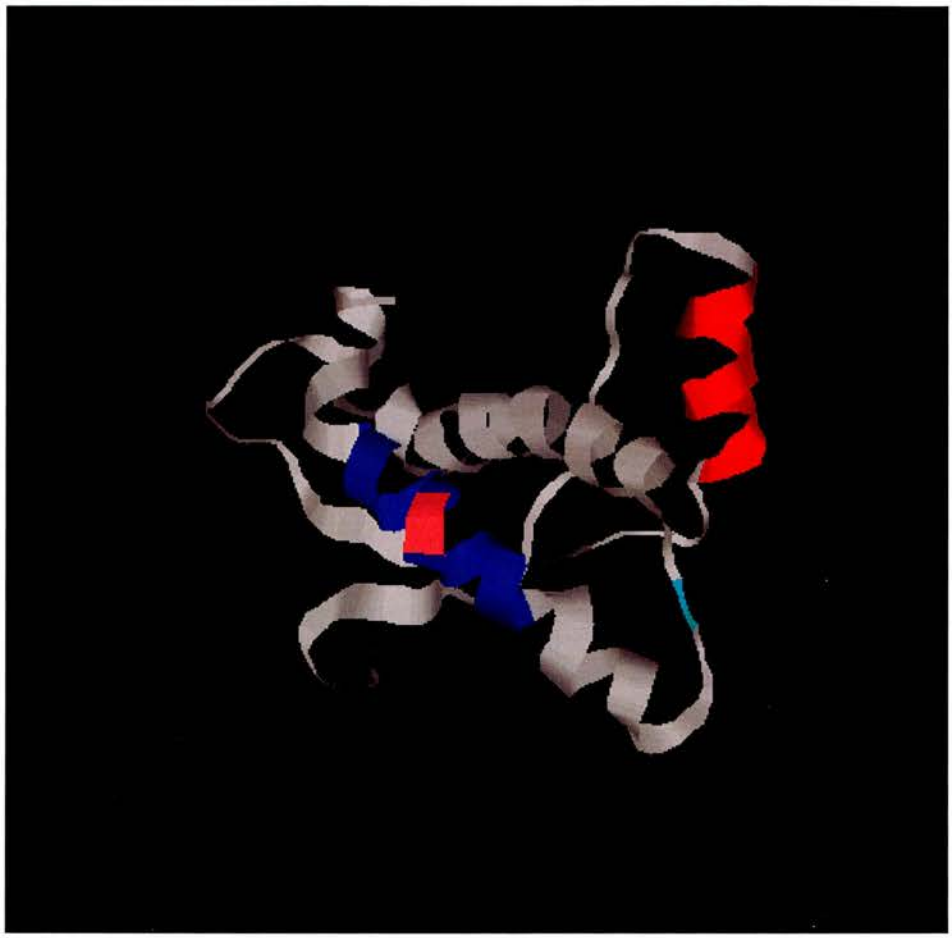

Localisation of the 6H4 and 8H4 epitopes on PrP (Based on the structure of murine PrP amino acid 121-231 published by Riek *et al* 2006). The epitope of anti-PrP antibody 6H4 is located in the first α-helix (amino acids 143-151 red)and the epitope of anti-PrP antibody 8H4 is located in the third α-helix (amino acids 175-185 blue) and includes the first N-glycan attachment site (N-glycan linked asaparagine[180] in pink), neither epitope is located near the second N-glycan attachment site (N-glycan linked asaparagine[196] cyan).

Appendix vii Titration of 6H4 in sporadic CJD MM type 2 challenged mice

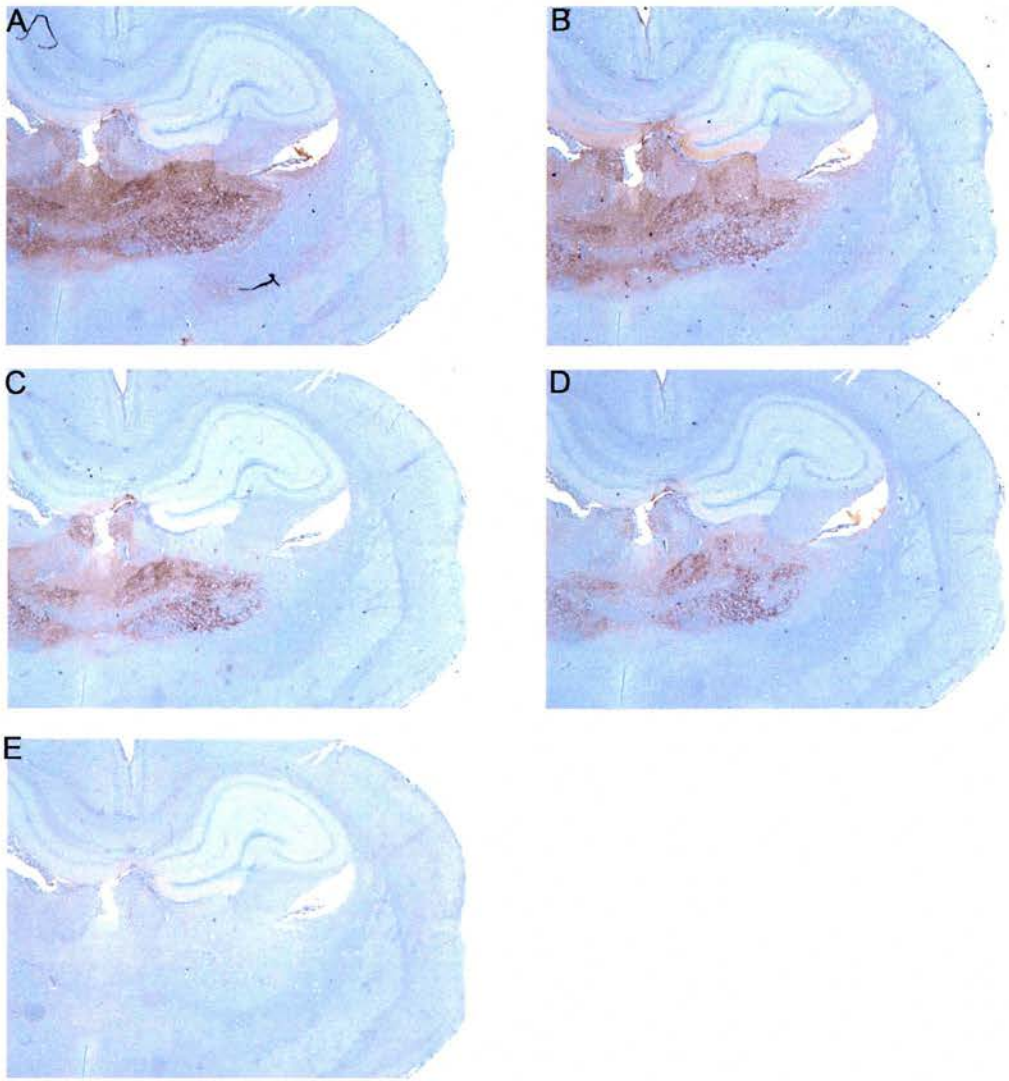

IHC performed on sections from a G2 transgenic challenged with sporadic CJD that were subjected to antigen retrival. Anti-PrP antibody (6H4) was used at (A) 1/10,000, (B) 1/20,000, (C)1/40,000, (D) 1/80,000. Normal mouse serum (1/20,000) was used as a negative control (E).

Appendix viii Titration of anti-PrP antibody (8H4) in sporadic CJD challenged mice

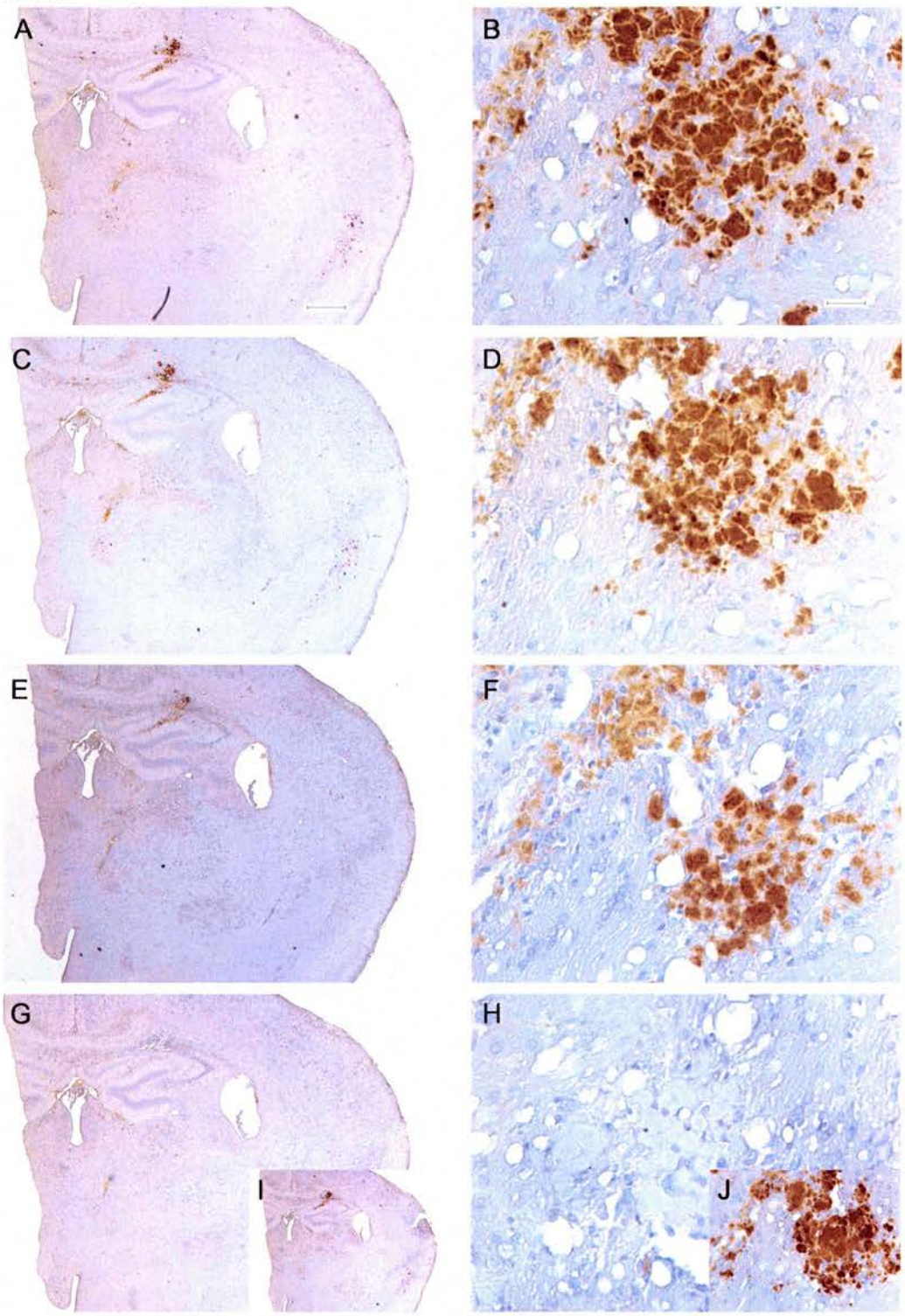

IHC performed on sections from a G2 transgenic challenged with sporadic CJD that were subjected to antigen retrival. Anti-PrP antibody (8H4) was used at (A & B) 1/5,000, (C & D) 1/10,000, (E & F)1/20,000. Normal mouse serum (1/20,000) was used as a negative control (G & H) and anti-PrP antibody (6H4 1/20,000) (I & J). Scale-bar 500 µm (A, C, E, G) and 50 µm (B, D, F, H).

Appendix ix Tritration of anti-PrP antibody 6H4 in variant CJD challenged mice

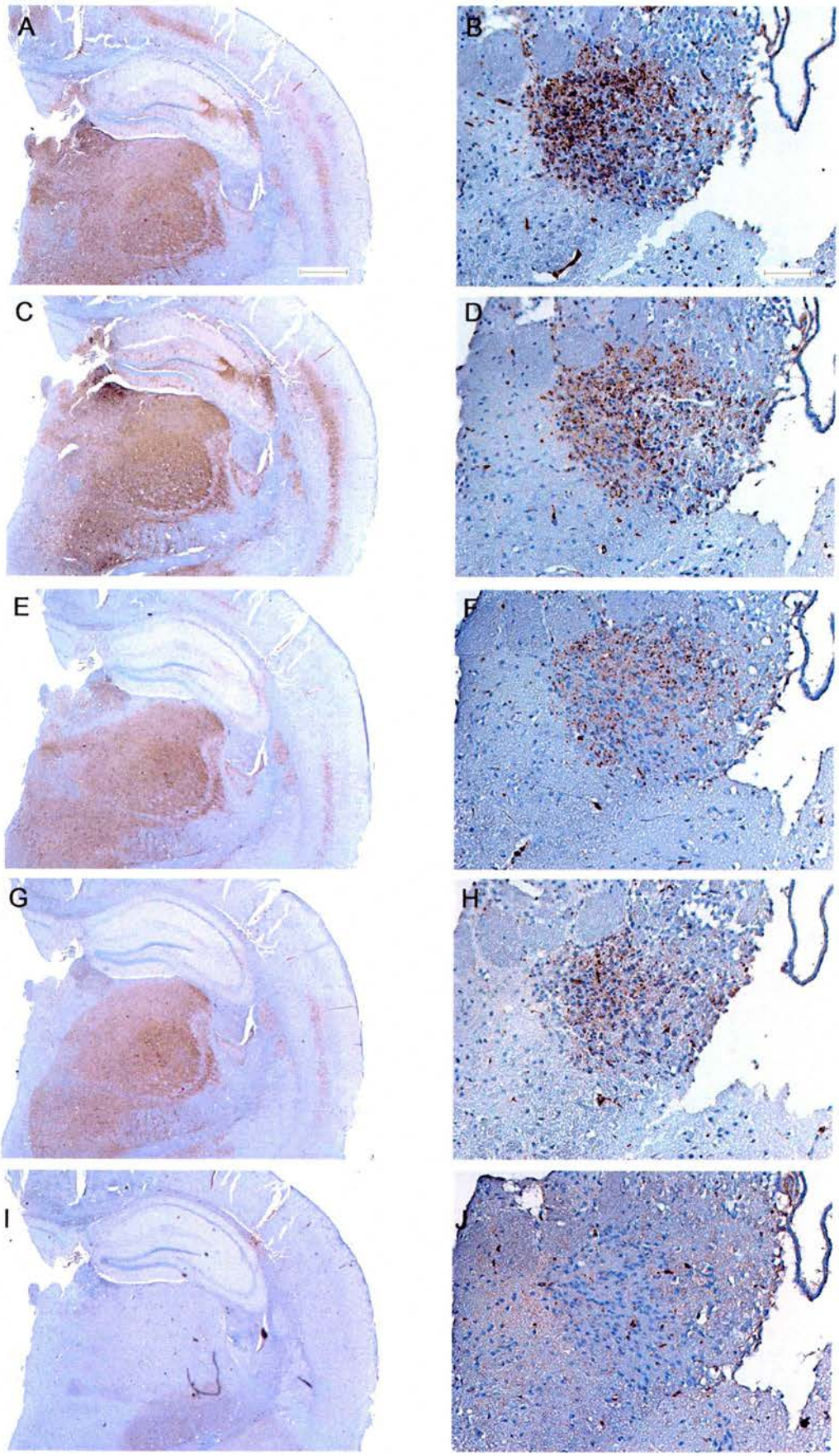

Appendix xTitration of anti-PrP anti-body in variant CJD challenged mice

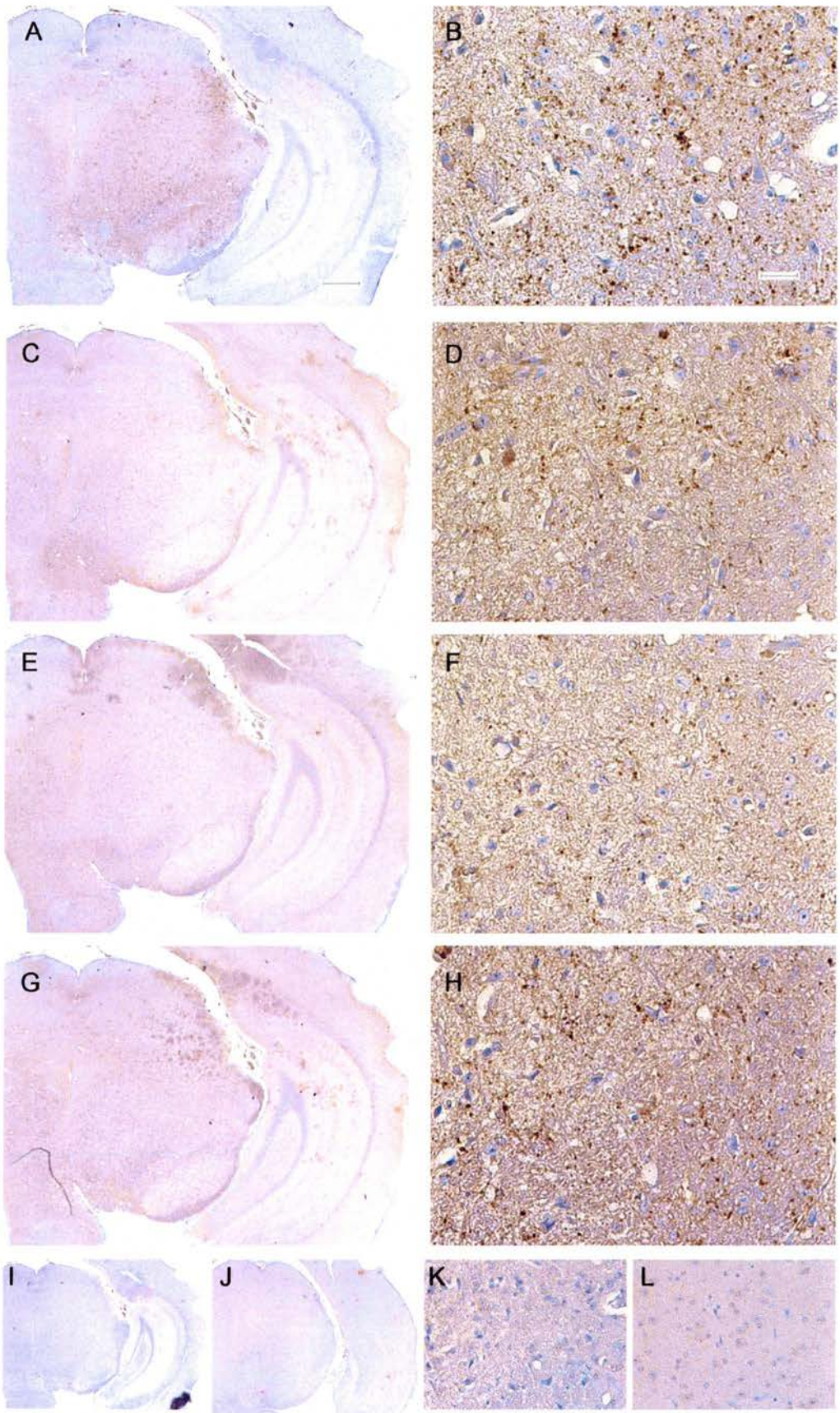

Appendix ix Titration 6H4 on variant CJD challenged mice

IHC was performed on sections from a clinical endpoint control mouse challenged with variant CJD that were subjected to antigen retrieval. Anti-PrP antibody (6H4) was used at (A & B) 1/10,000, (C & D) 1/20,000, (E & F) 1/40,000 and (G & H) 1/80,000. Normal mouse serum (I & J) 1/20,000 was used as a negative control. Scale bar 500 μm (A, C, E, G) and 50 μm (B, D, F, H).

Appendix x Titration 8H4 on variant CJD challenged mice

IHC was performed on sections from a clinical endpoint control mouse challenged with variant CJD that were subjected to antigen retrieval. Anti-PrP antibody (8H4) was used at (C & D) 1/2,500, (E & F) 1/5,000 and (G & H) 1/10,000. Anti-PrP antibody 6H4 1/20,000 was used as a positive control (A & B). Normal mouse serum 1/20,000 (I & K) and 8H4 (1/5,000) staining of section from a PrP null mouse (J & L) were used as a negative controls; non-specific binding to PrP null section was observed at 8H4 (1/2,500) data not shown. Scale bar 500 μm (A, C, E, G) and 50 μm (B, D, F, H).

Appendix xi Western bot of false positive ME7 seeded G1 PrP^C substrate PMCA

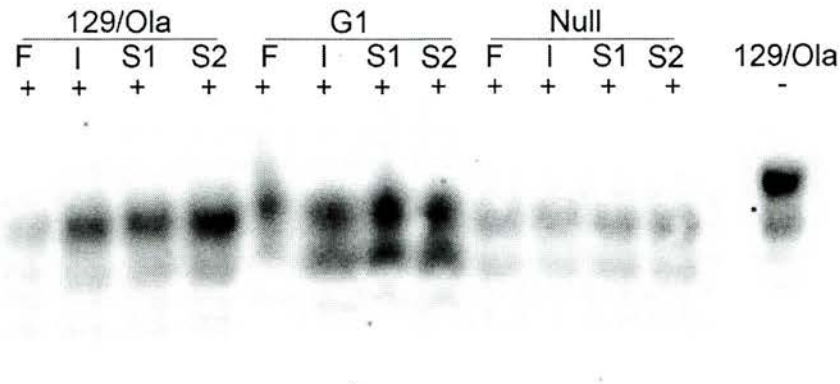

Western blot of ME7 seeded PMCA reactions in duplicate (S1 & S2), non-sonicated controls incubated at 37 °C (I) or frozen (F). Using normal brain homogenate as source of PrP^C from a PrP null, G1 transgenic and a normally glycosylated 129/Ola mouse, as indicated. A ratio of 1:100 ME7 to normal brain homogenate (5 mM EDTA) was used. Samples were digested with PK (50 µg/ml, 37 °C, 1 hour). Although by densitometric criteria the G1 PMCA reactions scored as positive amplifications, this appears to be an experimental artefact, incomplete PK digestion may have occured in these samples, additionally the frozen control in particular has not resolved during electrophoresis perhaps because of an excess of loaded protien in this sample.

Appendix xii list of publications resulting from this thesis

Cancellotti, E., Barron, R.M., Bishop, M.T., Hart, P., Wiseman, F. and Manson, J.C. (2006) The role of host PrP in Transmissible Spongiform Encephalopathies. *Biochimica et Biophysica Acta*.

Cancellotti, E., Wiseman, F., Tuzi, N.L., Baybutt, H., Monaghan, P., Aitchison, L., Simpson, J. and Manson, J.C. (2005) Altered glycosylated PrP proteins can have different neuronal trafficking in brain but do not acquire scrapie-like properties. *The Journal of Biological Chemistry*, **280**, 42909-42918.

Wiseman, F., Cancellotti, E. and Manson, J. (2005) Glycosylation and misfolding of PrP. *Biochemical Society Transactions*, **33**, 1094-1095.